ORNL-3945
UC-10 – Chemical Separations Processes
for Plutonium and Uranium

CHEMICAL TECHNOLOGY DIVISION
ANNUAL PROGRESS REPORT
FOR PERIOD ENDING MAY 31, 1966

OAK RIDGE NATIONAL LABORATORY
operated by
UNION CARBIDE CORPORATION
for the
U.S. ATOMIC ENERGY COMMISSION

Printed in USA. Price $6.00. Available from the Clearinghouse for Federal Scientific and Technical Information, National Bureau of Standards, U.S. Department of Commerce, Springfield, Virginia 22151

LEGAL NOTICE

This report was prepared as an account of Government sponsored work. Neither the United States, nor the Commission, nor any person acting on behalf of the Commission:

A. Makes any warranty or representation, expressed or implied, with respect to the accuracy, completeness, or usefulness of the information contained in this report, or that the use of any information, apparatus, method, or process disclosed in this report may not infringe privately owned rights; or

B. Assumes any liabilities with respect to the use of, or for damages resulting from the use of any information, apparatus, method, or process disclosed in this report.

As used in the above, "person acting on behalf of the Commission" includes any employee or contractor of the Commission, or employee of such contractor, to the extent that such employee or contractor of the Commission, or employee of such contractor prepares, disseminates, or provides access to, any information pursuant to his employment or contract with the Commission, or his employment with such contractor.

ORNL-3945

Contract No. W-7405-eng-26

CHEMICAL TECHNOLOGY DIVISION
ANNUAL PROGRESS REPORT
for Period Ending May 31, 1966

D. E. Ferguson – Division Director
R. G. Wymer – Chemical Development Section A Chief
R. E. Blanco – Chemical Development Section B Chief
K. B. Brown – Chemical Development Section C Chief
M. E. Whatley – Unit Operations Section Chief
H. E. Goeller – Process Design Section Chief
R. E. Brooksbank – Pilot Plant Section Chief

SEPTEMBER 1966

OAK RIDGE NATIONAL LABORATORY
Oak Ridge, Tennessee
operated by
UNION CARBIDE CORPORATION
for the
U. S. ATOMIC ENERGY COMMISSION

Contents

SUMMARY 1

1. POWER-REACTOR FUEL PROCESSING 27
   - 1.1 Development of Processes for Graphite-Base Fuels 28
   - 1.2 Development of Mechanical Processes 33
   - 1.3 Development of Processes for Heavy-Water-Moderated, Organic-Cooled Reactor Fuel 40
   - 1.4 Studies of the Adsorption of Protactinium 42
   - 1.5 Close-Coupled Process Development 43
   - 1.6 Hydrolysis of Uranium, Thorium, and Fission Product Carbides 47

2. FLUORIDE-VOLATILITY PROCESSING 48
   - 2.1 Fluidized-Bed Volatility Process Development: Laboratory Studies for Stainless-Steel- and Zircaloy-Clad UO_2 Fuels 48
   - 2.2 FBVPD: Small-Scale Engineering Studies 52
   - 2.3 Design of the Fluidized-Bed Volatility Pilot Plant for Zircaloy- and Stainless-Steel-Clad UO_2 Power-Reactor Fuels 54
   - 2.4 Corrosion Studies Related to the FBVPP, and More Corrosion Data from the Molten-Salt Volatility Pilot Plant 60
   - 2.5 Continuous In-Line Monitoring of Gas Streams in the Fluidized-Bed Fluoride-Volatility Process 64
   - 2.6 Sorption of Plutonium Hexafluoride by Metal Fluorides 66
   - 2.7 Separation of Uranium Hexafluoride from Bromine Fluorides 67
   - 2.8 Chromium Chemistry and the Behavior of Chromium in Volatility Processing 68
   - 2.9 Vapor-Liquid Equilibria of UF_6-NbF_5 System 69

3. MOLTEN-SALT REACTOR PROCESSING 72
   - 3.1 Continuous Fluorination of Molten Salt 72
   - 3.2 Distillation of Molten Salt 73
   - 3.3 Alternative Processing Methods for a Molten-Salt Breeder Reactor 75

4. WASTE TREATMENT AND DISPOSAL 79
   - 4.1 High-Level Radioactive Waste 79
   - 4.2 Intermediate-Level Radioactive Waste 88
   - 4.3 Low-Level Radioactive Waste 93
   - 4.4 Engineering, Economic, and Safety Evaluation 97

5. TRANSURANIUM-ELEMENT PROCESSING 107
5.1 Development of Chemical Processes 107
5.2 Development of Process Equipment 118
5.3 Design and Fabrication of Process Equipment 119
5.4 Construction of TRU 121
5.5 TRU Operations 125

6. CURIUM PROCESSING 129
6.1 Process Development 129
6.2 Solvent Extraction Processing of ^{243}Am-^{244}Cm 131
6.3 Processing of the $^{241}AmO_2$ Targets 133
6.4 Curium Recovery Facility Equipment 138

7. DEVELOPMENT OF THE THORIUM FUEL CYCLE 141
7.1 ^{233}U Storage and Distribution Facility 141
7.2 Sol-Gel Process: Further Development and New Applications 141
7.3 Development of Methods for Producing Microspheres 146
7.4 Construction of Thorium-Uranium Recycle Facility 153
7.5 Design of Process Equipment 155

8. SOL-GEL PROCESSES FOR THE URANIUM FUEL CYCLE 157
8.1 Uranium Sol-Gel Processes 157
8.2 Plutonia Sol-Gel Process 170

9. SEPARATIONS CHEMISTRY RESEARCH 176
9.1 Extraction of Metal Chlorides by Amines 176
9.2 New Separations Agents 176
9.3 Performance of Degraded Reagents and Diluents 179
9.4 Comparative Chemistry of Lanthanides and Trivalent Actinides 181
9.5 Recovery of Beryllium from Ores 182
9.6 Extraction of Alkalies by Di(2-ethylhexyl)phosphoric Acid (HDEHP) 183
9.7 Extraction of Cesium by 4-sec-Butyl-2-α-methylbenzylphenol (BAMBP) Plus Organic Acids 184
9.8 Kinetics of Metal-Ion Extractions by Di(2-ethylhexyl)phosphoric Acid (HDEHP) 185
9.9 Aggregation and Activity Coefficients in Solvent Phases 186

10. CHEMICAL APPLICATIONS OF NUCLEAR EXPLOSIONS 189
10.1 Copper Ores 189
10.2 Magnesium Ores 192
10.3 Stimulation of Natural Gas Wells 192
10.4 Production of Oil from Shale 193
10.5 Development of Hypervelocity Jet Samplers 193

11. RECOVERY OF FISSION PRODUCTS BY SOLVENT EXTRACTION 195
11.1 Hot-Cell Tests 195
11.2 Isolation of Promethium 197
11.3 New Flowsheet for Recovering Strontium, Rare Earths, and Cesium 197

12. BIOCHEMICAL SEPARATIONS 199
12.1 Biochemical Separations Research 199
12.2 Biological Macromolecular Separations Technology 202
12.3 Molecular Weights of Transfer Ribonucleic Acids 202
12.4 Body-Fluid Analyses 204

13. CHEMISTRY OF PROTACTINIUM 209
13.1 Chemical Behavior in Sulfuric Acid Solutions 209
13.2 Absorption Spectra in Sulfuric Acid Solutions 210
13.3 Studies with Hydrochloric Acid Solutions 216

14. IRRADIATION EFFECTS ON HETEROGENEOUS SYSTEMS 218
14.1 Radiolysis of Water in the Adsorbed State 218

15. HIGH-TEMPERATURE CHEMISTRY 221
15.1 Fabrication and Installation of the Spectrophotometer System for Use with High Levels of Alpha-Active Elements 221
15.2 Spectral Studies of Ionic Systems 224
15.3 Measurement of Densities of Liquids at High Temperatures and High Pressures 226

16. MECHANISMS OF SEPARATIONS PROCESSES 228
16.1 Activities of Tri-*n*-butyl Phosphate (TBP) in TBP-HNO_3-H_2O Solutions 228
16.2 Determination of Radioisotopes by Resolution of Gamma-Ray Spectra 228

17. CHEMICAL ENGINEERING RESEARCH 230
17.1 The Stacked-Clone Contactor 230

18. REACTOR EVALUATION STUDIES 234
18.1 Studies of the Cost of Shipping Reactor Fuels 234
18.2 Costs of Preparing Nuclear Fuel Materials 236
18.3 Cost Studies of Spent-Fuel Processing 237
18.4 Computer Code for Studies of Overall Power Costs 240
18.5 Shielding Design Code for Fuel-Handling Facilities 240

19. PREPARATION AND PROPERTIES OF ACTINIDE-ELEMENT OXIDES 241
19.1 Fundamental Studies of Thoria Sols and Gels 241
19.2 Surface and Sintering Properties of Sol-Gel-Derived Thoria 245
19.3 Urania Gel Oxidation 247

20. ASSISTANCE PROGRAMS 248
20.1 Eurochemic Assistance Program 248

20.2 Demonstration of the Disposal of Solid, High-Level Radioactive Waste in Salt 248
20.3 High-Level Alpha Laboratory 249
20.4 Fuel-Shipping Safety Studies 249
20.5 Evaluation of Radiation Resistance and Decontaminability of Selected Protective Coatings 250

21. WATER RESEARCH PROGRAM 256

22. CHEMISTRY OF CARBIDES AND NITRIDES 257

23. INDUSTRIAL APPLICATIONS OF NUCLEAR ENERGY 259
23.1 Economics of Hydrogen and Ammonia Production via the Electrolysis of Water, Using Low-Cost Nuclear Power 259
23.2 Production of Hydrogen by the Electrolysis of Water 263
23.3 Direct Fixation of Nitrogen with a Plasma Torch 266
23.4 Waste-Water Treatment 268

PUBLICATIONS, SPEECHES, AND SEMINARS 270

Summary

1. POWER-REACTOR FUEL PROCESSING

In the development of new nuclear-power-reactor concepts, fuels that can be used for long times and at high temperatures are continuously being sought. This sometimes leads to the use of fuels and cladding materials for which existing fuel processing methods are not applicable. The development of new recovery processes for such fuels is directed toward the demonstration of chemical methods and engineering practices for recovering and decontaminating the uranium, thorium, and plutonium. In the studies described here, development is centered on head-end methods designed to produce suitable aqueous feeds for solvent extraction and includes both mechanical and chemical treatments.

1.1 Development of Processes for Graphite-Base Fuels

Work on graphite-base fuels last year was devoted to the laboratory and engineering development of a grind-leach process for pyrolytic-carbon-coated ThC_2-UC_2 fuel particles contained in graphite (Peach Bottom reactor fuel, for the high-temperature reactor at Peach Bottom, Pennsylvania). In this process, the fuel compacts are broken in a hammer mill to -6 mesh, ground to -140 mesh in a double-roll crusher to ensure the rupture of the pyrolytic-carbon coating on all fuel particles, and leached in 13 *M* HNO_3 which may or may not contain fluoride, depending on conditions. The leached uranium and thorium nitrates are then filtered and washed from the graphite residue.

Tests with a commercial roll crusher demonstrated the feasibility of crushing broken fuel to -140 mesh, and an improved unit has now been built and is being used in further tests. Subsequent work with a batch-fed leacher-filter test facility (nominal capacity, 3 to 5 kg of fuel) demonstrated a satisfactory pneumatic method for controlled addition of ground fuel to the leacher, good solution loadings, satisfactory suspension of a concentrated slurry of ground fuel and leachant during leaching, rapid transfer of the slurry to a filtration column, and reasonable rates for separation of leachate and washes from the graphite. The uranium and thorium losses to the filtered and washed graphite were 0.35 and 0.67% respectively.

1.2 Development of Mechanical Processes

Unirradiated fuel assemblies from three second-generation power reactors (Dresden, type IV; Elk River, core II; and Consolidated Edison, core B) were successfully sheared into 1- and 2-in. lengths without prior disassembly except for the removal of end boxes.

A computer code was developed and used to calculate the temperature buildup from fission product heat generation in various steps in the shear-leach process. For fuel irradiated to 50,000 Mwd/metric ton and cooled 180 days, a permissible maximum temperature of 1586°F was calculated to exist at the center of a 10-in.-diam fuel-storage basket. It was also determined that the pressure developed in the dissolver would be less than 1 psi when this fuel is quenched by the acid.

Further safety studies with finely divided zirconium produced in the abrasive-disk sawing and in the shearing of Zircaloy-2-clad fuel assemblies showed that fines produced by sawing were always safe because of a high degree of conversion to ZrO_2 and a high dilution (7:1) with debris from the saw. Fines less than 149 μ in diameter produced by shearing are unsafe and must ultimately be dissolved in HNO_3-HF. A full-sized delayed-neutron leached-hull monitor was built and tested. This monitor is sensitive to as little as 5 mg of

^{235}U, ^{233}U, or ^{239}Pu in an 8-in. vertical increment of an 8-in.-diam basket. Monitoring time per increment is 40 sec. The monitor operated successfully in a ^{60}Co background of 1100 r/hr.

Hot-cell tests were made to measure the release of tritium and ^{85}Kr during shearing, leaching, and feed preparation. With stainless-steel-clad ThO_2-UO_2 fuel samples irradiated to 25,000 Mwd/metric ton, 0.2% of the ^{3}T and 1% of the ^{85}Kr were released as gases during shearing; in our system, another 0.2% of the ^{3}T and the remainder of the ^{85}Kr were released to the atmosphere during dissolution. About 70% of the remaining ^{3}T was volatilized and collected in condensates during evaporation and feed adjustment steps. Similar releases were measured with a Zircaloy-2-clad UO_2 PWR (pressurized-water reactor) fuel specimen irradiated to 40,000 Mwd/metric ton, except for a 9% release of ^{3}T during shearing. Each of the sediments produced during leaching and feed adjustment, respectively, amounted to 0.6% of the fuel; most of the fission products (Mo, Zr, Nb, Sb, and Ru) were found in the sediments.

1.3 Development of Processes for Heavy-Water-Moderated, Organic-Cooled Reactor Fuel

This year, studies were initiated on the processing of heavy-water-moderated, organic-cooled reactor (HWOCR) fuels. Most of the effort was centered on SAP-clad UC because this is a leading candidate for an HWOCR fuel. SAP is a sintered dispersion of 5 to 15% Al_2O_3 in aluminum. Several potentially feasible aqueous processing methods were investigated cursorily. These included: (1) decladding of the fuel with NaOH or NaOH-$NaNO_3$ solution, followed by dissolution of the residue (hydrous UO_2 and UC respectively) in nitric acid; (2) shearing of the fuel, followed by nitric acid leaching; (3) direct dissolution in nitric acid or mercury-catalyzed nitric acid; and (4) shearing, pyrohydrolysis of the UC to UO_2 at 750 to 780°C, and dissolution of the residue in nitric acid. None of these methods has received sufficient development to allow selection of the optimum process.

1.4 Studies on the Adsorption of Protactinium

Isotopically pure ^{233}U has high value because of its low gamma-activity level. The selective separation of its 27.4-day precursor ^{233}Pa would produce a source of such high-purity uranium and at the same time remove a large fraction of the beta and gamma radioactivity associated with short-decayed thorium.

Hot-cell experiments have demonstrated the practicability of recovering ^{233}Pa by adsorption on unfired powdered Vycor glass from nitric acid solutions. Sol-gel thoria, irradiated to about 5000 Mwd/metric ton and cooled 27 days, was dissolved in 13 *M* HNO_3–0.05 *M* HF–0.1 *M* Al, and the protactinium was preferentially adsorbed on unfired Vycor glass. About 97% of the protactinium was adsorbed at a loading of 3.1 mg of ^{233}Pa per gram of glass. The protactinium was eluted from the glass with 0.5 *M* oxalic acid, yielding product solutions with protactinium concentrations of about 1.5 mg/ml. Decontamination factors for zirconium-niobium, total rare earths, thorium, and uranium were 5.5, 4.8×10^3, $\geqq 1 \times 10^4$, and $\geqq 5.7 \times 10^2$ respectively. The ^{233}U that would be present after the decay of the protactinium would contain only 0.1 to 0.5 ppm of ^{232}U.

Similar experiments showed that silica gel was also an effective adsorbent, although the capacity values and decontamination factors were lower than those obtained with the unfired Vycor. Zirconium phosphate (ZP-1) had about half the capacity of unfired Vycor at 99% adsorption and was not amenable to elution.

Laboratory experiments showed that protactinium is also adsorbed by unfired Vycor glass from hydrochloric acid solutions. The protactinium distribution coefficients between 60- to 80-mesh glass and 1 to 10 *M* HCl ranged from 120 to 410, with 7.6 to 2.1% of the protactinium unadsorbable.

1.5 Close-Coupled Process Development

Development work on close-coupled processes included the completion of a survey to determine whether methods other than solvent extraction were capable of providing low-cost low-decontamination (factors of 1000) processes. Only anion exchange appeared to be a contender, and even here certain problems existed. Therefore, further work has been limited to modifying and improving existing solvent extraction technology for use in close-coupled processes. Batch differential extraction, which appeared to have some advantages in laboratory studies, was found to be inferior to continuous methods when scaled up in engineering

tests. Although use of tri-*n*-pentyl phosphate and triisopentyl phosphate in *n*-dodecane alleviated to some extent the second-organic-phase problem, both solvents were inferior to TBP in other respects. An engineering design study also indicated that the capital and operating costs for a batch differential and a continuous solvent extraction plant were nearly equal at the same capacity; however, the batch-type plant would be more expensive to operate.

2. FLUORIDE-VOLATILITY PROCESSING

This effort is part of an intersite program to develop fluoride-volatility processes as alternatives to aqueous methods for recovering valuable components present in spent UO_2 fuel from power reactors. The AEC's goal is to have the technology for low-enrichment fuel processing developed through "cold" engineering, "cold" semiworks, and "hot" pilot-plant programs so that design of a full-scale plant can begin by July 1, 1969. Our main contribution will be the installation and operation of a pilot plant in several of the shielded cells in Building 3019.

Laboratory- and small-engineering-scale studies were made in support of the fluidized-bed volatility process, particularly the HF-O_2 method for stainless-steel-clad fuels. Work is now under way on studies of the HCl process for Zircaloy-clad fuels.

Design of process vessels needed in the pilot plant for the decladding, oxidation, and fluorination of the UO_2-PuO_2, and cold trapping of the volatile hexafluorides is nearly complete. Fabrication is under way, and cell preparation has begun. Design of mechanical equipment, instrumentation, and electrical gear is proceeding. Process design for the product separation and purification steps has begun.

2.1 Fluidized-Bed Volatility Process Development: Laboratory Studies for Stainless-Steel- and Zircaloy-Clad UO_2 Fuels

Bench-scale tests have continued in support of the fluidized-bed volatility process for low-enrichment UO_2 fuel clad in stainless steel or Zircaloy-2. A portion of these tests were with the ½-in.-OD mini-bed reactor (bed weight, 5 to 8 g), and part were with a 1-in.-OD fluidized-bed reactor (bed weight, 40 g) equipped with blowback filters. The tests in the larger reactor were concerned with the physical state of the fuel and cladding during the decladding and fluorination steps, and the effect of large amounts of fluoride in the bed on these two steps. With the small reactor, emphasis was on the chemical behavior of plutonium as PuO_2 during the decladding cycle and in subsequent volatilization as PuF_6 with fluorine. In the decladding cycle, the effects of stainless steel decladding products, relative proportions of HF and oxygen, elimination of HF, and pretreatment of the bed with fluorine were related to plutonium retention. In the fluorination cycle, the effects of fluorination time, pyrohydrolysis, and type of bed materials were related to plutonium retention. The studies also included the fixation characteristics of plutonium on alumina during fluidization at high temperature.

Studies with small reactors were temporarily abandoned in favor of a 1-in.-OD reactor similar to that now being used for uranium decladding and fluorination tests.

When stainless-steel-clad UO_2 is declad with mixtures of HF and oxygen, lumps of U_3O_8 are formed if expansion of the fuel is prevented. To avoid lumping, the fuel should not occupy more than 10% of the reactor cross-sectional area.

A procedure that adequately pulverizes the pieces of "stainless steel oxide" without sintering the bed consists of contact for 15 min each with 10, 20, 40, and 80 vol % fluorine, all at 450 to 500°C. Then, 80 vol % fluorine is used at 500°C for 3 hr. With this method, about 99.9% of the uranium is removed.

Large amounts of "stainless steel fluoride" in the alumina bed accelerated the already rapid reaction of stainless steel cladding with mixtures of HF and oxygen. The stainless steel fluorides did not interfere with uranium removal during the fluorination step. Fluidized beds of pure ZrF_4 were used in the oxidation and fluorination of UO_2, with the uranium concentration in the fluorinated bed being one-fourth that found when alumina was used: 0.0074%, compared with 0.03% for alumina. Sintering was no problem when ZrF_4 was used; none occurred at 550°C even with a settled-bed fluorination.

2.2 FBVPD: Small-Scale Engineering Studies

Experience in remotely operating fluidized-bed equipment in the absence of fission products or plutonium is necessary before operating the FBVPP.

An engineering facility for acquiring such experience has been built in a cell, with all controls and instruments located externally. Two fluidized-bed reactors, one 2 in. in inner diameter and the other 4 in., are included, and metered inputs of HCl, HF, oxygen, fluorine, and nitrogen are provided. The reactors were made of nickel pipe. The effluent streams can be monitored for flow rate, temperature, and pressure, as well as for certain specific component concentrations. Gas chromatography, infrared and ultraviolet spectrometry, thermal conductivity, gas density, and paramagnetic susceptibility instruments are available.

During preliminary experiments in decladding stainless-steel-clad UO_2 fuel elements with HF-O_2, the Al_2O_3 bed often caked, causing incomplete reaction. Fluorination experiments were successful and provided data on in-line monitoring (see Sect. 2.5). Work will continue with both stainless-steel- and Zircaloy-clad fuels until instruments and operating methods are adequately developed.

2.3 Design of the Fluidized-Bed Volatility Pilot Plant for Zircaloy- and Stainless-Steel-Clad UO_2 Power-Reactor Fuels

A fluidized-bed fluoride-volatility pilot plant is being designed for installation in Building 3019. The processing of Zircaloy- and stainless-steel-clad UO_2 power reactor fuels will be studied in the facility at irradiation levels up to about 30,000 Mwd/ton with 140-day cooling. The primary goal of such studies will be to obtain data needed in the design of a full-scale commercial plant.

First in importance is the demonstration of the ANL process that includes the following steps: removal of Zircaloy cladding from UO_2 with HCl, oxidation of UO_2 to U_3O_8, formation of volatile hexafluorides by reaction of the uranium and plutonium with fluorine, and separation and purification of the product streams from each other and from fission products by different combinations of thermal decomposition of the PuF_6 and distillation. Near the end of this report period a decision was made to add equipment for studying the use of BrF_5 or BrF_3 for producing UF_6 prior to forming and removing PuF_6 with fluorine. Of secondary importance is the demonstration of the use of HF-O_2 for removing stainless steel cladding and oxidizing the UO_2.

Design of the major equipment items required in the decladding, pulverization, and fluorination steps (phase 1) was completed, except for the equipment related to the interhalogen method. Fabrication of equipment and cell preparation were begun. Design studies were made of problems related to accountability, handling of plutonium, containment, shielding, and fuel procurement. In phase 2 (separation and purification of product streams, and sampling and leaching of waste solids), design studies are under way. Ways of sampling and leaching waste solids are being studied, and some experimental development work is being planned. Studies are under way to aid in choosing a constructional material for the leacher.

2.4 Corrosion Studies Related to the FBVPP, and More Corrosion Data from the Molten-Salt Volatility Pilot Plant

Because of the highly reactive fluids used and the elevated temperatures required in volatility processes, corrosion of process equipment and piping must be carefully considered. As a supplement to corrosion studies at each of the participating sites, we have a subcontract with Battelle Memorial Institute, Columbus laboratories (BMI), to study volatility corrosion problems. Results of their corrosion studies specific to the FBVPP are presented, plus additional information on corrosion experienced in the Molten-Salt Fluoride-Volatility Pilot Plant (VPP).

Battelle workers compiled corrosion data related to the fluidized-bed volatility process obtained from the National Laboratories, ORGDP, and the published literature. The survey confirmed earlier choices for materials of construction. Metallographic studies revealed intergranular modifications in specimens of nickel that had been exposed to process conditions. Subsequent studies at BMI showed that similar modifications in nickel 200 and 201 were produced by exposing coupons to alumina. Different types of alumina produced varying degrees of modification, usually in proportion to their sulfur content. Tensile tests on specimens with modifications produced by repeated exposure to type 38 Norton alumina showed a significant loss of ductility as compared with that observed in tests of coupons from unexposed nickel.

Leaching will be used as a verification of sampling methods required to determine uranium and

plutonium retention in waste solids from the primary reactor. Also, the equipment will be designed so that leaching of fuel after oxidation may be studied following the all-volatility program, if desired. The high fluoride content of the waste solids will result in severely corrosive conditions with concentrated HNO_3, the proposed leachant.

A corrosion study was begun at BMI to determine the best material of construction for the leaching equipment. Of the 18 types of specimens tested, Corronel 230 (36 Cr, 58 Ni, 1 Mn, and 5 Fe, nominal) (in wt %) and HAPO alloys 17, 20, and 21 (25 Cr, 50 Ni, 0.6 Mn, with varying amounts of Mo, Cu, and Fe) (in wt %) were most resistant to 13 M HNO_3–0.1 M HF at the boiling point (120°C) in 24- or 48-hr tests. Rates for welded coupons submerged in liquid were 17 to 29 mils/month. Since pure chromium corroded at only 4 mils/month, alloys high in chromium, such as 60% Cr–40% Ni and 50% Cr–50% Ni, will be tested for corrosion and fabricability. Other experimental alloys may be prepared at BMI for testing.

Ultrasonic measurements were made to determine the extent of corrosion that occurred in the VPP dissolver during the aluminum program. Total corrosion for the ten dissolvings and aqueous decontamination was 5 mils. An inspection of the dissolver interior by telescope showed pits and two cracks, apparently shallow. Wall-thickness measurements of the fluorinator after the aluminum program showed average and maximum attacks of $\frac{1}{2}$ and $\frac{3}{4}$ mil, respectively, for each of the 40 fluorinations made in both the zirconium and aluminum programs. No allowance was made for corrosion during aqueous decontaminations.

2.5 Continuous In-Line Monitoring of Gas Streams in the Fluidized-Bed Fluoride-Volatility Process

For proper control of the various phases of the fluoride-volatility process, continuous in-line monitoring devices must be developed for use with multicomponent corrosive gas streams. Three instruments have been tested in connection with experiments on the HF-O_2 flowsheet for stainless steel: a gas chromatograph, a nondispersive infrared (IR) spectrophotometer, and an ultraviolet (uv) spectrophotometer. The gas chromatograph will analyze for fluorine or HF in a mixed O_2-N_2 stream. Infrared analysis for UF_6 in streams containing fluorine was not successful because of the variable content of a contaminant (probably CF_4) that absorbs strongly at a wavelength very close to that for UF_6. This contaminant probably comes from reaction of fluorine with carbon electrodes in the electrolytic cell used to produce fluorine. Fluorination experiments were monitored with a uv spectrophotometer equipped with a flow-through sample cell having a 0.5-mm optical path length and synthetic sapphire windows.

The uv spectrophotometer shows definite promise as a continuous UF_6 monitor during fluorination, and the gas chromatograph shows promise as an intermittent but general-purpose analyzer. The IR analyzer is not so promising but would be useful as a UF_6 monitor if an absorbance peak for UF_6 could be found with which absorbance of contaminants would not interfere.

2.6 Sorption of Plutonium Hexafluoride by Metal Fluorides

The separation of gaseous PuF_6 and UF_6 and removal of fission products by sorption-desorption steps could significantly enhance volatility methods for processing nuclear fuels. Of 31 metal fluorides (sorbents) first tested, 21 were eliminated when static tests with submilligram samples demonstrated failure to react with or sorb significant amounts of PuF_6. The remaining ten (the fluorides of the group I-A and II-A metals) have now had more extensive dynamic sorption testing, using 2-g sorbent samples. In no case did PuF_6 desorb as rapidly as UF_6 does from NaF. Lithium fluoride, NaF, and CaF_2 were studied most exhaustively for possible desorption of PuF_6 in the presence of fluorine, with LiF showing the most promise. No significant desorption from NaF could be measured even after 10 hr at 600°C. Desorption from CaF_2 could be detected only at 600°C, where 7 and 15% desorbed in 10 hr. With LiF, 97% desorbed in 9 hr at 400°C, and in 4 hr at 500°.

The valence of plutonium in lithium, sodium, and calcium compounds produced by reaction of the fluorides with PuF_6 lies between 4 and 5. This accounts for the difficulty in desorbing the plutonium as PuF_6, even in the presence of fluorine.

Application of the LiF sorption process to the volatility system appears promising. Optimization of sorption and desorption conditions, evaluation of separation from fission products, and preparation of the LiF in suitable form for large-scale testing are required.

2.7 Separation of Uranium Hexafluoride from Bromine Fluorides

In support of the interhalogen fluoride-volatility process for recovering uranium and plutonium from low-enrichment power-reactor fuels clad in either Zircaloy-2 or stainless steel, it was necessary to develop a method for separating UF_6 from BrF_3 and BrF_5 present in the product gas stream. Separation of the UF_6 by selective sorption from the product stream using NaF was precluded, unfortunately, by cosorption of the reduction product, BrF_3. (Bromine pentafluoride does not form a complex with NaF under these conditions.) A successful approach to this separation was found, however, by sorbing the UF_6 on a bed of NaF at 150°C, flushing the bed with fluorine to eliminate cosorbed bromine compounds, and then following up with additional fluorine in a series of pressurization-depressurization cycles. With this method, UF_6 containing less than 14 ppm of bromine was recovered. AEC specifications fix the limits of bromine contamination in UF_6 at 5 ppm. Based on the results of tests completed to date, it is expected that this stringent specification can be met.

2.8 Chromium Chemistry and the Behavior of Chromium in Volatility Processing

In processing stainless-steel-clad UO_2 fuel the behavior of the contained chromium in the HF-O_2 decladding step, and in the fluorination or UF_6 volatilization step, is of interest. Development studies showed essentially no chromium volatilization in the HF-O_2 decladding procedure; that is, the chromium remains in the fluidized alumina bed, probably as nonvolatile CrF_3. Appreciable chromium volatilization does occur, however, in the fluorination step. The volatile chromium compounds of interest here are CrO_2F_2, CrF_4, and CrF_5. The relative amounts of these three compounds were not determined. An appreciable amount of chromium was observed to cosorb with UF_6 in NaF sorption beds.

In chemical studies an effort was made to synthesize and characterize the NaF-CrF_4 compounds that are most likely to form in an NaF sorption system. This work revealed and identified one NaF-CrF_4 phase that was isostructural with K_2CrF_6 but of somewhat smaller unit-cell size. A method for generating CrO_2F_2 was also devised and studied. The NaF sorption system has promise as a means of removing CrO_2F_2 from the UF_6 product.

2.9 Vapor-Liquid Equilibria of UF_6-NbF_5 System

As a part of continuing studies on fluoride-volatility methods of processing nuclear fuels, the separation of UF_6 from volatile impurities by distillation is being considered. For this reason, the vapor-liquid equilibria of UF_6 and one such impurity, NbF_5, were determined. The 150°C isothermal data previously reported and the 5.92-atm isobaric data were fitted to three simplified forms of the Wohl four-suffix equation. The data were corrected for nonideal vapor-phase conditions by an empirical equation.

3. MOLTEN-SALT REACTOR PROCESSING

3.1 Continuous Fluorination of Molten Salt

Processing of both the fuel salt and the fertile salt of a molten-salt breeder reactor (MSBR) requires the continuous and complete removal of the uranium from the salt by fluorination. The principal problems are control of corrosion and conformity to high recovery specifications. It is anticipated that corrosion can be controlled by keeping a layer of frozen salt on the fluorinator walls, using the internal heat generation from fission product decay to provide the thermal gradient. The high recovery specifications may be met by using a tower in which a countercurrent flow of molten salt is contacted with dispersed, rising fluorine. Present work is aimed at showing that the fluorination rate is satisfactory and that the axial concentration gradient will not be destroyed by the inherent axial mixing in such towers. Recoveries of 96 to 99.4% have been achieved in 1-in.-diam towers containing salt to a depth of 48 in.

3.2 Distillation of Molten Salt

Removal of the fission product poisons from the fuel salt of the molten-salt breeder reactor will be accomplished, primarily, by vacuum distillation of the carrier salt (after the uranium has been removed by fluorination) to remove the valuable ^7LiF and BeF_2 from the less-volatile fission products. An equilibrium still was built and operated at 0.5 mm Hg and 1000°C to determine the relative volatility of CeF_3, NdF_3, and LaF_3 in an LiF–rare-earth fluoride system. After several operational difficulties were resolved, consistent results showed

these fluorides to have relative volatilities in the range 0.0005 to 0.003, with cerium showing the higher values. These values are low enough to permit the use of a batch still without difficulty.

3.3 Alternative Processing Methods for a Molten-Salt Breeder Reactor

Reductive coprecipitation and liquid-metal extraction are being studied as possible methods for decontaminating MSBR carrier salt (Li_2BeF_4) after removing uranium by fluorination. Adequate removal of La and Gd is achieved by treatment with near-theoretical quantities of Be to form beryllides of the type $LnBe_{13}$. Either excess Be, up to 243 times theoretical, or a stronger reductant, Li, is necessary to remove Zr at trace level. Zirconium is removed as free metal from 5 mole % ZrF_4 solutions in Li_2BeF_4, but from dilute solutions a beryllide, $ZrBe_2$, has also been identified. Neodymium, estimated to constitute 50% (by weight) of the lanthanides present, will require a 40-fold excess of Be for removal, corresponding to 11 g of Be per kilogram of salt being processed. To date, little success has been achieved in removal of Sm, Eu, or Sr with either Li or Be.

Lithium-bismuth (liquid-metal) extraction experiments were also continued. Significant removals were observed for La, Sm, Gd, Sr, and Eu – the last principally by extraction into the metal phase, the others by deposition as interfacial solids, as previously reported for other metal extraction tests.

4. WASTE TREATMENT AND DISPOSAL

4.1 High-Level Radioactive Waste

Laboratory Studies. – The ORNL work on the fixation of highly radioactive aqueous waste was summarized in an operating manual for use in the Waste Solidification Engineering Prototype at Pacific Northwest Laboratory (PNL). Melt compositions were developed for the two new waste types designated as Purex-1 and Purex-2. Lead borosilicate melts appear to be preferable to phosphate melts for fixing Purex-1 waste because of their lower corrosivity, but their thermal conductivities are also much lower. Viscosities were measured as a function of temperature for one aluminum (TBP-25) and three high-sulfate Purex (FTW-65) waste melts. For the latter type, viscosity increased with increase in the content of process oxides and with the addition of simulated fission products. Seven semiengineering-scale tests were made with phosphate melts for Purex-1 and Purex-2 types of waste, and one semiengineering-scale test of the Con-Potglass process was made with a lead borosilicate melt. The practicality of controlling ruthenium volatilization by recycling the overhead from the fixation vessel to the waste evaporator was confirmed in laboratory tests.

Scoping studies indicated the feasibility of dispersing fluidized-bed waste in a glass matrix and, alternatively, the probable feasibility of incorporating (dissolving) such waste in a homogeneous glass. Fluoride was volatilized from the bed when a fluoride-containing waste was dispersed in a lead borosilicate matrix.

Engineering Studies. – Four Rising-Level Potglass tests were made during this report period, two (R-89, -90) with FTW-65 Purex (with sulfate) waste and two with PW-1 Purex waste (R-91, -92). Particular emphasis was placed on determining the best method of adding the glass-making additives and evaluating the pot-corrosion problem. Test R-89, with an 8-in.-diam pot at 900°C, showed an excessively high corrosion rate; but a duplicate test, R-90, at 850°C, was completely successful, with negligible corrosion. A similar test in an 8-in.-diam pot at PNL also showed negligible corrosion. Test R-90, with an 8-in.-diam pot at 900°C, was also successful, and the corrosion rate was low. A similar test in a 12-in.-diam pot showed excessive corrosion, up to 239 mils. The proportional feeding of a solution of glass-making additives (LiOH, NaOH, and H_3PO_4) to the waste feed line is recommended as preferable to mixing directly with the waste in the feed tank. It was concluded that additional definition of the corrosion mechanism is required before attempting large-scale tests of the Rising-Level Potglass process with radioactive wastes.

4.2 Intermediate-Level Radioactive Waste

Immobilization of intermediate-level radioactive wastes (ILW's) by incorporation into a cheap, inert, and insoluble material before storage or burial offers safety and economic advantages to an expanding nuclear industry. Considerable

world-wide interest has been shown in the use of asphalt as a material for incorporating all types of ILW's. These wastes include second- and third-cycle raffinates; solutions from fuel decladding, solvent cleanup, and off-gas scrubbers; and slurries and solids from low-level treatment processes. The asphalt process being developed at ORNL consists in adding the waste directly to emulsified road asphalt in a stirred evaporater at any temperature up to the boiling point of the solution, evaporating the water and heating the product to about 160°C while stirring, and finally draining the product into a steel drum. The latter serves to contain the product during preliminary storage and shipment.

Mixtures of asphalt and waste salts products containing 10 to 80 wt % salts have been prepared in the laboratory with ORNL ILW, fuel dejacketing waste (FDW), and a Purex second-plutonium-cycle waste. Also, products containing 20 to 60 wt % salts from ORNL ILW have been prepared on an engineering scale. These wastes are principally nitrate solutions of sodium, aluminum, and iron and often contain sulfate, fluoride, chloride, and phosphate. The asphalt-salt products are very insoluble in water, and less than $^1/_{10,000}$ of the radioactive material is leached per day from a given sample. At present, cement is widely used as a matrix, but the leach rate is 50 to 100 times higher. Asphalt has a further advantage: the final volume of waste is only half the original; for cement, it is increased 50%.

The resistance of asphalt to radiation is found to limit the amount of radioactivity that can be incorporated and the degree of applicability of this disposal method. Studies show that asphalt should be satisfactory up to at least 10^8 rads of absorbed dose, a dose equivalent to that expected from an initial 10 curies per gallon of product over an infinite period. No increase of leach rates in water occurred at 10^8 rads with samples containing 60 wt % salts from ORNL waste. Hard asphalts swell about 36% at 10^8 rads, but soft asphalts allow gas to escape; swelling is probably not a problem at these dose levels.

The incorporation of inert solids in asphalt does not appear to increase the hazards that are normal in the handling of material that has a high flash point. However, the hazards involved in incorporating nitrates were studied intensively. A comprehensive series of tests (drop-weight, autoignition, shock sensitivity, flame propagation) on small and 30-gal-drum samples showed that the asphalt-salt mixtures burn, as expected, but that they do not explode or show a significant increase in burning rate over pure asphalt.

Laboratory, hot-cell, and engineering development studies are planned to determine the kinds and quantities of waste that can be incorporated, the levels of radioactivity that can be tolerated, and the engineering variables involved in operating a mixer-evaporator to produce this asphalt-bonded waste.

4.3 Low-Level Radioactive Waste

Water recycle is considered an improvement over the present method of dealing with the low-level radioactive waste problem. The current method consists in relatively inefficient decontamination treatment, discharge to nearby streams, and dependence on these streams to dilute the remaining radioactivity to maximum permissible concentrations. In the recycle approach, a more efficient treatment of low-salt-content waste water is designed to directly reduce the radioactivity levels to U.S. Public Health Service radiochemical specifications for drinking water, and the water can be returned for reuse in a nuclear installation.

Micro pilot plant experiments at ORNL have been based on a flowsheet that includes flocculation by alum, demineralization by ion exchange, and final cleanup by activated carbon. These experiments demonstrated decontamination factors (DF's) of 1000 to 10,000 for all major radioactive species for up to 2400 volumes of recycle water treated per volume of cation resin. This process has provided the highest DF's for cobalt and ruthenium ever attained in the ORNL development program. Operation of the water-recycle process for several more cycles is needed to determine whether a buildup of contaminants occurs. Pilot plant tests of the process are now warranted.

4.4 Engineering, Economic, and Safety Evaluation

Three studies are presented: costs of "perpetual" storage, safety of tank storage, and an analysis of the management of wastes from volatility processes.

The costs of perpetual tank storage of both acid and alkaline wastes were estimated as a function

of tank size, tank life, and fission product concentration in the waste for three representative types of financing. For acid wastes, the optimum tank capacity is about 1,000,000 gal, and minimum total costs range from 0.0165 to 0.0272 mill/kwhr. For alkaline wastes, the optimum tank capacity is 2,500,000 gal, and minimum total costs range from 0.0177 to 0.0294 mill/kwhr. Reducing the volume of wastes, as stored, by doubling the concentration of fission products reduces the total costs between 15 and 30%. The total costs for storing cladding wastes ranged from 0.0215 to 0.0398 mill/kwhr. These costs were greater than those for raffinate wastes because of the greater volumes of cladding wastes.

In a study of the safety of tank storage, consideration of the nature and extent of tank failure indicates that the most likely mechanism of release would be through loss of cooling and that the atmosphere would constitute the major exposure pathway. Two incidents leading to major releases were postulated, and total radiation exposures to neighboring populations at various distances downwind were estimated, based on dosage to the lungs resulting from inhalation, subsequent exposure to the fallout from the passing cloud, and exposure to direct radiation from the passing cloud. Exposure due to direct radiation from the passing cloud was found to be only a few percent of that from the other two sources, and may be considered negligible.

Costs were estimated for management of the major wastes from fluidized-bed volatility processing of Zircaloy- and stainless-steel-clad UO_2 reactor fuels. Management alternatives consist of encapsulating the wastes without additional treatment, encapsulation following preparation of glassy solids, and encapsulation of the fission products as a "glass" following their separation from the inerts by a phosphoric acid leach. In all cases, the final products are shipped to a salt mine for final disposal. It was concluded that there is not a clear-cut economic incentive to make glasses or to leach the fission products but that, if these conversions are desirable for greater safety in handling and shipping, a substantial credit from cheaper management of the products can be applied against the cost of the treatment step. Also, it was concluded that more economic waste management cannot be cited as an advantage of volatility over aqueous processing in the fluidized-bed method for low-enrichment fuel.

5. TRANSURANIUM-ELEMENT PROCESSING

The High Flux Isotope Reactor (HFIR) and the Transuranium Processing Plant (TRU) have been built at ORNL to produce large quantities of the heavy actinide elements as part of the USAEC Heavy Element Production Program. These materials will be used in basic research in laboratories throughout the country. The HFIR went critical early in the fall of 1965 and was approaching full power at the end of this report period. Construction of TRU was completed, essentially all equipment was installed, and "cold" checkout of this equipment was done. The initial radioactive processing will begin almost immediately. Special irradiations of more than 500 g of ^{242}Pu in a Savannah River reactor, beginning in February 1965, produced about 2 mg of californium. One target rod containing 5 μg of californium was processed at ORNL this year. The remaining targets will be processed in TRU in the coming year. Design and development work on the target elements, to be remotely fabricated in TRU, is under the direction of the Metals and Ceramics Division. The major phases of the project, including design and construction of the building, the development of the chemical separations processes, and the design, fabrication, and installation of the chemical process equipment are the responsibilities of the Chemical Technology Division and are reported here.

5.1 Development of Chemical Processes

During the past year additional Clanex, Tramex, and ion exchange processing runs were made at full-scale radioactivity levels in the Curium Recovery Facility (CRF). This work is reported in Sect. 6.

Methods for dissolving irradiated and unirradiated PuO_2 were investigated. Results indicate that irradiated PuO_2 dissolves more readily than unirradiated PuO_2; however, fluoride, which is not compatible with the main-line TRU process equipment, will probably be required for total PuO_2 dissolution. In turn, it will then be necessary to reduce the fluoride concentration to less than 5 ppm following dissolution; thus fluoride removal methods were studied. Simple hydroxide precipitations and washing appear to be adequate. Recovery and purification of plutonium by HCl anion exchange are convenient for TRU operations, and scouting

tests on a laboratory scale indicate that this method will provide acceptable plutonium recovery; however, additional purification may be required.

About 286 g of ^{242}Pu was prepared as PuO_2 for incorporation into HFIR targets. Thirty-one targets comprise the first loading of the HFIR.

The preparation of plutonia by a sol-gel method offers several process advantages over the hydroxide precipitation method used previously for preparing dense, coarse particles of PuO_2, and gives a product of greater uniformity. Plutonia sol-gel development was therefore continued, and significant progress was made in the preparation of uniform sols of desirable characteristics. This work is reported in Sect. 8.2.

A sol-gel method appears to be equally attractive for the preparation of 20- to 200-μ particles of dense americium-curium oxide for incorporation into HFIR targets. The ability to prepare oxide microspheres of controlled particle size from rare-earth sols as stand-ins for americium and curium was reported last year; and during this report period, the techniques developed were successfully applied to the preparation of ^{241}Am, ^{244}Cm, and mixed ^{243}Am-^{244}Cm sols. In all cases, dense oxide microspheres could be formed from these sols.

Rare-earth sol-gel development was continued both as an aid to HFIR target preparation and because the oxide forms produced have potential as control rod materials in reactors and as burnable poisons in fuel elements. During this investigation, modifications were developed that greatly simplify the process and make it more amenable for in-cell preparation of ^{243}Am and ^{244}Cm sols and microspheres. Studies to evaluate these modifications in the preparation of americium and curium sols are needed.

Since separation of californium-einsteinium-fermium and purification of some final products will be effected by ion exchange, two such processes were investigated at high activity levels. About 0.5 g of ^{242}Cm in miscellaneous recycle solutions from the CRF was satisfactorily purified by LiCl anion exchange. Although an attempt to separate 0.5 g of ^{242}Cm from $\sim$1.5 g of ^{241}Am by elution from cation exchange resin with α-hydroxyisobutyrate was not completely successful, results indicated that this method will probably be satisfactory with 100-mg quantities of ^{252}Cf. Additional high-activity-level runs will be required to prove the acceptability of this process.

One of the HFIR prototype target rods, TRU-SRL irradiation element No. 26, was discharged from the Savannah River High Flux Reactor after an estimated irradiation of 3.7×10^{22} *nvt*. This target, which originally contained 10 g of plutonium (95.66% ^{242}Pu) as oxide, was dissolved, analyzed for transplutonium-element content, and processed to recover the heavy elements. Analyses by the best available methods indicated that the irradiated targets contained 5.45 g of plutonium, 1.58 g of americium, 2.64 g of curium, about 5 μg of ^{252}Cf, about 2 μg of ^{249}Bk, and about 0.2 μg of ^{253}Es at the time of discharge from the reactor.

5.2 Development of Process Equipment

The full-scale Zircaloy-2 pulsed-column rack for the Tramex process was "cold" tested before it was installed in the plant. Emulsions stabilized by zirconia sols were minimized by control of temperature and acidity in the feed adjustment step. The batch spray column for berkelium separation was shown to be adequate in regard to hydraulics and efficiency. Testing of pulsed columns for separation of americium and curium from other transuranic elements was begun, but problems with plate wetting by the organic and subsequent flooding were very severe. Purification of the solvent only partially corrected the problem. Successful operation with the organic phase continuous was demonstrated, but the TRU rack is not operable in that manner without major revisions.

5.3 Design and Fabrication of Process Equipment

Equipment in TRU for recovery, separation, and purification of the actinide elements from irradiated HFIR targets includes dissolution and feed adjustment tanks, a centrifuge for feed clarification, two cycles of solvent extraction equipment, ion exchange columns for recovery of plutonium and miscellaneous special separations, plus numerous process and storage tanks.

With the exception of equipment for precipitation of the recycle actinide oxides, all process equipment has been designed and fabricated.

In the past year, equipment racks for the first-cycle solvent extraction system and for the chromatographic separation of californium, einsteinium,

and fermium were fabricated. In addition, an extensive in-line process instrument system for detection of losses in waste streams and product monitoring was designed, and the components were built in the ORNL instrument shop.

Several miscellaneous equipment items, including the all-Zircaloy-2 centrifuge, target carriers, solid-waste handling equipment, and a periscope, were procured or fabricated.

5.4 Construction of TRU

Construction of TRU is now essentially complete.

Equipment was installed in two phases. The first phase was a cost-plus-fixed-fee contract involving the installation of a major portion of the piping, structural, and service items required for operation of the process equipment. This work began in May 1965 and was completed in 5 ½ months. The second phase followed immediately, beginning November 1, 1965, utilizing ORNL craft forces for the installation of the prefabricated process equipment and piping. The major portion of this work was completed in January 1966, at which time "cold" shakedown runs were begun.

An office wing was added; a shielded alpha cave is being constructed in an existing laboratory; and a 50-ton crane, an emergency generator, and a data-logging system are being acquired for this facility.

5.5 TRU Operations

The TRU operating group was assembled and is engaged in getting TRU ready for operation. Air balancing and leak testing for the cells and the building were completed. Equipment and operating procedures were tested for dissolving HFIR targets, for removing excess aluminum from the feed by caustic precipitation and centrifugation, for the plutonium removal process (Plurix), for metering radioactive feed to the process, for the first solvent extraction cycle (Tramex), and for recovering berkelium by batch solvent extraction (Berlex). Second-cycle solvent extraction (Pharex) has not yet been operated successfully.

A safety analysis of the proposed operations was reviewed by the ORNL Director's Radiochemical Plants Committee, and operation of the processing plant was approved.

The first feed for TRU will be prototype targets and special slugs that were irradiated in the Savannah River Plant (SRP) reactors, and some solution (containing about 500 g of americium and curium) that was recovered from the wastes from the ^{242}Pu processing at SRP. About 2 mg of ^{252}Cf will become available from these materials late in 1966. The first HFIR targets will not be ready for processing until late 1966 or early 1967.

6. CURIUM PROCESSING

The Curium Program was jointly undertaken by the Isotopes Division and the Chemical Technology Division to prepare curium for fabrication into heat sources. The heat sources are desired to develop the techniques of incorporating curium into thermoelectric converters for evaluation as SNAP-type generators. The Chemical Technology Division is responsible for the purification of the curium, and for delivery of the refined product to the Isotopes Division. A number of process methods, facilities, and source materials were used for both the Curium Program and the closely related Transuranium-Element Program (Sect. 5).

The Curium Recovery Facility (CRF) was originally designed for laboratory-scale testing of transuranium-element processes at high levels of radioactivity. It went through several phases of modification to improve its operation and to increase its capacity to the multigram level. During the Program, the Clanex, Dapex, and Tramex recovery processes were tested at high levels of radioactivity, while about 35 g each of highly refined ^{243}Am and ^{244}Cm and about 25 g of ^{242}Cm were recovered from irradiated target materials. At the conclusion of the ^{242}Cm Program early next year, the CRF will be converted to a laboratory facility in which to continue the development, testing, and evaluation of separations processes useful in the separation and recovery of the transuranium elements.

6.1 Process Development

Two adverse effects of alpha radiolysis in high-activity-level Tramex feed – the rapid loss of acid from adjusted feed and the formation of oxidants that convert cerium to the extractable tetravalent state – were studied in laboratory-scale tests in the past year. Methyl alcohol was found to be effective for preventing acid loss only when

it is added to feed which already contains appreciable concentrations of the oxidants formed by radiolysis. Stannous chloride, which can be used as a reductant in high-activity-level Tramex feed to keep cerium in the unextractable trivalent state, is oxidized at the rate of 1.0 meq/whr and accelerates the rate of acid loss by radiolysis.

6.2 Solvent Extraction Processing of ^{243}Am-^{244}Cm

Approximately 16 g each of highly refined ^{243}Am and ^{244}Cm were recovered from Savannah River Plant concentrates, a residual solution developed during the separation and recovery of the ^{242}Pu contained in 10 kg of ^{239}Pu that had been irradiated to >99% burnup. Process losses, recoveries, and decontamination from fission products duplicated those reported previously. After the ^{243}Am-^{244}Cm campaign, a short series of promising chemical flowsheet modifications was tested at high activity levels. The results of the tests with the Dapex flowsheet indicated that it was superior to Clanex as a primary solvent extraction cycle. Other tests indicated that the Talspeak and Cerex flowsheets are still promising but need further study.

6.3 Processing of the $^{241}AmO_2$ Targets

Two campaigns were completed during the year in which two types of irradiated $^{241}AmO_2$ targets were processed to recover approximately 25 g of highly purified ^{242}Cm. Feed material for the first campaign consisted of 18 aluminum canned targets that had been irradiated in the ORR; that for the second campaign consisted of five Martin Company targets that had been irradiated in the MTR, plus an additional 18 ORR targets. Each ORR target contained about 3.3 g of ^{241}Am as AmO_2 compressed in an aluminum matrix and canned in aluminum. Similarly, the ^{241}Am content of the MTR targets was 3.6 g. At reactor discharge, each target contained the following amount of ^{242}Cm: MTR, 1.2 g; ORR (first set of 18), 0.8 g; and ORR (last set), 1.1 g.

The first lot of ORR targets was processed directly through one cycle of Tramex solvent extraction in batches of three targets, yielding a product contaminated with ^{144}Ce. The second campaign featured the continuous addition of reductant to the feed stream, as well as a combined Dapex-Tramex two-cycle process. Even though the targets were processed after a decay period of only 15 to 30 days, a curium product of exceptional purity was recovered with low losses.

6.4 Curium Recovery Facility Equipment

The Curium Recovery Facility, originally designed and constructed to recover gram quantities of curium and smaller amounts of the heavier transuranium elements, was modified during the year to improve its operation. Included was the replacement of the solvent extraction contactors fabricated from Zircaloy-2 with a set fabricated from tantalum. Similarly, two glass-lined tanks were replaced with tantalum-lined tanks. These resulted in improved capacity and ease of operation and eliminated the spalling of the glass into the process solutions, which occurred with solutions of high power density. Other modifications included piping changes and installation of a vacuum filter-transfer system and a phase separator. All these contributed to increasing the on-stream efficiency of the facility, and materially shortened the processing time required, a significant consideration in processing the relatively short-lived ^{242}Cm.

7. DEVELOPMENT OF THE THORIUM FUEL CYCLE

The Thorium Fuel Cycle work is part of the Thorium Utilization Program of ORNL. The overall objective is the development of the fuel-cycle technology required for economical power production in thorium-fueled reactors. Much of the work carried out in this program by the Chemical Technology Division has been in close cooperation with the Metals and Ceramics Division. Oxide fuels and the preparation of microspheres of those fuels are being emphasized, but some work on preparation of thorium-uranium carbides and other systems is being done to exploit the versatility of the sol-gel process.

7.1 ^{233}U Storage and Distribution Facility

Oak Ridge National Laboratory serves as a storage, purification, and dispensing center for ^{233}U. During the past year, the ^{233}U handling facility

has received 63.4 kg of ^{233}U as oxide, metal, and nitrate solution, including 50 kg as UO_2 containing less than 5 ppm of ^{232}U. Shipments during the same period amounted to 18.3 kg of ^{233}U as purified nitrate solution or oxide powder.

Recent modifications to the Building 3019 facility increased the storage capacity to 117 kg of ^{233}U as oxide or metal and to 400 kg as nitrate solution. A 1-kg/day single-cycle solvent extraction glove box to complement the 6-kg/day solvent extraction facility was placed in operation. In addition, a 5-kg/day dissolver-leacher, limited in size to "ever-safe" criticality dimensions, was designed and installed for use as a metal or oxide dissolver, or as a leacher for chopped, metal-clad fuel elements.

7.2 Sol-Gel Process: Further Development and New Applications

Laboratory studies were made of sol-gel methods for preparing dense UO_2-ThO_2 bodies containing more than 10 wt % UO_2 and for preparing dense thorium dicarbides from thoria-carbon sols. Fluid, stable urania-thoria sols of any composition can be prepared simply by mixing urania sols with thoria sols. Nearly theoretically dense UO_2-ThO_2 microspheres with thorium:uranium atom ratios of 3.5:1 have been prepared in 300-g lots. Basic studies of the nature of ThO_2-C sols and ThO_2-C gels are being made, and the conversion of ThO_2-C mixtures to the carbide is being studied in an attempt to prepare thorium dicarbides suitable for use as reactor fuels. At present, only porous, low-density (<90% of theoretical crystal density) carbides are obtained by using ThO_2-C sols as the starting material.

7.3 Development of Methods for Producing Microspheres

A process was developed for preparing thoria and thoria-urania spheres 50 to about 800 μ in diameter, of high strength and nearly theoretical density. In this process, colloidal oxide sols were dispersed in an organic liquid and converted to gel spheres by extraction of water. To fluidize the sol drops and to avoid coalescence, clustering, and deposition on the wall, the use of surfactants in the solvent and of special vessel configurations was necessary. The gel spheres were separated from the solvent, dried, and fired to 1150°C. Microspheres were prepared by using 2-ethyl-1-hexanol as the drying solvent in continuous column systems, including solvent recovery. Demonstrated capacities of these systems were up to 1200 g of thoria microspheres per hour.

A variety of nozzles for dispersing sol into uniform droplets were designed, built, and tested. Several appear to be satisfactory for plant use. Gel microsphere drying and firing continues to occupy our attention, especially in the case of urania and uranium-containing spheres, where we are constrained from using strongly oxidizing atmospheres during firing. In these cases, residual carbon in the product spheres may be too high for some possible applications for the fuel. Continuous operation of the microsphere forming column over a period of five days showed that the column reaches essentially steady state in that length of time. Changes in the composition of the drying alcohol used in the column, such as buildup of nitric acid, depletion of surfactant concentrations, and possible accumulation of degradation products from distilling the alcohol to dry it, do not prevent satisfactory operation over that time interval.

7.4 Construction of the Thorium-Uranium Recycle Facility

The Thorium-Uranium Recycle Facility (TURF) is to provide adequate shielded space for development of processes and equipment for remotely processing and fabricating Th-^{233}U fuels of various types. Sufficient shielding is being provided to accommodate highly irradiated fuel assemblies after a three-month decay period. The four operating cells that make up the facility are each 20 ft wide and have a combined length of 106 ft.

The construction contract for TURF was modified to provide for completion of the building by February 10, 1967. The building is now enclosed; much of the major equipment is installed; and the cell walls are poured and lined to an elevation near the midpoint between floor and ceiling. It is estimated that the job is 60% complete. Procurement of over $1.5 million of special equipment has proceeded smoothly except for three steel shielding doors. All other items have been, or can be, made available to the contractor prior to his need for them.

7.5 Design of Process Equipment

The type of fuel to be produced in the first line of equipment to be installed in TURF was changed

from metal tubes filled with vibratorily compacted oxide fragments to carbon-coated microspheres. This change in objective either revised or placed a restraint on design of all equipment except that being designed for handling liquids. Preliminary designs were made of the various major items of process equipment to guide the process development effort. Detailed designs were made of small-scale urania sol formation equipment for fabrication of process development equipment. Work yet to be accomplished includes additional preliminary design and fabrication plus final design of the equipment to be installed in the facility.

8. SOL-GEL PROCESSES FOR THE URANIUM FUEL CYCLE

The uranium fuel cycle, especially as it relates to fast reactors, occupies a position of primary importance in the reactor development program of the United States. Fuel preparation is an important part of the uranium fuel cycle, and the work reported in this section was carried out as part of our effort to apply the sol-gel techniques (initially developed for the thorium fuel cycle) to the uranium cycle.

Emphasis in this work was on urania and plutonia sol preparation because these sols are readily made into UO_2-PuO_2 mixtures that are useful as reactor fuels. However, some studies were made on other materials which show potential of being prepared by sol-gel techniques, such as UN and ZrO_2, and this work is included in this section.

8.1 Uranium Sol-Gel Processes

The urania work proceeded in two phases. The first consisted of (1) the development of a laboratory process for preparing aqueous urania sols by a precipitation-peptization method and (2) the production of more than 15 kg of urania microspheres. Details of the development of the sol preparation method and microsphere forming, drying, and firing studies of this phase have been published; some of the results are summarized in this section.

The second phase consisted of the chemical development of improvements in the laboratory flowsheet, investigations of other methods of urania sol preparation that are more amenable to engineering scaleup, and a study of an alternative method of preparing gel microspheres. In this work it was found that the uranium concentration in the sols could be increased by increasing the formate and the uranium concentrations in the uranous nitrate-formate solution from which the hydrous oxide was precipitated. Our developments have included a modified precipitation-peptization method for preparing urania sols, in which the hydrous oxide precipitate is washed and the washed solids are peptized by resuspending and adjusting the NO_3^- concentration, and a method of microsphere preparation that includes chemical gelation of dispersed sol droplets. In the latter procedure hydrous oxide sols are dispersed as droplets into an organic liquid floating on a layer of 15 *M* NH_4OH, and gelation occurs when the droplets descend into the ammonia solution.

To obtain a better understanding of the chemical and physical changes taking place during the urania sol preparation, samples were taken at various stages in the precipitation-peptization process and examined by electron microscopy and selected-area electron diffraction to measure the size, shape, and crystallinity of the particles. In addition, the visible and ultraviolet spectra of the diluted sols were measured, and approximate sizes of particle aggregates were calculated from the turbidities. The final sols consisted of cubic UO_2 crystals having an edge length of 10 to 20 A.

The preparation of uranium nitride microspheres from gel microspheres of mixed uranium oxide and carbon was investigated. The gel spherules were converted to the nitride by heating them in a stream of nitrogen at 1600°C or, alternatively, by heating them initially in a stream of argon at 1600°C and then in nitrogen.

An objective in the chemical development of zirconia sol procedures was to prepare urania-zirconia sols by a simple mixing of sols. Clear sols that had nitrate-zirconium ratios as low as 0.7 were prepared by adding formaldehyde to a boiling zirconyl nitrate solution, drying the resulting solution or sol, and resuspending the residue in water. In other experiments, hydrous zirconia was precipitated with ammonia from a nitrate-rich zirconia sol, washed with methyl alcohol, and peptized by adding nitric acid to the dried product. The best sols were made by adding formic acid to the starting material before precipitation. In one experiment, a sol 1.8 *M* in zirconium and having nitrate:zirconium and formate:zirconium ratios of 0.39 and 0.30, respectively, was prepared.

8.2 Plutonia Sol-Gel Process

Efforts to develop a sol-gel process for the preparation of dense oxide forms of PuO_2 were con-

tinued. The objective of this work is to develop a process for preparing plutonia sols that would (1) be compatible with other actinide sols and (2) afford versatility in forming techniques. Currently, the process utilizes polymerization of tetravalent plutonium to produce crystallites of colloidal size and to ensure valence stability. The final sols are 1 to 3 *M* in plutonium and have NO_3^-/Pu mole ratios of 0.1 to 0.15. They are stable for many months and are compatible with thoria and urania sols which have been produced at ORNL. The ability to produce dense plutonia, as well as homogeneous plutonia-urania or plutonia-thoria, microspheres at any desired ratio has been demonstrated on a laboratory scale. Pilot plant equipment capable of producing 100-g batches of plutonia sol was designed, fabricated, and successfully used in preparing such sols having uniform characteristics.

The plutonia sol is prepared by precipitating the hydrous oxide from a nitrate solution with ammonium hydroxide. After it is washed, the hydrous oxide is peptized by the addition of nitric acid to give a nitrate-rich plutonia sol containing a nitrate:plutonium ratio greater than or equal to 1. The nitrate level is reduced by drying and baking the sol. The residue is then resuspended in water to give a dilute sol, which is concentrated by evaporation to the desired plutonium concentration. Numerous 5- to 20-g batches of sol were prepared, and 560 g of plutonium was processed in 50- to 100-g batches in a small pilot facility.

It was established by spectral analysis that the sol that formed during the peptization of the hydroxide precipitate with nitric acid contained plutonium polymer and that the polymeric form stabilized the plutonium valence in the tetravalent state. X-ray line broadening measurements indicated the diameters of the plutonia crystallites in the product sols to be about 80 A. Micropore filtration techniques indicated a range of micelle sizes, with some aggregates as large as 1000 A.

The product sols could be dried to dense, hard fragments or formed into microspheres which calcine to dense oxide spheres at 1150°C. Microspheres of PuO_2-UO_2 containing 15, 20, and 25 wt % PuO_2 were prepared from mixed sols. After firing in H_2 at 1150°C, the densities of the mixed oxide products varied from 94 to 96% of the theoretical density. We have assembled equipment capable of producing 100 to 200 g of mixed oxide microspheres per day.

9. SEPARATIONS CHEMISTRY RESEARCH

New separations methods and reagents are being developed, principally for uses in radiochemical processing but also for other purposes extending from extractive metallurgy to biochemical separations. Solvent extraction technology retains the principal emphasis, while other separation methods are receiving a growing share of attention. Reagents that were developed in the former raw-materials program at ORNL continue to show extended utility. Additional reagents have also been discovered in more recent evaluation studies. The present program in separations chemistry can be divided into three interdependent types of research activity: (1) descriptive chemical studies (Sects. 9.1 to 9.4) of the reactions of substances to be separated and of separations reagents, of the controlling variables in particular separations, and of new compounds that may be potential reagents; (2) development (Sects. 9.5 and 9.6) of selected separations into specific complete processes, both where no workable process yet exists and where existing processes can be improved, carried where warranted to the point that large-scale performance can be predicted; (3) fundamental chemical studies (Sects. 9.7 to 9.10) of the equilibria and reaction mechanisms involved in separation systems, both to increase knowledge and to help define potential applications.

9.1 Extraction of Metal Chlorides by Amines

As part of the program surveying the extraction characteristics of many metals from various systems with representative amines, data were obtained for the extraction of Ir(IV) and Pt(IV) from HCl and LiCl–0.2 *M* HCl solutions over the range 0.5 to 10 *M* total chloride. Maximum extraction coefficients (obtained with the quaternary amine Aliquat 336) were about 10 and more than 1000 for Ir(IV) and Pt(IV) respectively.

9.2 New Separations Agents

Investigation for potential utility in solvent extraction or other separations methods continues on compounds that are (1) newly available commercially, (2) submitted by manufacturers for testing, or (3) specially procured for testing class or structure.

Tests with water-soluble (or marginally immiscible) carboxylic and sulfonic acids indicated that high-molecular-weight acids of suitable structure should be good cation exchange extractants. For example, strontium extraction and separation from sodium were higher with a medium-weight carboxylic acid than with HDEHP. Higher-weight carboxylic acids are being sought, and a small sample of di-*n*-dodecylnaphthalenesulfonic acid was synthesized.

Reported selective complexing of lithium by water-soluble sterically hindered β-diketones suggested that a high-molecular-weight analog might be an effective lithium extractant. Diketones are being procured for examination of the effects of structure in complexing, and the synthesis of bis(α,α-dimethyloctadecanoyl)methane is in progress.

The extensive complexing of metal ions by dimethyl sulfoxide in aqueous solution suggested that high-molecular-weight dialkyl sulfoxides (R_2SO) might be correspondingly extensive extractants. However, a series of symmetrical dialkyl sulfoxides extracted only a few metals (Au, Ag, Hg, Pu, and Cu), apparently via sulfur rather than oxygen coordination. The results suggest that an unsymmetrical sulfoxide R(Me)SO might give wider extraction through oxygen coordination; thus 2-ethylhexyl methyl sulfoxide is in preparation.

A new commercial primary amine of unstated composition, Amberlite XLA-3 (Rohm and Haas Company), showed good thorium extraction and low loss to the aqueous phase, resembling the extractant obtained from the commercial primary amine mixture Primene JM-T (Rohm and Haas Company) by scrubbing out the more-water-soluble fraction.

A laboratory supply of 1-(3-ethylpentyl)-4-ethyloctylamine, an excellent extractant formerly available as a research chemical, was prepared from the corresponding heptadecyl alcohol via conversion through ketone and oxime.

Samples of two new inorganic ion exchangers (titanium and tin phosphates) advertised for selective cesium sorption, when compared with ammonium molybdophosphate ion exchanger, showed lower selectivity for cesium (especially with respect to iron) and greater loss by solubility in 1 *M* HNO_3.

9.3 Performance of Degraded Reagents and Diluents

Identification of the three principal products resulting from the degradation of diethylbenzene (DEB) with nitric acid was completed. Each results from reaction at the α-carbon atom of one ethyl group to become (1-hydroxyethyl)ethylbenzene, (1-nitroethyl)ethylbenzene, or (1-ketoethyl)-ethylbenzene (ethylacetophenone). The role of the degradation products in extraction processing was studied. In severely degraded 1 *M* TBP(tri-*n*-butyl phosphate)–DEB solution, the products depress uranium extraction slightly and impair phase separation. Dissolved metals in the two-phase system TBP-DEB–2 *M* HNO_3 retarded degradation.

In further studies of the stability of di-*sec*-butyl phenylphosphonate (DSBPP) in nitric acid, a 1 *M* DSBPP–DEB solution was irradiated to 70 whr/liter while being stirred with 2 *M* HNO_3. Nitrogen uptake and hafnium extraction by the degraded reagent phase were lower than by a 1 *M* TBP solution treated similarly.

Isolation and identification of products from the degradation of *sec*-butyl-α-methylbenzylphenol by nitrate solutions were started. Nuclear magnetic resonance and infrared spectra of the principal product concentrated by column chromatography indicated nitro compound formation, most probably on the tertiary carbon atom of the *sec*-butyl group.

9.4 Comparative Chemistry of Lanthanides and Trivalent Actinides

Large differences between lanthanides and trivalent actinides in extraction by di(2-ethylhexyl)-phosphoric acid from organic-complexed aqueous solutions persist over large ranges of pH, complexant concentration, and nitrate concentration.

In a survey of several support materials for use in applying extraction chromatography to actinide and lanthanide separation, a polyamide powder gave superior performance.

9.5 Recovery of Beryllium from Ores

In continued studies of a primary-amine extraction process for recovering beryllium from low-grade-ore sulfate leach liquors, reagent costs were improved by optimizing the stripping and product-preparation procedures. The process includes extraction of beryllium with 1-(3-ethylpentyl)-4-ethyloctylamine, scrubbing with dilute sulfuric acid, and stripping with either dilute sulfuric acid or fluoride solutions. The product is recovered from the strip solution by hydrolytic precipitation

and upgraded to a relatively high-grade concentrate by dissolving the precipitate in caustic and diluting and heating to precipitate beryllium hydroxide.

9.6 Extraction of Alkalies by Di(2-ethylhexyl)phosphoric Acid (HDEHP)

The previous study of sodium extraction by HDEHP (HA) was extended to other alkalies. Extractions of tracers (K, Rb, Cs) from 3 *M* $NaNO_3$ and two-phase titrations of HA with MOH (K, Li) in 3 *M* MNO_3 showed that lithium, potassium, and rubidium (like sodium) follow the extraction reaction

$$M^+ + \underset{\cdots\cdots}{2(HA)_2} \rightleftharpoons \underset{\cdots\cdots}{MA\cdot 3HA} + H^+ ,$$

while the extractant remains mostly in the acid form $(HA)_2$, shifting toward $(MA)_n$ as more of the extractant is consumed. Cesium coordinates more than four A. (Dotted underlines represent the organic phase.)

The relative extractabilities at 0.1 *M* HA and $MA/\Sigma A = 0.1$ are:

Alkali	$\frac{E_M[H^+]}{E_{Na}[H^+]}$
Lithium	15
Sodium	1
Potassium	0.6
Rubidium	0.3
Cesium	0.35

in good agreement with previous results of simultaneous extraction from mixed solution.

9.7 Extraction of Cesium by 4-*sec*-Butyl-2-α-methylbenzylphenol (BAMBP) plus Organic Acids

The study of the synergistic extraction of cesium by BAMBP plus organic acids was completed. Increasing di(2-ethylhexyl)phosphoric acid (HA) concentration causes an increase of the extraction coefficient to a maximum, then a decrease. The rate of decrease approaches proportionality to the square of the HA concentration, suggesting that BAMBP and HA interact to form a 1:2 complex in addition to the 1:1 complex previously identified. Nuclear magnetic resonance spectra also suggest that BAMBP is hydrogen-bonded to the anion A^- when both are present in the complex with cesium. If this bonding forms $A^-\cdot 2BAMBP$, it should contribute to the stability of the synergistic complex.

9.8 Kinetics of Metal-Ion Extractions by Di(2-ethylhexyl)phosphoric Acid (HDEHP)

Six metal ions tested in extraction with 0.1 *M* HDEHP from $HClO_4$-$NaClO_4$ solutions, at ionic strength = 2, divided into two groups. The extraction rate constants of iron(III), beryllium, and strontium decreased linearly in inverse proportion to the aqueous acidity, while those of uranyl, europium, and zinc (all relatively fast extractions) were nearly independent of acidity. The iron extraction rates over a range of conditions are fairly closely summarized by the proportionalities

$$\text{rate constant} \propto [Fe^{3+}][HDEHP]^{0.3}/[H^+], \qquad [HDEHP] < 0.2\ M ,$$

$$\text{rate constant} \propto [Fe^{3+}][HDEHP]^{1.5}/[H^+]^2, \qquad [HDEHP] > 0.5\ M .$$

The inverse dependence on acidity appears to rule out the possibility that the iron extraction is slow because of slow dissociation of either hydrolytic species or hydrates. An alternative explanation, that the iron reacts readily (at the interface) only with the surface-active anion $DEHP^-$ (i.e., Na^+DEHP^-, its concentration inversely proportional to the acidity), is supported by the finding that the iron extraction is faster at pH 1 and 2 when the gross cation Na^+ is replaced by Sr^{2+}, which is extracted to a greater extent and produces more $DEHP^-$.

9.9 Aggregation and Activity Coefficients in Solvent Phases

Measurements continued of the departures from ideality in the behavior of organic solutions in solvent extraction systems via diluent vapor-pressure lowering determined by direct differential pressure measurement or by isopiestic balancing. The results are expressed as stoichiometric activity coefficients of (real or hypothetical) compounds and/or as apparent mean aggregation

numbers of polymeric species assumed to behave ideally.

In the system tri-*n*-octylamine (TOA)–benzene–sulfuric acid–water, being studied in an attempt to explain apparent deviations from the mass action law, two subsystems were examined: (1) dry TOA-benzene-H_2SO_4 and (2) undiluted TOA-H_2SO_4-H_2O. In the dry benzene solutions the aggregation number for the amine bisulfate increased rapidly with molality from about 2 near 0.003 *m* to about 3.3 at 0.1 *m* (well fitted by an empirical equation,

$$\bar{n}_{TOAH \cdot HSO_4} = 4.66\,[m_{TOAH \cdot HSO_4}]^{0.145})$$

and then more slowly to about 3.8 at 0.5 *m*. By means of these data the dissociation of the amine normal sulfate, indicated by $\bar{n}_{(TOAH)_2SO_4}$ slightly below 1, was estimated as 0.7% at 0.1 *m* and 4% at 0.4 *m*. In the undiluted TOA-H_2SO_4-H_2O system, the water content of TOA·0.765H_2SO_4 increased with increasing water activity to mole fraction $X_{H_2O} = 0.8$ at $a_{H_2O} = 1$ (the standard state being pure H_2O), while the activity of the amine sulfate (taken as solvent, the standard state being pure TOA·0.765H_2SO_4) decreased to 0.15. The water-content curve deviated considerably from Henry's law, but neither it nor the amine sulfate activity curve showed any discontinuity or region of critical sensitivity.

The activity coefficients of tri-*n*-butyl phosphate (TBP) in *n*-hexane at 25°C, needed in a study of synergistic strontium extraction by HDEHP-TBP, were determined by isopiestic balancing to decrease from 1 at 0 *m* to 0.66 at 0.2 *m* and 0.5 at 0.44 *m*. The curve is similar to, and slightly lower than, a literature curve for TBP in cyclohexane at about 6°C.

10. CHEMICAL APPLICATIONS OF NUCLEAR EXPLOSIVES

10.1 Copper Ores

Measurement of the distribution of various radionuclides between acid leach liquors and copper ore solids showed that the ion exchange properties of the ore would be important in minimizing the amounts of certain radionuclides (Cs, Zr-Nb, etc.) taken into solution by in-situ leaching of nuclear-broken ore with dilute sulfuric acid. Although several radionuclides contaminated the copper product recovered by cementation on detinned cans, only ^{106}Ru appears to be a significant problem. Ruthenium contamination was decreased by treating the leach liquor with lime or activated carbon, or more effectively, by solvent-extracting the copper. Tritium, in the form of tritiated water, was readily washed from a column of copper ore with a relatively small volume of leach solution, and most of it could be discarded before dissolving any copper. Radionuclides formed by neutron activation of the ore are apparently of little concern since most of those formed are not leached effectively and do not follow the copper in the cementation step. Based on the studies to date, the potential problems associated with the presence of radioactivity in the system do not appear to pose a preventive obstacle to the use of nuclear explosives in copper processing.

10.2 Magnesium Ores

Paper evaluation of past work on recovery of magnesium from olivine indicated that considerable improvement of the developed processes and extensive pilot operation would probably be required to establish economic feasibility. Also, it is not clear that the use of nuclear explosives could be advantageous in processing olivine deposits.

10.3 Stimulation of Natural Gas Wells

Laboratory measurements of tritium-hydrogen exchange in water-methane systems indicate that the rate of exchange will probably be low during methane production from a natural gas well which has been stimulated under the conditions of proposed Project Gasbuggy. The exchange from water to methane was equal to or less than 2×10^{-6} mc liter^{-1} day^{-1} at 100°C when the tritium concentration was 1 mc/liter. If fusion devices were used in gas stimulation rather than the Gasbuggy tritium-spiked fission device, tritium concentrations would be higher and radiation-induced exchange would probably occur.

10.4 Production of Oil from Shale

The use of a nuclear device to crush oil shale in place has been proposed. The recovery of the

oil from the crushed shale in the nuclear chimney would then involve in-situ retorting. A small furnace has been constructed in which the distribution and possible fate of radionuclides resulting from the nuclear detonation can be studied during the retorting process.

10.5 Development of Hypervelocity Jet Samplers

Efforts are continuing on feasibility studies of hypervelocity jets as means of transporting specimens, irradiated about 1 m from a nuclear detonation, to a remote recovery area that is relatively free from the destructive effects of the detonation. Copper and iron targets have been jetted successfully. Tests demonstrated that at least 50% of a target was formed into a jet in about 15 μsec. The jet traveled with a velocity equal to, or faster than, the estimated velocity of a nuclear shock front in rock.

From these results it is concluded that the following factors are important for efficient recovery of targets: the precision with which the target assembly is made; the precision with which the explosive is cast around this assembly; the symmetry of the detonation-wave front; and the alignment of the charge, target assembly, and flight chamber.

11. RECOVERY OF FISSION PRODUCTS BY SOLVENT EXTRACTION

11.1 Hot-Cell Tests

Several recovery processes developed and tested previously, but only with simulated reactor-fuel-reprocessing waste solutions at tracer level, have now been demonstrated successfully with Purex STW (sugar-treated waste) solution from Hanford. In a mixer-settler demonstration of the Phenex process for recovering cesium by extraction with 4-sec-butyl-2-(α-methylbenzyl)phenol (BAMBP), cesium recovery was more than 98%, and separations of cesium from other fission products and from bulk metals were efficient. No changes in extraction performance occurred in about 80 extraction-strip cycles, and analyses of the solvent showed no significant deterioration of the BAMBP.

In batch tests, cerium was separated selectively from a mixed fission product rare-earths solution (obtained by extracting rare earths from Purex STW and stripping with HNO_3) by oxidizing the cerium with silver-catalyzed persulfate and extracting with di(2-ethylhexyl)phosphoric acid (D2EHPA).

Ruthenium recoveries from Purex STW solution by extraction with a tertiary amine (Alamine 336) were much more effective than those obtained previously from simulated waste solutions. About 95% of the ruthenium was extracted from nitrite-treated STW in a single batch contact. The ruthenium was stripped readily with dilute caustic.

More than 95% of the ^{95}Zr-Nb was batch-extracted from Purex STW (0.3 M H^+) solution in 5 min at room temperature with D2EHPA. This is in contrast to the very slow extractions obtained earlier from high-acid Purex waste.

11.2 Isolation of Promethium

The first cycle of a two-cycle D2EHPA process for separating promethium from mixed fission product rare earths was demonstrated at tracer level in miniature mixer-settler equipment. Results were reasonably good but poorer than expected because of low stage efficiencies in the contactor. In 32 mechanical (16 to 18 ideal) extraction-scrub stages, about 65% of the promethium (along with heavier rare earths) was extracted and separated from rare earths lighter than promethium with D2EHPA in diisopropylbenzene diluent. The decontamination factor of promethium from neodymium was about 400.

11.3 New Flowsheet for Recovering Strontium, Rare Earths, and Cesium

A new and simplified flowsheet was tentatively outlined for recovering rare earths, strontium, and cesium from Purex waste. The proposed process provides less-pure products than processes developed earlier but has the potential advantages of greater simplicity and lower consumption of chemical reagents. The process includes single-stage extraction of the rare earths with sodium di(2-ethylhexyl)phosphate (Na-D2EHP) at pH 2.5 followed by extraction of strontium with Na-D2EHP–D2EHPA at pH 4. Cesium is then extracted from the waste at pH 12 with a substituted phenol.

12. BIOCHEMICAL SEPARATIONS

12.1 Biochemical Separations Research

Transfer ribonucleic acids (tRNA's) are intermediates in the process of protein synthesis in living cells. Each tRNA contains "information," coded in the chemical composition and physical configuration of the tRNA, that identifies the specific tRNA and participates in producing the correct amino acid sequence in proteins. To learn more about this "information" storage and action, samples of pure tRNA's are being prepared.

Two samples of individual tRNA's from *E. coli* B, the one for phenylalanine ($tRNA^{Phe}$) and one of the four for leucine ($tRNA_4^{Leu}$), were prepared by column chromatography. They were first separated from all other tRNA's by reversed-phase chromatography. However, they still contained some higher-molecular-weight RNA. To remove this, the samples were desalted by gel filtration, using Bio-Gel P-2 polyacrylamide gel columns, and concentrated by flash evaporation. Final purification was obtained by gel filtration on columns of Bio-Gel P-100, which achieves separation from RNA on the basis of molecular size.

Sample purity was determined both by amino acid incorporation and terminal nucleoside content. For both $tRNA^{Phe}$ and $tRNA_4^{Leu}$ the values were in agreement, indicating that the samples were very nearly pure. This is the first time that large (100-mg) samples of pure tRNA's have been prepared. Biochemical and physical experiments are now being done to determine the molecular weight, nucleotide composition, and mechanism of interaction with the corresponding aminoacyl-RNA synthetase enzymes.

An alternative method for fractionating tRNA's has been developed: chromatography on columns of hydroxylapatite, a calcium hydroxyphosphate inorganic ion exchanger. Resolution of 14 *E. coli* B tRNA's was obtained at room temperature by using phosphate gradient (concentration gradient) elution techniques. Since the sequence of elution of tRNA's is considerably different from that obtained on the reversed-phase columns, it is anticipated that combinations of these methods will be useful in preparing a number of pure tRNA's.

12.2 Biological Macromolecular Separations Technology

An engineering-scale program has been initiated to fill the need for new methods and facilities for preparing significant amounts of purified macromolecules from biological materials.

During the past year, the construction of facilities and acquisition of much of the equipment were completed. The production of large amounts of mixed tRNA's has been scaled up successfully. In one campaign, 300 kg of *E. coli* W cells were harvested, following continuous fermentation, and processed to yield 630 g of mixed tRNA's. Attention is now being directed toward scaling up the chromatographic methods for preparing gram-size samples of individual pure tRNA's from this large batch.

12.3 Molecular Weights of Transfer Ribonucleic Acids

The feasibility of measuring the molecular weight of tRNA by membrane osmometry was demonstrated. Preliminary data on crude, mixed tRNA's gave molecular weights ranging from 33,200 to 36,500 in the temperature range 37 to 17°C. Subsequent work showed the presence of a high-molecular-weight impurity; thus these values are not representative of pure tRNA.

Gel-permeation chromatography of unfractionated tRNA, phenylalanine tRNA, and a leucine tRNA on polyacrylamide gels (Bio-Gel P-150 and P-300) was used to estimate the size of the molecules. Molecular weights of 27,000 for the phenylalanine tRNA, 29,500 for the leucine-4 tRNA, and 26,000 to 26,500 for unfractionated tRNA were obtained.

12.4 Body-Fluid Analyses

An automatic high-resolution analyzer capable of quantifying ultraviolet-absorbing molecular constituents of urine is being developed for use as a clinical tool and in human biochemical research. This analyzer, which is a modified nucleotide analyzer, gives reproducible results, and it has separated up to 93 ultraviolet-absorbing urine constituents, of which 11 have been tentatively identified. Use of anion exchange resin in the size range 5 to 10 μ as the separating medium has greatly increased the resolution of the system.

13. CHEMISTRY OF PROTACTINIUM

Protactinium, whose isotope 233 is the precursor of ^{233}U, is a significant radionuclide in thorium-

breeder technology, and it also occupies a key position in the actinide series. Thus, better knowledge of its properties is imperative.

During this report period, solubility studies were carried out in both hydrochloric and sulfuric acid solutions, and, in most cases, reproducibility of results was still a problem. In hydrochloric acid, the addition of fluoride or silicofluoride increased the solubility markedly, but in a complicated manner.

A small-scale preparation of a sulfate compound, reported to be $H_3PaO(SO_4)_3$, yielded a product that gave a similar x-ray diffraction pattern but a much higher sulfate-to-protactinium ratio. The larger amount of sulfate might result from inadequate removal of sulfuric acid from the solid.

Spectrophotometric studies were continued, and resolution of some of the complex spectra by means of a computer code was initiated. In 10 *M* HCl the reported band near 2150 A could not be verified when carefully purified reagents were used; the absorption increased steadily with decreasing wavelength to below 2100 A. In concentrated sulfuric acid solution, three spectra were observed, depending on the source of the protactinium. In dilute acid a broad band is ordinarily observed near 2000 A, with a shoulder at 2800 and perhaps other shoulders in between. However, one case was different: Dilution of concentrated sulfuric acid solutions heated to fuming resulted in a sharp band near 2000 A and a second band near 2800. Resolution of spectra in 2.5 *M* H_2SO_4 solutions indicated that three to five Gaussian bands are required to account for the observed spectra.

14. IRRADIATION EFFECTS ON HETEROGENEOUS SYSTEMS

The study of the radiolysis of adsorbed water was continued, using silica-alumina, alumina, and some molecular sieves as adsorbents. The $G(H_2)$ values were measured as a function of the electron fraction of sorbed water and were found to be greatly enhanced over those for liquid water, especially for the silica-alumina-water system. Surface acidity seems to play a part in the efficiency of the adsorbent to sensitize or to transfer energy to the adsorbed water.

15. HIGH-TEMPERATURE CHEMISTRY

15.1 Fabrication and Installation of the Spectrophotometer System for Use with High Levels of Alpha-Active Elements

A spectrophotometer, associated cells, and related systems were specially designed by Applied Physics Corporation (APC) of Monrovia, California. The spectrophotometer was built by APC, and the related equipment was built by shops at Oak Ridge. The system will be used to study the aqueous solution chemistry of uranium and transuranium elements – including some isotopes of such alpha-active elements as curium – over a range of temperatures which may include the solution critical temperature.

Installation of the spectrophotometer and its related systems is now essentially complete in a "cold" area. At the conclusion of "cold" testing, the system will be installed in an area where high levels of alpha activity can be tolerated.

Numerous modifications were made in the system, both during construction and after installation and preliminary testing. The principal shortcomings were found in the absorption cell design and in the temperature control and programming unit. The cells were underdesigned in that some window flexure occurred under pressure. This was corrected by a redesign of the window retaining flange. The temperature control and programming unit did not meet the specifications set, and an extensive modification of the entire unit was required. In addition to these problems, the fluid-line disconnects originally specified for the heating system of the absorption cell were found to be incapable of operating at the required temperatures because of failure of the elastomer seals. Consequently, a new disconnect whose use required brazing stainless steel to titanium was selected. Fortunately, a useful brazing technique, which was recently developed by NASA, could be applied.

15.2 Spectral Studies of Ionic Systems

Aqueous solutions of uranyl perchlorate and UO_2^{2+} hydrolysis products are being studied to verify the experimental and computer techniques that will be used with the new spectrophotometer system. Until this system becomes operable,

spectral studies are being made at 25 to 95°C with a standard Cary model 14 spectrophotometer and the same digital data output equipment that will be used with the new system.

Spectral studies led to an assignment of bands into the various levels of a proposed triplet excited state which is different from the assignment made previously. The ultraviolet spectrum of the uranyl ion was measured to 1860 A and showed much previously unreported band structure.

We also measured the effect of hydrolysis on the UO_2^{2+} spectrum. We found that the frequencies of the peaks of the resolved bands do not shift as hydrolysis progresses, and thus conclude that hydrolysis does not affect the O – U – O structure. Our data suggest that there are fewer hydrolyzed species than were proposed in previous work and that hydrolysis involves the water of hydration in the equatorial positions.

15.3 Measurement of Densities of Liquids at High Temperatures and High Pressures

Density measurements were made for water up to 370°C and for uranyl perchlorate solutions up to about 300°C with the dilatometer described in the last annual report. Improvements on the dilatometer during the past year include a new design of the pressure seal at the top of the dilatometer (autoclave), which is based on the Haskel seal design. This modification has solved a small leak problem that existed in the earlier seals, probably because the autoclave is made of titanium. Also, several computer programs were written that greatly simplify and expedite the conversion of raw data to actual solution densities. We believe that we can measure the density of water at temperatures to 370°C with a maximum error of 1.5%, and that below 325°C the error will not exceed 0.6%. Our results confirm steam-table values to within these limits of error. Working with solutions that do not decompose, we should be able to maintain this accuracy.

16. MECHANISMS OF SEPARATIONS PROCESSES

The first three paragraphs below are abstracts of completed work, already reported. The literature citations can be found in Sect. 16 of this report. The last paragraph summarizes work still in progress.

16.1 Activities of Tri-*n*-butyl Phosphate (TBP) in TBP-HNO_3-H_2O Solutions

New experimental data are presented on the distribution of nitric acid and water between aqueous acid and 100% TBP solutions. A table of smoothed distribution data, obtained by a hand smoothing procedure from these data combined with other literature data, is also presented. Several different mathematical representations of the data in terms of the Gibbs-Duhem relation are described, and the resulting activities of TBP, obtained by graphical integration, are compared. A table of rational activities of TBP (based on pure anhydrous TBP as the standard state) is presented for aqueous nitric acid concentrations ranging from 0 to 15 *M*. Partial molar volumes of the components in the TBP phase, determined by least-squares analysis of the density data, are 16.5, 43.3, and 273.9 ml/mole, respectively, for H_2O, HNO_3, and TBP.

16.2 Determination of Radioisotopes by Resolution of Gamma-Ray Spectra

A FORTRAN-63 computer program, ALPHA, was developed for the quantitative analysis of radioactive samples by the least-squares resolution of the gamma-ray spectra. As the result of thousands of analyses, ALPHA was found to be fast, accurate, and relatively inexpensive. The program was designed to handle a small or a large number of samples. The samples can have different radioactivity levels (from 0.1 to 10^4 counts/sec), isotope compositions, and input formats. Also, they can be on cards or magnetic tape. ALPHA takes into account several corrections, such as background subtraction, counting time, decay, dead time, automatic compensation for gain and threshold shifts, sample fraction, and volume reduction prior to counting. Typical computation times for samples containing from six to ten isotopes are about 5 to 15 sec. The cost per analysis is about 20¢ (this includes only the CDC 1604 computer charges and not the cost of sample preparation and counting).

The determination of concentrations of radioactive nuclides having short half-lives is important in several radiochemical problems. Since the concentrations calculated by the least-squares resolution of gamma-ray spectra are accurate for long-half-life isotopes, the same technique was extended to short-half-life isotopes. In particular, two ways

of minimizing the estimated error in the individual radioisotope concentrations were studied. First, an equation was derived to express the errors of each component of a mixture as a function of the radioactivities of the other isotopes present, of the background counting rate, of the counting duration of solution and background, of half-life, of irradiation time (whether the nuclide is produced by nuclear fission or activation), and of decay time. To obtain optimum conditions for a particular isotope, the relative error can be minimized by graphical, analytical, or standard numerical methods.

Recent work on improving the accuracy in the determinations of radioisotopes may be summarized as follows: The use of coincidence gamma counting has been shown in one case to improve the accuracy of analysis 20-fold. This is for a mixture of ^{106}Ru and ^{131}I (one part ^{106}Ru and 1000 parts ^{131}I).

17. CHEMICAL ENGINEERING RESEARCH

17.1 The Stacked-Clone Contactor

An experimental seven-stage stainless steel stacked-clone contactor has undergone further testing with a variety of chemical systems including hexone–acetic acid (in which a solution residence time of 2 sec per theoretical stage was realized) and mineral oil–dilute HNO_3 (in which the dispersed phase had a very high viscosity). Operation in the organic-continuous mode was demonstrated with Amsco–dilute HNO_3, and further tests involved the high aqueous-phase viscosities of glycerol and dextrose solutions. The effects of solid-particle impurities in the aqueous feed were also noted. A 14-stage stacked-clone contactor (plant prototype) with integral pumps has been fabricated and installed; it is now being tested with the system TBP-Amsco-$NaNO_3$-$UO_2(NO_3)_2$-water.

18. REACTOR EVALUATION STUDIES

This program is supported jointly by the Reactor Division and the Chemical Technology Division. It consists of studies on various proposed advanced reactor and fuel-cycle systems to evaluate their technical and economic feasibility. The work in this Division during the past year included estimation of the costs of fuel shipping and processing and of preparing sol-gel oxides and other fuel materials in connection with the ^{233}U value study, the HWOCR (Heavy-Water Moderated, Organic-Cooled Reactor) evaluation, and the new nuclear power evaluation handbook. In addition, computer codes were developed for calculating shipping and processing costs and the overall cost of nuclear power, and for calculating the gamma-shielding requirements of fuel-handling facilities. The optimization of the size of fuel processing plants in a growing economy was also studied.

19. PREPARATION AND PROPERTIES OF ACTINIDE-ELEMENT OXIDES

The chemistry underlying the current sol-gel process for making dense nuclear-fuel oxides includes the physical chemistry of colloidal thoria, urania, and plutonia, and of other colloidal oxides of interest. The purpose of our effort in the Actinide Oxides Program is to determine the properties that control the behavior of these oxides during their preparation.

Viscosity measurements of dilute thoria sols demonstrated that a pH of 2.70 is more favorable for dispersing thoria sols than that of 2.0 or 3.6. At pH 2.70, the axial ratios at solids volume fractions of 0.00513 and higher are similar to those at pH 2; below this concentration, however, the flocs of particles tend to come apart, unlike the flocs at pH 2 or 3.6.

At concentrations of 4 through 7 *M*, thoria sol behaved as a simple pseudoplastic. At higher concentrations (8.0 and 8.8 *M*), the colloid was a gel that was pseudoplastic above the yield stress.

Studies of the electrophoretic behavior of thoria sols with a moving-boundary apparatus repeatedly showed at least two different electrophoretic mobilities for the same thoria sols, indicating that all the sol particles do not possess the same effective charge density.

The initial densification of thoria gel prepared from steam-denitrated thorium nitrate occurred by shrinkage from loss of water below 600°C and shrinkage from plastic flow and grain-boundary diffusion sintering from 600 to 1000°C. An activation energy of 39.0 kcal/mole was determined for the grain-boundary diffusion sintering in air.

Since urania sols and gels are sensitive to air oxidation, efforts were made to ascertain what precautions must be taken to obtain valid results when such materials are studied.

20. ASSISTANCE PROGRAMS

20.1 Eurochemic Assistance Program

The Laboratory continued to coordinate the exchange of technical information between Eurochemic and the AEC production sites and National Laboratories for the AEC Division of International Affairs. E. M. Shank completed his fourth year at Mol, Belgium, as U.S. Technical Advisor to Eurochemic during the construction and start-up of the Eurochemic fuel-processing plant. Construction of the plant and its auxiliary facilities is now complete. Cold start-up has begun, and hot start-up is scheduled for the end of 1966.

20.2 Demonstration of the Disposal of Solid, High-Level Radioactive Waste in Salt

Assistance was provided by the Division on the experiment concerning the disposal of highly radioactive, solid waste in salt (Project Salt Vault). The experiment is being conducted by the Health Physics Division in a salt mine at Lyons, Kansas. The first tests have included the use of fully irradiated, 90-day-cooled Engineering Test Reactor (ETR) fuel assemblies to simulate the heat and radiation from solid-waste containers. All equipment for transporting the fuel assemblies from Idaho to Kansas and handling them at and in the mine has been completed. The first set of ETR assemblies was successfully transported to and installed in the mine during November 1965.

20.3 High-Level Alpha Laboratory

A detailed design and cost study was made for a new alpha laboratory facility for joint use by the Analytical Chemistry, Chemical Technology, and Metals and Ceramics Divisions. The laboratory would contain thirty 16- by 32-ft alpha laboratories, two supporting "cold" laboratories, a 32- by 88-ft deep-bay area for large alpha experiments, a 32- by 64-ft shielded cave area, and office and service facilities. The facility, which would be administered by the Analytical Chemistry Division, is estimated to cost about $5,000,000. A preliminary design package, suitable for an architect-engineer, was completed. Since this project was relegated to fiscal year 1968, no further detailed design will be done for about a year; however, alternative layouts are being prepared to determine whether any further cost savings can be realized.

20.4 Fuel-Shipping Safety Studies

To provide technical backup data for Federal Regulations (10 CFR 72) designed to ensure the safety of spent fuel shipments by public carriers, both theoretical and experimental studies are being made. The scope of this program was increased materially during the past year. An analysis of the stresses produced by internal pressures in a cask was completed, and a report was issued. Studies on cover closures, lifting and tie-down devices, and cask shell thicknesses required to resist puncture have been completed, and reports on this work are in preparation. The shipping cask manual (ORNL-TM-681) prepared last year is being upgraded for issuance by the AEC as a monograph; this work is being done jointly by ORNL and Battelle Memorial Institute.

20.5 Evaluation of Radiation Resistance and Decontaminability of Selected Protective Coatings

Commercial coatings are still being tested for their resistance to gamma radiation. Exposures were made in air and in demineralized water. Three new coatings, a modified phenolic type and two epoxy types, were still in good condition after an exposure of 8×10^9 r in water. Nineteen coatings resisted exposures, in air, of $\geqq 1 \times 10^{10}$ r. A series of samples was exposed in the Nuclear Safety Pilot Plant to the plasma-jet volatilization of irradiated UO_2 to simulate a reactor excursion. The degree of contamination of the various specimens was measured. A new decontamination procedure to avoid chemical degradation of the coatings was developed and tested.

21. WATER RESEARCH PROGRAM

Oak Ridge National Laboratory is carrying out a program of basic research on the properties of water and its solutions under the auspices of the Office of Saline Water, Department of the Interior. This program has as its long-range goal the development of methods for the economical purification

of water in such amounts and of such purity that it may be used for irrigation and for drinking. Work in the program is under the direction of K. A. Kraus and is interdivisional. It is reported in part in a series of reports issued annually by the Department of the Interior. The most recent report in the series is *Saline Water Conversion Report, 1965*. Because the work is reported formally in the above series, only this abstract of the work carried out by Chemical Technology Division personnel is presented in this report.

Studies carried out in the Chemical Technology Division have followed several lines. One has been measurements of thermodynamic properties of water-organic liquid mixtures, in the hope that such mixtures will exhibit the properties of, and so serve as models for, salt-excluding organic membranes. This hope has been reinforced by the finding that the distributive selectivity and the activity coefficients of inorganic salts in the mixtures are similar functions of their water contents over a wide range of organic structures, from esters to amides and organic salts. Correlations of activity coefficients and miscibility gaps with dielectric constants, salt types, and water thermodynamic activity have contributed to the information necessary to establish the utility of organic liquids as membrane models.

In another line of study, methods are being sought to alter the hydrodynamic conditions near a solid surface to promote rates of mass transfer of a solute between the surface and the circulating fluid. (This study is under the direct supervision of D. G. Thomas, Reactor Division, ORNL.) This research is specifically intended to reduce the concentration polarization problems encountered in reverse osmosis and electrodialysis of brackish waters. The study is focused upon measurements of mass-transfer promotion from wires or cylinders supported above the mass-transfer surface near the edge of the hydrodynamic boundary layer. The experimental work uses an electrochemical technique with the ferricyanide-ferrocyanide redox system. The test surface is polarized with a large excess of supporting electrolyte so that the electric current is diffusion or mass-transfer controlled. Several promoter sizes and arrangements have been investigated over a range of Reynolds numbers. At certain points, the mass-transfer rates may be more than eight times higher than those observed without promoters, and the average rate over the entire test surfaces may be more than three times higher. These improvements are somewhat better than Thomas has found in an air-naphthalene system, indicating that the high Schmidt numbers of aqueous systems at least do not hinder the application of detached turbulence promoters.

A hyperfiltration (reverse osmosis) unit for desalination of brackish waters was designed and is under construction. It has the capability of circulating salt solutions at the rate of 20 gpm. The materials of construction are stainless steel and rubber hose. The purposes of the unit are: (1) to find out if hyperfiltration membranes are workable in the presence of large amounts of stainless steel, (2) to investigate long-term behavior of dynamically cast membranes, and (3) to investigate the effects of cross-flow velocities that are higher than those previously attainable on flux and rejection.

22. CHEMISTRY OF CARBIDES AND NITRIDES

In the current phase of this program, the basic chemistry of carefully characterized uranium and thorium carbides is being studied. This year's work consisted of studies of the reactions of thorium carbides with sodium hydroxide solutions, hydrolysis of uranium monocarbide–uranium dicarbide mixtures, and elucidation of the high-temperature region of the uranium-carbon phase diagram, where uranium monocarbide and dicarbide exhibit solid immiscibility. The results of these studies were reported in the open literature.

23. INDUSTRIAL APPLICATIONS OF NUCLEAR ENERGY

23.1 Economics of Hydrogen and Ammonia Production via the Electrolysis of Water, Using Low-Cost Nuclear Power

One example of the use of large blocks of low-cost nuclear power predicted for the foreseeable future would be the production of hydrogen by the electrolysis of water, and then the use of the hydrogen in the synthesis of ammonia for fertilizer. The market potential for nitrogen fertilizers is already very great due to the increase in world population and food consumption. The cost of ammonia made from electrolytic hydrogen, assuming

that the electrical power is produced by a desalination reactor, was compared with the cost of producing it by the conventional steam-methane reforming process. It was also assumed that the fertilizer plant would be located near the reactor. Factors studied included cost of power, cost of natural gas, production rate, return on investment, type of electrolytic cell, credit for by-product oxygen, and transportation cost.

Our study showed that, with recently developed electrolytic cells that operate at very high current densities, ammonia can be produced for $39 per ton with power at 2.5 to 3.0 mills/kwhr. Such power costs are obtainable on an incremental basis from commercial light-water reactors. Large, advanced reactors producing power at 1.6 mills/kwhr may allow an ammonia plant using such hydrogen to compete (assuming a credit for by-product oxygen) with steam-methane reforming plants that use natural gas at 29 to 33¢ per million Btu's. (The average U.S. price of industrial natural gas in 1963 was 34¢ per million Btu's.)

23.2 Production of Hydrogen by the Electrolysis of Water

The proposed use of large dual-purpose nuclear reactors to desalt seawater called for studies of on-site utilization of the huge block of by-product energy. The proposed amount of energy available [3000 to 5000 Mw (electrical)] is, in most cases, too large to be used in the immediate vicinity, and electrical losses over a 100-mile transmission line would amount to 10 to 20% of the production cost. But the synthesis of useful chemicals, such as NH_3, in closely integrated industrial-nuclear installations would overcome both problems. The hydrogen for ammonia synthesis can be produced by the electrolysis of water; thus its production in a new, advanced electrolysis cell is being studied in the laboratory. The cell incorporates porous nickel electrodes with a thin (0.010 in.) asbestos membrane containing 26 to 35% aqueous KOH serving as the ion-transfer medium. It has been operated at current densities up to 1633 ma/cm^2 (1517 amp/ft^2) with good cell efficiency as measured by the total voltage drop across the cell (2.18 v at 90°C).

Electrolysis cells that have metal-plate electrodes evolve the two product gases (oxygen and hydrogen) between the electrodes, causing increases in electrolyte resistivity, which can be attributed to bubble formation, and resulting in steep increases in cell voltage at high current densities. With the advanced cell, these gases are released behind each electrode; thus resistivity is not affected by bubble formation, and high current densities are attainable at low cell voltages.

In addition to laboratory evaluations of this new cell, studies are being performed on the relative merits of pulsed, unidirectional current (half-wave rectified ac) and direct current.

23.3 Direct Fixation of Nitrogen with a Plasma Torch

Laboratory study is in progress on the production of nitrogenous fertilizers via the direct fixation of nitrogen from oxygen-nitrogen mixtures, using a high-temperature plasma torch. Yields of fixed nitrogen, expressed as mole % nitric oxide in the final gas, have been as high as 5.3%, which may be compared with a theoretical maximum equilibrium concentration of 6.6% nitric oxide.

23.4 Waste-Water Treatment

Additional studies include a survey of the chemical, metallurgical, and waste-water-treatment industries to determine other processes which appear attractive for inclusion at a nuclear industrial complex.

1. Power-Reactor Fuel Processing

Laboratory and engineering-scale development of processes for recovering fissionable and fertile material from spent power-reactor fuels is continuing. This work has included basic chemical studies on unirradiated samples of new types of fuel and cladding materials, chemical and engineering development of mechanical and aqueous chemical processes for present-day and advanced fuels, and hot-cell testing of new processes to determine the effect of radiation and fission products on the chemical reactions. The major processes studied this year included a grind-leach process for uranium-thorium-graphite HTGR (high-temperature gas-cooled reactor) fuel, the shear-leach process for metal-clad oxide fuels, and caustic decladding and shear-leach for SAP-clad UC fuel for an HWOCR (heavy-water moderated, organic-cooled reactor). Work on fuel recovery processes for LMFBR (liquid-metal fast-breeder reactor) fuel was begun, and efforts on close-coupled processes were continued.

Grind-leach process development included laboratory and engineering-scale work with unirradiated Peach Bottom HTGR fuel compacts. In this process, the graphite fuel, which contains pyrolytic-carbon-coated ThC_2-UC_2 fuel particles, is broken to -6 mesh, ground to -140 mesh, and leached in 13 *M* HNO_3–0.05 *M* F^-. The uranium and thorium nitrate solution is then recovered from the graphite by filtering and washing. All steps of the process were proved feasible, and processing times and fuel recovery were satisfactory. Although this process appears to be inferior to the burn-leach process for carbon-coated fuels, further tests are planned for fuels containing particles coated with SiC or other incombustible refractories.

New work involved tests of the shear-leach process, in which tubular stainless-steel-clad and Zircaloy-2-clad UO_2 and ThO_2-UO_2 fuels are sheared into short lengths to facilitate nitric acid leaching of the fuel oxide. These studies indicated the feasibility of shearing intact second-generation power-reactor fuel assemblies. Calculations indicated that the fission product heat generation of stored, sheared fuel is insufficient to produce either dangerously high temperatures or pressurization of a batch leacher when the thermally hot fuel is quenched by the dissolvent. Further safety studies on the finely divided zirconium produced by sawing and shearing of Zircaloy-2-clad fuels proved that sawing is perfectly safe and that, although a problem exists with shearing fines, it is controllable. A full-scale model of the delayed-neutron leached-hull monitor was built, tested, and found to be satisfactory for rapidly and accurately checking the fissionable-material content of leached stainless steel and Zircaloy hulls. Hot-cell tests were made with irradiated Consolidated Edison and PWR (pressurized-water reactor) fuel samples to determine the amount of tritium and ^{85}Kr released during shearing, leaching, and feed adjustment. The tests indicated that the tritium release to the atmosphere is within established limits but that a problem exists in disposal of aqueous effluents. The sediments from fuel dissolution and feed adjustment were found to contain appreciable quantities of fission product molybdenum and zirconium.

Several methods for recovering uranium from SAP-clad UC fuel for an HWOCR were investigated. SAP is a cermet of Al_2O_3 and aluminum. Both shear-leach and an NaOH or NaOH-$NaNO_3$ decladding process appear feasible. Work will be continued on both processes.

Development of a process to adsorb protactinium on unfired Vycor glass was concluded in hot-cell experiments with highly irradiated 27-day-cooled ThO_2-UO_2. The adsorbed protactinium is eluted with oxalic acid. Satisfactory loadings on the powdered glass (3 mg of Pa per milliliter) and

eluate concentrations (2.8 mg of Pa per milliliter of oxalic acid) were achieved. Higher concentrations are not practical because the solution is self-heating. Hot-cell tests with silica gel and zirconium phosphate (Bio-Rad ZP-1) as adsorbent and hydrochloric acid as the fuel dissolvent were also conducted.

Close-coupled processing development included the completion of a survey to determine whether methods other than solvent extraction were suitable for low-cost, low-decontamination fuel processing. Only anion exchange seemed to qualify, and that only marginally. Experiments with stirred-pot and static-column batch-differential solvent extraction systems indicated that they were more difficult to operate than continuous solvent-extraction systems. Conceptual plant studies of batch and continuous solvent-extraction systems indicated that they were equally expensive; therefore, the continuous method is preferred because of its greater ease of operation.

1.1 DEVELOPMENT OF PROCESSES FOR GRAPHITE-BASE FUELS

Development of processes for recovering fuel materials from spent thorium-uranium-graphite fuels was continued. Major attention was focused on the laboratory and engineering development of a grind-leach process using unirradiated Peach Bottom fuel compacts. The reactor at Peach Bottom, Pennsylvania, is an HTGR. Hot-cell tests on the alternative burn-leach process[1,2] were commenced; work on the pressurized aqueous combustion process[3] for graphite fuels was discontinued because of corrosion and chemical problems that make the method appear definitely inferior to the burn-leach process.

Grind-Leach Process

The grind-leach process for coated ThC_2-UC_2 or ThO_2-UO_2 fuel particles, either admixed with or free of diluent graphite, includes the breaking of the fuel matrix to −6 mesh and subsequent roll-crushing of the broken fuel to −100 to −140 mesh in order to rupture all fuel-bead coatings. The crushed fuel is then leached in boiling 13 *M* HNO_3–0.05 *M* F^-, and the solubilized uranium and thorium nitrates are filtered and washed from the insoluble graphite. With pyrolytic-carbon-coated ThC_2-UC_2 fuel particles, the entire fuel matrix would be crushed; with SiC- or Al_2O_3-coated particles, it may be feasible to burn the graphite component of the fuel before grinding. Work done thus far has been with unirradiated Peach Bottom fuel compacts containing 150- to 420-μ-diam (+100 −40 mesh) ThC_2-UC_2 particles with a 55-μ-thick pyrocarbon coating.

Feed for the roll-crushing experiments was prepared in a conventional hammer mill (fixed hammers on a 15-in.-diam by 8-in.-long rotor operating at 845 rpm with discharge bars set for $\frac{1}{8}$-in.-wide slots). It produced, in a single pass, a 75% yield of −6 mesh material. A brief series of tests on ball-milling[4] the −6 mesh material indicated that this method is undesirable because of the low grinding rate, batchwise operation, and lack of positive size classification of the product.

Preliminary roll-crushing experiments were made with a small commercial roll crusher having 8-in.-diam by 2-in.-wide rolls. Nip angle (Fig. 1.1) and

[1]E. L. Nicholson, L. M. Ferris, and J. T. Roberts, *Burn-Leach Processes for Graphite-Base Reactor Fuels Containing Carbon-Coated Carbides or Oxide Particles*, ORNL-TM-1096 (Apr. 2, 1965).

[2]*Chem. Technol. Div. Ann. Progr. Rept. May 31, 1965*, ORNL-3830, pp. 34–36.

[3]*Ibid.*, pp. 36–39.

[4]H. O. Witte and L. M. Ferris, *Ball-Milling of Graphite-Bed Reactor Fuel*, ORNL-TM-1412 (Feb. 3, 1966).

ORNL-DWG 66-7555

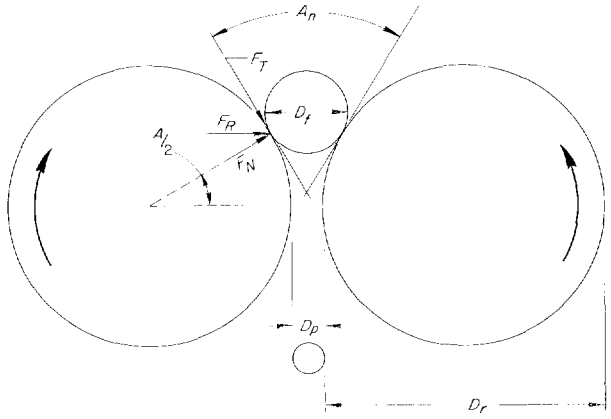

Fig. 1.1. Schematic Diagram of a Double-Roll Crusher. Angle of nip, A_n, is defined by $\cos A_n/2 = (D_r + D_p)/(D_r + D_f)$, for this critical condition in which F_R is horizontal. F_T is the tangential force on the particle, F_N is the normal force on the particle, and F_R is the resultant force on the particle.

throughput rates were determined. Nip angle is a measure of the coefficient of friction between the rolls and the material being ground. The position of one roll was adjustable, for varying the roll spacing (nominally equivalent to the maximum product diameter, D_p; see Fig. 1.1). Both rolls were chain-driven at the same speed by a variable-speed motor. The nip angle was found to be about 12° for Peach Bottom fuel, based on experiments at nominal roll spacings of 0.045 and 0.003 in.; the nip angle for ordinary rock is about 32°. Because of excessive play in the bearings of the rolls and the lack of rigidity in the machine frame, the true nip angle may be even smaller than 12°. The determination of the correct value is important for predicting the maximum size-reduction ratio per pass.

In tests with unfueled graphite, the throughput was measured at several values of roll spacing, roll speed, and nominal feed size, but the data were somewhat inconclusive. It was tentatively concluded, however, that, with the spacing set at the critical spacing for a particular feed size, the throughput was proportional to roll speed up to about 200 rpm (7-fps peripheral speed with the 8-in.-diam rolls). Increasing the speed from 200 to 300 rpm resulted in only a slight further increase in throughput. Typical grinding rates for unfueled graphite were 50 g/min through a nominal 0.003-in. gap, and 200 g/min for a 0.045-in. gap.

For HTGR coated fuel particles, the indicated roll spacing is about 150 μ (0.006 in.). At a nominal 0.002- to 0.003-in. spacing, a 90% yield of −100 mesh product was achieved after four successive passes through the rolls; incomplete reduction was attributed mainly to deficiencies in the machine. An unexpected result of recycling fuel through the rolls was the production of relatively large flakes. These flakes were up to 3000 μ in diameter but were only about 50 to 140 μ thick, as determined by optical measurements. Thus the effectiveness of a roll crusher in fracturing coated particles may be much greater than is indicated by a simple sieve analysis of the product.

Despite the deficiencies of this particular machine, it has demonstrated that roll-crushing of HTGR fuel is feasible. On the basis of information obtained in these tests, a new machine (Fig. 1.2) was designed and built and is currently being evaluated.

To obtain data for designing an engineering-scale crushed-fuel leacher, leaching experiments with feed prepared by the small commercial roll crusher were conducted in the laboratory. These tests demonstrated the need for continuous, controlled addition of ground fuel to the leachant, intimate contact between ground fuel and leachant to obtain maximum possible slurry concentrations and solution loadings, and a separate solid-liquid separation device after leaching. Experience in the laboratory led to an engineering test facility with a nominal capacity of 3 kg of ground HTGR fuel per batch. As shown in Fig. 1.3, the facility consisted of a ground-fuel feeder, a 4-in.-diam leacher, and a 6-in.-diam filter. The equipment had an actual capacity of 5 kg of fuel in 10 liters of graphite-acid slurry.

In the leaching and washing tests in the laboratory, samples of unirradiated, ground Peach Bottom fuel (3% U, 14% Th, 83% C) were leached for 5 hr in boiling 2 to 13 *M* HNO_3 (Table 1.1); uranium recoveries varied from 99.6 to 99.8%, and thorium recoveries from 98.2 to 99.2%. Similar recoveries were achieved with nitric acid made 0.05 *M* in HF, which shows that fluoride is not required as a catalyst for dissolving ThC_2-UC_2 (but would be needed for ThO_2-UO_2). The U-plus-Th concentration in the leachate was 0.2 *M*. When washed with 10 *M* HNO_3 instead of water, the recoveries were increased to 99.9%; this, however, may only indicate that leaching is incomplete in 5 hr. Subsidiary tests in which the fuel was leached with two successive batches of fresh boiling 13 *M* HNO_3 also resulted in recovery of 99.9% of both uranium and thorium. In these experiments, 13 to 50% of the carbide carbon was solubilized.

In experiments with the engineering test equipment, −140 mesh roll-crusher product was air-lifted from the feeder by fluidizing the material at the base of the feeder while injecting air into the vertical lift tube. The ground fuel flowed out of the upper feeder section into the leacher; and the air for lifting, plus the air purge to the upper section, prevented vapor generated by the boiling acid in the leacher from entering the fuel-addition line. The rate of addition of ground fuel was limited to about 75 g/min because of the foam generated by the initial reaction of fuel with the boiling 13 *M* HNO_3–0.05 *M* F^-. During the 7-hr leaching period, the powdered fuel was suspended by boiling and by injecting air into the

draft tube of the leacher. Subsequent transfer of the slurry to the filter vessel was effected in 30 sec by applying a vacuum of about 20 in. Hg to the filter vessel. In the filter, the flow rate of product solution and three water washes through the 6-in.-diam bed of ground fuel in the filtration vessel ranged from an initial rate of 320 ml/min to a final rate as low as 80 ml/min, for a total time of 48 min.

Flowsheet conditions and leaching and filtration results are summarized in Fig. 1.4. Uranium and thorium losses to the graphite residue after washing were 0.35 and 0.67% respectively. Additional washing of a portion of the residue with 0.1 *M* HNO_3 lowered the losses to about 0.2 and 0.5%. This additional washing would have increased the total volume of the mixed solution from 12.6 liters to 22.5 liters; therefore, the additional uranium and thorium recoveries were achieved at the expense of doubling not only the volume of mixed solution requiring feed adjustment but also the time required for washing.

Solution samples taken during leaching showed that the concentration of dissolved carbon reached

ORNL-DWG 66-149R

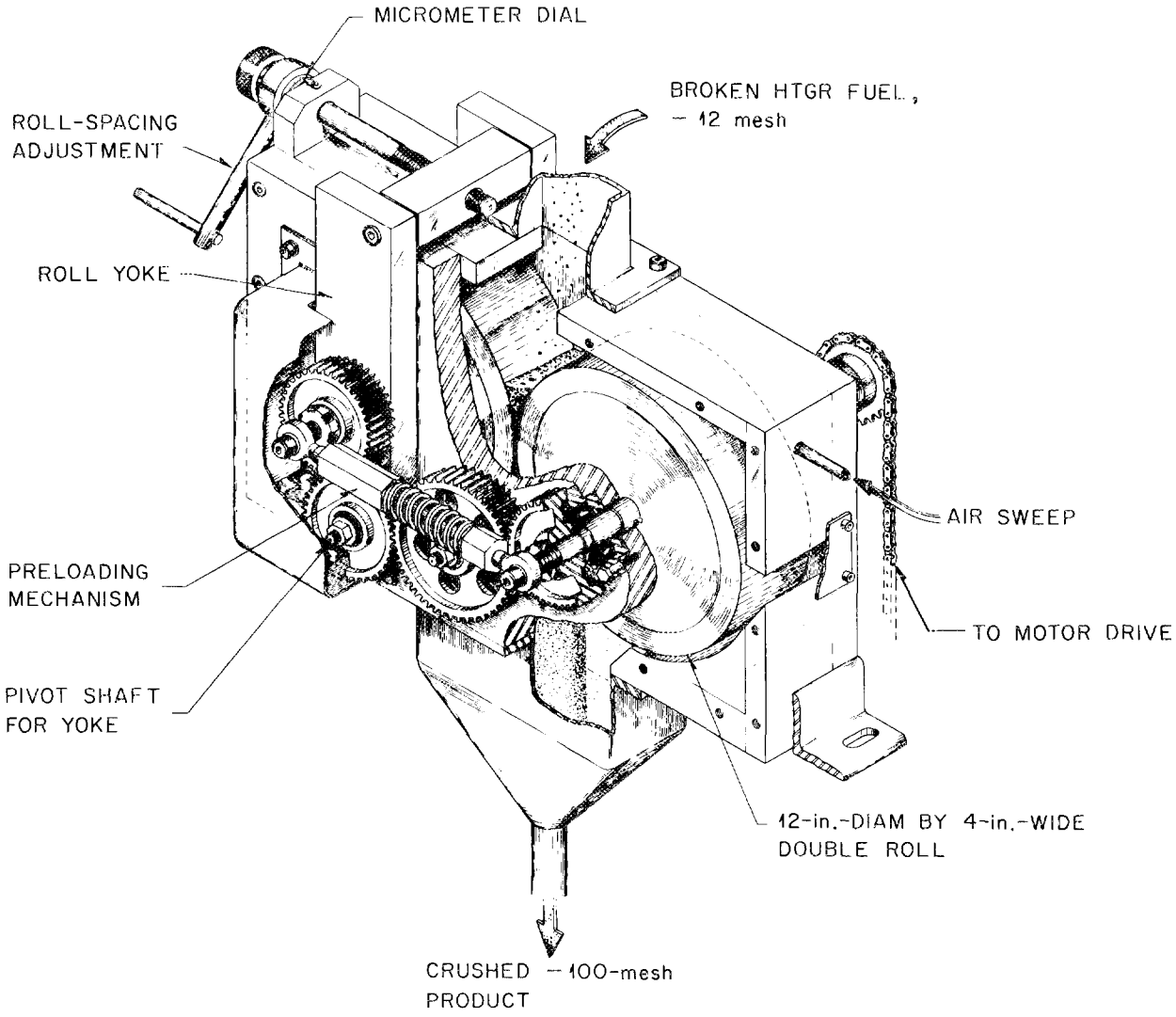

Fig. 1.2. Experimental Double-Roll Crusher for Final Size Reduction of Graphite Fuel.

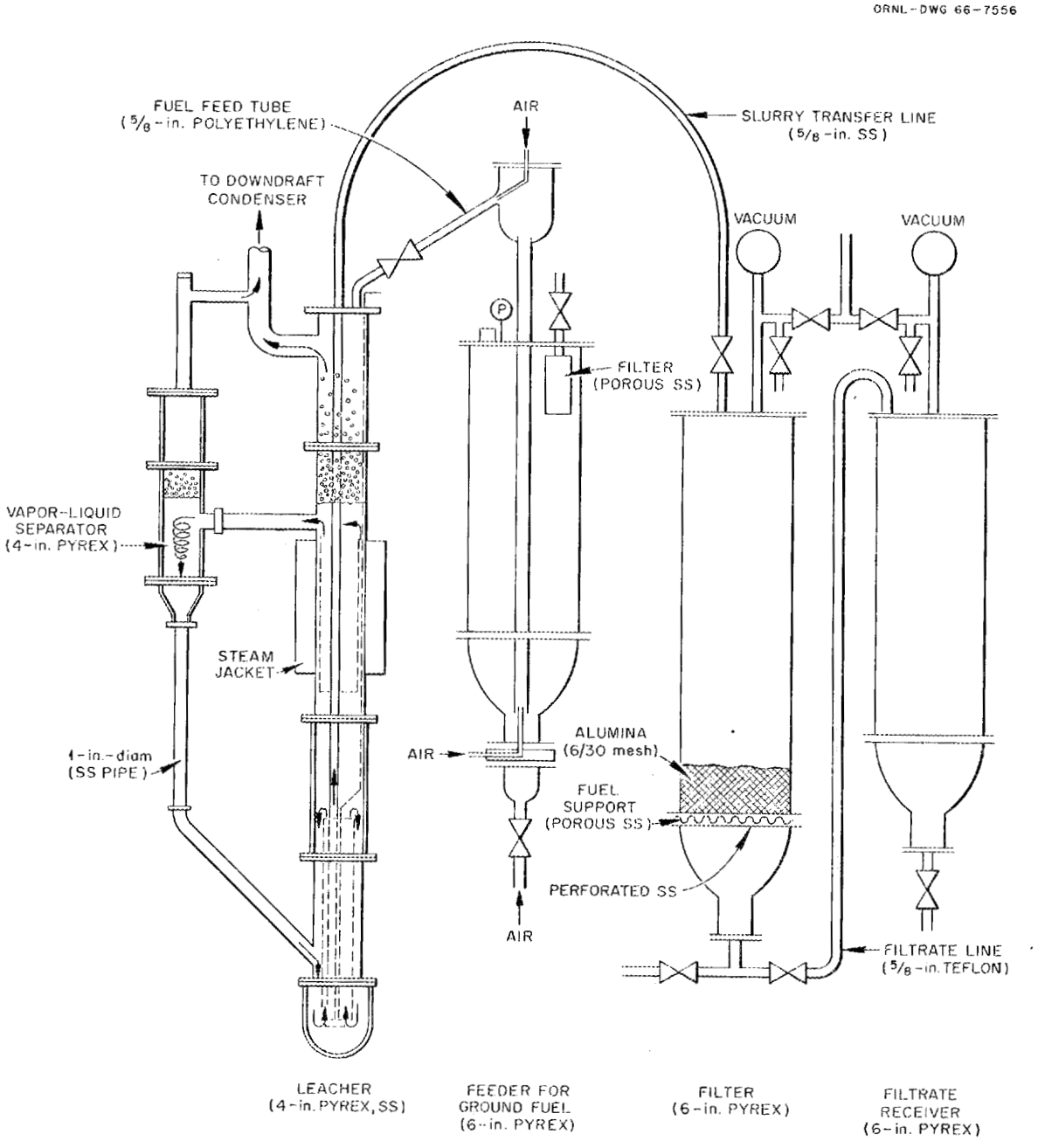

Fig. 1.3. Engineering-Scale Leaching and Filtering Apparatus for Finely Ground HTGR Fuel.

Table 1.1. Uranium and Thorium Recoveries After Leaching of Roll-Crushed Peach Bottom Fuel

Fuel crushed to −140 mesh. Boiling leachant used in each case.
Leaching time, 5 hr

Leachant Composition (M)		Wash	Recovery (%)		Carbide Carbon in Leachate (% of original)
HNO_3	HF		U	Th	
2.0	0	Water	99.6	98.2	24
5.0	0	Water	99.7	99.1	31
13.0	0	Water	99.8	99.2	13
15.8	0	Water	99.8	98.8	
2.0	0.05	Water	99.8	96.9	50
5.0	0.05	Water	99.8	99.0	32
13.0	0.05	Water	99.8	99.4	
13.0	0.05	Water	99.7	99.5	22
13.0	0.05	10 M HNO_3	99.9	99.9	
13.0	0.05	10 M HNO_3	99.8	99.9	52

a peak value of about 3.5 g/liter at 1.5 hr and slowly decreased to 1.15 g/liter at 7 hr. This indicates that the composite solution may require feed adjustment, for example, permanganate oxidation of the soluble compounds of carbon if their presence causes difficulties in subsequent solvent extraction.

Measurements of the permeability (Fig. 1.5) of 1- to 2.5-ft-deep beds of leached graphite residue to 0.1 M HNO_3 wash solution were well correlated by the equation $V = 0.9\ (\Delta P/L)\ (1/\mu)$, where V is in gal hr^{-1} ft^{-2}, $(\Delta P/L)$ is in psi per ft of bed depth, and μ is in centipoises. Bed depth, L, can be calculated from this equation by assuming the bulk density of the leached graphite to be 0.8 g/cm^3. Range of $(\Delta P/L)$ was 6 to 28 psi/ft.

The results of this work indicate that the grind-leach process for graphite-base fuels is feasible but probably not competitive with the burn-leach process for reactor fuels containing pyrolytic-carbon-coated fuel particles, particularly if scheduled hot-cell tests on the latter process indicate no serious fission product volatilization in the burner off-gases. The best application for the grind-leach process appears to be for fuels containing fuel particles coated with SiC or other highly refractory materials.

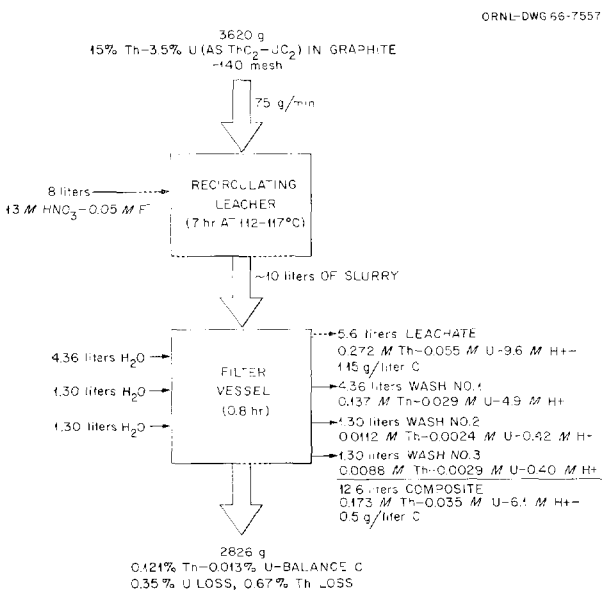

Fig. 1.4. Grind-Leach Process Flowsheet for Peach Bottom HTGR Fuel.

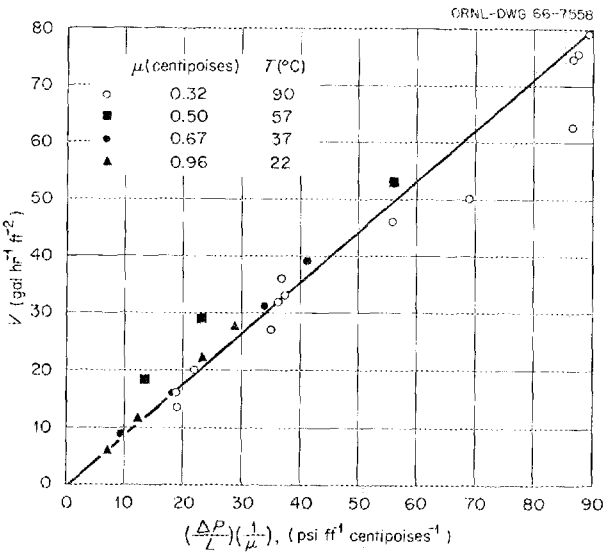

Fig. 1.5. Permeability of −140 Mesh Leached Graphite to 0.1 *M* Nitric Acid. Measurements made in $1\frac{1}{2}$-in.-ID cylinder for bed depths of 1 to 2.5 ft.

1.2 DEVELOPMENT OF MECHANICAL PROCESSES

Development of the basic technology of the shear-leach process[5–7] (for full-size unirradiated first- and second-generation stainless-steel-clad and Zircaloy-clad UO_2 and ThO_2-UO_2 power reactor fuel elements) has been completed on a full engineering scale. The process is now being used by Nuclear Fuel Services, Inc., in their reactor fuel processing plant near Buffalo, New York.

Work this year included: final verification of the process for second-generation fuels; evaluation of the fission product heat generation problem in various steps of the process; further evaluation of the zirconium-fines safety problem; continued development of a leached-hull monitor; and hot-cell experiments with irradiated fuel samples, to determine the release rate of tritium and ^{85}Kr during shearing and leaching and to characterize the residues obtained during leaching and feed adjustment.

Shearing of Second-Generation Fuels

The feasibility of shearing intact unirradiated second-generation power reactor fuel assemblies (after the end hardware has been removed) was investigated by using Dresden type IV, Elk River core II, and Consolidated Edison core B fuel assemblies. The Dresden fuel assembly (Fig. 1.6*a*) consisted of a 6-by-6 array of porcelain-filled Zircaloy-2 tubes (outer diameter, 0.52 in.; wall thickness, 0.035 in.; length, 115 in.) secured by crossed-wire grids, on approximately 19-in. centers. The Elk River assembly (Fig. 1.6*b*) consisted of 25 stainless steel tubes (outer diameter, 0.452 in.; wall thickness, 20 mils; length, 62 in.) filled with porcelain pellets. Two leaf-spring grid sections on 21-in. centers separated the tubes. The Consolidated Edison assembly (Fig. 1.6*c*) contained 231 porcelain-filled stainless steel tubes (outer diameter, 0.30 in.; wall thickness, 0.01 in.; length, 105 in.); the tubes were held in place with stainless steel leaf-spring grids.

The Dresden fuel assembly was successfully sheared into 1- and 2-in. lengths, with the terminal pieces varying from $1\frac{1}{2}$ to $2\frac{1}{2}$ in. The grids were easily broken during shearing, and the shearing force varied from 40 to 55 tons. Typical sheared fuel is shown in Fig. 1.7*a*. The Elk River assembly was also easily sheared into 1-in. sections (Fig. 1.7*b*). The results for these two fuels indicate that intact shearing of assemblies with the end hardware removed is feasible, provided that irradiation does not create special unforeseen problems.

The shearing tests with Consolidated Edison fuel were made with several short fuel-assembly sections 15 to 36 in. long. In one test, in which a 3-ft-long section containing four stainless steel leaf-spring grid sections was sheared, the fuel jammed in the fixed blade and could not be fed properly. After the tubes were pulled from the grid section, the terminal piece consisted of a section of sheath 4 to 5 in. wide, plus pieces of tubing $2\frac{1}{2}$ to 6 in. long. This test demonstrated that a dull shear blade and excessive clearance (20 mils) between the moving and fixed blade produced a poor product and did not cut the

---

[5] *Chem. Technol. Div. Ann. Progr. Rept. May 31, 1963*, ORNL-3452, pp. 17–25.

[6] *Chem. Technol. Div. Ann. Progr. Rept. May 31, 1964*, ORNL-3627, pp. 21–27.

[7] *Chem. Technol. Div. Ann. Progr. Rept. May 31, 1965*, ORNL-3830, pp. 48–59.

sheath completely. When the moving blade was replaced and the clearance was decreased to 3 to 5 mils, an excellent product and a good terminal cut were achieved. Material obtained with the 20-mil clearance is shown in Fig. 1.8*a*; typical product and the end pieces obtained with the 3- to 5-mil clearance are shown in Fig. 1.8*b* and c respectively. Unlike the moving blade, the fixed blade of the shear is not easily dulled and has not been replaced during the several years of use. It was concluded that the intact Consolidated Edison core B fuel can be sheared satisfactorily if the blade is reasonably sharp, if blade clearance is 3 to 5 mils, and if some "chunking" of fuel at the grids can be tolerated, along with some terminal pieces up to 3 in. long.

PHOTO 83597

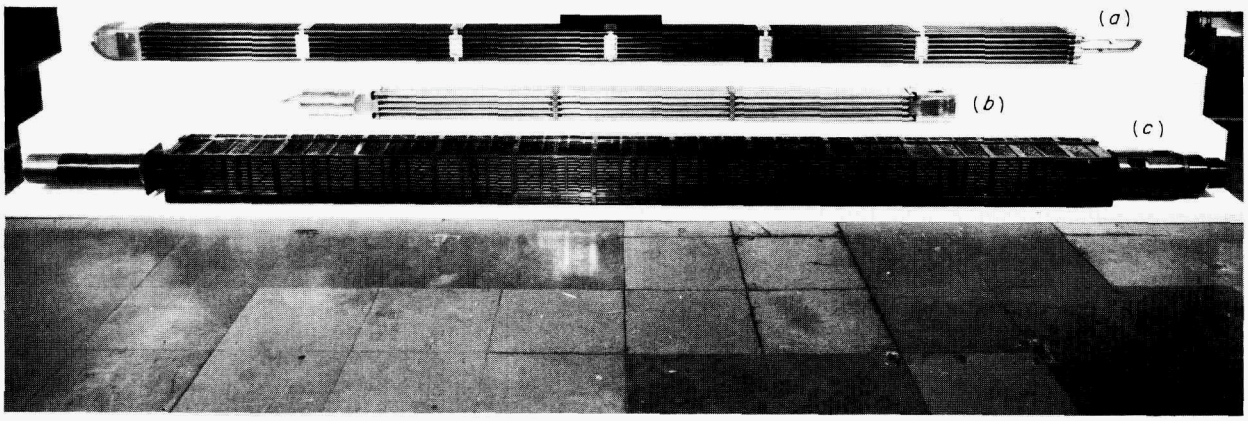

Fig. 1.6. Fuel Assemblies Used in Shearing Tests on Second-Generation Power Reactor Fuels. (*a*) Dresden type IV; (*b*) Elk River core II; (*c*) Consolidated Edison core B.

PHOTO 84318

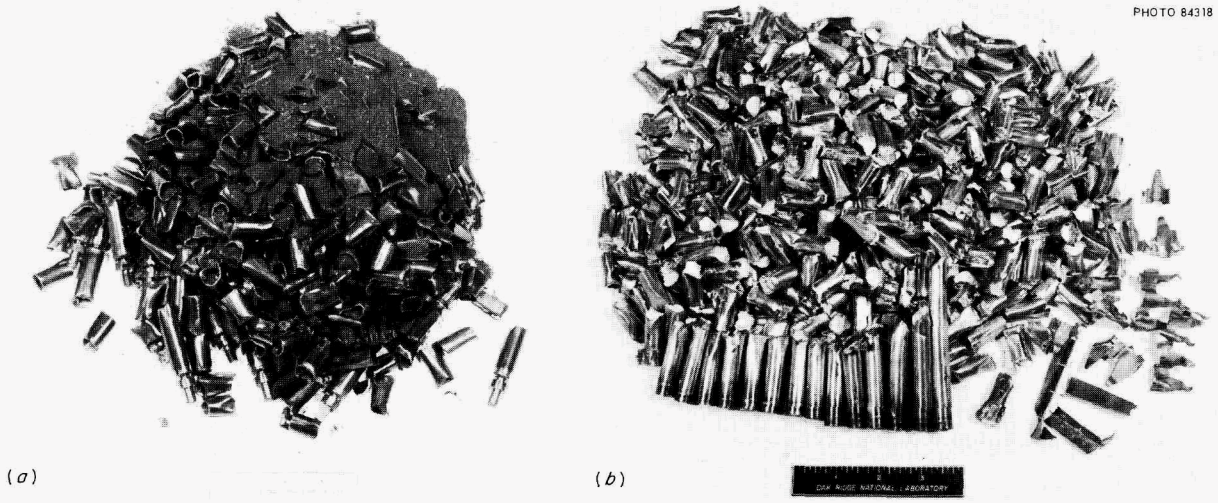

Fig. 1.7. Sheared Fuel from (*a*) Dresden Type IV and (*b*) Elk River Core II Shearing Tests.

Fig. 1.8. Sheared Fuel from Consolidated Edison Core B Shearing Tests. (*a*) Sheared with 20-mil clearance; (*b*) sheared with 3- to 5-mil clearance; (*c*) end piece from shearing with 3- to 5-mil clearance.

Fuel Element Heat Generation Studies

During the mechanical processing of spent power reactor fuels in air, internally generated heat from fission products may build up and produce temperatures detrimental to the fuel or equipment in the shear-leach process. To study this problem, a FORTRAN computer code, BIGDEAL, was developed[8] to cover fuel burnups ranging from 8000 to 50,000 Mwd/metric ton, specific powers of 10 to 70 w/g, and decay times of 180 to 1080 days. The decay code used was a modification of PHOEBE. For these calculations, a Yankee Atomic type subassembly (36 UO_2-filled stainless steel fuel tubes, 0.302 in. in outer diameter, 120 in. long, on 0.422-in. centers) was selected as a typical power reactor fuel. The fuel-handling operations that were evaluated have included: suspension of an intact assembly vertically in water; suspension horizontally in air; horizontal positioning in the shear feed envelope; basket storage of sheared material in an array of 16 baskets of 5, 7.75, and 10 in. inner diameter on 12-in. centers; and suspension of six filled baskets in a dissolver at the start of a batch dissolution. In addition to calculating the maximum anticipated temperature in each of the above situations, an estimation was made of the pressure rise in a vented batch dissolver caused by acid vaporization (from the quenching of the six baskets of thermally hot fuel by cold acid). The calculations also assumed steady-state heat-transfer conditions and heat loss by natural convection and radiation only. Temperatures calculated for minimum, typical, and maximum conditions are given in Table 1.2.

The highest temperature encountered (1586°F) is far below the melting point of both UO_2 (3947°F) and stainless steel (2642°F); therefore, it is assumed that the fuel and cladding will not melt during processing if the burnup, specific power, and cooling time are within the limits specified. By providing for longer decay times and forced cooling, lower temperatures could be maintained during mechanical disassembly, in the shear feed envelope, or during storage.

If the six fuel baskets were placed in an empty dissolver equipped with a 6-in.-diam off-gas line, an acid flow rate of 1.16×10^5 lb/hr would be required to develop a pressure of 1 psig in the dissolver when processing fuel at the maximum heat generating conditions. Such an acid flow rate is impractical; therefore, it is concluded that pressure buildup in the dissolver will not be a problem under normal operating conditions.

As part of this study, the thermal conductivity in air was determined for UO_2-filled stainless steel tubing (0.5 in. in outer diameter, with a wall thickness of 0.035 in.) sheared into 1-in. sections (and including the dislodged fines). The mean particle size of the UO_2 fines was 120 μ, and voidage was 40.3%. The thermal con-

[8]G. E. Abraham III and B. C. Finney, *Calculated Maximum Temperatures of Spent Yankee Atomic Type of Power Reactor Fuel During Shear-Leach Processing*, ORNL-3948 (in press).

Table 1.2. Minimum, Typical, and Maximum Temperatures Achieved by Reactor Fuel in Various Steps of the Shear-Leach Process

Operation or Process Step		Minimum Temperature[a] (°F)	Typical Temperature[b] (°F)	Maximum Temperature[c] (°F)
Receiving-canal storage		68.5	71.5	75.5
Mechanical disassembly		123	150	191
Shear feed envelope		143	350	548
Storage in baskets of various internal diameters:				
5 in.	Center	160	491	852
	Surface	140	324	548
7.75 in.	Center	196	720	1244
	Surface	155	453	773
10 in.	Center	232	924	1586
	Surface	171	575	979

[a]Burnup, 8000 Mwd/metric ton; specific power, 10 w/g; cooled for 1080 days.
[b]Burnup, 20,000 Mwd/metric ton; specific power, 23 w/g; cooled for 180 days.
[c]Burnup, 50,000 Mwd/metric ton; specific power, 70 w/g; cooled for 180 days.

ductivity is temperature dependent and can be expressed as:

$$k = 0.0280 \times 0.6209 \times 10^{-3}\ (t)\ ,$$

where k is the thermal conductivity in Btu hr^{-1} ft^{-1} $°F^{-1}$, and t is temperature in °F. The data were correlated for the temperature range 200 to 1500°F.

Safety Studies on Finely Divided Zirconium

Tests were conducted to evaluate the safety of handling zirconium particles produced (1) by abrasive-disk sawing of Zircaloy-2-clad fuel assemblies to remove inert end boxes and (2) by shearing of Zircaloy-2-clad fuel rods and then leaching the core material from the sheared pieces. Material for these tests was produced by both wet and dry abrasive-disk sawing and shearing of reactor-grade Zircaloy-2 tubing filled with UO_2 pellets. All samples were then sieved into eight particle-size fractions between 4760 and <44 μ. No attempt was made to separate the abrasive-disk debris from the zirconium fines in the sawed material, where the volume ratio of loose abrasive to fines was 7:1. The UO_2 in the sheared material was dissolved with 6 M HNO_3.

Ignition tests were made on small samples of each size fraction with a 20,000-v, 0.35-amp spark discharged from a "testacoil" probe. In the ignition tests none of the *sawing* fines, and only the <149-μ-diam particles produced by *shearing*, could be ignited. The results of the spark test on each size fraction were as follows:

Diametral Range of Zircaloy-2 Fines (μ)	Results
4760 to 2000	No reaction
2000 to 1190	No reaction
1190 to 590	No reaction
590 to 297	One flash, apparently from a finer particle clinging to this size fraction
297 to 149	One flash, as above
149 to 74	Brilliant flash produced
74 to 44	Brilliant flash produced (more pronounced)
<44	Brilliant flash produced (instantaneous and more pronounced)

The samples were also tested with a Phillips electron-probe analyzer to determine the extent of zirconium conversion to ZrO_2 during mechanical processing. The analysis showed that most of the sawing fines are apparently converted to oxide but that the Zircaloy-2 shearing fines are not oxidized by either shearing or leaching. Thus, the shearing operation itself does not constitute a fire or explosion hazard.

The results of these tests indicate that the fines resulting from sawing are safe because they are largely converted to ZrO_2 and are highly diluted with debris from the abrasive disk. It was also concluded that sheared particles larger than 149 μ in diameter are safe but that smaller ones should be periodically removed from the dissolver and dissolved in HNO_3-HF. In an experiment in which leached Zircaloy cladding and fines were dissolved, 80% of the −10 mesh fines and 5% of the bulk cladding were dissolved in 2 to 3 hr.

The size-distribution data presented below indicate the amount of zirconium fines that would be produced by leaching 1400 kg of sheared fuel (19% of which is cladding) containing 1 metric ton of uranium:

Particle Size (μ)	Zirconium (kg)
<44	0.106
<149	0.266
<297	0.372
<590	0.532
<1000	0.745
<2000	1.410

The volume of leached hulls produced was equivalent to about 75 gal per ton of uranium processed.

Monitoring of Leached Hulls

To be assured that the leaching of uranium, plutonium, or thorium from stainless steel or Zircaloy-2 cladding in the shear-leach process is complete, it is necessary for a fuel processor to have available a reliable monitor for testing the leached hulls.

The fabrication and testing of a prototype delayed-neutron monitor[9] was completed, and a full-scale monitor was built[10] and is now being tested. The new one is capable of monitoring an 8-in.-diam basket in 8-in. vertical increments. Each increment can be monitored in 40 sec, making it possible to monitor a 5-ft-long basket in about 6 min. For each measurement, the hulls are irradiated with thermalized neutrons for 20 sec, and the delayed neutrons are then counted for 20 sec. The monitor is sensitive to as little as 5 mg of fissionable isotopes.

First, the neutron flux in the empty basket was measured by indium dosimeters. Then the basket was loaded with hulls that had been filled with inert ceramic (no fuel), and the neutron flux was measured again. Typical results for both measurements are given in Fig. 1.9. Next, to simulate incompletely leached cladding, empty hulls containing known amounts of residual fuel were placed in known positions in the basketful of ceramic-filled hulls and monitored. The results are shown in Fig. 1.10 for one hull containing 6 mg of ^{235}U (left) and for a hull containing 100 mg of ^{235}U (right).

Figure 1.11 shows the response obtained when each 8-in. segment of the basket contained a uniformly distributed 100 mg of fuel and, in addition, one hull on the center line of the basket. This hull contained 500 mg of ^{235}U.

The full-scale monitor contained six special 2-in.-diam BF_3 detector tubes incorporating charcoal getters that provided the necessary efficiency and ensured long life (many months or even years). The getters remove the fluoride ions produced by the gamma radiolysis of the BF_3. These ions interfere with operation of the tube, and the gamma radiation comes from the ^{60}Co formed during irradiation of stainless-steel-clad fuel in the reactor. The estimated gamma-ray dose at the tubes, when a basket containing hulls from processing fuel burned to 25,000 Mwd/metric ton is monitored, is 450 r/hr. The gamma dependence of the monitor was evaluated by using a 110-curie ^{60}Co source that provided 1100 r/hr of gamma radiation at the tubes. The gamma pulses were 20 v, and the neutron pulses were 80 v. A neutron-counting circuit that we believe will discriminate more completely against the gamma pulses is currently being assembled. The source of the high background, which is equivalent to 15 mg of ^{235}U, is being sought; it is tentatively

[9] *Chem. Technol. Div. Ann. Progr. Rept. May 31, 1965*, ORNL-3830, pp. 56–59.

[10] *Ibid.*, Fig. 1.13, p. 58.

believed to be caused by activated sodium in the aluminum parts of the detector tubes.

A new type of neutron generator, which employs a rechargeable sealed-tube target that is continuously regenerated by a gas stream, is being tested; the new design gives a continuous flux of 10^9 neutrons/sec for 60 hr.

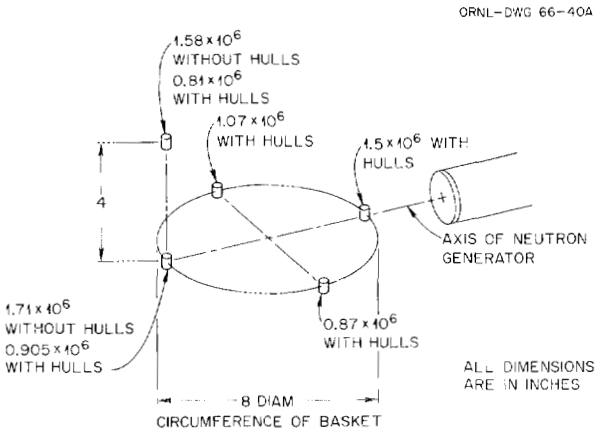

Fig. 1.9. Neutron Irradiation Flux (*neutrons cm*$^{-2}$ sec^{-1}) in the Basket Was Measured by Indium Dosimeters. The presence of hulls reduces the flux by only 50%.

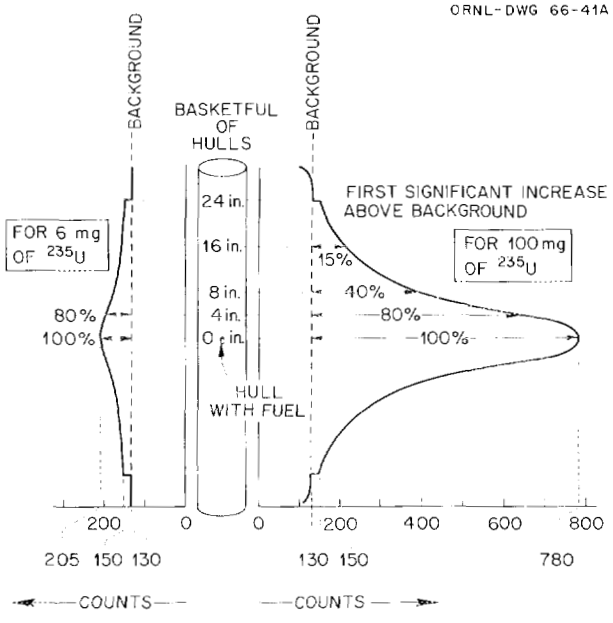

Fig. 1.10. The Monitor's Response to Fuel Drops Only 20% at the Boundaries of the 8-in.-long Segment of Basket Being Monitored.

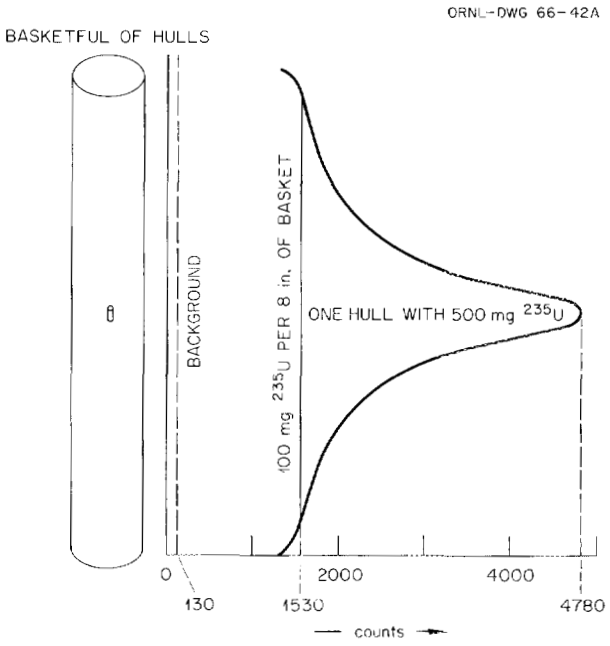

Fig. 1.11. It Is Estimated That a Small Amount of Fuel Uniformly Distributed in the Hulls Will Displace the Pulse from a Large Amount of Fuel in a Single Hull Without Changing the Pulse Profile.

Hot-Cell Tests

Hot-cell experiments were made with stainless-steel-clad Consolidated Edison and Zircaloy-2-clad PWR fuel samples, irradiated to 25,000 and 40,000 Mwd/metric ton, respectively, to evaluate the release of fission product tritium[11–15] and ^{85}Kr during shearing, leaching, and leach-product feed adjustment.[14] The samples were 4.5 in. long and $^5/_{16}$ in. in diameter. Each Consolidated Edison fuel pin contained 27 g of ThO_2 and 1.3 g of highly enriched $^{235}UO_2$; each PWR pin contained 36 g of UO_2. Residues obtained during

[11] E. L. Albenesius, *Phys. Rev. Letters* **3**, 274 (1959).

[12] E. L. Albenesius and R. S. Ondrejcin, *Nucleonics* **18**(9), 100 (1960).

[13] E. N. Sloth *et al.*, *J. Inorg. Nucl. Chem.* **24**, 337 (1962).

[14] D. L. Horrocks, *Trans. Am. Nucl. Soc.* **8**(1), 12–14 (1965).

[15] J. H. Goode, *Hot Cell Evaluation of the Release of Tritium and ^{85}Kr During Processing of ThO_2-UO_2 Fuels*, ORNL-3956 (in preparation).

the leaching and feed adjustment of the Consolidated Edison samples were then filtered from the solutions and analyzed. These data are important to fuel processors using the shear-leach process, particularly in association with the management of gaseous and liquid wastes.

Multiple shearing of the Consolidated Edison fuel rods released 0.2% of the tritium and 1% of the ^{85}Kr to the shear off-gas, based on calculated fission yields. Another 0.2% of the tritium and the balance of the ^{85}Kr were released to the dissolver off-gas when the exposed fuel was dissolved in fluoride-catalyzed nitric acid. Extrapolation of these results indicates that at this irradiation level about 1 curie of tritium per metric ton of uranium plus thorium would be liberated to the atmosphere during shearing and leaching. This quantity represents 0.5% of the amount calculated by Blomeke[16] that could safely be discharged from a 6-ton-per-day plant at $\frac{1}{10}$ MPC_a through a 100-m stack when the mean wind speed is 3 mph. In further experiments, about 70% of the tritium remaining in the dissolved fuel solution as THO was carried overhead when this strongly acid solution was distilled. In a processing plant, most of the THO released during feed adjustment would report to the low- or intermediate-level radioactive waste stream.

Multiple shearing and subsequent leaching with 4 *M* HNO_3 of the PWR fuel specimens released 9% of the tritium to the off-gas; this is equivalent to 18.5% of the maximum amount that could safely be discharged from a 6-ton-per-day plant.

In the shearing experiment, single rods were sectioned in a vacuum-tight hydraulic shear, and the released fission gases were flushed with hydrogen through hot copper oxide to convert the tritium to THO for counting in a liquid scintillation spectrometer. The hydrogen purged served as a carrier gas and also exchanged isotopically with tritium adsorbed on the vessel walls. The tritiated water was condensed with liquid nitrogen, and the remaining gases were sampled for ^{85}Kr determination.

When only the end plugs were sheared from five Consolidated Edison fuel samples, the amount of tritium released varied from 0.006 to 0.018% of the theoretical amount present. Two specimens sheared in eight places released 0.03 and 0.22% of the tritium present. About 0.5% of the ^{85}Kr was released from specimens receiving a single cut; 0.87 and 1.07% were released from the two samples receiving eight cuts. When two PWR fuel samples were sheared into $\frac{1}{2}$-in. sections, 9.27% of the tritium was released; one-fourth was released immediately, and the remaining three-fourths diffused in two days.

The sheared fuel was then dissolved in 13 *M* HNO_3–0.05 *M* HF–0.1 *M* $Al(NO_3)_3$ to release additional tritium and krypton. A purge gas of He–0.2% H_2 carried the dissolution off-gas through an NaOH scrubber, a cold trap held at −77°C, and then through heated copper oxide to convert any residual tritium to THO, which was condensed in a second cold trap. About 0.20 and 0.13% of the tritium were released during dissolution of the Consolidated Edison and PWR fuel samples respectively. In addition, the remainder of the ^{85}Kr from both samples was released.

The dissolved-fuel solutions and caustic scrubber solutions were distilled twice to separate the tritium from other fission products, and the tritium contents of the condensates were determined by scintillation spectrometry. In one experiment, 70% of the tritium was evaporated from the dissolver solution during feed adjustment.

In an actual 6-ton-per-day Thorex solvent extraction plant, the solvent extraction feed would contain an estimated 30% of the tritium, the acid rectifier overhead about 47%, and the concentrated acid about 23%. The rectifier overhead would have to be diluted with 18,000,000 gal of water to permit discharge at concentrations less than $\frac{1}{10}$ the MPC_w for tritium (3×10^{-3} $\mu c/ml$). Then, to qualify as potable water, further dilution to 1×10^{-3} μc of tritium per milliliter would be required. An alternative control measure would be volatilization of the tritiated water and dispersal in the atmosphere.

Insoluble residues were present in both the dissolver and feed-adjustment solutions obtained in the Consolidated Edison shear-leach tests described. These were collected by filtration, washed, dried, weighed, and analyzed. In these experiments, a typical radioactive leach solution was obtained by a 6-hr dissolution of the sheared ThO_2-UO_2 in boiling Thorex reagent. The solution was 8.5 *M* in HNO_3, 1.39 *M* in Th, and 0.05 *M* in U; gross gamma, 1.23×10^{10} counts min^{-1} ml^{-1}. Filtration recovered the residue, which,

[16] *Chem. Technol. Div. Ann. Progr. Rept. May 31, 1964*, ORNL-3627, pp. 110–12.

after washing and drying, amounted to 0.58 wt % of the original fuel core. The residue contained 0.23 wt % U, 7.45 wt % Th (representing a thorium and uranium loss of 0.05% each), 0.74 wt % Mo, and 0.23 wt % Zr. The remainder of the residue consisted of silica, alumina, and stainless steel corrosion products.

To remove excess nitric acid from the leach solution, it was evaporated until the boiling point was a little higher than 136°C. Approximately a 70% reduction in volume resulted. The concentrate was diluted with water to nearly the original volume, producing an acid-deficient feed solution of composition: 0.09 *M* acid deficient, 1.36 *M* in Th, 0.05 *M* in U; gross gamma, 1.49×10^{10} counts min^{-1} ml^{-1}. A precipitate formed during this feed adjustment was removed by filtration and analyzed. This second residue, representing about 0.6% wt % of the original core, contained 7.7 wt % Th (another thorium loss of 0.05%), 4.63 wt % Mo, 0.32 wt % Zr, and 0.19 wt % U (0.02% loss).

These experiments verify the relative insolubilities of the fission products molybdenum and zirconium encountered during head-end aqueous processing of the high-burnup fuels[17] and, specifically, the precipitation of these fission products from the strongly acid concentrate resulting from acid boil-off.

1.3 DEVELOPMENT OF PROCESSES FOR HEAVY-WATER-MODERATED, ORGANIC-COOLED REACTOR FUEL

One of the advanced reactor types being considered by the Atomic Energy Commission is a heavy-water-moderated, organic-cooled reactor (HWOCR). A prototype will possibly be built in the mid-1970's. Several zirconium-clad fuels, including ThO_2-UO_2, Th-U alloy, and UC, are being considered for the HWOCR; but, at present, SAP-clad UC appears to be the leading candidate. SAP (sintered aluminum product) is a sintered dispersion of Al_2O_3 (5 to 15%) in an aluminum matrix.

Studies were initiated this year on the development of aqueous methods for processing SAP-clad UC fuel. Several possible processing methods, such as caustic decladding, shear-leach, and others, were partially evaluated in the laboratory. At the present stage of development, caustic decladding appears to be the most practical method, although none of the processes studied have received sufficient development for a final evaluation to be made.

SAP cladding (6% Al_2O_3) dissolved rapidly (about 20 mg min^{-1} cm^{-2}) in boiling 2 *M* NaOH–2 *M* $NaNO_3$ solutions. Rate constants for each experiment were calculated from the expression given by Wymer and Blanco,[18]

$$-\frac{dN_{OH}}{dt} = \frac{dN_{Al}}{dt} = \frac{kSN_{OH}}{V},$$

in which dN_{Al}/dt is the initial rate of appearance of aluminum in solution (moles/min); k is the rate constant; S is the initial surface area of the specimen (cm^2); N_{OH} is the initial number of moles of hydroxyl ion; and V is the initial volume of the solution (liters). The rate constants obtained with SAP were about 4×10^{-4} liter min^{-1} cm^{-2}; these values, when compared with those obtained for pure aluminum (about 2.6×10^{-4}), show that the SAP cermet used in these experiments dissolved at about the same rate as pure aluminum.

Decladding of simulated SAP-clad UC fuel with both NaOH-$NaNO_3$ and NaOH solutions, followed by nitric acid dissolution of the residue, was studied briefly. In each experiment the UC/SAP weight ratio was about 8. The SAP cladding was readily dissolved in 4 hr in boiling 2 *M* NaOH–2 *M* $NaNO_3$, leaving UC (which is practically inert to this reagent) and some of the Al_2O_3 from the SAP as a residue. The uranium loss to the decladding solution was less than 0.07%. However, this approach has the disadvantage that, after the UC is dissolved in the nitric acid, up to 50% of the carbide carbon remains in solution as soluble organic compounds.[19] These could possibly have a deleterious effect in the subsequent solvent extraction step of the process. It is expected that decladding in NaOH solution, which

[17] J. H. Goode and J. R. Flanary, *Dissolution of Irradiated, Stainless-Steel-Clad ThO_2-UO_2 in Fluoride-Catalyzed Nitric Acid Solutions: Hot-Cell Studies on Pelletized, Arc-Fused, and Sol-Gel Derived Oxides*, ORNL-3725 (January 1965).

[18] R. G. Wymer and R. E. Blanco, *Ind. Eng. Chem.* 49, 59 (1957).

[19] L. M. Ferris and M. J. Bradley, *J. Am. Chem. Soc.* 87, 1710 (1965).

Table 1.3. Approximate Rates of Dissolution of SAP (6% Al_2O_3–94% Al) in Boiling Nitric Acid and Nitric Acid Containing Either HF Or $Hg(NO_3)_2$

Experiment	Concentration in Reagent (*M*)			Dissolution Time (hr)	Amount Dissolved (%)	Average Dissolution Rate (mg min^{-1} cm^{-2})
	HNO_3	HF	Hg			
1	8	0	0	4	18	0.2
2	10	0	0	6	25	
3	13	0.05	0	6	54	0.4
4	4	0	0.005	20	99	0.5
5	6	0	0.005	1	18	0.7
6	10	0	0.005	1	19	0.7
7	13	0	0.005	1	14	0.6
8	6	0	0.05	1	16	0.6
9	10	0	0.05	1	15	0.6
10	13	0	0.05	1	14	0.4

should provide for both dissolution of the SAP and hydrolysis of the UC even if it has been irradiated,[20] will circumvent this problem. Hydrolysis of the UC would be desirable since not only is the carbide carbon converted to gaseous hydrocarbons but the uranium in the carbide is converted to hydrous UO_2, which readily dissolves in nitric acid. Only preliminary experiments on the decladding of SAP-clad UC with NaOH solutions have been made. The method appears to work well except that the rate of reaction of UC with NaOH and sodium aluminate solutions is relatively low. Work on this method is continuing.

Shearing (followed by acid leaching) and direct dissolution in nitric acid were considered as processing methods for SAP-clad UC fuel. Both approaches could be made to work, but each process has disadvantages stemming from the relatively low rate of dissolution of SAP in nitric acid. SAP, in the absence of UC, dissolves in nitric acid at about 0.2 mg min^{-1} cm^{-2}. Mercuric nitrate, which catalyzes the dissolution of aluminum in nitric acid, was not effective as a catalyst for SAP even at a concentration of 0.05 *M*, ten times the concentration usually required (Table 1.3). The presence of HF at a concentration of 0.05 *M* did not significantly increase the rate of reaction. These results are in good agreement with those obtained by Italian workers.[21,22] Thus, in a shear-leach process, some, but not all, of the SAP cladding would be dissolved in nitric acid along with the UC. The residual cladding could be disposed of as a solid waste, but the dissolver solution would require analysis for aluminum before proceeding with feed adjustment and solvent extraction. On the other hand, complete dissolution of the SAP and the UC could be achieved, but only after quite long dissolving periods – 20 hr or more. Even if the fuel could be dissolved completely in a short time, the presence of all the aluminum from the cladding could be undesirable in a feed-adjustment step and from the waste-management viewpoint. After complete dissolution, uranium and aluminum would be present in solution in approximately equimolar concentrations.

Another method considered for the processing of SAP-clad UC fuel consists of shearing, pyrohydrol-

[20] M. J. Bradley *et al.*, *Nucl. Sci. Eng.* **21**, 159 (1965).

[21] G. Beone, *Comportamento del S.A.P. all'attacco di soluzioni di acido nitrico e nitrato mercurio*, RT/CHI(63)34 (October 1963).

[22] G. Beone, *Energia Nucl.* (Milan) **12**(5), 273 (1965).

ysis, and dissolution of the residue. This approach has the advantage that the carbide carbon is removed as CO and CO_2 during pyrohydrolysis and the uranium is converted to a reactive UO_2. This technique worked very well in the laboratory but could present problems on an engineering scale in that the temperatures required for rapid pyrohydrolysis of UC (750 to 780°C) are well above the melting point of SAP. In laboratory tests of this approach, SAP and UC (at a UC/SAP weight ratio of about 8) were allowed to react with steam for 4 hr at about 750°C. The resulting residue dissolved completely in about 5 hr in boiling 5 *M* HNO_3. Since SAP dissolved only slowly in nitric acid, it was tentatively concluded that, during pyrohydrolysis, the SAP had been converted to a low-temperature form of Al_2O_3, soluble in nitric acid. However, other experiments showed that this was not so. Heating SAP and type 2S aluminum above the melting point (about 690°C) in either steam or pure argon did not result in detectable chemical attack; however, the samples so treated dissolved rapidly in boiling 8 *M* HNO_3; heating above the melting point was essential to rapid dissolution in nitric acid. Samples that were heat-treated at temperatures up to 650°C dissolved at about the same low rates as those that were not heat-treated.

Other potential methods for processing SAP-clad UC and possible processes for other HWOCR fuels will be evaluated during the coming year.

1.4 STUDIES OF THE ADSORPTION OF PROTACTINIUM

Previous hot-cell experiments showed the feasibility of recovering nearly isotopically pure ^{233}U by adsorbing ^{233}Pa, its 27.4-day precursor, on powdered unfired Vycor glass from nitric acid solutions of highly irradiated short-cooled ThO_2-UO_2.[23] Since the protactinium accounts for a large fraction of the beta and gamma radioactivity associated with short-decayed thorium, the removal of this isotope greatly decreases the radioactivity of the aqueous thorium-uranium solution.

During the past year, the protactinium adsorption studies were completed, culminating in hot-cell experiments that demonstrated the practicability of the process for recovering protactinium. These experiments showed the maximum practical capacity of Vycor glass, silica gel, and zirconium phosphate under process conditions, as well as concentration factors obtained with oxalic acid elution and the effects of mesh size of the Vycor, flow rate, and repeated cycles of loading-washing-eluting.[24] Also, laboratory studies were made to measure the distribution coefficient of ^{233}Pa between unfired Vycor and hydrochloric acid solutions.

In the hot-cell work, the recovery of ^{233}Pa by adsorption on unfired Vycor, silica gel, or zirconium phosphate was demonstrated by using sol-gel thoria fuel specimens that had been irradiated to about 5000 Mwd per metric ton of thorium in an average neutron flux of 2.6×10^{14}. After a 27-day decay period, the thoria was dissolved by refluxing for 20 to 24 hr in 13 *M* HNO_3–0.05 *M* HF–0.1 *M* Al. This produced a solution with the following composition: HNO_3, 11.4 *M*; HF, 0.05 *M*; Al, 0.1 *M*; Th, 126 mg/ml; U, 0.82 mg/ml; ^{233}Pa, 0.054 mg/ml; and gamma emitters equivalent to 1.4×10^{12} counts/min. About 97% of the protactinium was adsorbed by passing this solution through a column 0.9 cm in diameter and 17 cm long containing 7 g of 100- to 120-mesh unfired Vycor. At a flow rate of about 1 ml/min, the column was loaded to 3.1 mg of ^{233}Pa per gram of glass (Fig. 1.12). The column had to be cooled with water to prevent boiling. It was washed with 10 *M* HNO_3–0.1 *M* Al, which removed about 1.5% of the protactinium. On eluting with 0.5 *M* oxalic acid, about 96% of the protactinium was recovered at an average concentration of 1.46 mg/ml – about 25 times the concentration of the protactinium in the feed. The most concentrated eluate fraction contained 2.86 mg/ml of ^{233}Pa and had to be diluted to prevent boiling. The protactinium product was decontaminated from zirconium-niobium, total rare earths, thorium, and uranium by factors of 5.5, 4.8×10^3, $\geq 1 \times 10^4$, and $\geq 5.7 \times 10^2$ respectively. The ^{233}U which would be obtained from the decay of the protactinium in this solution would contain only 0.1 to 0.5 ppm of ^{232}U.

A single adsorption-elution cycle appeared to have little or no effect on the unfired Vycor glass,

[23] J. G. Moore *et al.*, *Adsorption of Protactinium on Unfired Vycor: Initial Hot-Cell Experiments*, ORNL-3773 (April 1965).

[24] J. H. Goode and J. G. Moore, *Adsorption of Protactinium: Final Hot-Cell Experiments*, ORNL-3950 (in preparation).

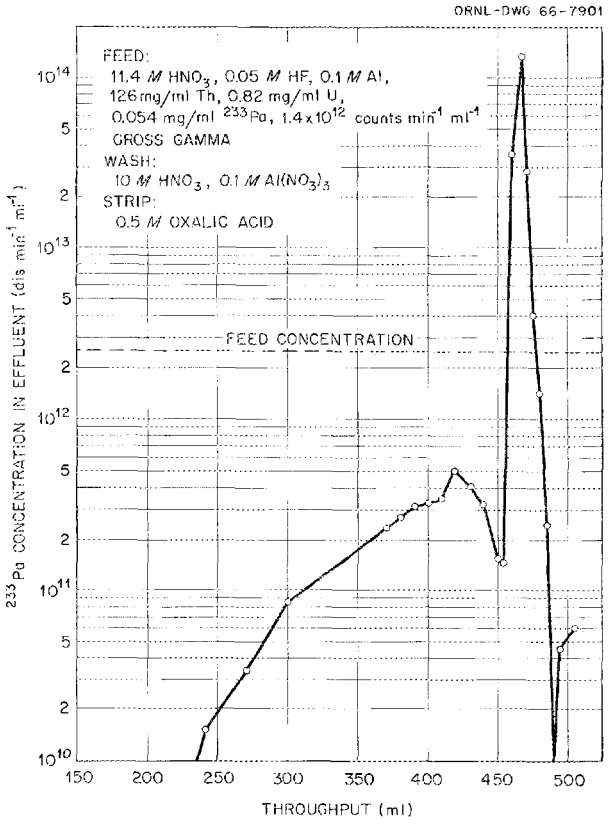

Fig. 1.12. Adsorption of Protactinium on 100- to 120-Mesh Unfired Vycor.

and a second experiment with the same column demonstrated practically the same adsorption and eluting characteristics. Increasing the particle size from 100–120 to 60–80 mesh decreased the column loading from 2.5 mg/g to about 2 mg/g. Increasing the flow rate from 1 ml/min to 2 ml/min decreased the loading by 10 to 15%.

Similar hot-cell tests were performed with 60- to 80-mesh silica gel and zirconium phosphate (Bio-Rad ZP-1). The columns were 0.6 cm in diameter, 11 cm long, and contained about 4 g of the adsorbent. At a flow rate of 0.5 ml/min and 99% protactinium adsorption, the silica gel adsorbed about 2 mg/g and the zirconium phosphate adsorbed 1.3 mg/g. For comparison, under the same conditions 60- to 80-mesh unfired Vycor adsorbed about 2.5 mg of ^{233}Pa per gram of glass.

The zirconium phosphate was not amenable to oxalic acid elution, so the protactinium was allowed to decay on the column and the ^{233}U was removed with nitric acid. The nitric acid elution severely damaged the zirconium phosphate, and it was not reusable. The protactinium on the silica gel, however, was easily eluted with oxalic acid. The elution characteristics were very similar to those of unfired Vycor, although the product was not quite so free from contaminants. The protactinium product from the silica gel had been decontaminated from zirconium-niobium total rare-earth beta emitters, thorium, and uranium by factors of about 1.5, 8.6×10^2, $\geqq 1.0 \times 10^4$, and >100 respectively.

The distribution coefficient of ^{233}Pa between 60- to 80-mesh unfired Vycor glass and 1.04 to 10.4 *M* HCl solutions containing about 3 g/liter of Th was measured by the Martin technique. The coefficient increased from 260 in 1 *M* HCl to a maximum value of 410 in about 4 *M* HCl, then decreased to 120 in 10 *M* HCl. The amount of unadsorbable protactinium ranged from 7.6% in the dilute acid to a minimum value of 2.1% in 6 to 8 *M* HCl. For comparison, the distribution coefficients for 1 to 10 *M* HNO_3 ranged from about 700 to 4000, respectively, with 6% to less than 2% of the protactinium unadsorbable.

1.5 CLOSE-COUPLED PROCESS DEVELOPMENT

During the growth of the nuclear power economy, when the recycling of highly irradiated ^{239}Pu and ^{233}U fuels is expected to become a common practice, the isotopic contaminants of these fuels will increase toward high equilibrium concentrations. The gamma or neutron radiations associated with these isotopic contaminants, or their daughters, will then necessitate shielded and remotely operated facilities for fuel fabrication. When such facilities become established, the current needs and practices of striving for complete fission product decontamination of the ^{239}Pu and ^{233}U products can be expected to diminish. These considerations are particularly important if the processing and fabrication plants are close-coupled and perhaps located at the reactor station. Such close-coupled systems are presently of interest to power producers desiring totally integrated and independent facilities and to the developers of the extremely large power stations that are expected to achieve very low unit power costs.

It is the purpose of this subprogram to develop and demonstrate low-cost fuel recovery processing methods that can be coupled to the sol-gel process for fuel reconstitution and refabrication. These methods will provide the necessary separation (a decontamination factor of about 1000) of the fuel from neutron poisons, chemical impurities, and fission products that might interfere with the fuel reconstitution process. Although incompletely decontaminated, the recovered fuel and the fuel assembly may then be prepared or manufactured in shielded and remotely operable facilities.

Chemical Development Studies for Close-Coupled Plants

Investigation of simple, low-cost methods that might be suitable for low-decontamination processing was completed. Separation methods which were investigated included precipitation, selective crystallization, ion exchange, electrodialysis, and solvent extraction. Except for solvent extraction, anion exchange was the only method that could be developed into a workable process. However, resin capacity was low and decontamination was poor, creating a recycle problem and requiring several cycles of anion exchange. We concluded that solvent extraction was the only operation that provided adequate product recovery and sufficient separation of the uranium and thorium from the contaminants to warrant further study.

Laboratory experiments showed that solvent extraction operations in a differential contactor resulted in satisfactory decontamination (Fig. 1.13). This contactor was simple and operated satisfactorily in laboratory-scale experiments in spite of the formation of a second organic phase. With 30% TBP (tributyl phosphate) in *n*-dodecane (NDD) as the solvent, more than 99.9% of the uranium and 48% of the thorium extracted in 3.3 vol of solvent (Fig. 1.14). The separation of uranium from gross gamma radioactivity was adequate, resulting in a decontamination factor (DF) of 1400. Continuing the extraction until 9.8 vol of solvent was used, extraction of 99.2% of the thorium and a DF of 68 were demonstrated. By extracting first with 3% TBP, then with 30% TBP, a more complete separation of uranium from thorium and fission products may be achieved, but operating with two solvent compositions is inconvenient.

During leaching of Zircaloy-2-clad ThO_2-UO_2 fuels with 13 *M* HNO_3–0.04 *M* HF, a small amount of cladding is dissolved. About 40% of this zirconium and 25% of the fluoride were extracted in the differential contactor. This was due to the high salting strength and the absence of a scrubbing step to remove these contaminants.

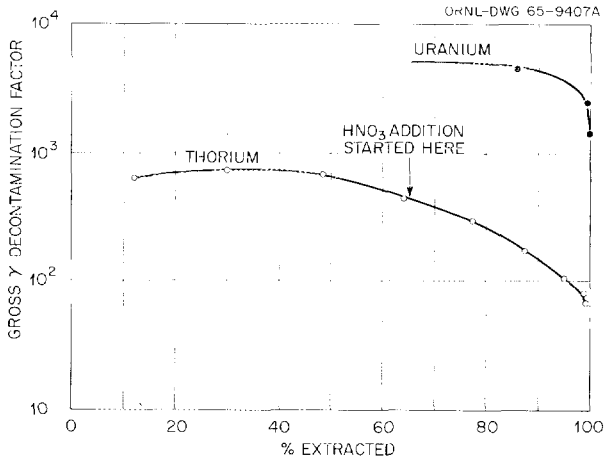

Fig. 1.13. Decontamination of Uranium and Thorium by Differential Extraction.

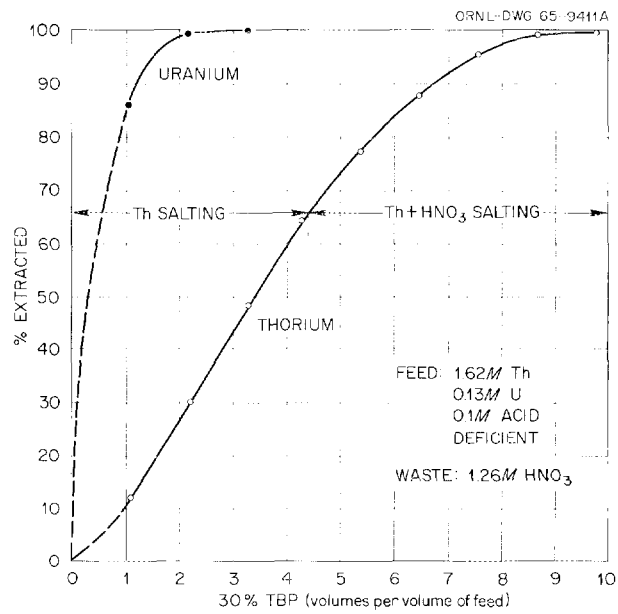

Fig. 1.14. Differential Extraction of Uranium and Thorium.

The fluoride, in particular, would be detrimental in the reconstitution or refabrication of the fuel product.

The second organic phase, sometimes called the third phase (Fig. 1.15), which is encountered in thorium extraction is due to the limited solubility of the thorium-TBP complex in aliphatic diluents. The use of any of the following three solvents, 80% TBP in NDD (which approximates the TBP content of the heavy third phase), 30% tri-*n*-pentyl phosphate (TNPP) in NDD, or 30% triisopentyl phosphate (TIPP) in NDD, decreases the difficulties with the second organic phase but presents other problems. When 80% TBP-NDD was used, the density difference ($\rho_{aq} - \rho_{org}$) was as small as 0.01 g/ml under some equilibrium conditions. The density of the scrub solution entering a countercurrent column would be less than the density of the pregnant organic leaving the column; consequently, operation of the system would be difficult. With either of the tripentylphosphates there is less probability of encountering a second organic phase than with TBP, but the distribution coefficient for thorium is less. The second organic phase is formed when 30% TBP or 30% TNPP is about 0.26 *M* in $Th(NO_3)_4$ but does not occur with 30% TIPP until it is 0.31 *M* in $Th(NO_3)_4$. The corresponding equilibrium aqueous phase in the 30% TIPP equilibration was more than 2 *M* in $Th(NO_3)_4$ (Fig. 1.15). Therefore, there is little possibility of encountering a second organic phase when TIPP is used as the solvent in a thorium extraction process. The effectiveness of these TBP substitutes in product decontamination from fission products has not been determined.

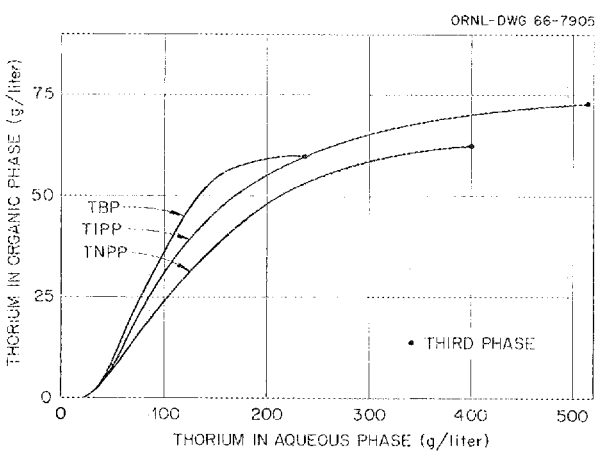

Fig. 1.15. Extraction of Unsalted $Th(NO_3)_4$ by 30% Tri-*n*-butyl Phosphate, 30% Tri-*n*-pentyl Phosphate, or 30% Triisopentyl Phosphate in *n*-Dodecane.

Accurate density equations were derived for aqueous and organic (TBP and NDD) solutions of thorium and nitric acid. The density of aqueous thorium nitrate–nitric acid solutions is given by the equation

$$\rho_{20^\circ C} = 0.382\ (M\ \mathrm{Th}) + 0.0289\ (M\ \mathrm{H}^+) + 1.0061\ ,$$

and the density of thorium–nitric acid solutions in TBP-NDD is given by:

$$\rho_{20^\circ C} = 0.373\ (M\ \mathrm{Th}) + 0.0234\ (M\ \mathrm{H}^+) + 0.9788\ (\mathrm{vol}\ \%\ \mathrm{TBP}) + 0.7479\ (\mathrm{vol}\ \%\ \mathrm{NDD})\ ,$$

where 0.9788 and 0.7479 are the densities of pure TBP and NDD respectively. When the thorium concentration was less than 1 *M* and the acid less than 4 *M*, these equations gave results that were with ±0.005 g/ml of the measured densities. This is about the limit of analytical accuracy.

Equipment Development for Close-Coupled Processes

A small pulsed column was tested as a batch solvent-extraction contactor to see whether it was more efficient than a stirred-tank batch differential contactor. Supposedly, it might have the desirable high throughput and multistage characteristics of a continuous pulsed column and thus be superior to the single-stage stirred-tank contactor. In the tests, a standard Thorex feed was extracted with acidified 30% TBP, which was injected at a pulse frequency of 30 cpm and an amplitude sufficient to provide organic flow rates of 52 to 207 gal hr^{-1} ft^{-2}. The tests were unsuccessful, even at the lowest flow rate, in that the organic holdup in the cartridge section approached 80% (even with supplemental pulsing). Also, the dense second organic phase formed an organic-continuous emulsion in the disengaging section, resulting in considerable aqueous entrainment in the extract. Good extraction performance was realized in the cartridge, as evidenced by little backmixing and a steep concentration gradient in the cartridge section, but this was largely negated by the excessive organic holdup and the formation of emulsions.

Also, a portion of the column changed from the aqueous-continuous to the organic-continuous mode during each run. We conclude that the problems of operating a large-scale batch-extraction system, either with a stirred-tank contactor or a pulsed-column contactor, are such that batch extraction should not be used for the close-coupled plant. This conclusion is reinforced by the fact of the undesirable extraction of zirconium and fluoride in batch extraction tests; and qualitative results of an engineering study indicate that the batch-extraction processing plant will cost about the same as the continuous-extraction plant and will be much more difficult to operate, even if the problem of the third phase were to be solved.

As part of the engineering development of batch extraction, a vortexing batch differential solvent-extraction contactor was invented and demonstrated. This contactor substantially reduced the required settler volume and hence the radiation exposure of the organic extractant. It is recommended for any radioactive process for which batch differential solvent extraction is feasible.

Studies of Conceptual Close-Coupled Plants

We have prepared a conceptual engineering design and preliminary economic evaluation of a small close-coupled plant for processing 165 kg/day of Zircaloy-clad, vibratorily packed sol-gel $(U\text{-}Th)O_2$ fuel irradiated to 20,000 Mwd/ton or more. This particular capacity and fuel type (that is, metal-clad oxide) were chosen to permit comparison of the close-coupled plant with a 165-kg/day on-site plant[25] for processing low-enrichment uranium fuel but designed to achieve high decontamination of the products and to permit conventional direct fabrication.

The study was based on essentially the same ground rules and cost assumptions that were used for the small-plant study. At first, we assumed that the processing plant used batch differential solvent extraction; but when this proved impractical for the technical reasons discussed previously, the study was repeated in order to estimate costs for a single-extraction-cycle continuous extraction system. The difference in cost between the batch and the continuous processes was insignificant in view of the probable accuracy of the estimates. The close-coupled plant was assumed to be fully integrated into a 1000-Mw (electrical) reactor station and included (1) underwater fuel-element storage and dismantling; (2) a remote maintenance shear-leach head-end treatment, with feed adjustment, acid recovery, high-level off-gas treatment, and high- and low-level waste evaporation equipment in the same area; (3) solvent extraction with 30% TBP followed by sol preparation by extracting the nitrate from the blended uranium and thorium nitrate product solutions with a long-chain amine; (4) gel formation, firing, and sizing; and (5) fuel fabrication in a remotely operated facility that is similar in design to TURF.

Capital costs for the processing plant were estimated from preliminary conceptual equipment and building layouts; the operating costs were derived by adjusting published data on the Nuclear Fuel Services plant to an integrated facility of relatively small size and adding perpetual-care waste-storage charges derived from computer calculations.

Capital costs for the fabrication plant were estimated by computer, and operating costs for the fabrication plant were estimated on roughly the same basis as for the chemical plant. Fully developed technology was assumed, and a frugal approach was used in estimating plant staffing and overhead.

The cost estimate is presented in Table 1.4. The results indicate a total processing and fabrication cost of about $156 per kilogram of (U + Th). This is a rather attractive cost in view of the small capacity of the plant and the present-day commercial fuel-processing costs for thorium fuels. The corresponding total cost for the small plant[26] was about $120 per kilogram of uranium, indicating that the more complex thorium processing system and remote fabrication plant cost about 30% more than similar operations with low-enriched uranium.

[25] *Chem. Technol. Div. Ann. Progr. Rept. May 31, 1965*, ORNL-3830, p. 66.

[26] W. E. Unger *et al.*, *On-Site Fuel Processing and Recycle Plant — Design Study*, ORNL-3959 (in press).

Table 1.4. Capital and Operating Costs for a Small Close-Coupled Processing Plant

Capital Cost	
Processing building and equipment	$ 7,430,000
Fabrication building and equipment	5,300,000
Startup cost, processing plant[a]	1,420,000
Startup cost, fabrication plant[a]	1,448,000
Total capital investment	$15,598,000
Annual Operating Cost[b]	
Capital amortization at $22\frac{1}{2}$%/year	$ 3,510,000
Processing plant (direct costs)	1,420,000
Fabrication plant (direct costs)	2,556,000
Solid waste	75,000
High-level waste storage	282,000
Medium-level waste storage	153,000
Total annual operating cost	$ 7,996,000
	$156 per kilogram of (U + Th)

[a]One year's operating cost, excluding waste-storage charges and fuel-element hardware.
[b]Exclusive of inventory charges and cost for (U + Th) makeup.

1.6 HYDROLYSIS OF URANIUM, THORIUM, AND FISSION PRODUCT CARBIDES

The carbides and nitrides of uranium, thorium, and plutonium have definite potential as reactor fuels. Pyrolytic-carbon-coated ThC_2-UC_2 particles in a graphite matrix are already being used as the fuel for the High-Temperature Gas-Cooled Reactor (HTGR, Peach Bottom, Pennsylvania). Uranium monocarbide is a leading candidate for the fuel in a heavy-water-moderated, organic-cooled reactor (HWOCR), and UC-PuC and UN-PuN are being considered as fuels for sodium-cooled fast breeder reactors. The chemistry of these and other carbides and nitrides is being studied to provide data basic to the development of processing methods for fuels of this type. Studies of the chemistry of uranium and thorium carbides that are directly pertinent to the processing of the specific types of fuel mentioned above are summarized in Sects. 1.1 and 1.3. In addition, the fundamental chemistry of uranium and thorium carbides in both aqueous and gaseous systems is being investigated in a separate but closely related program. Work done under this latter program is summarized in Sect. 22.

2. Fluoride-Volatility Processing

This effort is part of an intersite program to develop fluoride-volatility processes as alternatives to aqueous methods for recovering valuable components present in spent UO_2 fuel from power reactors. The AEC's goal is to have the technology for low-enrichment fuel processing developed through "cold" engineering, "cold" semiworks, and "hot" pilot-plant programs so that design of a full-scale plant can begin by July 1, 1969. Our main contribution will be the installation and operation of a pilot plant in several of the shielded cells in Building 3019. Process details and priorities, relationship to work at other sites, and possible advantages of volatility methods were presented in last year's annual report.

Laboratory- and small-engineering-scale studies were made in support of the fluidized-bed volatility process, particularly the $HF-O_2$ method for stainless-steel-clad fuels. Work is now under way on studies of the HCl process for Zircaloy-clad fuels.

Design and installation of the Fluidized-Bed Volatility Pilot Plant (FBVPP) is divided into phase I (decladding, oxidation, and fluorination of the UO_2-PuO_2, and cold trapping of the volatile hexafluorides) and phase II (product separation and purification). For phase I, design of process vessels is nearly complete, their fabrication is under way, and cell preparation has begun. Design of mechanical equipment, instrumentation, and electrical gear is proceeding. About 26% of the labor man-days estimated as being required for phase I was expended.

Process design for phase II has begun.

2.1 FLUIDIZED-BED VOLATILITY PROCESS DEVELOPMENT: LABORATORY STUDIES FOR STAINLESS-STEEL- AND ZIRCALOY-CLAD UO_2 FUELS

This study is intended to complement chemical process development work on a fluidized-bed volatility process for recovering uranium and plutonium from low-enrichment UO_2 power reactor fuels that are clad in either Zircaloy or stainless steel. Other work is being done at Argonne National Laboratory, primarily on the HCl process for Zircaloy-clad fuels, and at Brookhaven National Laboratory, where the emphasis is on operational problems related to the $HF-O_2$ process at an engineering scale. Our main task at Oak Ridge National Laboratory will be to provide a pilot-plant demonstration of the fluidized-bed process with highly irradiated fuel, and these studies are specifically intended to support this effort.

Bench-scale tests of the fluidized-bed volatility process, to be used for low-enrichment UO_2 fuels that are clad in stainless steel or Zircaloy-2, were made with a $\frac{1}{2}$-in.-OD mini-bed reactor that was not equipped with off-gas filters and with a 1-in.-OD fluidized-bed reactor equipped with blowback filters.

With the smaller reactor, emphasis was on the chemical behavior of plutonium during the decladding cycle and in subsequent volatilization as PuF_6 with fluorine. Studies of plutonium retention in the bed included the effect of stainless steel decladding products, the use of $HF-O_2$ mixtures, pyrohydrolysis, the presence of UO_2, and variations in the temperature of fluorination. We concluded that both diffusion into the alumina surface and fluoride-oxide interaction contribute to the difficulty of achieving complete plutonium volatilization.

In the 1-in.-OD reactor, studies were made of the $HF-O_2$ process for decladding stainless-steel-clad UO_2 fuel. The principal conclusion was that the fuel should not occupy more than 10% of the reactor cross-sectional area to prevent formation of lumps of U_3O_8. In studies of the bed produced in the $HF-O_2$ process, a fluorination program was developed to give maximum pulverization of the stainless steel oxide in conversion to fluoride.

Other work with the 1-in.-OD reactor demonstrated the feasibility of achieving high uranium recovery when using stainless steel fluorides or ZrF_4 (in place of alumina) as the fluidized-bed material.

Work with the ½-in.-OD mini-bed reactor has been discontinued. A second 1-in.-OD reactor, installed in a glove box for plutonium tests, will be used instead. It will test flowsheet proposals with plutonium-bearing fuel after uranium tests have been conducted in the other 1-in. reactor. Emphasis is now being placed on studies of the use of alumina and all-fluoride beds, the recovery of uranium with BrF_3 or BrF_5, and other development work required for the engineering design and operation of the Fluidized-Bed Volatility Pilot Plant (FBVPP).

Description of Fluidized-Bed Volatility Processes

In fluidized-bed volatility processes, the chemical steps for decladding and oxidation (pulverization) of the fuel are performed in a fluidized bed of alumina. The fluidized bed serves as a heat-transfer medium to distribute the heat of reaction.

Zircaloy-clad fuel can be reacted with gaseous HCl at about 400°C to yield volatile $ZrCl_4$, or it can be oxidized with mixtures of HF and oxygen at 550 to 600°C, to yield ZrO_2. The $ZrCl_4$ formed during decladding with HCl can subsequently be converted to ZrO_2 by hydrolysis with steam in a separate fluidized bed. Or, in the upper portion of the primary fluidized bed, it can be reacted with gaseous HF to form nonvolatile ZrF_4. The UO_2 fuel is pulverized by reacting with oxygen.

Stainless-steel-clad fuel can be treated with mixtures of HF and oxygen at 550 to 600°C to convert the cladding to oxides. The UO_2 fuel reacts with the oxygen and HF, causing pulverization and conversion to U_3O_8, UO_2F_2, and UF_4.

According to one proposed flowsheet, the oxides and fluorides of the uranium and plutonium are converted to the volatile hexafluorides by reaction with fluorine in the same bed. The UF_6 and PuF_6 are then collected in a cold trap and, later, separated by distillation or thermal decomposition, or both. An alternative flowsheet calls for conversion of the uranium to UF_6 by contacting with BrF_5, thus separating it from the plutonium (not volatilized by BrF_5). Subsequently, a stream of fluorine converts the nonvolatile fluorides of plutonium to PuF_6.

1-in.-OD Fluidized-Bed Unit

A 1-in.-OD fluidized-bed reactor was designed and used in many tests of uranium processes. A similar unit, which will be used for test runs of simulated plutonium processes, is shown in Fig. 2.1. It consists of a machined 30°-cone bottom welded to a 5½-in.-long, 1-in.-OD nickel tube. This tube is connected to a 10-in.-long, 2-in.-OD disengaging section by a tapered expansion section. Mounted in the disengaging section are two blowback filters, each consisting of a 1-in.-diam sintered nickel disk. The mean pore size is 20 μ. On an alternating cycle, each filter is blown back every 7 sec with a pulse of 10-psig nitrogen. The 1-in. fluidized-bed section is heated to the reaction temperature in a furnace, and the disengaging section and filters are heated to about 170°C by a coil of Nichrome wire. About 40 g of bed medium, 13 g of UO_2, and 4 g of cladding are used in a standard experiment. A typical stainless-steel-clad fuel unit, shown in Fig. 2.2, consists of a 6.5-g plate of UO_2 wrapped in a 2-g sheet of 5-mil-thick type 302 stainless steel.

Processing of Stainless-Steel-Clad UO_2 in Fluidized Beds

Lumps of U_3O_8 May Form During Decladding with HF-O_2 Mixtures. – The decladding treatment for stainless-steel-clad UO_2 consists of a 30-min treatment with 20% HF in oxygen followed by 1 hr with 40% HF in oxygen, both at 600°C. Studies in the 1-in.-OD unit showed that, if the fuel is prevented from expanding during the decladding, unpulverizable lumps of U_3O_8 are formed. Some UO_2F_2 and UF_4 are, of course, formed. If a large amount of lumps is present, bed fusion and loss of fluidization can occur during fluorination. The fraction of the fuel in lumps greater than 20 mesh ranges from none when the fuel initially occupies about 7% of the cross-sectional area to 100% when the fuel occupies about 22% of this area. Since small amounts of uranium oxide lumps do not interfere with fluorination, in most of the experiments the fuel occupied about 10% of the reactor cross-sectional area. When 10% of the cross-sectional area is occupied by fuel, the alumina-to-fuel weight ratio is about 2:1.

Fluorination Procedure Must Prevent Sintering and Promote Pulverization of "Stainless Steel Oxide." – During the HF-O_2 treatment to remove

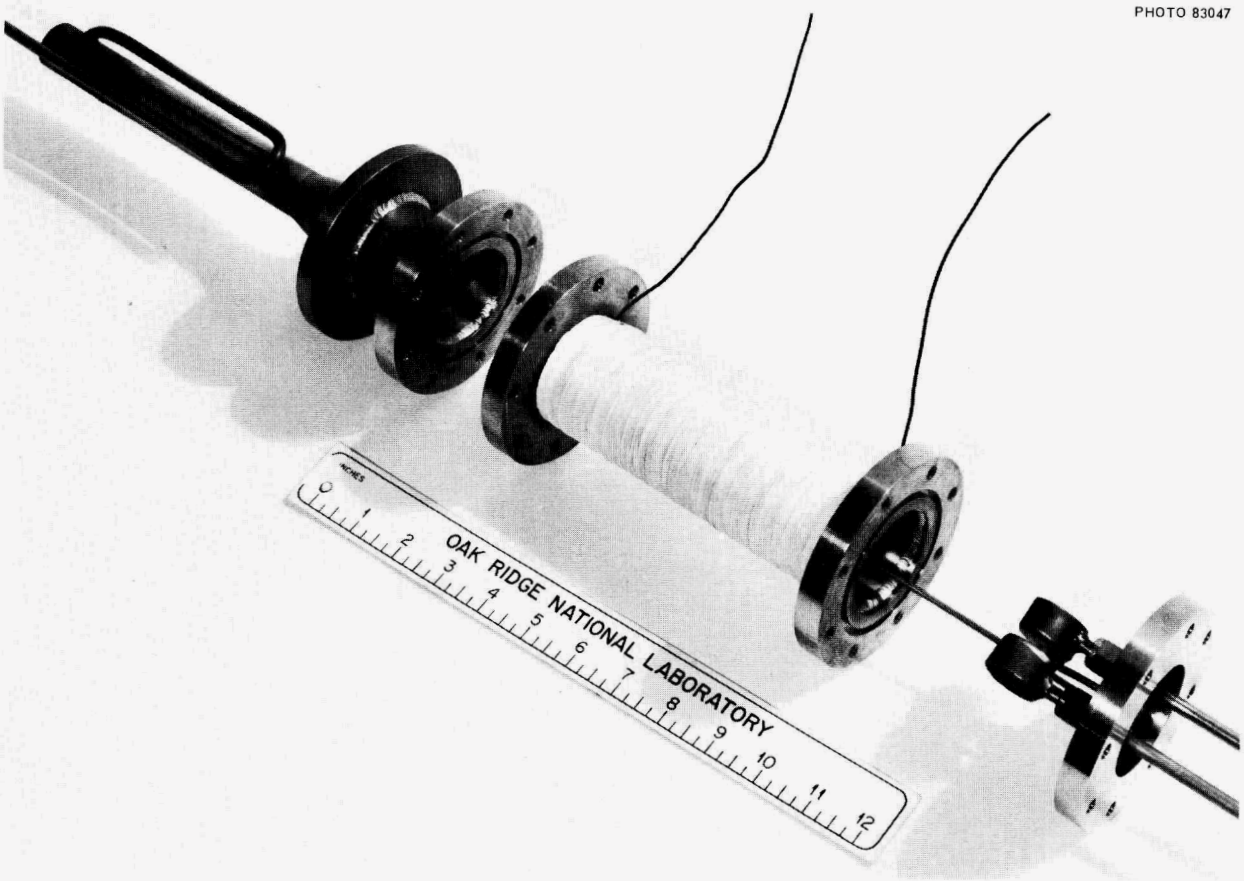

Fig. 2.1. View of the 1-in.-OD Fluidized-Bed Reactor, Including Disengaging Section and Blowback Filters.

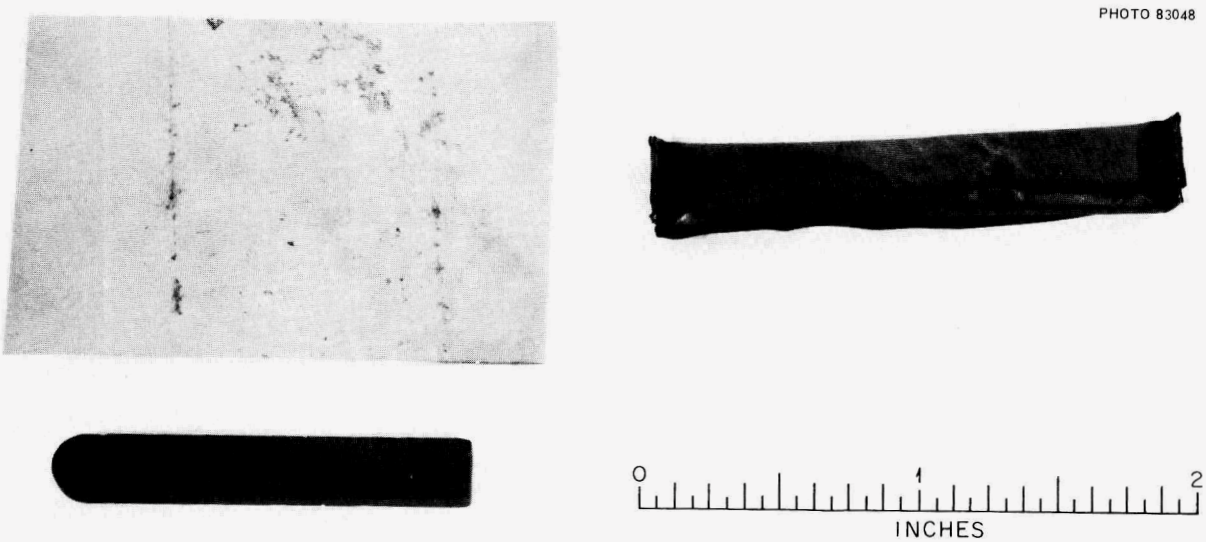

Fig. 2.2. Stainless Steel Fuel Specimen with UO_2 Plate and Sheet of Type 302 Stainless Steel.

stainless steel cladding, the cladding is converted to oxides but is not pulverized. These pieces of oxide must be pulverized during fluorination. An additional restriction on the fluorination procedure is that it must not cause sintering of the bed. Tests in the 1-in.-OD bed showed that sintering invariably occurs when the initial fluorination is carried out at 600°C or greater, or when a high initial concentration of fluorine is used at a low temperature – 450 to 500°C. Consequently, a low concentration of fluorine at a relatively low temperature must be used initially. A procedure that results in excellent uranium removal with no sintering and good pulverization of the stainless steel oxide consists of contact for 15 min each with 10, 20, 40, and 80 vol % fluorine, all at 450 to 500°C. The temperature is then raised to 550°C, and fluorination with 80 vol % fluorine is continued for 3 hr. With this method, about 99.9% of the uranium is removed from the alumina bed; a very small residue (0.03% of bed weight) remains.

Behavior of Chromium During Fluorination. – The chromium contained in the stainless steel cladding remains in the bed during treatment with the HF-O_2 mixture, but it is volatilized in an undetermined form during fluorination. Unfortunately, at least part of the chromium compound formed has only moderate volatility at 100°C, the temperature of the off-gas lines, and most of it is initially deposited in the first section of the off-gas system. Later, chromium-poor gas will transfer it to the cold traps, where the chromium may hold up plutonium (see Sect. 2.8).

Large Amounts of Fluoride in the Alumina Bed Cause Little Difficulty. – Although initially the fluidized bed is pure alumina, its use with stainless-steel-clad fuel results in the accumulation of solid fluorides, principally iron and nickel, since most of the chromium is volatilized during fluorination. Because reuse of the bed for many decladding cycles is an economic necessity, the effect of large amounts of stainless steel fluorides on the properties of the bed must be known. A series of studies was made in which five decladding and fluorination cycles led to a final iron-plus-nickel fluoride concentration in the alumina bed of nearly 50%. In another experiment, a complete decladding and fluorination cycle was performed in a bed containing only stainless steel fluoride. In these two studies, no serious difficulty was encountered. The decladding rate was more rapid than usual, probably because solid fluorides promoted the oxidation of stainless steel. Uranium removal was about 99.9% complete; and after 4 hr of fluorination, 0.056% of the original uranium remained on the pure stainless steel fluoride bed. These results indicate that, although a modified decladding program may be necessary in the presence of solid fluorides, a fluidized bed should be reusable many times. Further, there is a possibility of operating the reactor with only stainless steel fluorides as the fluidized medium.

Retention of Plutonium by the Fluidized Bed Presents a Problem. – Studies of the proposed fluidized-bed process for stainless-steel-clad UO_2 power-reactor fuel containing plutonium were continued with the ½-in.-OD mini-bed reactor unit. The results indicated that plutonium retention is influenced appreciably by diffusion effects and by fluoride-oxide interactions within the alumina bed.

The effects of diffusion of PuO_2 into alumina were studied in a series of tests in which about 0.1-g quantities of the material were fluidized with helium at 650°C for 0.1, 2.5, 5.0, and 10.0 hr. After subsequent 1-hr fluorinations at 450°C, the plutonium retentions reached a limiting value of about 2% in about 2.5 hr. The respective values were 0.8, 2.4, 1.7, and 2.1%.

The effect of fluoride-oxide interactions on plutonium retention due, in part, to the presence of uranium compounds was studied on a relative basis by varying conditions in the decladding cycle while standardizing subsequent fluorinations at 450°C for 1-hr periods. The tests were made with 0.1 g of PuO_2, 0.4 g of UO_2, and 0.3 g of stainless steel (type 304) in 5 g of fused alumina (Norton RR 120 mesh). In one test, we showed that plutonium retention was not appreciably affected by the stainless steel decladding products that form during the oxidation cycle. When stainless steel was omitted, the final plutonium retention was 21.9%, compared with a corresponding retention of 21.0% when stainless steel was present. In another test, with stainless steel present, the HF-O_2 ratio was changed from 40:60 vol % to 20:80 vol %. This, likewise, had no significant effect on retention. The final value was 17.6%. The complete absence of HF in the decladding cycle, however, had a marked influence on retention. When 100% O_2 was substituted for a 40:60 vol % mixture of HF-O_2, a subsequent 1-hr fluorination at 450°C reduced the retention to 5.1%. A comparable decrease was achieved by pretreatment

of the alumina with fluorine at 450°C for 1 hr prior to decladding with a 40:60 vol % mixture of $HF-O_2$. The plutonium retention here was 7.5%. More extensive pretreatment of the alumina with fluorine did not contribute to any further decrease.

Testing of other prospective bed materials as substitutes for alumina has included, to date, crystalline AlF_3 and sol-gel thoria. The use of AlF_3 resulted in plutonium retention very similar to that obtained when alumina preconditioned with fluorine was used. After the decladding cycle and a 1-hr fluorination at 450°C, it amounted to 8.7%. In two previous tests where preconditioned alumina was used, corresponding retentions were 7.5 and 9.6%. No improvement was achieved in the use of sol-gel thoria as bed material. A similar test resulted in plutonium retention of 7.5%.

Some decrease in retention was achieved by pyrohydrolyzing alumina that contained plutonium remaining after a 1-hr fluorination. The residual plutonium in a bed was reduced from 6.7 to 2.5% by hydrolysis with 73% steam in helium at 500°C for 2 hr followed by a second 1-hr fluorination. By comparison, a similar test in which the pyrohydrolysis step was omitted demonstrated a retention of 5.9% after 2 hr of fluorination.

Use of a Fluidized Bed of ZrF_4

The successful decladding and fluorination in the stainless steel fluoride bed led to investigation of the use of a ZrF_4 bed (commercial ZrF_4, less than 20 mesh). It was fluidized for 1 hr with a gas velocity of ½ fps to elutriate the fine particles. Thirty-five percent of the resulting material was still finer than 325 mesh. Pretreatment of this material with HF or fluorine to convert oxides to fluorides was necessary to prevent excessive powdering of the bed during processing of fuel. Plates of UO_2 were successfully oxidized to U_3O_8 and fluorinated in this bed with no sintering. About 99.97% of the uranium was removed during a standard 4-hr fluorination, with a residual uranium concentration of 0.0074%, based on the initial bed weight. This is about one-fourth the amount found after similar treatment in an alumina bed. Only a very slight powdering of the bed was found during oxidation and fluorination. Another advantage of the ZrF_4 bed is that it resists sintering. Cleanup fluorinations of a settled ZrF_4 bed at 450 and 550°C caused no sintering. Perhaps the final cleanup of plutonium can be done with the bed settled, requiring a much smaller flow of fluorine.

Zircaloy can possibly be volatilized as $ZrCl_4$ and converted to ZrF_4 in a fluidized bed of ZrF_4 by the following scheme.[1] A two-zone fluidized bed would be used, with HCl reacting with the Zircaloy in the lower zone to form volatile $ZrCl_4$. In the upper zone, this $ZrCl_4$ would react with HF to form nonvolatile ZrF_4. Such a scheme eliminates the hydrolysis reactor for disposal of $ZrCl_4$, does not require transfer of $ZrCl_4$ through filters and lines, and eliminates the use of the relatively expensive alumina as the bed. Only a single main waste stream exists, and its volume is minimal, depending only on the weight of Zircaloy processed.

This particular method of treating Zircaloy-clad UO_2 is a possible alternative to processing in alumina followed by hydrolysis of the $ZrCl_4$. As such, it will be explored in small-scale process tests to examine whether the particle-size range is suitable for fluidized-bed operation, and to study the retention of plutonium in ZrF_4 formed in situ. If successful, the decladding of stainless-steel-clad fuel will be studied with beds consisting of ZrF_4 and mixtures of ZrF_4 and stainless steel fluorides.

2.2 FBVPD: SMALL-SCALE ENGINEERING STUDIES

A small-scale engineering test facility, located in a cell in Building 3503, contains two fluidized-bed reactors, one made of 2-in. sched 40 nickel pipe and the other of 4-in. sched 40 nickel pipe, and the necessary process equipment for decladding with HCl and $HF-O_2$, followed by oxidation and fluorination. Instrumentation and control of this facility duplicates that to be used in the pilot plant as closely as possible, and all operations except fuel-element charging and process steps involving plutonium or irradiated fuel will be the same as in the pilot plant. The purpose of the facility is to test instrumentation and control equipment and to develop operating procedures.

[1] *Argonne National Laboratory Chemical Engineering Division Summary Report, April, May, June, 1961,* ANL-6379, pp. 134–45.

Construction, installation, and calibration of the reactors and their auxiliaries were completed. Testing of the HF-O_2 flowsheet for stainless steel fuel was begun. The initial results were unsuccessful, mostly because of caking of the bed material. This effect was more noticeable during decladding than during fluorination.

Results of Decladding and Fluorinating Stainless-Steel-Clad UO_2

A series of tests was run on 1-ft-long segments of Consolidated Edison type fuel bundles such as those shown in Fig. 2.3. The fuel tubes were 0.3 in. OD $\times$ 0.010 in. wall thickness and spaced 0.45 in. center-to-center in a square array. The tubes and the outer cage structure were of type 304 stainless steel, and the tubes were filled with UO_2 pellets. This type of element is very difficult to process in a fluidized bed because of the narrow internal channels. We found that when the cross-sectional area of the rectangle surrounding the fuel tubes in an element segment exceeded 20% of the reactor cross section (i.e., more than four tubes in the 2-in.-ID reactor) the change in volume resulting from oxidation of the steel and the UO_2 pellets was sufficient to plug the reactor and stop the gas flow. Several tests were unsuccessful because of caking of the alumina (the bed material), particularly when more than 30% of the solids would pass through a 140-mesh screen. In one completely successful test, decladding and fluorination were finished in 3 and 3.6 hr respectively. The uranium recovery was 99.6%, and the uranium material balance was 104%. In both successful and unsuccessful tests, the pressure, temperature, and flow-indicating and -controlling equipment performed well, although the necessity of keeping the HF system hot to prevent condensation resulted in more frequent maintenance of the differential-pressure cells.

Incomplete decladding of the fuel was the commonly observed result in the unsuccessful tests. In some runs this was obviously because hard cakes of alumina prevented contact between the metal and the HF-O_2 gas stream, but in other runs such cakes were not found when the reactor was opened. We thought the incomplete reaction might have resulted because of the low temperature at the surface of the element (caused by irregularities in fluidization of the alumina bed). To test this hypothesis, a fuel element equipped with six thermocouples was heated in the 2-in.-ID reactor

PHOTO 83788

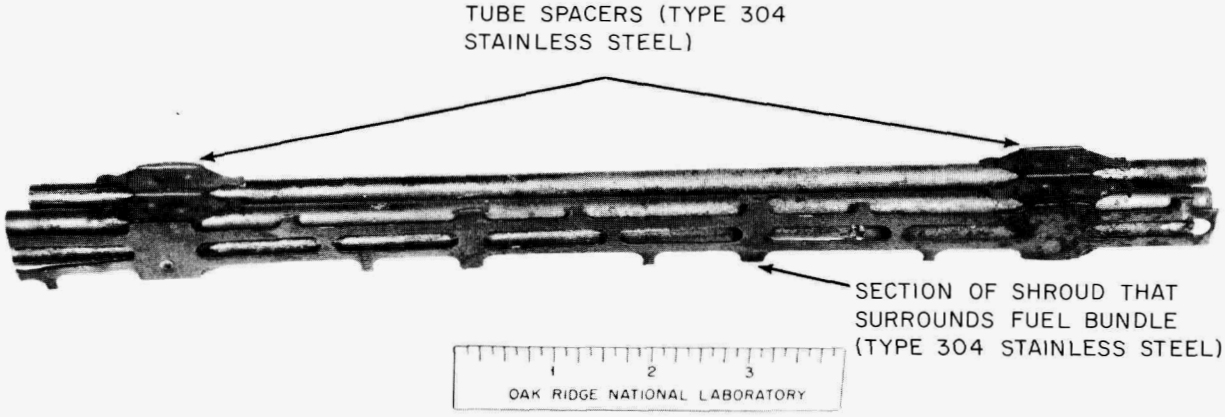

Fig. 2.3. Typical Four-Tube Segment of Fuel Element Used in Small-Scale Engineering Tests. Fuel element is of the type used in the Consolidated Edison Reactor. Rods are type 304 stainless steel tubes (0.3 in. in outside diameter; 10-mil wall thickness) filled with UO_2 pellets.

during five tests. In four of the tests, the particle size and type of alumina were varied, and in the other test no alumina was used. In all five tests, the fluidizing gas flow was constant at 1.0 fps, and the power input to the wall heater was constant. Results showed that the element temperature increased at almost the same rate in each test. Thus, we conclude (1) that low element temperature was not the explanation for incomplete decladding; and (2) that, under the conditions described, the fluidized bed was not an effective heat-transfer medium.

2.3 DESIGN OF THE FLUIDIZED-BED VOLATILITY PILOT PLANT FOR ZIRCALOY- AND STAINLESS-STEEL-CLAD UO_2 POWER-REACTOR FUELS

The Fluidized-Bed Volatility Pilot Plant (FBVPP) is being designed for installation in Building 3019. The processing of Zircaloy- and stainless-steel-clad UO_2 power reactor fuels will be studied in the facility at irradiation levels up to about 30,000 Mwd/ton with 140-day cooling.

The primary goal of such studies will be to obtain data needed in the design of a full-scale commercial plant. Some of the specific benefits to be derived include the following: a determination of the behavior of actual fission products in the process, particularly during the purification of plutonium; acquisition of experience in operating and maintaining a fluidized-bed processing plant under conditions of intense radioactivity; and demonstration of the safety of the fluidized-bed fluoride-volatility method.

The process flowsheet as of May 18, 1966, is shown in Fig. 2.4. Shortly after that date, a decision was made to add equipment for studying the interhalogen flowsheet (see "Process Description"). Provisions for supplying BrF_5 or BrF_3 to the primary reactor will be required, as will a method for reconverting and recycling the spent interhalogen. The distillation system will be designed to handle either a UF_6–fission-product–interhalogen mixture or, as originally planned, a UF_6–fission-product mixture, with or without PuF_6, depending on which of the two thermal decomposers is used. Meanwhile, laboratory studies will be concentrated on developing a method – hopefully, sorption-desorption – for recovering plutonium immediately after it leaves the primary reactor (see Sect. 2.6).

Design of the major equipment items required in the decladding, pulverization, and fluorination steps (phase 1) was completed, except for the equipment related to the interhalogen method. Fabrication of equipment and cell preparation were

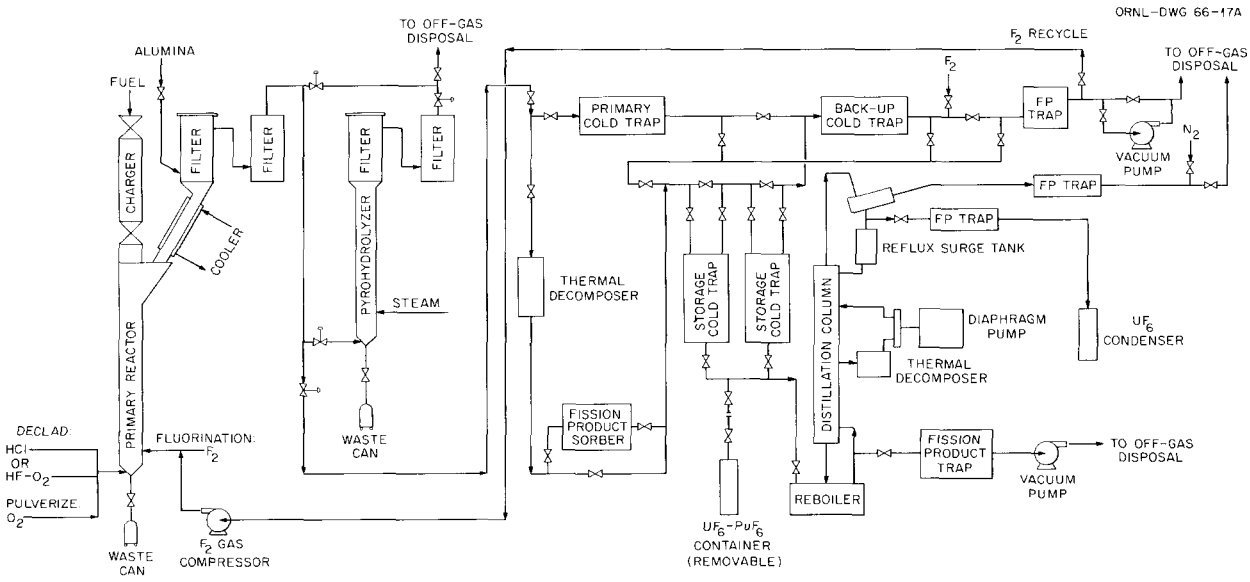

Fig. 2.4. Flowsheet for ORNL Fluidized-Bed Volatility Pilot Plant as of May 18, 1966.

begun. Design studies were made of problems related to accountability, handling of plutonium, containment, shielding, and fuel procurement.

In phase 2 (separation and purification of product streams, and sampling and leaching of waste solids), design studies are under way. A digital computer program was written to simulate distillation of a UF_6–PuF_6–fission-product mixture, with NbF_5 as a heel, while operating a thermal decomposer loop for PuF_6 off the fractionating tower.

Ways of sampling and leaching waste solids in the FBVPP are being studied, and some experimental development work is being planned. Studies are under way at Battelle Memorial Institute to aid in choosing a constructional material for the leacher (see Sect. 2.4).

Process Description

In the HCl process for Zircaloy-clad UO_2 (highest priority for FBVPP studies), the cladding is removed by reacting it with HCl to form volatile $ZrCl_4$. The $ZrCl_4$ flows to a separate vessel and is converted to ZrO_2 by reaction with steam in a fluidized bed of alumina or sand. After decladding and following pulverization of the UO_2 pellets by reaction with dilute oxygen to form U_3O_8, the uranium and plutonium compounds are converted to their respective hexafluorides by reaction with fluorine. The volatile fluorides from the fluorination steps are collected in cold traps and then revolatilized either through a thermal decomposer, where the plutonium is separated from the other salts by selective thermal decomposition, or to the storage cold traps for storage. The material in the storage cold traps is melted and drained to the batch distillation system, where the fission products are selectively removed. Niobium pentafluoride is added to the reboiler to serve as a heel during distillation. The low-boiling fission products are vented from the still overhead through sorbent traps to the off-gas disposal scrubber. The high-boiling fission products are collected in the reboiler, from which they are finally vaporized to fission product traps. If the plutonium is not removed prior to desublimation in the storage cold traps, it is separated from the uranium during the distillation process by recycling a side stream from the still through a thermal decomposer and back to the still. After sufficient decontamination from plutonium is achieved, the UF_6 is vaporized from the still through a cleanup fission product trap to a UF_6 container for removal from the system.

The processing of stainless-steel-clad fuels will be done in a manner similar to that described above for the Zircaloy-clad fuels except that the cladding will be removed by oxidation with HF-O_2. The "stainless steel oxide" product of the decladding will remain in the fluidized bed as relatively large particles that powder during the subsequent fluorination step.

Provisions will also be made to study the use of gaseous BrF_5 or BrF_3 instead of fluorine to selectively volatilize the uranium. The plutonium, then, is converted to PuF_6 by fluorine and collected separately. The method for purifying this PuF_6, however, has not been selected.

The facility is sized to process a charge of about 40 kg of UO_2 and 1250 g of plutonium. The primary reactor will be 8 in. in inner diameter, about 12 ft high, and will accommodate a fuel element 60 in. high with a 5.4-in. square cross section.

Status of Design, Fabrication, Procurement, and Installation

Engineering flowsheets for phase 1 (cell 3 equipment) were completed, but will require modification to show interhalogen equipment. The flowsheets show process equipment, flow paths, and instrumentation, and they identify all process and instrument piping.

Conceptual design studies of equipment for the uranium-plutonium separation and the product purification steps are proceeding. This equipment is a major part of phase 2 and will be installed in cell 2. The most significant design study related to uranium-plutonium separation and product purification was the writing of a digital computer program to perform the calculations necessary in the analysis of a dynamic-batch distillation–thermal-decomposition system.[2] Decomposition of PuF_6 to PuF_4 was assumed to occur in a decomposer located in a loop off the fractionating tower, with no decomposition in the tower. For one set of conditions where NbF_5 was added as a reboiler heel (about 2.5 mole % of the original charge), results of calculations showed that the reboiler

[2]Written by D. I. Dunthorn, Engineering Development Department, ORGDP.

could be operated at less than 100°C. This low an operating temperature should result in very slow thermal decomposition of PuF_6 to PuF_4 in the reboiler and in the fractionating tower.

Certified construction drawings have been issued for all the process vessels to be located in cell 3, except those required for interhalogens. These vessels are phase 1 equipment and will be operated first. Design of the cooler for the off-gas from the primary reactor and design of the transition zone between the cooler and the primary filter are being modified slightly to minimize the possibility of fines retention.

The shielding drawings for the phase 1 equipment in cell 3 were completed. Shielding steel was ordered and received precut and ready for installation.

Preparation of piping drawings for cell 3 is about 85% complete.

Fabrication of process equipment was begun in ORNL and ORGDP shops. The surge tank and scrub tower for disposing of HF, HCl, and fluorine are finished. The pyrohydrolyzer, cold traps, and primary reactor and pyrohydrolyzer backup filters are about 75% complete. The primary reactor is about one-fourth finished. The peripheral compressor required for recirculation of fluorine was completed. This unit was designed by the Mechanical Development Department, and a prototype was tested in the Engineering Development Department (EDD). (Both departments are in the Technical Division, ORGDP.) It uses a motor-generator set to develop 165-cycle alternating current required to drive an ac motor and, in turn, the compressor at 9900 rpm.

Procurement of all phase 1 process equipment is either finished or progressing. The furnace for the primary reactor is being made by Marshall Products Company and will be insulated with lightweight, high-temperature insulation as opposed to conventional firebrick and diatomaceous-earth–asbestos in series. The low-temperature refrigeration unit required for the cold traps will be supplied by Harris Manufacturing Company. It will be capable of removing 12,000 Btu/hr from circulating brine at −75°C, and will use ethane as the refrigerant in the low stage of the cascade of two 7.5-hp compressors. Tests were completed in the EDD on filter tubes fabricated from sintered nickel fibers and reinforced with nickel mesh, as supplied by the Huyck Metals Company. More conventional filter tubes made from sintered nickel powder without the mesh reinforcement failed at the welds. The sintered-fiber tubes to be used in the primary and backup filters for both the primary reactor and the pyrohydrolyzer have been ordered from Huyck.

A sliding-disk, full-opening valve normally used for high-vacuum service was modified and purchased from Mill Lane Engineering Company for use as the prototype for the valve in the charging chute to the reactor. On the basis of satisfactory leak-test results in the EDD, this basic design will be used in the FBVPP.

Numerous items of mechanical equipment are required for loading fuel elements into the carrier-charger, and, after transporting it from the storage canal to Building 3019, to charge the fuel element into the primary reactor; other equipment is required to remotely remove waste solids from the primary reactor and pyrohydrolyzer, move these wastes from the cell, from there to cell 1 for sampling and perhaps leaching, and finally to the burial ground. An existing carrier (the Pu-Al carrier) will be modified for use as a charger-carrier. Modifications of the upper end, including addition of a reel, have been designed but not drawn in final form. Design of modifications to the shutter has been completed. Fuel elements will be lowered from the carrier-charger on a zirconium wire into the primary reactor. A swaging die was developed to attach an aluminum ferrule to the wire to support the fuel elements; a punch-and-die-type forming tool was also designed for splicing the wire during the underwater loading operation. As the fuel element is lowered out of the carrier-charger, it passes through a shielded enclosure equipped with gloves and a viewing port. This enclosure is located on top of the charging chute. Designs are complete for the enclosure, its shielding, windows, port covers, split-flange charging valve, fuel element guide, and remote mirror, but final drawings have not yet been issued. The assembly view of the entire charging system remains to be drawn.

Equipment is being designed to transfer the porous metal filters from inside the reactor enclosure to carriers for disposal. Conceptual designs are nearly finished for the change-out method and carriers, but detailed design is only beginning. Improvements in the former may be necessary before the latter can proceed.

Conceptual design of a system for storing empty waste cans, positioning them under the primary reactor and the pyrohydrolyzer, disconnecting them,

and removing them from the cell is practically complete. Detailing of the handling machine is about 40% complete, with some subassemblies designed.

Design of process instrumentation is proceeding. Instrumentation was specified on engineering flowsheets as noted above. Six sections of the graphic panelboard as required for cell 3 equipment were designed. A preliminary drawing was started for the main transmitter rack. The necessity for enclosing the transmitter rack to contain possible releases of alpha emitters will complicate maintenance and routine adjustments. Heating the enclosure may also be required to prevent condensation of BrF_3 inside the transmitters.

Process and analytical instruments costing about $45,000 were received or are on order. This includes all analytical instruments (except an off-gas fluorine analyzer), as follows: (1) a gas-density detector to show the trend in the quantity of metal fluorides produced during fluorination, (2) an off-gas oxygen analyzer, (3) an off-gas hydrogen analyzer, (4) an analyzer to measure fluorine concentration downstream from the cold traps, and (5) a portable detector to monitor airborne fluorides.

Work is proceeding on the assumption that a Dextir data-handling system will be installed for use with the Oak Ridge Research Reactor and surrounding facilities, including Building 3019. With this system, selected instrument readings will be logged on magnetic tape. The tapes will be processed later on the IBM 360 digital computer in accordance with programs to be developed.

Electrical design for phase 1 included: the heating method for the upper part of the primary reactor, the pyrohydrolyzer, and the filter enclosures; wireways between cell 3 and the control area; and the lighting of cell 3. Design of the electrical power distribution system was started, and methods of heating process lines are being studied.

Modifications to improve the containment features of the Building 3019 penthouse (a secondary containment area) were completed. The penthouse can now be held at 0.3 in. vacuum (water gage) relative to atmospheric pressure. Additional capacity will be provided in the cell ventilation system by installing a new filter bank and rerouting ducts.

In preparation for installation of FBVPP equipment, all highly contaminated equipment from earlier programs was removed from cells 1, 2, and 3 of Building 3019. The walls, ceiling, and floor of cell 3 were decontaminated. The concrete retained some embedded contamination, however, that must be considered each time drilling of concrete starts. The cell was painted, and the need for masks has been infrequent, even when drilling. The cost-plus-fixed-fee contractor started work in cell 3 during April. The first task was the drilling of holes from the sample gallery into cell 3 and from cell 3 to cell 2. Work began on foundations for shielding at the lowest level.

Project Planning, Scheduling, and Reporting. – The project is being planned and scheduled using the critical-path method. Within the last year a cost reporting system has been placed into operation that allows expenditures of labor and material to be related to activities on the network diagram. The integrated system allows much flexibility in grouping and reporting actual costs. Based on the labor estimates now recorded on the network diagram, phase 1 is 26% complete.

Miscellaneous Design Studies

Accountability. – Early in the preliminary design of the FBVPP, plans were made to study accountability methods for the pilot plant and make whatever application possible to a full-scale plant situation.

The results of the study indicate that the most feasible method of handling accountability in the pilot plant is by analysis of product and waste streams. An accuracy of ±2% for plutonium at the 95% confidence level was estimated.

Measurement of the quantities of uranium and plutonium entering the process would be much more difficult and less accurate. Two possible methods were proposed for these measurements. With the first method, the uranium content of the fuel would be determined by either weighing the fuel element and subtracting the calculated weight of cladding and hardware, or by using the value for uranium content as supplied by the fuel element manufacturer. Next, the $^{235}U/U$ and Pu/U ratios would be determined by sampling the bed in the primary reactor. Such sampling would be possible only between the oxidation and fluorination steps of a two-step process; it would not be possible with the two-zone process employing simultaneous oxidation and fluorination. ANL personnel, fortunately, have recently recommended the two-step

process. Assuming that the peak-to-average ratio of the $^{235}U/U$ and the Pu/U ratios in the fuel is greater than 2, sampling errors in determining the average value of these ratios in the fuel were guessed to be within 10% precision and 5% bias at the 95% confidence level. Assuming further (1) that three samples are taken for analysis, (2) that the $^{235}U/U$ and Pu/U ratios may be determined within 1% by mass spectrometer and coulometric titration, respectively, and (3) that the total uranium is known within 1.5%, calculations showed that the ^{235}U and plutonium content of the fuel element might be determined within 7.5% at the 95% confidence level.

The second method proposed for measuring inputs of uranium and plutonium would rely on gamma scanning the fuel element prior to charging it to the primary reactor. First, the weight of total uranium in the fuel element would be determined as before. Then the relative levels of gross gamma activity and several fission products would be determined as a function of position in the element by scanning the element with an ion chamber and a multichannel scintillation chamber. Samples would be cut from the fuel element and analyzed to determine absolute concentrations of uranium, plutonium, and fission products and isotopic ratios of the uranium and plutonium. Finally, the average $^{235}U/U$ and Pu/U ratios in the fuel element would be determined by relating laboratory analyses of the samples to the relative spatial distribution of fission products indicated by the gamma scanner. For a typical power reactor element having axial peak-to-average burnup ratios of 2 to 4, the effect of the combined errors is estimated to be such that the average $^{235}U/U$ and Pu/U content of the fuel could be determined within ±10% at the 95% confidence level. Since this error dominates the error in measurement of the weight of total uranium, the ^{235}U and ^{239}Pu content of the fuel would be determined within 10%. Since the gamma scan method would require a lengthy and relatively costly development program far removed from the main objectives of the FBVPP, this approach was abandoned.

A program is under way here to study analytical and sampling problems anticipated in the FBVPP. Particular emphasis is being placed on sampling solids directly from the fluidized bed of the primary reactor, the gaseous UF_6-PuF_6 product stream, and the reactor waste solids. Recirculation of solids from the primary reactor through the sample container with a gas jet exhauster is being considered. This method is similar to the conventional method used in aqueous processes, and is currently being used successfully in the Waste Calcining Facility of the Idaho Chemical Processing Plant. A thief sampler is being considered for sampling waste solids in the waste container. A grinding and fusion method was recommended and outlined for analysis of samples of solids, with a detection limit for plutonium possibly as low as 0.00001 wt %. Equipment is being designed for acid leaching of waste solids from the pilot plant as a means of strengthening material balance data. Battelle Memorial Institute is investigating corrosion problems associated with the leaching step prior to selecting the material of construction (see "Choice of Material of Construction for FBVPP Leaching Equipment," Sect. 2.4).

Reference Fuel Element and Fuel Procurement. – The preliminary version of the accountability study distributed to project personnel for comments stated that the most nearly typical power-reactor fuel material to be processed in the FBVPP was fuel from the BONUS reactor irradiated to 11,000 Mwd/ton and cooled about 180 days. This burnup was generally not thought to be sufficient for the most rigorous demonstration runs to be made in the pilot plant. The problem was studied further, and a reference fuel element (similar to one from Oyster Creek) was adopted as the basis for calculations. Its characteristics are:

Burnup	23,000 Mwd/ton
Irradiation time	1492 days
Specific power	15.45 kw/kg
Thermal power	1600 Mw

Since the plant can only process an element less than 5 ft long, that will fit in an envelope 7.3 in. in diameter, only part of a fuel element was assumed. Based on a maximum of 40 kg of uranium per charge, quantities of other constituents would be as follows: 45 kg of UO_2, 59 kg of UF_6, 293 g of plutonium (total), 195 g of plutonium (fission), 9.2 kg of zirconium, and 336 g of ^{235}U.

A number of irradiated power-reactor fuel elements have been reserved for processing in the FBVPP. These elements are listed and described in Table 2.1.

Problems of Handling Plutonium in the FBVPP. – A study is being made of the problems that the

Table 2.1. Irradiated Fuel (Zircaloy-Clad) Elements Requisitioned for Processing in the FBVPP

Source of Element	Number Requested	Date Available (approx)	Description			
			Length (in.)	Cross Section (in. × in.)	^{238}U Content (kg)	Burnup (Mwd/ton)
BONUS (boiler)	4	6/69	30[a]	3.8 × 3.8	19.8	11,000
Shippingport (blanket)	12	6/66	10.25	5.2 × 5.2	15.5	8,000 to 23,000
Saxton (core II)	4	6/67	36.6	5.3 × 5.3	35.1[b]	18,000

[a]After cutting 60-in.-long element in half through nonfueled zone.

[b]Plutonium content before irradiation estimated to be 5.8% of mixed oxide fuel.

presence of plutonium is expected to cause in the pilot plant. The report, when issued, will include a description of the pilot plant equipment, a review of the pertinent characteristics of plutonium and plutonium compounds of interest, a tabulation of the quantities of plutonium and its daughters to be handled and the associated shielding problems, the containment design policy, and the design criteria for vessels containing plutonium.

The amount of plutonium required in a fuel charge to each FBVPP run was estimated. It had to be sufficient to cover expected losses to waste streams, samples, and holdup in equipment, and still provide enough product for reasonable material balances. Because of the uncertainties involved, estimates were made for both a pessimistic case and an optimistic one. The two values were 1235 and 530 g per run. Since these quantities exceed the amount present in a normal fuel charge, PuO_2-UO_2 additions will be needed.

Calculations were made to determine the required thickness of the gamma shield for the primary and backup cold traps in the FBVPP. The reference fuel charge was assumed, and the shielding calculations were made with the digital computer code SDC.[3] Only fission products with fluorides having significant vapor pressures at 650°C were used. Results indicated that 6 in. of lead would reduce the radiation background to 50 millirems/hr at a point in the personnel access area 59 in. from the nearer trap (primary). Six inches of lead was also recommended as shielding for the backup trap because of its proximity to the primary trap, and because of the physical arrangement of the two traps in cell 3.

Another investigation related to the problem of handling plutonium in the FBVPP was that of containing plutonium and uranium hexafluorides (MF_6) in the event of a major release. Release could conceivably occur if a line downstream from the primary reactor were to leak during a fluorination step, or if a pressurized cold trap were to rupture or develop a leak. Results of calculations indicated that if one-half of the MF_6 in one typical pilot plant run (20 kg of uranium and 500 g of plutonium) were released instantaneously, the concentration of plutonium at ground level in the ORNL area would exceed the maximum permissible concentration for plutonium (6×10^{-13} μc/cc) by a factor of 2 for only 10 min. This result is based on removing MF_6 by three mechanisms in series as follows: (1) deposition of one-half the total amount in cell 3, (2) a decontamination factor of 10^6 on the absolute filters, and (3) a maximum average dispersion factor of 4.6×10^{-5} (curies/m^3) (curies/sec) for the 3020 stack. On the basis of studies of PuF_6 releases at ANL, the decontamination factor of 10^6 should be achievable by filtering the air through two HEPA (high-efficiency particulate air) filters in series at 30 to 40% of rated flow, with sufficient water vapor present in the air to give a mole ratio (MF_6:H_2O) less than the

[3]E. D. Arnold and B. F. Maskewitz, *SDC, a Shielding-Design Calculation Code for Fuel-Handling Facilities*, ORNL-3041 (Mar. 31, 1966).

theoretical requirement of 0.5. The water vapor reacts with the MF_6 to form MO_2F_2, which deposits on the filters as particulate matter.

Preparation of Hazards Evaluation Report. – One engineer now has as his primary work responsibility the preparation of this report; another is working on it part-time. Thus far, a draft for the Chemical Process section of the report includes evaluations that extend through the fluorination step of each of the various methods to be demonstrated. Much of the work done in the studies described above should be directly applicable to the report.

2.4 CORROSION STUDIES RELATED TO THE FBVPP, AND MORE CORROSION DATA FROM THE MOLTEN-SALT VOLATILITY PILOT PLANT

Because of the elevated temperatures and the highly reactive nature of the principal fluids used in the fluidized-bed volatility process, corrosion of equipment and piping must be carefully considered. As part of the development program, corrosion data have been gathered at each of the participating sites. In the molten-salt fluoride-volatility program, data were collected in the major experimental facilities at ORNL, particularly in the Volatility Pilot Plant (VPP).[4] At the same time we have had a subcontract with the Columbus laboratories of Battelle Memorial Institute (BMI) to study specific problems related to corrosion in volatility processes and to aid in evaluating specimens exposed in our experimental facilities. In this section we discuss corrosion studies specific to the FBVPP, and present additional information on corrosion experienced in the VPP during the demonstration of the process for aluminum-based fuels.

BMI compiled corrosion data related to the fluidized-bed volatility process, with contributions obtained from Argonne, Brookhaven, and Oak Ridge National Laboratories, from ORGDP, and from the published literature. The survey confirmed earlier choices for materials of construction. Metallographic studies, part of which were made at the originating sites but mostly at BMI, revealed intergranular modification in specimens of nickel that had been exposed to process conditions. Subsequent studies at BMI showed that similar modifications in nickel 200 and 201 were produced by exposing coupons to alumina that might be used as the fluidized medium. Different types of alumina produced varying degrees of modifications, usually in proportion to their sulfur content. Sulfur, identified in the affected areas of the coupons and in portions of process equipment from Brookhaven, by both a chemical spot test and microprobe analysis, is thought to be the offender. Results of tensile tests on specimens with modifications produced by repeated exposure to type 38 Norton alumina (a relatively pure grade) showed a significant loss of ductility compared with that observed in tests of coupons from unexposed nickel. Attempts to solve the problem will be by: alloying nickel, seeking sulfur-free raw materials, developing purification methods, or a combination of these methods. Modifying nickel will probably be most effective because of sulfur-related fission products that will always be present. Cyclic exposure to fluorine may lessen the adverse effect of sulfur and sulfur-related elements that embrittle nickel, because of the volatility of the higher fluorides of these elements.

Leaching will be used as a verification of sampling methods required to determine uranium and plutonium retention in waste solids from the primary reactor. Also, the equipment will be designed so that leaching of fuel after oxidation may be studied following the all-volatility program, if desired. The high fluoride content of the waste solids will result in severely corrosive conditions with concentrated HNO_3, the proposed leachant.

A corrosion study was started at BMI to determine the best structural material for the leaching equipment. Of the 18 types of specimens tested, Corronel 230 (36 Cr, 58 Ni, 1 Mn, and 5 Fe, nominal)(in wt %) and HAPO alloys 17, 20, and 21 (25 Cr, 50 Ni, with varying amounts of Mo, Cu, Mn, and Fe) (in wt %) were more resistant to 13 *M* HNO_3–0.1 *M* HF at the boiling point (120°C) in 24- or 48-hr tests. Rates for welded coupons submerged in liquid were 17 to 29 mils/month. Since pure chromium corroded at only 4 mils/month, alloys high in chromium, such as 60% Cr–40% Ni and 50% Cr–50% Ni, will be tested for corrosion and fabricability. If these scouting tests continue to show superiority in one direction, small heats of special compositions will be produced at BMI for more extensive testing.

[4] *Chem. Technol. Div. Ann. Progr. Rept. May 31, 1965*, ORNL-3830, p. 34.

At the end of the demonstration of the aluminum process in the molten-salt fluoride-volatility program, the thickness of the dissolver (hydrofluorinator) walls was measured ultrasonically. After decontamination, corrosion rods were removed from the fluorinator, and sections of pipe and equipment were obtained for corrosion studies. These items are still quite radioactive, so detailed examination by micrometry and metallography, as appropriate, still remains to be done.

Survey of Corrosion Expected in the Fluidized-Bed Volatility Process

The survey of corrosion data applicable to the fluidized-bed volatility process confirmed the earlier choice of nickel 200 or 201 as the most nearly optimum material for use at 400 to 600°C in the decladding, oxidation, and fluorination steps of the HCl process for zirconium-clad fuels, and for use in the HF-O_2 processes for both zirconium- and stainless-steel-clad fuels. Maximum penetration rates in the HCl process calculated from relatively short exposures were less than 4 mils/month on the basis of weight change. Limited data for the HF-O_2 process indicated, on the same basis, corrosion of somewhat greater extent. Results indicated that Duranickel alloy 301 would probably be satisfactory for making the flanges. The corrosion resistance of austenitic stainless steel and Inconel was superior to that of nickel in the pyrohydrolyzer used in the HCl process. In some instances, welds made with nickel filler metal 61 corroded much faster than those made with nickel 200 or 201. Porous nickel filters corroded at acceptable rates in loop tests at ORGDP when exposed to H_2-HCl at 315°C and N_2-F_2 at 205°C. Uranium and plutonium hexafluorides in the presence of fluorine did not appear to accelerate attack at temperatures below 500°C.

Intergranular Modifications of Nickel in Fluidized-Bed Volatility Process

While compiling the corrosion data available from fluidized-bed experiments, BMI workers examined portions of nickel equipment and some of the nickel specimens exposed at other sites. These specimens were polished and then etched with 1:1 HNO_3-CH_3COOH. In some cases, intergranular modifications to a depth of 10 mils were observed. In an attempt to determine the cause of the modifications, laboratory studies were begun at BMI. After early experimental difficulties, similar modifications were produced in both nickel 200 and 201 by exposing the coupons to several of the types of alumina that might be used as bed material. Table 2.2 summarizes data from the experiments. Of special interest are the progression of modifications found when nickel 201 was exposed to Norton 38 Alundum and the relatively deep modifications produced by Norton Regular Alundum. Apparently, Alcoa T-61 alumina and Norton RR alumina contain only small amounts of the offending agent. In control experiments without alumina, no modifications were observed in coupons exposed to an atmosphere of water and in a vacuum; traces of modifications were observed when specimens were exposed in nitrogen.

Sulfur in the alumina is thought to cause the intergranular modifications. When the various grades of alumina were analyzed by combustion with oxygen and titration of the evolved SO_2, the following concentrations of sulfur were measured (ppm):

Norton Regular	190
Norton 38	< 30 (probably about 10)
Norton RR	< 50 (probably about 30)
Alcoa T-61	< 50 (probably about 20)

A spot test[5] with sodium azide (NaN_3) also showed sulfur present at the grain boundaries of coupons with modifications present in the Norton Regular Alundum. Results of microprobe analyses showed sulfur, iron, and oxygen at the surface of nickel specimens with intergranular modifications, but sulfur could not be detected to a significant depth in the grain boundaries.

A study was made to determine if intergranular modifications produced by exposing nickel 201 to Norton type 38 Alundum adversely affected the strength of the nickel. Norton type 38 is not necessarily the preferred bed medium, but it is advertised as being relatively pure, is cheaper than Norton RR, and is less friable than Alcoa T-61 alumina.

Tensile specimens measuring 0.5 × 2.75 × 0.055 in. were exposed to the alumina in evacuated capsules in two groups. The first group was exposed

[5] I. F. Feigl, *Qualitative Analysis by Spot Tests*, 2d ed., Nordeman, New York, 1939.

for 25 hr at 520°C and produced modifications to a nominal depth of 5 mils (10 mils, total). The second group was exposed to fresh alumina six different times for a total exposure of 350 hr at 520°C and a nominal penetration of 20 mils (a total of 40 mils of the 55-mil-thick specimens). Three specimens were exposed for each condition, and tensile tests were made at room temperature and at 520°C. Base-line data for specimens not exposed to the alumina were obtained from tensile tests of as-received specimens and after exposure in vacuum at 520°C for 350 hr.

Average values of tensile properties are presented in Table 2.3. Note that the intergranular modifications had significant effects on strength characteristics. Specimens exposed for 350 hr and pulled at room temperature showed reductions of 58 and 88%, respectively, for ultimate tensile strength and elongation. Corresponding values for specimens pulled at 520°C were 31 and 91%.

Table 2.2. Depths of Intergranular Modifications of Nickel As Affected by Alumina Type and Duration of Exposure

Nickel specimens sealed in a Vycor capsule in a vacuum

Temperature: 520°C

Time (hr)	Depth of Intergranular Modifications (mils)							
	Alcoa T-61		Norton 38		Norton Regular		Norton RR	
	Ni-200	Ni-201	Ni-200	Ni-201	Ni-200	Ni-201	Ni-200	Ni-201
25	0.5	<0.5	4.0	4.0	7.0	7.5		
50	1.0	1.0	6.0	4.5	7.0	7.5		
100	1.2	1.0	7.0	6.0	7.0	7.0	0.6	0.4
200	1.6	1.4	9.0	8.0	7.5	7.0		

Note: After 100-hr exposures with no alumina present and various atmospheres, traces of modifications were noted with nitrogen; none were noted with water or in vacuum.

Table 2.3. Effect of Intergranular Changes on Tensile Properties of Nickel 201

Tensile results are averages from three specimens

Exposure Conditions			Intergranular Penetration, Nominal (mils)	Measurements Made at Tensile Test Conditions					
				Yield Strength, 0.2% Offset (psi)		Tensile Strength (psi)		Elongation in 1 in. (%)	
Environment	Temperature (°C)	Time (hr)		RT[a]	520°C	RT[a]	520°C	RT[a]	520°C
				$\times 10^3$	$\times 10^3$	$\times 10^3$	$\times 10^3$	$\times 10^3$	$\times 10^3$
As-received	RT[a]	0	0	34.7	27.4	57.0	37.2	37.5	33.8
Vacuum only	520	350	0	23.0	18.7	57.4	35.4	42.2	24.0
38 Al_2O_3	520	25	10	24.3	19.0	51.1	32.2	33.9	24.9
38 Al_2O_3	520	350	40	22.0	17.2	24.0	24.9	4.3	2.5

[a]RT = room temperature.

Thus, the nickel containing grain-boundary modifications was shown to be severely embrittled.

Although sulfur apparently caused the modifications, the first, and rather insensitive, analyses indicated a low sulfur content for Norton 38 alumina. The analyses will be repeated using more refined analytical methods.

Choice of Material of Construction for FBVPP Leaching Equipment

Screening studies were started at BMI to find an alloy from which leaching equipment for the FBVPP can be fabricated. Eighteen alloys or forms of alloys were tested. All specimens except one were about ½ × 2 in., and most were welded. The exposures were conducted in 13 *M* HNO_3–0.1 *M* HF under refluxing conditions (bp, about 120°C) in an all-Teflon container equipped with Teflon support rods. Specimens of all alloys were immersed in liquid; Corronel 230 coupons were also located in the condenser, in the vapor above the liquid, and at the vapor-liquid interface.

The alloys with most favorable corrosion rates based on either 24- or 48-hr exposures were Corronel 230 and Hanford alloys 17, 20, and 21.[6] Nominal compositions are (in %):

Alloy	Cr	Ni	Co	Mn	Fe	W	Mo	Cu
Corronel 230	36	58		1	5			
Hanford 17	25	50		0.6	21.5		1.5	
Hanford 20	25	50		0.6	16.0		6.0	1
Hanford 21	25	50		0.6	18.5		1.5	3

Corrosion rates (mils/month) for welded coupons of Corronel 230 exposed for 48 hr were: 4.8 in the condenser, 22 in the vapor, 26 at the vapor-liquid interface, and about 27 for submerged coupons. After exposure in the liquid for 24 hr, welded specimens of Hanford 17 had corroded at the rate (mils/month) of 24, Hanford 20 at 17 and 27, and Hanford 21 at 24. Pure chromium corroded at 4 mils/month. Illium R, Nichrome V, Rexalloy 33, Haynes 21 (cast), and types 309, 310, and 446 stainless steel corroded at exceptionally high rates. Types 309 and 310 stainless steel were unstabilized; specimens of 309SCb will be tested further. Alloys with intermediate rates of attack were Vitallium (rolled), Haynes 21 (rolled), Hanford 22, 23, and 24, and Hastelloy F.

The excellent results from chromium prompted tests of samples of 60% Cr–40% Ni, 50% Cr–50% Ni, and 28% Cr–50% Ni–5% W–17% Fe received from the Blaw-Knox Company. These compositions have been developed for use as hangers in high-temperature boilers, but their fabrication properties are in question.

More Corrosion Data from the Molten-Salt Volatility Pilot Plant

The VPP dissolver (hydrofluorinator) and fluorinator were used throughout the programs to demonstrate molten-salt fluoride-volatility methods for processing zirconium- and aluminum-based fuels. Corrosion data from the zirconium program have been reported.[7,8] The aluminum program included ten dissolvings and a final cleanup with aqueous solutions to decontaminate the equipment.

Dissolver corrosion during the aluminum program was measured by pulse-echo and Vidigage techniques. Both methods indicated that total corrosion for the ten dissolvings and aqueous decontamination was 5 mils. The interior of the dissolver, inspected by telescope, revealed many small pits; a few wide, shallow pits; two parallel cracks, apparently shallow, ½ in. long and ½ in. apart, perpendicular to a girth weld 3 ft above the distributor plate; and a similar crack in the cone, observed after the zirconium program but which showed no significant change as a result of the aluminum program.

The fluorinator was not examined between the zirconium and aluminum programs. A total of 40 fluorinations were conducted in both programs. Wall thickness measurements after the aluminum program showed that the average attack in the salt region (the most vulnerable) was ½ mil per run for the 40 fluorinations, with no allowance for corrosion during the aqueous decontaminations. Maximum measured attack (on the same basis) was less than ¾ mil per run. Visual examination of the inside of the fluorinator revealed no evidence of excessive attack.

---

[6] R. E. Burns *et al.*, *Ind. Eng. Chem., Prod. Res. Develop.* 2(2), 163 (1963).

[7] *Chem. Technol. Div. Ann. Progr. Rept. May 31, 1964*, ORNL-3627, p. 34.

[8] E. L. Youngblood *et al.*, *Corrosion of the Volatility Pilot Plant INOR-8 Hydrofluorinator and Nickel 201 Fluorinator During 40 Fuel Processing Runs with Zirconium-Uranium Alloy*, ORNL-3623 (March 1965).

2.5 CONTINUOUS IN-LINE MONITORING OF GAS STREAMS IN THE FLUIDIZED-BED FLUORIDE-VOLATILITY PROCESS

One of the primary goals of the Fluidized-Bed Fluoride-Volatility Process Development Program is the selection and adaptation of instrumentation for monitoring and controlling operating conditions. Additionally, during the development of a process, analyzing reactor off-gas and other streams during an experiment helps show the response to changes in operating conditions and indicates needed changes. Selection, adaption, and evaluation of in-line analytical instrumentation is, therefore, a major part of the effort.

Three instruments have been investigated thus far in the Unit Operations Section: a gas chromatograph, an infrared (IR) spectrophotometer, and an ultraviolet (uv) spectrophotometer. To date only the HF-O_2 process has been tested, but the equipment for testing the HCl flowsheet is being installed, and experimental work will begin soon. To be included in future testing is the evaluation of thermal-conductivity cells and gas-density detectors.

The gas chromatograph was successful in monitoring HF or fluorine in O_2-N_2 streams and shows promise for use as an occasional but general-purpose analyzer. The IR analyzer had difficulty with interfering contaminants in the fluorine during attempts to monitor UF_6 in fluorination off-gas streams. The uv spectrophotometer successfully monitored UF_6 during fluorination experiments.

Tests of Gas Chromatograph for Analyzing Fluorine and HF in Oxygen-Nitrogen Mixture

The chromatograph being tested is a series 5000 Barber-Colman dual-column gas chromatograph with programmed temperature-control capabilities and a thermal-conductivity detector. One of the columns is a ½-in.-OD by 20-ft-long nickel tube packed with a 30- to 40-mesh Kel-F molding powder substrate and 20% No. 10 Kel-F oil absorbent. (The other column is not in use.) This packed column gives good separation between the HF and O_2-N_2 peaks and fair separation between the fluorine and O_2-N_2 peaks. Hydrogen fluoride tends to be held on this packing, and its peak tails rather severely unless the column is pretreated with fluorine and then ClF_3. With pretreatment, the tailing is reduced but not eliminated. Typical chromatograms for two systems, HF–O_2-N_2 and F_2–O_2-N_2, are shown in Fig. 2.5.

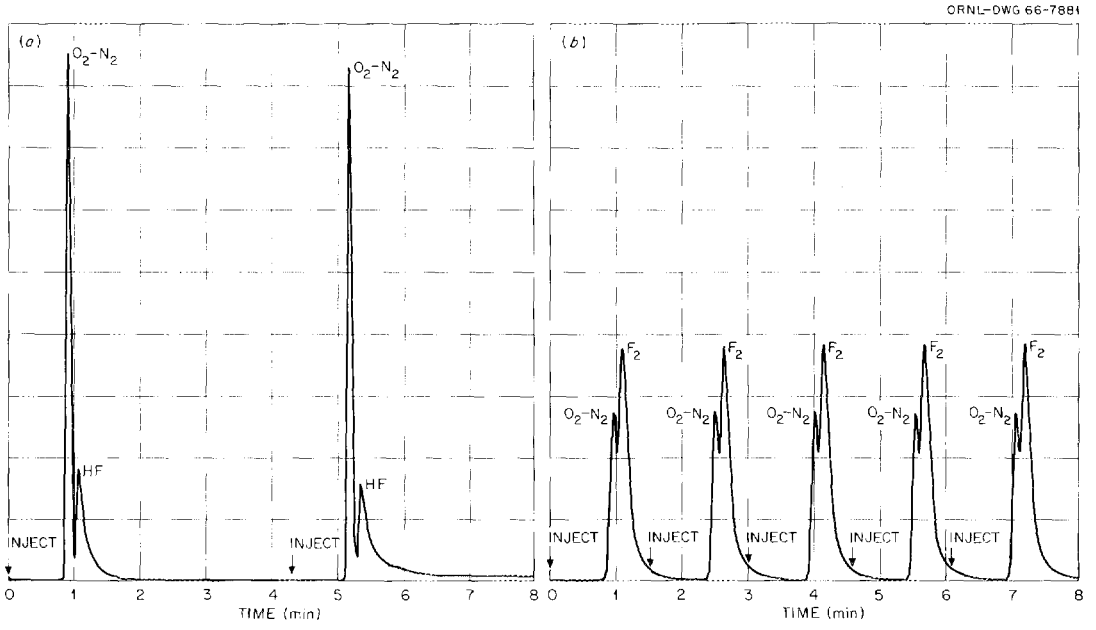

Fig. 2.5. Typical Chromatograms. (a) HF–O_2-N_2 mixture: 39% HF; (b) F_2–O_2-N_2 mixture: unknown concentrations, about 25% O_2-N_2.

Overlap of Absorbance Peaks for CF_4 and UF_6

Two infrared (IR) spectrophotometers have been tested: a Mine Safety Appliances model 300 LIRA and a Beckman model 215. Both are Luft-type, nondispersive IR analyzers, with selective detectors. Since UF_6 is very corrosive, the detectors of both instruments were filled with gases that have an IR absorption peak corresponding to one of the absorption peaks of UF_6, rather than UF_6 itself. These detector gases are SO_2 (8.6 μ) in the Beckman instrument and N_2O (7.7 μ) in the LIRA. Both instruments had nickel flow-through gas cells with CaF_2 windows and detected UF_6 in nitrogen streams. However, during attempts at calibration with F_2-UF_6 mixtures, an interfering contaminant was observed in the fluorine. The contaminant was thought to be CF_4,[9] which absorbs energy very strongly around 8 μ and is known to be in the fluorine produced at the Oak Ridge Gaseous Diffusion Plant in concentrations up to 0.1%. Since there is no simple means of removing CF_4 from fluorine, experiments with these instruments were suspended. If a selective absorbance peak for UF_6 (perhaps 16.0 μ) can be found, the development of an IR instrument will be resumed.

[9]Suggested by D. F. Smith, Physics Department, Technical Division, ORGDP.

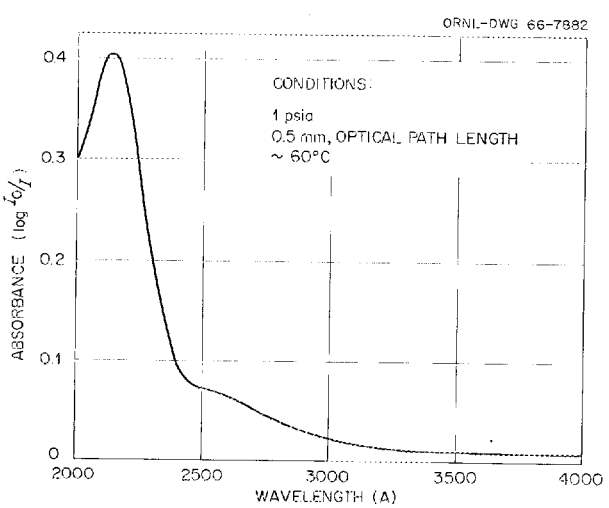

Fig. 2.6. Ultraviolet Absorbance Spectra of UF_6.

Ultraviolet Spectrophotometer Successfully Follows Fluorine Concentrations in Off-Gas from Two Fluorinations

A flow-through gas cell with a 0.5-mm optical path length and synthetic sapphire windows was fabricated for use with a Bausch and Lomb model 505 Spectronic uv spectrophotometer. After pretreating the cell with fluorine and ClF_3, the uv absorbance of UF_6 between 2000 and 5000 A was measured (Fig. 2.6). The 40.5% absorbance at 2140 A corresponds to a molar absorptivity of

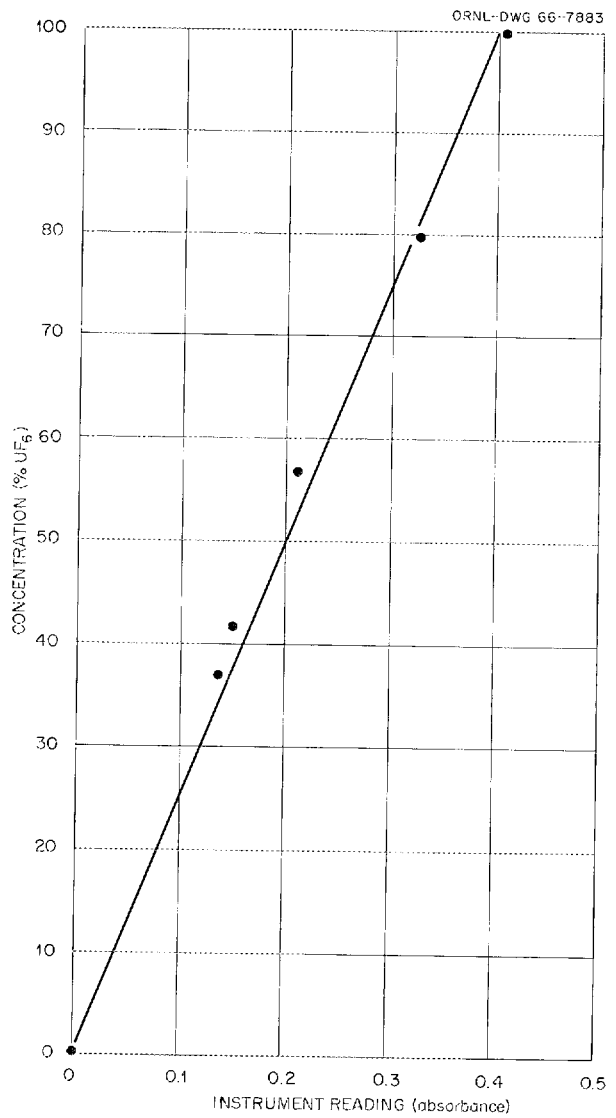

Fig. 2.7. Calibration of Bausch and Lomb Model 505 Spectronic Ultraviolet Spectrophotometer for Concentration of UF_6 in Fluorine at 2140 A.

3200 liters $mole^{-1}$ cm^{-1}, compared with 3600 ± 1000 reported previously.[10] The results of a calibration run with F_2-UF_6 mixtures at 1 psia are shown in Fig. 2.7. One difficulty experienced with the uv instrument is the clouding of the windows with a powdery film that probably resulted from incomplete preconditioning. In spite of this, the uv instrument was used to follow the UF_6 concentration in the off-gas from two fluorination experiments. The clouding caused about a 2% shift of the zero point during the run and, hence, an uncertainty in the point where UF_6 concentration returned to zero at the end of the run.

2.6 SORPTION OF PLUTONIUM HEXAFLUORIDE BY METAL FLUORIDES

The possibility exists that a sorption-desorption system can be found for PuF_6 comparable to the one whereby UF_6 is sorbed by and desorbed from NaF. Such a system would be of great advantage in the volatility processing of nuclear fuels.

The search for a PuF_6 sorption-desorption system progressed in three stages, resulting in the selection of ten sorbents (fluorides of the group I-A and II-A metals) as likely candidates for further study. Of the 31 fluorides tested, only these ten reacted with or sorbed significant amounts of plutonium. This led to 15-min dynamic tests that showed that sorption still occurred at all temperatures from 100 to 700°C. The hoped-for rapid desorption was not observed. The third phase of the investigation, long-term dynamic tests, showed relatively slow desorption from CaF_2 and LiF, leading to the current studies of LiF. Sorption at 280°C and desorption at 500°C appear to be likely conditions of operation. Additionally, the effort is being broadened (1) to consider other than the simple metal fluorides as sorbents, (2) to evaluate temperature, fluorine pressure, and other conditions that may favor the hexavalent state, and (3) to test physical and mechanical arrangements that may improve desorption.

The chief difficulty in achieving high desorption rates for PuF_6 appears related to the stability of the compounds holding the plutonium in a valence of less than 6.

[10] J. Winnick, personal communication.

Tests for Sorption and Desorption of Plutonium Hexafluoride

The fluorides of the metals of groups I-A and II-A that were shown to statically react with or sorb significant amounts of PuF_6[11] were tested in a dynamic system at temperatures of 100 to 700°C for retention of PuF_6. For these tests, about 1 to 7 mg of PuF_6 was passed through 2 g of the test sorbent during a 15-min period, using a fluorine carrier (60 ml/min). An NaF trap at 500°C collected the plutonium not retained in the test trap. The data of Table 2.4 show that for NaF, CsF, CaF_2, SrF_2, and BaF_2 the retention was high at all temperatures; at no temperature and with no sorbent was retention very low (i.e., desorption high).

Since rapid desorption, such as the rate in the UF_6-NaF system, does not occur with the plutonium complexes, long-term tests for desorption were undertaken. For these tests, about 40 mg of PuF_6 was first sorbed on the 2-g test sorbent; the desorption test included a fluorine flow of 60 ml/min into a backup trap of NaF at 200°C to collect any desorbed PuF_6. With NaF, insignificant quantities of PuF_6 were desorbed in 2-hr tests at 20, 100, 200, 300, 400, and 500°C; at 600°C in 10 hr, less than 0.5% was desorbed. With CaF_2, in tests similar to those described for NaF, the results were comparable except that, in duplicate 10-hr tests at 600°C, 7 and 15% desorption was obtained. For the NaF and CaF_2, no improvement in desorption was derived from reversing the flow of fluorine (opposite to that during sorption) for temperatures of 100 to 600°C. With LiF, significant but slow desorption was noted at 400°C (about 9 hr to desorb 97%) and at 500°C (about 4 hr to desorb more than 97%).

Properties of Compounds Formed by Sorbing Plutonium Hexafluoride

The static reactions of PuF_6 with fluorides of group I-A and II-A metals described previously[11] were repeated with equipment and methods modified to eliminate cross contamination and to improve contact between the gaseous and solid phases. The atom ratios achieved were 0.90 for LiF, 1.13

[11] *Chem. Technol. Div. Ann. Progr. Rept. May 31, 1965*, ORNL-3830, p. 85.

Table 2.4. Temperature Dependence for Retention of PuF_6 on Group I-A and II-A Metal Fluorides

Sorbent	Percentage of Plutonium Retained at Temperature (°C)						
	100	200	300	400	500	600	700
LiF	29.4	46.8	87.5	88.7	96.9	89.7	90.4
NaF	98.6	99.8	99.6	99.92	99.94	99.97	98.2
KF	97.1	98.5	97.6	97.5	94.2	94.4	98.0
RbF	83.6	90.4	93.8	99.9	99.9		98.5
CsF	99.6	98.6		97.9	99.8		95.8
BeF_2	29.1	20.1	76.6	70.9	71.0	73.4	87.1
MgF_2	98.8	98.2	96.3	96.9	98.6	98.6	94.5
CaF_2	99.99	99.995	99.994	99.997	99.98		99.996
SrF_2	99.95	99.97	99.7	98.9	99.97	99.96	99.97
BaF_2	99.4	99.95	99.95	99.99	99.97	93.93	99.99

for NaF, 1.31 for KF, 1.35 for RbF, 1.06 for CsF, 0.04 for BeF_2, 0.16 for MgF_2, 0.49 for CaF_2, 0.42 for SrF_2, and 0.37 for BaF_2. The thin films of compound formed with NaF, RbF, and CsF sorbents were reddish-brown; all others appeared white or opaque.

The oxidation state of plutonium sorbed as PuF_6 was studied by using oxidimetric titrations, infrared absorption, and x-ray methods. For these studies, the sample was prepared by passing PuF_6 in a stream of fluorine through a bed of sorbent at the test temperature. The sample containing plutonium was then transferred either to a solution of excess KI for back-titration of the liberated iodine or to a standard ferrous sulfate solution for back-titration with standard ceric sulfate solution. For the infrared studies the solid was dissolved in 2 *N* HNO_3 saturated with boric acid, and for the x-ray studies the solid was pulverized and transferred to a capillary. The average valence of the sorbed plutonium as a function of the preparation temperature was found by titrations to be 4.75 for 20, 100, 150, and 200°C, and 4.0 for 500 to 700°C; a value of 4.55 was obtained from infrared absorption for a sample prepared at 100°C. The sample prepared at 600°C gave an x-ray pattern that coincides with that of Na_3UF_7.

From the titration experiments, the oxidation numbers of the plutonium sorbed by CaF_2 were similar to those noted for NaF sorbent. With LiF sorbent, however, the plutonium had a valence of 4.0 for all temperatures of preparation.

The colors of the complexes prepared with NaF and CaF_2 depended on the preparation temperature, whereas those prepared with LiF were pink for all preparation temperatures. With NaF at the low temperatures (up to 300°C) the complex was tan, and at high temperatures it was green. With CaF_2, the comparable colors were white and violet.

2.7 SEPARATION OF URANIUM HEXAFLUORIDE FROM BROMINE FLUORIDES

The study reported here was made in support of the interhalogen fluoride-volatility process for recovering uranium and plutonium from low-enrichment UO_2 power-reactor fuels clad in either Zircaloy-2 or stainless steel. In this process, uranium (as the hexafluoride) is separated from plutonium by volatilization from a fluidized bed with BrF_5 or BrF_3. The plutonium remains in the bed for subsequent recovery with fluorine. The product stream, consisting of UF_6, BrF_3, BrF_5, Br_2, and an inert diluent such as helium, is then passed through a bed of NaF at 150°C, on which the UF_6 and BrF_3 are cosorbed. The BrF_3 is removed from the sorbent with a stream of fluorine that converts the BrF_3 to the nonsorbing BrF_5, leaving the UF_6 on the bed. After this, more fluorine is used in a series of pressurization-depressurization pulses to obtain the high degree of separation required.

Exploratory work demonstrated the feasibility of recovering UF_6 with minimal bromine contamination (14 ppm) by sorption on NaF. Fluorine is

used to remove bromine contamination, either as Br_2 or BrF_3, from the NaF bed. Pressure pulsation and the use of small NaF particles minimize the adverse effect of slow diffusion of bromine or bromine-fluorine compounds from the interior of the solid. We are planning further tests to see whether the specified bromine contamination of 5 ppm[12] is attainable by this method, and to determine whether the process objective is best accomplished by use of a fluidized bed of NaF.

Studies of Sorption-Desorption Methods for Lowering Bromine Content of UF_6

Studies on the evaluation of sorption on NaF as a means of separating UF_6 from BrF_3 and BrF_5 in the interhalogen fluoride-volatility process consisted generally of experiments in which 2-g quantities of UF_4 were fluorinated with a 20-80 mixture (vol %) of BrF_5 and helium. The product stream, consisting of UF_6, BrF_3, and BrF_5, was passed through a 4-g bed of granular NaF (activated Harshaw material). In most cases, the UF_4 was placed in a nickel boat contained in a 1-in.-OD nickel tube reactor, and was fluorinated for 2 hr. In a preliminary test, sorption of the product UF_6 and BrF_3 on NaF (−12 +20 mesh) at 100°C resulted in severe caking of the bed. Raising the bed temperature to 150°C in a second test eliminated the caking and resulted in complete sorption of the UF_6. The bromine contamination, based on the weight of UF_6 sorbed, was 6.3%. Subsequent desorption of the UF_6 onto a second bed of NaF by flushing with fluorine at 375°C for 1 hr reduced the corresponding bromine contamination to 54 ppm, based on UF_6. In another test, using a single bed of NaF (−12 +20 mesh) at 150°C, UF_6 was sorbed from a product stream as previously. A 1-hr fluorine flush, with the temperature held at 150°C, reduced the bromine content to 44 ppm. Changing the particle size from −12 +20 to −20 +40 mesh in a similar test further reduced the bromine contamination to less than 18 ppm. Additional improvement in the desorption of residual BrF_3 was obtained by ten cycles of pressurization-depressurization of an NaF bed (−12 +20 mesh) in the 1-hr fluorine treatment step. The cycles were of 1-min duration at 15 psig. The final bromine contamination in this test, based on the weight of UF_6, was less than 14 ppm (the analytical limit).

These data indicate that a cyclic fluorine pulsation, combined with NaF of the correct particle size, very probably will result in the required degree of separation.

2.8 CHROMIUM CHEMISTRY AND THE BEHAVIOR OF CHROMIUM IN VOLATILITY PROCESSING

In processing stainless-steel-clad UO_2 fuel by the fluidized-bed method, appreciable chromium volatilization occurs in the fluorination or UF_6 volatilization step but not in the HF-O_2 decladding step. The volatile chromium compounds of concern are CrF_4, CrF_5, and CrO_2F_2. Process development tests were conducted to define the problem; supporting chemical investigative work was done principally on the behavior of chromium in the NaF sorption step.

Preliminary work partially defined the behavior of the volatile compounds, CrF_4 and CrO_2F_2, formed in the fluorination step of the process. Sorption on NaF appears to have promise as a means of separating CrO_2F_2 from UF_6. Further work is planned on this system to identify the chemical complex involved and to ascertain the optimum temperature of operation. Work is also planned to define vapor pressure–temperature equilibria for the three volatile chromium compounds discussed above.

Chromium Volatilization in Process Testing

In a typical fluidized-bed test in a 1-in.-OD reactor, fluorination for 4 hr at 550°C produced the following disposition of chromium: 16% was left in the alumina bed, 4% was deposited in the disengaging section and on the filter, 53% was sorbed in the 100°C NaF bed, and about 8% was deposited in the filter blowback valves. The remainder was believed deposited throughout the gas tubing system, and this usually resulted in some chromium contamination of the HF used in a subsequent HF-O_2 decladding test. The composition of the alumina bed used in the above test was approximately 25% UO_2 and 8% type 304 stainless steel, resulting in a chromium content of about 1.6%.

[12] *Federal Register* 30, 14821 (1965).

Destructive oxidation of 20 g of type 302 stainless steel by $HF-O_2$ was accomplished in a boat test. Results showed that essentially no chromium volatilization occurred in the decladding step. Less than 0.5% of the chromium was found in the HF waste after treatment for 2 hr at 600°C.

Chromium Tetrafluoride Synthesis and Interaction with NaF

To provide the volatile chromium compounds needed for the studies, methods of synthesis were investigated. Free-energy estimates[13] indicated that the reaction

$$AgF_2 + CrF_3 \longrightarrow CrF_4 + AgF,$$

$$\Delta F^\circ = -29 \text{ kcal}, \quad (1)$$

might be used for synthesizing CrF_4. In laboratory tests, we found that dense blue-black CrF_4 vapors were evolved above 400°C, the boiling point of the compound. This procedure proved useful for small-scale preparation of CrF_4 when used directly for experiments performed inside a controlled-atmosphere glove box.

Exposure of NaF to CrF_4 vapor at 400 to 500°C yielded a pale-green solid phase with a face-centered cubic structure and a lattice constant of 7.90 A. Since it is isostructural with the high-temperature form of K_2CrF_6,[14] the compound is believed to be Na_2CrF_6.

Chromyl Fluoride Synthesis and Interaction with NaF

Chromyl fluoride was prepared by reacting CrO_3 with CoF_3, and the characteristics of the reaction were determined by transpiration with helium. Although this synthesis was used previously,[15] the conditions for the reaction were inaccurately defined. For example, we obtained substantial amounts of CrO_2F_2 at 200°C, the temperature used by previous workers to outgas the system before further heating to the temperature (450°C) they regarded necessary for synthesis.

Chromyl fluoride vapor was sorbed on active NaF, and the equilibrium pressure was determined by transpiration. At 23 and 168°C the pressures over the $NaF-CrO_2F_2$ were found to be 0.00153 and 0.00656 mm Hg respectively. The temperature-pressure equilibrium is therefore expressed as

$$\log P_{\text{mm Hg}} = -0.865 - \frac{579}{T}.$$

In contrast, the pressure of UF_6 over $UF_6 \cdot 2NaF$ is expressed by

$$\log P_{\text{mm Hg}} = 10.88 - \frac{5090}{T}.$$

These expressions show that the dissociation pressures are about equal at 100°C, and that at 150°C the UF_6 pressure is more than ten times the pressure of CrO_2F_2; consequently, UF_6 might be desorbed from NaF in the usual sorption-desorption purification procedures (about 300°C) without significant contamination by chromium.

2.9 VAPOR-LIQUID EQUILIBRIA OF UF_6-NbF_5 SYSTEM

During the recovery of uranium from spent nuclear fuels by a fluoride-volatility process, the UF_6 is contaminated by other volatile metal fluorides. One such impurity is NbF_5. Distillation is being considered as a method for separating the UF_6 from these impurities, but, to design the distillation system, more must be known about the vapor-liquid equilibria of the impurities and the UF_6.

An investigation was completed that determined the vapor-liquid equilibria of UF_6-NbF_5 in the region 0 to 13 atm at 114 to 315°C.

Vapor-Liquid Equilibria Experimentally Determined and Correlated by a Wohl-Type Equation

Specifically, the 150°C isotherm and the 5.92-atm isobar were determined experimentally in an isothermal still in which the vapors were circulated

[13] A. Glassner, *The Thermochemical Properties of the Oxides, Fluorides, and Chlorides at 2500°K*, ANL-5750 (1957).

[14] R. A. Oriani and C. P. Smyth, *J. Am. Chem. Soc.* 70, 125 (1948).

[15] G. D. Flesch and H. J. Svec, *J. Am. Chem. Soc.* 80, 3189 (1958).

mechanically[16] and in an isobaric still in which the vapors were circulated thermally.[17] The data were fitted by the method of least squares to three simplified forms of the Wohl[18] four-suffix equation. The simplified forms of these equations[19] are all fairly similar and differ only in the assumption made about the ratio of effective volumes of the two components. These equations are nonlinear, and curve fitting was accomplished on the CDC 1604 digital computer by a nonlinear regression technique developed by Law and Bailey.[20]

Since the data used were indirect, that is, liquid composition vs total pressure in the case of the isothermal data, and liquid composition vs boiling point in the case of the isobaric data, it was necessary to calculate the partial pressure P_i of each component from the "adjusted vapor pressure."[21] The "adjusted vapor pressure" is the vapor pressure of component i corrected for the nonideality of the vapor phase in the following manner:

$$P_i^* = P_i^0 \theta_i ,$$

where P_i^0 is the vapor pressure of component i, and θ_i is the nonideality correction factor for component i. This correction factor, calculated by means of an empirical equation developed by Black,[22] is a function of the critical constants and liquid molar volume of component i, the mole fraction of i in the vapor, and the temperature and pressure of the system.

The isothermal data and the calculated curves are shown in Fig. 2.8. The isobaric data and calculated curves for the best fit of that data are shown in Fig. 2.9. Table 2.5 lists the values of the constants that give the best fit for each set of data and each type of equation. The table also

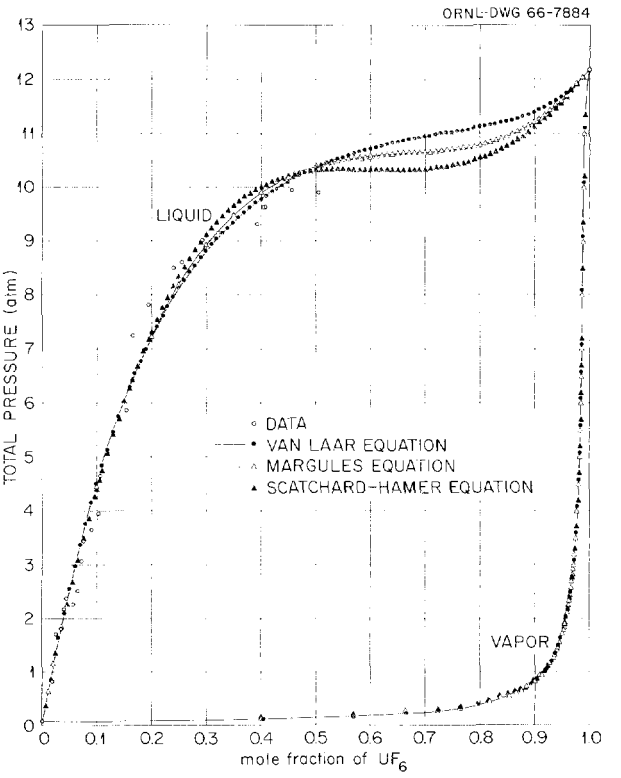

Fig. 2.8. Isothermal Pressure-Composition Diagram for UF_6-NbF_5 System at 150°C.

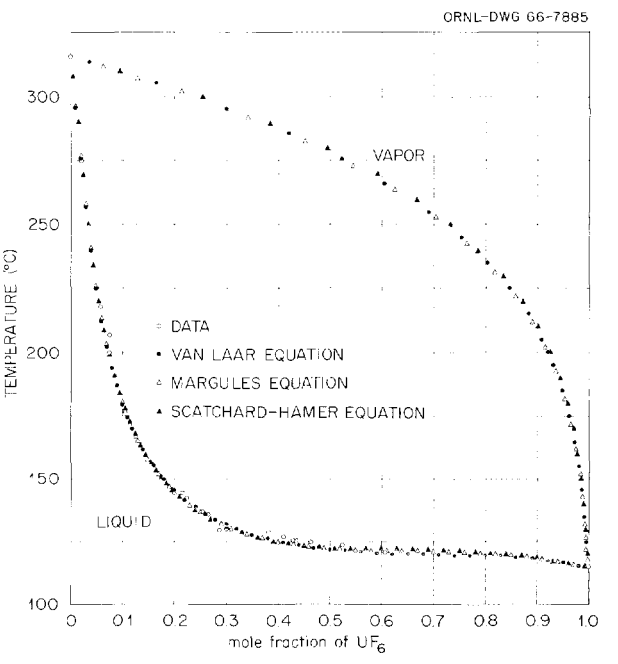

Fig. 2.9. Isobaric Temperature-Composition Diagram for UF_6-NbF_5 at 5.92 atm.

[16] R. C. Liimatainen, *Vapor-Liquid Equilibrium in the System Bromine Pentafluoride–Uranium Hexafluoride*, ANL-6003 (May 1959).

[17] D. F. Othmer and T. R. Morley, *Ind. Eng. Chem.* **38**, 751 (1946).

[18] K. Wohl, *Trans. Am. Inst. Chem. Engr.* **42**, 215–49 (1946).

[19] E. Hala *et al.*, *Vapor Liquid Equilibrium*, pp. 52–53, Pergamon, New York, 1958.

[20] V. J. Law and R. V. Bailey, *Chem. Eng. Sci.* **18** (1963).

[21] O. Redlich, A. T. Kister, and C. E. Turnquist, *Chem. Eng. Progr., Symp. Ser.* **48**, No. 2, 49 (1952).

[22] C. Black, *Ind. Eng. Chem.* **50**(3), 400–401 (1958).

shows the computed standard deviation of the dependent variable (either temperature or pressure) for each type. With the standard deviation as the criterion for choice, the van Laar equation is best. The van Laar equation is preferred also on the basis of the least peculiarity in shape of the curve between 0.6 and 1.0 m.f. UF_6 in the liquid. Since the calculated standard deviation for any of the simplified equations is not greater than the expected error in the data, any of the simplified four-suffix equations is satisfactory for computing the activity coefficients.

Table 2.5. Calculated Constants for Simplified Forms of the Four-Suffix Wohl Equation

Simplified Forms	Isothermal				Isobaric			
	A	B	D	σ (atm)	A	B	D	σ (°C)
Margules	0.737	1.023	0.239	0.12	0.58	0.95	0.04	3.0
van Laar	0.739	1.170	0.309	0.103	0.59	1.04	0.01	3.0
Scatchard-Hamer	0.729	0.929	0.479	0.38	0.53	0.88	0.34	3.2

σ = Standard deviation.

3. Molten-Salt Reactor Processing

The development of a molten-salt breeder reactor (MSBR) is among the long-range projects of the Oak Ridge National Laboratory. The Chemical Technology Division is participating by developing processes for continuously removing fission products from the core salt and recovering the newly produced ^{233}U from the blanket salt. The reference reactor for this study is a 1000-Mw (electrical) MSBR which is a two-region system with an $LiF-ThF_4$ (71-29 mole %) blanket and an $LiF-BeF_2-UF_4$ (about 65.5-31.2-3 mole %) fuel stream. In order to optimize breeding performance, the ^{233}U must not be allowed to reach high concentrations in the blanket (design concentrations will be about 0.012 mole %). Because of the low power density in the blanket, it is only necessary to remove the fission products by a small purge (one blanket volume per 40 years). The blanket is processed for uranium removal every 21 days.

Fission product poisons accumulate in the fuel salt at a much higher rate and must be removed on about a 39.4-day cycle. The most attractive process for the fuel salt consists of fluorination of the salt to remove the uranium and subsequent distillation of the carrier salt to separate the valuable ^7LiF and BeF_2 from the less-volatile fission products. The UF_6 from the fluorination is purified by sorption on NaF pellets, desorption, and collection in a cold trap. It is subsequently combined with the purified carrier salt by bubbling it into the liquid phase, reacting the UF_6 with UF_4, and subsequently adjusting the valence state by reduction with hydrogen. This processing scheme was previously described[1] and was subjected to a preliminary cost estimate that showed it to be economically feasible.[2] Advances in the technology this year, which will be reported here, involve the continuous fluorination and the vacuum distillation of the molten salt and studies of alternative methods of processing the fuel salt.

3.1 CONTINUOUS FLUORINATION OF MOLTEN SALT

The use of fluorination to recover uranium from a molten salt has been repeatedly demonstrated, particularly in the Molten-Salt Volatility Pilot Plant at Oak Ridge. Fluorination converts the UF_4 in the salt to volatile UF_6 according to the reaction:

$$UF_4 + F_2 \longrightarrow UF_6 .$$

The few fission products that become volatile by fluorination can be separated from the uranium by selective sorption on packed beds of MgF_2 and NaF. Problems that arise in applying fluorination to molten-salt reactor processing are concerned with the control of corrosion, the conformity to high recovery specifications, and the necessity for continuous operation. It is anticipated that corrosion can be controlled by operation of a continuous fluorinator with a layer of frozen salt on the vessel walls. This is made possible by the high rate of internal heat generation from fission product decay[1] in the MSBR fuel.

The attainment of consistently high recovery of the uranium is the subject of present study. The continuous fluorinator is envisioned as a tower through which salt will pass countercurrent to a rising, dispersed stream of fluorine. Problems of the equilibrium distribution of UF_6 between the gas and liquid phase, the rate of fluorination, and the degree to which axial mixing will destroy

[1] D. E. Ferguson, *Chem. Technol. Div. Ann. Progr. Rept. May 31, 1965*, ORNL-3830, pp. 301–2.

[2] C. D. Scott and W. L. Carter, *Preliminary Design Study of a Continuous Fluorination–Vacuum-Distillation System for Regenerating Fuel and Fertile Streams in a Molten Salt Breeder Reactor*, ORNL-3791 (January 1966).

the concentration gradient and negate the countercurrent effect are being considered.

Experimental studies of continuous fluorination of molten salt are being made in a 1-in.-diam nickel column having a salt depth of 48 in. No provision is being made in the present work for corrosion protection by a frozen layer of salt (Fig. 3.1). Fluorination tests in which molten salt (NaF-LiF-ZrF_4) containing 0.5 wt % UF_6 was contacted countercurrently with fluorine at 600°C demonstrated removal of uranium from the salt with 96 to 99.4% efficiency in a 1-hr period of continuous operation. The flow rates (cc/min) for the molten salt and the fluorine were 15 and 70 (STP) respectively. Material balances were complicated by the inevitable corrosion of the nickel vessel. Complete removal of uranium from the salt with no corrosion would yield, for the above conditions, a UF_6 concentration of 17.6 mole % in the off-gas. Observed concentrations ranged as high as 35 mole % UF_6.

These results indicate that subsequent development can be expected to produce acceptable recoveries of uranium by continuous fluorination.

3.2 DISTILLATION OF MOLTEN SALT

A flowsheet for the proposed MSBR uses a semicontinuous distillation process to remove rare-earth fission products from the reactor fuel. In this process the uranium-free salt is fed continuously to a still pot that accumulates the less-volatile fission products while the BeF_2

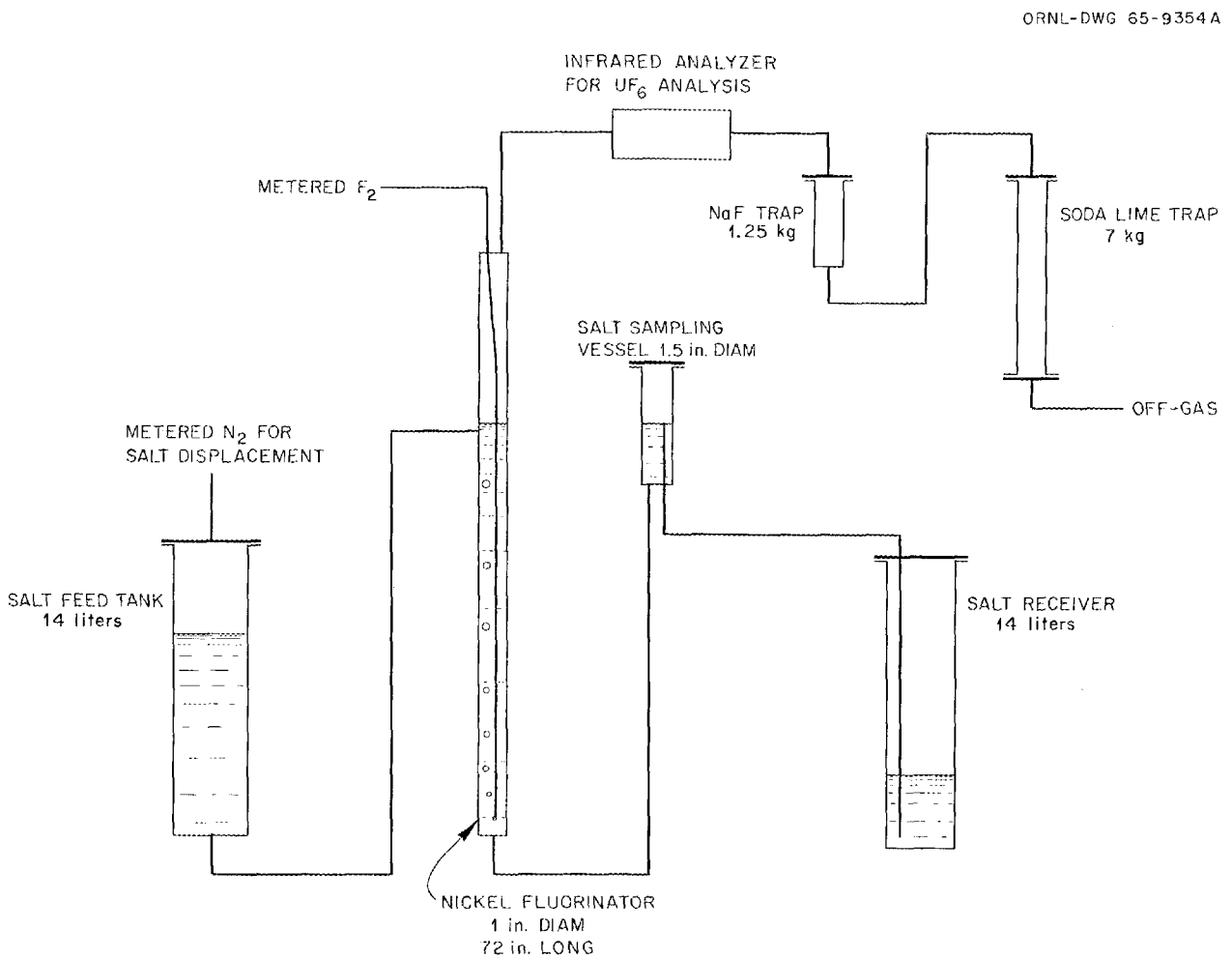

Fig. 3.1. Equipment for Removal of Uranium from Molten Salt by Continuous Fluorination.

and ^{7}LiF are boiled off.[2] The contents of the still pot are then discharged periodically with a cycle time determined probably by the rate of heat generation by the accumulated fission products.

Accurate vapor-liquid equilibrium data, mass- and heat-transfer data for boiling and condensing molten salts, and rates of entrainment of salt from the boiling surface are necessary to design the full-scale facility for processing molten salts. Vapor-liquid equilibrium data can be expressed as relative volatilities of the fuel-stream component with respect to LiF. The relative volatility, α_{AB}, of component A with respect to component B is defined as:

$$\alpha_{AB} = \frac{Y_A/X_A}{Y_B/X_B}, \qquad (1)$$

where A and B refer to the two components, and Y and X are the vapor-phase and the liquid-phase mole fractions respectively. The lower the relative volatility of the fission products with respect to LiF, the more effective will be the separation.

Values for the relative volatilities of the rare-earth fluorides with respect to LiF were measured with various temperatures and fission product concentrations by using a cold-finger technique.[1] These values, ranging from 0.01 to 0.05, are high enough to warrant reconsideration of the proposed simple distillation process.

To verify the relative volatility data, a recirculating vapor-liquid equilibrium still was used. This device (Fig. 3.2) was not as simple to operate as the cold-finger apparatus, but it was not subject to the same experimental biases.

ORNL-DWG 66-3933

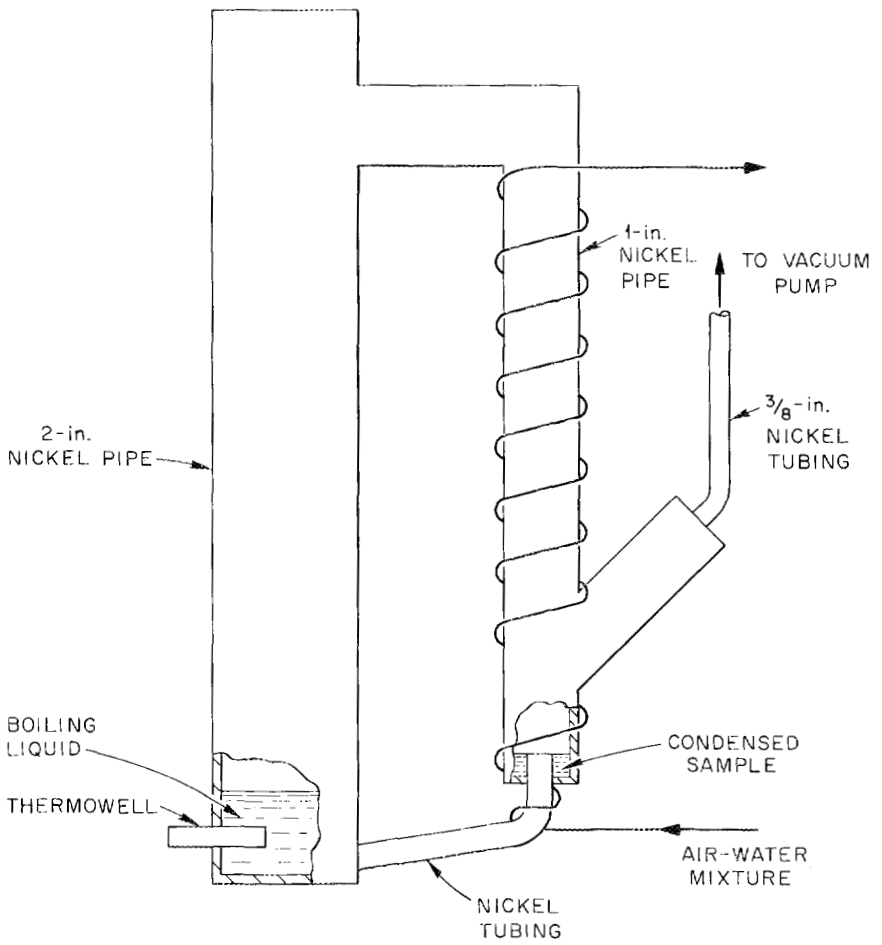

Fig. 3.2. Schematic Diagram of Molten-Salt Equilibrium Still.

Vapor was continuously generated in the 2-in. still pot, condensed in the 1-in. condenser, and returned as liquid to the still pot. When concentrations reach steady state, the concentration of the liquid in the still pot and that of the liquid in the condenser will be equilibrium values from which relative volatilities can be determined, provided the liquid volumes in the condenser and boiler sections are well mixed. Measurements were made by freezing the salt and cutting the still in pieces to take samples.

Several runs lasting from 2 to 30 hr were made with this still at 1000°C and 0.5 mm Hg. Relative volatilities for systems of LiF containing from 1 to 2% selected rare-earth fluorides were measured. The relative volatility of cerium apparently lies between 0.0014 and 0.003; the relative volatility of neodymium lies between 0.00055 and 0.00089; and lanthanum has a relative volatility of about 0.00067. These results were reproducible after initial difficulties with still operation were resolved. The principal problems appeared to be: (1) avoiding excessive contamination of the condensate collector when charging the salt to the system, and (2) salt clinging to the walls where it could not be mixed with the bulk of the salt.

The relative volatility of CeF_3 determined by the equilibrium still is about one-tenth of that reported previously from cold-finger measurements, and the relative volatilities of NdF_3 and LaF_3 are one-fiftieth of those previously reported. These more accurate values are low enough to permit comfortable operation of a batch distillation system in the fuel-salt flowsheet.

A number of other aspects of still operation were tested in these experiments. These experiments demonstrated that long-term operation of a unit for boiling and condensing fluoride salts can be performed with relatively simple controls for temperature and pressure. In the case of the small-scale equipment used in these experiments, the temperature in the condensing section was controlled by manually adjusting the flow of a mixture of air and water. Temperature in the still pot was regulated by an electronic on-off temperature controller connected to the furnace enclosing the still. A simple manostat controlled the pressure to within ±0.05 mm.

The formation of fluoride salt "snow" in the vacuum line from the still was once thought to be a potential problem in the operation of a distillation process. In these experiments we saw no "snow" or other type of salt deposition in the vacuum line.

Tentative tests that could have detected a corrosion rate of 0.1 mil/day indicated no corrosion.

We will continue these studies to collect good relative volatility data for all the rare-earth fluorides and to help provide heat- and mass-transfer data for design of an operational distillation unit.

3.3 ALTERNATIVE PROCESSING METHODS FOR A MOLTEN-SALT BREEDER REACTOR

Liquid-metal extraction has been under study as a possible substitute for vacuum distillation. Earlier tests with Li_2BeF_4 salt showed that the lanthanides were removed, in most cases, by a reductive coprecipitation with Be to yield refractory insoluble beryllides that deposited at the salt-metal interface. The scope of the study was extended to include reductive precipitation using minimum quantities of Li or Be as reductant followed by simple physical separation of the precipitated metals by filtration or settling. Decontamination factors were determined by using initial concentrations of 30 to 1000 ppm of Zr, Nd, La, Sm, Eu, Gd, and Sr, either singly or in various combinations.

Further studies of the liquid-metal extraction method were made with Li-Bi alloys to test removal of the same elements, with the exception of Zr and Nd.

Procedure

The reduction-coprecipitation studies were made of 15-g (7.5-cc) samples of Li_2BeF_4 spiked with "cold" neutron poisons (as fluorides). These samples were contained in mild-steel containers under a protective atmosphere of argon. A typical test included: preparing and sampling the original salt while it was molten; reducing with between 1 and 243 times the theoretical amount of Li or Be at temperatures in the range 500 to 1000°C for about 90 min, with stirring by an argon sparge; filtering through a sintered-Cu filter stick; recovering frozen samples of treated salt from the filter and, when possible, recovering the precipitated metals from the bottom of the reactor. Salt samples were analyzed for lanthanides and Zr

by neutron activation analysis, spark-source mass spectrometry, or emission spectrometry. The metal precipitates were examined by x-ray diffraction.

Liquid-metal extraction tests with solutions of Li in Bi were made in the same equipment but without filtration of either phase. Samples were recovered after settling, quenching to room temperature, and sacrificing the crucible. Before the salt and the metal slugs were sampled for analysis, they were cleaned of surface deposits.

Results

Reductive Precipitation. – The decontamination factors (DF's) for La and Gd (Table 3.1), when compared with the indicated process requirement at the bottom of each column, show that adequate removals could be achieved with both Li and Be by using excess reductant in the range of one to four times the theoretical requirement for depositing $LnBe_{13}$. The low values obtained in experiment 8 reflect the incomplete removal of Zr, present in this experiment as a major component, 11.7%. In this case the final concentration of Zr (500 ppm) was comparable to the initial concentrations of La and Gd, and was, therefore, sufficient to inhibit their reduction. The species identified in the recovered metal precipitates (see Table 3.1; experiments 1, 3, and 10) indicate that reduction of lanthanides in Li_2BeF_4 with either Li or Be leads exclusively to beryllides of the type $LnBe_{13}$. The x-ray identifications listed in Table 3.1 represent only the specific beryllide that is most likely, since the $LnBe_{13}$ compounds are indistinguishable from each other when codeposited from a mixture.

Examination of the DF's for Zr (Table 3.1) shows that Zr can be removed easily from solutions in Li_2BeF_4 over a broad range of concentrations by treatment with either Li or Be. It is deposited either as free metal or, from very dilute solutions (70 ppm), as $ZrBe_2$ (Table 3.1; experiment 4). The rather high theoretical excesses of Be used here do not represent optimized values. Based on the above work, the consumption of Be to obtain a DF (Zr) = 1.43 at an initial Zr concentration of 28 ppm would require only 0.2 g of Be per kilogram of salt being processed, even allowing a 100-fold excess. The value of DF (Zr) = 11 obtained at 1000°C in experiment 7 is of special interest since it suggests a solution to the high volatility of ZrF_4, a major problem encountered at this temperature in the vacuum-distillation salt recovery method. The technique would be to use Li or Be as a reductant to retain Zr in the still pot as nonvolatile free metal.

The reduction of Nd with Be (Table 3.1; experiments 2 and 4) required a 40-fold excess of reagent, as indicated by interpolation between the values shown. In the process, an initial concentration of 311 ppm of Nd [which is 50% (by weight) of the total lanthanides] would require 11 g of Be per kilogram of salt being processed. In experiment 4, Nd deposited in the form of $NdBe_{13}$ (identified by x-ray analysis). In this test, deposition of one of several possible Zr beryllides might be expected because of the low Zr concentration (70 ppm). This was confirmed when $ZrBe_2$ was identified along with α-Zr.

In addition to the elements listed in Table 3.1, Sm, Eu, and Sr were studied as parts of the mixtures used in experiments 1, 3, and 8, as well as in other tests not listed. Results with these elements are, generally, not encouraging. The value DF(Sm) = 2 obtained in experiment 3 is among the highest observed.

Li-Bi Alloy Extraction. – The DF's and distribution coefficients, K_D's, obtained in liquid-metal extractions of "spiked" carrier salt using Li-Bi alloys are summarized in Table 3.2. Except for Sm, adequate decontamination was achieved for all elements (La, Sm, Eu, Gd, and Sr) in the "spike." The generally high DF's cannot be explained in most cases by a true extraction mechanism, as is indicated by the low distribution coefficients shown in Table 3.2. Also, poor material balances were obtained when only samples of the salt and metal phases were used. The mechanism for the removal of the elements in question is precipitation as interfacial solids, which were later isolated and identified by x-ray analysis to be beryllides of the $LnBe_{13}$ type. The high K_D observed for Eu, however, indicates that this element was removed almost exclusively by extraction when 30 at. % Li-Bi alloy was used.

Table 3.1. Reductive Precipitation of Neutron Poisons from Li_2BeF_4

Initial concentrations: Zr = 70 ppm; Nd = 400 ppm; others 600 to 900 ppm

Experiment No.	Reductant	Factor of Excess Reductant	Temperature (°C)	DF = ppm of "spike" in original salt / ppm of "spike" in treated salt				Species Identified in Metal Precipitates by X-Ray Analysis
				Zr	La	Nd	Gd	
1	Be	1	550–600		2.4		2.3	Be; α-Zr (trace); $LaBe_{13}$ (trace)
2	Be	4.2 (Nd), 243 (Zr)	550–560	55		2.1		Not examined
3	Be	4.4	550–595		9.0		8.0	$LaBe_{13}$ and Be (trace)
4	Be	103	550–580			52		α-Zr, $ZrBe_2$, Be, $NdBe_{13}$
5	Be	121	550–560	395[a]				Be
6	Be	104	800	36				Cu (from filter) + unidentified lines
7	Be	162	1000	11				Not examined
8	Li	1.28	550–575	234[b]	1.1		1.3	α-Zr; LiF + Li_2BeF_4 in salt
9	Li	105	550–580	51				Cu (from filter)
10	Li	4.1	550		13		6	Be, $LaBe_{13}$, $FeBe_5$ (from crucible)[c]
	DF required for process			1.43	1.7	20	1.05	

[a]Initial concentration = 400 ppm of Zr.

[b]Initial concentration = 11.7% Zr.

[c]Separation by settling.

Table 3.2. Li-Bi Alloy Extraction of Lanthanides from Molten Li_2BeF_4

Initial concentration: Lanthanides = 800 to 1000 ppm each; Sr, about 200 ppm

Alloy Composition (at. %)	Contacting Conditions			$DF = \frac{C_{original\ salt}}{C_{treated\ salt}}$					$K_D = \frac{\text{mole fraction in metal}}{\text{mole fraction in salt}}$				
	Temperature (°C)	Time (min)	Volume Ratio (alloy/salt)	La	Sm	Eu	Gd	Sr	La	Sm	Eu	Gd	Sr
5.9 Li–94.1 Bi (C_{final} = 2.56 at. % Li)	550–560	160	0.71	3.0	3.5	1.0	2.0	1.5	0.85	2.2	0.54	0.32	0.18
30 Li–70 Bi (C_{final} = 10.05 at. % Li)	550–560	120	1.1	6.0	2.0	8.0	5.0	2.0	1.1	3.1	17.1	2.00	0.97
DF required				1.7	5.0	1.43	1.05	1.04					

4. Waste Treatment and Disposal

The waste treatment and disposal development program is designed to develop a comprehensive waste-management system for nuclear wastes, including their final disposal, and to estimate the cost of this operation. Economical management of radioactive effluents is a prerequisite to the natural growth of a nuclear power industry. A comprehensive waste-management flowsheet was presented previously.[1] High-level radioactive wastes (HLW), which contain nearly all the fission products, are converted to solids. Intermediate-level radioactive wastes (ILW), characterized by their generally high salt content, are incorporated in asphalt; any contained water is simultaneously volatilized. Low-level radioactive wastes (LLW) are treated to remove the radionuclides, and the decontaminated water is discharged to the environment or recycled for reuse. The recovered solids are combined with the ILW. Both the HLW and ILW solid products can be shipped to an ultimate disposal site.

4.1 HIGH-LEVEL RADIOACTIVE WASTE

Status and Progress

Development of the Rising-Level Potglass (RL-Potglass) process continues. Two new prototype waste compositions, PW-1 and PW-2, were studied, and phosphate-type glasses or ceramics were explored further. These prototype wastes will be the standards for the development program in the United States. They differ considerably from the previous standard waste, FTW-65, because of the high iron content of PW-1 and the increase in the fission product concentration of both wastes to that equivalent to a burnup of 20,000 Mwd/metric ton. This change necessitated additional melt-development studies and small-scale rising-level tests in the laboratory to develop a melt with a suitably low melting point and low degree of corrosivity. Additional large-scale tests were also required to define pumping, heat transfer, corrosion, and other engineering variables in 8- and 12-in.-diam pots. Some successful small- and large-scale runs were made, and corrosion was negligible, but in several instances it was severe. Consequently, evaluation of the RL-Potglass process in the Waste Solidification Engineering Prototype (WSEP) with radioactive waste at Pacific Northwest Laboratory (PNL) was not recommended until the corrosion mechanism is more clearly defined.[2] Low-melting silicate mixes were also developed to incorporate Purex wastes. Initial corrosion tests in a small-scale continuous melter were promising. It may prove possible to use Inconel, Nichrome, or similar commercial alloys, instead of platinum, to make a continuous melter.

Previous work with HLW's was confined to aqueous wastes. A new program was started to develop suitable treatment methods for the solid wastes from the fluidized-bed fluoride-volatility process (Sect. 2). An economic survey was made to define the parameters for this work (Sect. 4.4). Thermal conductivities were derived to assist in determining whether the waste bed should merely be sealed in a disposable stainless steel pot or dispersed in a glassy matrix in a pot. It appears feasible to place powdered glass over the waste bed in a pot and to melt the glass and cause it to flow into the voids.

[1] D. E. Ferguson *et al.*, *Chem. Technol. Div. Ann. Progr. Rept. May 31, 1965*, ORNL-3830, p. 96.

[2] R. E. Blanco and F. L. Parker, *Waste Treatment and Disposal Semiannual Progress Report, July–December 1965*, ORNL-TM-1465 (in press).

Laboratory Studies

Disposal of Aqueous Wastes. – The ORNL work on waste solidification was summarized in the ORNL section of the operating manual for the WSEP at PNL. A revised version will be issued as a final report summarizing the ORNL work on solidification of highly radioactive aqueous wastes.[3]

Melt-Development Studies. – Waste types studied during 1966 included Purex FTW-65, Purex-1, and Purex-2 (Table 4.1) in addition to melt viscosity measurements of a single TBP-25 melt. Work on the Purex melts covered a range of simulated fission product compositions from zero to that expected from a burnup of 20,000 Mwd/metric ton (Table 4.2). The compositions of melts[4] from FTW-65 Purex waste were varied systematically, and the leach rates of the products were determined. The results confirm that melts of this type that contain calcium are more insoluble than those without it. Further correlation of melt composition with physical properties is continuing.

The adoption of Purex-1 and Purex-2 as new standard compositions for Purex waste, with and without sulfate, and both containing simulated fission products from 20,000 Mwd/metric ton burnups (Tables 4.1 and 4.2), necessitated additional development of melt compositions. Reasonably satisfactory phosphate melt compositions

[3] W. E. Clark *et al.*, *Development of Processes for Solidification of Aqueous, Highly Radioactive Waste. Summary Report for Pot-Calcination and Rising-Level Potglass Processes*, ORNL-3961 (in preparation).

[4] C. L. Fitzgerald *et al.*, *A Computer Code for Storing and Retrieving Data and Developing Improved Solids for Fixation of Highly Radioactive Wastes*, ORNL-3824 (March 1966).

Table 4.1. Simulated Wastes (Without Fission Products) Used in Melt-Development Studies

Constituent	Gram-Moles per Liter of Waste			
	Purex FTW-65	Purex-1	Purex-2	TBP-25
H^+	0.5	5.0	5.0	0.5
Na^+	0.3	0.138	0.93	
Al^{3+}	0.05	0.001	0.001	1.6
Fe^{3+}	0.10	0.93	0.445	0.002
Cr^{3+}	0.02	0.12	0.024	
Ni^{2+}	0.01	0.05	0.01	
Hg^{2+}	0.0035	0.001	0.001	0.01
Ru	0.002			
Mn^{2+}				
SO_4^{2-}	0.15		0.870	0.026
PO_4^{3-}	0.005	0.003	0.006	
SiO_3^{2-}	0.01	0.01	0.01	
F^-	0.0005	<0.001	<0.001	
NO_3^-	~1.0	~8.8	~6.44	~5.4
Cl^-				
Gallons per unit weight	82 per 10^3 kg of U	100 per 10^3 kg of U	100 per 10^3 kg of U	106 per kilogram of ^{235}U

were readily available from previous melt-development work recorded in the ORNL melt catalog.[4] Difficulty was encountered with corrosion from Purex-1 waste which is high in iron. (See "Corrosion with Phosphate Melts," below.) Lead silicate melts were also developed for this waste type. The best of these were more homogeneous in appearance, had lower softening and operating temperatures, were less corrosive, and gave higher volume reductions than the phosphate melts (Table 4.3). Thermal conductivity was much lower than for the phosphate melts though still about twice as high as for calcined waste (Fig. 4.1).

Viscosity Measurements. – Viscosities of selected phosphate melts were measured by the falling-sphere method described previously.[4] The viscosity of TBP melt 263[4] decreased from 429 poises at 800°C to 207 at 900°C (Fig. 4.2). Viscosities of the FTW-65 melts were lower than those of TBP melt 263 by at least an order of magnitude. The effectiveness of fission products in increasing viscosity is shown by the fact that FTW-65 melt 392 without fission products decreased in viscosity from 11 poises at 800°C to about 6 at 850°C and to 3.5 at 900°C, while a melt of the same composition except for the addi-

Table 4.2. Simulated Fission Products Used in Melt-Development Studies

	Composition Number		
	1[a]	2[b]	3[c]
Burnup, Mwd/metric ton	10,000	10,000	20,000
Thermal neutron flux		3×10^{13}	
Irradiation time, months		11.4	
Decay time, months		3.8	
Percent ^{235}U in fuel		2	
Fission product concentrations, gram-atoms ($\times 10^2$) per liter of waste			
Rb	0.7	0.6	0.71
Cs	0.7	1.9	3.45
Sr	0.53	1.4	1.55
Ba	0.53	0.8	1.95
Rare earths	0.45	8.1	11.9
Zr	2.1	4.5	6.5
Mo (and Tc)	2.3	4.4	7.9
Ru, Rh, Pd	2.8	1.6	5.66
Ag			0.08
I		0.17	
Total fission products, gram-atoms per liter of waste	0.144	0.2347	0.397

[a]This composition was used in the earlier developmental studies, and its use was continued in some FTW-65 experiments to provide continuity. The figure of 10,000 Mwd/metric ton is only nominal.

[b]Calculated from ORNL-2127 (J. O. Blomeke and Mary F. Todd).

[c]C. R. Cooley, letter to W. G. Belter *et al.*, "Projected Waste Compositions for WSEP Studies," May 6, 1965.

Table 4.3. Summary of Semiengineering-Scale Tests of the RL-Potglass and Con-Potglass Processes

	Melt Numbers (see ref. 3)[a]							
	422	423	473	478	478[b]	479[c]	480	481
Process tested	RL-Purex-1	RL-Purex-1	RL-Purex-1	RL-Purex-1	RL-Purex-1	RL-Purex-2	RL-Purex-2	Con-Purex-1
Additives, g-moles per liter of waste solution								
H_3PO_4	2.0	2.5	3.5	2.4	2.4	2.4	2.2	
$LiOH \cdot H_2O$	1.1	1.4	1.9	1.4	1.4	1.37	1.37	
NaOH	1.1	1.4	1.9	1.3	1.3	1.27	1.27	1.0
$Ca(NO_3)_2 \cdot 4H_2O$	0.1							
NaH_2PO_2				0.1	0.1	0.1	0.1	
H_3BO_3			0.2					0.8
Silicic acid (80% SiO_2)								0.8
PbO								0.9
Operating temperature, °C	900–950	900–950	900–950	900–950	900–950	800–850	800–850	900
Time at operating temperature, hr	14.0	15.0	13.0	13.8	14.0	14.0	14.0	60.0
Volume reduction								
volume waste/volume solid	9.0	7.7	5.7	7.7	7.7	7.0	7.0	12.0
gallons solid per metric ton of U processed	11.1	13.0	17.5	13.0	13.0	14.3	14.3	9.0
Container corrosion	Negligible	High[d]	High[d]	Moderate	High[d]	Moderate	Moderate	Negligible[e]
Solid product (solubility and general appearance)	Soluble	Satisfactory	Satisfactory	Satisfactory	Satisfactory	Porous	Satisfactory	Satisfactory
Volatility and entrainment, % of total present								
Li	0.01	3.6	0.20	0.18	15.2	1.00	0.18	
Fe	0.12	3.3	0.17	0.13	15.6	1.80	0.27	0.34
PO_4	0.10	3.4	0.41	0.41	12.0	0.28	0.15	
Mo	0.63	4.6	0.59	0.70	12.7	1.71	0.96	1.38
Cs		4.4	0.63	0.49	14.6	0.26		9.0
Ru	53.3	38.4	39.5	34.4	38.6	27.7	30.8	12.5
Zr	1.9		<0.37	0.26		0.39	0.32	0.09
SO_4						15.0	11.3	

[a]Melts numbered 478 and higher are not included in this initial publication (ref. 3).

[b]Operated under flowing NO. Fluctuation in flow rate caused upsets in operation, resulting in excessive entrainment and excessive corrosion.

[c]The ratio chemical equivalents (alkalies + alkaline earths)/chemical equivalents (nonvolatile anions) < 1.

[d]Thermocouple wells corroded through.

[e]See Table 4.4 for detailed corrosion data.

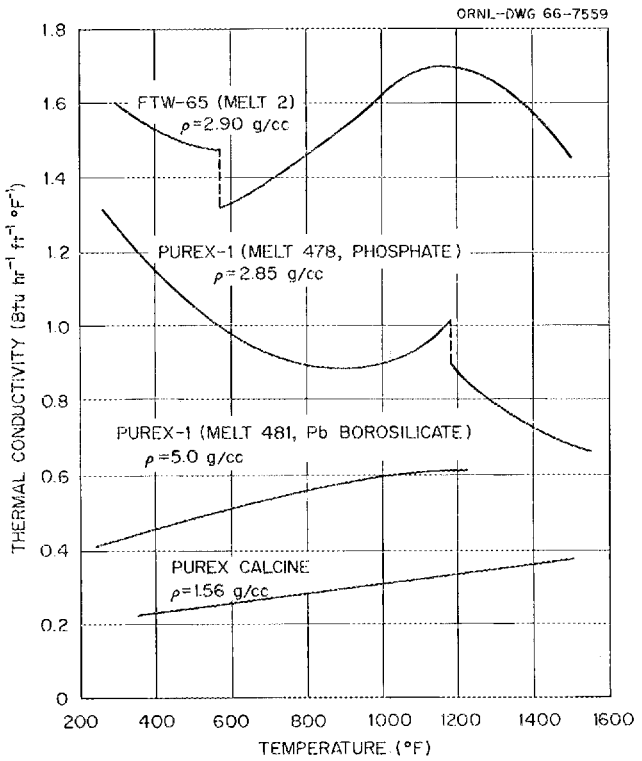

Fig. 4.1. Thermal Conductivities of Purex Disposal Solids.

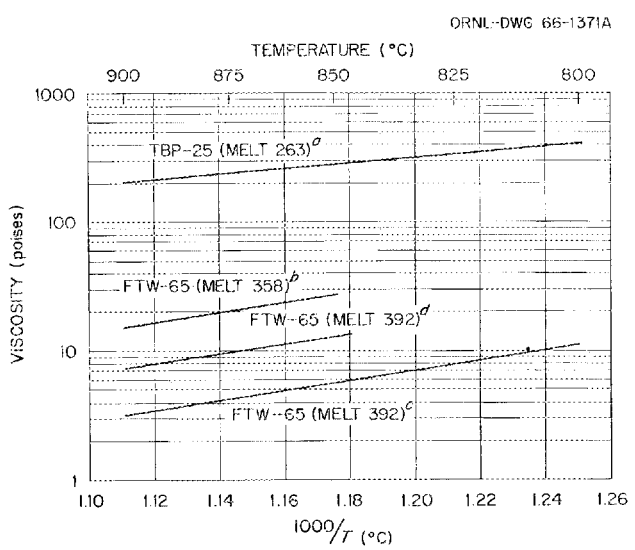

Fig. 4.2. Viscosities of Phosphate Melts Incorporating Simulated Radioactive Wastes. For melt compositions, see ref. 4. (*a*) 26.1% process oxides; (*b*) 40% process oxides, no simulated fission products; (*c*) 20% process oxides, no simulated fission products; (*d*) c plus simulated fission products equivalent to a burnup of 10,000 Mwd/metric ton.

tion of simulated fission products equivalent to a burnup of 10,000 Mwd/metric ton (composition 1, Table 4.2) decreased in viscosity from 13 poises at 850°C to 7 at 900°C.

Small-Scale Rising-Level Process Tests. – Seven semiengineering-scale Rising-Level (RL) Potglass tests were made, using phosphate melts: five with Purex-1 and two with Purex-2. The wastes contained simulated fission products equivalent to a burnup of 20,000 Mwd/metric ton. Fixation of Purex-1 waste in these melts required a higher temperature (900 to 950°C) than the 900°C maximum that is desirable when stainless steel pots are used. At about 950°C, corrosion was correspondingly severe (see below, "Corrosion with Phosphate Melts") except in melt 422, which contained added calcium and which solidified to form a product with rather unsatisfactory properties (Table 4.3). Substitution of 0.1 *M* NaH_2PO_2 (melt 478) for a small fraction of the Na^+ and PO_4^{3-} in a melt containing no added Ca^{2+} (melt 423) decreased the corrosiveness somewhat (Table 4.3). Further development is required to obtain Purex-1 melts that have suitably low corrosion rates and melting points.

Corrosion with Phosphate Melts. – The occasional unexplained cases of severe corrosion that have occurred in RL-Potglass experiments and during thermal conductivity tests on phosphate melts have resulted in the postponement of tests planned for this process in the WSEP at PNL. Corrosion incidents which contributed to this decision are summarized below (see also ref. 2).

1. Purex-1 Waste (High Iron Content, No Sulfate):
   (*a*) Melt 478. Crushed solid material from engineering run 91 (see "Demonstration of Rising-Level Potglass Process," below) corroded through the ¼-in. walls of the thermocouple wells (type 304L stainless steel) during 4 hr at 850 to 900°C. In a second experiment, severe corrosion did not occur after 2 hr at 850 to 900°C followed by cooling to room temperature and then a slow rise in temperature (for thermal conductivity measurement), ending at 830°C for 24 hr.
   (*b*) Melt 478. In two engineering-scale tests at 900°C, run 91 showed negligible corrosion, while run 92 showed heavy corrosion (see Demonstration of Rising-Level Potglass Process," below).

(c) Specimens of types 304L and 310 stainless steels ($\frac{1}{4}$-in.-diam rods) were partially immersed in melt 478 at 950°C for 69 hr under an atmosphere of air. The 310 steel was completely destroyed, and the 304L was heavily corroded. In similar tests at about 850°C for 24 to 72 hr in air and in argon, corrosion was generally less severe. Less corrosion occurred under argon than in air, and the B 10 steel was more heavily corroded than the 304L. Quantitative measurement of corrosion was not possible.

2. FTW-65 Waste (High Sulfate Content, Medium Iron Content):
   (a) Melt 2.[4] A thermal conductivity test on RL-Potglass "glass" in situ resulted in failure of the $\frac{1}{16}$-in.-wall center tube (304L) when kept at 830°C for 24 hr.
   (b) Melt 358. Crushed solid material was melted down for thermal conductivity measurements. The $\frac{1}{16}$-in. wall of the heater well (304L) failed during the second of two successive periods of heating to 850°C for 3 to 4 hr.
   (c) Melt 357. Of two engineering-scale tests at ORNL and one at PNL, one test at ORNL at 900°C showed heavy corrosion, but corrosion was negligible in the other two at 825 to 850°C (see Sect. 4.3).

Many of the above tests are not truly representative of the conditions prevailing during the actual RL-Potglass solidification process. However, when combined with the occasional cases of severe corrosion observed in small-scale RL-Potglass experiments (Table 4.3), they indicate the need for further study of corrosion under varying RL-Potglass conditions, and particularly the need for a knowledge of the corrosion mechanism.

Ruthenium Volatility Studies. – In the pot processes, it is expected that the volatilization of ruthenium will be controlled by recycle of the pot off-gas to the evaporator. In the evaporator, the nitric acid is steam stripped from the combined feed and pot condensate to yield a condensate containing very little ruthenium. Engineering-scale tests have indicated the validity of this approach,[1] and more recent laboratory tests further confirm it.[2] For example, variation of ruthenium concentration from 0 to 1.0 mg/ml in a simulated pot off-gas stream recycled to the evaporator resulted in volatilization of less than 1% of the ruthenium in all cases. If necessary, small concentrations of a reductant (e.g., NaH_2PO_2) can be added to reduce the volatility by factors of 38 to 2500.[5]

Volatility-Waste-Process Development Program. – The fluidized-bed volatility process for recovering uranium and plutonium from spent fuel elements produces substantial quantities of highly radioactive solid wastes (see Sect. 2). These wastes consist of alumina powder (bed material) with fission product fluorides. The purpose of this program is to develop and demonstrate laboratory-scale processes for converting these waste powders into a form suitable for permanent disposal.

Three primary alternatives are being considered: (1) sealing the contaminated alumina powder in a stainless steel can, omitting any kind of processing; (2) dispersing the powder in a glass, metal, or polycrystalline solid and canning it; and (3) incorporating the powder in a glass or polycrystalline solid and canning the product. Any of these forms would be suitable for shipment to a salt mine for permanent disposal (see Sect. 4.4).

Dispersion in Glass. – Initial studies were concentrated on dispersing the bed material in a glass. Tests with 60- to 300-mesh alumina or alumina containing 25 wt % "stainless steel oxides," plus stand-ins for fission products to simulate the solid wastes, showed that dispersion in glass is feasible by simply melting a high-density glass placed on top of the powder. The glass flows down into the powder to form a continuous matrix surrounding the particles. The method was also tested with bed material (alumina containing a mixture of stainless steel oxides and fluorides) obtained from "cold" engineering tests (see Sect. 2.2). The glass was a powdered commercial lead borosilicate glass (Corning No. 8463; density, 6.2 g/cc). It was placed on top of the bed material, melted, and held for 1 hr at 600°C. The product was mechanically strong, but the homogeneity was uncertain, as indicated by color variations, presumably resulting from the iron. This same effect was noticed with a glass consisting of 12.5% B_2O_3–87.5% PbO (by weight).

Optimum glass/bed weight ratios for the dispersion experiments (i.e., no reaction between bed material and glass) were about 2/1. The weight

[5] H. W. Godbee and W. E. Clark, "Use of Phosphate and Hypophosphite to Fix Ruthenium from High-Activity Waste in Solid Media," *Ind. Eng. Chem. Prod. Res. Develop.* 2, 157 (1963).

of bed material varied from 25 to 120 g, and dispersion times and temperatures varied from ½ to 1 hr at 600 to 650°C, depending upon the size of the bed particles. Under the same conditions, faster removal of air bubbles and faster mixing occurred when vacuum was applied at the bottom of the container. The engineering feasibility of, or the need for, the vacuum has not been determined.

Since ZrF_4 is one of the possible solid wastes requiring disposal, and also one of the fission product fluorides, its behavior in contact with low-melting (500 to 600°C) lead borosilicate glasses must be known. Thermodynamic analysis shows that the reaction between ZrF_4 and SiO_2, B_2O_3, or PbO is highly probable at the temperatures mentioned above. To determine whether these oxides, when present as a glass, will react with ZrF_4 at these temperatures, a thermogravimetric analysis (weight loss with temperature) was run with a mixture of ZrF_4 powder and a powdered commercial lead borosilicate glass. A sample containing 2.1378 g of ZrF_4 and 4.2690 g of glass was heated to 600°C and held at this temperature for 2 hr. An exothermic reaction occurred between 450 and 500°C. The weight loss over this 50° interval was about half the total weight loss of 3.63%.

Dispersion in a glass without premixing of the bed material and powdered glass was studied by two additional techniques. The first was to premelt the high-density glass and pour it on the bed material, and the second was to place the bed powder over a solid low-density glass and then melt the glass. The first technique produced the same quality product as obtained by melting the high-density glass on top of the bed material. Initial attempts with sinking the bed powder in a low-density glass were unsuccessful since the type of glass tested (Na_2O-P_2O_5 eutectic, density about 2.5 g/cc) reacted with the bed material to form an extremely viscous melt that prevented further mixing.

Incorporation Studies. – Scouting studies were made of the feasibility of preparing homogeneous glasses by contacting the bed material with various fluxes. Among the latter were the Na_2O-P_2O_5 eutectic and the PbO-B_2O_3 melts, as well as the combination of additives (NaH_2PO_4, Na_2HPO_4, $Na_4B_2O_7$) necessary to produce the aluminum borophosphate glass listed in the ORNL melt catalog as melt 284. The Na_2O-P_2O_5 and PbO-B_2O_3 melts did not produce satisfactory materials at 800°C. Melt 284, containing 35.4% (by weight) of waste cladding oxides, produced a seemingly homogeneous glass. Here, the powders were mixed, melted, and held at 900°C for 1 hr.

Characterization studies were started on simulated bed materials obtained from the ANL, BNL, and ORNL fluidized-bed development programs (see Sect. 2). These studies include the measurement of bulk density of the bed powder in the as-poured state and after compaction; chemical and physical stability determinations as a function of temperature, using thermogravimetric and differential thermal analysis; thermal conductivity measurements on the as-poured and compacted bed material as a function of temperature; and solubility and other physical measurements.

The effective thermal conductivities, k_e, of the various two-phase systems considered for disposal of the bed material were estimated by using theoretical equations for the thermal conductivity of mixtures.[6] These estimated values of k_e show that the thermal conductivity of the bed material could be increased by factors of 10 to 230 over that in air by judicious selection of the matrix in which the bed material is dispersed (Table 4.4). Reasonable values of conductivity (see, for example, Fig. 4.1) for the bed material incorporated into a glass or crystalline solid – single phase – are also given in Table 4.4. These values show that the conductivity of the bed material is increased over that in air (by factors of 2 to 3), but not nearly so much as with the dispersions.

The maximum volume percent of Al_2O_3 that can be readily incorporated in glasses or polycrystalline solids is 15 to 25% (Table 4.4). This is economically important since it shows that the number of storage cans required to contain a given amount of waste will be two to six times larger if the alumina is incorporated (dissolved) rather than dispersed. Therefore, it was tentatively concluded that dispersions are better than solid solutions because they have higher thermal conductivities, smaller volumes, and probably equally low solubilities.

---

[6]H. W. Godbee, *Thermal Conductivity of Magnesia, Alumina, and Zirconia Powders in Air at Atmospheric Pressure from 200°F to 1500°F*, ORNL-3510 (April 1966).

Table 4.4. Estimated[a] Thermal Conductivity of Fluidized-Bed Waste Solids in Various Media at 500°F

Continuous Phase	Discontinuous Phase	Volume Percent Al_2O_3	Thermal Conductivity (Btu hr^{-1} ft^{-1} $°F^{-1}$)		
			Continuous Phase, k_c	Discontinuous Phase, k_d	Mixture or Single Phase, k_e
		Two-Phase Systems			
Air	Al_2O_3	60	0.025	11	0.32
Aluminum	Al_2O_3	60	130	11	74
Glass	Al_2O_3	60	0.5	11	3.2
Crystalline solid	Al_2O_3	60	2	11	5.6
		Single-Phase Systems			
Glass		15–25			0.5
Crystalline solid		10–15			1

[a]Using mixture equations given in ref. 6.

Engineering Studies

Demonstration of RL-Potglass Process – *FTW-65 Purex Waste.* – A final test (R-90) of the RL-Potglass process with FTW-65 Purex waste was made in an 8-in.-diam × 96-in.-high pot, using melt 357[4] (Table 4.5). The operating temperature was limited to 850°C since laboratory studies had indicated that the viscosity and corrosivity of the melt were satisfactorily low at this temperature. Also, a previous test at 900°C (R-89) in an 8-in.-diam pot had shown that the corrosion rate was excessive (Table 4.6). Test R-90 proceeded smoothly, and the corrosion was negligible – 15 mils. The original wall thickness of the pot was 320 mils. The same melt was also successfully tested at PNL in a 12-in.-diam pot. In this test, a dense solid product was formed, and there was no evidence of any corrosion.

PW-1 Purex Waste. – Test R-91 was an RL-Potglass test made in an 8-in.-diam pot, using simulated PW-1 waste and lithium and sodium phosphates as glass-making additives (Table 4.7). Phosphite was also added to provide a reductant to decrease corrosion (see "Small-Scale Rising-Level Process Tests," above). The waste, additives, and simulated fission products were combined in the feed tank and fed to the pot as a single stream, as in all previous tests. A precipitate formed in the feed tank, making it difficult to control the flow rate of the resultant slurry to the pot. However, the test was completed, and a satisfactorily dense glassy product was formed. Corrosion was negligible, less than 5 mils (Table 4.6).

Test R-92 was a duplicate of R-91, with two exceptions: (1) a 12-in.-diam pot was used to determine the effect of pot diameter on processing rate, and (2) the glass-making additives and phosphite were added as a separate, proportionated stream in the waste feed line to the pot. Test R-92, which lasted for 100 hr, was conducted in a stainless steel (304LC) pot, 12 in. in diameter and 6 ft high. The pot was heated in an induction furnace having a 15-in.-diam susceptor.

Because of malfunction of the proportional feed system, an excess of about 26% of the additive phosphate solution was added during the first 20 hr of operation, and the proper feed ratios were not reached until the 44th hour. This may have caused the excessive corrosion observed in the bottom of the pot, since laboratory experience indicates that an excess of phosphate frequently leads to excessive corrosion. Undoubtedly, these

Table 4.5. Composition of FTW-65-X3[a] Simulated Purex Waste and Additives for Runs R-89, R-90

Expressed as gram-moles per liter of original waste

Melt 357;[4] approximate mp 800°C

Constituent	Concentration	Constituent	Concentration
H^+	1.5	SO_4^{2-}	0.45
Na^+	0.9	PO_4^{3-}	0.015
Al^{3+}	0.15	SiO_3^{2-}	0.03
Fe^{3+}	0.30	F^-	0.0015
Cr^{3+}	0.06	NO_3^-	~3.1
Ni^{2+}	0.03	Fission products[b]	0.5
Hg^{2+}	0.0105		
Additives		Additives	
H_3PO_4	3.6	NaOH	2.7
LiOH	2.4	$Al(NO_3)_3$	0.75

[a]The FTW-65-X3 represents the highest concentration of this waste type that can be conveniently simulated by direct makeup from laboratory reagents without heating the solution.

[b]Hanford-BNL simulated-fission-product composition equivalent to a burnup of 10,000 Mwd/metric ton (Table 4.2). Total waste oxides = 30 wt %.

Table 4.6. Corrosion Results in Rising-Level Potglass Engineering-Scale Test

Diameter of pot, 8 in.

Run	Waste Type	Equivalent Fission Product Level (Mwd/metric ton)	Additive[a]	Operation Temperature (°C)	Operation Time (hr)	Additive Addition Method	Maximum Corrosion Depth (mils)
R-89	FTW-65-3X	10,000	Type 1	900	45[b]	Pre-mix	320
R-90	FTW-65-3X	10,000	Type 1	850	97	Pre-mix	15[c]
R-91	PW-1	20,000	Type 2	900	64	Pre-mix	<5[d]
R-92[e]	PW-1	20,000	Type 2	900	100	Feed line	239

[a]Type 1: 2.7 moles NaOH, 2.4 moles LiOH, 0.75 moles $Al(NO_3)_3$, and 3.6 moles H_3PO_4 per liter of waste. Type 2: 1.27 moles NaOH, 1.37 moles LiOH, 2.4 moles H_3PO_4, and 0.1 mole NaH_2PO_2 per liter of waste.

[b]Failure occurred.

[c]Pot cooled and solids remelted and held at 700 to 800°C for 30 additional hours.

[d]Crushing and remelting caused failure of 28-mil-wall tubing.

[e]Pot diameter, 12 in.

Table 4.7. Composition of Purex-1 Simulated Purex Waste and Additives for Runs R-91, R-92

Expressed as gram-mole per liter of original waste

Melt 478 (Table 4.3)

Constituent	Concentration	Constituent	Concentration
H^+	5.0	Fission products	
Fe^{3+}	0.93	Sr^{2+}	0.015
Na^+	0.14	Ba^{2+}	0.019
H_3PO_4	0.003	Rare earths	0.118
NO_3^-	7.8	Zr^{4+}	0.065
Ni^{2+}	0.005	MoO_3	0.065
Al^{3+}	0.001		
Cr^{3+}	0.012		
Additives		Additives	
NaOH	1.27	H_3PO_4	2.40
LiOH	1.37	NaH_2PO_2	0.10

variations in proportional feed rates can be controlled and prevented by suitable modifications of the equipment. Consequently, proportional addition of the glass-making additives is recommended. Severe corrosion (up to 239 mils) occurred in the bottom zone of the pot and decreased to nearly zero at the top. The exact reason for the high corrosion rate in test R-92 compared with the rate for R-91 is unknown but could have been caused by (1) improper mixing of waste and additives, (2) additional length of operating time at temperature, or (3) unpredictable corrosivity at high temperatures. It was concluded that sharper definition of the corrosion mechanism is required before large-scale tests with radioactive feeds are attempted.

4.2 INTERMEDIATE-LEVEL RADIOACTIVE WASTE

The intermediate-level wastes (ILW's) generated in nuclear installations generally have been stored in tanks or mixed with cement. These wastes include second- and third-cycle raffinates; solutions from decladding, solvent cleanup, and off-gas scrubbers; and slurries and solids from processes for decontaminating process waters. These wastes are characterized by their modest levels of radioactivity (heating and radiation dose levels are not serious problems) and by their high salts or solids content, which prevents their efficient treatment by conventional methods such as ion exchange or precipitation. Still, neither tank storage nor solidification in cement is completely satisfactory. Tank storage is only a temporary measure, and the products formed by mixing the waste with cement are only moderately insoluble and represent a volume increase. In addition, most operations with cement are dusty, good mixing is difficult to achieve, and the operations are cumbersome.

A promising recent development is the use of asphalt to solidify and insolubilize these wastes. Immobilization of wastes by incorporation into such a cheap, insoluble material as asphalt before burial or other storage can reduce not only treatment costs but also the flow of radioactivity to the environment. Plants for incorporating ILW in asphalt have been developed in Belgium[7] and France.[8] In the process being developed at

[7] P. Dejonghe, in *Third United Nations International Conference on the Peaceful Uses of Atomic Energy*, A/CONF. 28/P/774 (May 1964).

[8] G. Wormser, J. Rodier, and E. de Robien, in *Third United Nations International Conference on the Peaceful Uses of Atomic Energy*, A/CONF. 28/P/86 (May 1964).

ORNL, wastes are introduced into an emulsified asphalt at any convenient temperature below the boiling point of the solution, water is volatilized by heating, the temperature of the product is raised so that it flows freely, and the product is drained into a steel drum for preliminary storage and shipment. Attractive features of the process include: use of emulsified asphalt, which flows readily at room temperature; evaporation at low temperatures to minimize entrainment of radiation emitters and thermal degradation of the asphalt; low agitation rates, which provide adequate mixing and keep the heated surfaces of the evaporator clean; operation in a batch or continuous manner; and incorporation of soluble or insoluble solids with equal effectiveness.

Status and Progress

Incorporating ILW in asphalt is a promising method for handling this type of waste, and no serious problems have been observed in the incorporation procedure. The products show acceptably low leach rates in water over long periods of time, with no significant increase at radiation levels up to 10^8 rads. A comprehensive hot-cell program is planned to determine the radiation limits for the asphalt system. Three prominent types of ILW will be tested and will contain 50 to 500 curies of mixed fission products per gallon. In particular, the effect of dose and dose rate on leaching of activity from the samples and on radiolytic gas formation in the samples will be studied. Engineering studies are planned with nonradioactive wastes; a 12-in.-diam by 16-in.-high Pfaudler wiped-film evaporator will be used. These studies will generate heat-transfer and flowsheet data as a function of waste type; flow rates, flow ratios, and speed of the rotor in the evaporator; and the temperature of the heated surface in the evaporator. Information will be gained on possible processing problems such as entrainment of asphalt, emulsifying agent, or radioactivity from the evaporator.

Process Description

The batch process consists in (1) adding the waste directly to emulsified asphalt in an evaporator, which contains a stirrer and a bottom outlet, at any convenient temperature up to about 100°C, with a low stirring rate (about 150 rpm); (2) evaporating the water and raising the temperature of the product to about 160°C; and (3) draining the product into a disposal container (Fig. 4.3). In the continuous process, the waste and asphalt are introduced at the top of a wiped-film evaporator, and the mixture flows down the walls of the evaporator where the water is evaporated and the temperature of the product is raised to about 160°C. Agitator paddles or blades sweep the walls continuously at about 150 to 300 rpm and provide good mixing and heat transfer. The process was demonstrated in the laboratory with nonradioactive and radioactive waste in a 4-in.-diam by 6-in.-high batch evaporator, and on an engineering-scale with a 12-in.-diam by 16-in.-high Pfaudler wiped-film evaporator with 4 ft^2 of heat-transfer surface. The processing rate in the large unit was about 4 gal/hr of product containing 60 wt % salts (Table 4.8).

Mixtures containing 10 to 80 wt % salts from waste have been prepared from ORNL ILW, fuel-dejacketing waste (FDW), and from a Purex second-plutonium-cycle waste (2CW) (Table 4.8). The asphalts were emulsified asphalts used in the surface treatment of roads (type RS-2, a rapid-setting, high-viscosity emulsified asphalt; type SS-1, a slow-setting, low-viscosity emulsified asphalt). Both types contained nominally 63 wt % asphalt, 35 wt % water, and 2 wt % emulsifying agent. No apparent difference was observed in the products obtained with either type. In the engineering-scale tests, more oil was in the condensate when SS-1 asphalt was used. The mixtures that contained 70 to 80 wt % salts represented high volume reductions (volumes of waste per volume of product), but were not always homogeneous and free flowing. The products containing 60 wt % salts (Table 4.8) represent a good compromise of properties – volume reduction, homogeneity, viscosity, etc. Therefore, they were studied in greatest detail.

Solubility of Asphalt Products

The uniformity of the asphalt coating on the waste particles is measured by determining the leach rate of elements from the asphalt-salts product. Leach tests were carried out with distilled water at 25°C, and the water was completely renewed each week. In some tests, the water was circulated, but in most it was stagnant.

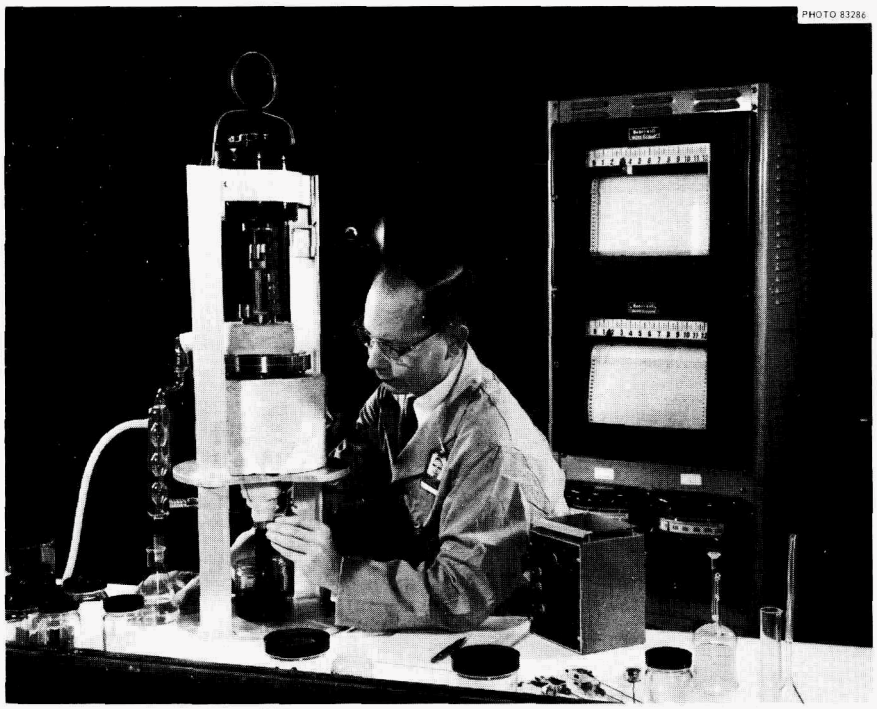

Fig. 4.3. Drawing a Sample of Asphalt-Containing Simulated ORNL Intermediate-Level Radioactive Waste from the Mixer-Evaporator Unit.

Table 4.8. Compositions of ILW's and the Asphalt Products Incorporating 60 wt % Salts from These Wastes

Component	ILW[a]		2CW + 1.1 NaOH[b]		FDW[c]	
	Waste (*M*)	Asphalt Product (wt %)	Waste (*M*)	Asphalt Product (wt %)	Waste (*M*)	Asphalt Product (wt %)
Sodium	6.61	18.5	9.66	17.0	4.16	18.6
Nitrate	4.64	34.9	6.2	29.5	2.2	26.5
Hydroxide	2.06	3.8	2.82	3.7	0.06	0.2
Sulfate	0.35	4.1	1.13	8.5		
Aluminum	0.22	0.7			1.9	10.0
Ammonium	0.19					
Chloride	0.056	0.2				
Iron			0.54	2.3		
Asphalt		37.8		39.0		44.7
Density at 25°C, g/ml	1.34	1.5	1.33	1.5	1.21	1.5
Volume of waste/ volume of product		2.0		1.7		2.6

[a]Oak Ridge National Laboratory intermediate-level waste (evaporator bottoms).
[b]Purex second-plutonium-cycle waste, neutralized with 10% excess NaOH.
[c]Aluminum fuel-dejacketing waste.

The leach rate, expressed as the fraction of the activity in the sample leached per day through unit specific surface, was calculated from the relation:

$$\frac{\text{(activity leached/total activity in sample)}}{\text{(surface area of sample/mass of sample) (time)}} = \frac{\text{fraction leached}}{(\text{cm}^2/\text{g})\ \text{day}} \equiv \text{fraction leached g cm}^{-2}\ \text{day}^{-1}\ .$$

The numerical value of this unit and the method of calculation are the same as those previously used,[9] but the terminology here appears better since it avoids the easily misinterpreted term – g cm^{-2} day^{-1}.

Asphalt products containing 20 to 60 wt % salts from simulated ORNL ILW were leached with water for periods of up to 16 months. The fraction of the ^{137}Cs or sodium leached per day through unit specific surface reached a steady-state value of 1.5×10^{-4} for the 20 wt % product and 3×10^{-4} for the 60 wt % product (Fig. 4.4). Hot-cell tests with actual ORNL ILW, containing 5 curies of mixed fission products per gallon, confirmed these tracer tests. After nine months of leaching, a product containing 60 wt % salts from ORNL ILW approached a steady-state value of 2×10^{-4} g cm^{-2} day^{-1} (Fig. 4.4).[10] After four months the fraction of the sodium leached from products containing 20 to 60 wt % salts from simulated dejacketing or second-cycle wastes was nearly the same as that obtained with simulated ORNL ILW. The fraction of ^{106}Ru leached from a product containing 60 wt % salts from simulated ORNL ILW reached a steady-state value of 7×10^{-6} g cm^{-2} day^{-1} (Fig. 4.4). Generally, the leach rates of asphalt products are 50 to 100 times lower than those of cement products containing similar amounts of waste salts.

Stability of Asphalt Products Toward Radiation

The radiation stability of asphalt products made with simulated wastes was determined by irradiation with a ^{60}Co source. Products containing 60 wt % salts from simulated ORNL ILW, FDW, and 2CW were prepared from a hard-base asphalt and irradiated to doses of 10^6 to 10^8 rads. As reported previously[9] for ILW, a dose of 10^6 rads showed negligible effect, a dose of 10^7 caused slight swelling (Fig. 4.5), and a dose of 10^8 rads caused a sample to swell about 36% in volume. The results with samples containing salts from FDW and 2CW are about the same as those with ILW. In contrast, similar samples prepared from a soft-base asphalt and irradiated to a dose of 10^8 rads showed only a slight increase in volume (Fig. 4.5). An asphalt product containing 10 curies/gal would receive a dose of 10^8 rads in an infinite period.[11] Thus, soft-base asphalt should be

[9] H. W. Godbee *et al.*, *Chem. Technol. Div. Ann. Progr. Rept. May 31, 1965*, ORNL-3830, pp. 116–117.

[10] J. H. Goode, *Fixation of Intermediate-Level Radioactive Waste in Asphalt: Hot-Cell Tests*, ORNL-TM-1343 (Nov. 18, 1965).

[11] H. W. Godbee *et al.*, *Chem. Technol. Div. Ann. Progr. Rept. May 31, 1964*, ORNL-3627, pp. 109–110.

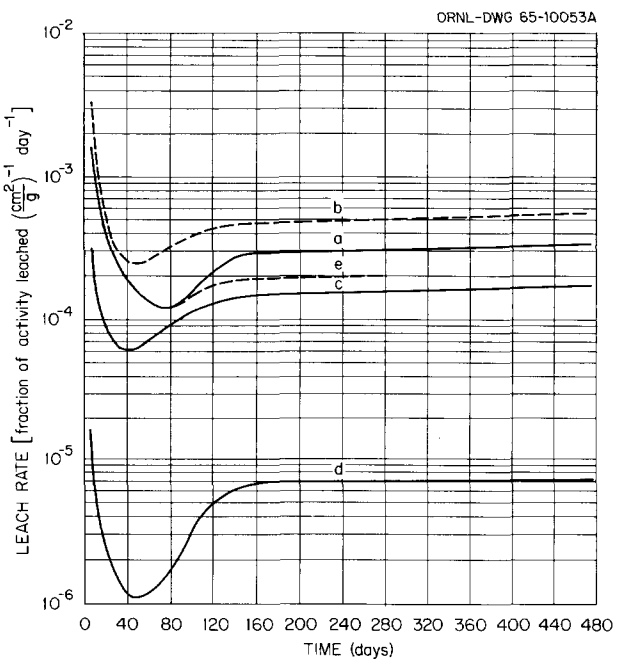

Fig. 4.4. Leach Rates of Asphalt Products Incorporating Simulated ORNL Intermediate-Level Waste. Sodium and ^{137}Cs from product containing 60 wt % solids with (*a*) stagnant and (*b*) flowing water and (*c*) containing 20 wt % solids with flowing and stagnant water. (*d*) ^{106}Ru from 60% product with stagnant water. (*e*) ^{137}Cs from product containing 10 curies/gal and 60 wt % salts from actual ORNL ILW.

PHOTO 81049R

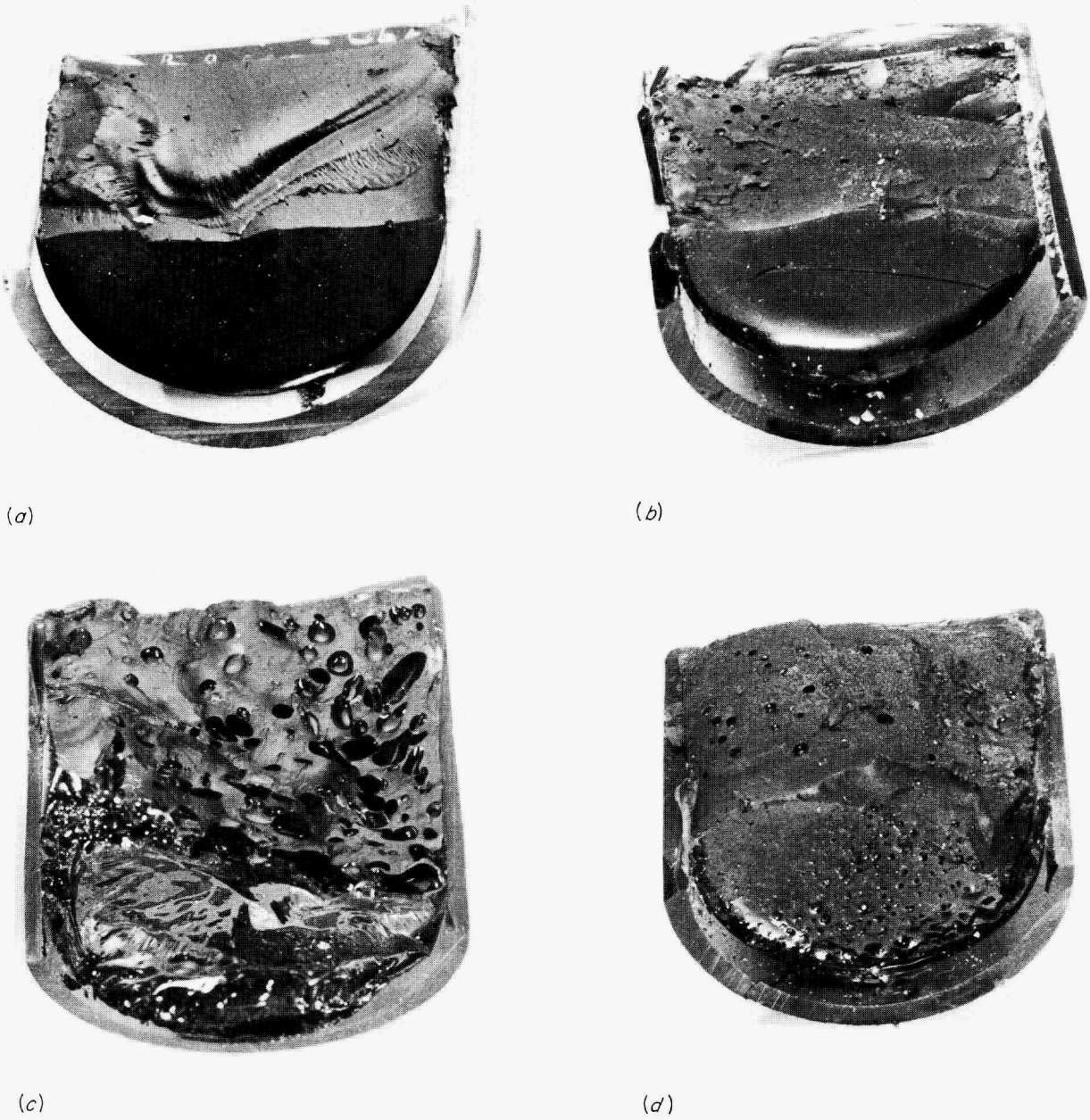

Fig. 4.5. Cross Sections of Asphalt Products Containing 60 wt % Salts from Simulated ORNL Intermediate-Level Waste. (*a*) Unirradiated; (*b*) hard asphalt irradiated to 10^7 rads; (*c*) hard asphalt irradiated to 10^8 rads; (*d*) soft asphalt irradiated to 10^8 rads.

satisfactory from the standpoint of radiation stability. A product containing about 10 curies per gallon of mixed fission products from ORNL ILW had, as mentioned above, about 2×10^{-4} fraction of the activity leached per day through unit specific surface after nine months (about 10^7 rads) (Fig. 4.4). This result is practically the same as that obtained with the nonradioactive products. No radiolytic gases were released over this period, and a volume increase was not visibly perceptible upon examining the sample in its container. However, a few small bubbles were observed in the product after breaking it open (Fig. 4.6). Leach tests on the ^{60}Co-irradiated samples indicate that irradiation to a dose of 10^8 rads does not affect the leach rate.

Hazards Survey

The incorporation of inert solids in asphalt does not appear to present any additional hazard to that normally present when processing, storing, or shipping an organic material with a high flash point. In fact, the flash point of an asphalt product should increase as the amount of inert solids increases. The hazards involved in incorporating an oxidant (nitrate salts) in asphalt were studied intensively. With small samples, the flash point of unirradiated asphalt, approximately 280°C, was lowered only about 50°C when the mixture contained 35 wt % nitrate and a total of 60 wt % salts. The flame was easily extinguished when the air was replaced by nitrogen, even though the solid-phase temperature was 400 to 500°C. Standard drop-weight, autoignition, shock sensitivity, and flame-propagation tests were made. Also, burning tests with 30-gal-drum samples showed that the asphalt-salt mixtures burn, as would be expected, but that they do not explode or show a significant increase in burning rate over that for pure asphalt. All these tests were made by a subcontractor.[12]

4.3 LOW-LEVEL RADIOACTIVE WASTE

Introduction

The objective in developing a water-recycle process is to provide a closed-circuit water-treatment system to decontaminate low-level radioactive waste (LLW) to drinking-water purity (with

[12]Subcontract 2604 with Atlantic Research Corporation, Alexandria, Va., "Safety Characteristics of Waste-Asphalt Product."

PHOTO 84320

Fig. 4.6. Asphalt Product Containing 10 Curies/gal and 60 wt % Salts from Actual ORNL ILW. Sample is broken to show bubbles formed on absorbing a dose of 10^7 rads.

respect to radioactivity) as specified by the U.S. Public Health Service (USPHS), and to permit the water to be returned to the nuclear installation for reuse. The remaining intermediate-level waste is mixed with asphalt and buried as solid waste. Reuse is in line with current United States policy, which encourages recirculation rather than discharge of waste water to rivers and streams.[13] This type of research and development is also directly applicable to the recycle of nonradioactive industrial and urban waste waters, where nearly complete clarification and demineralization are required.

Status and Progress

A micro pilot plant test with low-salt-content recycle water gave results that were very promising and that agreed well with those projected from tests with high-salt-content LLW.[14] Decontamination factors (DF's) of 1000 to 10,000 were obtained for all major radioactive species for up to 2400 volumes of waste treated per bed volume (BV) of cation resin; they were in the thousands for ^{131}I, ^{106}Ru, ^{90}Sr, and total rare earths, and in the ten-thousand range for ^{60}Co and ^{137}Cs; other radiation emitters – ^{144}Ce, ^{125}Sb, and ^{95}Zr-Nb – were reduced to the analytical limits of detection (Table 4.9). The product water also met USPHS standards for those nonradioactive elements determined. The usual salt content was reduced to less than 2 ppm, a greater than 20-fold reduction. Several more cycles will be run to determine whether buildup of contaminants occurs. The results will be used to predict the cost of processing and reusing water in a full-scale plant. The prospects seem good because results from small-scale laboratory work have been largely confirmed in the micro pilot plant tests.

Experimental Work and Results

The process consists in (1) coagulating by zeta-potential-controlled additions of the coagulant, alum, and the coagulant aids, activated silica and a nonionic organic polyelectrolyte; (2) clarifying by upflow through a fluidized bed of sludge (upflow clarifier) followed by filtering through a bed of anthracite coal and sand; (3) demineralizing by cation-anion exchange; and (4) sorbing the remaining radioactive and nonradioactive contaminants on granular activated carbon (Fig. 4.7).

A micro pilot plant test was made with synthetic recycle waste water – a low-salt-content water consisting of decontaminated and demineralized LLW treated by this process (80%), raw LLW (20%), and radioactive tracers. Continuous operation of the coagulation-clarification system under optimum conditions was important to the maintenance of high DF's for radionuclides such as cobalt and ruthenium which, in neutral waste, exist in several forms, including colloidal and ionic. The efficient removal of colloids is associated with the neutralization of their mutually repelling surface charges, as measured by zeta potentials (ZP).[15] For synthetic recycle water, the successive addition of activated silica (0.5 ppm as SiO_2) and alum [2 to 3 ppm as $Al_2(SO_4)_3$] in the flash mixer changed the ZP from -20 mv to $+3$ mv. The alum dose was one-tenth of that required for treating the high-salt-content LLW. Stirring at 1750 rpm effectively enmeshed the colloids within the freshly formed aluminum hydroxide floc. The addition of 75 ppb of a nonionic organic polyelectrolyte (Purifloc N-12, made by Dow Chemical Company) at the flocculator enhanced the growth and settling properties of the floc (Fig. 4.8) and accomplished the desired filtering action in the upflow clarifier (the primary filtering medium) by maintaining a fluidized bed of sludge. The final ZP was -2 mv. After coal-sand filtration, the water had a clarity comparable to that of distilled water, representing a greater than 100-fold decrease in turbidity.

In the demineralization-carbon system, specific conductance was a simple indicator of resin-bed exhaustion because ionic breakthrough precedes breakthrough of the radioelements, as in the treatment of standard LLW.[14] As expected, the DF for bulk ions was less than that obtained for standard LLW: 100 to 200 instead of 500, simply because the specific conductance of the recycle water, at 80 to 100 micromhos/cm, was only one-fourth to one-third of that for LLW, while the value for water after demineralization was the same in both cases.

---

[13] J. W. Gossett, *Chem. Process. (Chicago)* **28**, 29 (1965).

[14] *Chem. Technol. Div. Ann. Progr. Rept. May 31, 1965*, ORNL-3830, p. 127.

[15] T. M. Riddick, *Tappi* **47**, 171 (1964).

Table 4.9. Product-Water Analysis of Low-Salt-Content Waste Treated by the Water Recycle Process[a]

A. Overall Decontamination Factors (DF's) for Radionuclides

	Individual Isotopes								Total Rare Earths	Gross Gamma	Gross Beta	Bulk Ions (specific conductance)
	^{144}Ce	^{60}Co	^{137}Cs	^{131}I	^{106}Ru	^{125}Sb	^{90}Sr	^{95}Zr-Nb				
Waste analysis, dis min^{-1} ml^{-1} or counts min^{-1} ml^{-1}	28.0	245	162	277	96	3.4	55.1	1.7	52.0	254	198	80[b]
DF's for product water	800[c]	37,000	14,000	3600	1230	210[c]	5700	350[c]	1900	270[c]	260[c]	200[b]

B. Wet Analysis

	Turbidity (JTU)[d]	Total Dissolved Solids (ppm)	Total Hardness (ppm $CaCO_3$)	Total Alkalinity (ppm $CaCO_3$)	Calcium Hardness (ppm $CaCO_3$	Na (ppm)	Al (ppm)	Si (ppm)	PO_4 (ppm)	SO_4 (ppm)	F (ppm)	Cl (ppm)	NO_3 (ppm)	C (ppm)
Waste water	10	e	24	19.6	21	3	<0.1	0.56	0.17	<2	0.26	<1	3	38
Product water	<0.05	<1	0.1	<1	<0.1	<0.1	<0.1	<0.1	0.02	<2	<0.02	<1	<1	<2
USPHS standards[f]	5	500	g	g	g	g	g	g	0.1[h]	250	1	250	45	1

[a]Alum–silica–nonionic polyelectrolyte clarification, cation-anion exchange, vegetable-based activated carbon. DF values for product water with a specific conductance of less than 1 micromho/cm.

[b]The dimensions of specific conductance are micromhos/cm.

[c]These are minimum values, since all of the radioactivity in the waste water was reduced to the analytical limits of detection (background).

[d]Jackson turbidity unit. Turbidities measured on low-angle turbidity meter. Ref.: A. P. Black and S. A. Hannah, *J. Am. Water Works Assoc.* **57**, 901 (1965).

[e]Not determined.

[f]U.S. Public Health Service Drinking Water Standards, 1962.

[g]No limits given

[h]No limit given. This figure is considered to represent the safe tolerance level in drinking water for man. Ref.: T. R. Camp, *Water and Its Impurities*, p. 93, Reinhold, New York, 1963.

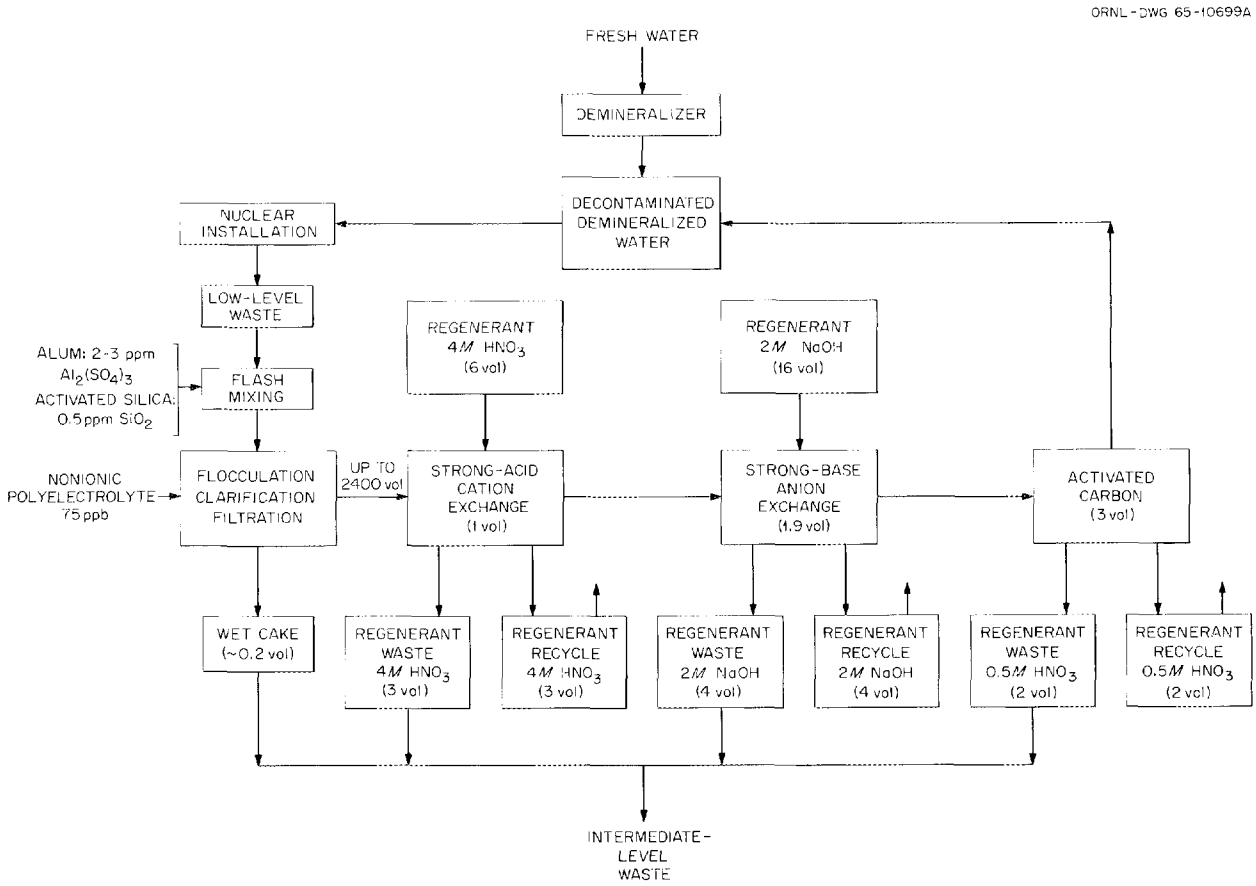

Fig. 4.7. Flowsheet for the Water Recycle Process.

A vegetable-based, granular activated carbon (Nuchar C-190, made by West Virginia Pulp and Paper Company) was used in preference to other commercial carbons because of its greater capacity for cobalt, according to the studies of Roberts and Abdel-Razek.[16] At the end of the run, ^{60}Co was eluted from the carbon column by 0.5 *N* HNO_3; 2.25 BV (equivalent to 6.75 cation resin volumes) decreased the activity to one one-hundredth of the original, while 4 BV (equivalent to 12 cation resin volumes) decreased it to one one-thousandth. However, cobalt elution is not really required during every resin-regeneration cycle because the carbon column is oversized to attain optimum contact time (equal to 3 cation resin volumes to give 12 min of contact time). No ^{60}Co breakthrough was evident at the conclusion of the run.

A principal objective of these runs was to accumulate a large inventory of decontaminated, demineralized water for a recycle test run. Data obtained in these runs demonstrated that (1) the pH of the raw waste must be in the range 7 to 8 prior to treatment (otherwise, poorly formed alum floc results in poor colloid removal, and a 35-fold decrease in the overall DF for ^{60}Co occurs), and (2) activated-carbon treatment should *follow*, not precede, cation-anion exchange. An additional carbon column inserted between the cation and anion exchange columns altered the chemical reactions of the ^{60}Co in the effluent from the cation exchanger and resulted in a 100-fold decrease in the DF for ^{60}Co.

[16] J. T. Roberts and I. Abdel-Razek, private communication about work being done at the University of Tennessee.

PHOTO 83266

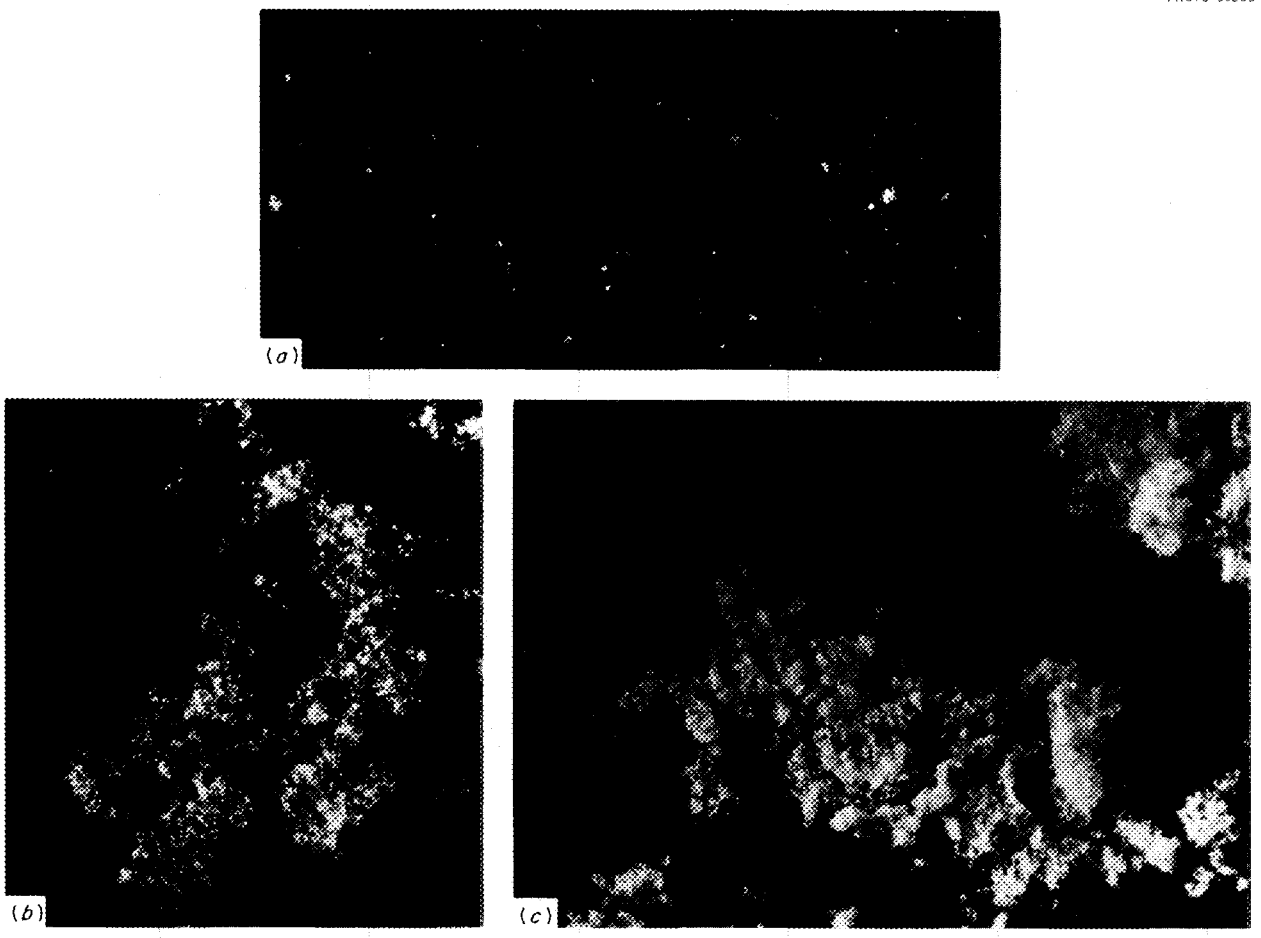

Fig. 4.8. Coagulation of Suspensoids by Use of Zeta-Potential Control. (*a*) Raw water contains suspended particles which have an average zeta potential (ZP) of −20 mv. (*b*) Alum [2 to 3 ppm $Al_2(SO_4)_3$] and activated silica (0.5 ppm, as SiO_2) are added with rapid stirring. Repulsive surface charges are neutralized to a ZP of +3 mv, and particles (the "stars") are enmeshed into the freshly formed small aggregates of aluminum hydroxide floc. (*c*) Floc growth is enhanced by the addition of a nonionic organic polyelectrolyte (75 ppb) which lowers the ZP to −2 mv. The water, after filtration, has a clarity comparable to that of distilled water.

4.4 ENGINEERING, ECONOMIC, AND SAFETY EVALUATION

During this report period, a study of the costs of perpetual storage of power-reactor fuel-processing wastes in tanks was completed, an analysis of the safety of tank storage was undertaken in cooperation with the Health Physics Division, and the economics of managing wastes from fluidized-bed volatility processing of power-reactor fuels was examined. The results of these studies are summarized below.

Costs of Perpetual Tank Storage

A study of the costs of perpetual storage of power-reactor fuel-processing wastes in tanks has been completed and published.[17] In this study, the costs are examined for three representative types of financing: government ownership, private ownership, and a combination of government and

[17] J. O. Blomeke *et al.*, *The Costs of Permanent Disposal of Power-Reactor Fuel-Processing Wastes in Tanks*, ORNL-2873 (September 1965).

private ownership. The case of government ownership includes only depreciation and interest on the investment capital; whereas, in the case of private ownership, costs reflect a 15% return on equity as well as allowances for depreciation, insurance, taxes, and interest. In the third case, private ownership is assumed during a 20-year period of waste accumulation, after which the government assumes responsibility for perpetual care of the tank farm. In each case, it is assumed that a permanent tax-free fund is established during the filling period and that the fund is of such size that the annual tax-free interest will be sufficient to provide for the periodic replacement of tanks and for the annual operating expense of the facility.

The tank farms were designed for storing raffinate wastes in both acid and alkaline forms, and in tanks ranging in capacity from 200,000 to 5,000,000 gal. Cladding wastes are neutralized and stored in 1,200,000-gal carbon-steel tanks. Capital costs were estimated for each case, then used in computer code TASCO to estimate total costs for each method of financing as a function of tank size, tank lifetime, and fission product concentration in the waste.

Raffinate Waste. – For the raffinate wastes, initial capital expenditures varied from $8 to $16 million, and the total over 20 years of waste accumulation ranged from $22 to $61 million. The annual operating expenses ranged from $0.3 to $0.4 million during the first year to $0.5 to $2.0 million during the 20th year. The magnitude of the permanent fund needed for "perpetual care" ranged from $22 to $72 million, and annual payments of $0.7 to $2.6 million are required to establish this fund. The total cost of perpetual storage of acid raffinate waste, in mills per kilowatt-hour of electricity generated, is plotted in Fig. 4.9 against tank capacity for tank lifetimes of 25, 50, and 75 years for the three cases of financing. Minima occur at a tank capacity of about 1,000,000 gal in all cases. These minima range from 0.0165 to 0.0184 mill/kwhr for case 1, from 0.0235 to 0.0253 mill/kwhr for case 2, and from 0.0251 to 0.0272 mill/kwhr for case 3. Total costs for alkaline waste storage are as much as 15% higher than the equivalent costs for acid

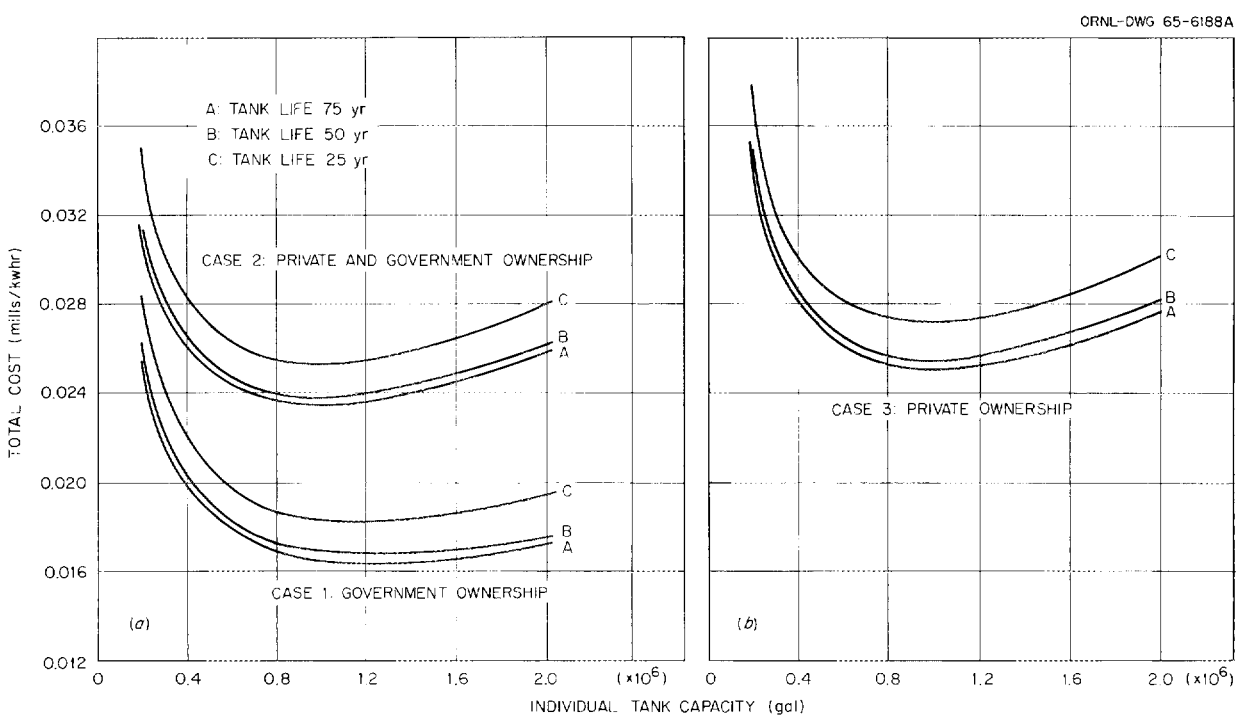

Fig. 4.9. Cost of Acid Waste Storage as a Function of Tank Capacity, Tank Life, and Method of Financing. (*a*) Case 1, government ownership; case 2, private and government ownership; and (*b*) case 3, private ownership.

storage (Fig. 4.10), and the optimum tank capacity is about 2,500,000 gal.

One of the least-certain aspects of the basis used for this study is the degree of fission product concentration that can be tolerated during storage. The concentrations adopted are based on a careful consideration of Savannah River and Hanford experience and are believed to be as great as practical for wastes of this type. To obtain an indication of the effect of fission product concentration on costs, a second set of costs was computed on the basis that the wastes are reduced to half the volume of the original design basis. In this instance, acid Purex and Thorex wastes are stored at 50 and 100 gal per ton of fuel, respectively, and alkaline Purex and Thorex wastes are stored at 300 and 600 gal/ton. This reduction in volumes caused a decrease of between 15 and 30% in total costs. The optimum tank size for acid-waste storage remained about 1,000,000 gal, whereas the optimum size for alkaline-waste storage dropped from about 2,500,000 to 1,500,000 gal.

These costs are about the same as those estimated for managing raffinate wastes by a series of operations including 30-year interim storage, conversion to solids, and shipment and final disposal of the solidified wastes in a salt mine.[18] The latter scheme is believed to offer greater safety than long-term tank storage and is the preferred approach.

Cladding Wastes. — The costs of cladding-waste storage were compiled independently of those for the raffinates. The initial capital cost in all cases was $3.5 million, and the total over 20 years was $52 million. The annual operating expenses ranged from $19,000 to $89,000 for the first year to $82,000 to $980,000 for the 20th year. The permanent fund varied from $17 to $78 million, and required annual deposits of $0.6 to $2.8 million. Total costs ranged from 0.0215 mill/kwhr

[18] J. O. Blomeke *et al.*, "Estimated Costs of High-Level Waste Management," *Symposium on the Solidification and Long-Term Storage of Highly Radioactive Wastes*, Richland, Wash., Feb. 14–18, 1966.

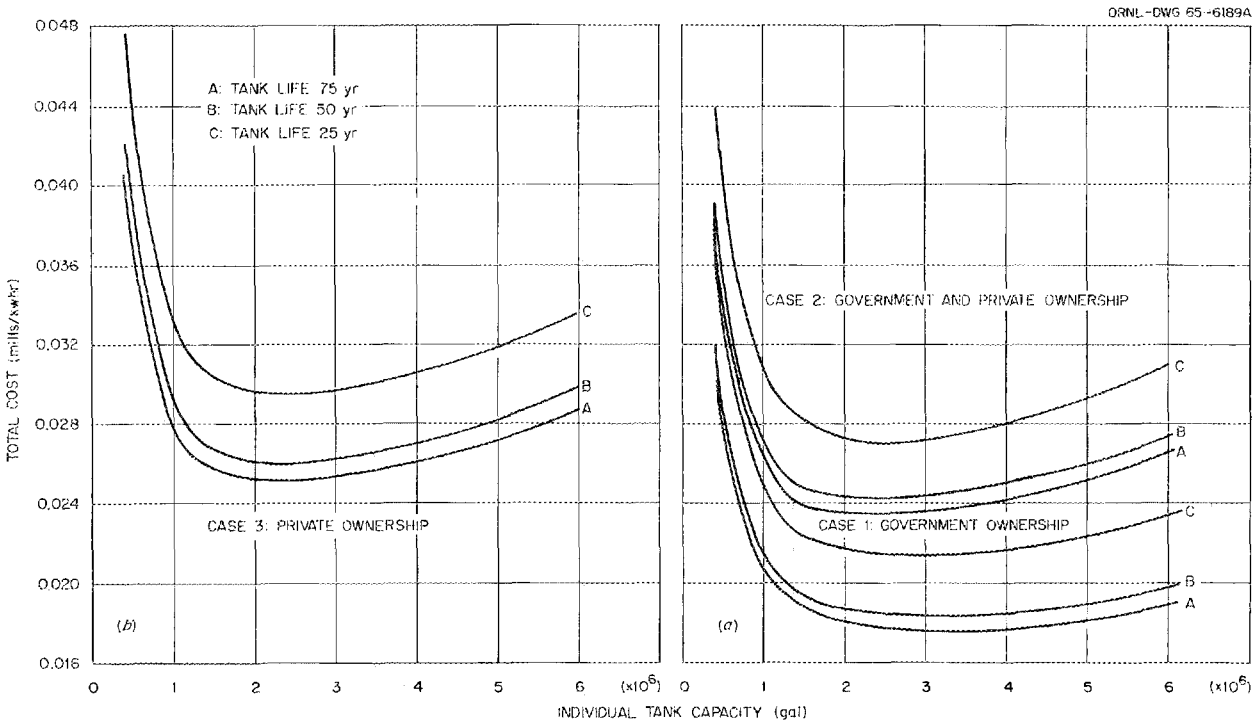

Fig. 4.10. Cost of Alkaline Waste Storage as a Function of Tank Capacity, Tank Life, and Method of Financing. (*a*) Case 1, government ownership; case 2, private and government ownership; and (*b*) case 3, private ownership.

for tanks of 75-year life with government ownership to 0.0398 mill/kwhr for tanks of 25-year life with private ownership. The total costs of cladding-waste storage, which are in every instance greater than the comparable costs for raffinate storage, are a consequence of the larger volumes.

A Safety Analysis of Tank Storage

A safety analysis of the tank storage of highly radioactive processing wastes from power-reactor fuels was undertaken, using the same basis as that adopted for the economic studies of waste management. A hypothetical tank farm is assumed to be located on the ORNL reservation, thus permitting a more detailed study to be made of the movement of accidentally released radionuclides by virtue of an existing thorough knowledge of the local environment. Tanks of Savannah River design with a capacity of 1,000,000 gal are assumed. When newly filled, they contain between 4 and 7 billion curies of radioactive fission products, depending on whether the wastes are stored as alkaline or acid solutions. Maximum heat generation rates range from about 40,000,000 to 70,000,000 Btu/hr.

The most likely mechanism of a major release is believed to be the loss of cooling. The worst possible time for this to occur would be when the tank is newly filled and the heat evolution rate is at its peak. In this event, the wastes would heat themselves to boiling in 10 to 20 hr. An additional 115 hr would be required for the acid waste to evaporate to dryness, and 240 hr would be required to evaporate the alkaline waste to dryness. It is estimated that decomposition of the inert and fission product salts would require 10 hr and 17 hr for acid and alkaline wastes, respectively, and that 24 to 47 hr would be needed for thermal decomposition of the concrete vaults. Assuming continued containment of the fission products (FP's) at this time, it is estimated that the maximum in-tank temperature would reach several thousand degrees Fahrenheit at the end of an additional hour.

Based on these considerations, two incidents are postulated (Table 4.10). In the first, it is assumed that cooling is interrupted for a time sufficient for the wastes to self-heat to boiling and that they boil for 10 hr with both the condenser and the filter out of service. Releases from an acid and an alkaline waste tank are as shown. This type of incident might be such as could be incurred by sabotage of the cooling and ventilation facilities above ground.

The second postulated incident assumes permanent loss of cooling, as might result from an explosion of radiolytic hydrogen in the tank. Hydrogen is produced in these tanks at such rates that, if the ventilation system failed, the lower explosive limit (4% H_2 in air) would be reached in only $1\frac{1}{2}$ to 3 hr, and our analyses indicate that quantities could accumulate which, if ignited, could rupture the tank and concrete encasement. In this event, if no effective remedial actions were taken, great atmospheric releases would be encountered over the ensuing 168 to 300 hr.

Assuming that the FP's associate with the normal dust particles in the air, and choosing a

Table 4.10. Postulated Incidents

Type of Incident	Quantities of Radioactive Fission Products Released to Atmosphere by:	
	Acid Waste	Alkaline Waste
1. Self-boiling for 10 hr without condenser and filter	300 curies/min of Ru; 10^3 curies/min of FP's (720,000 curies)	300 curies/min of FP's (180,000 curies)
2. Permanent loss of cooling	90% of Ru, Cs, and Te; 5% of other FP's – over 168 hr (1.1×10^9 curies)	50% of Ru; 25% of Cs and Te; 1% of other FP's – over 300 hr (1.5×10^8 curies)

typical particle size (that is to say, deposition rate), the gamma exposure rate (in r/hr) due to fallout is estimated to be that shown in Fig. 4.11 as a function of the distance downwind from an acid-waste tank. This is for incident 1 under conditions of rainfall and dry weather, at night. Here, it is assumed that the emitters do not lie directly on the surface but are distributed exponentially throughout the topmost layers, as in weapons fallout. Figure 4.12 shows similar curves for incident 2. The ground exposure rates for incident 2 are about 5000 times those for incident 1.

Figure 4.13 shows the ground-level concentration ($\mu c/cm^3$) at various distances downwind following the first incident, and the resulting exposure to the lungs from breathing the contamination over the duration of the incident. These dose equivalents are the result of integration over the first year.

Figure 4.14 gives the same information for incident 2. These results are about 1000 times those shown in Fig. 4.13.

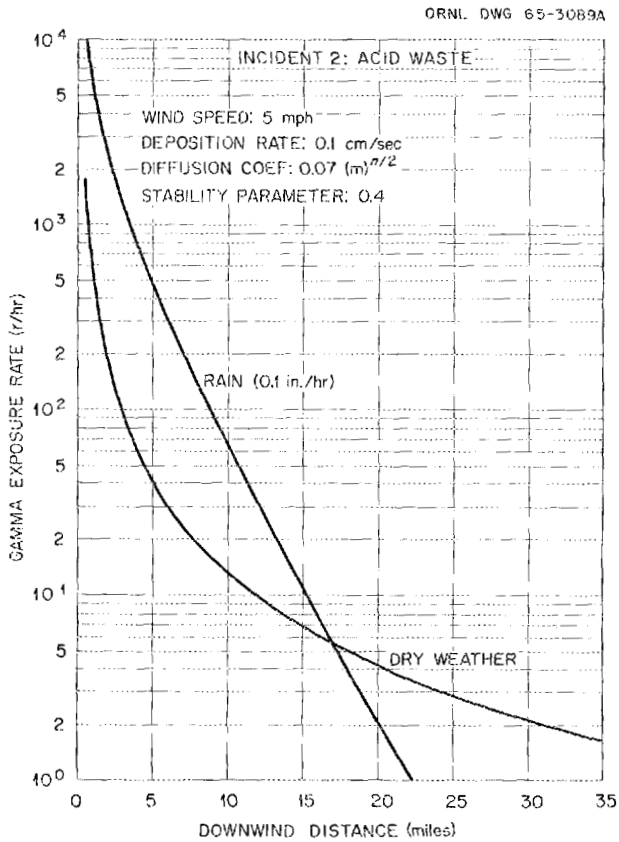

Fig. 4.12. Ground-Level Exposure Rate as a Function of Distance Downwind from an Acid Waste Tank Following Permanent Loss of Cooling.

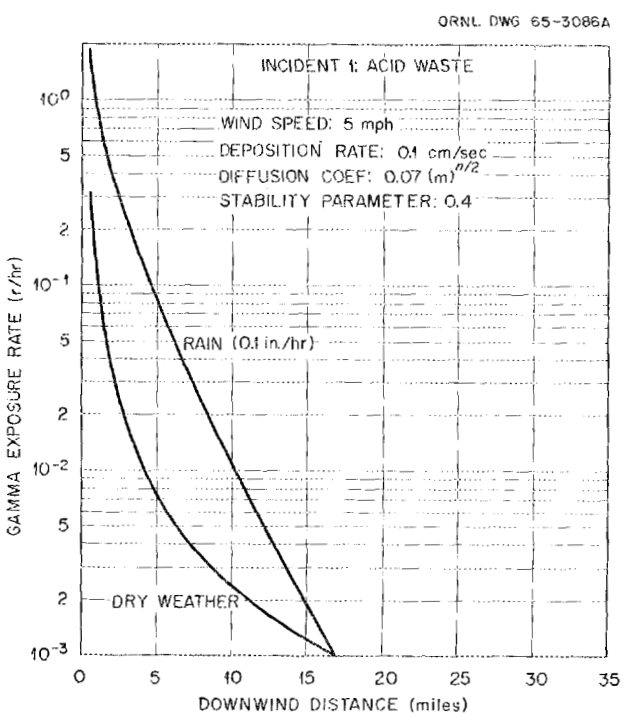

Fig. 4.11. Ground-Level Exposure Rate as a Function of Distance Downwind from an Acid Waste Tank Following Temporary Loss of Cooling.

Similar analyses of incidents 1 and 2 for the case of alkaline waste gave results from one-fifth to one-half of those for acid wastes.

A third source of exposure to the surrounding population is that which would result from direct radiation from the passing radioactive cloud. This has been found to be only a few percent of that from the two sources already treated and consequently is considered to be of negligible importance.

Another phase of this study, which is still in progress, is a consideration of a large-scale release of radioactive materials to the geological environment, and the resultant contamination of the ground and surface waters. From a consideration of all known exposure pathways, and the corrective measures necessary, we expect to estimate the extent of liabilities incurred by these releases.

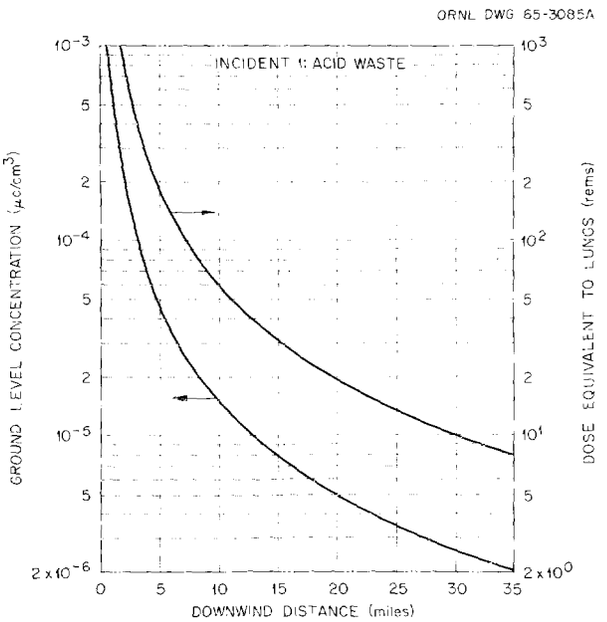

Fig. 4.13. Ground-Level Concentration as a Function of Distance Downwind from an Acid Waste Tank Following Temporary Loss of Cooling.

Fluidized-Bed Volatility Wastes[19]

An analysis was made to determine economically preferred methods of managing fluidized-bed volatility wastes from processes based on the removal of Zircaloy cladding by anhydrous HCl and on the removal of stainless steel cladding by HF-O_2. Costs were estimated for management (1) by encapsulating the primary reactor beds without additional treatment, (2) by encapsulating the beds after their conversion to glassy solids having lower solubility and better thermal properties than the original bed, and (3) by encapsulating the fission products as a glass after their separation from the bed by a phosphoric acid leach. In all cases, the final products are shipped to a salt mine for final disposal.

Although the characteristics of the glassy products that might be produced from volatility wastes can be predicted from the technology developed for vitrifying aqueous wastes, the engineering details of the processes and the equipment required have not been established. Therefore, the costs of making the "glasses," or of the proposed fission product leaching step that might precede it, were not included in this study.

The characteristics of the principal wastes from the HCl-volatility process, and the possibilities for management, are given in Fig. 4.15. The effective thermal conductivities, k (Btu hr^{-1} ft^{-1} $°F^{-1}$), were estimated over the range 200 to 900°F. The alumina bed is used for five cladding-removal and fluorination cycles, following which the fission product heat generation rate, 120 days after fuel discharge from the power reactor, is nearly 10,000 Btu hr^{-1} ft^{-3}.

The high-level (HL) radioactive waste may be stored in air-cooled annular bins for decay of short- and intermediate-lived fission products, then packaged in stainless steel cans (6, 12, or 24 in. in diameter and 10 ft long), and shipped to a salt mine for final disposal. Alternatively, this

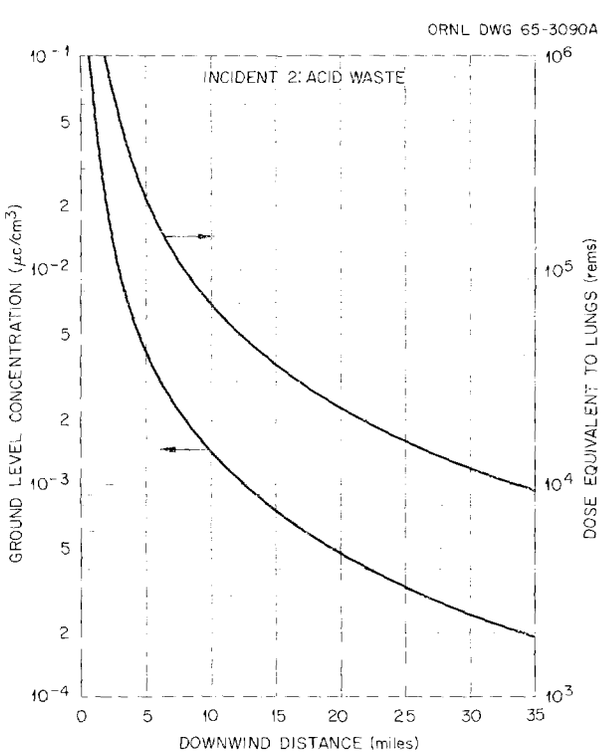

Fig. 4.14. Ground-Level Concentration as a Function of Distance Downwind from an Acid Waste Tank Following Permanent Loss of Cooling.

[19] J. C. Suddath and J. O. Blomeke, *An Economic Analysis of High-Level Waste Management for Fluidized-Bed Volatility Processing of Power Reactor Fuels*, ORNL-TM-1441 (April 1966).

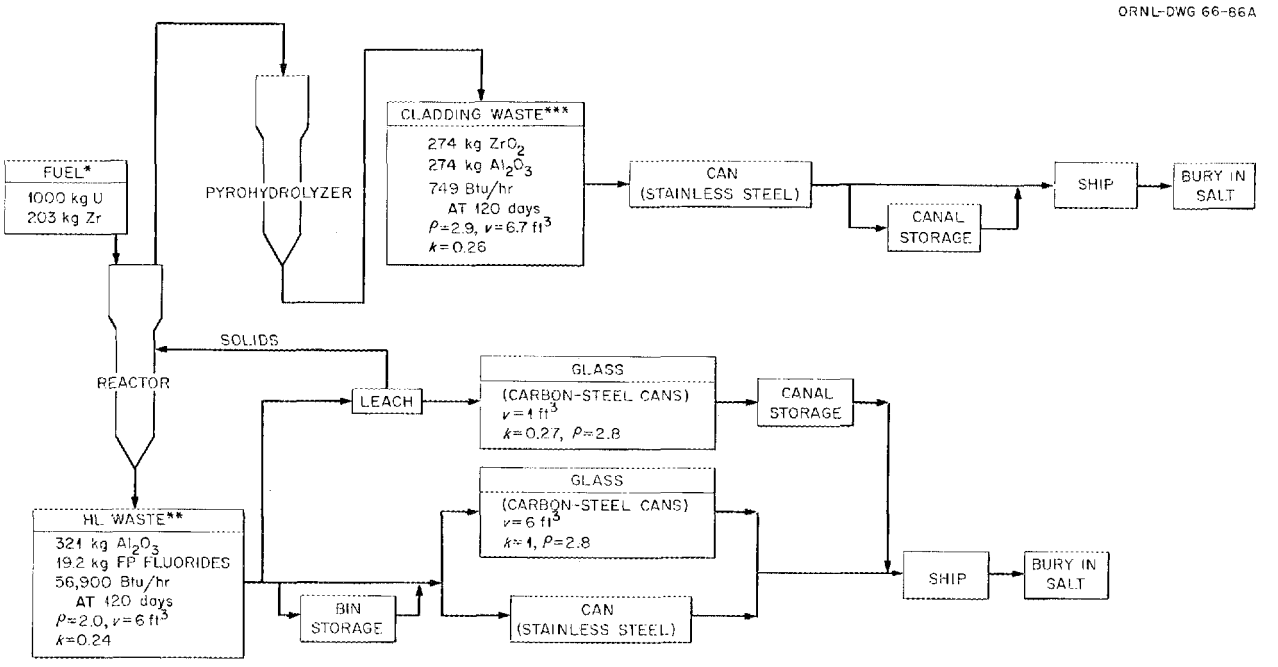

* UO_2 FUEL RODS 0.369 in. IN DIAMETER, WITH ZIRCALOY CLADDING 0.0215 in. THICK. 21,000 Mwd/metric ton (ORNL-3686).
**BASED ON $\frac{Al_2O_3}{FUEL}$ = 1.2 AND USE OF BED FOR FIVE CYCLES.
***ASSUMES THE PRESENCE OF 1% OF FISSION PRODUCTS PLUS 5300 curies OF INDUCED ^{95}Zr-Nb ACTIVITY PER metric ton OF URANIUM.

Fig. 4.15. Management of Wastes from HCl Volatility Process.

waste may be converted to a less-soluble microcrystalline glassy solid having a better thermal conductivity, then packaged in less-expensive carbon-steel cans, and shipped to a salt mine. Carbon-steel containers are considered to offer adequate containment for the low-solubility glassy materials; whereas stainless steel is stipulated for the untreated wastes.

A third choice for management of HCl-volatility waste is to leach more than 95% of the fission products with 85% H_3PO_4, return the alumina to the reactor, and convert the leach liquor into a phosphate glass.[20] This glass is stored in water-filled canals for fission product decay before shipment to a salt mine.

The cladding waste after pyrohydrolysis contains 50% ZrO_2 in Al_2O_3, and its fission product level is 1% of that of the reactor-bed waste. This waste is canned in 24-in.-diam stainless steel containers and may be stored temporarily in canals or shipped immediately to a salt mine.

[20] L. C. Emma, BNL, personal communication, Nov. 18, 1965.

The characteristics and management of the high-level waste from the HF-O_2 process are given in Fig. 4.16. This waste contains 23% by weight of "stainless steel fluorides," equivalent to using the Al_2O_3 bed for two decladding-fluorination cycles. The fission product heat generation rate is about 4000 Btu hr^{-1} ft^{-3}. It is stored for fission product decay in air-cooled annular bins, after which it is either canned directly in 24-in.-diam stainless steel containers or converted to a microcrystalline "glass" and encapsulated in carbon-steel vessels. The packaged products are shipped to a salt mine for final disposal.

Costs. – The costs for each management operation were based on earlier economic analyses made here and at the Idaho Chemical Processing Plant (ICPP), and were computed as a function of age of the wastes. The operating life of the processing plant was taken as 20 years, and present-worth costs were computed on the basis of recovering all capital and operating expenses during this 20-year period of waste production. An annual interest rate of 4% was assigned.

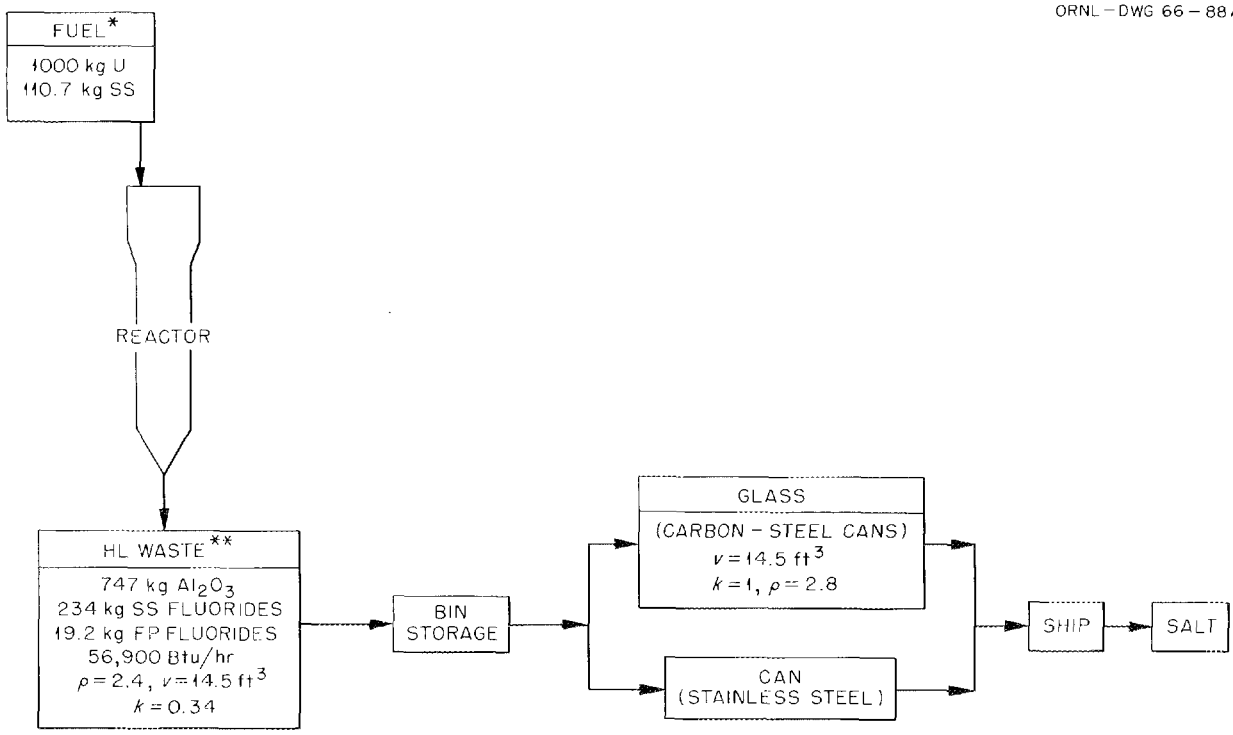

* UO_2 FUEL RODS 0.342 in. IN DIAMETER, WITH STAINLESS STEEL CLADDING 0.010 in. THICK; 21,000 Mwd/metric ton. (SEE REPORT WCAP-2385).

** BASED ON $\frac{Al_2O_3}{FUEL} = 1.2$ AND USE OF BED TWO TIMES (23% STAINLESS STEEL FLUORIDES).

Fig. 4.16. Management of Wastes from HF-O_2 Volatility Process.

Air-cooled annular bins of the ICPP design[21] were used for interim storage of the wastes prior to treatment and encapsulation. The HCl-process HL waste was stored in 4-in.-thick bins, and the HF-O_2-process waste was stored in 8-in.-thick bins. The costs of stainless steel containers, 6, 12, and 24 in. in diameter by 10 ft long, were taken as $500, $855, and $2500.[22] Glassy solids can be encapsulated in the largest vessels (24 in. in diameter) at relatively early ages: 1.3 years in the case of HCl-process wastes, and 0.6 year in the case of HF-O_2-process wastes. Therefore, only 24-in.-diam containers were considered for these products, and the cost of the cans was taken as $1250 each. The costs for shipping the wastes 1000 miles were based on published data.[23] The shipping casks contain thirty-six 6-in.-diam vessels, nine 12-in.-diam vessels, or four 24-in.-diam vessels. The costs for disposal of the wastes in salt mines are based on unpublished data[24] for burial of the containers in the floor of a mine 1000 ft below the surface.

The minimum total costs for management of these wastes in untreated form and as glassy solids are given in Fig. 4.17. For the HL and

[21] J. I. Stevens, *An Economic Evaluation of Ultimate Disposal of Liquid Radioactive Wastes by the Fluidized Bed Calcination Process*, IDO-14595 (October 1962).

[22] J. J. Perona *et al.*, *Evaluation of Ultimate Disposal Methods for Liquid and Solid Radioactive Wastes. Part II. Conversion to Solid by Pot Calcination*, ORNL-3192 (September 1961).

[23] J. J. Perona *et al.*, *Evaluation of Ultimate Disposal Methods for Liquid and Solid Radioactive Wastes: Shipment of Calcined Solids*, ORNL-3356 (October 1962).

[24] R. L. Bradshaw, J. O. Blomeke, and J. J. Perona, *Evaluation of Ultimate Disposal Methods for Liquid and Solid Wastes. Part VI. Disposal of Solidified Wastes in Salt Formations*, ORNL-3358 (in preparation).

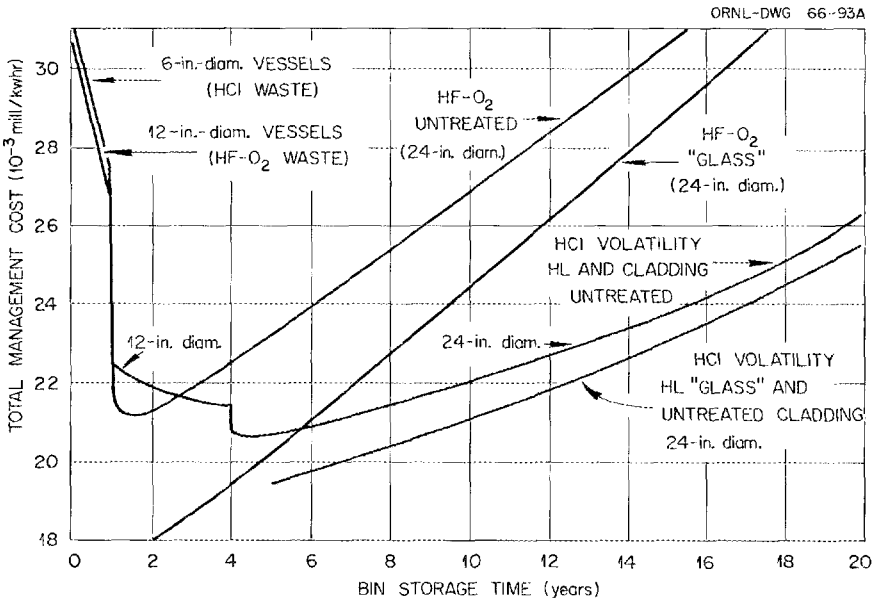

Fig. 4.17. Total Management Costs as a Function of Bin-Storage Time.

cladding wastes from the HCl volatility process, the minimum total cost of 0.0206 mill/kwhr is obtained, using four to five years of bin storage followed by encapsulation in 24-in.-diam vessels. The minimum cost for managing this waste as a "glass" is 0.0194 mill/kwhr, with 5-year bin storage before treatment and encapsulation. In the case of the waste from HF-O_2 processing, minimum costs for management in untreated form and as a "glass" are 0.0212 and 0.0180 mill/kwhr, respectively, at bin-storage times of 1.5 and 2.0 years.

The incremental and total costs for managing phosphate glass prepared from the HCl-volatility HL waste following a phosphoric acid leach, and including the costs for cladding-waste management, are given in Table 4.11. In this scheme, the fission products are leached from the reactor bed, and the liquor is made into a phosphate glass. The glass is encapsulated in 6-in.-diam carbon-steel vessels ($240 each), which are subsequently stored in water-filled canals[25] for 3, 10, and 30 years before shipment to a salt mine for burial. Minimum total costs of about 0.013 mill/kwhr are obtained with 10 to 30 years' interim solid storage.

[25] J. O. Blomeke *et al.*, *Evaluation of Ultimate Disposal Methods for Liquid and Solid Radioactive Wastes. Part III. Interim Storage of Solidified Wastes*, ORNL-3355 (October 1963).

Discussion and Conclusions. – In this study, the important consideration is the *difference* between minimum total costs of managing the wastes in untreated form and as a glassy product. The costs for untreated wastes in each case may be taken as a nearly complete cost. Although they do not include costs for a container-filling station

Table 4.11. Management Costs in Thousandths of a Mill per Electrical Kilowatt-Hour for Phosphate Glass and Cladding Wastes from HCl Volatility Process

	Interim Solid Storage in Canals for:		
	3 Years	10 Years	30 Years
Containers	4.1	4.1	4.1
Interim solid storage	2.5	5.0	7.2
Shipment 1000 miles	2.0	0.8	0.4
Disposal in salt	6.2	3.6	1.6
Total	14.8	13.5	13.3

and a remote welder for sealing the vessels, these items are of minor economic importance and should not alter the totals substantially. On the other hand, the costs of management after incorporation in glass are exclusive of the possibly more significant costs of the glass-preparation step and of the leaching step preceding phosphate-glass production.

The largest cost difference is in the handling of the HCl volatility waste as a phosphate glass. Almost $1200 per metric ton of uranium processed (0.0012 mill/kwhr) is available to pay for leaching the HL waste from the reactor bed, for producing a glass from the resulting aqueous phosphate leach liquor, and for preparing the solids for reuse in the reactor bed. We doubt if this is sufficient to pay for these steps, but it certainly represents a major part of the potential cost. Inherent in these estimates, of course, is the assumption that the leached solids can be recycled to the reactor over a long term of operations.

There is $520 per ton of uranium (0.0032 mill/kwhr) available to pay for producing microcrystalline solids from the HF-O_2 volatility process waste. This should be much simpler than the combination leaching and phosphate-glass production, and it may be possible to accomplish it for the money available.

The least cost difference is associated with making microcrystalline solids from HL HCl volatility waste: $190 per ton (0.0012 mill/kwhr). However, in terms of cost, the same amount of money is available as for HF-O_2 waste, $30 per cubic foot of glassy product.

The uncertainties in the volatility process flowsheets, as well as in the waste characteristics, temper any conclusions that can be drawn from an economic analysis of proposed waste management schemes at this time. The following general observations are made, however.

1. There is not a clear-cut economic incentive to do anything with the wastes other than to encapsulate them after several years of bulk storage and to ship them to a salt mine for final disposal. If, for greater safety during handling and shipment, it is desirable to incorporate them in glass, a substantial credit from cheaper management can be applied against the cost of the treatment step, but the total management cost will probably be increased.

2. One of the major imponderables to be resolved is the potential difficulty arising from the presence of fluoride in these wastes. Early laboratory data indicate that volatile fluorides are evolved during the glass-encapsulation operations. It seems entirely possible that a pyrohydrolysis step may be required for fluoride removal to produce either an acceptably safe granular product for interim storage and shipment, or as a pretreatment step before incorporation in glass.

3. The most significant factor presently affecting the management costs of these wastes is the volume of waste per unit of fuel processed. Volatility process development should be directed toward reducing these volumes.

4. The total cost of high-level waste management from volatility processing may be equal to or more than the costs estimated for aqueous process wastes. More economic waste management cannot be cited as an advantage of volatility over aqueous processing in the fluidized-bed method for low-enrichment fuel.

5. Transuranium-Element Processing

The Transuranium Processing Plant (TRU) and the High Flux Isotope Reactor (HFIR) were built at ORNL as production facilities to provide gram quantities of many of the transuranium elements and milligram quantities of some of the transcalifornium isotopes. These materials will be used in research work in laboratories throughout the country. This part of the USAEC Heavy Element Production Program began with the long-term irradiation of ^{239}Pu in a Savannah River production reactor. This irradiation program has produced nearly 1 kg of ^{242}Pu and 300 g each of ^{243}Am and ^{244}Cm. The ^{242}Pu was recovered and decontaminated at Savannah River, and some of the americium and curium was processed at the Curium Recovery Facility (CRF) at ORNL. Over a one-year period beginning in February 1965, about 525 g of ^{242}Pu was irradiated in a special High Flux Demonstration Run in one of the Savannah River production reactors. This reactor, with a special fuel loading, was operated at a thermal-neutron flux exceeding 2×10^{15} neutrons cm^{-2} sec^{-1}. In this run, 6 prototype HFIR targets containing 10 g each of ^{242}Pu, 18 actual HFIR target rods also containing 10 g of ^{242}Pu, and 8 special slugs fabricated at Savannah River were irradiated. This irradiation produced about 2 mg of californium along with the other associated heavy actinide elements. One of the HFIR prototype rods, which contained about 5 μg of californium, was processed at ORNL this past winter; the remaining rods will be processed in the immediate future in TRU.

The major main-line chemical processes were developed and tested at high activity levels, and equipment was designed and installed in the facility to do the essential processing. Within this past year, essentially all construction in connection with the facility was concluded, and the "cold" checkout of the equipment is now essentially complete. This report summarizes the development work and other phases of the program in the Chemical Technology Division during the past year. Development of the procedures and equipment for remotely fabricating target rods is under the direction of the Metals and Ceramics Division and is not reported here.

Additional small quantities of ^{243}Am and ^{244}Cm were recovered in the CRF during this report period. All processing activities in this facility have now been concluded, however, and all additional processing will be done in TRU. Work in the CRF during the past year is reported in Sect. 6.

5.1 DEVELOPMENT OF CHEMICAL PROCESSES

Chemical processes are required for preparation of oxides used in HFIR targets and for recovery of heavy elements from irradiated targets. Material for HFIR targets was obtained from irradiating, to greater than 99.9% burnup of ^{239}Pu, batches of plutonium as plutonium-aluminum alloy in a Savannah River production reactor. About 1000 g of residual plutonium (primarily the 242 isotope) has been recovered and purified at Savannah River. About 286 g of this material was used for the initial HFIR loading, and the remaining plutonium was irradiated at Savannah River in a reactor having a special fuel loading designed to maximize the flux. In addition, about 300 g of ^{243}Am and 300 g of ^{244}Cm, along with rare-earth fission products in nitric acid, were recovered as a crude product from the raffinate of the plutonium recovery step at Savannah River. About 75 g of this material was processed for americium-curium recovery at ORNL in the CRF; the remainder will be processed in TRU. In the processing in the CRF, americium, curium, and rare earths are concentrated and converted to a chloride system by the Clanex process, and the actinides are then isolated from the lanthanides and other fission products by the Tramex process. Purified ^{242}Pu, ^{243}Am, and ^{244}Cm will

be converted to dense oxides in the particle-size range 20 to 200 μ, made into targets in TRU, and irradiated.

The main-line HFIR target processing method consists in dissolving the target in HCl; separating the actinides from fission products and aluminum by the Tramex process; extracting the transcurium elements from americium and curium in dilute HCl; separating berkelium from californium, einsteinium, and fermium by dialkyl phosphate extraction of Bk^{4+} from concentrated HNO_3; and isolating californium, einsteinium, and fermium by chromatographic elution from a cation exchange resin.

Status and Progress

During the past year, additional Clanex, Tramex, and ion exchange processing was demonstrated at full-scale radioactivity levels in the CRF. This work is reported in Sect. 6.

Since residual PuO_2 will remain in the targets irradiated in the Savannah River High Flux Reactor, a study was made of methods for dissolving irradiated and unirradiated refractory PuO_2. Results indicate that irradiated PuO_2 dissolves more readily than the unirradiated PuO_2; however, fluoride, which is not compatible with the main-line TRU process equipment, will probably be required for total PuO_2 dissolution. Since it will be necessary to reduce the fluoride concentration to less than 5 ppm following dissolution, fluoride removal methods were also studied. Simple hydroxide precipitation appears to work satisfactorily.

Although the HNO_3 anion exchange method for plutonium isolation can be used in TRU operations, it may be convenient to separate plutonium from HCl solutions. Scouting tests on a laboratory scale showed that an HCl anion exchange method will give acceptable plutonium recovery; however, the product may require additional processing to remove residual fission products.

The sol-gel method for the preparation of 20- to 100-μ particles of dense americium-curium oxide for incorporation into HFIR targets has several inherent advantages over alternate processes. Laboratory efforts to perfect the process, with lanthanides as stand-ins for americium and curium, were continued. The techniques developed were successfully applied to the preparation of ^{241}Am, ^{244}Cm, and mixed ^{243}Am-^{244}Cm sols. In all cases it was possible to form these sols into microspheres that calcine to dense oxide spheres. Significant steps were made toward adapting the process for easier operation in the shielded facilities required for americium and curium processing.

Chromatographic elution from cation exchange resin with α-hydroxyisobutyrate solutions will be used to separate californium, einsteinium, and fermium in TRU. The method was tested by separating americium from curium at high activity levels. While the results obtained in these tests were not completely satisfactory, they indicated that this method can be scaled up to handle 100-mg quantities of ^{252}Cf. Experimental studies with rare earths as stand-ins for the heavy elements are needed to optimize column scale-up, and additional high-activity-level runs are required to fully prove this process.

One of the HFIR prototype target rods was discharged from the Savannah River High Flux Reactor on September 7, 1965, after an estimated irradiation of 3.7×10^{22} *nvt*. This target, which originally contained 10 g of plutonium (95.66% ^{242}Pu) as oxide, was dissolved, analyzed for transplutonium-element content, and processed to recover the heavy elements. Analyses indicated that the irradiated target contained 5.45 g of plutonium, 1.58 g of americium, 2.64 g of curium, about 5 μg of ^{252}Cf, about 2 μg of ^{249}Bk, and about 0.2 μg of ^{253}Es at the time of discharge from the reactor.

Plutonium Recovery from Irradiated HFIR Targets

The $^{242}PuO_2$ in HFIR targets and in aluminum-matrix slugs now being irradiated in the Savannah River reactor will not be completely burned before it is processed; also, in the future it may be necessary to process some targets from the HFIR before the $^{242}PuO_2$ is completely burned. Unfortunately, the dissolution methods for unburned or partially burned PuO_2 normally require fluoride, which is not compatible with Zircaloy-2 processing equipment in TRU. For these reasons, a study of dissolution methods for irradiated and unirradiated refractory PuO_2 was made. This work included rate studies of methods that require fluoride, as well as an investigation of nonfluoride methods.

Results indicated that fluoride-catalyzed dissolutions will probably be required; accordingly, a stainless steel dissolver was installed in TRU. However, when fluoride is used, it will be necessary to reduce the fluoride concentration to less than 5 ppm before subsequent processing is done

in Zircaloy-2 equipment. Thus, fluoride removal methods, as well as analytical methods to detect fluoride at low concentrations, are being investigated.

During normal processing of irradiated HFIR targets, the plutonium will be completely burned, and the entire target can be readily dissolved in HCl. Since it will be necessary to recover ^{244}Pu from these targets, an HCl anion exchange system for recovery and purification of plutonium is being investigated.

PuO_2 Dissolution Studies

Phosphoric acid and anhydrous HCl gas in molten $KCl\text{-}AlCl_3$ were the only effective reagents found for dissolving unirradiated PuO_2 without fluoride; however, irradiated PuO_2 dissolved much more readily than the unirradiated PuO_2. Total dissolution of an irradiated specimen (~64 at. % of the plutonium fissioned) was accomplished by refluxing with 3 *M* HCl. This reagent dissolved about 65% of the plutonium in a specimen irradiated to about 30 at. % fissioned. These results indicate that it should be possible to process HFIR targets containing significant quantities of plutonium by nonfluoride methods if sufficient burnup has been accomplished; however, fluoride will probably be required for total PuO_2 dissolution of less highly irradiated material.

Unirradiated PuO_2 Dissolution Studies. – The PuO_2 used for these studies was identical with that used in HFIR prototype fuel targets. This refractory PuO_2 was made from plutonium that had been purified by anion exchange, precipitated as the hydroxide, washed, dried at 90°C, and calcined at 1100°C for 5 hr. The particle size was 177 to 200 μ. In all dissolution experiments which required fluoride, periodic additions were made to replenish HF, which was rapidly lost by volatilization and in corrosion of glass equipment.

Phosphoric acid, concentrated HNO_3 0.1 *M* in HF, and anhydrous HCl in molten $KCl\text{-}AlCl_3$ effectively dissolved refractory PuO_2. Nine-molar HBr 0.1 *M* in HF, or 6 *M* HCl 0.1 *M* in CuF_2 is probably effective, although tests with these solutions were not continued long enough for complete dissolution.

Complete dissolution of 192 mg of PuO_2 was achieved by refluxing with 50 ml of 15.8 *M* HNO–0.1 *M* HF for 22 hr. Hourly additions of sufficient HF to keep the solution at 0.1 *M* were necessary to maintain the dissolution rate. In experiments in which periodic additions of HF were not made, dissolution rates decreased drastically within 2 hr. Rapid dissolution rates were also obtained with 9 *M* HBr–0.1 *M* HF and 6 *M* HCl–0.12 *M* CuF_2. Dissolutions of 32 and 28%, respectively, were achieved by these reagents in 1 hr. However, as in the previous experiment, rates decreased rapidly after the first hour because of fluoride loss. Total dissolution with periodic additions of fluoride was not attempted.

A number of additional reagents that did not require fluoride were investigated; however, concentrated H_3PO_4 proved to be the only effective aqueous reagent. In this case, PuO_2 was added to 50 ml of 85% H_3PO_4, and the H_3PO_4 was concentrated by evaporation until a temperature of 260 to 270°C was obtained. At these conditions, PuO_2 completely dissolved in about 6 hr, and plutonium was recovered from the phosphate solution by precipitation with NaOH. After a single precipitation and wash, the PO_4^{3-}/Pu mole ratio was 0.18. A second precipitation should reduce the phosphate content to an acceptably low level.

In the investigation of nonaqueous dissolution methods, plutonia was found to be dissolved rapidly and completely by anhydrous HCl gas in molten $KCl\text{-}AlCl_3$ (50-50 mole %) at 500°C. In similar experiments without HCl, a plutonia dissolution rate of only 8%/hr was obtained.

Additional reagents investigated and the average dissolution rates obtained are listed in Table 5.1.

Irradiated PuO_2 Dissolution Studies. – These experiments were conducted with ½-in. segments of prototype HFIR target rods that were irradiated in the Engineering Test Reactor (ETR). The target rods are designated as TRU-1 (~31 at. % of the plutonium fissioned), TRU-2 (~64 at. % of the plutonium fissioned), and TRU-3 (~62 at. % of the plutonium fissioned).

The TRU-1 target rod had an unperturbed peak exposure of 1.7×10^{21} neutrons/cm^2 and was exposed to an average heat flux of 640,000 Btu hr^{-1} ft^{-2}. The TRU-2 target rod had an estimated integrated, unperturbed peak exposure of 3.2×10^{21} neutrons/cm^2 and was exposed at a higher average flux of 3.7×10^{14} neutrons cm^{-2} sec^{-1} (peak, unperturbed), for one ETR cycle. The TRU-2 target was exposed to extreme heat-flux conditions of greater than 1,000,000 Btu hr^{-1} ft^{-2}. The TRU-3 target received a burnup greater than that received by TRU-1, but at approximately the same heat flux.

Table 5.1. PuO_2 Dissolution in Various Solutions

Aqueous Reagent	Dissolution Time (hr)	Average Dissolution Rate (%/hr)
4 *M* HNO_3–0.5 *M* $K_2S_2O_7$–0.005 *M* $AgNO_3$	2	0.51
12 *M* LiCl–1 *M* HCl	2.5	0.019
9.6 *M* LiCl–0.8 *M* HCl–2 *M* H_2O_2	1	0.013
10 *M* LiCl–0.5 *M* HCl–0.23 *M* NaOCl	3	0.28
12 *M* LiCl–1 *M* HCl–0.5 *M* $NH_2OH{\cdot}HCl$	2	0.007
29% H_3PO_4–5% H_2O_2	4	0.11
9 *M* HBr	11	0.07
Fused Li_2CO_3 at 700°C		0.04[a]
Fused Li_2CO_3–$LiNO_3$ at 650°C		0.31[a]

[a]Total amount of plutonium that was dissolved by fusing PuO_2 in reagents, followed by cooling and dissolving the solidified salts in water.

All irradiated specimens were more readily dissolved than those that were unirradiated. Dissolution in HNO_3-HF was considerably more rapid for irradiated PuO_2 (Fig. 5.1), and TRU-2 was completely soluble in 2 to 3 *M* HCl, while unirradiated PuO_2 is virtually insoluble in this reagent. Dissolution data obtained for these targets are shown in Table 5.2. All dissolutions were conducted under reflux conditions. When HNO_3 was used without HF, the aluminum portion (jacket and matrix) of the target segment was first dissolved in 1.2 *M* NaOH–1.5 *M* $NaNO_3$.

The PuO_2 residue from the HCl dissolutions of TRU-1 and TRU-3 was readily dissolved in refluxing 6 *M* HCl–0.1 *M* CuF_2. An HNO_3 dissolution of TRU-2 without fluoride was not attempted.

In most experiments a small amount of residue remained that was soluble in aqua regia and H_2SO_4. It consisted primarily of aluminum, silicon, palladium, ruthenium, and rhodium, with some molybdenum and zirconium and traces of calcium, copper, iron, magnesium, silver, titanium, and nickel.

Dissolution tests were also made with a pellet cut from the HFIR prototype target rod, TRU-SRL irradiation element No. 26, which was irradiated to $\sim 3.7 \times 10^{22}$ *nvt* in the Savannah River High Flux Reactor. About 45% of the original 10 g of plutonium (95.66% ^{242}Pu) was burned out by the irradiations. When a large excess of 2.6 *M* HCl was added to the pellet, only about 25% of the residual plutonium was dissolved. However, the solid residue was readily soluble in 15.6 *M* HNO_3–0.1 *M* HF. Because this test showed incomplete dissolution of plutonium in 2.6 *M* HCl, the target rod was processed by dissolving the aluminum in caustic and by dissolving the residue in 8 *M* HCl containing 0.1 *M* CuF_2 catalyst. More experience

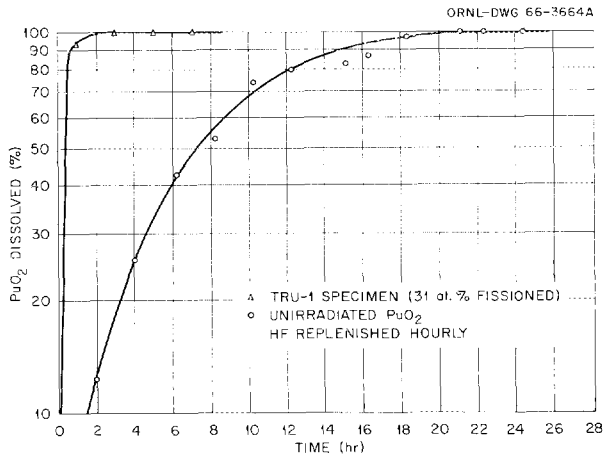

Fig. 5.1. Comparison of the Dissolution Rates of Irradiated and Unirradiated $^{239}PuO_2$ in 15.8 *M* HNO_3-0.1 *M* HF.

Table 5.2. Dissolution of Irradiated $^{239}PuO_2$ in Various Solutions

Reagent	Percentage of PuO_2 Dissolved		
	TRU-1	TRU-2	TRU-3
15.8 *M* HNO_3–0.1 *M* HF	99.96	99.94	99.5
15.8 *M* HNO_3	45		68.0
2 to 3 *M* HCl	65	99.85	87.2

is needed to determine the burnup necessary before the residual PuO_2 can be dissolved without fluoride.

Fluoride Removal Following Target Dissolution

Laboratory tests indicate that fluoride can be effectively removed from HFIR target dissolver solutions by hydroxide precipitation, filtration, and redissolution. In studies made with simulated dissolver solution that contained thorium as a stand-in for plutonium, fluoride was reduced to 3 ppm by two precipitation cycles. Fluoride decontamination factors of about 54 and 14 were obtained for the first and second cycles respectively. Results were comparable for solutions with and without aluminum.

Plutonium Isolation by HCl Anion Exchange

Plutonium can be isolated from HFIR target dissolver solution by sorption on anion exchange resin from 6 to 8 *M* HCl at 60°C. Under these conditions the trivalent actinides and rare-earth fission products do not load, and the HCl effluent from the plutonium column can readily be converted to feed suitable for Tramex processing.

Since Pu^{3+} will not load, the stability of Pu^{4+} in concentrated HCl was investigated. Tetravalent plutonium was found by spectrophotometric analysis to be stable for several days in both 6 and 8 *M* HCl at room temperature, and there was no evidence of disproportionation after heating to 75°C for 1 hr.

In small-scale laboratory experiments, column loadings of greater than 99% were obtained from both 6 and 8 *M* HCl feed solutions on Dowex 1-8X resin at 60°C. After loading, the column was washed with ten column displacement volumes of 6 or 8 *M* HCl without significant plutonium losses (~0.1%).

Plutonium can be eluted from the column with either dilute or concentrated acid that contains sufficient reductant to reduce Pu^{4+} to Pu^{3+}. Since eluting with concentrated acid may afford significant decontamination from fission product ruthenium and zirconium, which load with the plutonium, several reductants were investigated. Ascorbic acid, U^{4+}, and NH_4I were effective in reducing plutonium. Under the conditions used (0.1 *M* reductant and 6 to 8 *M* HCl), NH_4I was the most effective. Complete plutonium elution was obtained in 7 column displacement volumes when NH_4I was used, while 12 column volumes were required when ascorbic acid was used; U^{4+} was even less effective. Adequate decontamination from fission products has not yet been demonstrated.

Preparation of Oxides for HFIR Targets

High Flux Isotope Reactor targets will be made from pressed pellets of aluminum powder and actinide oxide, with the aluminum phase continuous to ensure satisfactory heat transfer during irradiation.

A process utilizing hydroxide precipitation for preparing dense, coarse particles of PuO_2 was reported previously.[1] During this past year it was used to prepare about 324 g of PuO_2, containing 286 g of ^{242}Pu. This material was subsequently made into targets for the first loading of the HFIR.

The preparation of plutonia by a sol-gel method offers several process advantages over the hydroxide precipitation method mentioned above, and gives a product of greater uniformity. Plutonia sol-gel development work was continued, and significant progress was made in the preparation of uniform sols of desirable characteristics. This work is reported in Sect. 8.

A sol-gel method appears to be equally attractive for the preparation of 20- to 200-μ particles of dense americium-curium oxide. The ability to prepare oxide microspheres of controlled particle size from rare-earth sols as stand-ins for americium and curium was reported last year.[2] This work

[1] F. L. Culler, Jr., *et al.*, *Chem. Technol. Div. Ann. Progr. Rept. May 31, 1964*, ORNL-3452, pp. 114–15.

[2] D. E. Ferguson *et al.*, *Chem. Technol. Div. Ann. Progr. Rept. May 31, 1965*, ORNL-3830, pp. 143–49.

was continued not only to provide processes for americium and curium oxide preparation but also because rare-earth oxide microspheres have potential as control rod materials and as burnable poisons in fuel elements for nuclear reactors. The sol preparation method as originally developed consists in (1) precipitating the metal hydroxide by adding NH_4OH or tetramethylammonium hydroxide (TMAH) to a rare-earth nitrate solution, (2) removing residual nitrate and soluble impurities by washing the precipitate with water, (3) forming a sol by adding a small amount of HNO_3 and digesting at 50°C, and (4) concentrating the sol by evaporation. Recent modifications, which have greatly simplified the process, make it more amenable to in-cell preparation of ^{243}Am and ^{244}Cm sols. In the modified procedure the metal hydroxide is prepared by a reverse "strike"; that is, a dilute solution of rare-earth nitrate (~0.02 *M*) is added to a 20-fold excess of 8 *M* NH_4OH. This results in a precipitate that is easier to filter and to wash. The lighter lanthanide hydroxides (up to neodymium) prepared in this way liquefy spontaneously into translucent sols, and the heavier lanthanide hydroxides are readily converted to sols by heating for 1 hr at 80°C.

The modified sol preparation method has not yet been tested for preparation of americium and curium sols, but the original rare-earth sol procedure was successfully applied to the preparation of ^{241}Am, ^{244}Cm, and mixed ^{243}Am-^{244}Cm sols. In all cases it was possible to form these sols into gel microspheres that calcine to dense oxide spheres. Future work will be directed at applying the simplified procedure to the preparation of americium-curium sols.

Preparation of $^{242}PuO_2$ for HFIR Targets. – Plutonium-242 oxide for the first HFIR targets was prepared by the hydroxide precipitation method[1] and was ground to the desired particle-size range with pestle and mortar. The following size distribution was obtained:

Screen Size	Wt %
−70 +100	45.8
−100 +200	22.4
−200 +325	12.6
−325	19.2

About 324 g of this oxide, containing 286 g of ^{242}Pu, was used in targets for the first HFIR loading. Although −325 mesh fines were not used in prototype targets previously fabricated, the inclusion of the 19.2 wt % fines in these targets presented no problems.

About 74 g of $^{242}PuO_2$ contained in reject aluminum pellets was recovered and recycled without dissolving the PuO_2. The aluminum matrix was dissolved in $NaOH$-$NaNO_3$ solution, and contaminant oxides, for example, Al_2O_3, were dissolved by refluxing in dilute HNO_3, which does not dissolve appreciable quantities of the high-fired PuO_2.

Original Rare-Earth Sol-Gel Process. – In this process the nitrate salt of the rare earth is dissolved in water and is precipitated by addition of a base, preferably TMAH. Although NH_4OH can be used, it is impossible to decrease the nitrate-to-metal mole ratio in the precipitate below 0.3 to 0.5, and sols prepared from this precipitate produce inferior microspheres. When TMAH is used to precipitate the metal hydroxide, essentially complete nitrate removal can be obtained. Six to ten washes are required to remove contaminant ions. Because of the amorphous character of the hydroxide, the precipitate cannot be filtered; and centrifugation is required in all washing operations. Carbon dioxide is readily sorbed by the basic hydroxide and prevents sol formation if it is present in sufficient quantity. As received, TMAH frequently contains excessive carbonate as an impurity, which must be removed prior to use. Atmospheric CO_2 can also be troublesome, and the best sols were prepared in a CO_2-free atmosphere. After a small addition of HNO_3, the washed hydroxide is peptized by digestion for 30 to 60 min at 50°C. The amount of HNO_3 required varies with the rare earth used. Nitrate:metal mole ratios of 0.03 to 0.05 are sufficient to produce good praseodymium and neodymium hydroxide sols, while ratios of 0.1 to 0.2 are necessary for europium hydroxide sols. After digestion, the sols can be concentrated to 2 *M* by evaporation at 50°C.

In all cases it was possible to produce microspheres that calcine to oxide spheres. Dense oxide microspheres were prepared from hydroxide sols of praseodymium, neodymium, gadolinium, and europium, as well as from mixed sols of praseodymium-neodymium and europium-gadolinium.

Spheres are readily formed from 1 to 2 *M* sols by the tapered-column technique. Good results were obtained with a dehydrating mixture consisting of 10 vol % 2-octanol, 89.9 vol % 2-methyl-1-pentanol, and 0.1 vol % Span 80. It is also possible to use

2-ethyl-1-hexanol containing a small amount of Span 80.

Resistance to crushing forces was determined as a function of sphere diameter for praseodymia and europia microspheres. In both cases it is proportional to the square of the sphere diameter (Fig. 5.2). The strengths of praseodymia and europia are quite comparable; however, higher calcination temperatures are necessary to obtain the maximum strength for europia. Praseodymia spheres attain the indicated resistance to crushing forces at a calcination temperature of 1050°C. A cubic crystal structure is indicated by x-ray analysis for this praseodymia. Increasing the temperature to 1250°C did not increase the resistance to crushing forces. For europia spheres, the maximum resistance to crushing forces is not attained until the calcination temperature exceeds 1200°C. X-ray analysis of europia spheres indicates a change in crystalline form from cubic to monoclinic at 1200 to 1300°C, and the monoclinic form is apparently required for maximum crush resistance. The crystallite size range for both 1500°C-fired europia and 1050°C-fired praseodymia spheres was determined by x-ray line broadening to be 500 to 600 A.

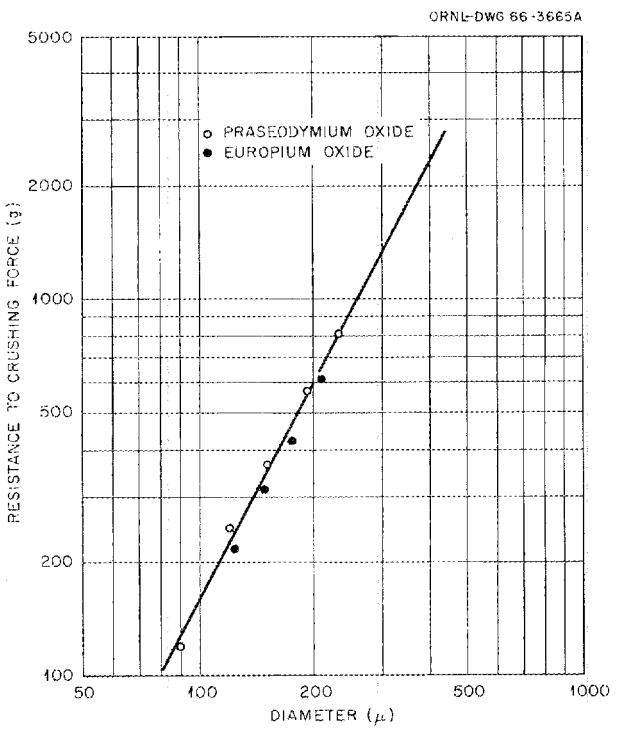

Fig. 5.2. Correlation of Resistance to Crushing Forces and Diameter for Praseodymium Oxide and Europium Oxide Microspheres.

Improved Rare-Earth Sol-Gel Process. – In recent development work it was discovered that, when the order of addition is reversed during precipitation of the rare-earth hydroxide, NH_4OH can be used as the precipitating base. The resulting precipitate is easier to filter, nitrate can be more completely removed, and there is a strong tendency toward spontaneous sol formation during washing. This behavior simplifies equipment requirements and makes possible a single-vessel operation. Since less time is required to prepare a sol and since all the steps can be done in one vessel, CO_2 sorption from the atmosphere is not a serious problem.

The modified sol process consists in the following steps:

1. The metal hydroxide is precipitated by the addition of a 0.02 *M* solution of the lanthanide nitrate to a 20-fold excess of 8 *M* NH_4OH, with stirring, at 25°C.

2. The precipitate is centrifuged and washed with CO_2-free distilled water five or six times (the precipitate is reslurried and recentrifuged, and the wash liquor is decanted, during each wash cycle); the pH of the wash liquor decreases from 11 to 9.

3. The damp paste is aged for 30 to 60 min for the lower lanthanides (up to neodymium), at which time it liquefies spontaneously into a translucent sol with a metal concentration of about 0.5 *M*, a nitrate-to-metal ratio of about 0.2, and a pH of 7. The viscous hydroxide pastes of the heavier lanthanides do not liquefy spontaneously at 25°C even after several days, but if they are heated for 1 hr at 80°C, the viscosity decreases sharply and the apparent pH decreases from 10 to about 7. This produces fluid sols about 0.5 *M* in metal, with a nitrate-to-metal mole ratio of 0.05 to 0.15.

4. The dilute sols can be concentrated to 2 to 2.5 *M* metal hydroxide in a rotary vacuum evaporator at 50°C.

Sols prepared in this manner can be formed into microspheres as previously described; for example, microspheres were prepared of a series of rare-earth oxides (La_2O_3, CeO_2, Pr_6O_{11}, Nd_2O_3, Eu_2O_3, Ho_2O_3, Er_2O_3). The gel microspheres are dried in vacuum for several hours at 120°C and heated to 500°C in vacuum to decompose the residual nitrate before sintering at 1000 to 1500°C in air (the final temperature depending on the

crystal form required). A sample of 150-μ-diam microspheres of monoclinic Eu_2O_3 heated to 1475°C for 3 hr is shown in Fig. 5.3. The products have high density (95% of the theoretical crystal density) and low surface area (0.01 to 0.1 m^2/g).

Samples of hydroxide sols of praseodymium, neodymium, and europium were examined by electron microscopy and selected-area electron diffraction to determine the size, shape, and crystallinity of the colloidal particles at various stages in the process. Electron micrographs of a praseodymium hydroxide sol at various times of aging at 25°C are shown in Fig. 5.4. The rapid decrease in viscosity and pH occurs between stages *B* and *C*, during which time the sol particles crystallize into rods and bundles of rods (400 to 1000 A long and 20 to 200 A wide) with a diffraction pattern characteristic of hexagonal $Pr(OH)_3$. Examination of a thin microtome section cut through a gel microsphere showed that the bundles of rods were randomly oriented and had a roughly square cross section.

Polished cross sections of calcined oxide microspheres reveal some fine internal pores, and methods are being developed to reduce this porosity and to increase the density above 95%.

^{241}Am Sol Preparations. -- The original sol-gel procedure as developed for the preparation of rare-earth microspheres was directly applicable to the preparation of ^{241}Am sols. Stable sols were prepared, and microspheres that calcined to oxide spheres at 1150°C could be produced.

Americium sols were made by precipitating the hydroxide from $Am(NO_3)_3$ solutions with NH_4OH and with TMAH. Unlike the results obtained with rare-earth precipitates, complete nitrate removal was achieved by NH_4OH precipitation, and the ability of the precipitate to form a sol indicated that NH_4OH is a satisfactory base for actinide sol preparations.

Small differences between americium and rare-earth behavior suggest that americium may be more amenable to sol formation and microsphere preparation than are the lanthanides. There was

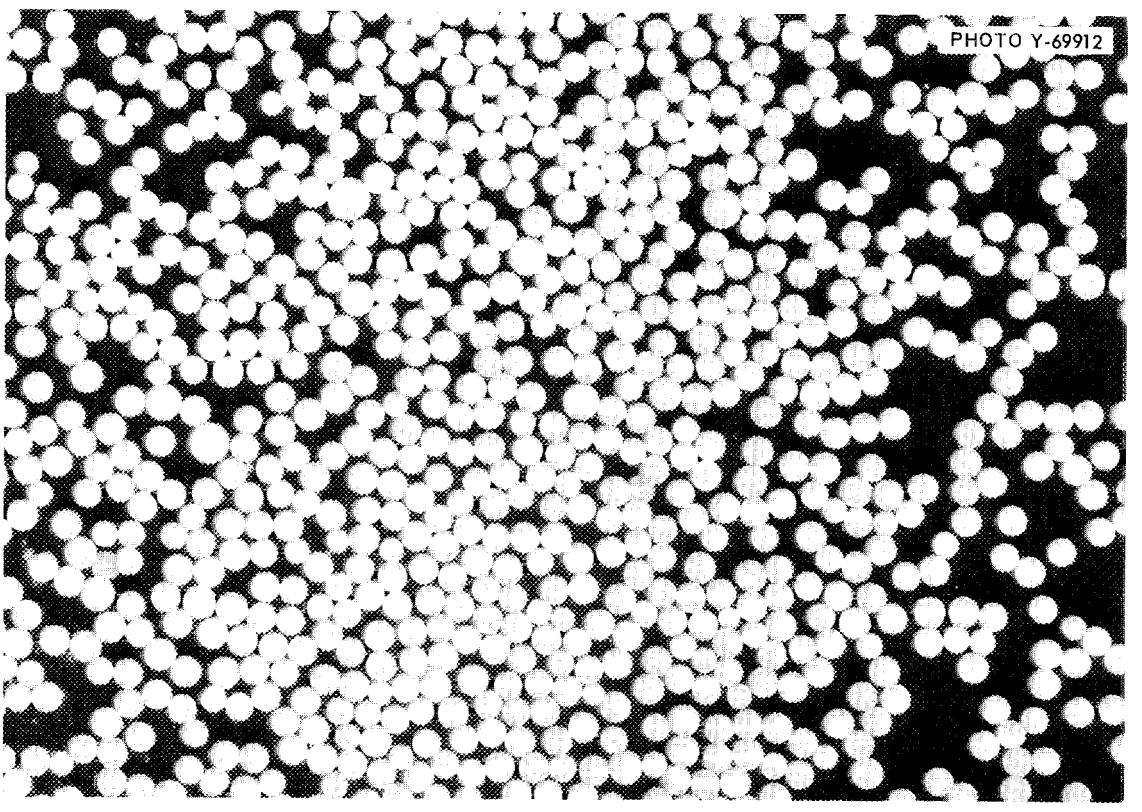

Fig. 5.3. Microspheres of 120-μ-diam Monoclinic Eu_2O_3 Calcined at 1475°C.

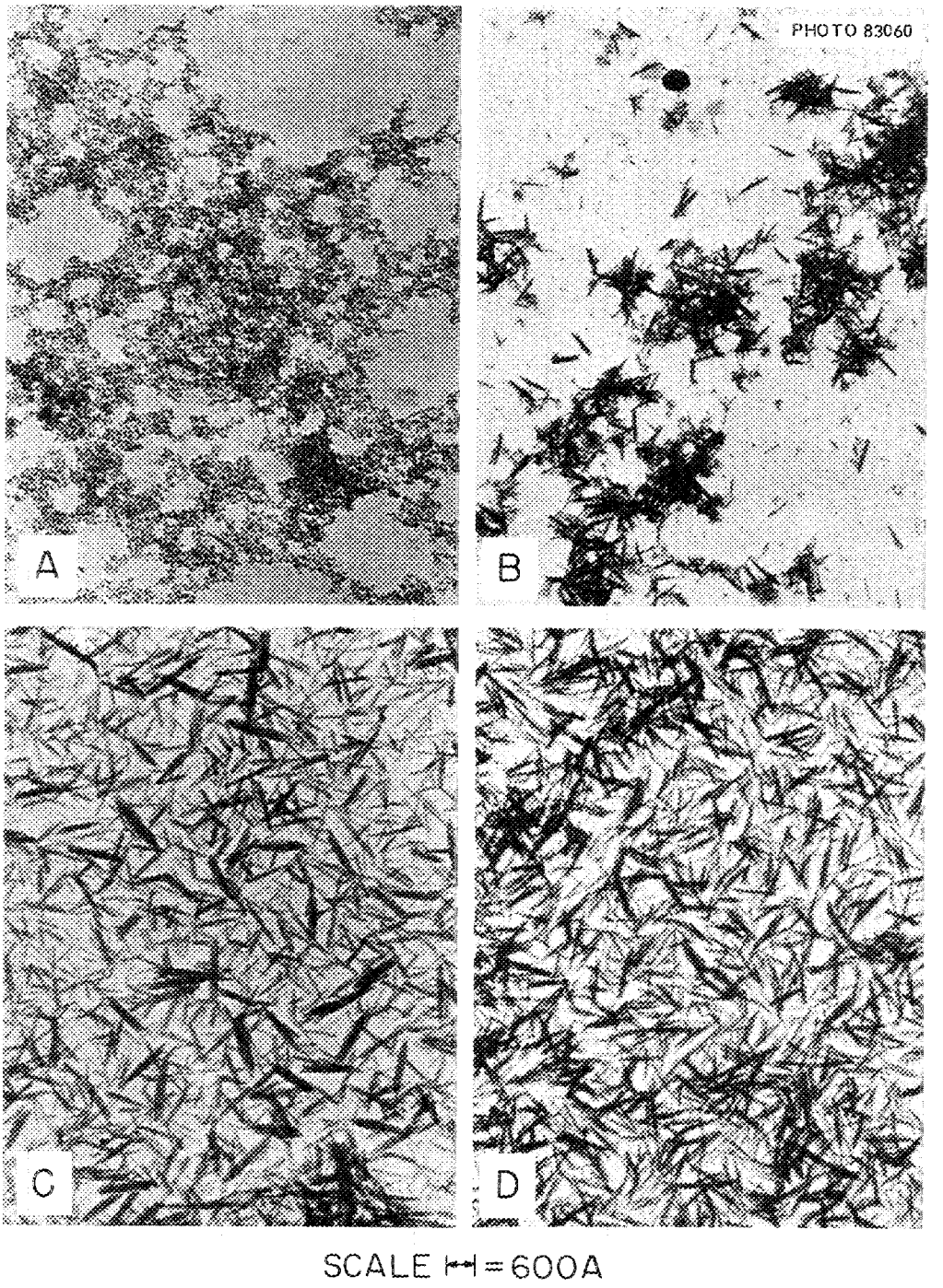

Fig. 5.4. Electron Micrographs of Praseodymium Hydroxide Sols. (A) Freshly precipitated, aged 18 min; (B) precipitate washed, aged 80 min; (C) precipitate washed, aged 140 min; (D) precipitate washed, aged 6 days.

much less tendency for americium hydroxide to peptize during the later stages of the washing procedure, and the sol formed during digestion was quite translucent, which is indicative of a small micelle size. A nitrate:americium mole ratio of 0.15 was required for good sol stability. After digestion, the sols were concentrated to nearly 2 *M* by evaporation.

Americium hydroxide microspheres were formed by introducing the concentrated sol from a syringe into a beaker of slowly agitating drying medium (20 vol % 2-octanol–80 vol % 2-ethyl-1-hexanol). The gel spheres calcined to stable oxide spheres at 1150°C.

Curium Sol Preparations. – Sols can be prepared from both ^{244}Cm and mixed ^{243}Am-^{244}Cm hydroxides by appropriate modifications of the rare-earth sol-gel procedure. Two radiolytic effects were encountered, but neither appears to limit the usefulness of the technique. (1) During sol concentration, severe foaming limits curium concentration to about 100 g/liter. (2) Considerable porosity can result from radiolytic decomposition of water in the set gel sphere. This latter effect is minimized by rapid drying and by calcining immediately after sphere formation. Dilute curium sols can be formed into uniform set gel spheres that calcine to very hard oxide microspheres.

Curium sols were produced by precipitating the hydroxide from an HNO_3 solution with NH_4OH, followed by two washes with 7 *M* NH_4OH to ensure complete removal of residual nitrate. The precipitate was further washed with distilled water until the pH of the filtrate was less than 8.0. This required six to eight washes. A high-speed centrifuge was used to separate the precipitate from the liquid.

After it was washed, the precipitate was transferred to a beaker as a thick slurry; and sufficient 0.1 *M* HNO_3 was added to give a nitrate:curium mole ratio of about 0.2. The slurry was stirred and heated at 50 to 70°C for 1 to 2 hr. During this digestion period the thick slurry became a thin sol characterized by the appearance of a foam layer. Digestion was continued until the volume of foam was equal to that of liquid. At this point a few milliliters of methanol was added, which quenched the foam and gave a thin, free-flowing sol. Because of the foaming, the maximum sol concentration was limited to about 100 g of curium per liter (300 w/liter). The sol generates radiolytic gas at a rate of about 8 liters/hr per liter of sol.

Sols prepared as described above can be formed by setting the sol in a drying solvent, either in a stirred pot or in a tapered column. However, preparing uniform microspheres by the stirred-pot method has not been possible, since the shearing action of the paddle breaks the dilute sol droplets into very small particles of various sizes. Improved uniformity and larger particles were obtained when a tapered column was used for sphere forming. Extensive agglomeration of the sol droplets during column drying was difficult to overcome; however, good results were obtained with a drying agent containing 79.3 vol % *n*-hexanol, 20 vol % *n*-octanol, 0.5 vol % Span 80, and 0.2 vol % Adogen 364. The Span 80 and the Adogen 364 were necessary to prevent agglomeration of the small droplets during dehydration. The set gel spheres were washed with methanol to remove residual drying agent and allowed to air dry. The resulting gel microspheres (average diameter of 100 to 200 μ) were free-flowing.

The gel particles must be calcined quickly, since water incorporated in the gel structure is decomposed by the intense alpha radiation, producing radiolytic gas and forming gas pockets in the gel spheres. The gel must be calcined at a temperature greater than 1050°C to produce oxide spheres that will retain their integrity. Spheres calcined at 800 to 1000°C tended to disintegrate. Calcination at 1200°C produced very hard, dense microspheres, which dissolved slowly in either 6 *M* HNO_3 or 6 *M* HCl at reflux. The gel spheres shrank in size about a factor of 3 during calcination at 1100°C, and the fired product was a free-flowing powder, with sphere diameters in the size range 40 to 80 μ.

Curium and mixed americium-curium oxides can also be prepared as hard fragments by drying and calcining their washed hydroxide precipitates. While oxide prepared in this fashion is suitable for HFIR targets, grinding and screening operations are necessary to obtain the desired particle size unless a mechanical method to form the hydroxide can be devised.

Ion Exchange Separations at High Activity Levels

Since the separation of californium-einsteinium-fermium and purification of some final products will be effected by ion exchange, recent work

was done with two such processes at high activity levels. About 0.5 g of ^{242}Cm in miscellaneous recycle solutions from the CRF was satisfactorily purified by LiCl anion exchange. An attempt to separate 0.5 g of ^{242}Cm from ~1.5 g of ^{241}Am by elution from cation exchange resin with α-hydroxyisobutyrate was less successful; however, results indicate that this method will probably be satisfactory with 100-mg quantities of ^{252}Cf.

The LiCl anion exchange purification of ~0.5 g of ^{242}Cm from recycle CRF solutions worked very well. During this processing, resin loadings were about 600 w/liter, which is substantially higher than any previously encountered. The product contained no detectable radiochemical contaminants.

In the chromatographic separation test, the resin was loaded up to 5000 w/liter with ^{242}Cm-^{241}Am. Methanol added to the process solutions effectively suppressed the formation of radiolytic gas so that no appreciable increase in pressure drop across the resin column was noted. However, resin degradation was severe, and about one-third of the ^{242}Cm became embedded in the charred resin and was not readily eluted. Essentially all this curium was recovered by slurrying the resin in 6 *M* HNO_3 and leaching for 24 hr. Even though the run was not successful, it appears that this procedure can be adapted for handling up to 100-mg amounts of ^{252}Cf. Further experiments are in progress to optimize column scale-up, and additional high-activity-level runs are planned.

Analysis and Processing of an Irradiated HFIR Prototype Target

One of the HFIR prototype target rods, TRU-SRL irradiation element No. 26, was discharged from the Savannah River High Flux Reactor on September 7, 1965, after an estimated irradiation of 3.7×10^{22} *nvt*. This target, which originally contained 10 g of plutonium (95.66% ^{242}Pu) as oxide, was dissolved, analyzed for transplutonium-element content, and processed to recover the heavy elements. Analyses by the best available methods indicated that the irradiated target contained 5.45 g of plutonium, 1.58 g of americium, 2.64 g of curium, about 5 μg of ^{252}Cf, about 2 μg of ^{249}Bk, and about 0.2 μg of ^{253}Es at the time of discharge from the reactor. Detailed analytical results, material balances, and other information about this rod have been published.[3]

The processing method consisted in dissolving the aluminum jacket and matrix in caustic–sodium nitrate solution, dissolving the residue in HCl containing CuF_2 catalyst, isolating the plutonium by sorption on anion exchange resin from HCl solution, effecting group and partial separation of the transplutonium elements by LiCl anion exchange, and separating berkelium-californium-einsteinium by chromatographic elution from cation exchange resin with a solution of ammonium α-hydroxyisobutyrate.

Target Dissolution. – The aluminum jacket and matrix of the target rod (~150 g of aluminum) were dissolved in 1 liter of 5.2 *M* NaOH–4.8 *M* $NaNO_3$. The reaction rate was easily controlled by regulating the amount of rod immersed in the caustic solution, and dissolution was complete in about 3 hr. The solution was filtered to recover the undissolved residue (residual PuO_2 and actinides). Loss of curium in the aluminum dissolver solution was <0.1%.

The actinides, including residual PuO_2, were essentially dissolved after being refluxed in 8 *M* HCl–0.1 *M* CuF_2 for 1 hr. Two additional passes with refluxing 8 *M* HCl–0.1 *M* CuF_2 were made to ensure complete dissolution of the PuO_2. These two passes contained less than 0.5% of the total plutonium recovered. All three of the solutions were combined for processing. This combined solution was carefully analyzed to determine the total amount of actinides in the irradiated target.

Plutonium Isolation. – Plutonium was separated from fission products and other actinides by loading a plutonium chloride complex on an anion exchange resin from an HCl solution. Final purification was obtained by the standard HNO_3 anion exchange process.

The dissolver solution was adjusted to 8 *M* HCl–1 *M* HNO_3 and passed through an anion exchange column at 60°C. Under these conditions, 95% of the plutonium (5.3 g) was loaded on the column and was later recovered as product. Attempts to elute plutonium by reducing Pu^{4+} to Pu^{3+} with 1 *M* $NH_2OH{\cdot}HCl$ in 8 *M* HCl were not successful, but satisfactory plutonium elution

[3] W. D. Burch, *Transuranium Quarterly Progress Report for Period Ending Oct. 31, 1965*, ORNL-3965 (in preparation).

was accomplished without valence change in 1 *M* HCl. Attempts were made to further purify the plutonium from ^{103}Ru and ^{95}Zr by reducing the plutonium to the trivalent state with 1 *M* $NH_2OH \cdot HCl$, adjusting the HCl to 8 *M*, and passing the adjusted feed through an anion exchange column. Under these conditions, ruthenium and zirconium sorb as chloride complexes while Pu^{3+} passes readily through the column. This procedure was not successful, since difficulty was experienced in reducing plutonium.

Final plutonium purification was obtained by anion exchange from HNO_3. The plutonium was precipitated from the chloride solution as the hydroxide, filtered, and washed with NH_4OH. The hydroxide was then dissolved in 8 *M* HNO_3, and the plutonium valence was adjusted by reduction with ferrous sulfamate, followed by oxidation to Pu^{4+} with $NaNO_2$. Plutonium was loaded on a Dowex 1-X4 (50- to 100-mesh) anion exchange resin at 80°C, washed with 8 *M* HNO_3–0.01 *M* HF, and eluted in 0.7 *M* HNO_3.

Transplutonium-Element Isolation. – The transplutonium elements were recovered by LiCl anion exchange. Eluate from the first plutonium ion exchange column was adjusted to 12.5 *M* LiCl and passed through an anion exchange column to load actinides and rare-earth fission products. Rare earths were eluted with seven column volumes of 10.5 *M* LiCl–0.1 *M* $NH_2OH \cdot HCl$–0.1 *M* HCl. This gave a rare-earth decontamination factor of $>10^3$ and a curium breakthrough loss of 0.3%. Partial separation of americium and curium from the transcurium elements was obtained by eluting with 9.5 *M* LiCl–0.1 *M* HCl until about 80% of the americium and curium was removed from the resin column. The remaining actinides were stripped from the resin column in 1 *M* HCl. This product fraction contained 420 mg of ^{244}Cm, 165 mg of ^{243}Am, and essentially all the berkelium, californium, and einsteinium. It was treated with NH_4OH to precipitate the metal hydroxides, which were filtered and washed. The precipitate was dissolved in 50 ml of 1 *M* HCl, evaporated to dryness, and redissolved in 50 ml of 0.05 *M* HCl to prepare feed for sorbing the actinides on a cation exchange resin column. The actinides were loaded at 80°C onto 200 ml of Dowex 50W-X12 resin (200 to 400 mesh) in a column 2.5 cm in diameter and 36 cm long. Flow rates throughout the run were maintained at 0.35 ml cm^{-2} min^{-1}.

After being loaded, the resin was washed with 50 ml of 0.05 *M* HCl, and the transplutonium elements were separated by chromatographic elution with 0.5 *M* ammonium α-hydroxyisobutyrate at pH 4.2 until the californium was eluted, and then with 0.4 *M* ammonium α-hydroxyisobutyrate at pH 4.6. Fractions were taken during this elution and were analyzed by alpha pulse to determine the actinide content.

Berkelium was recovered from the center column fraction that preceded curium elution by converting to 8 *M* HNO_3 solution, oxidizing to Bk^{4+} with $KBrO_3$, extracting with 0.3 *M* di-(2-ethylhexyl)phosphoric acid in decane, and stripping with 8 *M* HNO_3–1 *M* H_2O_2.

5.2 DEVELOPMENT OF PROCESS EQUIPMENT

Engineering studies are being conducted to develop equipment and operating procedures for the TRU. The development of solvent extraction equipment was concerned mainly with glass prototype pulse columns in which the flowsheets were tested to determine flow capacity, mass transfer efficiency, and revisions to the chemical flowsheets. Two of the equipment racks for the plant were tested.

Status and Progress

In the Tramex flowsheet, emulsions stabilized by zirconia sol were minimized by revising the feed adjustment step. Final testing of the Zircaloy-2 pulse-column rack was completed before it was installed in the plant. The batch spray column for berkelium separation was satisfactorily "cold" tested. Work was started on the flowsheet for separation of americium and curium from other transuranic elements. Severe plate wetting by the solvent was partially eliminated by purification of the organic reagents, but the only completely successful operation was with the organic phase continuous. Studies will be continued on this flowsheet.

Tramex Process

Testing of the Tramex process showed that emulsions can be minimized by careful feed adjustment and that operation in the full-scale

pulse columns is satisfactory with synthetic process solutions. Both zirconia and silica sols emulsify when they are mixed with the Tramex solvent. The sols are formed by hydrolysis during the boildown feed adjustment step. The amount of sol and subsequent emulsion is minimized by keeping the temperature below 120°C during the boildown and then by adjusting the free acid to 0.2 *M* or higher. Addition of complexing agents such as tartrate or sulfate was not adequate. Addition of a flocculating agent (Polyox 205) reduced the amount of emulsion, but gel "strikes" that were useful in other flowsheets caused heavy emulsions.

Final testing of the full-scale pulse columns before installation in the process building was completed. Continuous operation was successful with solutions that were typical, except for radioactivity, for the Tramex process. The LiCl feed contained about 100 ppm of zirconium, and its concentration was adjusted by boildown. Several pump diaphragms made of Zircaloy-2 failed; however, none of the replacements made of a tantalum–10% tungsten alloy failed. The efficiency of the columns, measured by using $NiCl_2$ as the solute, agreed with that previously obtained in the small glass columns in which most of the development work was done.

Berkelium Separation Equipment

The semicontinuous spray column designed for separation of berkelium from the other transuranic elements was tested with typical nonradioactive solutions. The equipment was demonstrated to be hydraulically adequate although one of the spray heads plugged. The hole sizes were subsequently enlarged. The efficiency was satisfactory in a test with cerium and europium as substitutes for berkelium and californium. After several revisions of the chemical flowsheet, greater than 98% recovery of cerium was obtained, with a decontamination factor greater than 1000 with respect to europium.

Separation of Americium and Curium from Other Transuranic Elements

Following the separation of actinides from lanthanides by the Tramex process, the actinides are separated by the Pharex process into two groups with 2-ethylhexylphenylphosphonic acid as the extraction agent. Study of this procedure in pulse columns is in progress. Severe plate wetting by the solvent, and consequent phase inversion, was a problem. Cleaning of the plates gave only temporary relief. Treatment of the diluent (Amsco) with activated alumina and scrubbing of the solvent with strong HCl removed unidentified surface-active agents and reduced plate wetting. This permitted operation for a short period, but the solvent cleanup was inconsistent and the tests could not be repeated.

Other means of circumventing the problem are under study. Flame-treating of the plates to form a heavy oxide film minimized the wetting phenomena and permitted operation of the columns with the aqueous phase continuous, as designed. It also appears satisfactory to operate the columns with the organic phase continuous.

5.3 DESIGN AND FABRICATION OF PROCESS EQUIPMENT

Equipment was designed and built to separate and recover the actinide elements from irradiated HFIR target rods. (Solvent extraction, ion exchange, and precipitation techniques are used.) Equipment fabricated of Zircaloy-2, tantalum, and Hastelloy C, for corrosion and resistance in HCl systems, is mounted on racks that are remotely replaceable if failures should occur or if new techniques should be required.

Status and Progress

After approximately three years of continuous effort, the design and fabrication of all main-line chemical process equipment were completed. One special equipment rack for preparing oxide precipitates for use in making recycle targets is being delayed until development of the sol-gel procedure is completed. Essentially all this equipment is now installed in the facility.

Equipment Racks

Two of the three equipment racks that were incomplete at the beginning of this year – the solvent extraction system and the californium-einsteinium-fermium separation system racks – were designed and fabricated. A flowsheet based

on the sol-gel technique was selected for the preparation of oxides for fabrication of HFIR targets, and design of this final equipment rack has just started.

The separation of californium, einsteinium, and fermium is accomplished by chromatographic elution from an ion exchange resin. The ion exchange column and related feed preparation and solution handling systems for this operation are made entirely of tantalum to minimize the contamination of the small quantities of products with impurities from corroding equipment. In-line alpha and neutron monitors on the elutriant stream from the ion exchange column show the elution peaks for the different specific alpha and neutron activities of the three products and allow the correct product cuts of the elutriant stream to be made.

To provide a more versatile first-cycle solvent extraction system, the equipment rack originally fabricated for this position was modified slightly for use as the second-cycle extraction system, and a new first-cycle rack was designed and made. The added versatility was desirable to allow a number of different head-end flowsheets to be run in the first cycle. The new first-cycle rack was designed with a number of piping jumpers on the front of the rack, to allow rerouting of inlet and recycle streams into alternate points of the three-column system.

In-Line Instrumentation

To maintain current information on such operating variables as losses, separation factors, and decontamination factors, a group of monitors (one alpha, one gamma, and four neutron) was installed for the process streams. The gamma monitor consists of a detector and a multichannel analyzer that scan the aqueous product stream from either the first- or the second-cycle strip column. Analysis of the gamma spectrum from this instrument gives a semicontinuous measure of product purity and fission product decontamination.

The alpha and neutron monitors are similar in design and make use of a solid-state detector of the surface-barrier type. As an alpha counter the solid-state element is relatively insensitive to both neutrons and beta-gamma radiation. For neutron detection, the face of the detector is covered with a polyethylene sheet, and the proton from the *n-p* reaction of fast neutrons is detected. Although its efficiency for neutron counting is only about 0.1%, the detector has the advantage that it is extremely directional and can be used in a relatively high general neutron background.

The waste aqueous and organic streams from each of the solvent extraction systems pass in front of a neutron detector that is able to detect losses in the range of 1%. A third neutron detector is located at the bottom section of the berkelium recovery column and monitors the californium content of the berkelium product during the separation steps. An alpha and a neutron monitor on the elutriant stream from the californium-einsteinium-fermium separation system show the activity peaks of these three components.

Centrifuge

Design and fabrication of the all-Zircaloy-2 centrifuge were completed, and the unit was tested thoroughly before installation. During the tests, minor vibrational problems were encountered that required a modification of the support bearing between the drive motor and the centrifuge bowl, and the addition of vertical and horizontal vanes in the centrifuge to prevent wave harmonics from developing. The centrifuge was operated at speeds up to a maximum of 4000 rpm. In preinstallation testing, removal efficiencies for appropriate rare-earth hydroxide simulants were measured and shown to be adequate. A centrifugal force exceeding $2500 \times g$ is developed at 4000 rpm.

Fabrication of Miscellaneous Equipment

Several items of miscellaneous equipment were procured or fabricated. Included are two components of the solid-waste handling system — a waste accumulation station and a carrier for transporting waste containers from the transfer cubicle to the accumulation station. The latter, which is installed in the limited-access area, incorporates a disposable 42-in. concrete cask inside a supplementary shield. Small waste items are accumulated in plastic containers 10 in. in diameter by 10 in. high. These are heat sealed at the transfer cubicle and then stored in the accumulation station, to be disposed of in groups of 30 to 40 in the concrete cask.

Fabrication of the Postirradiation Carrier, which provides sufficient shielding (4 ft of limonite concrete) to handle 1 g of californium, was completed, except for the addition of the shielding material. An existing cask was modified for use as a Preirradiation Carrier, where gram amounts of curium are handled in each target. Specifications for a periscope were prepared, and an order was placed for one unit. Periscope sleeves are provided in all cells, and the periscope can be used at any cell after installation of a viewing dome. This dome can be installed from the operating area without jeopardizing containment.

5.4 CONSTRUCTION OF TRU

The Transuranium Processing Plant, containing nine shielded cells, eight laboratories, and related service areas, is essentially complete.

Status and Progress

The lump-sum contractor completed construction of the basic building in June 1965. From May 17, 1965, through October 1965, the H. K. Ferguson Company installed, on a cost-plus-fixed-fee contract, certain portions of the equipment required for operation of the processing equipment. On October 18, 1965, ORNL craft forces began installation of the shop-fabricated processing equipment. The major part of this phase was completed in January 1966, at which time "cold" shakedown runs were begun.

An office addition to TRU was also constructed during this time and was occupied by ORNL personnel during the latter part of February. A shielded alpha cave is being constructed; also, a 50-ton crane to transfer equipment from trucks to the building handling facilities, an emergency

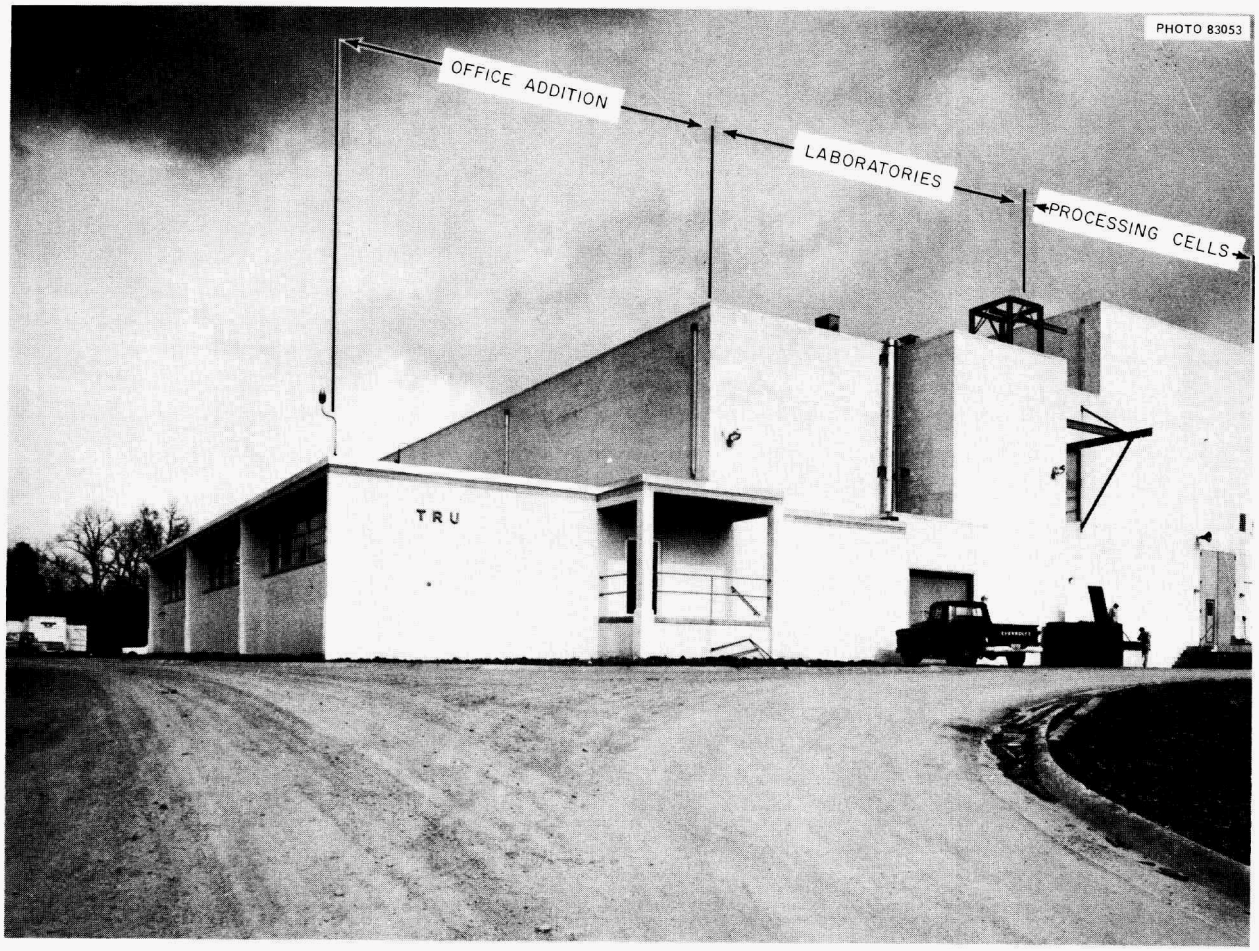

Fig. 5.5. Transuranium Processing Plant.

generator, and a data-logging system are being purchased for incorporation into TRU.

Building Construction

An overall view of TRU, showing the process cell area, laboratory wing, and office annex, is shown in Fig. 5.5.

Installation of Process Equipment

The installation of processing equipment was divided into two phases. The first phase, comprising approximately 80%, was done on a cost-plus-fixed-fee contract. On May 17, 1965, the H. K. Ferguson Company began the installation of the instrument racks, piping, electrical, and structural equipment required for final placement and operation of the prefabricated processing equipment to be installed in the cell tank pits and the cubicles. A major part of this work was in the Chemical Makeup Area, and this is depicted in Fig. 5.6. This work was completed on November 1, 1965, as originally scheduled.

Phase 2, the installation of the processing equipment in the cubicles and cell tank pits, was begun on October 18, 1965, by ORNL craft forces. This work included the intercell conveyor, processing equipment in the nine cubicles and seven cell tank pits, and miscellaneous process auxiliaries.

Locating all equipment in the cell tank pits and the cubicles from a set of grid bars in the

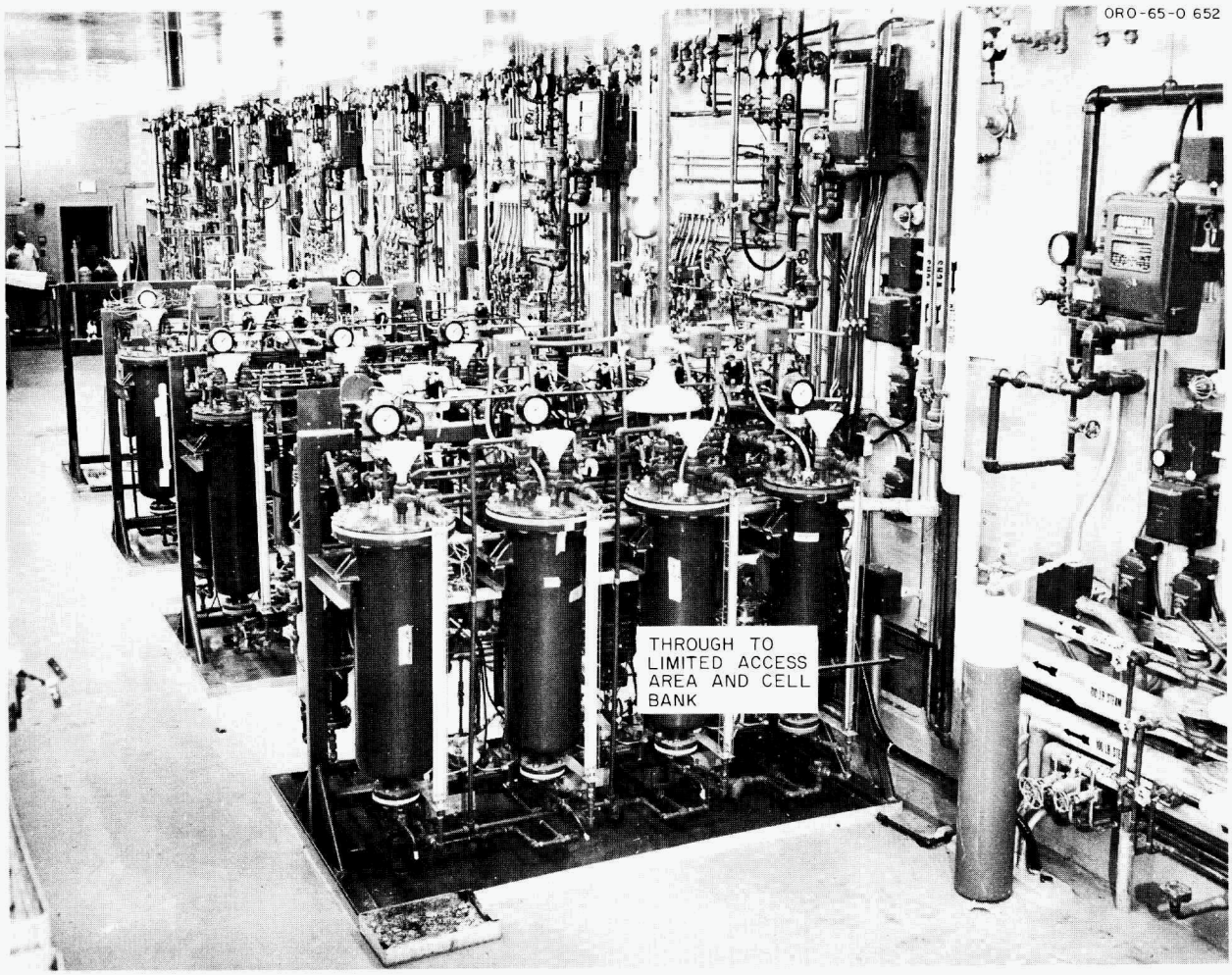

Fig. 5.6. Chemical Makeup Equipment and Service Piping in Chemical Makeup Area.

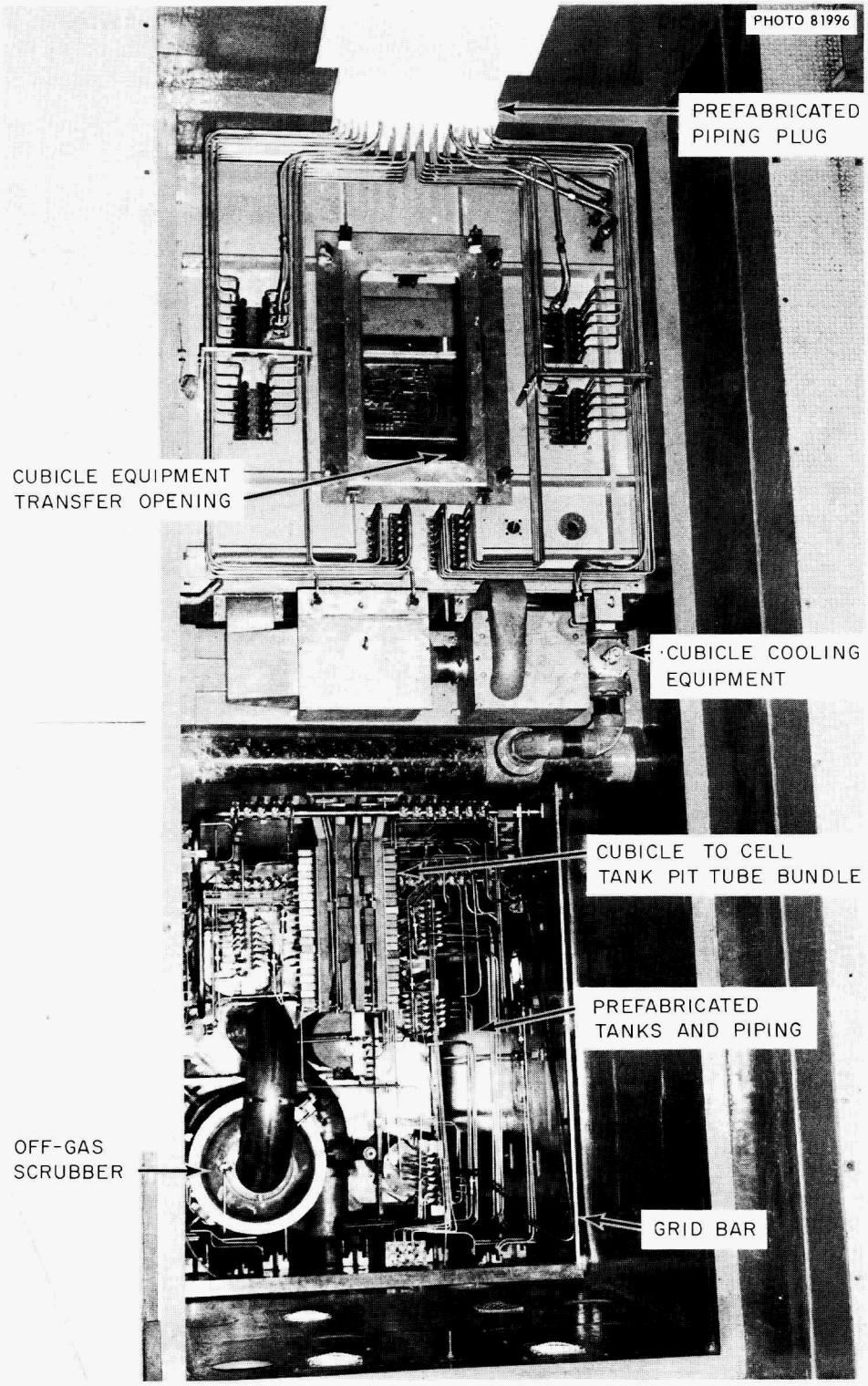

Fig. 5.7. Overall View Looking Down at Chemical Processing Equipment in Cell 7.

pits proved to be a very workable arrangement. The few inevitable errors were quickly isolated, and adjustments were made with appropriate jigs or other devices to relocate the item in question.

The equipment in the cubicles and tank pits, shown in Figs. 5.7–5.9, was originally fabricated in mockups and jigs, utilizing the convenience of shop facilities. The prefabricated tubing was readily installed in the facility; it required only bolting in place and leak checking in this final phase of construction.

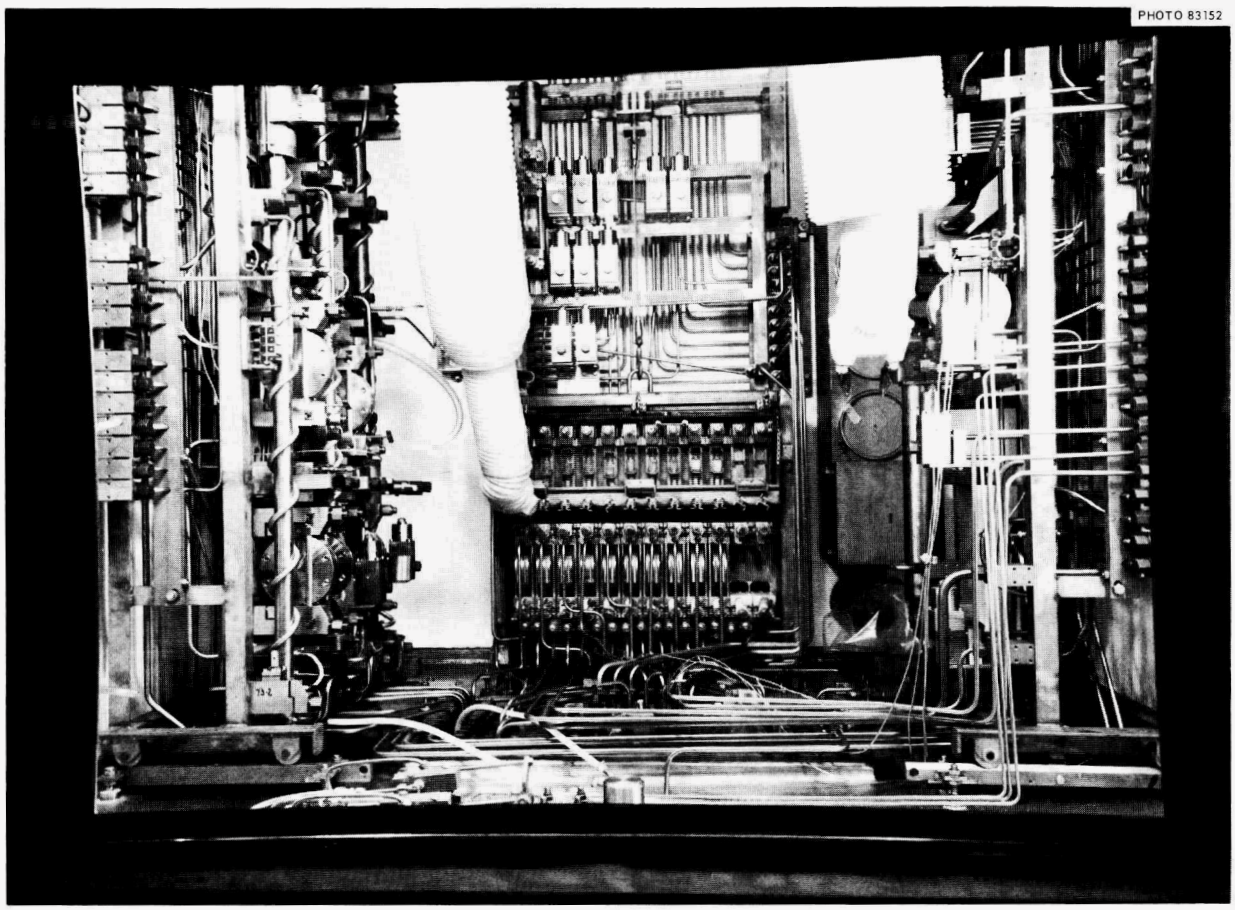

Fig. 5.8. View of Chemical Processing Cell Through Front Window. Solvent extraction equipment rack on left, sampler station at back of cell.

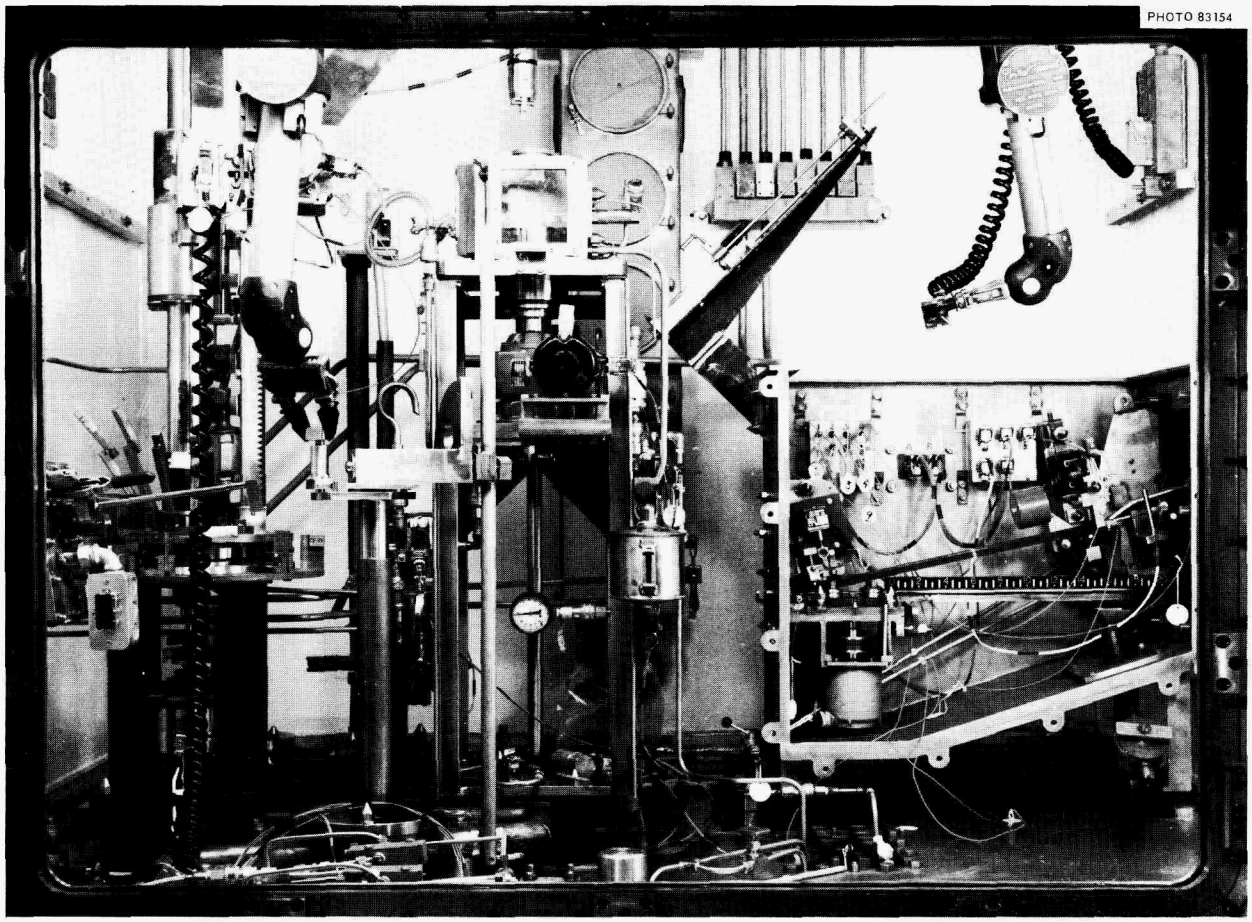

Fig. 5.9. View of Target Fabrication Cell Showing Pellet Loader on the Right and Welder in the Center.

5.5 TRU OPERATIONS

Construction of TRU and installation of much of the processing equipment was completed this year. Building and process equipment checkout was started simultaneously with the start of final equipment installation by ORNL craft forces.

Status and Progress

The TRU operating group was assembled and is engaged in training and in pre-startup checking of TRU. The plant and the equipment were checked for conformity with the drawings, and all building service systems are in operation. Cell and building air balancing and leak testing were completed. Equipment and operating procedures were tested for all "cold" chemical makeup, for dissolving HFIR targets, for removing excess aluminum from the feed by caustic precipitation followed by centrifugation, for recovering the plutonium by ion exchange (Plurix), for metering radioactive feed to the process, for the first cycle of solvent extraction (Tramex process), and for recovering berkelium by batch solvent extraction (Berlex process). Second-cycle solvent extraction (Pharex) has not been operated successfully; certain changes must be made and development work must be extended. The equipment for separating californium, einsteinium, and fermium has just been completed and is ready for checkout.

A safety analysis of TRU and of the proposed operations was prepared and was reviewed by the ORNL Director's Radiochemical Plants Committee. Operation of the processing plant was approved.

Available Feed Materials

The normal feed for TRU will be HFIR-discharged targets containing varying amounts of the heavy-element oxides dispersed in aluminum. However, there is a backlog of actinide materials from some special irradiations at Savannah River that will supply feed to TRU until the irradiations in the HFIR become routine. These sources include the following:

1. Four "prototype" targets that have an active region equal in size to that of HFIR targets, but with a different external configuration to make the targets more convenient to irradiate in one of the Savannah River Plant (SRP) reactors.
2. Eight SRP slugs that contain all available ^{242}Pu not already committed to HFIR targets.
3. About 250 gal of HNO_3 solution containing 260 g of ^{242}Cm and 220 g of ^{243}Am. This material was recovered at Savannah River from the wastes from the original ^{242}Pu processing.

Table 5.3 indicates the expected quantities of actinides in these special feeds.

Inspection of 18 HFIR Targets

About 100 to 200 μg of californium is contained in 18 target rods that were irradiated at SRP and are now stored in the HFIR pool. There is no incentive to process these targets to recover the transuranic actinides in the near future, since the feeds listed in Table 5.3 are far more valuable. However, the rods have the equivalent of three months' full-power irradiation in the HFIR, and they will be put in the first HFIR target loading if their integrity can be assured. Preliminary inspections revealed some damage to the spacer fins that center the rods in an outer sheath, but a method for installing an additional spacer is being investigated and will probably prove acceptable.

The targets will be brought from the HFIR pool to the TRU facility, inspected in cubicle 1, and returned to the HFIR. Ten separate inspections or operations will be performed on each rod.

Proposed Program

The plant will begin operating with radioactive feed during June. The special feeds will be

Table 5.3. Expected Compositions of Special Feeds for TRU

	Total Mass in All Feed Material of Indicated Type		
	Four TRU-SRP Prototypes	Eight SRP Slugs	250 gal of HNO_3 Solution
Al, g	1000	2000	
^{242}Pu, g	12	92	0
^{243}Am, g	6	37	220
^{244}Cm, g	14	93	260
^{248}Cm, g	0.002	0.05	
^{249}Bk, mg	0.04	0.7	
^{252}Cf, mg	0.2	1.7	0.2
Mixed fission products, g	8	50	5000[a]

[a]Almost all gamma-ray activity has decayed or has been separated except that from ^{154}Eu and ^{144}Ce.

processed first; then the main program will begin. This involves recovering transcurium elements and recycling americium and curium to the HFIR. The exact schedule of processing and irradiation will depend on the demands for the various transuranium isotopes.

Special Target Dissolver

Hot-cell tests on irradiated plutonium specimens indicated that HCl was not effective in dissolving high-fired PuO_2 particles that had been irradiated to less than 65% burnup. At lower burnups, even the conventional 15 *M* HNO_3–0.1 *M* HF is very slow in dissolving PuO_2. Because of our complete inability to handle fluoride-containing reagents in the nearly all-Zircaloy-2 TRU equipment, a new stainless steel dissolver system was designed and installed in cell 6 on an unused portion of one rack.

This system consisted of a dissolver, a condenser, an off-gas scrubber, a filter, and a sampler. We intend to use this system to dissolve the partially irradiated targets we now have, plus any HFIR targets that might be pulled early. At a later date, when we will expect no more of these targets that are difficult to dissolve, we will remove the stainless steel dissolver system.

The target dissolution method consists in dissolving the aluminum matrix in caustic, dissolving the residue in refluxing 15 *M* HNO_3–0.1 *M* HF, removing the fluoride by precipitating the actinide elements and withdrawing the fluoride-containing supernatant, and then dissolving the residue of actinide elements in dilute HNO_3 for transfer to the main part of the plant. No fluoride will leave the stainless steel system except in a basic solution, where it is not harmful to the Zircaloy-2.

This new dissolver system was checked out by dissolving dummy targets containing CeO_2 as a stand-in for PuO_2. The first of the irradiated targets is now ready to be dissolved.

Feed Precipitation and Centrifugation

The all-Zircaloy-2 centrifuge will be used for feed clarification and recovery of precipitated hydroxides in nitrate-to-chloride conversion processes. Slurries are fed by steam jet, and a control-board-mounted steam regulating system was required before adequate metering could be achieved. All components of this system now function satisfactorily.

Plutonium Removal and Recovery (Plurix)

This portion of the system was tested and operated successfully. Chemical runs were made with iron as a stand-in for plutonium. However, plutonium is so different from iron that only "hot" operations can provide a real test of efficiency or recovery. An improved seal (O-ring) was installed on the top, movable, resin retainer screen to prevent a small loss of resin into the piping system.

First Solvent Extraction Cycle (Tramex)

The pulse columns and auxiliaries for the first cycle of solvent extraction were successfully operated on the Tramex flowsheet at flow rates of 0.5 liter/hr for synthetic feed, 0.7 liter/hr for scrub, and 1.5 liters/hr for extractant. Although slightly lower than originally intended, this throughput is still completely adequate.

Second Solvent Extraction Cycle (Pharex)

This process equipment, which is nearly identical to that used in the first cycle, was also successfully operated. However, the Pharex reagent (2-ethylhexylphenylphosphonic acid), which was custom prepared for us by a commercial firm, cannot be used with this equipment. Apparently, either the material or an impurity in this material reacts with the metal surfaces in the pulse columns and makes them organophilic. When significant amounts of organic "wet" the pulse plates, flow through the aqueous-continuous column is restricted, and the columns "flood." Methods of circumventing the problem are being studied by the development groups.

Berkelium Recovery Process (Berlex)

Hydraulic behavior of the berkelium recovery system was satisfactory during a "cold" run in which stable cerium and europium were added to

the feed as stand-ins for berkelium and californium. Analytical results showed no detectable cerium in the raffinate and no detectable europium in the product. This indicates a maximum product loss of 1.9% of the cerium to the raffinate, a decontamination factor for europium of at least 245, and an overall separation factor greater than 1.5×10^4. Material balances for cerium and europium were 80 and 117% respectively.

If the chemistry of berkelium is like that of cerium, performance of this equipment under "hot" conditions should be quite satisfactory.

6. Curium Processing

The Curium Program was jointly undertaken by the Isotopes Division and the Chemical Technology Division to prepare curium for fabrication into heat sources. The heat sources are desired to develop the techniques of incorporating curium into thermoelectric converters for evaluation as SNAP-type generators. The Chemical Technology Division is responsible for the purification of the curium, and for delivery of the refined product to the Isotopes Division. A number of process methods, facilities, and source materials were used for both the Curium Program and the closely related Transuranium-Element Program (Sect. 5).

The Curium Recovery Facility (CRF) was originally designed for laboratory-scale testing of transuranium-element processes at high levels of radioactivity. It went through several phases of modification to improve its operation and to increase its capacity to the multigram level. During the program, the Clanex, Dapex, and Tramex recovery processes were tested at high levels of radioactivity, while about 35 g each of ^{243}Am and ^{244}Cm and about 25 g of ^{242}Cm were recovered. Details of the processes will be discussed below, followed by sections devoted to ^{242}Cm and ^{244}Cm recoveries in the CRF and a series of tests conducted at high radiation levels to evaluate a number of alternate flowsheets. A brief description of equipment, modifications, and operating experience in the CRF concludes this section.

6.1 PROCESS DEVELOPMENT

The principal out-of-cell development work on this Program was a laboratory-scale study of adverse radiation effects on Tramex feed solution. Although the radiolytic mechanism is not known, practical methods for overcoming the adverse effects were developed and successfully used during CRF operations. Other studies with transuranium elements are reported in the previous section (Sect. 5).

Study of Radiolytic Effects on Tramex Feed

During ^{242}Cm processing in the CRF, two important effects of alpha radiolysis in high-activity-level feed were noted. These were (1) the rapid loss of acid from adjusted feed and (2) the formation of oxidants that converted cerium to the extractable tetravalent state, making good cerium decontamination impossible. During the initial CRF runs, methyl alcohol added to the feed decreased the rate of acid loss only slightly compared with the very effective stabilization of feed acidity demonstrated in previous tests.[1,2] Laboratory-scale tests made to resolve this discrepancy showed that, to be effective, methyl alcohol must be added to feed already containing an appreciable concentration of the oxidants formed by radiolysis. As a result of these studies, the CRF operating procedure was changed to allow oxidants to accumulate for about 100 whr after boiling before adding the methyl alcohol. This usually resulted in effective stabilization of the acid. Also studied was the effect of $SnCl_2$, a reductant added in CRF processes to keep cerium in a trivalent state.

Radiolytic Effects in Tramex Feed

Acid loss and oxidant formation as a function of alpha radiation dose were determined for a sample

[1] D. E. Ferguson *et al.*, *Chem. Technol. Div. Ann. Progr. Rept. May 31, 1965*, ORNL-3830, pp. 157–73.

[2] B. Weaver and F. A. Kappelmann, *Talspeak: A New Method of Separating Americium and Curium from the Lanthanides by Extraction from an Aqueous Solution of an Aminopolyacetic Acid Complex with a Monoacidic Organophosphate*, ORNL-3559 (August 1964).

of Tramex feed prepared in the CRF. The feed was 10.1 *M* LiCl containing hydrolyzable metal impurities (aluminum, fission products, rare earths, and corrosion products) at a concentration of 0.2 equivalent/liter and ^{242}Cm at a concentration of 96 mg/liter (11.5 w/liter). The initial tests were made by following the procedure previously used in the CRF. Immediately before starting the experiment, dissolved chlorine was removed by heating the sample to boiling. Then the sample was cooled to room temperature, and a final acid adjustment was made. Solution acidity and the oxidant concentration, expressed as available chlorine, were determined at various times. The results plotted as a function of total radiation dose in watt-hours per liter of feed are presented in Fig. 6.1.

The acid concentration of the solution dropped from 0.40 *M* to zero, and hydrolyzable metal ions, including curium, precipitated in 57 hr or at a total radiation dose of 660 whr/liter. These results are in good agreement with operating experience in the CRF. It can be noted in Fig. 6.1 that the rate of acid depletion decreased as the free-acid concentration decreased. At a free-acid concentration of 0.35 *M* the rate of acid loss was 1.0 meq/whr; at 0.10 *M* the rate was 0.60 meq/whr.

The lower curve in Fig. 6.1 shows the oxidant concentration, which was determined as available chlorine as a function of alpha-radiation exposure. The initial increase in oxidant concentration, which should approximate the initial production rate of oxidant, was about 1.0 meq/whr. A maximum oxidant concentration of 0.021 equivalent/liter was reached at a dose of 120 whr/liter. Oxidant concentration in the feed solution then decreased at a rate of 0.025 meq/whr. The reason for this increase to a maximum followed by a decrease upon further exposure is not known.

Behavior of Stannous Chloride in Tramex Feed

Since stannous chloride is used in CRF operations to keep cerium in the unextractable trivalent state, a laboratory-scale test was made to investigate $SnCl_2$ behavior in Tramex feed. Here the stannous ion was oxidized at the rate of 1.0 meq/whr, which agrees with the initial rate of oxidant formation in the previous experiment (Fig. 6.1). Stannous ions in Tramex feed caused about a 50% increase in the acid depletion rate (~1.5 meq/whr instead of 1.0 meq/whr at 0.35 *M* H^+) but greatly decreased the production rate of radiolytic gas. After all the stannous ions were oxidized, the rate of radiolytic gas formation increased, the rate of acid loss decreased to that observed for untreated feed solution, and oxidants accumulated in the solution.

Effect of Methanol in Tramex Feed

Effective acid protection with methanol in Tramex feed was found to depend upon the presence of radiolytically formed oxidants at the time of the methanol addition. In a typical laboratory

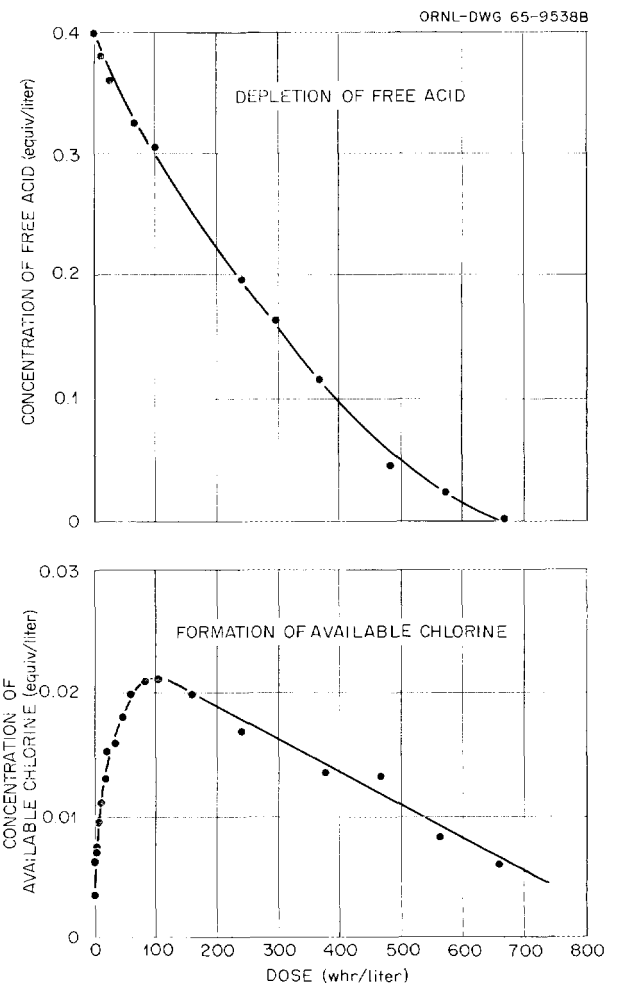

Fig. 6.1. Effect of Alpha Radiation on Tramex Feed Solution. Medium: 10.1 *M* LiCl; power level: 11.5 w/liter.

test, the final acid adjustment was made, and 5 vol % methanol was added immediately after the Tramex feed sample was heated to boiling to remove oxidants. The rate of acid depletion measured at 0.1 *M* H^+ was 0.3 meq/whr compared with 0.6 meq/whr previously observed for untreated feed. The acid concentration decreased from 0.3 *M* to zero, and metal hydroxides precipitated at an alpha radiation dose of 880 whr/liter, which is only slightly more than the 660-whr/liter exposure that reduced the acid concentration of untreated feed from 0.4 *M* to zero. Throughout the test with methanol, the oxidant concentration measured as available chlorine was 2 meq/liter (one-tenth the maximum concentration observed for untreated feed).

Effective acid stabilization was demonstrated in a test in which the oxidant concentration was allowed to reach a maximum before methanol was added. Five volume percent methanol, added to feed (containing the radiolytically formed oxidants) at 15.8 w/liter (132 mg of ^{242}Cm/liter), stabilized the acid concentration during an exposure of about 2000 whr/liter (Fig. 6.2), after which the acid was depleted at a rate equal to that observed for untreated feed. Assuming that all the alcohol (~1.2 moles/liter) was consumed during the exposure, the estimated rate of methanol destruction is 0.6 meq/whr, a rate comparable to that for acid destruction in untreated feed.

Also plotted in Fig. 6.2 is the oxidant concentration as a function of dose. The oxidant concentration was essentially constant at ~0.5 meq/liter during the time that the acid was stabilized. It reached a maximum of 2 meq/liter at an exposure of about 1800 whr/liter, which roughly corresponds to the dose at which most of the methanol was consumed.

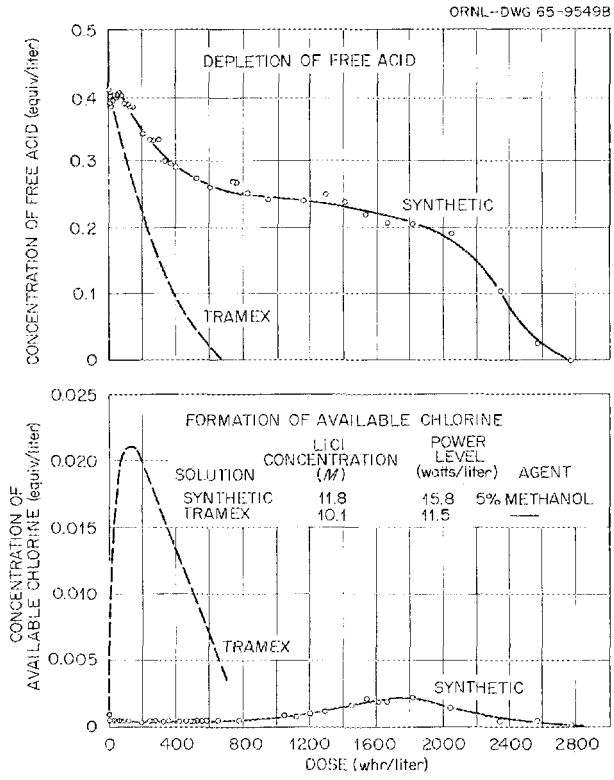

Fig. 6.2. Effects of Alpha Radiation on Concentrated LiCl Solutions Stabilized with Methanol.

Combined Effect of Methanol and Stannous Chloride in Tramex Feed

A single scouting experiment was done to determine the feasibility of using methanol to retard acid loss from Tramex feed containing stannous chloride to keep cerium in the trivalent state. As the rate of acid loss was decreased only slightly, storing adjusted Tramex feed containing stannous chloride for more than a few hours does not appear to be feasible even if methanol is added. The most satisfactory procedure was to protect adjusted Tramex feed from acid loss by adding methanol. The stannous chloride was then added as the feed entered the extraction contactor.

6.2 SOLVENT EXTRACTION PROCESSING OF ^{243}Am-^{244}Cm

Feed materials processed for americium and curium recovery during the past year included Savannah River Plant (SRP) concentrates containing ^{243}Am-^{244}Cm, and irradiated $^{241}AmO_2$ targets. The source and previous history of the SRP concentrates were described previously.[1] The $^{241}AmO_2$ targets are discussed in Sect. 6.3. After the ^{243}Am-^{244}Cm campaign, a short series of promising chemical flowsheet modifications were tested at high activity levels. The results of the tests with the Dapex flowsheet indicated that it was superior to the Clanex as a primary solvent extraction cycle. Other tests indicated that the Talspeak and Cerex flowsheets are still promising but need further study.

Status and Progress

A short campaign to recover approximately 16 g each of ^{243}Am and ^{244}Cm from 175 liters of SRP concentrate was completed. This highly purified material was desired as a readily available stock to meet future needs of research and development for quantities of ^{243}Am and ^{244}Cm. The process was conducted according to the Clanex-Tramex flowsheet, with recoveries, losses, and decontamination essentially the same as those reported previously.[1]

After solvent extraction processing, additional decontamination of the curium product was obtained by LiCl anion exchange techniques. Quantities of ^{243}Am, ^{244}Cm, and ionic impurities in the solvent extraction product and in the final purification product are shown in Table 6.1.

The americium-curium product was stored as an HCl solution and was available to supply various requests for gram amounts of americium or curium.

Flowsheet Testing

At the conclusion of the ^{243}Am-^{244}Cm campaign, a short series of in-cell development runs was conducted with partially purified ^{243}Am-^{244}Cm as feed stock to test three proposed chemical flowsheets: the Dapex, the Cerex, and the Talspeak.

Table 6.1. Purified ^{244}Cm Product

Constituents	Solvent Extraction Product (g)	Final Purification Product (g)
^{243}Am	15.5	15.2
^{244}Cm	15.3	15.0
Li	96	5
Ca	2	0.02
Cr	0.3	<0.02
Cu	1.2	<0.01
Fe	0.5	<0.02
Rare earths	~10	<0.01
Ni	3.7	0.05
Zr	6	<0.01

Dapex. – The Dapex flowsheet, featuring 0.7 *M* di-(2-ethylhexyl)phosphoric acid (HDEHP) in Amsco 125-81 (alphatic hydrocarbon diluent) as extractant, was shown to be superior to the Clanex flowsheet for converting nitrate feed stock to Tramex feed; in addition, it is also compatible with aluminum-containing chloride feed (dissolver solution). With either feed, the solvent extraction losses were low, and decontamination from zirconium was high.

Cerex. – A test of the Cerex flowsheet (a modification to the Tramex flowsheet that includes an oxidant, $KBrO_4$, in the wash I stream of the stripping bank to maintain any extracted Ce^{4+} in the tetravalent state) showed that conditions for the oxidation step were poor and that Ce^{3+} appeared in the product. The partial success obtained in this test, however, indicated that further development of a suitable oxidant system might yield a useful flowsheet.

Talspeak. – The Talspeak flowsheet,[2] which could replace both the present cycles of solvent extraction, features extraction of the lanthanides in the first bank with HDEHP in diisopropyl benzene, extraction of the actinides in the second bank with HDEHP in Amsco diluent, and stripping of the actinides in the third bank. The actinides are initially prevented from extracting by complexes of lactic acid and diethylenetriaminepentaacetic acid (DTPA). These complexes are broken by pH control in the second contactor. A simple acid strip is used for actinide recovery.

The advantages of the flowsheet are that the chemical system is noncorrosive to stainless steel, and that aluminum-based target materials can be dissolved in HNO_3 without fear of the hydrogen explosion hazard. The disadvantage lies in the fact that the lactate-DTPA complexing agent is relatively unstable to radiation degradation and can form heavy polymeric substances under certain conditions.

The chemistry involved in the experimental flowsheet was successfully tested with americium and europium tracers in laboratory mixer-settler equipment having only a few stages. The waste organic from the rare-earth extraction section (two scrub, one feed, three extraction stages) contained 49% europium and 0.1% americium. The product organic from the actinide extraction section (two scrub, one feed, three extraction stages) contained 96.5% americium and 1% europium; there was a 3.5% americium loss to the raffinate waste.

The hot-cell tests were conducted with two banks of mixer-settlers designed for Tramex flowsheets. The product was stripped by washing with acid in the waste-organic catch tank. The lactate-DTPA solution was continuously metered to the feed solution (0.3 *M* in HNO_3, 0.16 *M* in rare earths and containing 0.193 g of ^{244}Cm per liter) as it entered the first-cycle solvent extraction contactor. This maintained the acidity in the pH range 3 to 3.5. No lactic acid was included in the feed to minimize radiation exposure. As was expected, contactor efficiencies were low, cross-contamination was high, and neither recovery nor decontamination was acceptable. However, no difficulties specifically due to high-level radiation were encountered in several 16-hr runs. This encourages further development aimed at increasing the decontamination and recoveries at high levels of beta-gamma and alpha activity.

SRP Concentrates. – During the past year the remainder of the first lot of unprocessed SRP concentrate, containing approximately 50 g each of ^{243}Am and ^{244}Cm, was transferred into the Curium Recovery Facility and evaporated to a small volume before storage in the tanks inside cell 4. A second lot of SRP concentrate, containing approximately 170 g of ^{243}Am and 216 g of ^{244}Cm, was received and transferred to the underground storage vessel.

Both these solutions will be combined and transferred to the Transuranium Processing Facility for recovery of the actinides.

6.3 PROCESSING OF THE $^{241}AmO_2$ TARGETS

Two ^{242}Cm recovery campaigns were completed during the year in which two types of targets were dissolved. Data for the last campaign are incomplete, and the results are extrapolated over the last six targets. Feed material for the first campaign consisted of 18 aluminum canned targets, 0.5 in. in diameter and 9 in. long, that had been irradiated in the ORR; that for the second campaign consisted of five Martin Company targets, 1.25 in. in diameter and 5 in. long, that had been irradiated in the MTR, plus an additional 18 ORR targets (10 in. long). Each ORR target contained about 3.3 g of ^{241}Am as AmO_2 compressed in an aluminum matrix and canned in aluminum. Similarly, the ^{241}Am content of the MTR targets was 3.6 g. At reactor discharge, each target contained the following amount of ^{242}Cm: MTR, 1.2 g; ORR (first set of 18), 0.8 g; and ORR (last set), 1.1 g.

The first lot of ORR targets was processed directly through one cycle of Tramex solvent extraction in batches of three targets. The product was contaminated with ^{144}Ce. The second campaign used continuous addition of reductant to the feed stream as well as a combined Dapex-Tramex two-cycle process. Even though the targets were processed after a decay period of only 15 to 30 days, the curium product was of exceptional purity.

Status and Progress

About 6.9 g of ^{242}Cm was recovered in the first campaign, of which 6.4 g met specifications for source fabrication (Table 6.2). Solvent extraction and process losses in the one-cycle Tramex flowsheet totaled about 4%; the rest was lost by decay. Decontamination from fission products was marginal; the main difficulty was insufficient cerium decontamination (Table 6.3). Hydroxylamine hydrochloride in the scrub step did not adequately remove the extracted Ce^{4+} before the solvent entered the stripping bank. The system was modified to permit a reductant to be added to the feed just before it entered the extraction bank so that Ce^{4+} would not be present in the original feed. The second campaign, which used the Dapex-Tramex (two-cycle) flowsheet, gave high-purity, specification-grade ^{242}Cm-product recoveries averaging 97% and solvent extraction losses totaling 3.4% (Table 6.4), of which 2.8% occurred the first time the Dapex cycle was used. The material balance for the campaign was 104%. The marked decrease in the Tramex-cycle losses (compared with losses in previous runs) is attributed to the improved design of the new contactors, the modified feed adjustment procedure that virtually eliminated formation of solids in the contactors, and to the elimination of leaky valves in the system. Decontamination factors for ^{103}Ru, ^{95}Zr-Nb, and ^{141}Ce averaged, over the two campaigns, $\sim 2.6 \times 10^3$, 3.5×10^3, and 900, respectively, for the ^{242}Cm product, which was recovered in the highest purity yet observed in the Program. The gamma-to-alpha ratios measured in the dissolver product (Dapex feed), Tramex feed (Dapex product), and final nitrate product are compared in Fig. 6.3. Here the gamma scan is normalized to the alpha disintegration rate and is plotted against photon energy

Table 6.2. Curium Product Purity

Constituents	Specification	Product		
		$^{241}AmO_2$ Targets		
		First 18, ORR	Second 18, ORR[a]	Five Martin
Cm, g/liter	0.25	0.25	0.25	0.25
HNO_3, *M*	1 to 4	1.4	2.5	3.5
Cl^-, g/liter	<0.1	<0.1	<0.1	<0.1
Ni, g/liter	<1	0.13	0.13	0.13
Bi, Pb, Ca, Si (total), g per g of Cm	<0.05	0.18[b]	0.16[b]	0.22[b]
Alkali metals (total), g/liter	<10	16.5	3.4	2.4
Other cations (total), g/liter	<1	<1	0.14	0.6
Suspended solids, g/liter	<0.01	c	c	c

[a]Data for first six of the campaign.

[b]Consists almost entirely of calcium present at the limit of detection.

[c]Filtered through 45- to 60-μ pore sintered glass filter initially. After the new tantalum-lined evaporator was installed, no solids could be found, and filtration was discontinued.

Table 6.3. Decontamination Factors: ^{242}Cm Recovery

Cycle	Gross Gamma	^{103}Ru	^{95}Zr-^{95}Nb	^{141}Ce	^{144}Ce	^{140}Ba
First 18 ORR Targets[a]						
Tramex	350	180	980	18	13	>500
Second 18 ORR Targets[b]						
Dapex	10	540	24	1	1	>7
Tramex	360	95	15	7.9×10^3	1.6×10^3	c
Overall	3.4×10^3	5.2×10^4	360	7.9×10^3	1.6×10^3	
Five Martin Targets						
Dapex	6	9	6	1	1	>30
Tramex	120	150	1.1×10^3	190	190	c
Overall	720	1.4×10^3	6.6×10^3	190	190	

[a]Processed through one cycle only.

[b]Processed at ~15 to 30 days after reactor discharge; based on first 12 targets.

[c]Not detected.

(Mev). The scan of the nitrate product indicates only ^{103}Ru (trace) and ^{95}Zr-Nb as contaminants. The other peaks are due to curium isotopes and fission gammas.

Important flowsheet and procedure modifications developed and reduced to practice during these campaigns included: (1) limiting the maximum temperature in the Tramex feed adjustment to 120°C, (2) continuously metering a reductant (0.15 *M* $SnCl_2$ in 10.8 *M* LiCl–0.03 *M* HCl) stream into the feed as it enters the extraction bank of the contactors, (3) increasing the HCl concentration to 8 *M* in the Tramex strip solution, and (4) scrubbing with 10.8 *M* LiCl–0.03 *M* HCl. These four modifications resulted in the following significant improvements respectively: eliminating the accumulation of solids in the contactors, maintaining the cerium in the inextractable (trivalent) state, increasing zirconium-niobium decontamination, and better europium scrubbing. The increase in on-stream time that resulted from the absence of solids became a significant factor in ^{242}Cm recovery because of its short half-life (160 days).

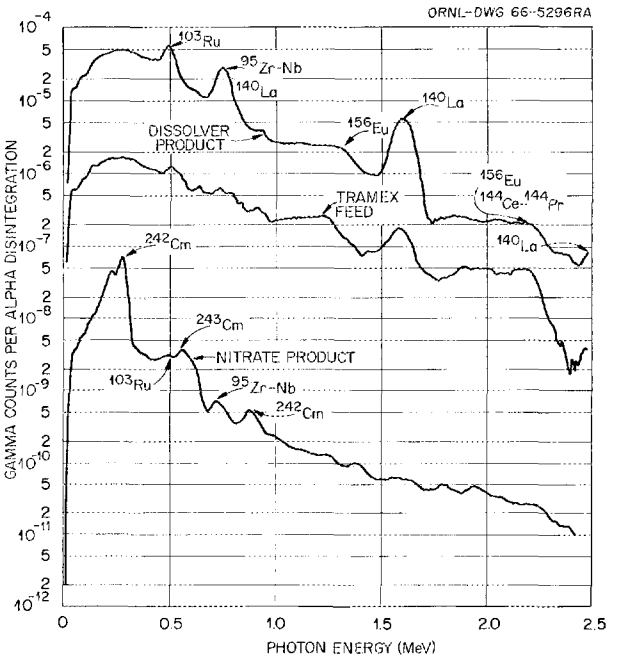

Fig. 6.3. Gamma Scans of the Principal Streams Handled in the ^{242}Cm Program.

Table 6.4. Curium Material Balance

(February to May 1966)

	^{242}Cm	
	g[a]	Percent of Dapex Feed
Dapex		
Dissolution	17.71	
Solvent extraction feed	18.46	100.00
Recovered product	17.85	96.67
Solvent extraction losses	0.51	2.77
Total accounted for	18.36	99.44
Tramex		
Solvent extraction feed	18.85	102.10
Recovered product	19.11	103.52
Solvent extraction losses	0.12	0.67
Total accounted for	19.23	104.19

[a]Each of the three runs was corrected for decay to the date that the product was recovered from the individual lot of feed material. Further decay of finished product during storage before delivery to user will reduce the amount delivered at the rate of about 0.5%/day.

These modifications, along with delaying the addition of the methanol to the Tramex solvent extraction feed for about 100 whr after the final evaporation and LiCl adjustment, permitted processing feeds of 15 to 20 w/liter without difficulty. These procedures, including recent modifications to the flowsheet, are presented below.

Dissolution of the Targets

The targets were dissolved in lots of three by metering 6 *M* HCl at 0.75 liter/hr into a dissolver vessel initially containing enough water to cover the targets. The temperature was held at 50°C throughout the run. The acid addition rate controlled the dissolution rate such that hydrogen evolution never exceeded 2 moles/hr. The solution was continuously sparged, and the evolved gases were further diluted with purge air to reduce the hydrogen concentration to less than 2 vol %. The noncondensable fraction of the evolved gas was scrubbed with 1 *M* NaOH and passed successively through beds of activated charcoal and silver mesh

to sorb acid vapor and radioiodine before discharging it to the gaseous-waste disposal system of the laboratory.[3] The off-gas was continuously monitored for particulate and gaseous fission products. As the cladding was breached, the trapped gases were released, resulting in momentary surges of activity, mostly ^{85}Kr. Of the ^{131}I released during dissolution, only a minute quantity escaped the scrubber-sorber system, even with targets that had decayed only 15 days. After all the acid was added to the system, the solution was digested for 2 hr at 50°C. Then the dissolver solution (~0.7 *M* free HCl) was filtered and stored until two lots were accumulated. The composited solution was digested at 95 to 100°C for 2 hr and adjusted to solvent extraction feed specifications as described in the next section. The adjustment of Tramex feed from dissolver solution was the same as that prepared from Dapex product, with care being taken to limit the aluminum concentration to <0.1 *M*.

Dapex Feed Adjustment

The raw dissolver solution, about 0.7 *M* in HCl, 0.7 *M* in Al, and containing approximately 0.3 g of ^{242}Cm per liter, was adjusted to Dapex feed specifications (0.5 *M* HCl initially) with 12 *M* HCl or by dilution with water. The power density, while not a controlling factor, was usually about 20 w/liter; the aluminum concentration in the ranges encountered did not vary significantly and was not controlled.

Dapex Solvent Extraction

The Dapex solvent extraction flowsheet is shown in Fig. 6.4. When feed material that had decayed less than 30 days after reactor discharge was being processed, 5 vol % of the Amsco diluent was replaced with diethylbenzene to help chemically fix radioiodine in the extractant. In spite of this, however, some ^{131}I was released from the solutions in the contactors to the cell atmosphere.

[3]The dissolution of the Martin target was conducted in a cell 4 vessel not equipped with a charcoal--silver mesh sorber, because these targets would not pass the target charging port of the dissolver. The data indicated >99.5% of the ^{131}I was removed in the scrubber.

Adjusted feed was metered at 0.6 liter/hr to the extraction bank of a 16-stage mixer-settler maintained at 50°C. Here the americium, curium, and most of the rare earths were extracted into 0.7 *M* HDEHP metered to the extraction bank at 2.2 liters/hr. Most of the extracted impurities were scrubbed from the extract with 0.03 *M* HCl metered to the scrubbing bank of the mixer-settler at 1.2 liters/hr. The americium, curium, and rare earths were stripped into 2 *M* HCl metered to the stripping bank of a second 16-stage mixer-settler. Traces of ^{95}Zr, ^{131}I, and other light fission products that stripped into the aqueous phase with the americium-curium and rare earths were preferentially reextracted into 0.7 *M* HDEHP metered to the washing bank of the second mixer-settler at 0.9 liter/hr. The aqueous product was collected and transferred in batches to an evaporator, where it was concentrated for the first step in the Tramex feed adjustment procedure which follows.

Tramex Feed Adjustment

The americium—curium—rare-earth product from the Dapex cycle (or raw dissolver solution) was evaporated to a small volume to remove the bulk of the excess HCl; sufficient 13.5 *M* LiCl was then added to give approximately an 11 *M* LiCl feed calculated to yield a power density of 30 to 40 w/liter. The remainder of the excess acid was removed by evaporation to 120°C, after which the calculated volumes of methyl alcohol, 12 *M* HCl, and the remaining 13.5 *M* LiCl required were added and mixed thoroughly to give a power density of 15 to 20 w/liter. After assay, the adjusted feed was filtered and transferred to the feed hold tank in batches sufficient for one day of solvent extraction operation. The remainder was withheld and sampled daily so that additional adjustment of the acid could be made (if required) to compensate for that destroyed by radiolysis.

Tramex Solvent Extraction

The Tramex cycle of solvent extraction was conducted according to the most recent Tramex flowsheet (Fig. 6.5), using the same equipment held at 50°C as that used in the Dapex cycle. The feed was metered to the extraction bank of the mixer-settler at 0.6 liter/hr. A 0.3-liter/hr stream of

ORNL-DWG 66-5297A

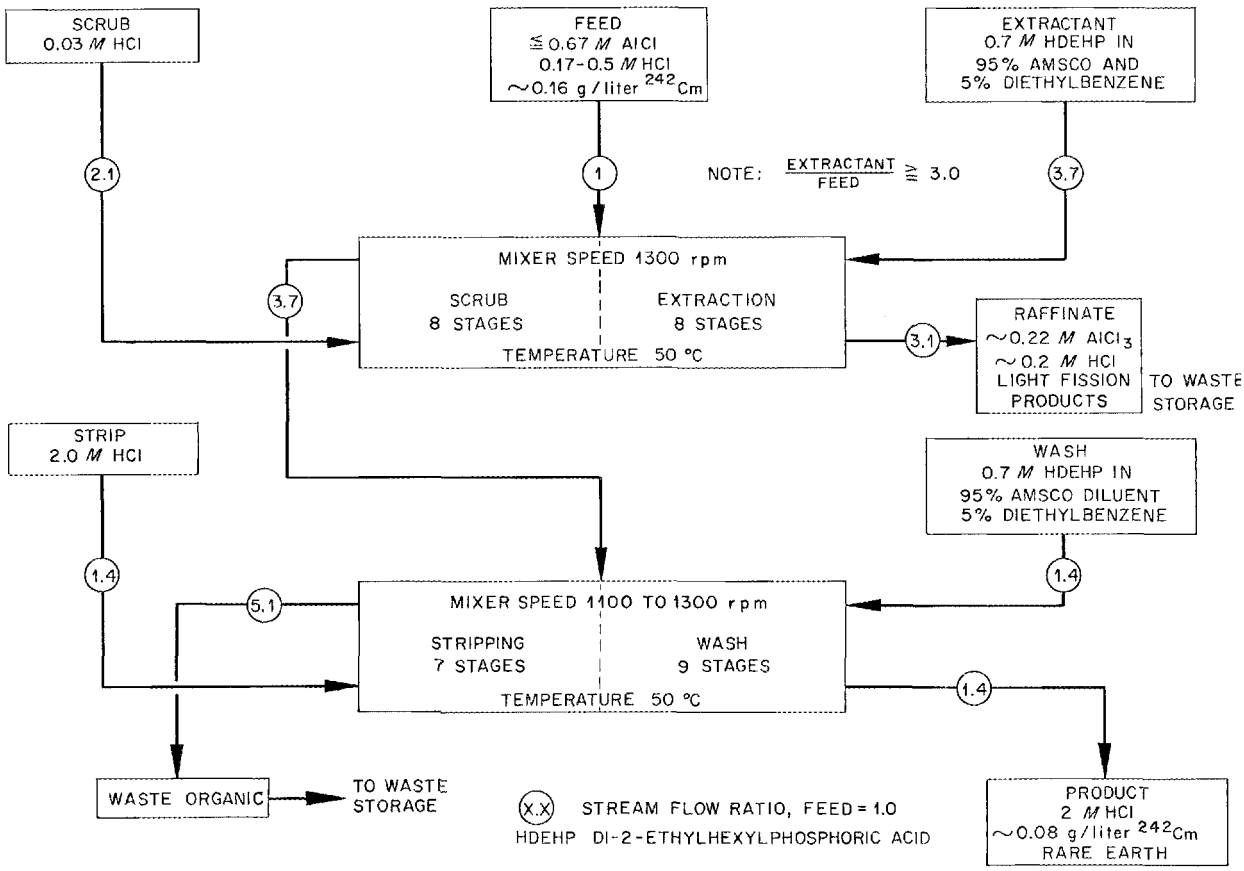

Fig. 6.4. Curium Recovery Flowsheet; Dapex (1966).

reductant (0.15 *M* $SnCl_2$ in 11 *M* LiCl–0.03 *M* HCl) was continuously mixed with the feed just before it entered the contactor to maintain cerium in the trivalent inextractable state. Americium and curium were extracted into 0.65 *M* amine–HCl metered to the extraction bank at 2.4 liters/hr; traces of impurities were scrubbed from the extract with 10.8 *M* LiCl–0.03 *M* HCl metered to the scrubbing bank of the mixer settler at 1 liter/hr. The americium and curium were stripped into ultrapure 8 *M* HCl metered to the stripping bank at 1.1 liters/hr. Ruthenium in the extract was hindered from stripping into the americium-curium fraction by including amine-nitrite in the backwash stream. This unstable reagent was kept chilled and was metered into an equal volume of the 0.65 *M* amine–HCl wash II stream and passed to the washing bank of the mixer-settler. The aqueous product stream was continuously evaporated to remove the excess acid and to reduce the volume of the solution to be handled in the chloride removal step which follows.

Chloride Removal

The concentrated chloride product solution (~6 g of ^{242}Cm in ~10 to 12 liters) was converted to the nitrate system by metering 10 *M* HNO_3 to the product evaporator at 0.75 liter/hr, while holding the volume in the evaporator constant. The HNO_3

ORNL-DWG 66-5298A

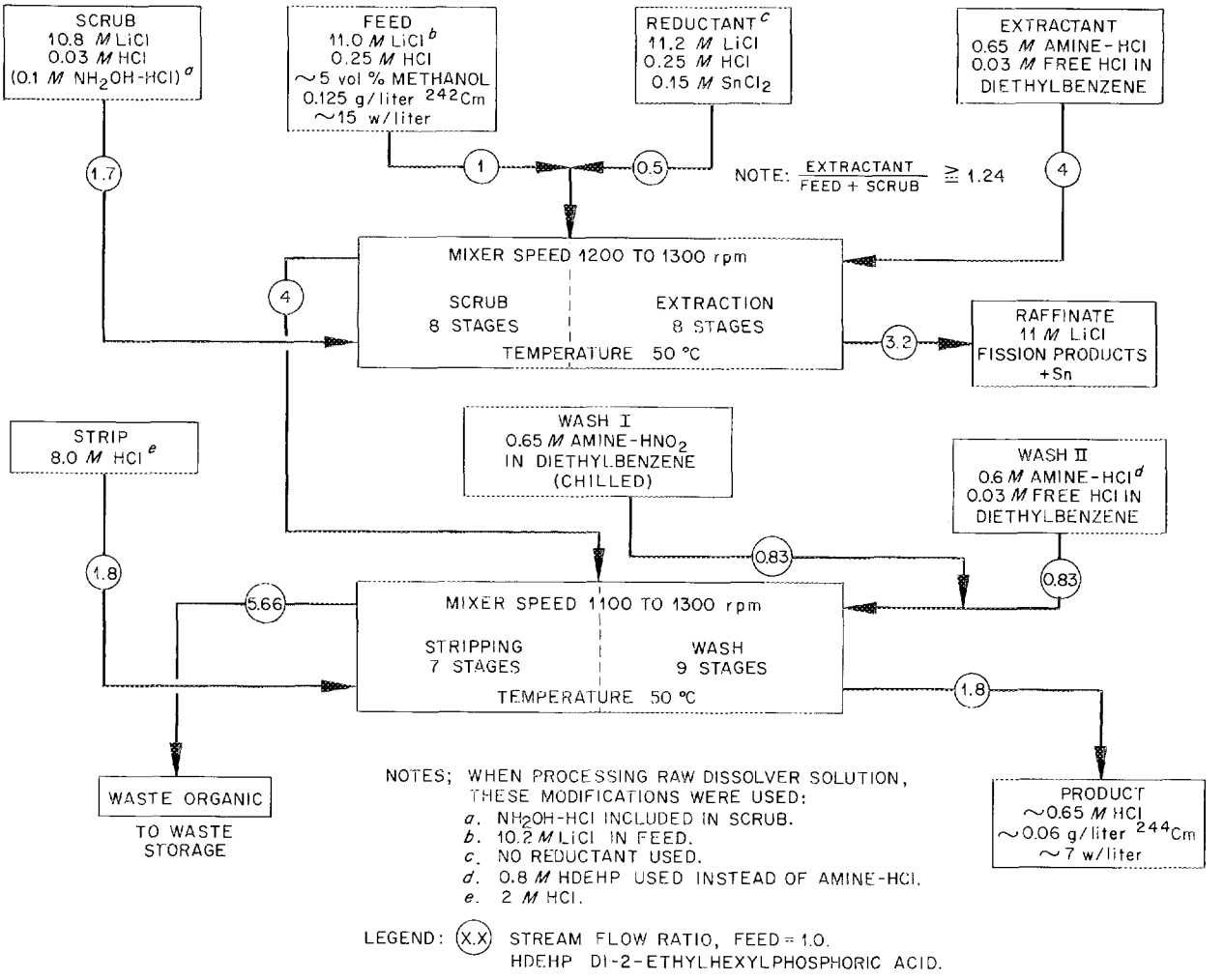

Fig. 6.5. Curium Recovery Flowsheet; Tramex (1966).

addition was discontinued when the chloride content of the residual solution reached 100 ppm, after which the evaporation was continued to a final volume of about 6 liters (~120 w/liter) to remove the excess nitric acid. The residual solution was then diluted to approximately 0.5 g of curium per liter, and stored until shipment. The final product contained ~0.25 g of ^{242}Cm per liter, and was about 4 *M* in HNO_3.

Curium Product Transfer

The curium product was transferred to the Isotopes Division facilities in a water-shielded and -cooled carrier. The product solution, stored at a power density of about 50 w/liter, was diluted with water rinses to about 30 to 40 w/liter in the carrier. In the last campaign, the filtration step was eliminated because the solids present in product recovered and held in glass-lined tanks were eliminated after the tantalum-lined vessels were placed in service.

6.4 CURIUM RECOVERY FACILITY EQUIPMENT

Progress and Status

The Curium Recovery Facility, designed and constructed to recover gram quantities of curium

and lesser amounts of the heavier transuranium elements, was described previously.[4] Experience gained over the past year and a half of operation with radioactive feed material led to incorporating modifications both to the design of the solvent extraction equipment and to the choice of material of construction. Revisions and modifications to the piping and the addition of several new pieces of equipment have greatly improved the ease of operation and minimized the downtime required for maintenance and repair. Included in the new equipment were two mixer-settlers made of tantalum, a new tantalum-lined product storage tank, a tantalum-lined product collection-evaporator tank, a tantalum-lined waste-organic collection tank, a vacuum filter and solution transfer system, a new reagent addition system, a phase separator, and a new lightweight feed metering pump. Piping changes consisted in extending the outlet nozzles of the process tanks above the operating deck for greater accessibility and flexibility of operation.

New Equipment

Tantalum Contactors. – A new set of mixer-settlers was fabricated that features longer mixing chambers and modified stirrer blades which improved the pump mixing characteristics. The mixer drive units were mounted on the support rack in the cell, eliminating the former cumbersome flexible-cable system driven through the cell roof. The new unit functions smoothly and has greater capacity than the older units. No corrosion attack was observed.

New Tanks. – Two glass-lined collection tanks were replaced with tantalum-lined vessels. One of these, the product collection tank (which also serves both as an evaporator and as a reaction vessel), is exposed to prolonged periods of intense bombardment with high-energy alpha particles and to corrosive attack by HCl-HNO_3 mixtures. It was observed that the glass "flanked" away from the lining upon continued exposure and contaminated the product with solids. Ultimate breaching of the glass liner was feared. The second tank, the spent-solvent collection tank, was replaced with one designed to accumulate the small volume of entrained aqueous product solution for the whole run, thereby eliminating the need for daily shutdowns to recover it. A separate phase separator was installed so that larger volumes that might occur could be handled without interrupting the run.

A new tantalum-lined curium product storage tank was installed in cell 3. The new tank allowed isolation or combination of successive lots of specification-grade product to be stored while operations were in progress. It also made another process vessel available for use in storing off-specification material for later recycle.

Piping Revisions. – The piping inside cell 4 was revised to provide easy access to the process tanks located below the deck. This consisted of extending tantalum outlet lines to above the edge of the deck near the suction manifold of the transfer pumps. With this system, only the insertion of a short pair of easily installed flexible jumpers to a pump was required to move the contents of any vessel to any other.

Reagent Addition System. – The reagent addition system was redesigned such that a pressure bottle located outside the glove box is used to transfer reagents into the process vessels. The discharge line from the pressure bottle leads to the glove box, where the terminals of the transfer lines to each cell vessel are located.

Vacuum Transfer-Filtration System. – A new vacuum transfer-filtration system was installed that resulted in rapid filtration and transfer of highly salted process solutions from the feed adjustment tank to the feed head tank. When used in conjunction with the revised piping terminating above the decking mentioned earlier, rapid transfers and the filtration of any solution from one vessel to any other vessel also became easy and rapid.

Feed Metering Pump. – A new, lightweight model of the reagent head of the feed metering pump was designed and fabricated that incorporated a handling yoke. This model is easily installed or replaced in the cell with manipulators in about 10% of the time required for the previous model.

Building Vacuum System. – The building vacuum system was upgraded to minimize a radiation-contamination hazard that existed. The wet-vacuum pump was replaced with a steam-jet evacuator and condenser system that is totally enclosed. The new system has ample capacity and gave satisfactory service in all respects.

Manipulator. – The design of the manipulator finger was modified to include a mechanically

[4] F. L. Culler *et al.*, *Chem. Technol. Div. Ann. Progr. Rept. May 31, 1964*, ORNL-3627, pp. 136–52.

fixed finger pad fabricated from one-ply fabric-reinforced neoprene rubber sheet. The pad covers the working face of the finger and is held with backing plates mounted on each side of the finger. These pads now have a useful service life.

Operations

Remote Maintenance. – Two in-cell tanks and the mixer-settlers were disconnected from their service piping, removed from the cell, and then replaced with new counterparts without delay or incident. The old equipment was lifted into the maintenance enclosure atop the cells and transferred into sealed steel containers of suitable size by means of a bagging technique. The new equipment was introduced into the maintenance enclosure from steel containers in a similar manner. Other items installed with this technique included the vacuum transfer system and the reagent head of the feed pump. Routine maintenance in glove boxes of in-cell valves and pumps was continued throughout the year.

7. Development of the Thorium Fuel Cycle

7.1 ^{233}U STORAGE AND DISTRIBUTION FACILITY

Oak Ridge National Laboratory serves as a storage, purification, and dispensing center for ^{233}U fuel. During the past year, approximately 63.4 kg of ^{233}U as oxide powder, metal residue, and nitrate solution was received in 12 shipments. During this same period, eight shipments, amounting to 18.3 kg of ^{233}U as purified nitrate solution or oxide powder, were made from the center. The receipts included 50 kg of ^{233}U containing less than 5 ppm of ^{232}U. The present inventory is 190 kg of ^{233}U varying in isotopic enrichment from 78 to 98.5% and containing from 2.6 to 250 ppm of ^{232}U.

The solution storage system, dry-solid storage wells, and 1 kg/day single-cycle glove-box purification system, which were described in last year's annual report, were placed in operation.

A dissolver-leacher (Fig. 7.1), limited in size to "ever-safe" criticality dimensions, was designed and installed for use as a metal or oxide dissolver or as a leacher for chopped metal-clad fuel elements containing ^{233}U. The leacher is capable of dissolving 1700 g of UO_2 to a final concentration of 100 g/liter in 2 hr.[1] The removable inner basket makes the unit attractive for leaching chopped stainless-steel-clad or zirconium-clad elements, as well as for dissolution of metal, slag, or oxide. This unit increased the dissolution rate in the solvent extraction facility[2] by a factor of 6 and, coupled with the glove-box solvent extraction system, eliminates the need for dissolution in thorium-containing solutions (thorium acts as a neutron poison) and for limiting feed concentrations to 10 g of ^{233}U per liter to avoid the possibility of criticality.

7.2 SOL-GEL PROCESS: FURTHER DEVELOPMENT AND NEW APPLICATIONS

Recent developments in sol-gel technology include extension of the process to the preparation of microspheres of ThO_2-UO_2 of all thorium:uranium ratios, and the preparation of thorium carbides from ThO_2-C sols.

Preparation of Thoria-Urania by Sol-Gel Methods

One objective of these studies is to see if sol-gel technology can be extended to include mixtures of thoria and urania in all ratios. We are concentrating our efforts on an approach where sols are mixed in the desired ratio, since this would be the most convenient approach to use with the variety of fuel compositions we anticipate will be studied in our development program in the TURF. The original sol-gel process, which uses thoria sol prepared by steam denitration of thorium nitrate, is limited to mixtures containing less than about 10% uranium, which is added to the thoria sol as uranyl nitrate or as UO_3.

In the present mixed-sol approach, a thoria sol is mixed directly with a urania sol. Laboratory-scale investigations are also under way on other possible methods for preparing mixed sols, such as solvent extraction of nitrate from mixed $Th(NO_3)_4$-$UO_2(NO_3)_2$ solutions, dispersal of precipitated $Th(OH)_4$ with $UO_2(NO_3)_2$, and coprecipitation of uranium and thorium hydroxides followed by peptization in HNO_3. We are concentrating our efforts on sols having a thorium:uranium atom ratio

[1] M. E. Whatley *et al.*, *Unit Operations Section Monthly Progress Report — January, 1964*, ORNL-TM-798 (July 1964).

[2] C. C. Haws *et. al.*, *Summary of Kilorod Project — A Semi-Remote 10 kg/day Vibratory-Compaction Method*, ORNL-3681 (August 1965).

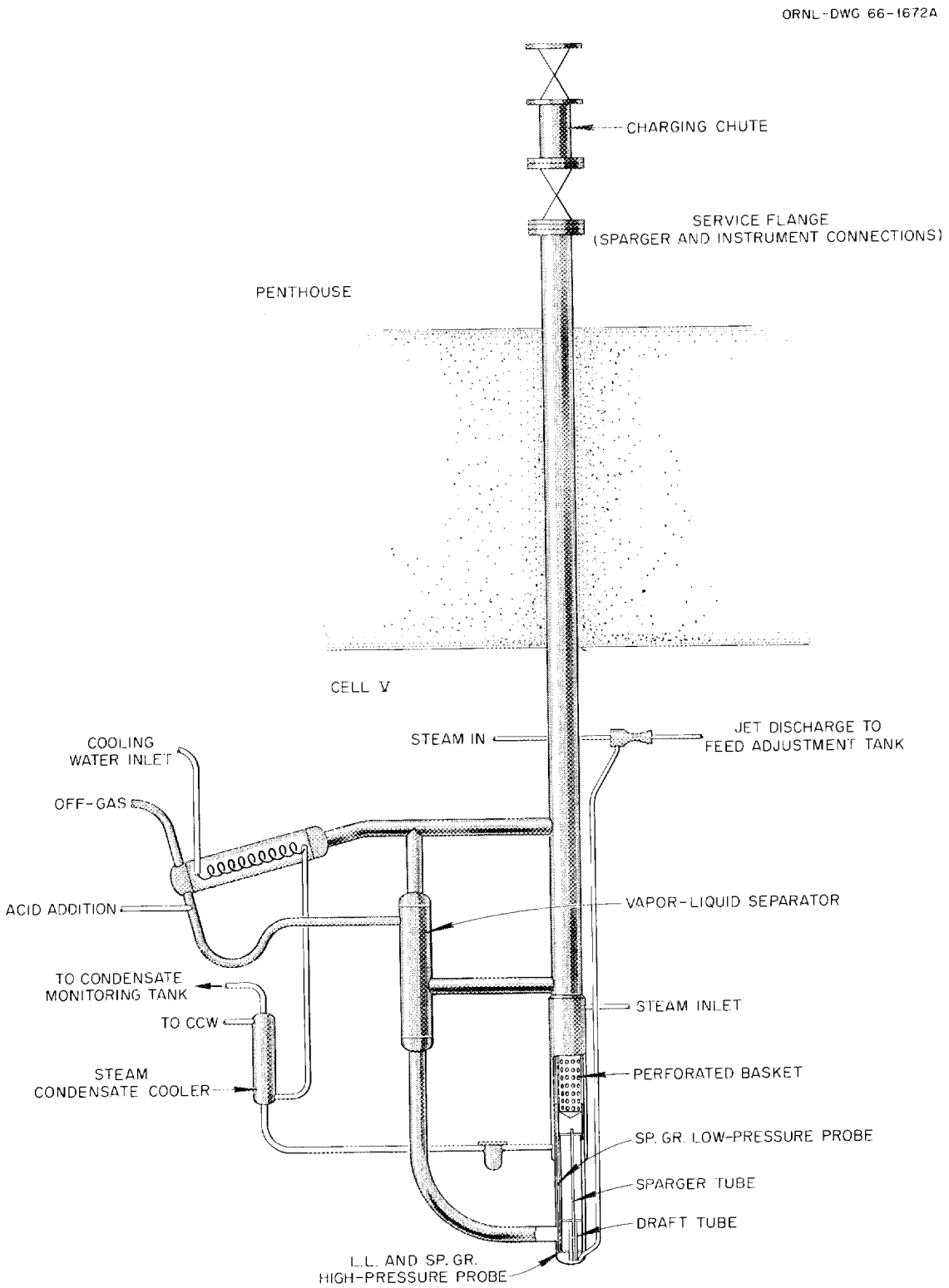

Fig. 7.1. ^{233}U Dissolver-Leacher.

of about 3.5:1, since this appears to be in the range of most interest for reactor fuels.

The thoria sols were prepared by several methods, each of which produces a sol having a different thoria crystallite size and a different optimum nitrate:thorium ratio. These sols were blended with urania sols, and conditions were found in each case where it is possible to make useful sol mixtures in the range of thorium:uranium atom ratios approximately equal to 3. In this way, we are obtaining insight into the fundamental nature of stable thoria-urania sol mixtures.

We prepared UO_2-ThO_2 sols by the following methods:

1. blending UO_2 sols with ThO_2 sols,
2. dispersing coprecipitated $Th(OH)_4$-$U(OH)_4$ with HNO_3,
3. dispersing $Th(OH)_4$ with $UO_2(NO_3)_2$.

Sols that are both fluid and stable can be prepared by any of these methods. The first method was used to prepare 300-g lots of calcined microspheres with thorium:uranium atom ratios up to 3.5:1. The last two methods were not as thoroughly examined for suitability of microsphere formation, although a few small-scale tests were performed.

Mixing UO_2 Sols with ThO_2 Sols. – Stable, fluid UO_2-ThO_2 sols over the entire composition range were successfully prepared by using UO_2 sols made either by the formate method or by the nitrate method,[3] and by using ThO_2 sols made by our standard method from steam-denitrated ThO_2.[4]

We prepared 300-g lots of microspheres with thorium:uranium atom ratios up to 3.5:1. The upper limit of concentration of (Th + U) appears to be about 1.6 *M* for fluid sols at a thorium:uranium ratio approximately equal to 3. Above this concentration the sols are too thick for easy microsphere formation. Typical chemical composition and crystallite sizes are shown in blend 6 (Table 7.1). This sol was formed into 200- to 300-μ-diam gel microspheres with 2-ethyl-1-hexanol containing 0.3% Span 80 and 0.5% Ethomeen S/15 surfactants. Excellent gel microspheres with shiny surfaces and no evidence of pitting were produced. These spheres could be dried to 125°C in argon with no evidence of cracking or deleterious pitting of the surface. After calcination at 1200°C, they were found to have near-theoretical density, excellent resistance to crushing forces, and low carbon contents (Fig. 7.2). The residual porosity remaining in the microspheres was shown to be less than 200 A by mercury porosimetry.

[3] J. P. McBride, *Preparation of UO_2 Microsphere by a Sol-Gel Technique*, ORNL-3874 (February 1966).

[4] D. E. Ferguson, *Status and Progress Report for Thorium Fuel Cycle Development for Period Ending December 31, 1962*, ORNL-3385 (Oct. 14, 1963).

Table 7.1. Preparations of UO_2-ThO_2 Sols

Preparation scale: ~300 g of combined oxides

Preparation Code	Th/U Atom Ratio	(Th + U) (*M*)	NO_3^-: (Th + U) Mole Ratio	U^{4+} (% of U)	X-Ray Crystallite Size (A)[a]		
					111 Plane	220 Plane	311 Plane
Blend 6[b]	3.45	1.6	0.11	65	65	64	68
CP-12	3.75	1.65	0.13	52.6	67	62	65
CP-13	3.69	2.0	0.13	63.5	72	63	62
CP-14A	3.04	1.8	0.14	62	66	58	69
CP-14B	2.59	1.7	0.15	47	67	67	68

[a] Crystallite sizes were determined by x-ray line broadening of the reflections from the 111, 220, and 311 planes, as shown.

[b] Blend 6 – prepared by blending a urania sol (1.32 *M* in U, 88% U^{4+}, and having a nitrate:uranium ratio of 0.16) with a thoria sol (3.07 *M* in Th, with a nitrate:thorium ratio of 0.099) prepared from steam-denitrated thoria. The urania sol was prepared by the formate method.

ORNL-DWG 66-111R

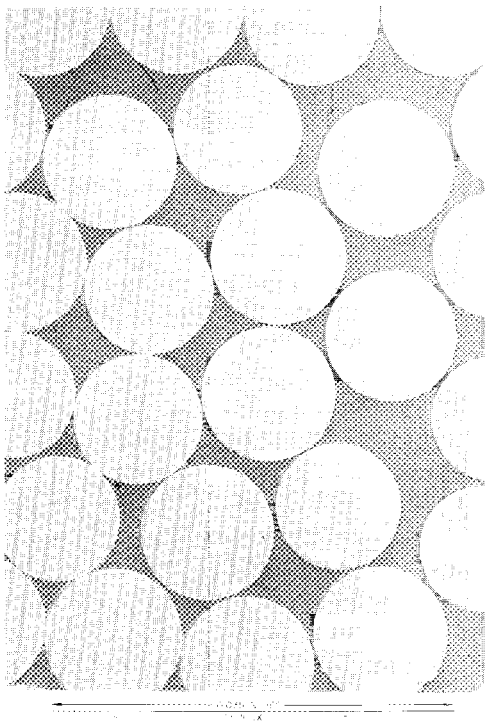

POLISHED SECTIONS OF 210 TO 297-μ-diam MICROSPHERES; THORIUM: URANIUM ATOM RATIO OF 3.5, DENSITY BY Hg POROSIMETRY OF 99% OF THEORETICAL; 30 ppm OF C; AND OXYGEN: URANIUM MOLE RATIO OF 2.016

Fig. 7.2. Calcined ThO_2-UO_2 Microspheres Prepared by Mixing Thoria and Urania Sols.

Sols having thorium:uranium atom ratios of $\frac{1}{3}$, 1, and 3 were made by using UO_2 sols prepared by the nitrate method. We have not characterized these sols or their resultant gels and fired products as extensively as the sols prepared from UO_2 sols by the formate method. However, we formed gel shards and gel microspheres from these sols in 5- to 15-g lots and calcined these products to near-theoretical density.

Coprecipitation Method. – Thoria-urania sols over the entire composition range were prepared by a coprecipitation method. In this method the hydrous oxides are precipitated from a solution containing $U(NO_3)_4$ and $Th(NO_3)_4$ by using NH_4OH. They are filtered, washed free of electrolyte, and dispersed into sols by warming the filter cake to 65°C and adjusting the nitrate concentration. Previous methods of sol formation depended on washing the filter cake until the nitrate reached the concentration for optimum sol formation on heating. Some of the hydroxide precipitates were exceptionally easy to filter and wash. Sols with 3:1, 1:1, 1:3, and 1:19 atom ratios of thorium: uranium were prepared. These sols are generally in the concentration range 0.7 to 1.0 *M* in combined oxides, and possess good fluid properties and stability. One of the sols (thorium:uranium ratio of 1) was concentrated to 3.3 *M* by vacuum evaporation at 55°C. The nitrate:metal atom ratios in the sols range from 0.1 to 0.4, and the average crystallite size varies from 20 to 30 A.

$Th(OH)_4$-UO_3 Method. – Sols with thorium: uranium atom ratios of 3.5 were prepared by this method, in which precipitated $Th(OH)_4$ filter cake is dispersed by adding solid $UO_2(NO_3)_2 \cdot 6H_2O$ to it. When the two solids are mixed, immediate liquefaction occurs and a yellow, fluid suspension is formed. Heating the suspension to 93°C yields a transparent ruby-red sol. Crystallization occurs on cooling, but the crystals redissolve and the sol remains fluid at room temperature when diluted with water to 2.16 *M* (thorium-uranium). The nitrate:thorium-uranium mole ratio was 0.434, and the crystallite size as measured by x-ray line broadening was <30 A for ThO_2 and <1000 A for UO_3. Attempts to form the sol into gel microspheres that would fire to a dense product were not successful. Excessive cracking occurred in gelation and on drying and firing. The high nitrate concentration of the sol probably caused the cracking problem. Some means of nitrate removal, either during or after gelation, would probably be required before this sol could be used for microsphere preparation.

Calcination studies of the gel microspheres showed that firing according to a specific sequence of temperatures and atmospheric environments was required to obtain a product of near-theoretical density and low carbon content. Firing under reducing conditions produced spheres of low density, high carbon content, and low resistance to crushing forces. The attainment of high density does not appear to be simply a matter of removing the carbon. Thermogravimetric analyses are being made in an attempt to determine the optimum firing conditions.

Thorium Dicarbide by Sol-Gel Methods

Thorium dicarbide microspheres are of interest for use in high-temperature gas-cooled reactors.

They can be prepared by a modification of the sol-gel process involving mixed thoria-carbon sols.[5,6] This method leads to a relatively low-density (<90% of theoretical) product; and, in the relatively few experiments that have been performed so far, small amounts of unreacted ThO_2 have been present in the product. Present studies are designed to ascertain what control can be exercised over density and residual oxide (or free carbon) content. In addition to being used in forming carbides, mixed oxide-carbon microspheres are precursors in some methods for nitride and sulfide synthesis. In initial work, we are concentrating principally on conversions of dried gel fragments to ThC_2 fragments, with the expectation of changing the emphasis to the formation of ThC_2 microspheres as we learn more about the conversion. Preparation of dicarbide microspheres is somewhat more complicated than that of shards in that the microsphere forming process introduces extraneous carbon into the ThO_2-C gels in the form of sorbed organic liquids. We are attempting to understand the basic conversion reactions between ThO_2 and carbon before proceeding too deeply into studies of conversion to dicarbide microspheres, where additional factors must be taken into account. Even in the relatively simple case of dried gel shards, side reactions that consume carbon, such as those between sorbed H_2O and carbon, and between nitrate ion and carbon, must be allowed for in the conversion step.

In preparation of ThO_2-C sols for conversion to mono- or dicarbides, we are examining different carbons as well as several methods of suspending the carbons in ThO_2 sols. The sol produced must have good fluidity for formation into microspheres and yield no gross segregation of carbon and ThO_2 upon gelation. In addition, it is likely that only certain arrangements of carbon and ThO_2 crystallites in the gel will lead to dense carbides and good conversions. Gross segregation of ThO_2 and carbon is likely to occur unless the carbon is arranged in such a manner that the thoria crystallites are prevented from sintering together to form gross thoria particles on heating to the conversion temperature (1150°C). The nature of the carbon, for example, acidic vs basic, plays a role in its interaction with ThO_2 sol.

The techniques studied for forming ThO_2-C sol mixtures include (1) dispersion of carbon in a ThO_2 sol via a pump recycle loop, (2) ultrasonic dispersion of carbon in ThO_2 sols, (3) addition of ThO_2 to a carbon suspension, and (4) ball milling a C-ThO_2 sol blend. The first two methods have been used successfully in the past at ORNL, and the third was developed at Southwest Research Institute. The ball-milling method, which has apparently not been used previously, gave the best results in terms of sol properties, that is, viscosity, sedimentation, and Newtonian behavior. Final evaluation must, of course, include sphere formation and conversion to carbide, which are still being studied. Preparation by this method involves ball milling the carbons with a 2 to 3 *M* ThO_2 sol for about 20 hr.

Five different channel black carbons were used in the above tests. The surface area of the channel blacks ranged from 100 to 1400 m^2/g. Spheron 9 (United Carbon Company), which had the lowest specific surface area, gave the most fluid sols. The viscosity of a 2 *M* ThO_2–8 *M* C sol is only 6 to 6.5 centipoises, compared with 4 centipoises for the ThO_2 sol prior to addition of Spheron. The other channel blacks at the same concentration gave sols (or pastes) with viscosities of 40 to 25,000 centipoises. If the viscosity is too high (above about 60 centipoises), the sols are not manageable. With Spheron 9, it appears that about 3.5 *M* is the practical upper limit of thoria concentration when the carbon:thoria mole ratio is 4. At a carbon:ThO_2 mole ratio of 2, Spheron 9 was still superior to the higher-surface-area channel blacks; and at this ratio, a 4 *M* ThO_2–8 *M* C sol is quite thick (~2000 centipoises) and non-Newtonian. Dilution to 3.4 *M* ThO_2 gives a usable sol (59 centipoises; Newtonian), and at 3 *M* the viscosity is 20 centipoises. The ThO_2-C sols prepared with Spheron 9 appear to form good microspheres in 2-ethyl-1-hexanol by using 0.3% Span 80 and 45% Ethomeen S/15 as surfactants.

Sols having carbon:thoria mole ratios of 4.17, 3.71, and 3.25 were prepared by the ball-milling method, using Spheron 9, and dried to gel shards that were used in carbide conversion studies. Several test conversions were made on these gels in an effort to define conditions for optimum conversion to the dicarbide (Tables 7.2 and 7.3). At temperatures of 1900°C and at carbon:thoria mole

---

[5] R. G. Wymer and D. A. Douglas, Jr., *Status and Progress Report for Thorium Fuel Cycle Development for Period Ending December 31, 1963*, ORNL-3611 (July 1965).

[6] J. L. Kelly *et al.*, *Ind. Eng. Chem., Process Design Develop.* **4**, 212–16 (1965).

Table 7.2. Composition of Fired Products Calculated from Elemental Analysis

Assumption: Thorium present only as ThO_2, ThC, or ThC_2; possibility that oxycarbide (ThOC) could be present is neglected

Run No.	$C:ThO_2$ Mole Ratio	Composition (%)				Composition Material Balance	Calculated[a] Density (g/cc)	Observed Hg Density (g/cc)		Percent of Theoretical Density	
		ThC_2	ThC	ThO_2	Free C			1 atm	544 atm	1 atm	544 atm
80	3.25	10.61	87.67	1.57	0.05	99.90	10.50	8.39	10.19	79.9	97.1
77	3.71	53.85	44.42	1.73	0.10	100.10	9.99	7.98	9.77	79.9	97.8
75	4.17	87.33	9.30	3.04	0.33	100.00	9.58	8.55	8.83	89.2	92.2

[a]Using x-ray densities: ThO_2 = 10.03; ThC_2 = 9.60; ThC = 10.64; C = 2.0.

ratios >4, conversion to the dicarbide appears to occur reasonably well. Only run 75 had enough carbon initially for complete conversion to dicarbide. Apparently, a side reaction, such as that between nitrate and carbon during the initial lower temperature portion of the heating cycle, consumed some of the carbon. The chemical analysis of the final product on run 75 indicates that a total of 0.123 mole of carbon per 100 g of starting material was consumed in side reactions; the free carbon remaining in the fired product would not be enough to convert the remaining ThO_2 and ThC to ThC_2. The free-carbon content in the final product increased as the initial carbon:thoria ratio was increased. Therefore, even when proper balance of carbon and ThO_2 is achieved, higher temperature and/or longer reaction times may be required to obtain complete conversion to ThC_2. The higher oxygen residues coincident with the higher carbon contents are puzzling but may be related to the intimacy of the solid-solid contact. The observed density of the product in run 75, where appreciable conversion to ThC_2 occurred, is about 90% of that theoretically possible for the analyzed compositions.

7.3 DEVELOPMENT OF METHODS FOR PRODUCING MICROSPHERES

Small, spherical particles of high-density oxide or dicarbide are the preferred fuel materials for proposed high-temperature gas-cooled reactors. The spherical shape is preferred because of the ease with which pyrolytic carbon coatings are applied. The coating serves as a small "pressure vessel" for fission product retention. The greater mechanical strength, the controlled void volume, the bulk flow properties, and the overall uniformity possible with spheres are important advantages for many applications. Therefore, we have emphasized the development of the sol-gel process for preparation of small, high-density spheres.

In the microsphere preparation process, drops of sol are gelled by extracting the water into an organic liquid, such as 2-ethyl-1-hexanol (2EH), called the "solvent."

The process for converting a sol into a fired microsphere includes the following six operations:

1. Disperse the sol into drops.
2. Suspend the drops in a solvent that extracts water to cause gelation.
3. Separate the gel microspheres from the solvent (organic liquid).
4. Recover the solvent for reuse.
5. Dry the gel microspheres.
6. Fire the microspheres to densify them and to bring about desired chemical reactions.

For a given sol concentration, the size of the product microsphere is determined in the first step. In the second step, the extraction of water causes gelation and thus converts the drop of sol into a solid sphere. This is the key process step.

Table 7.3. Conversion of Dried ThO_2-C Gels to Thorium Carbides

Conditions: 15 to 20 g of gel shards; vacuum induction furnace
Heating Schedule: to 1100°C in ⅓ hr; to 1700°C in 1 hr; to 1900°C in 1 hr; hold at 1900°C for about 30 min

Run No.	C:ThO_2 Mole Ratio	Maximum Temperature (°C)	Final Gas Pressure (μ)	Weight Loss[a] (%)	X-Ray Analyses			Chemical Analyses[b] (wt %)					Totals (O + C + Th)	Porosity (%)
					ThO_2	ThC_2	ThC	Total C	Free C	Total Th	Soluble Th	O		
73[c]	3.25	1170	7000	19.4	Major	Minor	Trace	6.91	0.60	90.18	89.25	3.15	100.24	3.74
80	3.25	1915	13	23.2	Not detected	Trace	Major	5.36	0.05	94.44	94.56	0.095	99.90	17.63
77	3.71	1920	14	22.2	Not detected	Minor	Major	7.34	0.10	92.65	92.27	0.105	100.10	18.28
75	4.17	1890	40	22.3	Not detected	Major	Trace	8.98	0.33	90.84	90.73	0.184	100.00	3.17

[a]Theoretical weight loss for conversion to ThC_2 is 17.94%; the reported values include approximately 5% volatiles present in the original gels as sorbed gases and water.

[b]Theoretical percentages:

	C	O	Th
ThO_2		12.16	87.85
ThC	4.92		95.08
ThC_2	9.38		90.62
ThOC	4.61	6.14	89.25

[c]This run had an air leak during firing.

The interfacial tension holds the drop in a spherical shape. This fixes the maximum microsphere size attainable, since very large drops will distort. Slow extraction of water is essential to obtain a microsphere with a high density and high strength. If the water is extracted too fast, the drop breaks into fragments or forms a hollow particle. The remaining four operations are simple in principle. However, the densification during firing and the amounts of carbon and volatile materials in the fired product can vary greatly, depending on the drying and firing conditions.

The first four process operations can be done in a continuous column system (Fig. 7.3). The sol is dispersed into drops that are released into the enlarged top of a tapered column. The drops are suspended or fluidized by a circulating upflowing stream of the organic liquid. As the water is extracted and the drops shrink and gel into solid microspheres, their settling velocity increases. The column configuration and the fluidizing flow rates are selected to permit the gelled particles to fall out continuously while sol drops are formed at the top of the column. The separation of the gel spheres from the organic liquid is completed by discharging them onto a filter and draining off the liquid. The spheres are then dried and fired. Fresh or purified solvent is continuously added to the column to displace wet solvent to a recovery system where water is removed by distillation. The columns may be operated batchwise without removal of product or recovery of solvent. Other types of equipment were used to form microspheres. For example, agitation in baffled vessels was used for dispersing and suspending the sol drops when microspheres less than 100 μ in diameter were desired. A mixer-settler system would be a simple and efficient microsphere preparation sys-

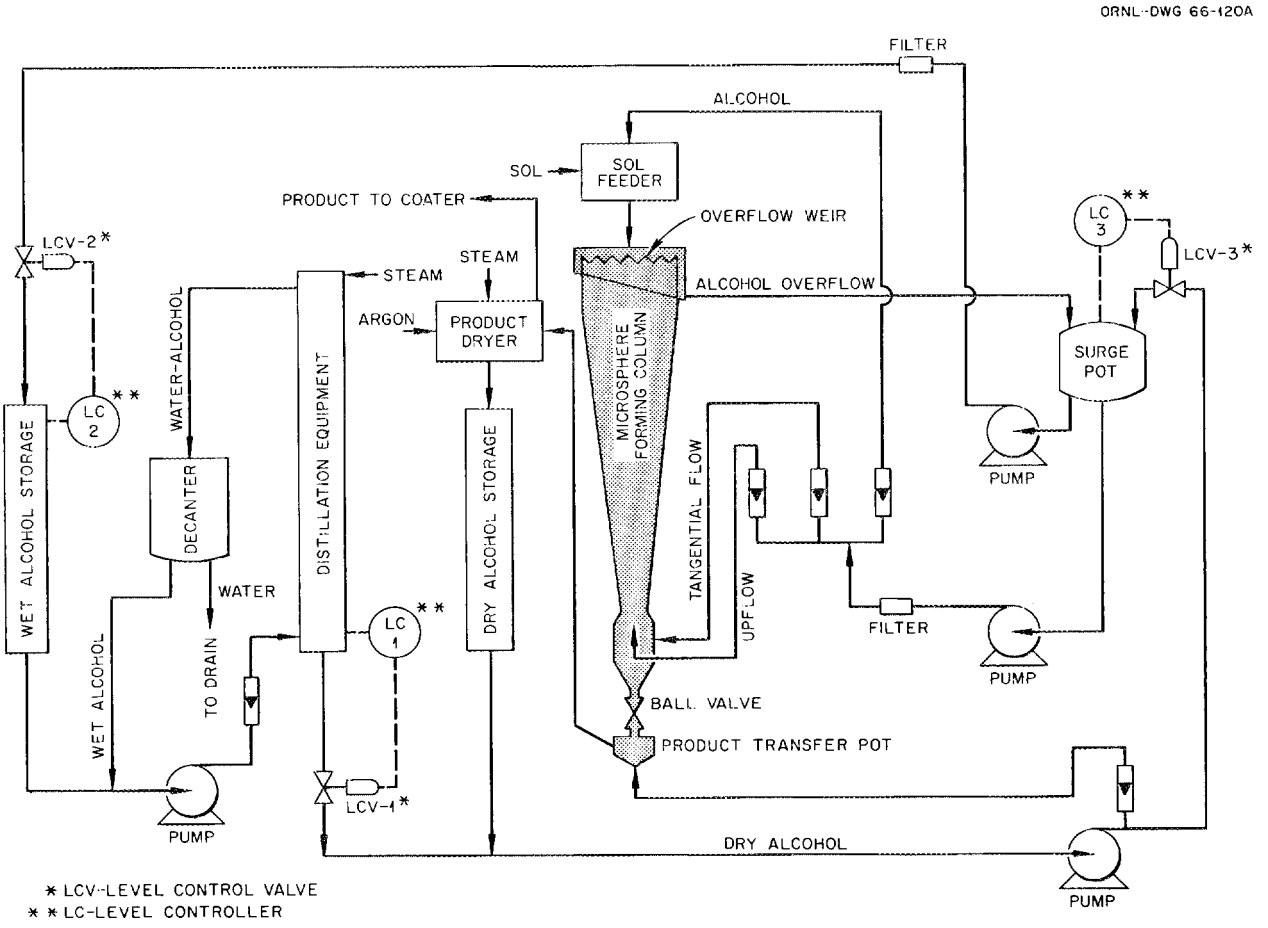

Fig. 7.3. Flow Diagram for Sol-Gel Microsphere Forming Process.

tem if a relatively nonuniform product was acceptable and a mean diameter of 80 μ or less was desired.

Dispersion of Sols

A major part of this study was the development of sol dispersers. None was optimum in all respects, but the important requirement can be met.

Sol drops may be formed from a larger mass of sol by applying one or more forces, such as gravity, centrifugal fields, shear, inertia, interfacial tension, and electrostatic repulsion. To obtain uniform drops and controlled diameters, both the force and the configuration of the sol where the force is applied must be uniform, and one or both must be controllable. With all the dispersers, the uniform sol configuration is obtained by feeding the sol through small orifices, 0.004 to 0.030 in. in diameter.

The two sol dispersion devices that gave the most uniform drops have important limitations. The first, which consists of flowing sol through small orifices immersed in the 2EH, is a practical and simple means of forming 1200- to 2000-μ drops by the falling-drop mechanism. But the orifice size necessary to produce sol drops smaller than 1000 μ is too small to be practical. The second, the two-fluid nozzle, described in the last annual report, gives excellent drop uniformity and simple, easy control of the drop size over a wide range. However, the maximum capacity per two-fluid nozzle (1 to 10 cc/min depending on the drop size) was restrictive, and the need for nonpulsating and accurately controlled flows was an important limitation for remote large-scale operation.

A recently developed and promising method for uniformly dispersing a sol on a large scale is to shear the sol stream emerging from an orifice, by maintaining a velocity gradient in the 2EH at the orifice. This method was tested with rotary feeders immersed in the top of the column. The sol stream leaving small orifices (0.010 or 0.016 in. in diameter) in the feeders is sheared off with most of the force from the velocity gradient in the relatively stagnant 2EH. In all the other devices studied to date, the orifices are stationary and the 2EH is pumped past the orifice through a confined flow channel.

An electrostatic sol disperser was developed on a laboratory scale and tested in the microsphere column. This device has 15 No. 24 hypodermic needles at a controlled positive potential with a copper ring at ground potential around each needle. The mode of dispersion varies with voltage with distinct transitions. As the voltage is increased, there is first an operating region with little effect, then an intermediate region characterized by a single stream of very uniform drops, and then a region wherein a fanlike spray of nonuniform drops is formed. For the intermediate region of uniform drops, the sol drop size is a function of voltage, sol flow rate, and sol concentration. With this disperser, the calcined-product size distributions for a 3 *M* thoria sol and a limited range of mean sizes (200 to 350 μ) were as good as for a two-fluid nozzle.

Column Design

Tapered columns (glass) were the most successful of several column configurations tested. Continuous addition of sol drops and removal of gel microspheres was possible for columns up to $\frac{1}{2}$ in. in minimum inner diameter by simply using smooth, gradual tapers and axial upflow of solvent. When the columns were scaled up to a minimum inner diameter larger than this, the suspension of the sol drops and gel spheres was unsatisfactory in several ways because of the laminar flow and parabolic velocity distribution. The problems associated with maintaining fluidization in the larger columns were eliminated by introducing a solvent stream tangentially at the bottom of the column below the point of minimum inner diameter (Fig. 7.3). This tangential stream produced a swirl that extended with decreasing intensity from 1 to 3 ft up the column. The mixing caused by the swirl prevents the accumulation of particles on one side of the column and the resultant axial flow. By controlling tangential and axial flows separately, the velocity profile across a diameter can be flattened, or the upflow rate at the center may even be relatively lower than that in the region between the center and the wall. The flattening of the velocity profile by the swirl reduced the amount of axial mixing so that the sol drops remained in the upper half of the column.

Drying and Firing Conditions

Drying and firing are necessary to remove volatile matter and to sinter the spheres to a high density, as well as to bring about desired chemical changes in some cases. The temperature and the atmosphere are controlled according to a program in which the gel spheres, as removed from the column, are heated to about 1200°C and then cooled to room temperature. The drying-firing operation is conveniently done in two steps in two separate pieces of equipment. At the present stage of development, drying is done with the spheres supported by a fritted-glass disk in a Pyrex vessel. The organic drying solvent (2EH) is drained off through the frit. The entire vessel is heated by a mantle, and heated gas is passed up through the frit. The dried spheres are fired in alumina crucibles inside laboratory muffle furnaces.

Cracking that occurs during firing and the amount of carbon in the dried gel spheres depend on the drying conditions. Cracking is much more troublesome with spheres having large diameters than with the smaller ones. The presence of steam in the drying atmosphere aids the removal of 2EH from the gel spheres and minimizes cracking. For thoria microspheres, the preferred conditions are:

Drying	Argon	25 to 110°C in 1 hr
	Argon + steam	110 to 200°C in 6 hr
Firing	Air	From 100 to 500°C at 100°C/hr
		From 500 to 1150°C at 300°C/hr
		At 1150°C for 4 hr

For thoria-urania sols made with $UO_2(NO_3)_2$ or UO_3 (limited to <10% urania), the urania is reduced to UO_2 by Ar–4% H_2 during the final 4 hr of firing and then is protected by an argon atmosphere during cooldown. If carbon black is added to the sol, carbide microspheres may be formed by reaction of the carbon with the oxides at temperatures of 1700°C or higher in an inert atmosphere or vacuum.

The rates of temperature rise listed for the thoria microspheres were slow enough to be safe for any of the gels. Much faster rates of temperature rise during either drying or firing sometimes resulted in fractured particles, or particles having greater porosity, larger surface areas, and lower resistances to crushing forces.

Solvents and Surfactants

The eight-carbon alcohol 2EH was used for all the microsphere preparation studies reported here. In general, the long-chain alcohols are the most satisfactory. Halogenated solvents were avoided because of possible halogen contamination of the product. Considering the many excellent properties of 2EH for this use, we are unlikely to find any solvent that is significantly better.

A surfactant must be dissolved in the solvent to prevent coalescence of the sol drops with each other, coalescence of the sol drops on the column walls, and clustering of partially dried drops. Surfactants also lower the interfacial tension between the sol and 2EH; the interfacial tension must be high enough to keep the drops spherical. The concentrations of surfactant used were 0.1 to 1 vol %. Span 80 (an Atlas Powder Company ester) was most effective for preventing coalescence and clustering, but it also gave a low interfacial tension and permitted distortion of the larger drops of sol. (Span 80 is, nominally, sorbitan monooleate.) Ethomeen S/15 and Amine O were successful for forming thoria spheres in all sizes. For sols other than pure thoria, Span 80 and Ethomeen S/15 were generally used together, with the most common concentration being 0.5 vol % of each.

Solvent Recycle

The solvent that overflows from the microsphere column to the wet-solvent tank is dried before it is returned to the column. The water content is efficiently reduced by a simple single-stage distillation. The boiling point of the 2EH changes rapidly with water content: from 183°C for pure 2EH to 150°C for 0.5 wt % H_2O, and to 98°C for the azeotrope when an aqueous phase is present. The solubilities at room temperature are 2.55 wt % for water in 2EH, and 0.1 wt % for 2EH in water.

Use of heat exchangers, a still heated with 90-psig steam, and a phase separator gives very simple and efficient operation. Only a small fraction of the liquid is vaporized. Most of the heat required is sensible heat, and a good heat exchanger minimizes the heating and cooling load. As water and 2EH are vaporized, the water content of the liquid decreases until the boiling point

approaches the condensation temperature of 90-psig steam (165°C). Thus the amount of boilup is automatically controlled, and no measurement or control devices are needed. After the vapors are condensed, the aqueous and 2EH phases separate by gravity and are discharged through jacklegs. This single-stage distillation with separation of the condensed liquids requires less heat than a multiple-stage column with reflux.

Gradual color changes of the solvents during sphere-forming operations indicate the accumulation of surfactant or solvent degradation products. The accumulation of these impurities did not cause any apparent deleterious effects during the longest runs (over 100 hr) that we made. One charge of 2EH was used for over 100 days in a pilot-plant system, with small additions of surfactants during every period of operation. If impurities do limit the recycle of solvent, the costs of solvent treatment vs replacement will have to be considered.

Characteristics of the Product

The product characteristics of principal importance are: shape, size, chemical composition, homogeneity, density, resistance to crushing forces, and amount and type (open or closed) of porosity present. Irradiation behavior is also of prime importance. Generally, nearly 100% of the particles produced in the product size range were spheres. Some of the nonstandard sol preparations and column conditions resulted in clustering or cracking into fragments. About 750-μ-diam thoria microspheres were the largest possible for the conditions used, as shown by the fact that the largest gel particles were slightly distorted. (The interfacial tension cannot maintain the spherical shape when the sol drop becomes very large, since the distorting forces become relatively larger.) The lower size limit is determined by the practicality of dispersing the sol into very small drops and collecting the product, which may be nearly colloidal.

The only impurity problem encountered so far concerns the presence of 2000 to 5000 ppm of carbon in urania microspheres fired in reducing or inert atmospheres. Since the nitrate, formate, and hydrazine are completely volatilized, this carbon must come from the 2EH and the surfactants. The 2EH and surfactants leave no residues except carbon, and the carbon can be completely oxidized during firing if an oxidizing atmosphere is acceptable. The concentrations of other impurities are the same as or less than those in the nitrate salts from which the sols are prepared. The sol-preparation, sphere-forming, and sphere-drying operations are not corrosive to stainless steel or glass apparatus, and the microspheres are inert toward alumina at 1200°C.

Most of our gel microspheres sinter to strong particles of nearly theoretical density at 1150°C. The pores remaining at this temperature are very fine and uniformly distributed. The results for pyrolytic carbon coating and irradiation of sol-gel microspheres are good.

Characteristics of thoria gel microspheres and their fired products were investigated as a function of time during continuous operation of the microsphere column for about five days. The primary objective of the investigation was to determine the effect of long-term use of the organic extractant, 2EH, on product characteristics. A second objective was to evaluate different gel sphere drying methods for removing carbon from the gel microspheres that were produced. A single ThO_2 sol preparation was used throughout the continuous run to eliminate any differences in product because of sol variability. The thoria particles dispersed in the sol had a crystallite size of 59 A when measured by x-ray line broadening, and a crystallite size of 68 A when calculated from surface area measurement by nitrogen adsorption.

Carbon content, density, and pore size distribution of the gel microspheres were measured; and density and carbon content of the calcined microspheres were measured. Pore size distribution is believed to be a good index of changes in the gel-setting mechanism. The presence of a population of pores significantly larger than the mean crystallite size could conceivably signal deleterious changes in the organic extractant. Such pores were observed in some previous preparations. Increases in the carbon content of the gel or calcined product from species that result from the organic extractant would not be desirable.

The carbon content of the gel and of the calcined product was approximately constant with time (Table 7.4). These data suggest that there is no buildup of species in the 2EH that can preferentially sorb on the thoria gel. Steam-stripping of the gel spheres produced calcined products of very low carbon content (30 to 45 ppm), as well as a high density (about 9.8 g/cm^3). Gel spheres

Table 7.4. Properties of Dried Thoria Gel and Calcined Thoria Microspheres (210 to 250 μ in Diameter when Calcined)

Column Operating Time (days)	Treatment Method	Carbon Content (ppm)		Pore Radius of the Gel (A)				Density (g/cm^3)	
		Gel	Fired Product	Mean Radius (No. av)	Percentile 80th	90th	95th	Gel	Fired Product[a]
Gel[b]	Oven dried	950–1200	30	23	23	24	27	5.39	9.85
1	c	5700	42	35	48	250	950	3.90	9.82
2	c	1500–2600	38	28	36	39	300	4.76	9.77
3	c	4300	44	25	31	34	37	5.07	9.64
4	c	4100	35	26	32	32	32	4.83	9.86
4	*d*	3700	91						9.84
4	e	3700	120						9.87

[a]Theoretical density is 10.00 g/cm^3.

[b]Sol evaporated and dried to gel in an oven at 80 to 100°C in air to produce gel fragments. This gel was not exposed to 2EH.

[c]Steam-stripped at 100°C with 50 g of steam per gram of microspheres. Gel microspheres then calcined by heating in hydrogen at 1200°C for 4 hr after a 300°C/hr heatup rate from room temperature in hydrogen.

[d]Steam-stripped at 100°C with ~5 g of steam per gram of microspheres, and then with argon and methanol vapor at 150°C for 1 hr. Calcination same as c.

[e]Same as *d*, except methanol vapor at 250°C was used.

dried in methanol vapor had about the same carbon content as those that had been stripped, but the carbon content of the fired product was twice as high. Washing gel spheres in acetone or methanol was examined as an alternative to steam-stripping. In both cases, excessive cracking and destruction of the microspheres resulted; thus this approach cannot be used for thoria. Steam-stripping the gel spheres prior to firing to high density produces a microsphere after calcination that is acceptable from the standpoint of both carbon content and density. When the gel is steam-stripped, firing of the gel in air is not required to achieve low carbon content. When argon drying is used, the gel microspheres contain 3 to 5 wt % carbon, the removal of which requires firing in air.

The measurements of pore radii show little change with time during column operation and, therefore, suggest that no species that will affect the gel-setting mechanism are building up in the organic extractant. A product of acceptable carbon content and density was obtained even with the gel formed after one day's operation. Radii of 10% of its pores were larger than 750 A. Coarse pores observed during the early operation are believed to result from excessive extraction of nitrate from the sol during gelling. The organic extractant appears to reach a near-equilibrium content of nitrate in a one- to two-day operation period.

Coated-Particle Development Facility (CPDF) Microsphere Column

A system including a tapered column with a minimum inside diameter of 3 in. was installed and operated with thoria sols (Fig. 7.3). The capacity, limited by the steam supply to the distillation system, is at least 25 cc/min of sol (1200 g of ThO_2 per hour for a 3 *M* thoria sol). All four types of sol dispersers were used, and the results are at least equal to those obtained in the development studies. Two two-fluid nozzles gave 85% yields of microspheres in the 210- to 250-μ range. For the

falling-drop mechanism with 0.022-in.-diam orifices, the products were 80% in the 590- to 849-μ range for one run and 60% in the 420- to 500-μ range for another run. This column system is being used to supply microspheres for other parts of the fuel-cycle program and to investigate the problems of long-term remote operation.

7.4 CONSTRUCTION OF THORIUM-URANIUM RECYCLE FACILITY

Building Construction

A contract for the construction of the Thorium-Uranium Recycle Facility (TURF) was signed with Blount Brothers Construction Company of Montgomery, Alabama, on May 6, 1965. The initial contract stipulated a completion date of December 28, 1966; however, some changes in drawings and the discovery of some drawing deficiencies have necessitated an extension of the contract to February 10, 1967. The facility is estimated to be about 60% complete.

The building has been completely enclosed since January 1966. Views of the exterior and interior of the facility, taken in mid-April, are shown in Figs. 7.4 and 7.5 respectively. Installation of stainless steel cell liners is the task that controls the rate of progress of construction. The contractor was unable to use metal–inert-gas welding exclusively for joining liner plates but did use this method for the first pass. Tungsten–inert-gas welding was used for the final pass. The protective coating system to be applied to the walls in most of the occupied areas and in cell F was upgraded from a vinyl to a modified phenolic at the request of the paint contractor, with no

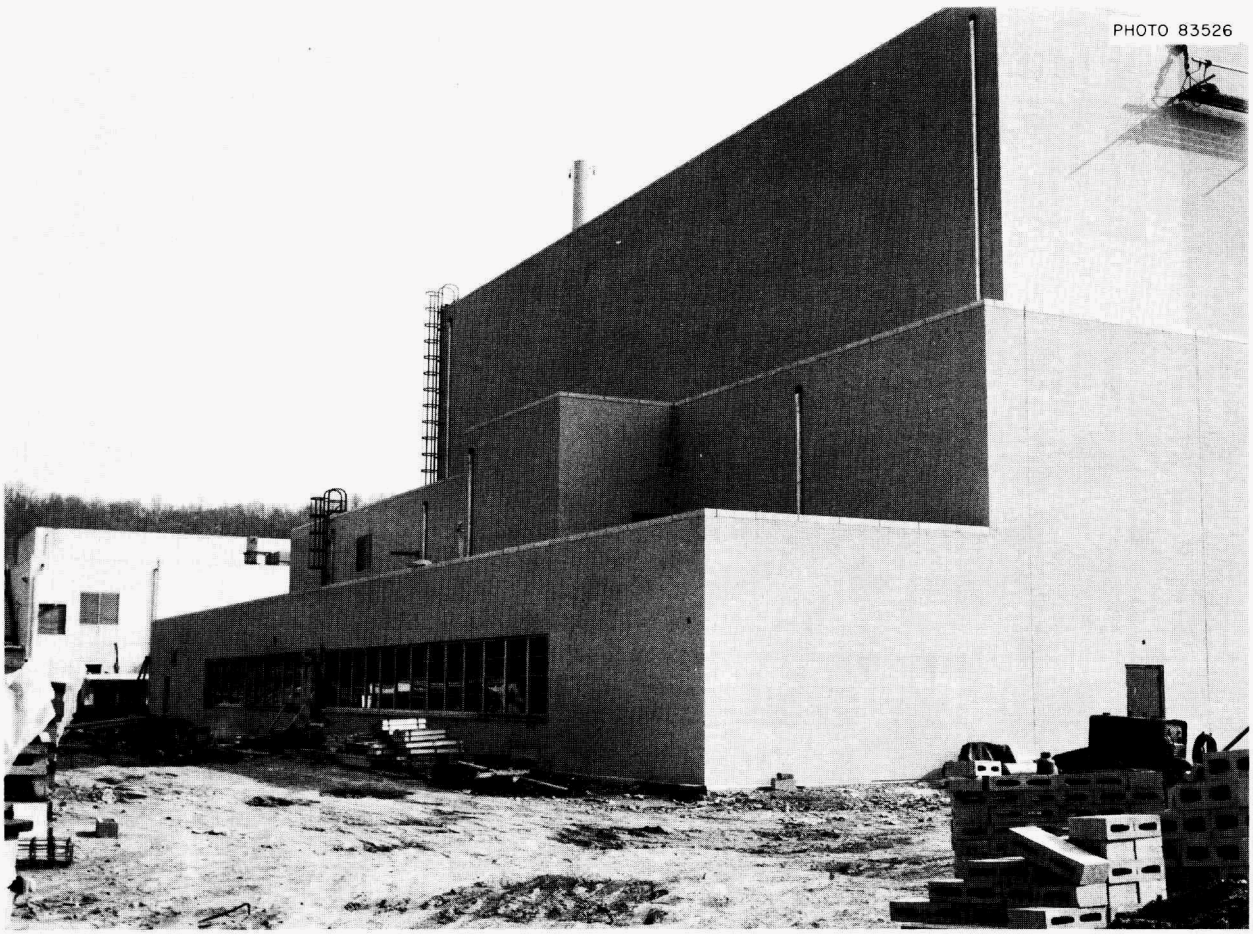

Fig. 7.4. Exterior View of TURF, April 1966.

Fig. 7.5. Interior View of TURF, April 1966.

additional cost to the government. Using essentially the same coating system in almost every area saves labor for the painting contractor and thus compensates for the cost of additional materials. Cell A, sometimes referred to as the glove maintenance room, is a structure consisting of $\frac{1}{4}$-in.-thick carbon-steel plates, supported by external steel structural members, into which are mounted a number of large (up to 3×4 ft) Plexiglas viewing panels. To minimize distortion we designed this structure to allow the various carbon-steel panels to be joined to each other by skip welding, with the space between the welds being sealed with epoxy cement. Argonne National Laboratory previously built a similar metal room in this fashion, and it has performed satisfactorily. All the panels for this room have been fabricated and have received two coats of paint at the painting contractor's shop.

The waste pit outside Building 7930 is under construction; the 30-in. main exhaust and the 8-in. process waste drain lines are in place; and the emergency generator shed has been erected.

Procurement of Fixtures Furnished by the Government

Those items that presented unusual problems in design and/or procurement and also those that required lead times that would delay the construction were deleted from the fixed-price contract and included in the ORNL procurement list. These include the in-cell crane and manipulator system; the three steel shielding doors; underground stainless steel duct work; highest-quality stainless steel pipe, valve, fittings, and eductors; viewing windows and window forms; special penetrations

through the cell walls; various untested items for the cell fire protection system; and other miscellaneous items. Equipment costing $565,000 has been delivered; equipment costing $980,000 is on order and is approximately 50% complete; and equipment estimated to cost $125,000 remains to be placed on order.

The major difficulty has been with the three steel shielding doors. Both the design and construction lagged behind the schedule. This work was expedited as much as possible, but unforeseen problems arose with the drives of the vertical lift doors and caused additional delay. We do not yet know whether the delay in door delivery will delay completion of the building.

The remainder of the procurement has proceeded essentially on schedule, and all other items have been available prior to the contractor's need. Particularly noteworthy is the design and construction of the in-cell crane and manipulator system; this $363,000 order for design and construction has proceeded smoothly with an increase of only $13,000 in contract price. While the proof of the system will be its performance in the facility, the manufacturer's tests of powering and linking devices are very encouraging. The pressure-reducing valve for the cell fire protection system was modified and tested; it was accepted by Factory Mutual Insurance Company during the year.

7.5 DESIGN OF PROCESS EQUIPMENT

Procedures and equipment are being developed to adapt the sol-gel process to remote operation as required for TURF.

During the year the function of the first line of equipment to be installed in TURF was changed from vibratorily compacted, oxide-filled metal tubes to carbon-coated microspheres. Preliminary plant-type designs were prepared for most of the major process steps; "cold" pilot-plant-scale equipment was designed for development of urania sol formation equipment; and work was completed on the equipment for handling liquids. The development of the vertical tube furnace for firing of oxide fragments was completed. Final design of both a dryer and a vertical tube furnace was discontinued, pending results of developmental work with microspheres.

A simplified flowsheet of the blocks of equipment to be installed in the facility is shown in Fig. 7.6. Of the process steps indicated, only urania sol preparation, microsphere formation, and microsphere drying and firing have received significant preliminary design study.

Small-scale precipitation-peptization test equipment was designed and fabricated for use by Unit Operations in the development of this method of urania sol preparation. The engineering flowsheet for this system was developed, with attention being given to problems peculiar to remote operation. Washing of the precipitate is done by countercurrent decantation rather than by filtration, to avoid handling solids. Also, pumps for the urania precipitate are of a novel design with no moving parts in the process stream. The system will have a capacity of approximately 1 kg per 8-hr day. Similar equipment is to be designed and fabricated for testing (by Unit Operations) the amine extraction method of preparing urania and urania-thoria sols.

The equipment located in Building 4508 for production of microspheres is, in principle, satisfactory for plant operation, although there are shortcomings or significant design problems remaining in the following areas: (1) installation and maintenance of the drop forming device; (2) means for predetermining the performance of the drying alcohol; (3) means for transfer of gel spheres from the bottom of the sphere forming column; (4) means for making the rough separation of spheres from the alcohol; and (5) means for inspecting spheres at the time of withdrawal from the column. All except (2) have been or are being designed, but none have yet been fabricated or tested. The design of the dryer for oxide fragments was approximately 75% complete when the objective was

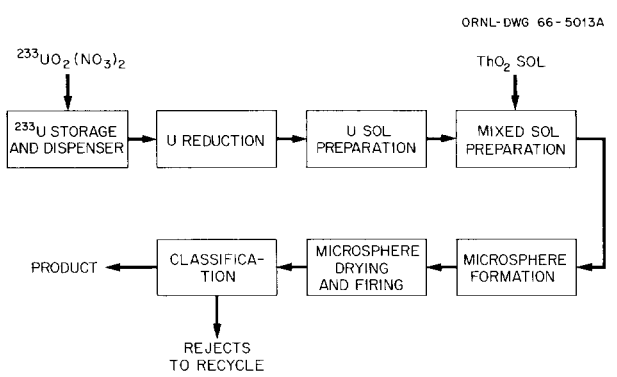

Fig. 7.6. Simplified Flowsheet of Microsphere Equipment for TURF.

changed. A tilting-pan carousel was being designed because both we and the drying-equipment manufacturers believed that it would be much simpler mechanically than the continuous tray dryer. A lack of bids from suitable fabricators to design and construct a dryer to our specifications forced us to assume the detailed design of this device. The requisite drying conditions for microspheres have not yet been established; however, preliminary indications are that this style of dryer is not suited to drying microspheres and that the unit under design was greatly oversized. A vertical tube dryer, similar to the vertical tube furnace tested for firing oxide fragments, appears at this time to be best suited for drying microspheres.

Testing of a 3-in.-ID prototype vertical tube furnace to be used for calcining sol-gel oxide fragments was successfully completed. The gel was introduced at the top of the furnace, calcined to 1150°C, and cooled while passing down through the tube. When uranium was present in the thoria used in the tests, it was reduced to UO_2 by Ar-H_2 flowing up the tube. The furnace, as tested in a final operating demonstration, was judged ready for adaptation to remote operation. Product quality from this calciner met or exceeded expectations, and mechanical reliability is judged adequate for our requirements. A number of problems concerning the operation of the calciner were solved or circumvented. The most troublesome of these was the breaking of the bore tube. This occurred when bridges of product collapsed with the furnace at operating temperature; it was alleviated by developing procedures that minimized the occurrence of bridging. For example, it was found that bridging did not occur if the bed was held static at 1150°C up to 4 hr. Periods of 8 to 12 hr at this temperature, however, caused bridging. Bridges intentionally formed, as described, could be broken repeatedly without damaging the tube, provided the furnace was cooled to room temperature before attempting to break the bridge. Instrumentation was developed to follow the progress of the bed down the tube. This equipment could reliably detect and signal a lack of movement of the bed downward (and therefore a bridge) in about 5 min, which is less time than is required, since detection of a bridge within 2 hr is adequate. Installation of this furnace for remote operation would require means of remotely breaking bridges and replacing the bore tube (or complete furnace). Frequency of breakage should be low enough that this would impose no severe handicap. The quality of the product was significantly improved as compared with that of the product from calcination in muffle furnaces. Using our standard method of measurement, gas release values measured on the furnace product were 0.003 to 0.008 cc/g as compared with 0.05 to 0.15 cc/g obtained previously on samples fired in muffle furnaces. The oxygen:uranium atom ratios were <2.015. Densities measured by mercury porosimetry at 500 psi were 9.97 to 10.12 g/cc. These are close to the theoretical crystal density of ThO_2. The product improvements are believed to be the result of better contact between the reducing gas and the solids, and the removal and handling of the product in Ar-H_2 without exposure to air.

Oxide fragments were to have been fired in a vertical tube furnace similar to the one tested. When the program objective was changed, all major decisions relative to furnace design had been made, and we were detailing the calcining system and preparing a bid package for the furnace, which was to have been a fully sealed unit, heated electrically by molybdenum resistors. Conceptual design of a Vezin-type sampler had been completed; a detailed design was in progress. We believe that this same general method will be adequate for firing microspheres and that no problem will be encountered with bridging of microspheres in the tube.

8. Sol-Gel Processes for the Uranium Fuel Cycle

The uranium fuel cycle, especially as it relates to fast reactors, occupies a position of primary importance in the reactor development program of the United States. Fuel preparation is an important part of the uranium fuel cycle, and the work reported in this section was carried out as part of our effort to apply the sol-gel techniques (originally developed for the thorium fuel cycle) to the uranium cycle.

Emphasis in this work was on urania and plutonia sol preparation because these sols are readily made into UO_2-PuO_2 mixtures, which are most important as reactor fuels. However, some studies have been carried out on other materials which show potential of being prepared by sol-gel techniques, such as UN and ZrO_2, and some of this work is also reported in this section.

8.1 URANIUM SOL-GEL PROCESSES

Chemical development of uranium sol-gel processes includes work on the preparation of urania, uranium nitride, and zirconia sols for use in urania-zirconia preparation. The urania work proceeded in two phases. The first consisted of (1) the development of a laboratory process for preparing aqueous urania sols by a precipitation-peptization method and (2) the production of more than 15 kg of urania microspheres (7 kg containing fully enriched uranium). Details of the development of the sol preparation method and microsphere forming, drying, and firing studies of this phase have been published.[1] A summary of the more important parts of this report is given below ("Preparation of Urania Sols and Microspheres"). The second phase was the chemical development of improvements in the laboratory process, investigation of other methods of urania sol preparation more amenable to engineering scaleup, and study of an alternative method of preparing gel microspheres. This is reported in "Development of Urania Sol-Gel Process," later in this section. Also discussed is the nature of urania sols and sol-forming phenomena indicated by electron micrograph, electron diffraction, and absorption spectra techniques ("Physical Chemistry of Urania Sol Formation") (summary of a report now in press[2]). A report on the laboratory preparation of uranium nitride microspheres by a sol-gel technique[3] is summarized in "Preparation of Uranium Nitride Microspheres." The final section describes the chemical development of zirconia sol preparation, the goal of which is preparation of sols suitable for mixing with urania sols to prepare the mixed oxides.

Preparation of Urania Sols and Microspheres[4]

The sols used in preparing 15 kg of UO_2 microspheres by the sol-gel technique were prepared by precipitating hydrous U(IV) oxide and then dispersing it in water. A flowsheet for the laboratory preparation of U(IV) sol is given in Fig. 8.1. It begins with the preparation of a uranous nitrate solution by the catalytic reduction with hydrogen of a uranyl nitrate solution containing excess nitric acid. The solution is filtered to remove the catalyst. In the preferred method of preparation (nitrate-formate), formic acid is added to the filtered solution and

[1] J. P. McBride, *Preparation of UO_2 Microspheres by a Sol-Gel Technique*, ORNL-3874 (February 1966).

[2] C. J. Hardy, *The Electron Microscope, Electron Diffraction, and Spectrophotometric Examination of Hydrous Uranium Dioxide Precipitates and Sols*, ORNL-3963 (in press).

[3] T. A. Gens, D. M. Helton, and S. D. Clinton, *Laboratory Preparation of Uranium Nitride Microspheres by a Sol-Gel Technique*, ORNL-3879 (November 1965).

[4] Summary of ref. 1.

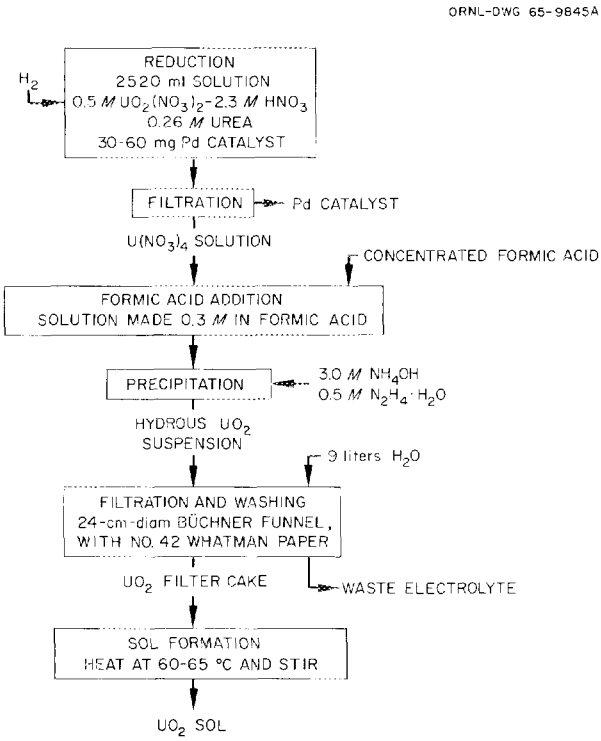

Fig. 8.1. Flowsheet for the Laboratory Preparation of Urania Sol.

the hydrous oxide is formed by precipitating U(IV) with an ammonia solution containing hydrazine. The precipitate is collected by filtration and then washed to remove excess electrolyte. The washed filter cake is then heated at 60 to 65°C to produce a fluid, stable sol. Sols were also prepared from the hydrous oxide precipitated from uranous nitrate solution without the addition of formic acid according to the nitrate method, but this method presented some problems (see below and ref. 1). Precautions were taken to protect the material from air oxidation by the use of a blanket gas (argon) during all stages of the process. Because it was desirable to work with enriched uranium, the sols were made batchwise, using 300 g of uranium in each lot. Thus, several batches could be worked with concurrently in the same area without fear of criticality incidents. Sol concentrations of 1.2 to 1.6 *M* UO_2 were achieved (Table 8.1).

In order that the washed filter cake can be liquefied to a sol by heating, it is necessary to add the ammonia in the precipitation step until a pH between 7 and 8 is achieved. The addition of formic acid to the U(IV) nitrate solution is necessary to maintain a high U(IV) content (more than 85% of the uranium) in the precipitate and the subsequent sol. In the absence of formic acid, the U(IV) content of the hydrous oxide would be down to about 80% of the total uranium, in contrast to better than 99% for the original U(IV) nitrate solution. In addition, the formic acid simplifies pH control in the precipitation step and accelerates the washing of the filter cake.

To form microspheres, the urania sol was dispersed into droplets at the top of a forming column (Fig. 7.3, Sect. 7.3), and the droplets fell through countercurrently flowing 2-ethyl-1-hexanol. As the droplets fell, water was extracted until a sufficient quantity had been removed and the drops were set to gel microspheres. Two organic surfactants, Amine O and Span 80, were added to the organic solvent at about a 0.5 vol % concentration to prevent spheres sticking to the column wall and to prevent clustering. The spheres settled to a product-collection vessel at the bottom of the column where they were collected batchwise.

Wet gel spheres were placed on a fritted disk, and blanket gas was passed through the fritted disk and from there through the bed of gelled spheres. The entire vessel was heated by a heating mantle. A variety of drying conditions were tested for effectiveness of removing the 2-ethyl-1-hexanol and surfactants from the gel microspheres.[1] Steam stripping appears to be best. Drying under argon at 150°C best preserved the U(IV) content of the gel, but the carbon content was about three times as high as with steam stripping. Vacuum drying at 100°C for 74 hr yielded gelled microspheres, still containing about 5 wt % carbon. In general, the carbon content of the dried gel spheres was 2 to 7 wt %.

Table 8.1. Properties of Typical Urania Sols

Specific Gravity (g/cc)	Uranium Concentration (*M*)	U(IV) Content (% of U)	NO_3^-/U Ratio	$HCOO^-$/U Ratio
1.317	1.23	87	0.13	0.44
1.319	1.27	85	0.07	0.38
1.369	1.48	86		0.45
1.373	1.49	84	0.14	0.45
1.404	1.61	86	0.11	0.31
1.405	1.62	87	0.11	

The UO_2 microspheres were fired at 1150 to 1250°C in high-purity Alundum boats inside a 2½-in.-ID furnace tube also made of high-purity Alundum. Two firing procedures were used. In one, the spheres were heated in H_2 at 300°C/hr to the firing temperature and held there for 4 hr. In the other, the spheres were heated to 950°C in CO_2, the heating continued in H_2 to firing temperature, usually 1150°C, and held for 4 hr.

Table 8.2 shows firing data for typical products. Microspheres from the straight H_2 firing and the CO_2-H_2 firing differed in carbon content, resistance to crushing forces (crush strength), and x-ray crystallite size as measured by x-ray diffraction line broadening. The H_2-fired products contained 2000 to 5000 ppm of carbon and generally had crush strengths between 1.3 and 2.3 lb. The CO_2-H_2 firing effectively lowered the carbon content but decreased the strength. The crystallite size obtained for microspheres of a typical H_2-fired product was 450 A, while that for a CO_2-H_2-fired product was 2500.

The method routinely produced yields of 90% of the calcined microspheres from a 300-g batch in the 125- to 177-μ-diam size. In this 125-to-177-μ fraction, about three-fourths of the spheres (by weight) were of 149- to 177-μ size. With urania, microsphere-forming experience at ORNL has primarily been in the 50-to-250-μ range.

Figure 8.2 shows typical urania microspheres. The bright spots are light reflections from the surfaces of the spheres. Polished sections of these same spheres are shown in Fig. 8.3. Although it does not appear at this magnification, there is a uniformly distributed microporosity in these spheres which tends to coalesce to form macropores at about 1700°C.

Development of Urania Sol-Gel Process

After the completion of the preparation of about 15 kg of urania microspheres, chemical development of the urania sol-gel process continued in an attempt to improve the laboratory process and to produce more concentrated urania sols. The incentive to produce more concentrated sols derives from the attendant decrease in volumes which must be handled, and from improvement in sphere-forming-column operations. In addition, other sol preparation methods more amenable to engineering scaleup were investigated. These included an improved precipitation-peptization process and a method based on solvent extraction. A new method of microsphere preparation involving the hydrolysis of sol droplets was also investigated.

Improvements in the Laboratory Process. – Sol preparation by the precipitation-peptization method begins with the preparation of a uranous nitrate solution by the catalytic reduction (with H_2) of a solution 0.5 *M* in UO_2^{2+} and 2.3 *M* in NO_3^-, containing 15 g of urea per liter. The excess nitric acid over the stoichiometric nitrate : uranium ratio of 2 is necessary to prevent precipitation during reduction. The effects on solution stability and sol formation of (1) substituting formic acid for the excess nitric acid and (2) of increasing the uranium concentration were studied.

Table 8.2. Firing Data for 125- to 177-μ-diam UO_2 Microspheres

Sintered in H_2 at indicated temperature for 4 hr

Heatup Schedule	Sintering Temperature (°C)	Weight Loss on Sintering Gel (wt %)	Weight Required to Crush (g)	Carbon Content (ppm)	Density of Product (% of theoretical)
a	1150	6.9	871	4600	97.8
a	1250		1050	4900	97.6
b	1150	10.2	354	460	~100
b	1250		313	200	~100
b	1250	9.4	354	<100	~100

[a] H_2 to firing temperature at 300°C/hr.

[b] CO_2 to 450°C at 50°C/hr; CO_2 to 600°C at 25°C/hr; CO_2 to 950°C at 50°C/hr; H_2 to firing temperature at 300°C/hr.

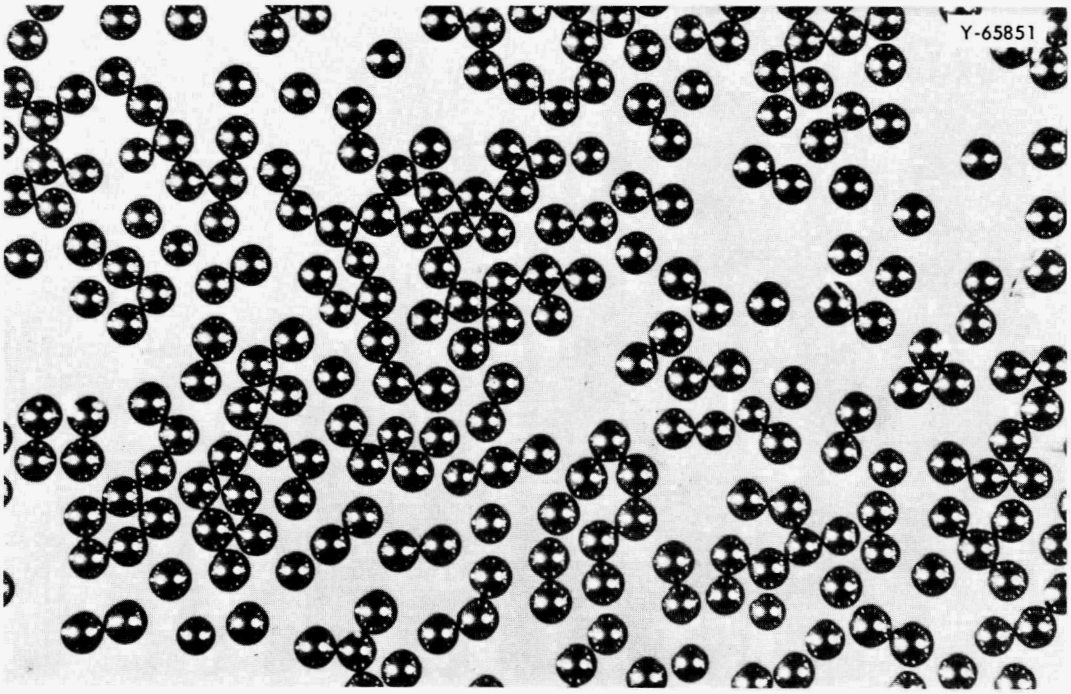

Fig. 8.2. Typical UO_2 Microspheres (Diameters, 125–177 μ).

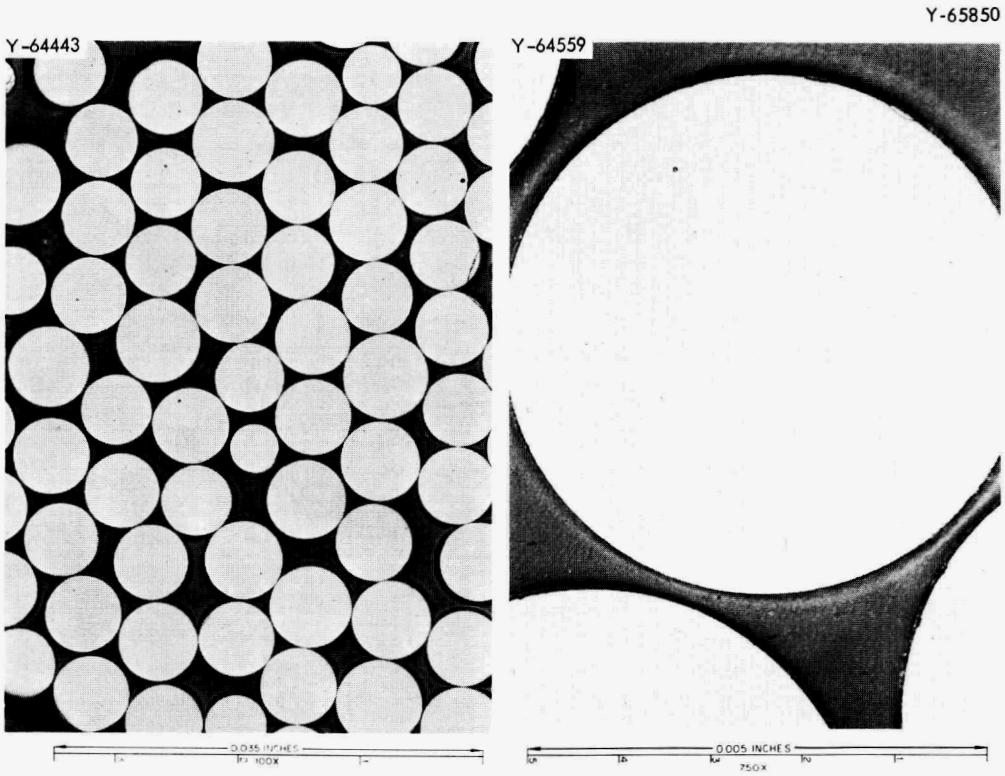

Fig. 8.3. Sections of UO_2 Microspheres. Density, 96% of theoretical; carbon content, less than 100 ppm; resisted crushing loads of 550 g.

Table 8.3 shows the results of experiments in which the uranium and nitrate contents of the solution to be reduced were held nearly constant at about 0.5 *M* and 1 *M*, respectively, and formic acid was added to give formate-to-uranium ratios of from about 0.8 to 1.6. In all experiments, the reduced solutions were stable and could be processed to form sols in the usual manner (see "Preparation of Urania Sols and Microspheres"). (Subsequent experience showed that stable solutions may be prepared with an $HCOO^-/U$ ratio of 0.5 and that urea need not be added.) The time required to produce a sol by heating the hydrous oxide filter cake increased markedly for the oxide precipitated from the reduced solutions that contained the higher formate concentrations (e.g., about 4 hr for $HCOO^-/U$ of 1; 8 hr for a ratio of 1.3; 16 hr for a ratio of 1.6).

Examination of Table 8.3 shows that optimal conditions for preparing a UO_2 sol of high uranium concentration and high U(IV) content were obtained when the sol was prepared from a solution containing an $HCOO^-/U$ ratio of 1.3. The final sol was 2.23 *M* in uranium, and the oxidation state of the uranium was represented by the formula $UO_{2.06}$. Sol product yields decreased with increasing $HCOO^-/U$ ratios. These results and previous experience[1] suggest that for high yields, an $HCOO^-/U$ ratio of 0.4 to 0.8 in the solution to be reduced may be desirable.

Reduced solutions were prepared from uranium solutions (0.5, 0.75, 1.06, and 1.34 *M* in uranium) with NO_3^-/U ratios of 2 and $HCOO^-/U$ ratios of 1; each contained a small amount of urea. Sols were prepared in the usual way by precipitating the uranium with ammonia (final pH, 7); the hydrous oxide was recovered by filtration and then washed and held at 60 to 65°C to form a sol. The results are shown in Table 8.4.

It is seen that uranium content of the sol increased with increase in the uranium concentration in the starting solution, without significantly affecting the U(IV) content or sol yields. The 2.8 *M* sol formed from the solution prepared at the highest uranium concentration showed a higher viscosity than the more dilute sols.

Engineering Scaleup. – Development of a process for making kilogram quantities of urania sol (enriched in ^{235}U) in criticality-proof equipment requires modification of the laboratory process. Scaleup of the method for making the uranium(IV) nitrate solution does not appear to be difficult, but filtering and washing present criticality and handling problems and make difficult the production of sols having a prescribed NO_3^-/U ratio. Hence, effort is being directed toward developing a process in which the hydrous oxide is precipitated and washed and the washed solids are peptized by adjusting the NO_3^- concentration. Preliminary results have been encouraging, and a completely continuous sol preparation process is foreseen.

In the present tentative process a U(IV) solution is prepared by catalytic reduction with H_2 of a 0.5 *M* UO_2^{2+} solution containing 1 *M* NO_3^- and 0.25 *M* $HCOO^-$. After reduction, the $HCOO^-$ concentration is adjusted to give an $HCOO^-/U$ ratio between 0.5 and 0.7 (this adjustment is necessary

Table 8.3. Effect on Sol Properties Produced by Substituting HCOOH for the Excess HNO_3 when Preparing Solutions of U(IV)

Reduction Conditions			Properties of the UO_2 Sols		
U Concentration (*M*)	NO_3^-/U Ratio	$HCOO^-/U$ Ratio	Specific Gravity (g/cc)	U Concentration (*M*)	U(IV) Content (% of U)
0.52	2.0	0.77	1.41	1.54	90
0.50	2.0	0.80	1.48	1.85	89
0.47	2.0	1.00	1.51	1.95	94
0.50	2.0	1.00	1.52	1.98	91
0.51	2.0	1.26	1.59	2.23	94
0.50	2.0	1.59	1.57	2.16	95

because part of the $HCOO^-$ is reduced in the reduction step). The hydrous oxide is then precipitated by adding 3.5 *M* NH_4OH. The precipitate is then washed several times to reduce the NO_3^- concentration. The washed precipitate is resuspended, the NO_3^- concentration is adjusted, and the suspension is stirred at 60 to 65°C until peptized. Table 8.5 shows the properties of urania sols prepared in this way. As indicated in the table, two preparations were made using a kilogram of uranium. Greater than 95% yields of sol were achieved in the large-scale preparations.

Uranium(IV) solutions of the above composition were readily prepared in a stainless steel reactor containing a fixed bed of 1 kg of platinized alumina catalyst in the form of ⅛- by ⅛-in. right cylinders. The reactor was made of 1½-in. sched 40 pipe. The catalyst occupied a 3-ft length of pipe. With H_2 at a pressure of 500 psi, more than 99% of the uranium was reduced at a solution flow rate of 1 liter/hr.

Development of Methods for Preparing Microspheres. – A method of microsphere preparation that includes chemical gelation of dispersed sol droplets has been developed for making spherules of the oxides of uranium, zirconium, and thorium.[5]

[5]T. A. Gens, *Formation of Uranium, Zirconium, and Thorium Oxide Microspheres by Hydrolysis of Droplets*, ORNL-TM-1508 (in press).

Table 8.4. Preparation of Uranium(IV) Nitrate Solutions: Effect of Uranium Concentration on Properties of the UO_2 Sol

Reduction conditions: mole ratios – UO_2^{2+}:NO_3^-:$HCOO^-$ = 1:2:1

Initial UO_2^{2+} Concentration	Sol Properties				
	UO_2 Sol Concentration (*M*)	U(IV) Content (% of U)	NO_3^-/U Ratio	$HCOO^-$/U Ratio	Yield (%)
0.5	1.98	91	0.05	0.51	91
0.75	2.18	86	0.09	0.68	87
1.06	2.56	91	0.06	0.63	90
1.34	2.79	90	0.09	0.55	89

Table 8.5. Properties of Urania Sols Prepared by the Modified Precipitation-Peptization Process

Precipitation conditions: 0.5 *M* U, 1 *M* NO_3^-, 0.25 to 0.35 *M* $HCOO^-$

Peptization conditions: NO_3^- concentration adjusted; mixture stirred at 60 to 65°C

Preparation	Specific Gravity (g/cc)	Uranium Concentration (*M*)	U(IV) Content (% of U)	NO_3^-/U Ratio	$HCOO^-$/U Ratio
NUFD-5[a]		0.67	88	0.15	0.07
F-9[b]	1.258	0.01	83	0.19	0.15
F-10[b]	1.205	0.81	87	0.18	0.17

[a]100 g of U.
[b]1 kg of U.

In this method, a hydroxide precipitate is prepared by bubbling ammonia into a salt solution, and the precipitate is heated to form a sol. Microspheres are then formed by jetting the sol onto a layer of organic liquid (usually 2-ethyl-1-hexanol) floating on a layer of 15 *M* NH_4OH. The sol stream disperses into droplets in the organic layer, and the droplets fall into the ammonia solution, where they are converted into gelled hydroxide microspheres. These spherules may then be dried and fired. Work is under way on the preparation of several kinds of microspheres and on controlling their porosity. Most of the effort has been directed toward applying this method to the preparation of uranium oxide microspheres, as briefly described below.

In a typical preparation 0.1 mole of UCl_3 is dissolved in 100 ml of water to yield a U(IV) solution; the nominal composition of the uranium compound is UCl_3OH. Ammonia, diluted with argon, is bubbled into the solution until the uranium precipitates, and the precipitate is melted at 50°C to form a sol. Gel microspheres are formed by using the layered-liquid system described above. The spherules are leached several times over a 20-hr period with a total of 5 liters of 15 *M* NH_4OH to reduce the chloride content below 10 ppm. The leached microspheres are oven-dried and fired for 1 hr at 1150°C in Ar–4% H_2. Porosity of the product, measured by mercury porosimetry, is typically about 1.2%. Figure 8.4 shows the fired UO_2 microspheres. A photomicrograph of a polished section of one of the fired microspheres appearing in Fig. 8.5 shows some internal porosity. Spheres 250 μ in diameter resisted a crushing force of 800 g.

Physical Chemistry of Urania Sol Formation[6,7]

In preparing urania sols by the precipitation-peptization method (see "Preparation of Urania Sols and Microspheres"), the washed hydrous

[6]Summary of ref. 2.

[7]This work was done by C. J. Hardy, guest scientist from the Chemistry Division, Atomic Energy Research Establishment, Harwell, England.

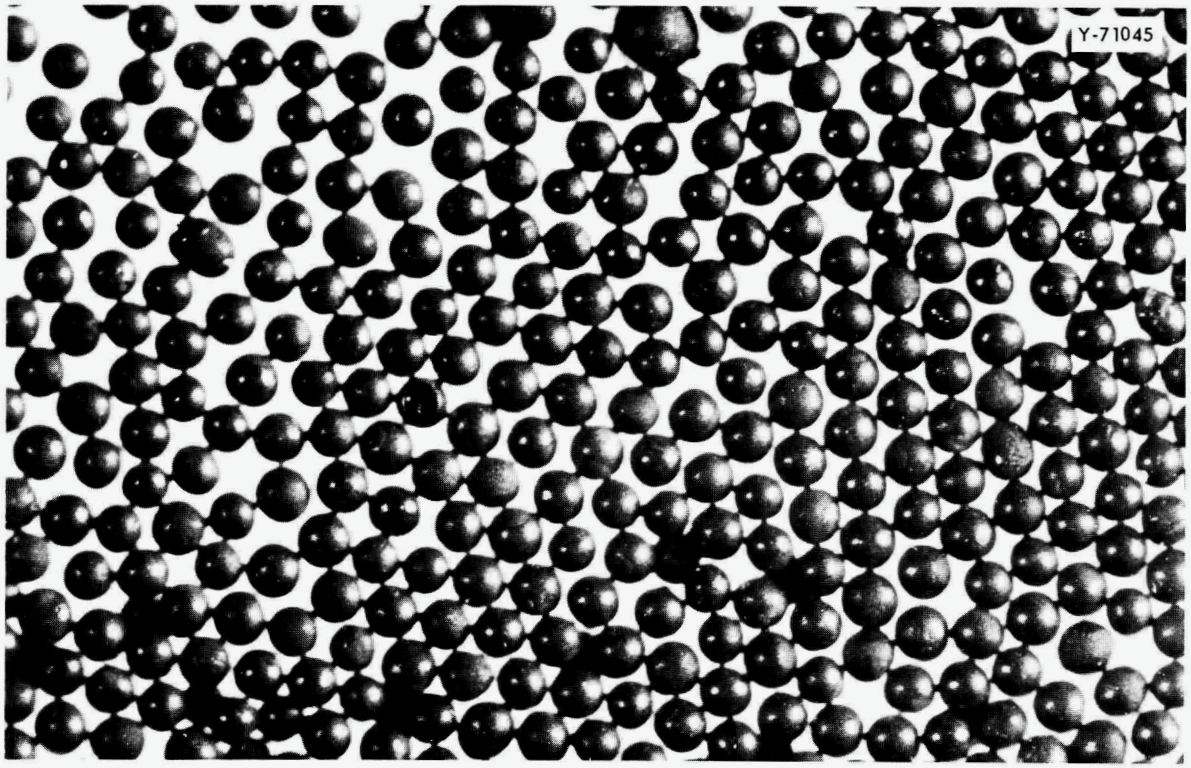

Fig. 8.4. Microspheres Formed from 1.3 *M* U(IV) Chloride Sol and Fired in Ar–4% H_2 at 1150°C.

oxide, prepared from either a uranous nitrate or nitrate-formate solution, is heated at 60 to 65°C to form a sol. Alternatively, the precipitate can be allowed to age at 25°C for several days, during which time a sol gradually forms. To obtain a better understanding of the chemical and physical changes occurring in the precipitate during the sol-forming process, samples were taken at various stages in both the nitrate and nitrate-formate processes and examined by electron microscopy and selected-area electron diffraction to measure the size, shape, and crystallinity of the fundamental particles. In addition, the visible and ultraviolet spectra of the diluted sols were measured, and approximate sizes of particle aggregates were calculated from the turbidities.

Fig. 8.5. Photomicrograph of a Polished Section of a UO_2 Microsphere Prepared from Chloride Sol. Fired in Ar–4% H_2 at 1150°C.

The initial precipitates consisted of irregularly shaped aggregates of 15- to 25-A-diam particles of hydrous uranium dioxide. The initially diffuse lines in the electron diffraction patterns became sharper with increased time of aging at 25°C. The black sols prepared by heating the filtered and washed precipitates at 60°C consisted of cubic UO_2 crystals having an edge length of 10 to 20 A. The presence of 0.4 mole of formate per mole of uranium in the sol prepared by the nitrate-formate method resulted in a more uniform dispersion on the electron microscope grid but did not appreciably affect the size or lattice spacing of the primary crystallites. Figure 8.6 is an electron micrograph of sol particles prepared by the nitrate-formate method, and Fig. 8.7 is its electron diffraction pattern, showing that the particles consist of crystalline UO_2.

The turbidities or apparent absorption spectra of the diluted sols were measured from 8000 to 3000 A, and the optical density was found to vary inversely as the 1.2 to 1.4 power of the wavelength from 8000 to 4000 A, and as the fourth power of the wavelength at less than 4000 A. The maximum size of the scattering particles calculated from the turbidity at 4000 A was of the order of 800 A, which agrees approximately with the size of the largest aggregates observed on the electron micrograph.

A model has been proposed (ORNL-3963) for the chemical and physical constitution of the particles in the nitrate-formate prepared sol in which formate ions bridge pairs of uranium atoms on the surface of primary cubic crystallites having an edge length of 10.9 A; these crystallites are then considered to form the aggregates that have diameters of up to 800 A.

Preparation of Uranium Nitride Microspheres[8]

The preparation of uranium nitride microspheres from gel microspheres of mixed uranium oxide and carbon was investigated. Spheron 9 carbon black was dispersed in urania sol at 0°C with a Bronson Sonifier (ultrasonic generator and sonic converter device) to give a mixed sol 0.55 *M* in urania with a carbon-to-uranium weight ratio of 2.3. The mixed sol was then formed into gel microspheres in a manner similar to that described previously for thoria (cf. Sect. 7.3). The gel spherules were converted to UN microspheres by heating them in a stream of nitrogen at 1600°C or, alternatively, by heating them in a stream of argon at 1600°C and then in nitrogen at 1600. Thermodynamic calculations were performed to guide the laboratory work.[9]

Either of the two firing methods (nitrogen or inert gas followed by nitrogen) yielded a satisfactory product. However, with the method employing only nitrogen, an impervious UN coating prevented complete conversion of the interiors of the microspheres. Temperature cycling from 1600°C to 1000 and back to 1600, in flowing nitrogen, rendered the coating permeable, and the reaction then proceeded rapidly. Spheres 200 μ in diameter, made by either method, resisted crushing loads of about 400 g.

Figure 8.8 is a photograph of microspheres prepared by heating the gel microspheres in nitrogen. Chemical and x-ray analyses showed that all the UO_2 had been converted to nitride, but the product contained 0.13 atom of residual carbon per atom of uranium. The density, measured by toluene displacement, was 13.66.

The major problem with these methods, if the desired product is pure UN, is that the amount of carbon in the UO_2-C gel microspheres must be carefully controlled since one atom of carbon is required per atom of oxygen. Additional carbon is unavoidably added to the microspheres during the forming operation, and further work is needed to control the final carbon-to-uranium ratio. In addition, the relative amount of U(VI) in the final gel should be known or predictable in order to establish the amount of carbon necessary for conversion to pure UN.

The methods described above appear promising for preparing UN microspheres for use in reactor fuels.

Development of Methods for Preparing Zirconia Sols

The increased strength of urania microspheres containing up to 20 vol % zirconia and the enhanced burnup potential obtained by adding such

[8]Summary of ref. 3.

[9]T. A. Gens, *Thermodynamic Calculations of the Yield of Uranium Nitride During Carbothermic Reduction of Uranium Oxide in the Presence of Pure Nitrogen or Nitrogen Mixed with Hydrogen or Inert Gas*, ORNL-TM-1264 (September 1965).

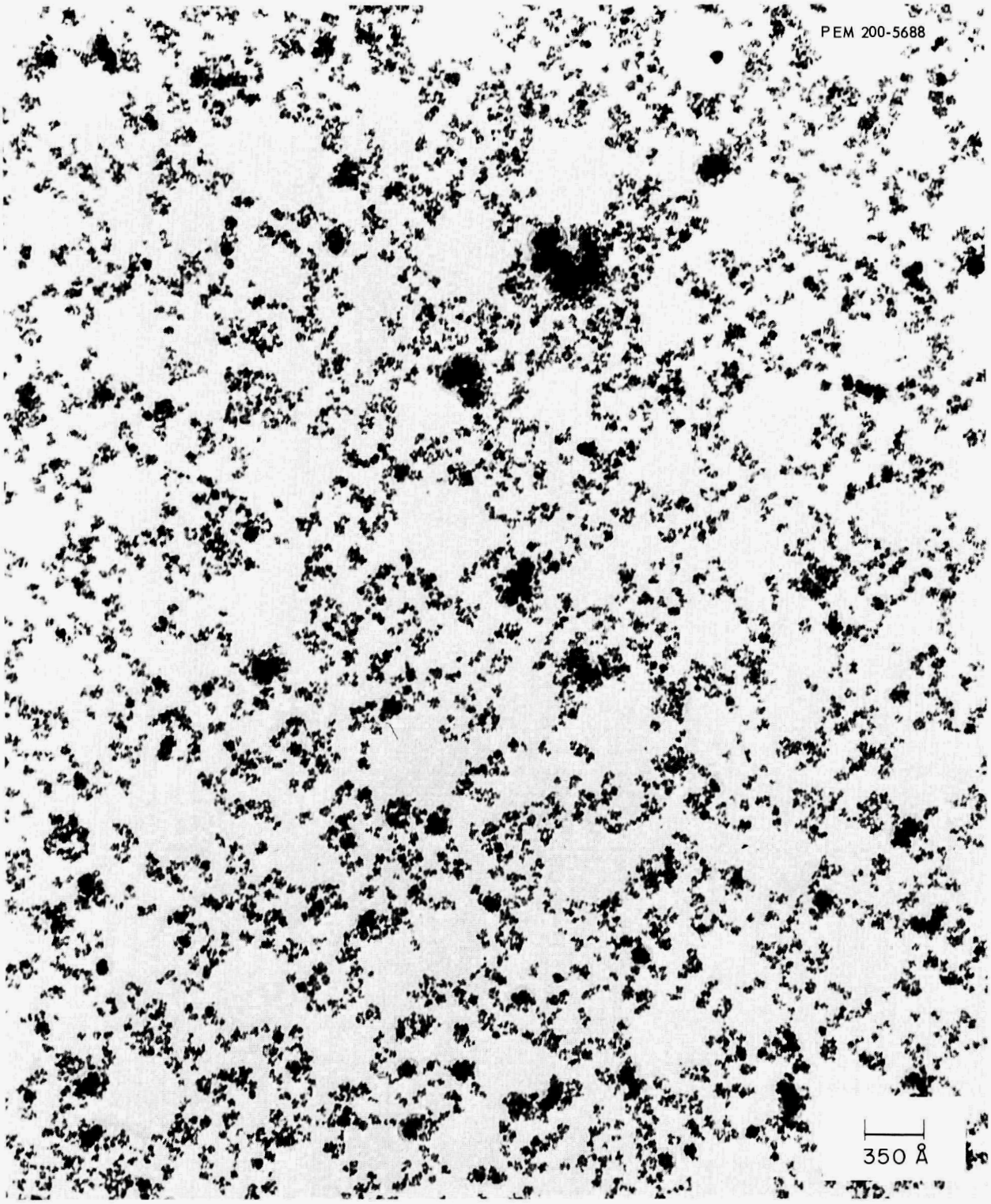

Fig. 8.6. Electron Micrograph of Urania Sol Prepared by Nitrate-Formate Method.

Fig. 8.7. Electron Diffraction Pattern of Urania Sol Prepared by Nitrate-Formate Method.

a diluent provide an incentive to study ways of making urania-zirconia sols. Chemical development of zirconia sol preparation was done with the objective of making such compound sols by simple mixing. Various methods of preparing concentrated zirconia sols containing low nitrate-to-zirconium ratios were investigated by using as starting materials a zirconyl nitrate solution and a nitrate-rich zirconia sol ("preformed zirconia sol") prepared by titrating a zirconyl nitrate solution to pH 1.5 with NH_4OH and boiling to form a sol. In one group of experiments, formaldehyde was added dropwise to a boiling zirconyl nitrate solution in an attempt to destroy the nitrate. The resulting solution or sol was dried, and the residue was resuspended in water. Clear solutions or sols that had nitrate:zirconium ratios as low as 0.7 were prepared this way. In other experiments, hydrous zirconia was precipitated with ammonia and washed with methyl alcohol; then peptization was attempted by adding nitric acid to the dried product. Attempts to prepare sols by this method with zirconyl nitrate solution were unsuccessful; but with the preformed zirconia, several sols were prepared. The best ones were made by adding formic acid to the preformed material before precipitation. In one experiment, a sol 1.8 *M* in zirconium and having nitrate:zirconium and formate: zirconium ratios of 0.39 and 0.30, respectively, was prepared. In a similar experiment, treatment

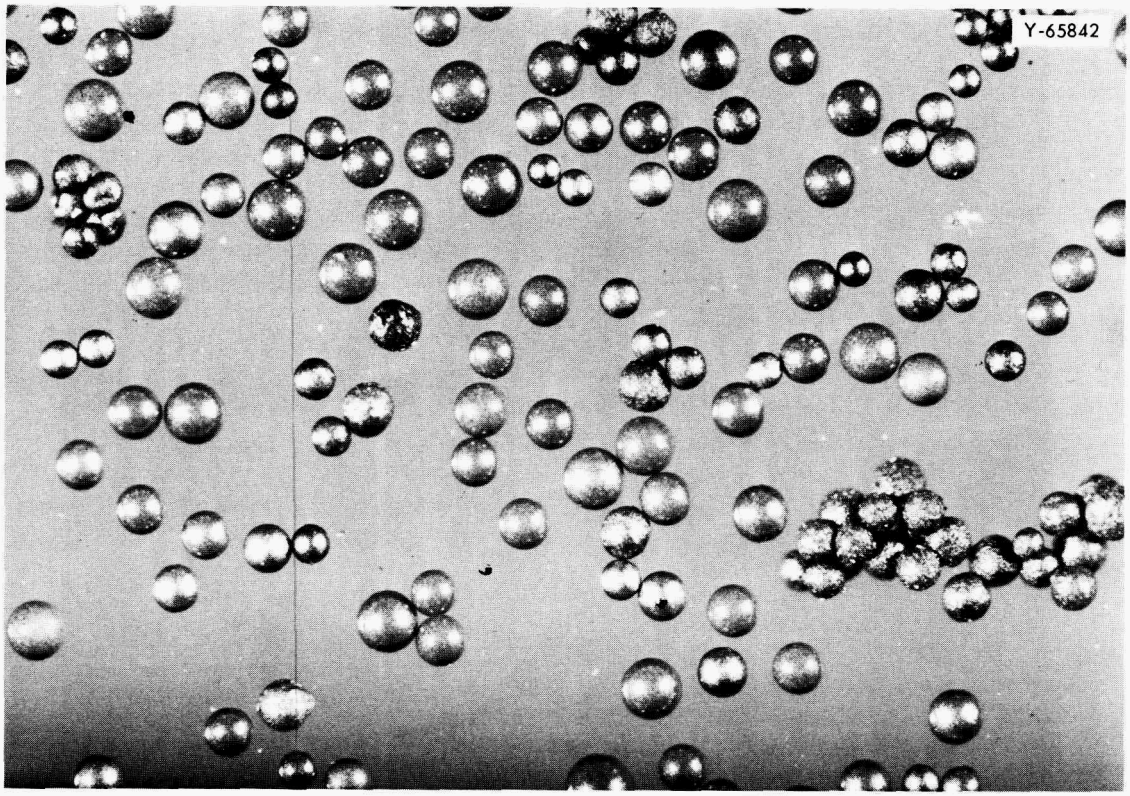

Fig. 8.8. Uranium Mononitride Microspheres Prepared by Firing UO_2-C Gel Microspheres Under Nitrogen.

of the final sol with Dowex 3 resin in the formate form yielded a sol with a nitrate:zirconium ratio of 0.27.

Figure 8.9 shows how the nitrate:zirconium ratio was affected by the dropwise addition of formaldehyde to a boiling 1.65 *M* $ZrO(NO_3)_2$ solution and then refluxing for 24 hr or longer. Even with excess formaldehyde (assuming the reaction: $2HNO_3 + HCHO = HCOOH + 2NO_2 + H_2O$), the ratio was only reduced to 0.7, and nitrate removal appeared to be leveling off. Table 8.6 gives the results obtained in several experiments in which solutions prepared as above were dried and the solids resuspended in water.

The most promising sols were prepared by adding formic acid to the cold, preformed zirconia sol (0.558 *M*), precipitating the hydrous oxide by adding this mixture to an excess of 1 *M* NH_4OH while keeping the mixture at 0°C, and peptizing the washed hydrous oxide with 0.6 *M* HNO_3. Ease of peptization was adversely affected by increasing the precipitation temperature, extending the aging period of the precipitate prior to washing, drying at 50°C rather than at room temperature, and grinding the dried powder. Table 8.7 gives the results obtained in several preparations. The following example is illustrative of the sol preparation method.

Eight and one-tenth grams of 97 to 100% HCOOH was added to 100 ml of cold preformed zirconia sol (Zr, 0.558 *M*; NO_3^-/Zr, 2.12), and the resulting sol was added with stirring to 305 ml of 1 *M* NH_4OH maintained at 0°C. The precipitate was allowed to age 1 hr at 0°C before filtering. It was washed several times by suspending in cold methyl alcohol and filtering on a Büchner funnel. The recovered solids were air-dried overnight at room temperature. Eighteen and eight-tenths milliliters of 0.6 *M* HNO_3 was added to the dried precipitate, and the suspension was heated and stirred for several hours to form a sol. The sol was 1.84 *M* in Zr and had NO_3^-/Zr and $HCOO^-/Zr$ ratios of 0.39 and 0.30 respectively.

Table 8.6. Preparation of Acid-Deficient Solutions or Sols by Reaction of Formaldehyde with Zirconyl Nitrate Solution

Preparation Method:
1. 200 ml of 1.65 *M* $ZrO(NO_3)_2$
2. Temperature, 100°C
3. Dropwise addition of HCHO
4. Reflux time $\geq$ 24 hr
5. Evaporation to dryness
6. Addition of H_2O

37% HCHO Added (g)	Drying Conditions	Composition of Final Sol		
		Zr Concentration (*M*)	NO_3^-/Zr Ratio	$HCOO^-/Zr$ Ratio
18.7	60°C, air	1.62	0.83	0.19
18.7	60°C, air	0.84	0.76	0.11
25.0	50°C, vacuum	1.53	0.72	0.34
19.0		1.13	0.61[a]	0.33

[a]Treated with 22.4 g of Dowex 3 resin in the OH^- form.

Table 8.7. Zirconia Sol Preparation with Preformed Zirconia Sol

Preparation Method:
1. 100 ml of 0.558 *M* zirconia sol; $NO_3^-/Zr = 2.12$
2. Addition of HCOOH (97 to 100%)
3. Addition at 0°C to 305 ml of 1 *M* NH_4OH
4. Cold CH_3OH wash
5. Evaporation to dryness at room temperature
6. Peptization with 0.6 *M* HNO_3

HCOOH Added (g)	Initial $HCOOH/NO_3^-$ Ratio	Sol Properties			
		Zr Concentration (*M*)	NO_3^-/Zr Ratio	NH_4^+/Zr Ratio	$HCOO^-/Zr$ Ratio
0	0	0.52	0.88	0.26	
5.4	1.0	1.41	0.65	0.28	0.45
8.1	1.5	3.5[a]	0.48	0.09	0.45
8.1	1.5	1.84	0.39	0.08	0.30
8.1	1.5	0.35[b]	0.27	0.08	1.28
10.8	2.0	4.3[a]	0.48	0.09	0.32

[a]Sols concentrated by heating in air to give fluid sols.

[b]Treated peptized sol with Dowex 3 resin in formate form to gelation; added HCOOH.

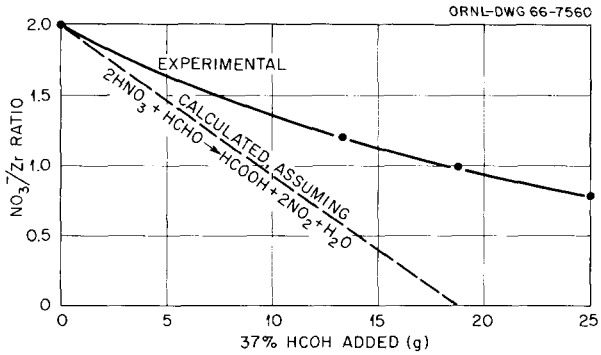

Fig. 8.9. Nitrate:Zirconium Ratio, as Affected by Dropwise Addition of 37% Formaldehyde to 200 ml of 1.65 *M* $ZrO(NO_3)_2$ Solution at 100°C. Reflux time ≧ 24 hr.

8.2 PLUTONIA SOL-GEL PROCESS

Efforts to develop a sol-gel process for the preparation of dense oxide forms of PuO_2 were continued. The objective of this work is to develop a process for preparing plutonia sols which (1) would be compatible with other actinide sols and (2) would afford versatility in forming techniques. These conditions require a nitrate medium and stable colloids of low nitrate concentration. Currently, the process utilizes polymerization of tetravalent plutonium to produce crystallites of colloidal size and to maintain valence stability. The final sols are 1 to 3 *M* in plutonium and have NO_3^-/Pu mole ratios of 0.1 to 0.15. They are stable for many months and are compatible with thoria and urania sols which have been produced at ORNL. The ability to produce dense plutonia, as well as homogeneous plutonia-urania or plutonia-thoria, microspheres at any desired ratio has been demonstrated on a laboratory scale.

Status and Progress

The ability to prepare plutonia sols on a laboratory scale (5 to 20 g) and to produce both pure PuO_2 and PuO_2-ThO_2 microspheres was reported last year.[10] During this report period, efforts were continued to improve and optimize the sol-making process; and studies were initiated to determine the nature of colloidal plutonia particles by spectrophotometric, microfiltration, x-ray line broadening, and electron-microscopic techniques. Pilot plant equipment capable of producing 100-g batches of plutonia sol was designed, fabricated, and successfully used in preparing such sols having uniform characteristics. In addition, the compatibility of plutonia sols with urania sols was demonstrated; and dense PuO_2-UO_2 microspheres containing up to 25 wt % PuO_2 were prepared from mixed sols. In future development work, efforts to define the nature of collodial plutonia particles will continue, and increased emphasis will be given to process modifications which are amenable to scaleup. Pilot plant equipment, which is nearly complete, will be used to prepare 100- to 300-g batches of PuO_2-UO_2 microspheres; and analytical equipment designed for alpha containment will be used to characterize oxide forms which contain PuO_2.

Sol Process

The flowsheet for the plutonia sol process is shown in Fig. 8.10. Hydrous plutonia is precipitated from a plutonium nitrate solution (containing 1 to 3 *M* excess HNO_3) by slow addition of the plutonium solution to a 100% excess of NH_4OH with rapid stirring. The plutonia is recovered by filtration, the filter cake is resuspended in water, and the suspension is filtered. Three washings are usually sufficient to reduce the pH of the filtrate to less than 8.0, indicating satisfactory removal of contaminant ions. The freshly precipitated plutonia is then peptized by digestion with dilute HNO_3. Complete peptization, characterized by a change from an opaque light-green slurry to a nearly transparent dark-green suspension, requires a minimum nitrate concentration of one mole of HNO_3 per mole of plutonium. At this HNO_3/Pu ratio, a digestion time of about 4 hr at 80°C is necessary. Higher nitrate concentrations, however, can be used to reduce the digestion time and temperature; for example, at NO_3^-/Pu mole ratios of 2 or more the digestion time is 10 to 15 min at room temperature.

The plutonia sol produced during digestion is a stable colloidal dispersion but is not suitable for fuel-particle preparation until the nitrate concentration has been reduced. This is accomplished by evaporating the sol to produce a gel, then baking the dried gel at 250°C for about 2 hr. Nitrate removal is a function of both time and temperature,

[10] *Chem. Technol. Div. Ann. Progr. Rept. May 31, 1965*, ORNL-3830, pp. 144–48.

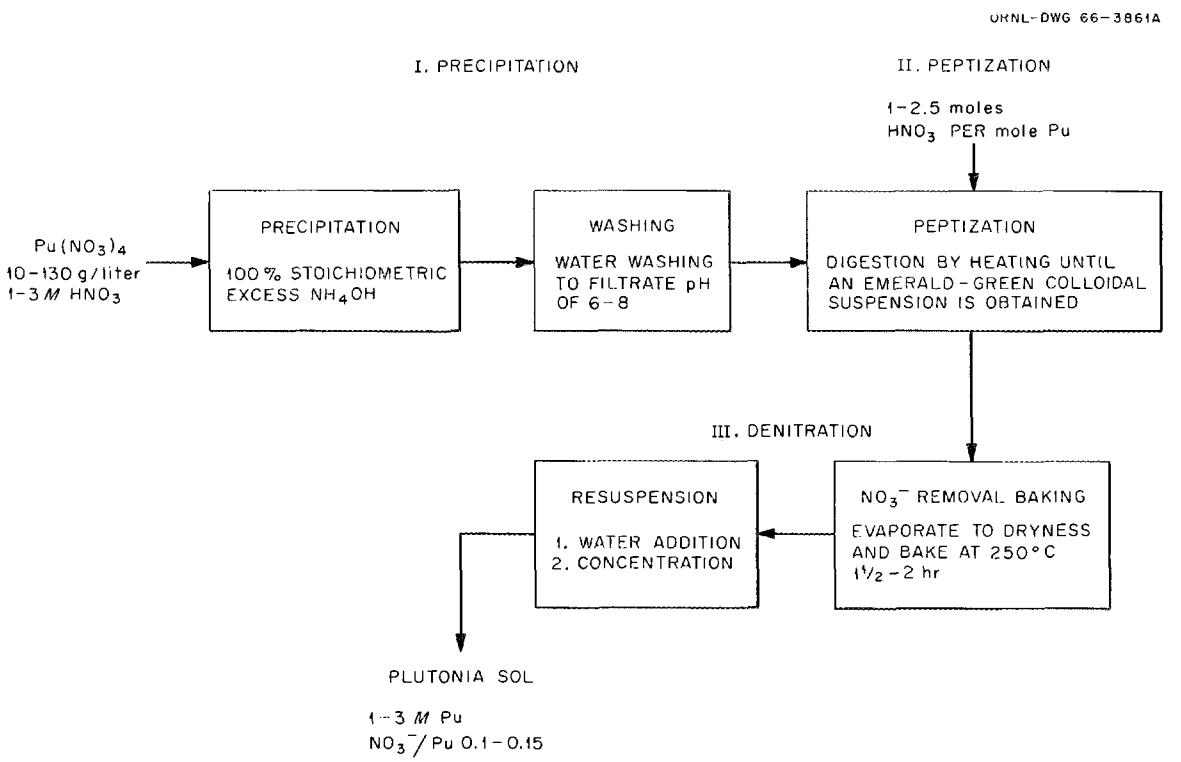

Fig. 8.10. Plutonia Sol-Gel Process.

and excessive baking will result in material which cannot be redispersed. For this reason, very uniform heating of plutonia solids is required during nitrate removal. The final sol is prepared by resuspending the baked gel in water and evaporating to the desired plutonium concentration. Sols with plutonium concentrations in excess of 2 *M* and with NO_3^-/Pu mole ratios between 0.1 and 0.15 are obtained.

Demonstration of the Process

Numerous small-scale batches of plutonia sol were prepared in batch sizes of 5 to 20 g of plutonium, and a small pilot facility capable of producing 100-g quantities of plutonia sol has recently been assembled and successfully used to process 560 g of plutonium in ten batches (50 to 100 g of plutonium per batch) (Table 8.8).

The sol-forming equipment was originally designed as a "single vessel," in which all processing – precipitation, filtration and washing, nitrate addition and sol formation, volume reduction, baking, and redispersion – was to be done. In practice, all steps through volume reduction were accomplished very effectively in this vessel as fabricated, but since stirring was required during baking to provide uniform denitration, the last two steps were performed with a specially designed open hot plate. Supporting equipment in the same glove box included a valence adjustment vessel, condensers, two waste tanks which also serve as a vacuum manifold, and an in-box vacuum pump. The valence adjustment vessel was also used as a holdup tank in which $Pu(NO_3)_4$ feed solution was diluted and metered into the NH_4OH in the sol-forming vessel. Valence adjustment of the $Pu(NO_3)_4$ stock solution was not required.

Dilute $Pu(NO_3)_4$ feed solutions were used at first, but later, higher concentrations were found to be practical and did not affect product quality (this is important since vessel size is extremely limited if critically safe equipment is to be employed). Nitrate feed solutions containing up to 115 g of Pu per liter were used, and NH_4OH concentrations were increased from 2 *M* to 6.3 *M*.

Table 8.8. Plutonia Sol Preparations

Preparation method:
1. Precipitation of $Pu(OH)_4$ with excess NH_4OH
2. Washing $Pu(OH)_4$ with H_2O
3. Peptization of $Pu(OH)_4$ with HNO_3
4. Drying and baking to reduce NO_3^- content
5. Addition of H_2O to form plutonia sol
6. Concentration of sol by evaporation

Preparation	Precipitation[a]						Peptization				Baking		Final Sol Properties	
	$Pu(NO_3)_4$ Solution			NH_4OH Solution										
	Volume (liters)	Pu Concentration (*M*)	NO_3^- Concentration (*M*)	Volume (liters)	Concentration (*M*)	Excess Added (%)	Volume (liters)	Pu Concentration (*M*)	NO_3^-/Pu Ratio	Time at 80°C (hr)	Temperature (°C)	Time[b] (hr)	Pu Concentration (*M*)	NO_3^-/Pu Ratio
PS-1	1.22	0.169	2.34	2.0	2.5	114	2.5	0.083	1.3	<6			1.18	0.33
PS-2	1.22	0.169	2.34	2.0	2.5	114	2.5	0.083	1.3	4.5	200	6.4	1.08	0.28
PS-3	1.22	0.169	2.34	2.0	2.5	114	2.5	0.083	1.3	4.1	205	5.9	1.71	0.22
PS-4	1.22	0.169	2.34	2.0	2.5	114	2.5	0.083	1.3	2.9	250	1.08	1.96	0.17
PS-5	1.22	0.169	2.34	2.0	2.5	114	2.5	0.083	2.5	0[c]	265	0.78	1.63	0.11
PS-6	1.22	0.169	2.34	2.0	2.5	114	2.5	0.083	2.5	0	250	1.80	1.88	0.11
PS-7	0.86	0.240	1.84	1.0	3.75	104	1.75	0.120	2.5	0	250	1.80	2.10	0.11
PS-8	0.65	0.318	1.84	0.63	5.0	72	1.25	0.165	2.5	0	300	0.20	0.98	0.095
PS-9	1.30	0.318	3.68	1.25	5.0	72	2.5	0.165	2.5	0	278	0.47	1.46	0.10
PS-10	0.53	0.476	2.25	0.53	6.3	48	1.15	0.219	1.7	0.5	225	2.62	1.28	0.18

[a] $Pu(NO_3)_4$ solution added to NH_4OH solution.
[b] Approximate time at temperature.
[c] Stirred at room temperature.

At NO_3^-/Pu ratios of 1.3 and 2.5, precipitated plutonia was repeptized at concentrations as high as 50 g of Pu per liter. At 2.5, peptization occurred while heating to 80°C even in dilute solutions; in concentrated solutions only ½ hr at 80°C was required at $NO_3^-/Pu = 1.7$. Extrapolating these data, it seems reasonable to assume that precipitation can be accomplished with feed containing 200 g of Pu per liter and 7 *M* in NH_4OH, and that peptization can be effected at 80 g of Pu per liter. If these conditions can be met, then 400-g Pu batches can be processed in a working volume of 5 liters; this is feasible even in 5-in.-diam critically safe equipment.

Discussion of Process Variables

During early development work it was established by spectral analysis that the sol that formed during digestion of the hydroxide contained plutonium polymer, that the polymeric form stabilized the plutonium valence in the tetravalent state, and that the crystallites formed by polymerization were of colloidal dimensions. While these characteristics were desirable, a high "nitrate demand" ($NO_3^-/Pu \geq 1$) for total conversion of precipitated plutonium to a stable polymeric colloid was indicated; therefore, a subsequent nitrate removal step in the sol process was required. Nitrate removal could be accomplished by baking the dried polymeric colloid at temperatures of 100 to 300°C, but this step constituted a major problem in that precise kinetic data and very uniform heating of the dried polymer were required to obtain a final sol of suitably low nitrate concentration without incurring excessive product losses due to nondispersible solids. Therefore, efforts were made to prepare a colloid having a nitrate-to-plutonium ratio of less than 1, and other nitrate-removal methods were investigated. The kinetics of nitrate ion removal by baking were also studied.

All efforts to prepare an initial plutonium polymeric colloid at a nitrate ratio of less than 1 were unsuccessful. Polymer was prepared from $Pu(NO_3)_4$-HNO_3 solutions by (1) extraction of nitrate with strong-base amines, (2) nitrate removal by electrodialysis, (3) dilution to low acid concentration followed by heating, (4) partial neutralization of excess acid followed by dilution, (5) neutralization of excess acid to low pH followed by heating, and (6) precipitation at various rates and concentrations followed by repeptization with dilute HNO_3. When polymerization was attempted by neutralization, dilution, or removal of excess nitrate, precipitation occurred as the nitrate-to-plutonium ratio approached 1; and when precipitated plutonium was repeptized with dilute HNO_3, a nitrate ratio of 1 or more was required.

The crystallite diameters of several polymer preparations have been determined by x-ray line broadening to be of the order of 20 A, regardless of the preparation method. This indicates that there may be considerable latitude in selecting a method for preparing the first high-nitrate polymeric colloid. Information concerning possible differences in the degree of aggregation of crystallites for various preparation methods is not available.

In attempts to remove nitrate from plutonia sols of high nitrate concentration, electrodialysis, neutralization, and amine extraction were briefly investigated. It appeared to be possible to partially denitrate dilute polymeric colloids by electrodialysis, but during subsequent evaporation the sols formed irreversible gels at low plutonium concentrations (0.3 *M*). Attempts to denitrate by neutralization and amine extraction resulted in precipitation of the polymer, and resuspension of the precipitated polymer again required one mole of nitrate per mole of plutonium.

During denitration by baking dried polymer, crystallite growth and agglomeration of crystallites occurred; these phenomena appear to be intimately associated with the ability to prepare a plutonia sol at low nitrate concentration. X-ray line broadening indicated a crystallite size of about 80 A for plutonia sols which were denitrated to ratios of 0.1 to 0.2. Micropore filtration techniques indicated a range of micelle sizes in the final sol, with some aggregates as large as 1000 A. Aggregates in various size ranges were separated by high-speed centrifugation, and x-ray analysis of such fractions indicated no variation in crystallite size as a function of aggregate size.

During baking, nitrate removal time decreases with increasing temperature and can vary from many days at 125°C to 13 min at 300°C. For this reason, uniform heating is essential, and a method to rapidly determine nitrate ratios during baking is required. An analytical technique was developed which employed titration with sodium hydroxide to determine nitrate concentration and application of an empirical gravimetric factor to a dried sample

to estimate plutonium concentration. Nitrate-to-plutonium ratios obtained in this way were in good agreement with ratios obtained by subsequent chemical analysis.

Kinetic data were collected by determining NO_3^-/Pu ratios as a function of baking time at various temperatures, and linear plots were obtained by assuming a second-order dependence on nitrate ion concentration (Fig. 8.11). The same rates were obtained when starting materials of different NO_3^-/Pu ratios were used. From a process standpoint, a baking temperature that would permit some latitude in baking time and still permit rapid nitrate removal is desired; 250°C appears to fulfill these requirements. As indicated in Fig. 8.11, at 250°C $1\frac{1}{2}$ to 2 hr of baking will provide product in the desired range (e.g., the NO_3^-/Pu ratio at $1\frac{1}{2}$ hr is about 0.14, and at 2 hr about 0.11).

Microsphere Preparation

Plutonium sols can be dried and calcined to dense, hard fragments, and they can be formed into microspheres which calcine to dense oxide spheres at 1150°C. Plutonia sols can also be mixed with thoria or urania sols and formed into microspheres or fragments.

Laboratory-scale preparation of PuO_2-ThO_2 microspheres containing 2, 10, 30, 50, and 80 wt %

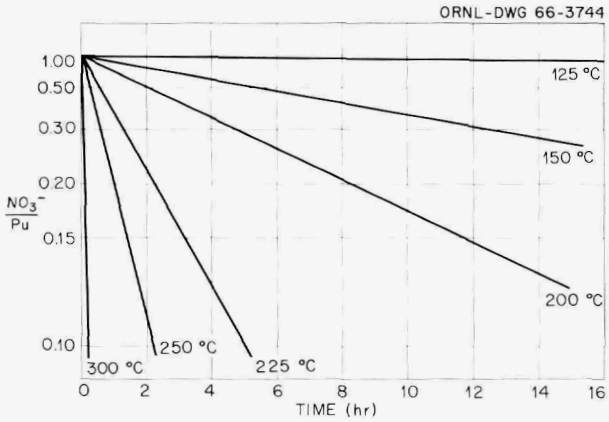

Fig. 8.11. Denitration of Plutonia Sols by Baking at Different Temperatures.

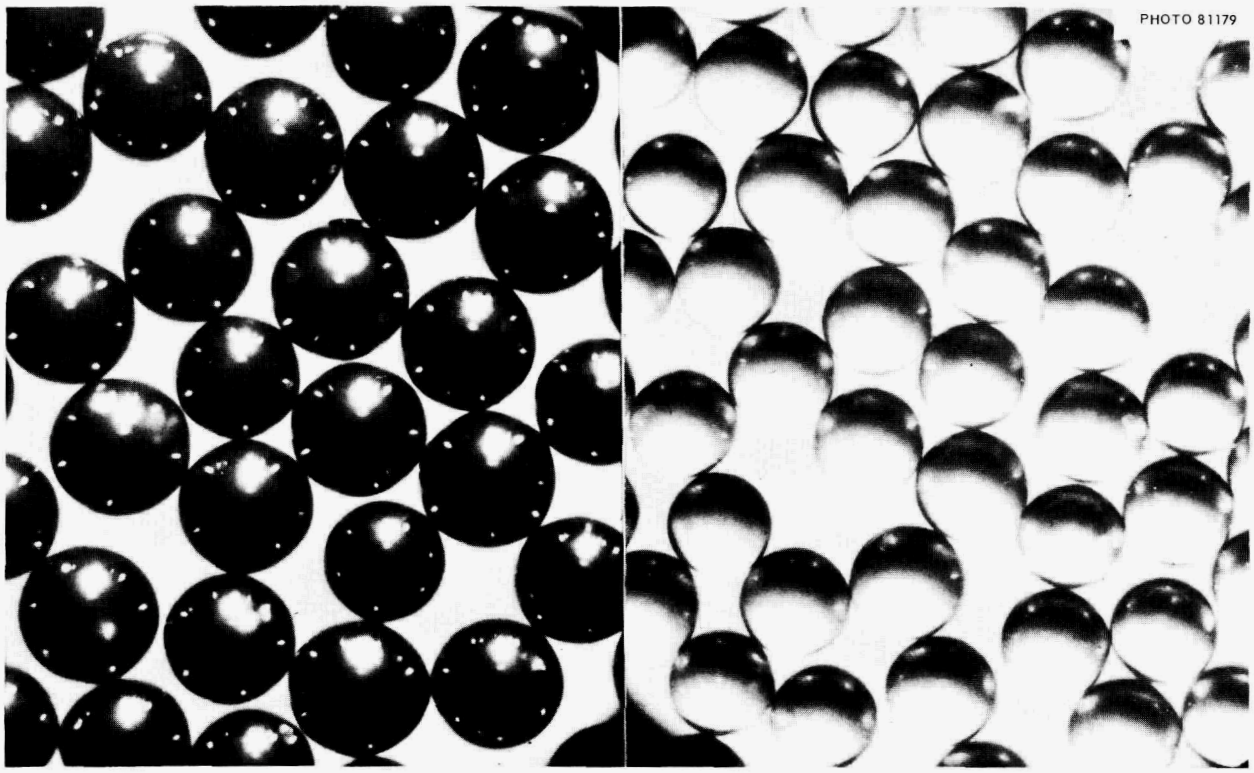

Fig. 8.12. 75% Urania–25% Plutonia Microspheres Before and After Firing at 1150°C in Hydrogen.

PuO_2 was reported last year.[10] During this report period, low-nitrate PuO_2 sols were found to be quite compatible with UO_2 sols, and microspheres of PuO_2-UO_2 containing 15, 20, and 25 wt % PuO_2 were prepared from mixed sols. As in the thoria microsphere preparation (Sect. 7.2), the microspheres of PuO_2-UO_2 were formed in a tapered column. The drying medium used was 2-ethyl-1-hexanol containing 0.5 vol % Amine O and 0.5 vol % Span 80.

The density of the mixed oxide products after firing in hydrogen at 1150°C varied from 94 to 96% of theoretical. (The theoretical density of the mixed oxides was taken as the weighted average of the densities of the components.) Photomicrographs of UO_2-PuO_2 microspheres before and after firing are shown in Fig. 8.12.

Equipment capable of producing 100 to 200 g of mixed oxide microspheres per day has been installed in two 6-ft glove boxes. The first is for sol blending, microsphere forming, and drying; the second is for calcination, separation, and packaging. This equipment will be used to prepare kilogram quantities of mixed UO_2-PuO_2 microspheres in the near future.

9. Separations Chemistry Research

9.1 EXTRACTION OF METAL CHLORIDES BY AMINES

In view of the potential for increased use of amine extractants, a systematic survey was made of the extraction characteristics of many metals from hydrochloric acid and acidified lithium chloride solutions with representative amines. Extraction coefficients for 61 metal ions were reported previously.[1] The data reported here complete the work planned for this survey.

Data are shown in Fig. 9.1 for the extraction of Ir(IV) and Pt(IV) from LiCl–0.2 *M* HCl and HCl solutions over the range 0.5 to 10 *M* total chloride with 0.1 *M* solutions of representative primary, secondary, tertiary, and quaternary amines in diethylbenzene. The extraction power of the amines for both metals varied in the order: Aliquat 336 (quaternary amine) > Alamine 336 (tertiary amine) > Amberlite LA-1 (secondary amine) > Primene JM (primary amine). The extraction coefficients showed relatively little dependence on chloride or acid concentration. Maximum coefficients were about 10 for Ir(IV) and more than 1000 for Pt(IV).

9.2 NEW SEPARATIONS AGENTS

Organic Acids

Previous tests with low-molecular-weight carboxylic and sulfonic acids (water soluble or of marginal immiscibility) indicated that high-molecular-weight acids of suitable structure should be good cation exchange extractants and, in addition, that sulfonic acids will give an unusually wide range of synergistically enhanced extractions. Branched structures are desired because straight-chain carboxylic acids are known to give excessive

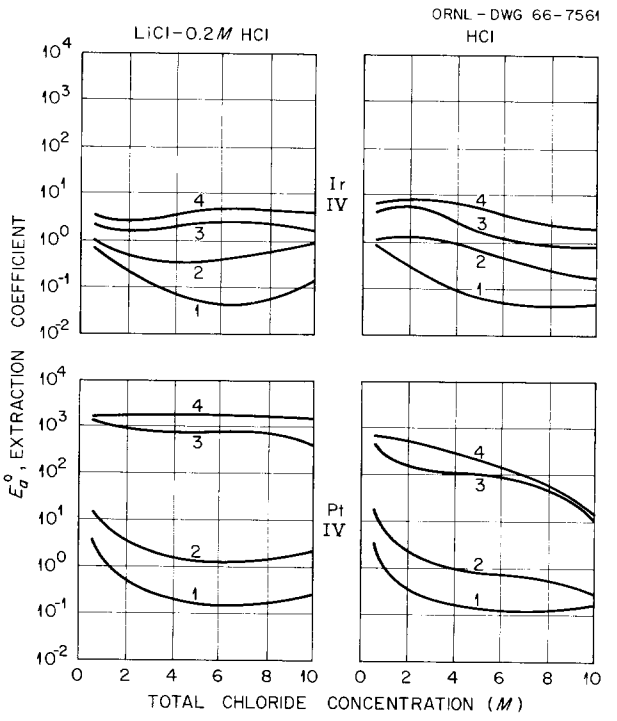

Fig. 9.1. Extraction of Metal Chlorides with Amines. Organic phase: 0.1 *M* solutions of (1) Primene JM ($RR'R''CNH_2$, 18 to 24 carbon atoms), (2) Amberlite LA-1 ($RR'R''CNHC_{12}H_{23}$, 24 to 27 carbon atoms), (3) Alamine 336 (R_3N, R = *n*-octyl, *n*-decyl mixture), and (4) Aliquat 336 [$R_3(CH_3)N^+$, R = *n*-octyl, *n*-decyl mixture] in diethylbenzene. With Aliquat 336, 3 vol % of tridecanol was added to the solvent phase to prevent the formation of a third phase. Amines were in the chloride form. Aqueous phase: 0.01 *M* metallic ion in HCl or LiCl–0.2 *M* HCl solutions (0.5 to 10 *M* in total chloride). Contact time: 10 min at a phase ratio of 1:1.

[1] *Chem. Technol. Div. Ann. Progr. Rept. June 30, 1962*, ORNL-3314, p. 104; *ibid., May 31, 1963*, ORNL-3452, p. 170; *ibid., May 31, 1964*, ORNL-3627, p. 179; *ibid., May 31, 1965*, ORNL-3830, p. 193.

precipitations and emulsions. A carboxylic acid (2,2-dimethyl-*n*-octadecanoic acid) is on order for custom synthesis, and di-*n*-dodecylnaphthalene-sulfonic acid is being prepared in this laboratory. A small sample has already been prepared and purified [neutral equivalent, 536 (theoretical, 545)] for use in preliminary tests.

Distributions of some "marginal" acids to aqueous phases are compared in Table 9.1. Preliminary tests of strontium and barium extractions from 4 to 7 *M* $NaNO_3$ solutions showed higher extraction coefficients and separation factors from sodium than those obtained when di(2-ethylhexyl)-phosphoric acid (HDEHP) was used. The extraction coefficients vs pH were similar to those with HDEHP, with the extraction maxima shifted from pH 4 to 5 to pH 9 to 10, as is to be expected for the weaker acids.

β-Diketones

At least two sterically hindered β-diketones (dibenzoyl- and dipivaloylmethane) have been reported as selective complexers for lithium ion, suggesting that a diketone of suitable size and structure for organic-phase solubility might give selective lithium extraction. Several diketones have been obtained to compare possible steric and other structural effects on lithium complexing. A higher-molecular-weight compound, bis(α, α-dimethyloctadecanoyl)methane, is being prepared in this laboratory for extraction tests.

Dialkyl Sulfoxides

The fact that dimethyl sulfoxide (Me_2SO) forms complexes in aqueous solution with many metal ions suggested that water-immiscible dialkyl sulfoxides (R_2SO) of sufficiently high molecular weight might be good extractants. However, a series of symmetrical dialkyl sulfoxides were found to extract relatively few metal ions from chloride and nitrate solutions, and the identity of these (Au, Hg, Ag, Pt, and Cu) suggests that here the association is through the sulfur, instead of through the oxygen, as was suggested by the wide range of complexes with Me_2SO. Moreover, the extractions fell off with increasing alkyl chain length in the symmetrical dialkyl sulfoxides. These two observations suggest that a wider range of extractable complexes might be obtained with an unsymmetrical alkyl methyl sulfoxide, R(Me)SO; thus 2-ethylhexyl methyl sulfoxide is being prepared.

Primary Amines

A new commercial primary amine, Amberlite XLA-3,[2] was obtained for examination. Analysis showed a content of >98% primary, <1% secondary, and <1% tertiary amine, with a neutral equivalent

[2] *Amberlite XLA-3/Preliminary Technical Notes*, IE-91-65, Rohm and Haas Co., Philadelphia, Pa. (August 1965).

Table 9.1. Distribution of Sodium Carboxylates to Aqueous Phases

Acid	Neutral Equivalent		Aqueous Solubility[b] of Sodium Salt (*M*)
	Found[a]	Theoretical	
"Koch acid" ($RR'R''$-C-CO_2H, "15–19 carbons")	627	240–300	<0.001
2-*n*-Dodecyloctadecanoic acid	469	453	Emulsion
"Versatic acid 15A" (R-C(Me_2)-CO_2H, "average 15 carbons")	271	~240	0.14

[a] By titration in aqueous alcohol.

[b] In 4 *M* $NaNO_3$ solution. All three $<10^{-4}$ *M* as free acid in water.

of 412 [manufacturer's value, neutral equivalent = 353 (ref. 2)]. Only 5.4% was lost by distribution from about 0.1 *M* solution in Amsco 123-15 to 30 vol of 0.2 *M* H_2SO_4, as compared with about 33% loss of Primene JM-T (ref. 3) when tested similarly. "Steady-state" loss to a simulated ore leach liquor at pH 1.8 was 16 ppm from 0.1 *M* solution, and the thorium extraction coefficient was considerably above 100 at 0.03 *M*. In both these respects, Amberlite XLA-3 resembles the extractant obtained by scrubbing out the lower-molecular-weight components from Primene JM-T.

1-(3-Ethylpentyl)-4-ethyloctylamine ("heptadecylamine," "HDA," "Amine 21F81") is a highly branched primary amine with excellent properties as an extractant. It was formerly available in small quantities as a research chemical from Union Carbide Chemical Company but is no longer available from that source. A supply was prepared[4] from 3,9-diethyltridecanol-6 by conversion of the alcohol (6 moles) to ketone and then oxime, and catalytic hydrogenation to amine. The crude product, as separated by fractional vacuum distillation, assayed 16% primary amine plus 4% secondary or tertiary amine. This was upgraded by cation exchange sorption-elution in isopropyl alcohol solution[5] to 75% primary amine, 6% secondary + tertiary amine (calculated at same equivalent weight as HDA), and 19% inert. The overall yield of HDA, based on starting alcohol, was about 10%.

Inorganic Ion Exchangers

Samples of two new ion exchangers advertised for selective cesium sorption,[6] titanium phosphate (Abedem Ti) and tin phosphate (Abedem Sn), were compared with commercial zirconium phosphate (ZP-1) and ammonium molybdophosphate (AMP-1) in sorption of cesium and several other metal ions from 1 *M* HNO_3 solutions (Table 9.2). The

[3]Primene JM-T, Rohm and Haas Co., described as $RC(CH_3)_2NH_2$, 18 to 22 carbon atoms.

[4]H. L. Holsopple and F. G. Seeley, *Synthesis of 3,9-Diethyltridecyl-6-amine*, ORNL-TM-1314 (Nov. 5, 1965).

[5]J. P. Nelson *et al.*, *Anal. Chem.* 33, 1882 (1951).

[6]Société d'Études, de Recherches et d'Applications pour l'Industrie (S.E.R.A.I.), Brussels, Belgium.

Table 9.2. Comparison of Sorption by Some Commercial Inorganic Ion Exchangers

Metal Ion (in 1 *M* HNO_3)	Distribution Coefficient[a] to:			
	Abedem Ti[b]	Abedem Sn[b]	ZP-1[c]	AMP-1[c]
Cs	1020	200	460	6700
K	3	2	4	4
Li	≦0.1	≦0.1	0.3	0.3
Fe(III)	280	107	29	1
Ba	22	≦0.1	0.2	0.2
Eu	6	10	0.3	0.9
Ce(III)	2	4	≦0.1	1
Am	4	8	0.2	3
Ca, Cr(III), Al	0.4–0.6	≦0.1–0.3	≦0.1	0.4–0.6
Cu(II), Co(II), Sr	0.1–0.3	≦0.1–0.2	≦0.1	≦0.1–0.4
Na, Ni(II), Zn, Cd	≦0.1	≦0.1	0.1	≦0.1–0.2

[a]Distribution coefficient = (moles per gram of solid)/(moles per milliliter of solution).

[b]Titanium and tin phosphates (S.E.R.A.I., Brussels, Belgium).

[c]Zirconium phosphate and ammonium molybdophosphate (Bio-Rad Laboratories, Richmond, Calif.).

selectivity of the Abedem exchangers for cesium was lower than that of ammonium molybdophosphate, especially with respect to iron. They also showed greater loss by solubility in nitric acid solution: Abedem Ti, 8%; Abedem Sn, 2%; ZP-1, 0.8%; and AMP-1, 0.2% in 20-hr contacts of 1 g of each with 10 ml of 1 *M* HNO_3.

In brief tests of the Abedem exchangers for chromatographic biochemical separations, almost no transfer ribonucleic acid was sorbed from phosphate medium, while it was sorbed too strongly from chloride medium for elution by 5 *M* NaCl.

9.3 PERFORMANCE OF DEGRADED REAGENTS AND DILUENTS

In radiochemical processing by solvent extraction, degradation of the solvent phase can cause unsatisfactory operation. The amount of degradation varies with the materials used and with the extent of their exposure to radiation and reactive chemicals during the processing of the aqueous feed.

Progress and Status

Studies of several aspects of diluent and reagent degradation have been made at ORNL, and summaries of prior work have been published.[7-9] This year, the identification of the principal products resulting from degradation of diethylbenzene (DEB) with nitric acid was completed, and the effects of their presence on the extraction process were studied. A brief study of the stability of di-*sec*-butyl phenylphosphonate (DSBPP) against degradation by nitric acid was finished, and studies were begun which aimed toward isolation and identification of the products formed when *sec*-butyl-α-methylbenzylphenol (BAMBP) is treated with nitric acid. The ORNL studies of the stabilities of several reagents and aromatic diluents were summarized and presented at the International Conference on the Chemistry of the Solvent Extraction of Metals, held at Harwell on September 27–29, 1965.[10]

Stability of Diethylbenzenes

(1-Hydroxyethyl)ethylbenzene, an alcohol, was identified in diethylbenzene degraded by nitric acid. This compound and the two identified previously[8,9] [ethylacetophenone and (1-nitroethyl)-ethylbenzene] are the major products of the degradation. Infrared spectra showed very little nitration of the benzene ring. The alcohol predominated in the early stages of degradation by boiling 2 *M* HNO_3, but its concentration reached a maximum and then decreased; subsequently, the formation of the ketone and nitro compound was favored. A suspected conversion of the nitro product to the ketone was proved when a sample of the former, purified by column chromatography, was heated in a sealed tube. A gas chromatograph of the mixture after 3 hr of heating at 110°C showed 50% conversion. The decrease in the alcohol concentration suggests that it also converts to either the ketone or the nitro compound, but this was not proved.

A commercial DEB, 1 *M* in TBP, was mixed with an aqueous 2 *M* HNO_3 solution containing dissolved metals, and the stirred two-phase system was irradiated to an exposure of 70 whr/liter. The objective was to simulate in laboratory tests a condition more nearly approximating the conditions prevailing in large processing equipment. Periodic analyses of the organic phase and that from a control test without metals present showed that the rate of DEB degradation was slightly lower in the presence of metals.

Degradation products from pure DEB's were shown last year[9] to be poor extractants for fission products. It has now been shown[10] that the presence of DEB products in severely degraded (4 hr of boiling with 2 *M* HNO_3 under reflux) 1 *M* TBP–DEB depresses the uranium extraction slightly. The products also have an adverse effect on disengagement of the organic and aqueous phases. For example, the degraded solution used above takes about twice as long as the undegraded

[7] C. A. Blake, W. Davis, Jr., and J. M. Schmitt, *Nucl. Sci. Eng.* **17**, 626–37 (1963).

[8] *Chem. Technol. Div. Ann. Progr. Rept. May 31, 1964*, ORNL-3627, p. 180.

[9] *Chem. Technol. Div. Ann. Progr. Rept. May 31, 1965*, ORNL-3830, p. 197.

[10] *Proceedings of the International Conference on the Chemistry of the Solvent Extraction of Metals, Sept. 27–29, 1965, Harwell, England*, to be published by Macmillan.

solution to separate at room temperature from 2 *M* HNO_3 (90 sec vs 45) and from 0.2 *M* Na_2CO_3 (60 sec vs 30). It is difficult to remove completely the DEB products from the organic phase. Scrubbing with water and aqueous alkaline solutions is only partly effective. Scrubbing with ethanolamine effectively removes the nitro compound, but this method of cleanup results in high reagent loss and is expensive. Further testing is required to determine the extent of product buildup in a continuous process.

Stability of Di-sec-butyl Phenylphosphonate

Undiluted DSBPP (di-sec-butyl phenylphosphonate), a solvent extraction reagent with excellent ability to separate uranium from thorium,[11] was irradiated with a ^{60}Co gamma-ray source last year to 100 whr/liter while being stirred with 2 *M* HNO_3. Although some of the reagent was nitrated, the fission product extraction power of the irradiated material was less than that of irradiated TBP in a comparable test. In further studies, solutions of TBP or DSBPP (each 1 *M*) in DEB were irradiated to 70 whr/liter while being stirred with 2 *M* HNO_3. Nitrogen uptake in the organic phases was 0.1 *M* and 0.07 *M*, respectively (Table 9.3), and gas chromatography indicated that the nitrogen was present almost completely in DEB-nitro compounds, described previously. Extraction of ^{181}Hf from 2 *M* HNO_3 (calcium test)[7] was slightly lower with DSBPP than with TBP ($D = 1.4$ vs $D = 1.7$). Organic-phase hafnium concentrations after extraction from 0.1 *M* Hf solution (traced with ^{181}Hf) were low.

Phenyl-substituted organophosphorus reagents have been reported[12] to be susceptible to formation of phenol groups on the benzene ring ortho to the attached phosphorus atom, and it has been reported[12] that the products extract fission products strongly. It is difficult to determine relative hafnium extractions by reagent and diluent degradation products, but the low extractions from the strong 0.1 *M* hafnium solution indicated low concentrations of any materials that extract hafnium (and presumably fission products) strongly.

Stability of sec-Butyl-(α-methylbenzyl)phenol

The substituted phenol sec-butyl-(α-methylbenzyl)phenol (BAMBP) has utility in recovering and separating cesium and rubidium from the other alkali metals by solvent extraction.[13] BAMBP, however, when in contact with aqueous acidified nitrite solutions, degrades with loss of extraction power. Gas chromatograms of the degraded BAMBP show several peaks not originally present, one of which is significant. Some concentration of the product has been achieved by column chromatography on neutral alumina. The concentrate contains nitrogen (infrared and elemental analysis),

[11] C. A. Blake *et al.*, *Comparison of Dialkyl Phenylphosphonates with TBP in Nitrate Systems*, ORNL-3374 (Jan. 8, 1963).

[12] E. S. Lane and A. Pilbeam, *The Radiation Decomposition of Some Phenyl Substituted Organo-Phosphorus(V) Extractant Systems*, AERE-M-1284 (January 1964).

[13] W. D. Arnold, D. J. Crouse, and K. B. Brown, *Ind. Eng. Chem., Process Design Develop.* 4, 249–54 (1965).

Table 9.3. Comparison of Hafnium Extractions by Degraded DSBPP and TBP

Degraded Solution[a]	Nitrogen Uptake (*M*)	Hafnium Extraction from 2 *M* HNO_3 with: ^{181}Hf Tracer, Distribution Coefficient (Calcium Test)[b]	0.1 *M* Hf, Moles Complexed per Liter of Organic Phase After: Na_2CO_3 Scrub	Calcium Test[b]
1 *M* DSBPP/DEB	0.07	1.4	0.0002	0.0006
1 *M* TBP/DEB	0.10	1.7	0.0002	0.0023

[a] Irradiated while stirring with 2 *M* HNO_3 in ^{60}Co source, 70 whr/liter exposure.
[b] See ref. 7.

and nuclear magnetic resonance spectra are consistent with nitration on the side chains, principally at the tertiary carbon atom of the sec-butyl group. Work will continue until this compound is positively identified.

9.4 COMPARATIVE CHEMISTRY OF LANTHANIDES AND TRIVALENT ACTINIDES

Studies of the comparative extraction chemistry of lanthanides and trivalent actinides have continued in support of and search for potentially useful processes for separating these elements.

In the development of the Talspeak process for removing lanthanides from trivalent actinides by extraction with di(2-ethylhexyl)phosphoric acid (HDEHP) from lactic acid containing sodium diethylenetriaminepentaacetate (Na_5DTPA) (see Sect. 6.5), it was observed that extraction of americium at fixed pH values from 2.6 to 3.0 was almost exactly inversely proportional to the DTPA concentration from 0.001 to 0.1 *M* DTPA (Fig. 9.2). Dependences of extraction of neodymium, samarium, and europium on DTPA concentration were only slightly different from that of americium. The large difference between americium and the whole lanthanide group persists even at very low DTPA concentrations, but not in its absence. At a constant DTPA concentration of 0.05 *M*, the difference in extractability of americium and several lanthanides decreases only slowly as the pH is decreased from 3.5 to 1.8 (Fig. 9.3).

Addition of neutral nitrates up to a concentration of 6 *N* nitrate in Talspeak aqueous solutions increased distribution coefficients of americium and lanthanides up to a factor of 2 without changing group separation factors.

Substitution of chlorinated hydrocarbons for aromatic hydrocarbons as diluents for HDEHP in Talspeak extractions did not change the group separation factors, but dilution by aliphatic hydrocarbons decreased separation by nearly a factor of 2.

Brief studies of extraction by hydrocarbons of compounds of americium, cerium, and europium with fluorinated derivatives of acetylacetone from alkaline solutions indicated that extractabilities were in the order: hexafluoroacetylacetonate > trifluoroacetylacetonate > acetylacetonate. Extractions by tributyl phosphate in diisopropylbenzene (DIPB) of the hexafluoroacetylacetonate were very high. No useful differences in extraction of the elements were observed. The fluorinated reagents are volatile and expensive and are too soluble in the aqueous phase.

In studies of the applicability of extraction chromatography to lanthanide-actinide separation, tests were made of the elution behavior of columns made by supporting HDEHP on various finely divided materials including polyethylene, Teflon, Kel-F, Saran, polyamide (Woelm), silicone-treated glass beads, silica gel, and diatomaceous earth. In all cases except with the polyamide powder, a small portion of the extracted cations failed to elute with the major part, thus decreasing separation. The polyamide powder also has unusually

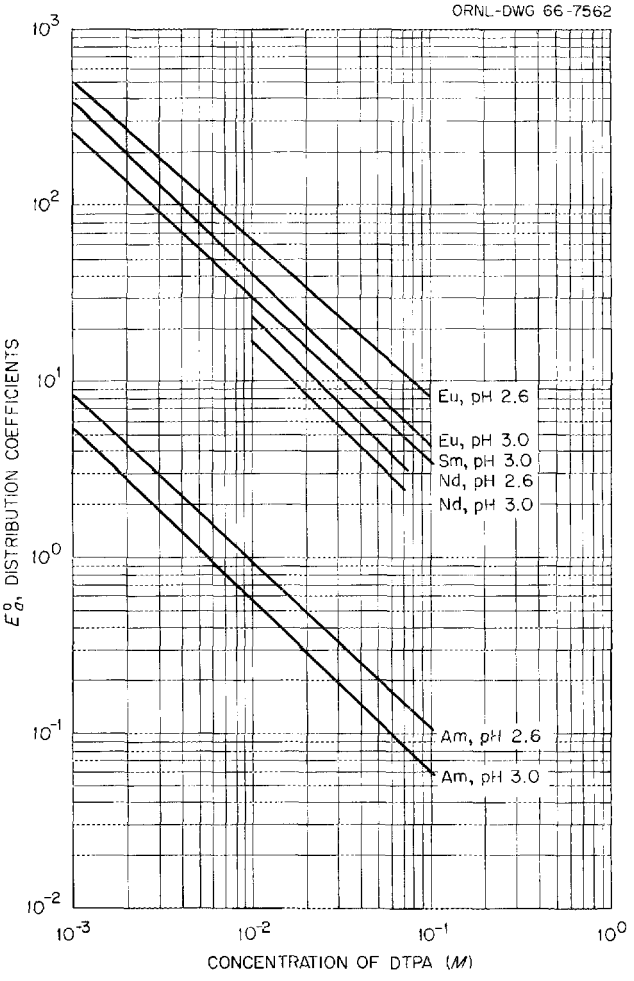

Fig. 9.2. Extractabilities Vary Inversely as Concentration of DTPA. Organic phase: 0.5 *M* HDEHP in DIPB. Aqueous phase: 1 *M* lactic acid plus DTPA.

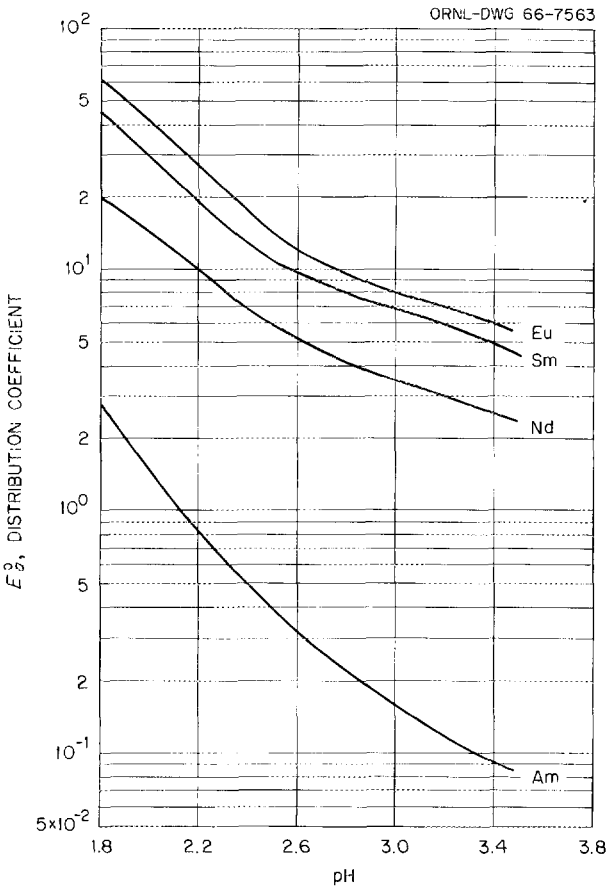

Fig. 9.3. Group Separation Is Effective over Wide pH Range. Organic phase: 0.5 *M* HDEHP in DIPB. Aqueous phase: 1 *M* lactic acid, 0.05 *M* DTPA.

high capacity for extractants. Complete separations of americium and lanthanides at tracer level were accomplished by application of the Talspeak system to polyamide columns. Separation of lanthanides at tracer level by elution with dilute mineral acids indicated stage heights of about 1 mm. Use of the polyamide is limited to systems in which the aqueous acidity is less than 3 *N* because of its solubility in more concentrated acid.

9.5 RECOVERY OF BERYLLIUM FROM ORES

In recent years, interest in beryllium has grown because of its extraordinary physical and chemical properties. The increasing demand for beryllium (for high-temperature alloys, atomic reactor use, etc.) and the apparent scarcity of high-grade ores have increased the need for processes capable of recovering the metal from the low-grade domestic ores. A tentative solvent extraction process was previously outlined for recovering beryllium from low-grade-ore sulfate liquors by extraction with a primary amine, scrubbing with dilute sulfuric acid, and stripping with either dilute sulfuric acid or dilute fluoride solutions.[14,15] One primary amine in particular, 1-(3-ethylpentyl)-4-ethyloctylamine (HDA), is superior to other primary amines tested. Further testing of this process continued to be encouraging. Both stripping flowsheets were optimized, resulting in considerable reduction in chemical reagent consumptions for the sulfuric acid stripping method, compared with those estimated previously.

Extraction of Beryllium

The effect of individual contaminants on the extraction of beryllium was studied by adding them to "pure" beryllium sulfate solutions. No significant change in the beryllium extraction coefficients occurred on addition of 10 g of Mg^{2+}, 1 g of Ca^{2+}, or 3.7 g of Si (as SiO_3^{2-}) per liter.

Stripping Beryllium with Fluoride Solutions

In a batch countercurrent test, more than 95% of the beryllium was stripped from 0.3 *M* HDA in Solvesso 100 (loaded with 0.3 g of beryllium per liter) in six stages with about 2 moles of NH_4F per mole of beryllium. In the process flowsheet, beryllium is then precipitated with ammonia, and part of the filtrate (which contains fluoride) is recycled to the stripping system to reduce requirements for makeup fluoride. In the six-stage countercurrent stripping system, all the fluoride was fed to the first stripping stage as NH_4F-$(NH_4)_2SO_4$ solution, and 0.01 *M* H_2SO_4 was fed to the sixth stage. Subsequent recovery of the beryllium by hydrolytic precipitation with ammonia was complicated by the fluoride content of the loaded strip solution (about 0.2 *M* F^-). At this

[14] *Chem. Technol. Div. Ann. Progr. Rept. May 31, 1964*, ORNL-3627, p. 211.

[15] *Chem. Technol. Div. Ann. Progr. Rept. May 31, 1965*, ORNL-3830, p. 225.

concentration, the presence of fluoride ion requires an unacceptably large amount of ammonia for the complete precipitation of $Be(OH)_2$. Stripping with $NaF\text{-}Na_2SO_4$ solution is now preferred since beryllium stripping is as effective as in the ammonium system, and beryllium can be precipitated completely (pH 10) with economic amounts of sodium hydroxide.

Stripping Beryllium with Sulfuric Acid

Acid requirements for stripping beryllium were decreased from about 18 lb per pound of BeO to about 9 lb by increasing the number of stages from four to six and changing the point of addition of the bulk of the acid. In the present flowsheet, 6 *M* H_2SO_4 is fed to the third stripping stage and 0.01 *M* H_2SO_4 to the sixth. The last three stages serve primarily to back-scrub acid from the amine (convert it from the bisulfate to the sulfate), thereby minimizing acid usage and converting the amine to a form that can be more readily recycled to the low-acid extraction system. The decrease in the amount of acid used for stripping also considerably decreased ammonia requirements for precipitating beryllium from the strip solution.

Product Upgrading

The products obtained by hydrolytic precipitation of beryllium from the strip solution usually contain a few percent of aluminum and other contaminants such as iron, magnesium, and calcium. To obtain a purer BeO concentrate, the original beryllium precipitate is dissolved in caustic, and the solution is filtered to separate most contaminants except aluminum. Diluting and heating the solution precipitates $Be(OH)_2$, well separated from aluminum. A product obtained by extraction of beryllium from a synthetic leach liquor with HDA, stripping with $NaF\text{-}Na_2SO_4$, precipitating with caustic, and upgrading the precipitate as described above showed the following impurities by spectrographic analysis (in percent): 0.05 Al, 0.01 Fe, 0.02 Mg, 0.03 Ca, 0.03 Cu, 0.005 K, 0.05 Si, 2.7 Na, and <0.02 V.

9.6 EXTRACTION OF ALKALIES BY DI(2-ETHYLHEXYL)PHOSPHORIC ACID (HDEHP)

The extraction of sodium by HDEHP (HA) in benzene was previously studied in connection with the study of strontium extraction as tracer ^{85}Sr from sodium nitrate solutions.[16] This study has been extended to the other alkalies (except francium). Tracers ^{42}K, ^{86}Rb, and ^{134}Cs were extracted from 3 *M* $NaNO_3$ solution, and potassium and lithium distributions were determined in two-phase titrations of HA with KOH and LiOH in the respective 3 *M* nitrate solutions. The results for potassium in tracer and macro concentrations agreed well.

At each of a series of reagent compositions $MA/\Sigma A$ (i.e., fraction of total DEHP in the salt form, NaDEHP, etc.), the apparent reagent dependence, as shown below, was obtained from the slope of the linear plot, log $E_M[H^+]$ vs log $[\Sigma A]$ (where E_M is the distribution coefficient, $[M]_o/[M]_a$):

Alkali	Apparent Reagent Dependence for $MA/\Sigma A$ Equal to:				
	0	0.1	0.2	0.5	0.8
Lithium	2	1.6	1.5	0.9	0.7
Sodium	2	1.6	1.5	0.8	0.6
Potassium	2	1.8	1.4	1.0	0.7
Rubidium	2	1.8	1.5	1.0	0.6
Cesium	2.6	2.4	2.0	1.6	1.0

The results show that for lithium, potassium, and rubidium, as for sodium, the extraction reaction at low pH, where most of the extractant remains in the acid form, is:

$$M^+ + \underset{\cdots\cdots}{2(HA)_2} \rightleftharpoons \underset{\cdots\cdots}{MA{\cdot}3HA} + H^+ .$$

(Dotted underlines represent the organic phase.) It shifts at higher pH toward formation of the (aggregated) simple salt, consistent with a net reaction:

$$M^+ + \underset{\cdots\cdots}{\frac{1}{2}(HA)_2} \rightleftharpoons \underset{\cdots\cdots}{(MA)_n} + H^+ .$$

The results for cesium indicate that it coordinates more than four A, not unexpected on the basis of the size of the cesium ion and its higher coordination number in some other complexes.

[16] W. J. McDowell and C. F. Coleman, *J. Inorg. Nucl. Chem.* 27, 117–39 (1965).

The relative extractabilities of the alkalies from these data are, at, for example, 0.1 *M* HA and MA/ΣA = 0.1:

Alkali	$\frac{E_M[H^+]}{E_{Na}[H^+]}$
Lithium	15
Sodium	1
Potassium	0.6
Rubidium	0.3
Cesium	0.35

These results agree well with those previously reported from the simultaneous extractions from a mixed solution 1 *M* in each alkali nitrate.[17]

9.7 EXTRACTION OF CESIUM BY 4-*sec*-BUTYL-2-α-METHYLBENZYLPHENOL (BAMBP) PLUS ORGANIC ACIDS

Study was completed of the synergistic extraction[18] of cesium by a substituted phenol (BAMBP) in combination with organic acids. At low pH and low concentration of the added organic acid, the cesium extraction coefficient varies linearly with both, as shown in Fig. 9.4 for di(2-ethylhexyl)phosphoric acid (HDEHP). This is consistent with formation of the species previously deduced,[18] $CsHX_2 \cdot 2BAMBP$ and $CsHX_2 \cdot 2(BAMBP)_2$, by cation exchange of Cs^+ with one H^+ from the acid dimer $(HX)_2$. As the concentration of HDEHP increases at a given pH (Fig. 9.4), the cesium extraction coefficient goes through a maximum and then decreases, at a rate becoming nearly proportional to the square of the HDEHP concentration. Since the synergistic cesium extraction coefficient varies with the square of the BAMBP concentration[18] while the BAMBP exists as a mixture of monomers and dimers,[19] this suggests that BAMBP and HDEHP interact to form a 1:2 complex, $BAMBP \cdot (HDEHP)_2$, in addition to the 1:1 complex, $(BAMBP)_2 \cdot (HDEHP)_2$ or BAMBP·HDEHP, previously identified by dielectric measurements and by infrared and nuclear magnetic resonance spectra.[20]

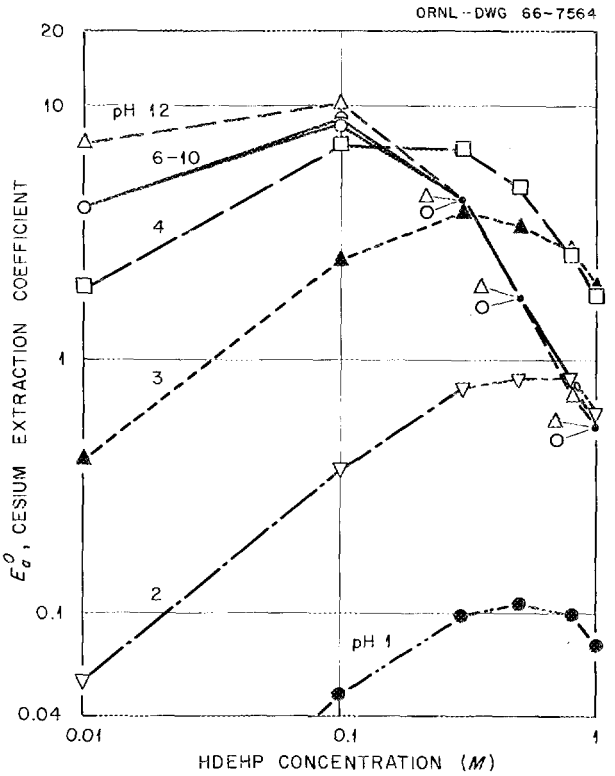

Fig. 9.4. Synergistic Cesium Extraction by BAMBP plus Di(2-ethylhexyl)phosphoric Acid. 1.0 *M* BAMBP and varying concentrations of HDEHP in Amsco 125-82; 10^{-3} $CsNO_3$ in 3 *M* $NaNO_3$ initial; equilibrium pH indicated. Extraction coefficient at zero HDEHP: <0.01 at pH 1-8, 0.09 at pH 10.3, 6.4 at pH 12.2.

Nuclear magnetic resonance spectra also suggest that BAMBP is hydrogen-bonded to the anion of the organic acid when both are present in the complex with cesium. It seems possible that the anion might form hydrogen bonds with two BAMBP molecules simultaneously, contributing further to the stability of the synergistic complex. Since the two oxygens are equivalent in the anion, their electron density is greater than in the un-ionized acid, so that they should form stronger bonds and in turn enhance the bonding between the phenolic oxygens and cesium.

In ref 19, an infrared absorption peak at 3542 cm^{-1} was ascribed to the OH in the hydrogen bond

[17] *Chem. Technol. Div. Ann. Progr. Rept. June 30, 1962*, ORNL-3314, p. 112.

[18] *Chem. Technol. Div. Ann. Progr. Rept. May 31, 1965*, ORNL-3830, pp. 214–17.

[19] B. Z. Egan, R. A. Zingaro, and B. M. Benjamin, *Inorg. Chem.* 4, 1055 (1965).

[20] *Chem. Technol. Div. Ann. Progr. Rept. May 31, 1965*, ORNL-3830, p. 212.

of the BAMBP dimer. Subsequently, Keder *et al.*[21] showed that this peak does not disappear with dilution, hence belongs to an intra- rather than intermolecular bond; they assign it to phenol OH bonded with the benzyl π electrons. None of the information derived in ref 19 from infrared absorption (e.g., the degree of dimerization as a function of BAMBP concentration) is affected by this correction.

9.8 KINETICS OF METAL-ION EXTRACTIONS BY DI(2-ETHYLHEXYL)PHOSPHORIC ACID (HDEHP)

Kinetic measurements continued in the extraction by HDEHP of iron(III), an important representative of several very slow extraction equilibria with this reagent. As previously reported,[22] the extraction rate is first order with respect to aqueous iron concentration under all conditions tested. In extraction from perchloric acid–sodium perchlorate solutions at constant ionic strength (e.g., 2), the pH and HDEHP concentration dependences change rather abruptly in the region $0.2\ M < [\text{HDEHP}] < 0.5\ M$. The results to date can be fairly closely summarized by the proportionalities

$$\text{rate constant} \propto [Fe^{3+}]\,[\text{HDEHP}]^{0.3}/[H^+]\ , \qquad [\text{HDEHP}] < 0.2\ M\ ,$$

$$\text{rate constant} \propto [Fe^{3+}]\,[\text{HDEHP}]^{1.5}/[H^+]^2\ , \qquad [\text{HDEHP}] > 0.5\ M\ .$$

We were surprised to find that the rate decreases with increasing acidity, because we had expected the slowness to prove due to either (1) slow dissociation of hydrolytic iron species, predicting rate *increasing* with acidity, or (2) slow dissociation of hydrates, predicting little dependence on acidity. Accordingly, the effect of acidity was determined in the extractions of several other metals (Fig. 9.5). The ions tested divided into two groups – iron, beryllium, and strontium, rates inversely proportional to acidity; and uranyl,

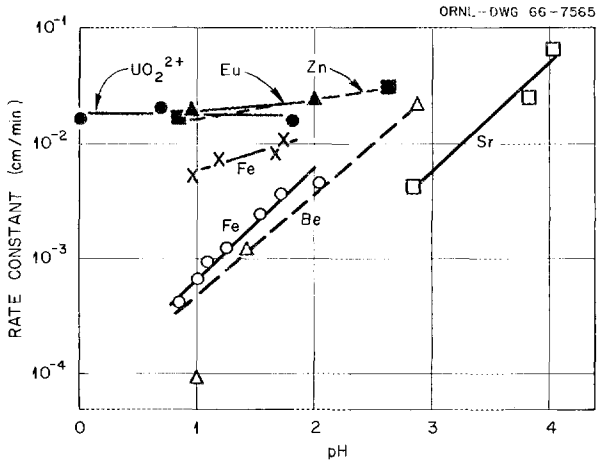

Fig. 9.5. Kinetics of Metal-Ion Extractions by HDEHP, 25°C. Organic phase, 0.1 *M* HDEHP in *n*-octane. Aqueous phases, ionic strength = 2, $HClO_4$ + $NaClO_4$ except *x*: $HClO_4 + Sr(ClO_4)_2$.

europium, and zinc (all relatively fast extractions), rates nearly independent of acidity.

A proposed explanation for the effect of acidity is that uranyl ion, etc., may react readily with either the anion or acid form of the extractant, but that iron, etc., may react readily (at the interface) only with the surface-active anion, which (in form of the salt Na^+DEHP^-) decreases linearly as the acidity increases. One attempted test of this hypothesis, by extraction with an appreciably water-soluble dialkylphosphoric acid, has so far failed because the acids tried (di-*n*-butyl- and di-sec-butylphosphoric acid) precipitate the iron. Another test, however, does appear to support the hypothesis. This consists in replacing sodium with strontium as the gross cation in the aqueous phase. More strontium than sodium is extracted by HDEHP at, for example, pH 1; that is, more of the extractant is ionized. Hence, the iron extraction should be faster,[23] as is indeed found (*X* points in Fig. 9.5). This test will be extended to still lower pH's; we expect that eventually the iron extraction rate will begin to drop steeply in inverse

[21] W. E. Keder, E. C. Martin, and L. A. Bray, *Separation of Alkali Metals by Solvent Extraction with Mixtures of Organic-Soluble Acids and Phenols*, BNWL-SA-273, p. 8.

[22] *Chem. Technol. Div. Ann. Progr. Rept. May 31, 1965*, ORNL-3830, p. 217.

[23] The higher affinity of strontium than sodium for HDEHP should provide more competition to the iron extraction and thus decrease its equilibrium extraction coefficient. However, this is not inconsistent with an increase of the iron extraction rate, since a large decrease of the resistance will overshadow the slight decrease in the driving force.

proportion to the *square* of the acidity, since the strontium extraction coefficient so decreases.

9.9 AGGREGATION AND ACTIVITY COEFFICIENTS IN SOLVENT PHASES

Diluent vapor-pressure lowering, determined by direct differential pressure measurement or by isopiestic balancing, has continued to be used for investigating departures from ideality in the behavior of organic solutions in solvent extraction systems. The departure from ideality is calculated optionally either as the stoichiometric activity coefficient of a specified (real or hypothetical) compound or as the apparent mean aggregation number of a polymeric species assumed to be behaving ideally. The following data for amine sulfates are calculated by both methods.

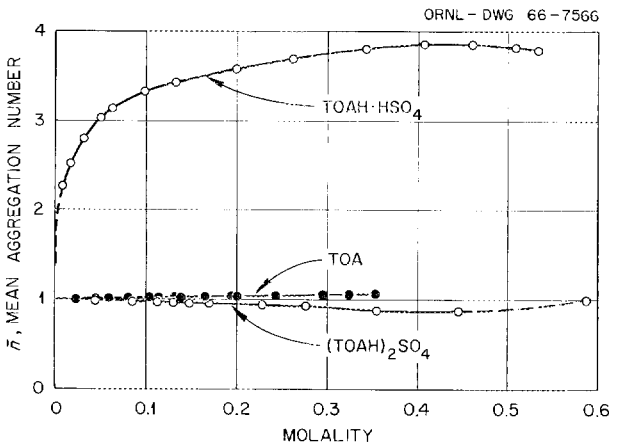

Fig. 9.6. Apparent Aggregation of Tri-*n*-octylamine and Its Sulfates in Dry Benzene, 25°C. Isopiestic vapor balancing: TOA vs triphenylmethane; its salts vs azobenzene.

Tri-*n*-octylamine–Benzene–Sulfuric Acid

As previously noted,[24] the explanation for apparent deviations of amine extraction systems from the mass action law is being sought in the aggregation behavior and activity coefficients of the various species involved in the extraction systems.

The apparent aggregation $\bar{n}$ of trioctylamine bisulfate (TOAH·HSO$_4$), as well as of the normal sulfate and the free-base amine, has now been measured in dry benzene at concentrations up to around 0.5 *m* (Fig. 9.6). While the $\bar{n}$'s for the latter remain rather close to unity throughout, $\bar{n}$ for the bisulfate rises rapidly toward 4. The points up to 0.1 *m* are well fitted by the empricial equation

$$\bar{n}_{\mathrm{TOAH\cdot HSO_4}} = 4.66\,(m_{\mathrm{TOAH\cdot HSO_4}})^{0.145}\,.$$

The small divergences of $\bar{n}_{\mathrm{TOA}}$ and $\bar{n}_{(\mathrm{TOAH})_2\mathrm{SO_4}}$ appear to be real and reproducible. The rising $\bar{n}_{\mathrm{TOA}}$ ($= 0.017\ m_{\mathrm{TOA}} + 1$) indicates a slight degree of intermolecular association. The falling $\bar{n}_{(\mathrm{TOAH})_2\mathrm{SO_4}}$ indicates dissociation, consistent with qualitative evidence from titration curves[25] that some free base and bisulfate coexist with normal trioctylamine sulfate in benzene solution. If no mixed bisulfate–normal sulfate aggregates are formed,[26] the dissociation reaction presumably is

$$(\mathrm{TOAH})_2\mathrm{SO_4} \rightleftharpoons \mathrm{TOA} + \frac{1}{n}(\mathrm{TOAH\cdot HSO_4})_{\bar{n}}\,.$$

(Here the slight association of TOA is negligible.) On the further assumption that the sulfate dissociation and bisulfate aggregation are not significantly changed in the mixed solutions, the data of Fig. 9.6 can be combined to estimate the degree of dissociation:

Molarity of $(\mathrm{TOAH})_2\mathrm{SO_4}$	Percent Dissociation
0.1	0.7
0.2	1.5
0.3	3
0.4	4
0.5	4

In the evaluation of the stoichiometric activity coefficients, there was no question that monomeric TOA and $(\mathrm{TOAH})_2\mathrm{SO_4}$ were the appropriate formulations for the free base amine and the normal

[24] *Chem. Technol. Div. Ann. Progr. Rept. May 31, 1964*, ORNL-3627, p. 206.

[25] K. A. Allen, *J. Phys. Chem.* **60**, 239 (1956).

[26] The linear rise found for $\bar{n}$ vs $\mathrm{H_2SO_4/TOA}$ (ref. 24, p. 207) suggests little if any direct association between normal sulfate and bisulfate.

sulfate, and evaluation of their activity coefficients through extrapolation of the osmotic coefficient function to $m = 0$ was straightforward.[27] However, it is not obvious whether the monomer or the tetramer will prove the more useful formulation for the bisulfate activity coefficients; hence they have been calculated both ways (Fig. 9.7). In this system the osmotic coefficients of the benzene solutions increased rapidly as the bisulfate concentration decreased, so that there was considerable uncertainty in extrapolation to $m = 0$. This does not affect the accuracy of the *slopes* of the $\gamma_{TOAH \cdot HSO_4}$ curves at concentrations above around 0.1 m monomer (0.025 m tetramer) but does make uncertain the vertical positioning of those curves in Fig. 9.7. A computer program is being prepared to provide a more suitable calculation.

Tri-*n*-octylamine–Sulfuric Acid–Water

In continued testing of the possible effects of water content on the activities of amine salts, water contents of an undiluted amine sulfate-bisulfate mixture were measured as a function of water activity. Tri-*n*-octylamine bisulfate was

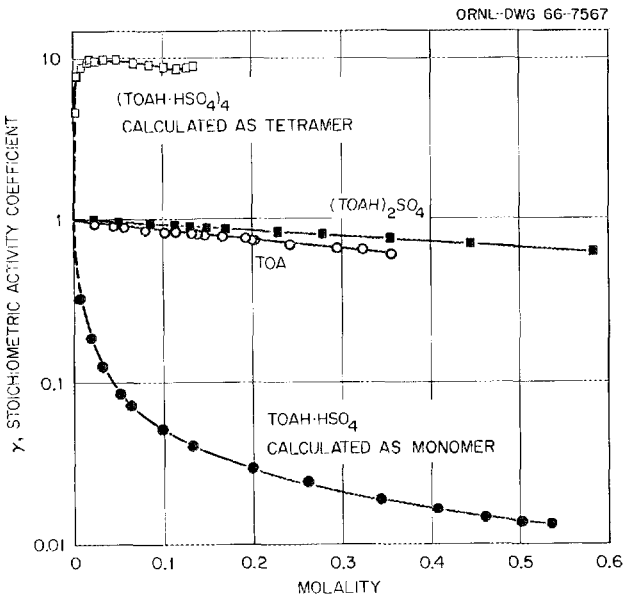

Fig. 9.7. Activity Coefficients of Tri-*n*-octylamine and Its Sulfates in Dry Benzene, 25°C. Isopiestic vapor balancing: TOA vs triphenylmethane, its salts vs azobenzene.

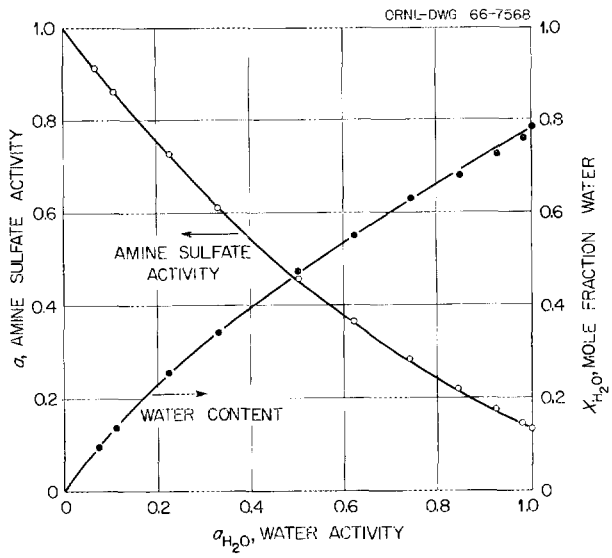

Fig. 9.8. Composition and Activities in the Undiluted $TOA-H_2SO_4-H_2O$ System, 25°C. The ratio H_2SO_4:TOA constant at 0.765. Isopiestic vapor-phase equilibration with various saturated aqueous salt solutions. Standard states: pure water for a_{H_2O}, pure dry TOA·0.765 H_2SO_4 for $a_{amine\ sulfate}$.

dried under high vacuum until some of its sulfuric acid content was volatilized (final mole ratio of normal sulfate to bisulfate = 0.44; TOA·0.765 H_2SO_4). This was equilibrated isopiestically with a series of saturated aqueous solutions of known water activity (Fig. 9.8). The activity of the (constant-ratio) amine sulfate mixture, taken as solvent, was then calculated as previously described.[27] The water-content curve deviates considerably from Henry's law, but neither it nor the amine sulfate activity curve shows any discontinuity or region of critical sensitivity.

Tributyl Phosphate–*n*-Hexane

The activities of TBP in dilute solutions in *n*-hexane, needed in the study of synergistic strontium extraction by HDEHP-TBP mixtures,[28] were determined by isopiestic balancing. The activity coefficient curve (Fig. 9.9) is similar to,

[27] *Chem. Technol. Div. Ann. Progr. Rept. May 31, 1965*, ORNL-3830, p. 219.

[28] *Chem. Technol. Div. Ann. Progr. Rept. May 31, 1965*, ORNL-3830, p. 213.

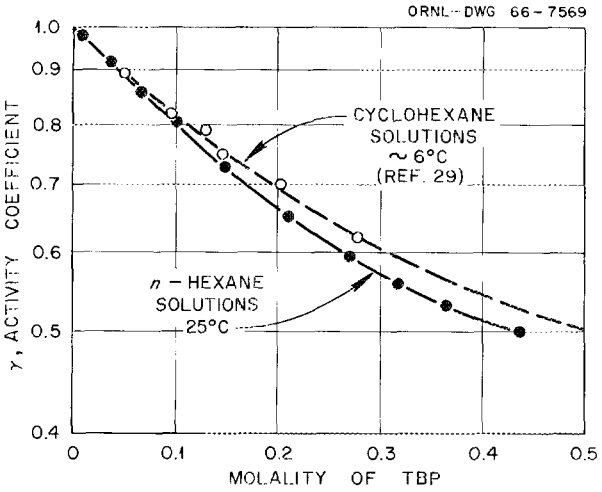

Fig. 9.9. Activity Coefficient of TBP in Dry *n*-Hexane Solution. Isopiestic vapor balancing vs azobenzene. Dashed curve: activity coefficient from freezing-point depression in cyclohexane, ref. 29.

and slightly lower than, that for TBP in cyclohexane as determined cryoscopically at around 6°C.[29] Neither curve can be fitted satisfactorily by the Scatchard-Hildebrand, van Laar, or Margules equations.[30]

Differential Pressure Gage

In a continuing program to improve the sensitivity and accuracy of differential vapor pressure measurements, a new commercial diaphragm instrument is being tested.[31] Pressure difference moves a stretched metal diaphragm, causing a change in capacity that is detected by a capacity bridge. Tests with standard aqueous solutions indicated accuracy within 0.5%. For example, water vs saturated KNO_3 showed 1.778 mm Hg at 25°C, and saturated KCl vs saturated NaCl showed 2.127, as compared with 1.786 and 2.133, respectively, calculated from the literature values.[32] However, there is some drifting with time, indicating real or virtual leakage, and this appears to be worse with organic than with aqueous solutions. Tests are continuing, to determine whether this difficulty is inherent or can be eliminated.

---

[29] W. F. Johnson and R. L. Dillon, *Physical Properties of Tributylphosphate-Diluent Solutions*, HW-29086 (Sept. 1, 1953).

[30] J. H. Hildebrand and R. L. Scott, *The Solubility of Nonelectrolytes*, 3d ed., pp. 34, 36, 131, Dover, New York, 1964.

[31] *MKS Baratron Electronic Pressure Meter*, Bulletin 77, MKS Instruments, Inc., Burlington, Mass.

[32] R. A. Robinson and R. H. Stokes, *Electrolyte Solutions*, 2d ed., p. 510, Butterworths, London, 1959.

10. Chemical Applications of Nuclear Explosions

The purpose of this program is to provide research and development in selected areas of the Plowshare Program, especially those areas requiring knowledge of chemistry or metallurgical engineering to determine feasibility. Areas in which research was performed last year included (1) studies of the distribution and possible fate of radionuclides formed during the use of nuclear devices to aid in the recovery of copper from ore deposits; (2) an examination of the potential for production of magnesium from olivine; (3) measurement of the rate of exchange of tritium and hydrogen in water and natural gas under conditions that may be encountered in the stimulation of gas production from wells by nuclear explosives; (4) studies of the distribution and possible fate of radionuclides formed during the use of nuclear devices to aid in the recovery of oil from shales; (5) hypervelocity jet sampling as a means of removing a specimen after irradiation in the neutron flux of a detonation, but ahead of the detonation shock wave.

10.1 COPPER ORES

Fracturing of copper ore deposits with nuclear explosives, followed by leaching in place, is being studied for the AEC by Lawrence Radiation Laboratory (LRL) and by the U. S. Bureau of Mines at Tucson, Arizona. The Oak Ridge National Laboratory is cooperating in this program by studying potential problems that might arise from the presence of radioactive contaminants in the processing cycle. The proposed flowsheet for recovering copper includes percolating a leaching solution of dilute sulfuric acid down through the nuclear-broken ore to dissolve the copper, collecting the leach liquor at the bottom of the ore body and pumping it to the surface, recovering a copper concentrate from the solution by cementation on iron, and returning the barren solution, after fortifying it with acid, for reuse in the leaching step.

Problems that might arise from the presence of radionuclides in the system are being considered under two main categories; first, evaluation of radioactive hazards to personnel; second, possible radiocontamination of the copper product, which, of course, could affect its marketability. Assessment of these problems requires some knowledge of the amounts of the different radionuclides that would be present in the system, their leachability under expected flowsheet conditions, and their behavior in certain processing steps, for example, the copper cementation step. The amounts of each of the fission products and tritium produced by detonation of a given yield depend, of course, on the type of device used. We have assumed in the initial evaluations that most of the energy might be derived from fusion and that leaching would not begin sooner than eight months after the shot; thus the tritium activity would be much higher than the total fission product activities. In addition, induced activities would be present, their amounts depending on the composition of the ore and conditions of the experiment.

Since nuclear-broken copper ore is not available for leaching tests, the paths of the radionuclides in the processing cycle are being studied by dosing the copper ore with soluble isotopes, with reactor-irradiated copper ore, and with radioactive debris from one of the Nevada test-site shots.

Status and Progress

At this stage of the studies, the potential problems associated with the introduction of radioactivity into the system do not appear to constitute a preventive obstacle to the use of nuclear explosives in copper processing. The anticipated concentration levels of the radiocontaminants in the process liquors should be far below the level that would require the shielding of equipment to avoid radiation exposure to personnel. Tritium will require special consideration (particularly with respect to underground operations) since it will be in a volatile form.

Ruthenium contamination of the copper is of concern but does not seem to represent a limiting problem. The level of contamination might be sufficiently low as to not represent a hazard to the customer population even if there is no rejection of ruthenium in going from the cement copper concentrate to the final product. However, this needs confirmation. If necessary, it appears that suitable means of reducing ruthenium contamination are available.

Leaching of Test-Shot Debris

In batch tests with radioactive debris, less than 2% of any of the long-lived radionuclides were dissolved under expected flowsheet conditions (pH 2 to 3) from a sample of "puddle glass" (Fig. 10.1). However, about 50% of the ^{90}Sr, about 20% of the ^{144}Ce, and 5 to 10% of the ^{106}Ru were dissolved from a sample of rubble.

Adsorption of Radionuclides by the Ore

The ion exchange properties of the copper ore are highly important in regulating the amounts of certain radionuclides that are dissolved. Batch distribution tests with soluble radionuclides showed that fission products, such as cesium and zirconium-niobium, and potential activation products, such as silver, are adsorbed very strongly by the ore from acid leach solutions (Fig. 10.2). Strontium, rare earths, and ruthenium are adsorbed much more weakly, although significantly. The chimney of broken ore can be pictured as an ion exchange column several hundred feet high. Radionuclides dissolved in the early phases of the leaching cycle tend to be adsorbed on the ore as the leach solution is recycled through the ore column. This would limit the buildup in concentrations of some radionuclides in the leach liquor to levels far below those that would be predicted on the basis of batch leaching experiments.

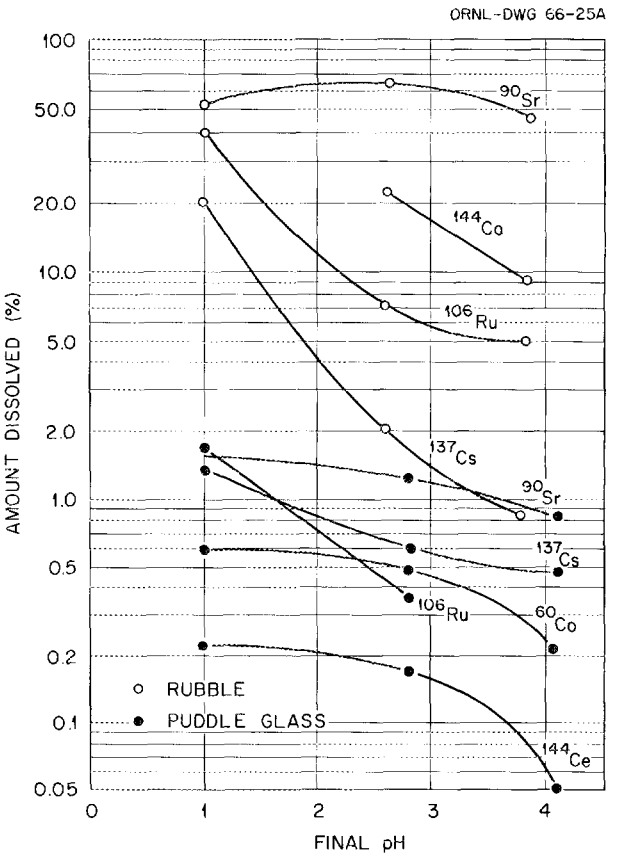

Fig. 10.1. Leaching of Test-Shot Debris with Sulfuric Acid. Procedure: 10-g samples of −4-mesh debris leached for two days at room temperature with 20 ml of dilute H_2SO_4; acid added during the leach to maintain the pH approximately constant at 1.0, 2.5, or 4. The supernatant was analyzed for the various radionuclides. The unleached debris contained (in dis/min × 10^4 per gram): puddle glass – 1.4 ^{137}Cs, 22 ^{144}Ce, 4.1 ^{90}Sr, 3.7 ^{60}Co, and 2.0 ^{106}Ru; rubble – 2.2 ^{137}Cs, 0.04 ^{144}Ce, 0.09 ^{90}Sr, 0.01 ^{60}Co, and 0.12 ^{106}Ru.

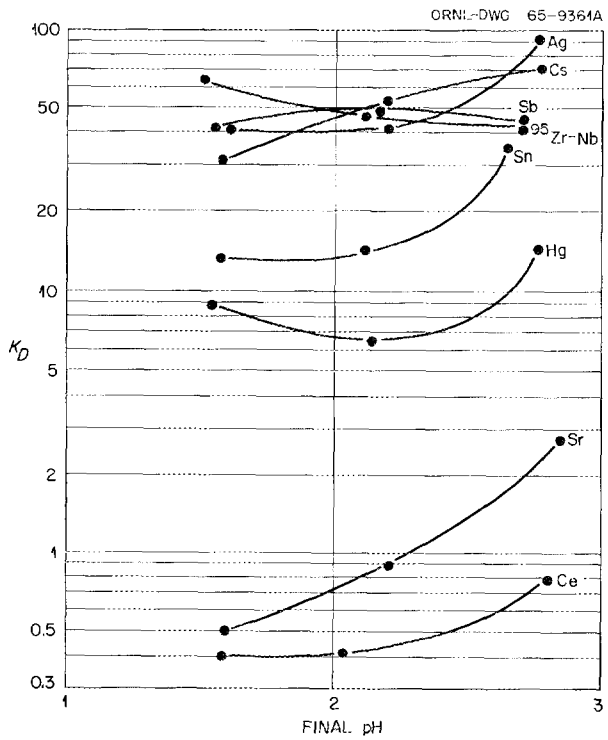

Fig. 10.2. Adsorption of Radionuclides by Arizona Copper Ore. Procedure: 5 ml of Arizona copper ore leach liquor (adjusted to different pH levels and spiked with the appropriate radioisotope) contacted 16 hr with 1 g of −20-mesh Arizona ore tailings; amount adsorbed calculated on basis of head solution and supernatant analyses. Less than 4% (K_D < 0.25) of Ru, Fe, Eu, Sc, Y, Cr, Co, Zr, and Cd were adsorbed in the pH range of 1.5 to 2.8.

Cementation Tests

Excessive radiocontamination of the cement copper could introduce complications in subsequent processing operations and, if not eliminated in these operations, could affect the marketability of the final copper product. In cementation tests with copper leach liquors dosed with radioisotopes, significant fractions of fission products such as ruthenium and zirconium-niobium cemented with the copper. Certain potential activation products such as silver cemented quantitatively. However, on the basis of the amounts of the various radionuclides that would be present in the system and other considerations, ^{106}Ru is the only radionuclide that appears important with respect to radiocontamination of the cement copper.

Column Leaching Tests

A number of tests were made in which a 4-in.-diam column of Arizona copper ore was leached with sulfuric acid by the open-drainage–trickle leach method. The dissolved copper was recovered from the column effluent by cementation on detinned cans, and the depleted solution was fortified with sulfuric acid and recycled to the column. In a test wherein test-shot rubble was added to the column (2000 g of rubble per 2500 g of copper ore), the gamma activity of the leach solution was only slightly above background. The copper products contained 0.005 to 0.01 μc of ^{106}Ru per gram of copper, but no other radioisotopes were detected.

To better follow the paths of the radionuclides in the processing cycle, another column run was made in which the ore was spiked with a solution containing equal numbers of curies of ^{134}Cs, ^{85}Sr, ^{95}Zr-Nb, ^{144}Ce, and ^{106}Ru. In the initial volumes of effluent collected, ^{85}Sr was the dominant isotope, but its concentration decreased rapidly as the solution was recycled through the column. Only a very small fraction of the total ^{134}Cs and ^{95}Zr-Nb was found in the effluent. After several cycles of the solution, about 54% of the total activity in the effluent was due to ^{144}Ce, 42% to ^{106}Ru, and 3% to ^{85}Sr. Ruthenium was the only radioisotope found in the cement copper in appreciable amounts, its concentration increasing with each successive product batch.

In another run, the ore was spiked with Arizona copper ore that had been irradiated in the Oak Ridge Research Reactor and cooled for 52 days. At that time, the concentrations of activation products in the irradiated ore, in microcuries per gram, were: 109 ^{46}Sc, 78 ^{59}Fe, 13 ^{60}Co, 12 ^{54}Mn, 11 ^{65}Zn, 7 ^{75}Se, and 1.4 ^{95}Zr. Only small fractions of any of these isotopes were dissolved in the column run. Based on analyses of the solution entering the cementation circuit and the copper products, less than 3% of the dissolved ^{95}Zr, ^{75}Se, and ^{46}Sc and less than 0.2% of the dissolved ^{54}Mn, ^{59}Fe, ^{60}Co, and ^{65}Zn were removed with the copper in the cementation step.

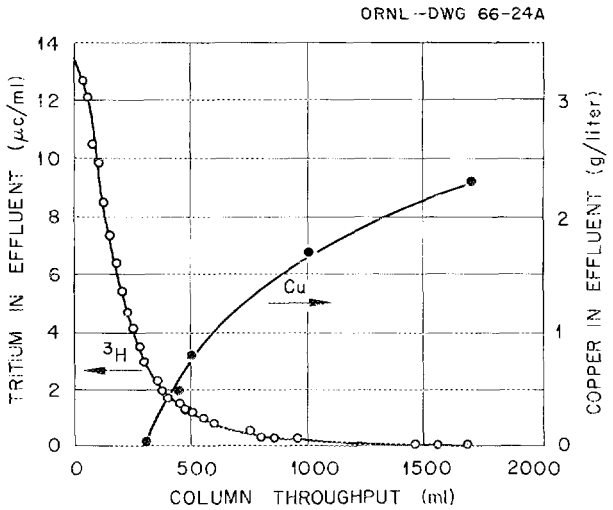

Fig. 10.3. Tritium and Copper Concentrations in the Column Effluent. The pH of the effluent was 4.7 at 500 ml, 4.6 at 1000 ml, and 4.5 at 1650 ml. Procedure: 4500 g of −0.5-in. Arizona copper ore, spiked with tritiated water containing 3 mc of ^{3}H, was leached at 0.5 ml/min with synthetic well water adjusted to pH 1.2.

Tritium

Following a nuclear shot, the tritium will adsorb on the ore rubble as tritiated water.[1] Practically all of it should eventually be taken into the leach solution. On leaching ore dosed with tritiated water in a column, most of the tritium was removed in the first portions of effluent (Fig. 10.3). This suggests that the tritium hazard might be appreciably lessened by discarding rather than recycling the initial effluent, which contains little copper. A significant fraction of the soluble ^{90}Sr also is removed early in the cycle and could be eliminated by this procedure.

Ruthenium Contamination of Copper Product

Preliminary tests showed that ruthenium contamination can be appreciably decreased by treating the leach liquor with activated carbon or by treating the recycle liquor with lime. Also, solvent extraction of copper[2] with LIX–64 (a new copper extractant of undisclosed structure) gave a clean separation of copper from radiocontaminants.

10.2 MAGNESIUM ORES

A survey was started to determine whether the Plowshare Program could benefit the minerals industry, and therefore, the economy, of the Appalachia region. Paper evaluation of past work by TVA on recovering magnesium (and possibly by-product nickel and chromium) from olivine indicated that establishing olivine as a competitive raw material for magnesium would require considerable improvement of the TVA process and probably an extensive pilot operation. Because of considerations with respect to the geography, nature, and size of the ore bodies and the nature of the subsequent recovery process, it was not clear that the use of nuclear explosives would be advantageous in processing olivine. Considerations of possible Plowshare applications in the Appalachia region are inactive for the present.

10.3 STIMULATION OF NATURAL GAS WELLS

In feasibility studies of the stimulation of gas production from wells by nuclear devices (Project Gasbuggy), it is important to consider the relative distributions of tritium gas (produced by the device) to the groundwater and to the natural gas (e.g., methane) initially present in the cavity, and to the gas that enters the well once gas production has started. Because of the extreme temperatures and pressures at the instant of detonation and shortly thereafter, the tritium distribution occurring during this phase can be measured realistically only in an actual nuclear test. However, laboratory measurements have been made which provide an indication of the tritium exchange to be expected during the gas production phase.

---

[1] F. W. Stead, "Distribution in Groundwater of Radionuclides from Underground Nuclear Explosions," *Third Plowshare Symposium, April 21–23, 1964*, TID-7695.

[2] D. W. Agers *et al.*, "A New Reagent for Liquid Ion Exchange of Copper," *Mining Eng.* 17, 76 (1965).

Such tests have shown that the formation of tritiated methane is probably low, provided that the tritium concentration in the gas phase is low and provided that there is no catalytic effect in the presence of cavity medium. Specifically, the tritium exchange with hydrogen in methane–water-vapor mixtures is equal to or less than 2×10^{-6} mc liter^{-1} day^{-1} at 100°C when the tritium concentration is 1 mc/liter, and is equal to or less than 2×10^{-8} mc liter^{-1} day^{-1} at room temperature when the tritium concentration is 0.2 mc/liter. The proposed Gasbuggy experiment involves a 10-kiloton fission device with a 10,000-curie tritium spike. The maximum gas-phase tritium concentration after the shot has been estimated at 0.3 mc/liter, and the present tests include this concentration. The laboratory exchange tests have been conducted for a period which exceeds the expected methane residence time in the well during actual production. These water-methane exchange rates are at least a factor of 10 lower than those predicted from the literature for tritium-gas–water and tritium-gas–methane systems, but the latter were determined at much higher tritium concentrations, where self-induced radiation exchange was significant.

A fusion Plowshare device would conceivably produce more tritium than the 10,000-curie spike. It is not clear that a gas-phase tritium concentration would be produced that would be sufficiently high to make radiation-induced tritium-hydrogen exchange a significant factor in determining the quality of the methane product. Nevertheless, experiments will be made to determine the extent of tritium and hydrogen exchange between water and methane at tritium concentrations between 1 and 100 mc/liter. In some of the tests, the gas phase will be in contact with shale from the formation in which the proposed Gasbuggy shot is to occur, in order to determine its possible catalytic effects on the exchange.

10.4 PRODUCTION OF OIL FROM SHALE

The use of a nuclear device to crush oil shale in place has been proposed under the Plowshare Program. The recovery of the oil from the crushed shale in the nuclear chimney involves in-situ retorting, and the feasibility of this concept is being studied at the Bureau of Mines Research Station in Laramie, Wyoming. As a part of this study, experiments have been started at ORNL which will examine the distribution and possible fate of radionuclides formed during the nuclear crushing and retorting steps. A small retort has been constructed which will have the capability of first retorting and then burning 100-g batches of crushed shale. The shale will be contaminated with the radionuclides (or their stand-ins) expected to be produced by the device, along with the activation products produced by irradiation. The product oil and gases will be analyzed for the contaminants.

10.5 DEVELOPMENT OF HYPERVELOCITY JET SAMPLERS

Hypervelocity jets are being studied as a means of transporting samples, irradiated about 1 m from a nuclear detonation, to a recovery area (about 100 m away) that is relatively free from the destructive effects of the detonation. The experiments are being conducted at the Frankford Arsenal, Vincentown, New Jersey, in an evacuated (1 mm Hg) flight chamber 18 in. in diameter and 55 ft long. The equipment has been modified to handle the $3\frac{1}{2}$-lb charges needed to focus and accelerate a jet formed from a 390-g copper cone that contains a 3-g target of gold. The gold simulates transplutonium materials. The jetted target is caught in a laminated wooden block 36 in. thick.

During the past year, preparatory to using the gold targets, tests were made with smaller cones of copper, iron, and aluminum, containing targets of the same metals. The results are summarized below:

1. At least 50% of the target and a portion of the supporting cone formed into a jet in about 15 μsec and traveled with a velocity equal to, or faster than, the estimated velocity of a nuclear shock front in rock.
2. The remainder of the target and most of the cone formed a "reaction slug" which followed the jet, but at a lower speed. (In the experiments, the reaction slug was also recovered in the receiver. In a nuclear detonation the slug would not be recovered because it would be overtaken and destroyed by the shock front.)

3. It is easier to catch jetted material when the jet consists of coarse particles, although this type of jet does not move to the receiver quite as fast and as accurately as a coherent jet. Jet breakup was controlled by the configuration of the target and the ductility of its material. When hardened copper was tested, x-ray photographs showed that 80 to 90% of the jet consisted of coarse particles.

4. Ten to twenty percent of the jetted material was vaporized and condensed on the walls of the flight chamber.

5. The jet was stopped by 13 in. of wood. Jet retrievals in ice, water, and gel were tried. These are impractical for the New Jersey test range because (1) the vessel of ice has to be prepared at the arsenal (in Philadelphia) and maintained in transit and on the range; (2) a reasonable quantity of water is difficult to contain under jet-impact conditions (the jet split a 55-gal drum of water), and the necessary filtration and sampling facility would be complicated for handling 100 to 200 gal of water; and (3) the many boxes of gel required for the series of shots are expensive. These considerations, however, need not preclude the use of any of these methods for recovery of the target in a nuclear explosion. Baffles installed in the chamber near the explosives end deflected most of the extraneous matter that had been getting into the receiver and which came primarily from the explosive charge.

From these results it is concluded that the precision with which the target assembly is made, the precision with which the explosive is cast around this assembly, the symmetry of the detonation-wave front, and the alignment of the charge, target assembly, and flight chamber are well suited to good recovery of future test targets.

11. Recovery of Fission Products by Solvent Extraction

The objective of the fission product recovery program is to develop processes applicable to large-scale recovery and purification of fission products from reactor-fuel-reprocessing wastes. Large quantities of certain fission products are being requested for industrial, space, and other applications, and there is evidence that the demand will increase. Also, aside from their utility for recovering useful fission products, the recovery methods developed are of interest for fractionating wastes to ease certain waste-disposal problems.

Since the inception of this program the principal emphasis has been on the development of solvent extraction methods, because they are particularly versatile and readily adaptable to large-scale operations. Thus far, a solvent extraction process using di(2-ethylhexyl)phosphoric acid (D2EHPA) has been successfully developed for recovering ^{90}Sr and mixed rare earths. A modification of this process has been developed and operated in plant scale at the Hanford Atomic Products Operation. New processes have also been developed in the laboratory for recovering cesium with substituted phenols and for recovering zirconium-niobium and ruthenium. The combination of these developments with previous studies of rare-earths separations and of the recovery of technetium, neptunium, and plutonium affords a possible integrated solvent extraction flowsheet for recovering nearly all valuable components from waste liquors. Current studies are aimed at consolidating, optimizing, and completing these developments and at devising new processes that might provide even greater advantages in operations and cost.

11.1 HOT-CELL TESTS

Several recovery processes developed and tested previously, but only with simulated waste solutions at tracer level, were demonstrated successfully in hot-cell tests with actual Purex STW (sugar-treated waste) solution from Hanford. The waste as received was about 0.3 *M* in free acid and 0.17 *M* in iron.

Cesium Recovery

In a mixer-settler run, more than 98% of the cesium was recovered from the Purex STW (complexed with tartrate and adjusted to pH 12) solution by extracting with 1 *M* 4-*sec*-butyl-2-(α-methylbenzyl)phenol (BAMBP) in Amsco 125-82 and stripping with 0.1 *M* HNO_3–0.02 *M* sulfamic acid. Overall decontamination factors for cesium were: 1000 from ^{90}Sr and Fe; 2200 from Al; 3000 from ^{144}Ce, ^{95}Zr-Nb, and ^{106}Ru; and more than 700 from Na. The principal purpose of the run was to test the chemical and radiation stability of BAMBP at full radiation level. No changes in extraction performance or physical characteristics of the solvent were noticed in about 80 extraction-strip cycles over a period of about 50 hr.

Spectrophotometric examination at 371 mμ of solvent samples withdrawn from the system periodically throughout the run indicated that the amount of nitrated BAMBP was negligible (less than 0.1%) in all samples. The titrated BAMBP concentration of the samples varied over a narrow range and was the same for the final sample and the original (Table 11.1). Standard cesium extraction tests showed a small increase in the cesium extraction coefficient with cycling of the solvent. For example, the extraction coefficient in the second of two extraction contacts was about 8 for the final solvent, compared with about 5 for the original solvent.

Separation of Cerium from Other Rare Earths

The efficient separation of cerium from other rare earths obtained previously[1] with cold feeds by

[1] *Chem. Technol. Div. Ann. Progr. Rept. May 31, 1965*, ORNL-3830, p. 224.

Table 11.1. Testing of Irradiated BAMBP

Procedure: Samples of stripped solvent from the continuous cesium recovery run were scrubbed with dilute nitric acid and then water; then they were contacted with two successive volumes of 3 *M* $NaNO_3$–0.0008 *M* Cs solution at pH 12.0, each contact at an aqueous/organic phase ratio of 2/1.

Solvent Exposure		BAMBP Concentration (*M*)	Standard Cesium Extraction Test		
			Final pH	Cesium Extraction Coefficient, E_a^o	
Time (hr)	Approximate Number of Cycles			First Contact	Second Contact
0	0	1.00	12.0	5.6	5.2
8	10	1.01	12.0	5.8	6.2
16	20	1.03	11.9	6.1	6.0
24	32	0.96	11.9	5.7	6.0
32	44	0.96	11.9	7.7	8.5
40	58	0.99	11.9	7.9	8.5
52	82	1.00	12.0	10.6	8.1

oxidizing the cerium with silver-catalyzed persulfate and extracting with di(2-ethylhexyl)phosphoric acid (D2EHPA) was achieved also in batch tests with Purex STW. A mixed rare-earths feed was first prepared by extracting rare earths from tartrate-complexed STW solution at pH 2.5 with D2EHPA and stripping with 2.5 *M* HNO_3. The cerium in the strip solution was oxidized by adding silver nitrate to 0.015 *M* concentration and sodium persulfate to 0.1 *M* concentration and heating for 20 min at 50°C. Batch contacting the oxidized solution with ½ vol of 0.3 *M* D2EHPA–Amsco 125-82 removed more than 97% of the cerium but only about 0.3% of the promethium from the aqueous phase. More than 99% of the cerium was stripped by contacting the extract with one-fourth its volume of 2 *M* HNO_3–1 *M* H_2O_2. The overall decontamination factor of cerium from promethium was more than 270.

Ruthenium Recovery

Ruthenium recoveries from Purex STW solution by tertiary amine extraction were much more efficient than those obtained previously[1] in tests with simulated wastes. Pretreatment of the STW, by adding sodium nitrite and heating, improved the ruthenium recoveries. For example, with 0.2 *M* Alamine 336 in 95% Amsco 125-82–5% tridecanol diluent, about 95% of the ruthenium was extracted from nitrite-treated STW in a single batch contact at an organic/aqueous phase ratio of 2/1, whereas only 39% was extracted from untreated waste under the same conditions. In the former test, less than 1% of the ^{95}Zr, ^{137}Cs, and ^{144}Ce were extracted with the ruthenium. About 90% of the ruthenium was stripped from the extract by contacting it with dilute caustic solution.

In addition to the favorable results with Alamine 336, better than 85% of the ruthenium was also extracted (organic/aqueous ratio of 2/1) from nitrite-treated STW with 100% TBP and with the quaternary amine Aliquat 336. No suitable method is known for stripping the ruthenium from Aliquat 336.

Zirconium-Niobium Recovery

In contrast to the slow extractions[2] of ^{95}Zr-Nb obtained from Purex 1WW solution (4 *M* H^+) with D2EHPA, extractions from the relatively low-acid

[2] *Chem. Technol. Div. Ann. Progr. Rept. May 31, 1963*, ORNL-3452, p. 193.

STW solution (about 0.5 *M* H^+) are rapid, with equilibrium being obtained at room temperature within 5 min. More than 95% of the ^{95}Zr-Nb was extracted from STW solution in a 5-min contact with 0.1 *M* D2EHPA in Amsco 125-82 at an aqueous/organic phase ratio of 2/1.

11.2 ISOLATION OF PROMETHIUM

The first cycle of a two-cycle process[3] for separating promethium from mixed fission product rare earths in a nitric acid system by extraction with D2EHPA was demonstrated in a tracer run in miniature mixer-settler equipment. In this system, extraction coefficients of the rare earths increase fairly uniformly with atomic number, with separation factors between adjacent elements being in the range of 2 to 2.5. About 65% of the promethium (along with heavier rare earths) was extracted and separated from rare earths lighter than promethium with 0.75 *M* D2EHPA in diisopropylbenzene in 16 extraction and 16 scrub stages. The decontamination factor for promethium from neodymium was about 400. Although not measured, decontamination factors should have been much greater than 400 from rare earths lighter than neodymium, which are extracted less strongly. Because of poor mixing, stage efficiencies in extraction and scrubbing were poor (50 to 60%), and the total number of ideal stages in the two units was, therefore, probably no greater than 18. This accounts for the relatively poor promethium recovery and somewhat lower decontamination efficiency than was expected. In this run the aqueous feed was a rare-earths nitrate solution containing ^{148}Pm tracer and, in g/liter: 9 La, 7 Pr, 20 Nd, 6 Sm, and 1.0 Eu. The nitric acid concentration was 0.55 *N*. The scrub solution was 0.4 *M* HNO_3, and 2 *M* NaOH was fed continuously to the feed stage to control the acidity in the extraction system at the desired level. The flow ratios of feed/organic/scrub/2 *M* NaOH were 1/10/5/0.1.

11.3 NEW FLOWSHEET FOR RECOVERING STRONTIUM, RARE EARTHS, AND CESIUM

A new and simplified flowsheet (Fig. 11.1) was tentatively outlined for recovering rare earths, strontium, and cesium from Purex waste. The proposed process provides less-pure rare earths and strontium products than processes developed earlier but requires less equipment and does not use large amounts of aqueous-phase complexing agents (e.g., tartrate, citrate). Also, problems associated with slow extractions of rare earths[4] from highly complexed solutions are avoided. In this flowsheet, the rare earths, as well as nearly all the iron and some aluminum, are extracted from unadjusted Purex STW solution in a single stage with the sodium salt of di(2-ethylhexyl)phosphoric acid (Na-D2EHP) in Amsco–tributyl phosphate diluent. The amount of Na-D2EHP fed to the system is regulated to provide a final extraction pH (5-min contact) of 2 to 2.5. Iron extraction, which is very slow at higher acidities, is rapid under these conditions. For example, in batch contacts, more than 99.8% of the iron was extracted in 1 min. The rare earths are selectively stripped from the solvent with dilute nitric acid, after which the solvent is prepared for recycle by single-stage contact with dilute caustic. In the second cycle, a small amount of DTPA is added to the aqueous phase to complex nickel and chromium. Strontium then is extracted with Na-D2EHP–D2EHPA and stripped with dilute HNO_3. The cesium is then extracted with a substituted phenol at pH 12. Alternatively, the strontium and cesium can be extracted together at pH 5 to 8 with a mixture of D2EHPA and a substituted phenol.

---

[3] *Chem. Technol. Div. Ann. Progr. Rept. May 31, 1965*, ORNL-3830, p. 225.

[4] *Chem. Technol. Div. Ann. Progr. Rept. May 31, 1964*, ORNL-3627, p. 211.

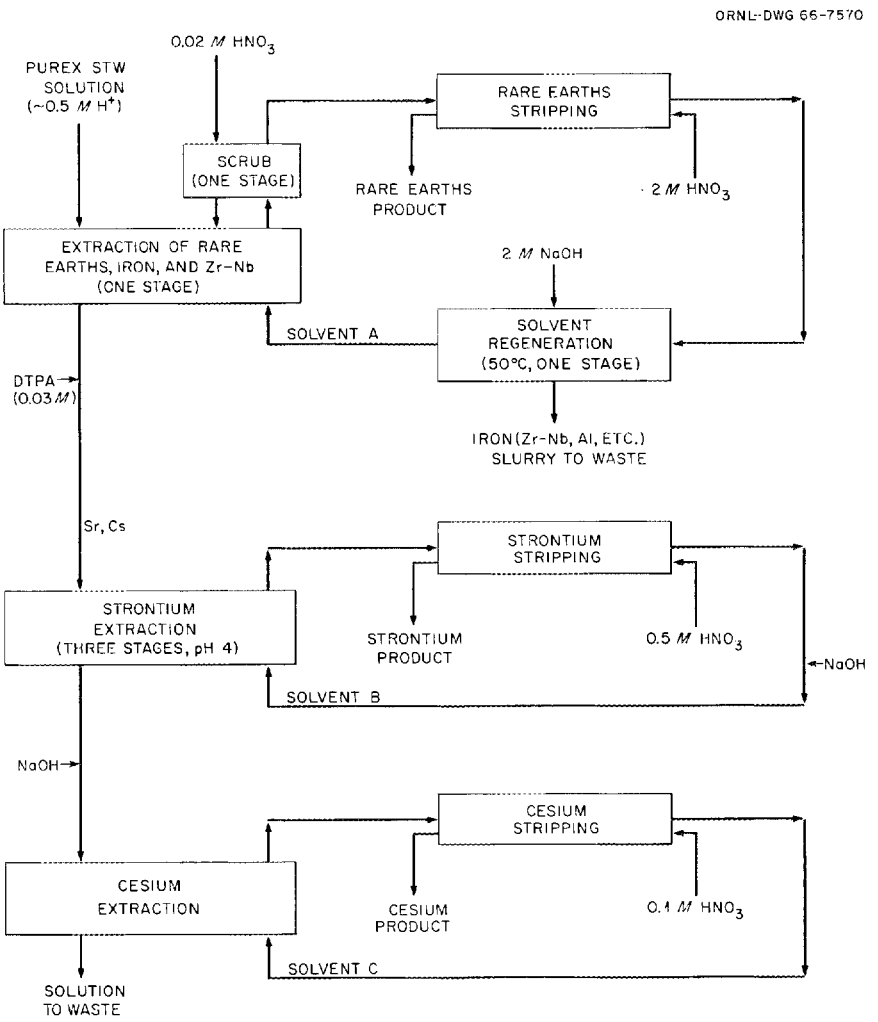

Fig. 11.1. Simplified Flowsheet (Tentative) for Recovering Rare Earths, Strontium, and Cesium from Purex STW. Solvent A, 0.75 *M* Na-D2EHP in TBP-Amsco diluent; solvent B, 0.06 *M* Na-D2EHP–0.24 *M* D2EHPA in TBP-Amsco diluent; solvent C, 1 *M* BAMBP in Amsco.

12. Biochemical Separations

12.1 BIOCHEMICAL SEPARATIONS RESEARCH

The recovery of purified macromolecules of biological interest can present formidable problems, since the wanted materials usually occur in minute quantities in complex biological systems and must be recovered in a biologically active or undamaged state. A need for methods for the recovery of such macromolecules has arisen from the increased attention being given to all phases of biological, biochemical, and medical research. The program at ORNL is broadly oriented toward the development of methods for recovering a variety of types of macromolecules; however, all the activities to date have been focused on the recovery of pure transfer ribonucleic acids (tRNA's). The tRNA's are intermediates in the process of protein synthesis; a specific tRNA transports each of the 20 amino acids to the site of protein synthesis and contains "information," coded in the chemical composition and physical configuration of the tRNA, that identifies the specific tRNA and participates in producing the correct amino acid sequence in the protein. Samples of pure tRNA's are being prepared for subsequent biochemical and physical chemical experiments so that more can be learned about the nature of "information" storage and action.

Two tRNA's, the one for the amino acid phenylalanine ($tRNA^{Phe}$) and one of the four for leucine ($tRNA_4^{Leu}$) from *E. coli* B, have been recovered in a highly purified state by reversed-phase column chromatography.[1] Conditions controlling the chromatographic resolution of these two tRNA's were optimized in a series of preliminary experiments. Increased resolution was obtained at increasing temperatures, from 10 to 37°C, and also when the sodium chloride gradient eluate was buffered at pH 4.5, compared with higher pH levels. The improved resolution at 37°C may be due to changes in the secondary structure of the tRNA, and at pH 4.5 it may be due to protonation of some of the bases in the tRNA. These changes may affect the ionic interaction between the tRNA and the column, thus shifting the position of the tRNA in the chromatogram.

Twenty grams of *E. coli* B mixed tRNA's were chromatogrammed in up to 4-g lots on coupled reversed-phase columns (Fig. 12.1). The results

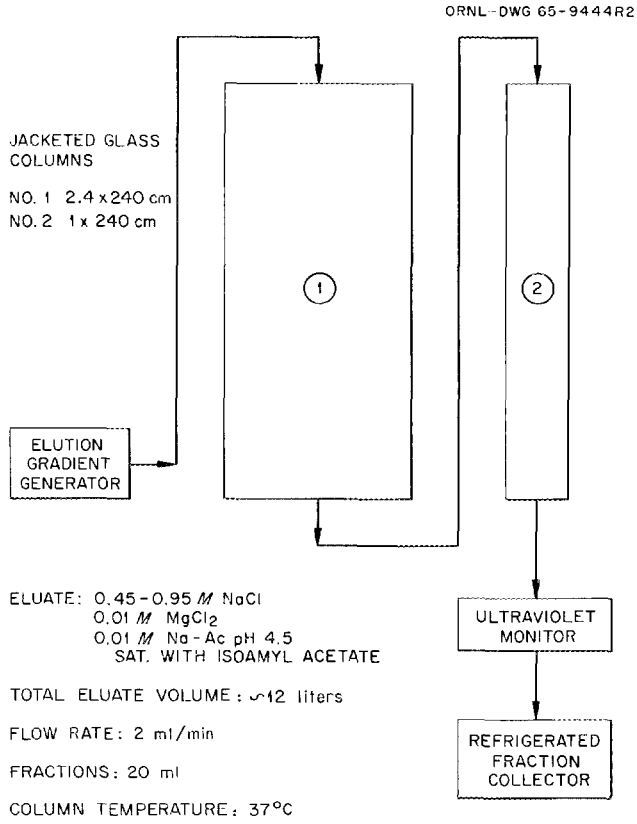

Fig. 12.1. Reversed-Phase Chromatographic System for Recovering $tRNA^{Phe}$ and $tRNA_4^{Leu}$.

[1] *Chem. Technol. Div. Ann. Progr. Rept. May 31, 1965*, ORNL-3830, p. 200.

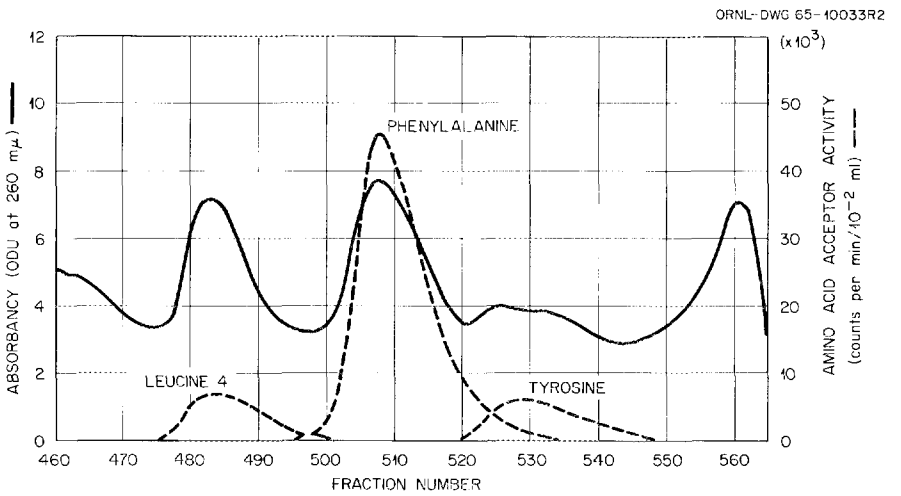

Fig. 12.2. Final Portion of Chromatogram from Reversed-Phase Chromatography Experiment.

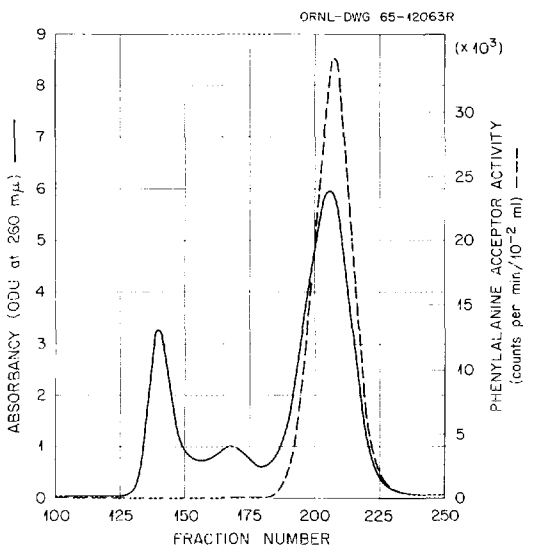

Fig. 12.3. Chromatographic Experiment with Bio-Gel P-100 for Final Purification of $tRNA^{Phe}$.

Table 12.1. Purity of Phenylalanine and Leucine-4 tRNA's

	Amino Acid Acceptance (micromicromoles/ absorbancy unit)	Terminal Adenosine Nucleoside[a] (micromicromoles/ absorbancy unit)
$tRNA^{Phe}$	1344 ± 4[b]	1322 ± 22
	1320 ± 10[c]	
$tRNA_4^{Leu}$	998 ± 25[b]	1120

[a]After basic hydrolysis.

[b]With crude aminoacyl-RNA synthetase.

[c]With purified phenylalanine aminoacyl-RNA synthetase.

of a typical experiment are shown in Fig. 12.2; for improved clarity, only the final portion of the chromatogram is shown. The $tRNA^{Phe}$ and $tRNA_4^{Leu}$ were separated from each other and from other tRNA's, but they were contaminated with a higher-molecular-weight RNA. The chromatographic fractions containing the $tRNA^{Phe}$ and $tRNA_4^{Leu}$ were separately pooled, desalted by gel filtration (molecular sieve chromatography) on Bio-Gel P-2 polyacrylamide gel columns, and concentrated by flash evaporation. Final purification was then achieved by gel filtration on Bio-Gel P-100 polyacrylamide gel columns, with results as shown in Fig. 12.3 for $tRNA^{Phe}$. On the latter column, the RNA's separated as a function of size, and the higher-molecular-weight contaminant eluted ahead of the $tRNA^{Phe}$ or $tRNA_4^{Leu}$.

Sample purity was determined both by amino acid acceptance and by terminal adenosine nucleoside content. In each case, the values were very nearly identical (Table 12.1), indicating that the final purified samples were all active $tRNA^{Phe}$ or $tRNA_4^{Leu}$.

This is the first time that relatively large (100-mg) samples of pure tRNA's have been prepared,

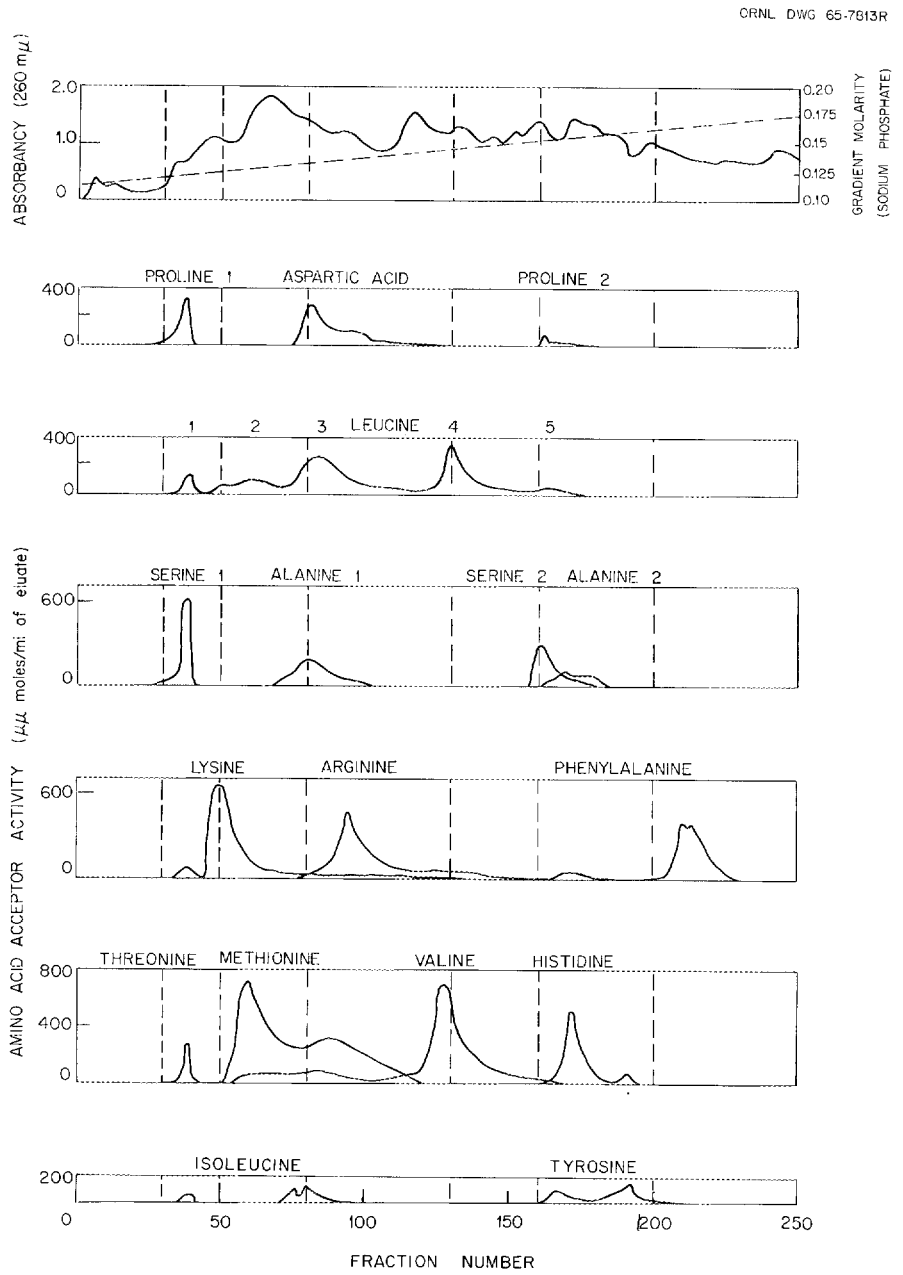

Fig. 12.4. Chromatographic Resolution of tRNA's by Hydroxylapatite Columns.

and they are now being used by investigators in the ORNL Chemical Technology and Biology Divisions to determine their molecular weight, nucleotide composition, and mechanism of interaction with the corresponding aminoacyl-RNA synthetase enzymes.

Studies have been made of the fractionation of tRNA's by an alternative method — chromatography on columns of hydroxylapatite, a calcium hydroxyphosphate inorganic ion exchanger. Resolution of 14 *E. coli* B tRNA's was obtained at room temperature by phosphate gradient elution at pH 6.8. A typical chromatogram is shown in Fig. 12.4. The ultraviolet absorbance curve shows partial resolution into a large number of peaks. Multiple tRNA peaks, well separated in the chromatogram, were

observed for proline, serine, and alanine. There also appeared to be two tRNA's for isoleucine, tyrosine, and phenylalanine. Five leucine tRNA's were indicated, confirming last year's results obtained with reversed-phase column chromatography. The sequence of elution of the tRNA's from the hydroxylapatite column is considerably different from that obtained with the reversed-phase system, and it is expected that combinations of these methods will be useful in separating several individual tRNA's.

12.2 BIOLOGICAL MACROMOLECULAR SEPARATIONS TECHNOLOGY

Since macromolecules of biological interest occur in complex biological systems in minute quantities, large volumes of starting materials must be processed to recover gram amounts of purified macromolecules. Further, because of their relatively large size and sensitivity to loss of biological activity, they cannot be treated by many of the more conventional chemical processing operations. To provide new capabilities and facilities for preparing significant amounts of purified macromolecules, an engineering-scale program has been started.

During the past year, major accomplishments included the construction of facilities, including a large controlled-temperature processing area, and the acquisition of major components, including several large refrigerated centrifuges.

All the activities thus far have been directed toward preparing gram-size samples of pure transfer ribonucleic acids (tRNA's) by scale-up of laboratory procedures developed under Biochemical Separations Research (Sect. 12.1). The tRNA's are intermediates in the process of protein synthesis in all living systems, and gram-size samples of pure tRNA's are needed to permit extensive concurrent biochemical and physical-chemical experiments.

A procedure for preparing mixed tRNA's from *E. coli* bacteria was successfully scaled up, and large amounts of mixed tRNA's were produced. The process flowsheet consists of the following four major steps:

1. Continuous Fermentation. A stainless steel flow sterilizer was devised and attached to the 300-liter fermenter in the Biology Division to permit continuous cell growth. The cells, in a rapid growth phase with a doubling time of about $1\frac{1}{2}$ hr, were semicontinuously harvested in a Wesphalia centrifuge.
2. Cell Breakage. The harvested cells were promptly broken in a phenol–aqueous-buffer mixture, and the aqueous solution, containing the nucleic acids, was recovered by batch centrifugation at 16,000 *g* in a refrigerated Sharples centrifuge with a 7-liter bowl. It was initially believed that centrifugation of this mixture (phenol, aqueous solution, and cell debris) would be the limiting step; however, under proper conditions, this operation can more than keep up with cell growth.
3. DNA-RNA Separation. Fractional precipitation in an aqueous-buffer–isopropyl alcohol mixture was used to remove undesirable DNA. This was done batchwise in the controlled-temperature processing area.
4. DEAE-Cellulose Extraction. Final purification of the mixed tRNA's was achieved by batch extraction onto DEAE-cellulose, an anion exchanger (cellulose modified by the addition of diethylaminoethyl groups), and preferential elution by 0.65 *M* NaCl solution. The product was precipitated and stored as a semidry powder at $-20°C$.

As experience was accumulated, larger campaigns were undertaken to achieve extended periods of cell growth, followed by batch processing of the material through to the mixed tRNA product. In one campaign, with *E. coli* W, fermentation was continued for 80 hr, and 300 kg of cells were harvested. They yielded 630 g of mixed tRNA's. Only a few such campaigns a year are anticipated in order to supply the mixed tRNA needed for further separation work.

Attention is now being directed toward scale-up of the chromatographic methods used in preparing pure phenylalanine and leucine-4 tRNA's as described in Sect. 12.1. The engineering variables affecting chromatographic resolution are being defined, and large reversed-phase columns (1, 2, and 3 in. by 8 ft) have been built.

12.3 MOLECULAR WEIGHTS OF TRANSFER RIBONUCLEIC ACIDS

It is generally accepted that tRNA molecules consist of about 75 to 80 nucleotides, giving a

calculated molecular weight of 25,000 to 30,000. However, published values based on sedimentation analysis, viscosity, and free diffusion range from as low as 11,000 to 14,000 to as high as 41,000.

Osmometry

A high-speed membrane osmometer was used to obtain osmotic pressure measurements of crude, mixed tRNA solutions. The van't Hoff equation, relating osmotic pressure to molecular weight, is applicable to ideal solutions only; therefore measurements were made at several tRNA concentrations, and the results were extrapolated to zero concentration from a plot of π/c vs c. Osmotic pressure measurements were made at 17 and 37°C. In one series of experiments, the solution of tRNA's was dialyzed against the buffer solvent, and osmotic pressure measurements were made at 25, 13, and 17°C (Fig. 12.5).

A plot of π/c vs c for the nondialyzed solutions showed a slight positive slope, while the dialyzed material showed less dependence on concentration, with a slope nearer zero. It appears from these limited data that dialysis reduces charge and ionic interactions. Also, there appeared to be a trend toward decreasing molecular weight with increasing temperature.

The apparent molecular weights of the crude, mixed tRNA's varied from 33,200 to 36,500. Under comparable conditions, the molecular weights of the dialyzed and nondialyzed material were 34,500

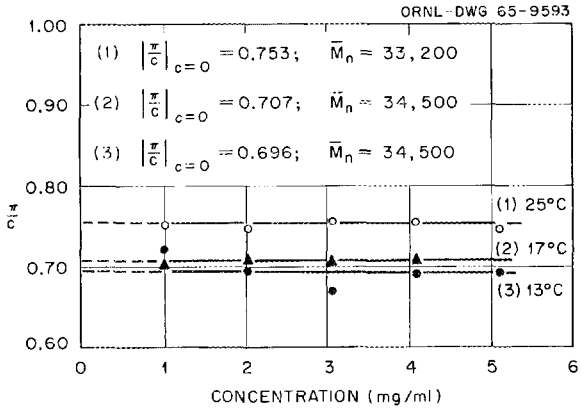

Fig. 12.5. Osmotic Pressure of Dialyzed tRNA in 0.1 *M* Phosphate Buffer, pH = 7.35.

and 36,500 respectively. Later studies, using gel-permeation chromatography, showed that these values were too high due to the presence of high-molecular-weight impurities in the crude tRNA. However, the experiments demonstrated the applicability of osmometry to molecular weight determinations of tRNA's.

Gel-Permeation Chromatography

Gel-permeation chromatography refers to the molecular sieving properties of porous gel particles. Excellent correlations between the molecular weights of several proteins and their elution volume on Sephadex and agar gel columns have been reported. Polyacrylamide gels were used in this work. These correlations are best applied to systems in which the other parameters relating to shape are known to be consistent, or "typical behavior" is assumed for a given series of solutes being compared. Since this is a comparative method of determining molecular weight, the most important factor is the choice of standards for comparison. Although values for the molecular weight of proteins found by different investigators differ by as much as 10%, proteins have been studied extensively, and their behavior on gel columns has been well documented. Serum albumin, egg albumin, and β-lactoglobulin, used as standards in these experiments, can be represented as ellipsoids of revolution, with axial ratios of about 4:1. It is believed that the tRNA molecule has an axial ratio of 4:1 or higher. Thus, gel-column behavior of tRNA and these proteins should be comparable.

Excellent linear correlation was obtained when the elution volume was plotted against the logarithm of the molecular weight, as shown in Fig. 12.6. The molecular weight of crude, mixed tRNA samples from General Biochemicals was 39,000, measured on a P-100 column (1 × 121 cm) by eluting with 0.1 *M* phosphate buffer. The good agreement of this value with the value of 36,500 obtained by osmometry at 17°C in 0.1 *M* phosphate buffer substantiates the validity of this method.

Only a single elution peak was observed on the P-100 column. However, other tests showed that two peaks were observed on P-150 and P-300 columns when eluting with a solution 0.4 *M* in NaCl, 0.01 *M* in $MgCl_2$, and 0.05 *M* in Tris buffer,

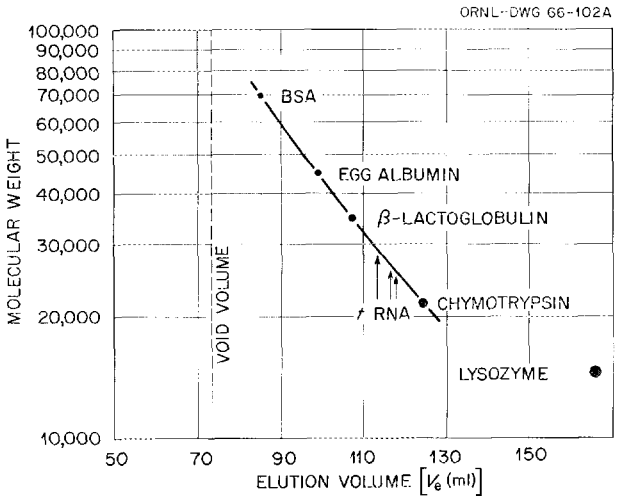

Fig. 12.6. Molecular Weights of Mixed tRNA, Phenylalanine tRNA, and Leucine-4 tRNA from Elution Volume on Bio-Gel P-150.

pH 7.35. This shows that the crude tRNA contained a high-molecular-weight impurity. The value of 39,000 is an average value of the mixed tRNA's and the higher-molecular-weight material.

The P-150 and P-300 columns separated the unfractionated tRNA from the high-molecular-weight material present in the initial crude, mixed tRNA's and gave good resoltuion of the pure phenylalanine and leucine-4 tRNA's. Therefore these columns were used to determine the molecular weight of these pure tRNA's (preparation described in Sect. 12.1). Values obtained from the P-150 column data for unfractionated tRNA (high-molecular-weight impurity removed), phenylalanine tRNA, and leucine-4 tRNA were 26,000, 27,000, and 29,500. The molecular weight of the unfractionated tRNA was also estimated by using the P-300 column. A value of 26,500 was obtained. In the case of the unfractionated tRNA, the values represent an average of all the specific tRNA's present. The values are in excellent agreement with reported values of 26,600 for pure yeast alanine tRNA, 26,500 for unfractionated yeast tRNA, and 28,000 to 32,000 for unfractionated wheat germ tRNA.

12.4 BODY-FLUID ANALYSES

The goal of the Body-Fluid Analyses Program is to develop systems for automatically analyzing complex human body fluids for their molecular constituents. This program is a part of the Molecular Anatomy (MAN) Program directed by N. G. Anderson of the ORNL Biology Division.

Of particular interest is the automatic analysis of human urine, since many of the molecular constituents of urine are known to have pathological significance. An automatic urine analyzer of high resolution would be valuable in the diagnosis of many diseases and would also be useful in the study of human biochemistry.

A literature search has been started on the subject of urinalysis and urine constituents, and the experimental program has been directed toward development of a modified nucleotide analyzer for analyzing the ultraviolet-absorbing constituents of urine. This analyzer gives reproducible results and has separated and detected up to 93 ultraviolet-absorbing urine constituents, of which 11 have been tentatively identified.

Literature Search

A search of the literature of the last ten years which deals with urinalysis and the significance of urine constituents is being made with assistance from the MEDLARS computer search system. Over 100 references have been found, and abstracts of these are being collected in an annotated bibliography. Reference to 54 molecular constituents of human urine with pathological significance has been found, and many of these constituents are ultraviolet absorbing.

Modified Nucleotide Analyzer

The major experimental effort has been to develop a modified, automatic nucleotide analyzer for urine analysis. This has included determination of reproducibility of the device, identification of some separated urine constituents, increasing the sensitivity of the ion exchange separation column, and development of equipment.

The analyzer is an automatic high-resolution device for analyzing mixtures of nucleotides, nucleosides, and purine and pyrimidine bases.[2] Gradient elution of an anion exchange column (0.6 cm inside diameter × 150 cm, with Dowex 1-X8 resin) is used for separation, and a continuous uv spectrophotometer operating alternately at two

[2]N. G. Anderson *et al.*, *Anal. Biochem.* 6(2), 153 (1963).

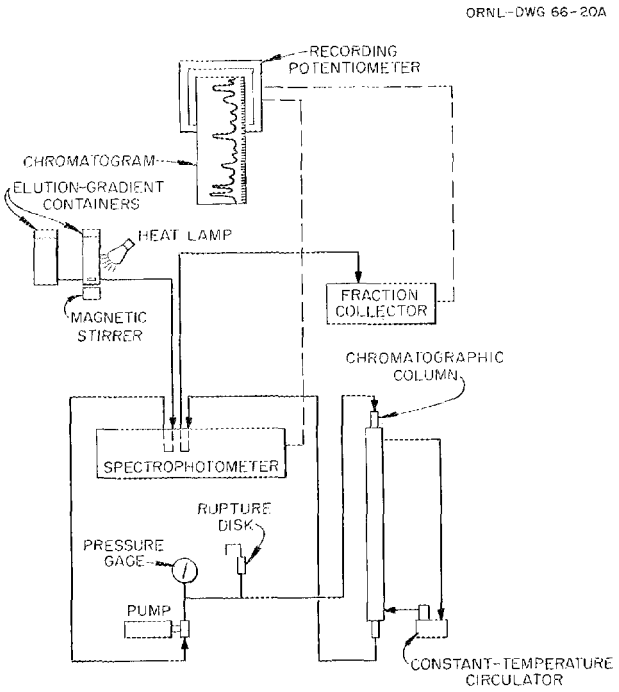

Fig. 12.7. Modified Nucleotide Analyzer for Urinalysis.

wavelengths is used for detection (Fig. 12.7). There are also provisions for temperature control of the column, volumetric measurement or collection of the column effluent, and continuous recording of the spectrophotometer output. A urine chromatogram is developed by placing a urine sample (1 to 2 cc) on the anion exchange column and eluting with ammonium acetate solutions ranging in concentration from 0.015 to 3 *M* at a pH of 4.4. A typical chromatogram takes about 40 hr and gives 60 to 80 peaks (Fig. 12.8).

Urine chromatograms from different people exhibit many differences but also many similarities, such as large peaks for uric acid and hippuric acid. Some of the differences can be attributed to diet. Figure 12.8 shows a comparison between the urine of a normal subject on a high-protein, low-vegetable diet and urine from the same subject on the same diet with the addition of coffee and aspirin. Several new chromatographic peaks appear with the addition of coffee and aspirin.

Twenty-seven urine samples (24-hr composites) from normal subjects have been collected and processed, and 48 tests with urine have been made with the analyzer. There has been no apparent loss of resolution, and reproducibility is adequate.

Identification of Separated Urine Constituents

Urine constituents indicated by the chromatogram are being tentatively identified by determining the position and the 280 mμ/260 mμ absorbance ratio of known standard peaks in the urine chromatogram and comparing them with unknown peaks. This gives two independent means of comparison, both of which should be characteristic of specific constituents. The positions of 20 standard peaks have been established, and 11 peaks have been tentatively identified in urine samples (Fig. 12.8). These are:

Xanthine	*p*-Hydroxycinnamic acid
Hypoxanthine	Homovanillic acid
Urocanic acid	Vanillic acid
Uric acid	Kynurenic acid
Hippuric acid	Salicylacetic acid
p-Hydroxybenzoic acid	

Identification depends on isolating very nearly pure components in each of the chromatographic peaks. Some tests were made in which effluent fractions were collected, and uv absorption spectra were made of several such fractions within a few of the single chromatographic peaks. The absorption spectra were different for some of the fractions collected within the same chromatographic peak, indicating more than one component in the single peak. Recent tests with ion exchange columns giving higher resolution also show that some chromatographic peaks are composed of several constituents. For example, the uric acid peak can be resolved into at least six others. This shows the importance of obtaining the greatest possible resolution in the anion exchange columns before definite identification can be made.

Another method for verifying the identity of the chromatographic peaks will be by a technique developed by Cohn[3] and others in which absorbance ratios of the purified unknown at different pH's are used for characterization.

Ion Exchange Properties and Column Resolution

The separating power of the ion exchange column must be increased to circumvent the problem of peak identification and to make it possible to quantify the urine constituents. Anderson *et al.*[2] found in their earlier work that different batches

[3]W. E. Cohn, *J. Biol. Chem.* 235, 1488 (1960).

of the same ion exchange material (Dowex 1-X8) had different separation powers for the nucleotides and related compounds; however, the reasons for these differences were not determined.

Recent results show that particle size of the ion exchange resin is very important. A continuous water elutriation system was designed and built to classify the resin. This system is composed of a 4-in.-ID elutriation column, a constant-level water feed system with flow rate control, a slurry pump for resin feed, and product receivers for the overhead and bottom fractions. The column is composed of a section of constant diameter at the top for feed introduction and particle sizing and a lower tapered section where fines are resuspended.

The system is capable of separating resin into different sizes in the diametral range of 5 to 50 μ. The overhead fraction is closely sized in one pass, but the bottom fraction usually requires two or three passes to remove all the small particles.

A batch of anion exchange resin (Dowex 1-X8), known to be good for nucleotide separation, was separated into three size ranges: 5 to 10 μ, 10 to 20, and larger than 20. These materials were loaded into identical stainless steel columns, 0.45 cm inside diameter $\times$ 150 cm, and urine samples were separated on each by using the same operating conditions except for pressure. The smaller resin particles gave much better separation. A semiquantitative indication of the separating power is a comparison of the number of chromatographic peaks resolved in each case:

Resin Size (μ)	Number of Peaks	Initial Pressure (psig)
5–10	66	1500
10–20	55	580
>20	42	350

The best separation was obtained with a stainless steel column, 0.62 cm inside diameter $\times$ 150 cm, filled with 5- to 10-μ resin and operating at 1500 psig. Ninety-three urine chromatographic peaks were resolved, compared with 60 for the original system.

Other properties of the ion exchange resin and the effects of different column parameters are also being investigated.

Development of Equipment

High-pressure operation is necessary to take advantage of the high resolution of small resin particles. Stainless steel columns were designed and built for operation at pressures up to 4000 psig. They are simple to make and use. A method of sample injection based on the use of two three-way valves also proved satisfactory. Here, part of the delivery line is used as a sample holder, and the sample is flushed through the line into the columns with the normal delivery of the elution system.

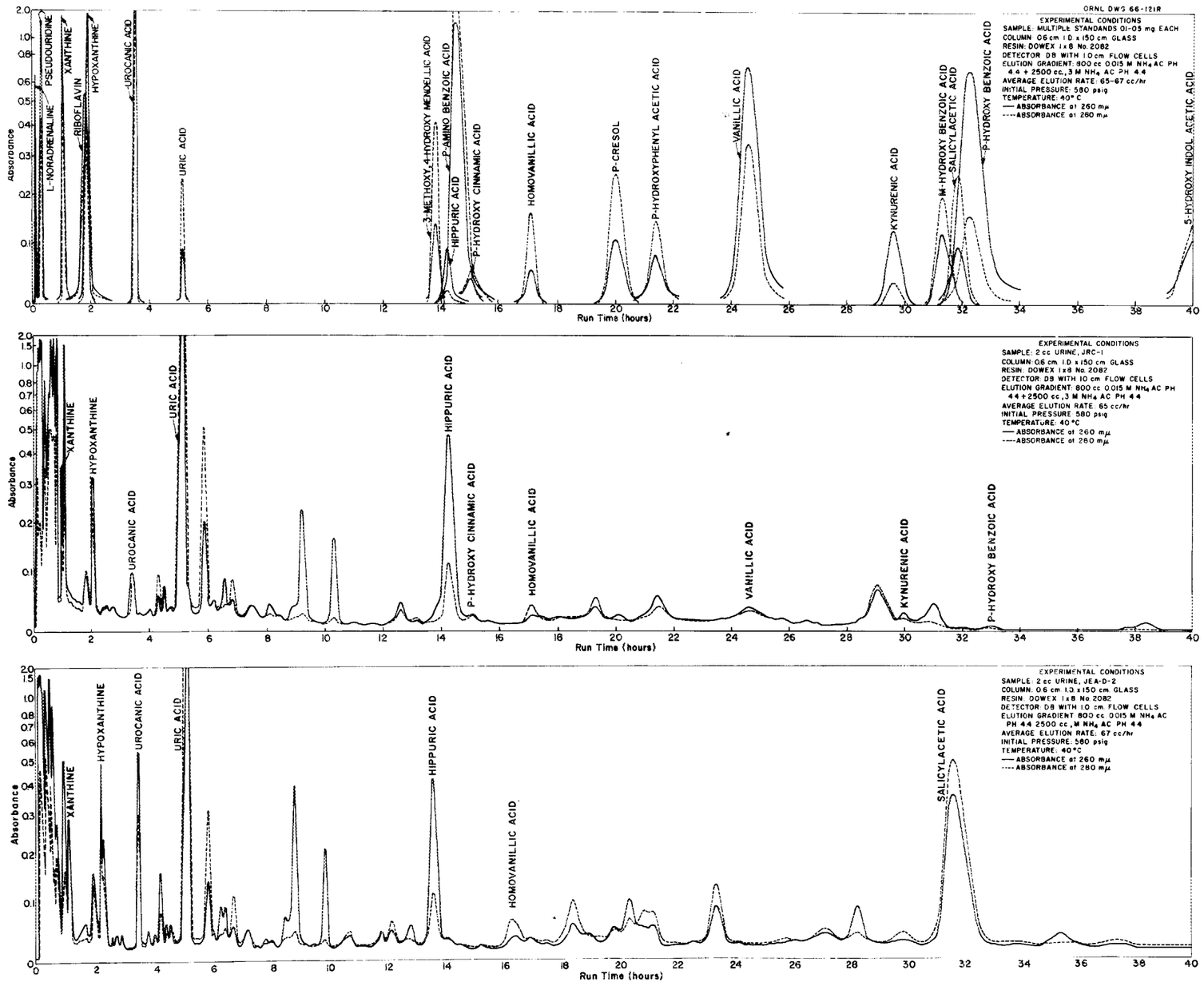

Fig. 12.8. Typical Urine Chromatograms and Tentative Identification of Eleven Peaks by Comparison with Chromatographic Positions of Standard Compounds. ——— absorbance at 260 mμ; ------ absorbance at 280 mμ.

13. Chemistry of Protactinium

The purpose of this program is to study the chemistry of protactinium, particularly in systems potentially applicable to chemical separations processes, and to relate its properties to those of the other actinides. In most aqueous solutions, protactinium does not behave in a simple or reproducible manner, and its chemistry cannot be predicted with much certainty. This program is being extended to the study of actinide elements other than protactinium, in certain cases, and the experimental techniques developed here will be applied to these studies.

13.1 CHEMICAL BEHAVIOR IN SULFURIC ACID SOLUTIONS

Study of sulfuric acid solutions of protactinium was continued, with emphasis on the preparation of a solid protactinium sulfate compound. Various measurements were made with the compound so that the initial state of the protactinium would be known better than it had been for previous work, in which the starting material was oxide or hydroxide. Solubility measurements were in reasonable agreement with previous ones, and indicate that minimum solubility occurs in concentrated sulfuric acid, with higher solubilities in either dilute or fuming acid.

Extraction experiments reported last year were continued in the system 2.5 *M* H_2SO_4 vs 0.03 *M* trilaurylamine in diethylbenzene solvent. Results were entirely consistent with those in last year's annual report[1] and further supported the conclusions discussed there. A summary of this work was presented at the Second International Symposium on Protactinium Chemistry, La Physicochemie du Protactinium, held at Orsay, France, in July 1965; the papers presented at the meeting have not yet been published.

Protactinium Sulfate Compound

A small amount of a protactinium sulfate compound (50 mg of protactinium) was made according to the procedure used by Bagnall and Brown at Harwell.[2] The method includes the addition of protactinium in HF solution to a large excess of concentrated sulfuric acid, followed by heating to distill away the HF and, finally, to fume away part of the sulfuric acid. Small crystals form as the HF is removed, and the solubility of protactinium in concentrated sulfuric acid is low enough that nearly all of it is recovered as the solid compound.

The solid is washed first with concentrated sulfuric acid, then with a few tenths of a milliliter of nitrobenzene to remove excess sulfuric acid, and finally with the same volume of benzene to remove the nitrobenzene. The final product is dried by warming gently under a vacuum. It is difficult to achieve quantitative removal of excess sulfuric acid from the crystals without contaminating them with water or other materials with which they might react.

Analysis of the product showed 69.0% sulfate and 34.8% protactinium, for a material balance of 103.8%. The sulfate/Pa mole ratio was 4.77, a value substantially different from that (3) reported by Bagnall and Brown. The high ratio might be explained by incomplete removal of sulfuric acid during washing.

With the cooperation of O. L. Keller, of the Chemistry Division, and R. L. Sherman, of the

[1] *Chem. Technol. Div. Ann. Progr. Rept. May 31, 1965*, ORNL-3830, p. 228.

[2] K. W. Bagnall, D. Brown, and P. J. Jones, *J. Chem. Soc.* 1965, p. 176.

Analytical Chemistry Division, a good x-ray diffraction pattern was obtained on this compound. It has not been examined in detail but is qualitatively very similar to that reported by the Harwell group for their compound, stated to be $H_3PaO(SO_4)_3$.

Since a single-crystal study would help to determine the structure of the compound, several attempts, all unsuccessful, were made to grow larger single crystals (up to several tenths of a millimeter). A preparation on a larger scale is planned, using carefully dried solvents to remove the excess sulfuric acid. Since the x-ray method of crystal-structure determination may be very useful, both for protactinium and other actinide work, an x-ray powder camera was purchased and modified for better containment of the sample so that it can be used to study alpha-active materials.[3]

Solubility of Protactinium in Sulfuric Acid Solutions

Previous solubility measurements of protactinium in sulfuric acid solutions, when the oxide or hydroxide was the saturating phase, were not reproducibile. In an attempt to obtain more consistent results, recent studies were made with the sulfate compound as the saturating phase and high concentrations of sulfuric acid (less favorable to hydrolysis). Reproducibility could be obtained from a given mixture under certain conditions; but some changes, particularly the addition of more of the solid protactinium compound, caused apparent increases in solubility which, in most cases, were reversed very slowly if at all.

Four acid concentrations between 11.6 and 19.5 *M* (fuming) H_2SO_4 were investigated in detail. In all except the most dilute, the solubilities reached a constant value after a few days; in the 11.6 *M* solution, however, they continued to increase. After a week all four solutions were heated to 250–300°C, mixed, and then cooled to room temperature. Measurements made the next day were all 50 to 100% higher than those made before heating. All subsequently decreased and became constant after about two weeks. Except for the most dilute acid, the constant value was about the same as that before heating. Additional measurements were made during a period of seven weeks, and consistent results were obtained (column 2 of Table 13.1).

Table 13.1. Protactinium Solubilities Observed in Sulfuric Acid Solutions

H_2SO_4 Concentration (*M*)	Pa Solubility (mg Pa/ml)			
		After Adding More Pa (days)		
	Initial	2	6	10
19.5	0.024	0.11	0.11	0.11
17.4	0.019	0.11	0.088	0.045
14.4	0.036	0.13	0.16	0.14
11.6	0.15	0.32	0.34	0.33

Although there was excess solid in all four solutions (determined by analysis and visual inspection), several milligrams more of the compound was added to each of the mixtures. Solubility increased substantially in each case (column 3); in only one, the 17.4 *M* acid, did it subsequently drop significantly and appear to be approaching its initial value.

This experiment demonstrates the difficulty in obtaining meaningful solubility data for protactinium. It is clear that such measurements are not promising as a means of gaining information about complexing or the molecular species in solution.

13.2 ABSORPTION SPECTRA IN SULFURIC ACID SOLUTIONS

Preliminary results of some absorption spectra of protactinium in concentrated sulfuric acid were reported last year. These studies were continued and extended to dilute acid solutions. Recent attempts to resolve the complex spectra into individual bands indicated that spectroscopy may yield information about the soluble species. Qualitatively, a striking similarity was observed for the spectra of protactinium and of uranyl ion in the same range of the ultraviolet spectrum.

Three distinctly different spectra were observed in concentrated sulfuric acid, depending on the source or treatment of the protactinium (Fig. 13.1). Curve *A* represents the usual spectrum, with a

[3]R. L. Sherman and O. L. Keller, *Rev. Sci. Instr.* **37**, 240 (1966).

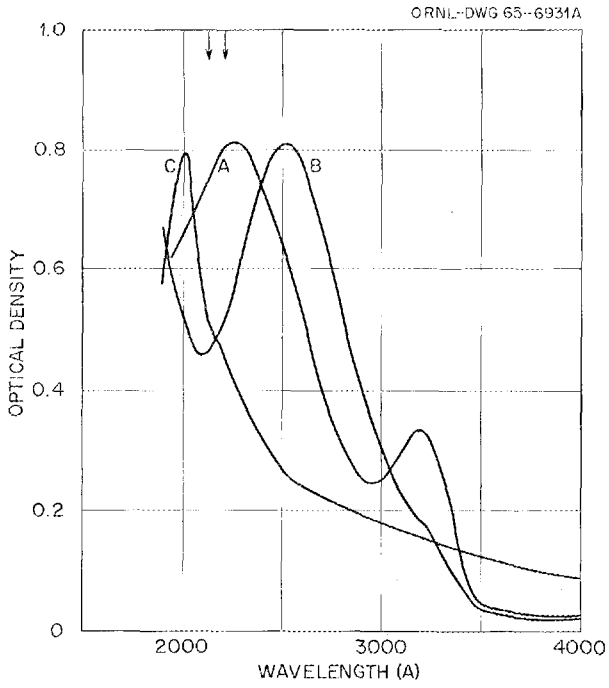

Fig. 13.1. Different Spectra Observed for Protactinium in 18 *M* H_2SO_4.

peak near 2260 A (the apparent peak at 3200 A results from the action of sulfuric acid on trace organic impurity). Such spectra are typically obtained from solutions prepared by dissolving purified protactinium hydroxide or oxide in concentrated sulfuric acid or by spiking concentrated sulfuric acid solutions with dilute acid solutions of protactinium. Leaching of the original Harwell oxide with concentrated sulfuric acid gave a solution having a similar absorption band, but displaced to 2180 A. With repeated leaching of the same oxide, the apparent solubility decreased, the peak height also decreased, and the peak moved to a slightly shorter wavelength.

Spectrum *B* resulted from a solution prepared by leaching a sample of impure oxide with concentrated sulfuric acid. Two peaks are noted: one at 2500 A (well defined) and one below 2000 A. This spectrum is distinctly different from any reported in the literature. Repeated leaching of the same oxide with fresh concentrated sulfuric acid gave solutions with similar spectra, except that the solubility and absorption were both markedly less and the peaks were not so well defined. We were unable to reproduce this spectrum when protactinium from any other source was used, or to convert this material, by any simple chemical treatment, to that which gave curve *A*. Neither hydroxide precipitation (after addition of chloride or fluoride) nor ignition to the oxide was effective. After repurification of the oxide by the standard ion exchange procedure, a spectrum similar to curve *A* was observed. We have no explanation for this spectrum (*B*), except that it might be the result of double-salt formation or of a complex of protactinium with some unknown impurity.

Spectrum *C* was obtained from either of the above solutions (that gave curve *A* or curve *B*) by heating to the temperature of fuming of sulfuric acid or, better, by fuming the solution nearly dry and redissolving in concentrated acid. As discussed previously, this is essentially the procedure used to prepare the solid compound, reported to be $H_3PaO(SO_4)_3$. Spectrum *C* is characterized by a very sharp (for protactinium) peak at about 2000 A and a shoulder near 2200. The solution that initially gave curve *B* (before heating) showed an additional shoulder near 2550 A.

All the spectra described were quite stable. The only change within several weeks occurred in the solution that gave spectrum *C*, and which was derived by heating the solution that initially gave spectrum *B*. After two weeks the major peak near 2000 A decreased in height about 20%, and the 2200-A shoulder grew somewhat.

Brief studies were made of the effect of dilution with water (simultaneous dilution of both acid and protactinium). Dilution of the solution that gave curve *A* yielded a broad band that was displaced to a shorter wavelength, about 2030 A, in 2.5 *M* acid. Dilution of the solution that gave curve *B* resulted in a rapid decrease in the peak at 2500 A and the appearance of shoulders (below 10 *M* acid) at about 2300 and 2800 A (Fig. 13.2). The spectra of both solutions, after dilution to 2.5 *M* acid, were quite similar; the difference observed for concentrated acid disappeared after dilution.

Dilution of the solution that gave curve *C* to 2.5 *M* acid, however, resulted in a different spectrum (Fig. 13.3). The peak near 2000 A remained reasonably sharp, and a second, well-defined peak appeared near 2800 A. A shoulder often occurs near 2800 A and is reported in the literature, but it is not so well defined as in this case.

Any explanation of the three different spectra is tentative at best. As stated above, none is

offered for spectrum *B*. The spectra *A* and *C*, however, are readily reproduced, and the difference between them is almost certainly related to the effect of heating. Fuming in concentrated sulfuric acid has an extremely strong dehydrating action, and is the operation used to yield the compound reported to be $H_3PaO(SO_4)_3$. Therefore, the sharp band observed in spectrum *C* is very likely associated with the $PaO(SO_4)_3^{3-}$ anion or a species in equilibrium with it. The difference between this band and spectrum *A*, to a first approximation a broadening of the band and a shift to longer wavelength, might result from hydration, polymerization, or both. Hydration would not ordinarily be expected in concentrated sulfuric acid, but condensed species of protactinium are unusually stable. These processes would result in Pa–OH or Pa–O–Pa bonds rather than in the Pa–sulfate and Pa=O configuration of the trisulfate ion. The latter might be somewhat like the metal-oxygen actinyl bond.

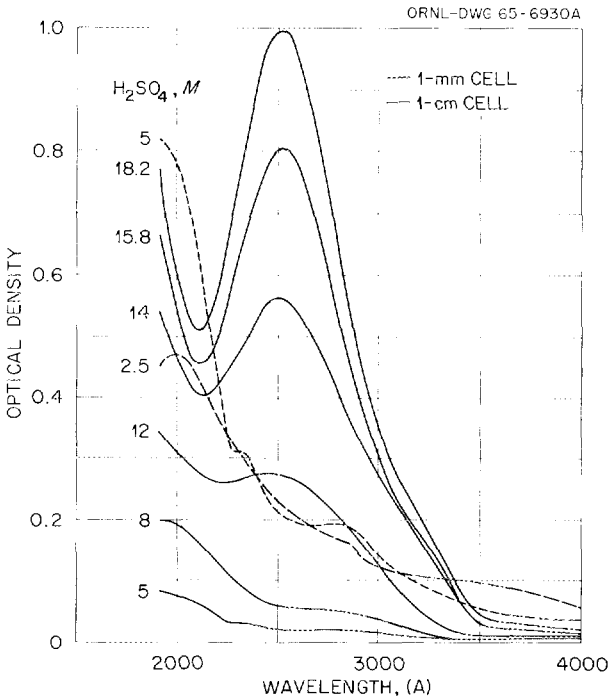

Fig. 13.2. Effect of Dilution on Protactinium with Absorption Peak at 2500 A.

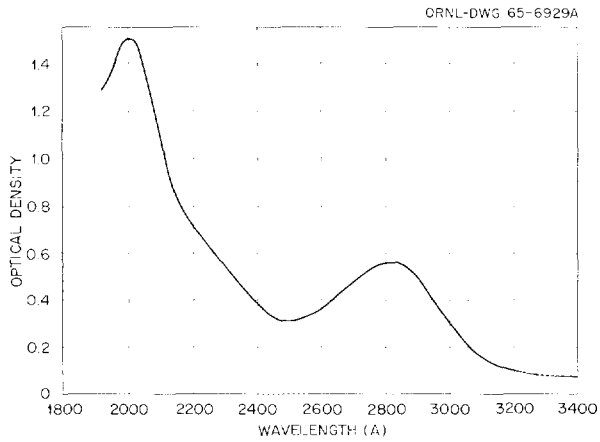

Fig. 13.3. Effect of Dilution on Protactinium with Absorption Peak at 2000 A. Compare with curve C, Fig. 13.1.

Resolution of Spectra

A computer code was developed at Oak Ridge National Laboratory for resolving overlapping spectra and was applied to the study of the absorption spectra of the uranyl ion[4] (Sect. 15.3). To date, only two protactinium spectra have been studied in this manner, but the work is continuing.

The first, the spectrum shown in Fig. 13.3, was studied after subtracting an estimated correction for light scattering (inverse fourth power of the wavelength, based on absorption in the range 3600 to 4000 A, in which protactinium does not absorb). Two band models were used. One included three bands, the obvious ones at 2800 and 2000 A, and a third near 2300 A, where a shoulder appears (Fig. 13.4; the stars are experimental points, and the lines are the individual bands and their sums). All subsequent discussion is in terms of wave numbers (cm^{-1}) rather than wavelengths (A) because the resolution is done in units of wave numbers: $cm^{-1} \cdot A = 10^8$. The result did not give a good fit to the band at 35,500 cm^{-1}. This band is not symmetrical, and it is necessary to postulate two bands in this region to better fit the data. A calculation with four bands (Fig. 13.5) gives a very good fit; the standard deviation is 0.0048 in absorbance units.

The second spectrum resolved by the computer code is a typical one for protactinium in 2.5 *M* H_2SO_4. The results for models using three bands (Fig. 13.6) and four bands (Fig. 13.7) show little difference in fit; thus there is small justification

[4]J. Bell and R. J. Biggers, *Mol. Spectr.* **18**, 247 (1965).

on this basis for a choice between them. Two bands could not account for the observed spectrum.

If the two resolved spectra are compared, it is clear that some bands are quite similar in position and width, while others are not. The source of the protactinium in the two cases is quite different, and it is not unreasonable that some of the bands should be different. We plan to continue this work in order to determine whether any similarities of band positions and shapes, and systematic changes in band intensities, can be correlated with changes in protactinium concentration, acidity, or other experimental variables.

The data farthest into the ultraviolet, near 50,000 cm^{-1} (2000 A), are subject to question because this is near the limit of the range of the spectrophotometer. As this limit is approached, the slits open rapidly and absorbance readings may be substantially in error. Calculations were made in which the data at the left-hand end of the curves were ignored, and the resulting parameters were not changed greatly. There was evidence, however, that the rather broad, experimentally observed band in the region of 50,000 cm^{-1} might result from two overlapping bands, one near 48,000 cm^{-1} and the other above 50,000. Since it is

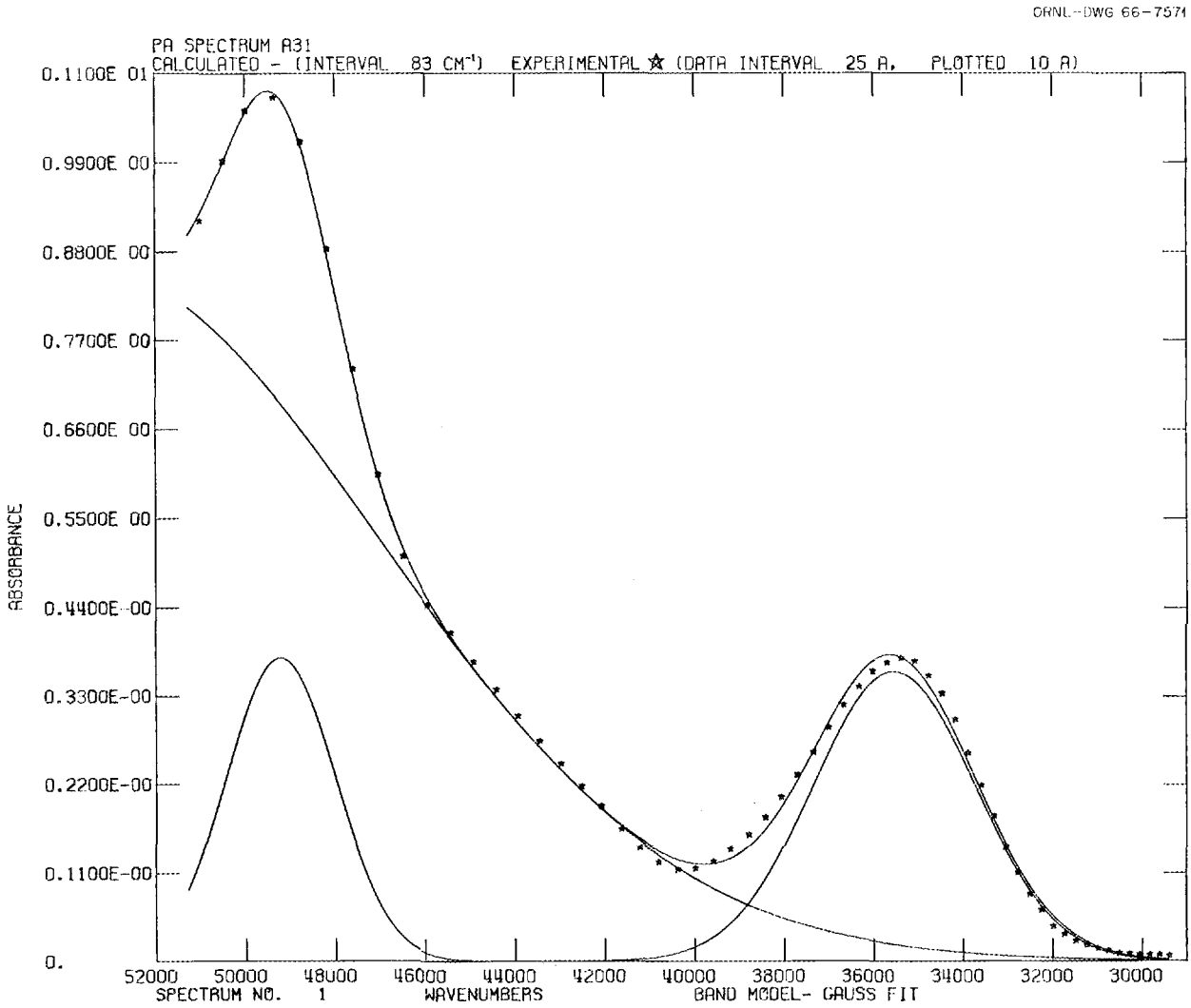

Fig. 13.4. Protactinium Spectrum Resolution with Three-Band Model.

probably impossible to obtain data much beyond 52,000 cm^{-1}, it is unlikely that this question can be resolved with certainty.

During the spectrum-resolution work described above, the observation was made that the ultraviolet spectrum of protactinium is strikingly similar to that of uranyl solutions in the same range of wavelength. Also, the resolved bands had roughly the same spacing. If this observation can be supported by additional study, it could have considerable significance, because uranium and protactinium presumably have very different structures. In particular, protactinium strongly resembles niobium and tantalum in solution, rather than uranium, and it is generally agreed in the literature that the PaO_2^+ ion is quite unstable if it exists at all.

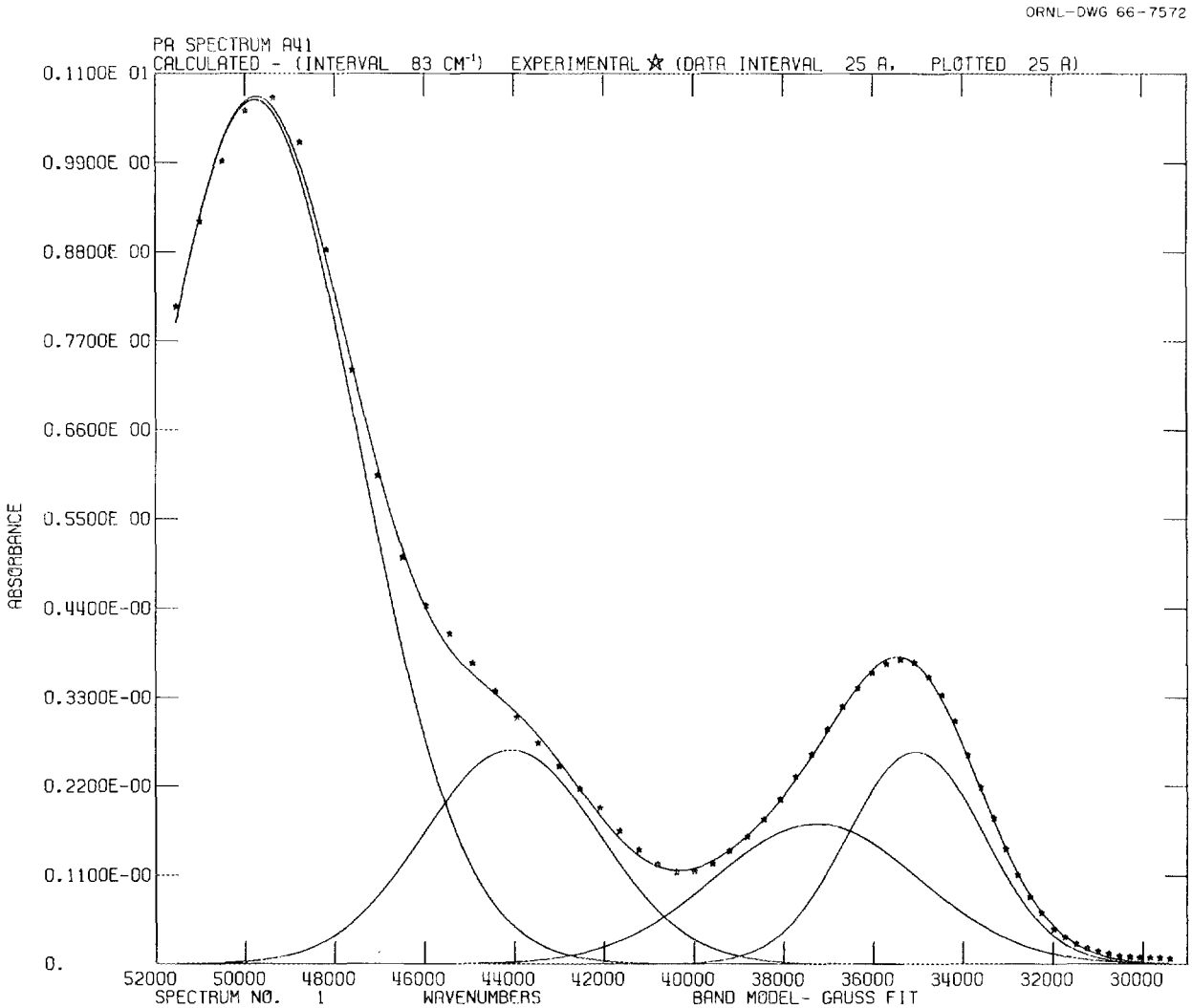

Fig. 13.5. Protactinium Spectrum Resolution with Four-Band Model.

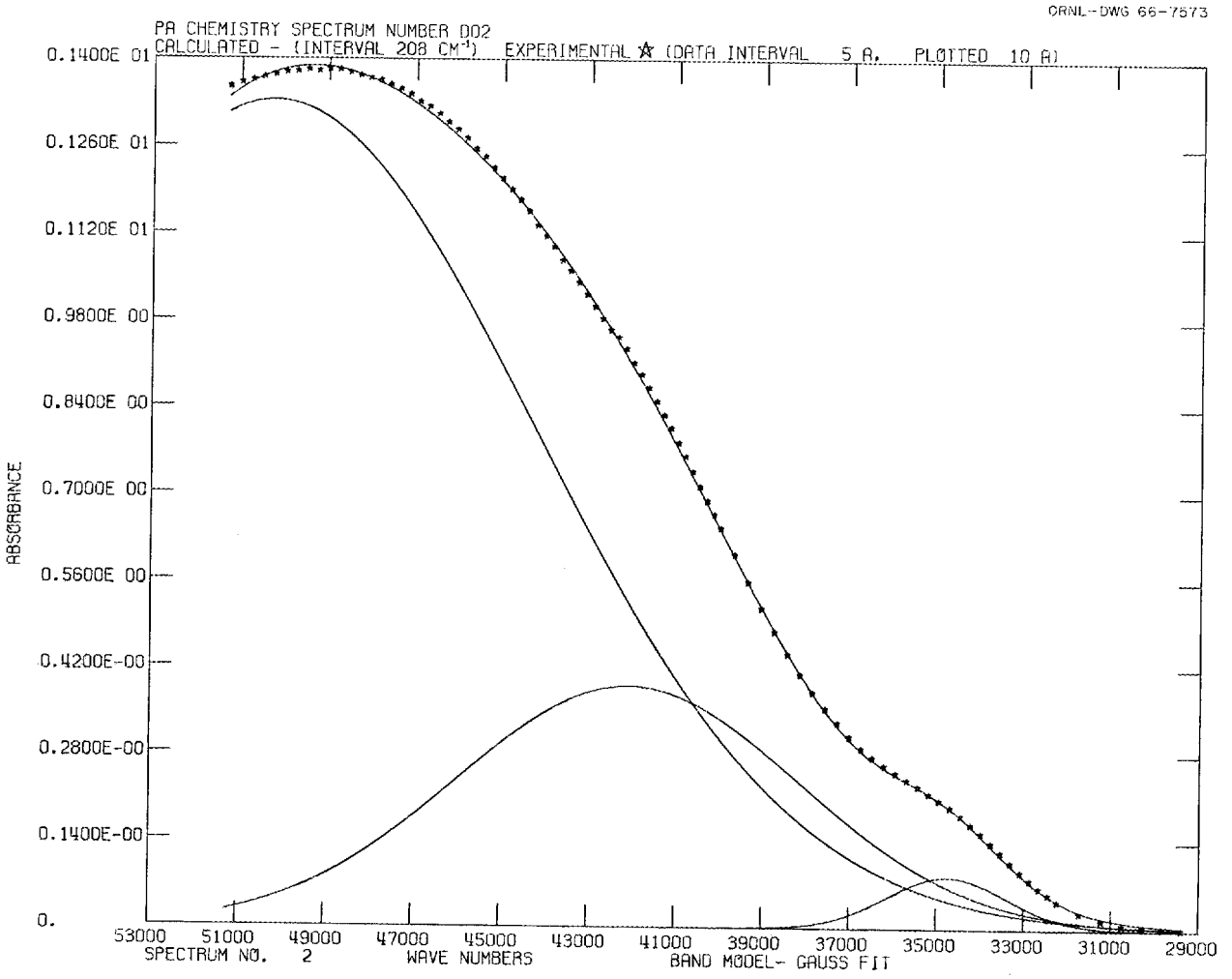

Fig. 13.6. Protactinium Spectrum Resolution with Three-Band Model.

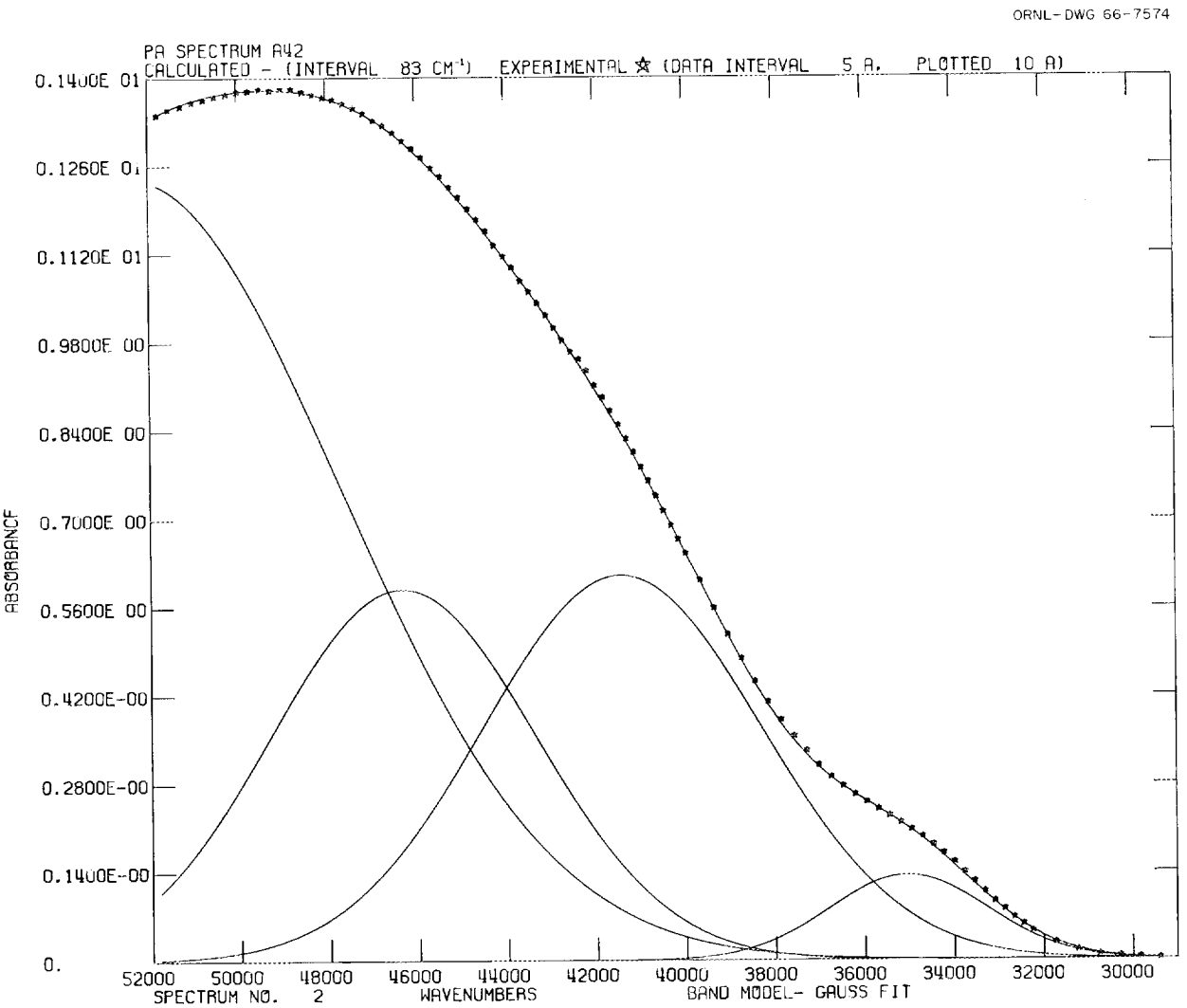

Fig. 13.7. Protactinium Spectrum Resolution with Four-Band Model.

13.3 STUDIES WITH HYDROCHLORIC ACID SOLUTIONS

Efforts to correlate ultraviolet absorption spectra with the nature of the protactinium ion present in strong HCl solutions were unsuccessful. No bands could be located which could be unambiguously ascribed to absorption by the protactinium. Solubility measurements in strong HCl showed that fluoride ion, or one of its complexes, is the only common inorganic ion that affects the solubility of protactinium oxide. An anion exchange procedure was shown to be useful in separating protactinium from a mixture of oxides, but the separation is very slow at room temperature.

Ultraviolet Spectrophotometric Studies

Several studies have been reported in the literature relating to the ultraviolet absorption spectrum of protactinium dissolved in strong (7 to 10 *M*) HCl.[5] These agree generally, but not precisely, and report a strong band centering approximately at 2130 A and a weaker band at approximately 2600; the latter is attributed to polymeric protactinium by some investigators. In the present study, all the first spectra obtained showed a

[5]D. Brown and A. D. Maddock, *Quart. Rev. (London)* 17, 325 (1963).

peak at 2700 A, which was approximately proportional to the protactinium concentration; some of the solutions showed a second, higher peak at 2085 A also. The height of this peak could not be correlated with the concentration of the protactinium.

Experiments were carried out in 10 *M* HCl solutions prepared from materials of the highest purity obtainable. The spectra were obtained immediately after preparation to minimize the effect of chlorine produced by radiolysis. During this investigation, the spectrum of HCl was determined down to the lower limit of the Cary model 14 spectrophotometer (approximately 1940 A). If the absorption was measured against water as a reference, then it increased steadily with decreasing wavelength below 2170 A. There was no evidence of a peak or a shoulder.

The final protactinium spectra were obtained by comparing the solutions with water (as a reference solution) and manually subtracting the spectrum of an identical HCl solution without the protactinium. These spectra showed no absorption above 2700 A and a steady increase in absorption at lower wavelengths. The molar extinction coefficient increased approximately linearly with decreasing wavelength to a value near 10^4 at 2100 A, but no absorption peak was observed.

Solubility in Hydrochloric Acid

The solubility of Pa_2O_5 in hydrochloric acid of various molarities was determined by batch equilibrations. At HCl concentrations below 6.5 *M*, the protactinium concentration was less than 5 mg/liter. Lower values could not be determined by alpha-pulse analysis because of preferential dissolution of the elements in the protactinium decay chain. Above 6.5 *M* the solubility increased markedly. For example, in 7.05 *M* HCl the solubility was 6.1 mg/liter; in 9.63 *M*, 29.0 mg; in 11.42 *M*, 67.8 mg.

Since it was believed that protactinium might form double ions with other inorganic ions and thus change its solubility, the amount dissolved in 9 *M* HCl containing 1 to 2 m*M* concentrations of various foreign ions was determined. None of these ions (Ca, NH_4, Al, K, Na) had any apparent effect on the solubility. However, silicofluoride ion, SiF_6^{2-}, in a concentration of 2.0 m*M*, increased the solubility tenfold over the solubility in acid without the impurity. This indicates qualitatively that the protactinium-fluoride complex is at least as strong as the silicon-fluoride complex. Studies on the solubility of Pa_2O_5 in 9 *M* HCl, 1 to 10 m*M* in fluoride ion, gave quite unexpected results. It was known from previous work in processing gram amounts of protactinium that, in 8 *M* HCl–0.4 *M* HF, solubilities greater than 5 g of protactinium per liter could be obtained easily (F/Pa approx = 18). In the present study, with an excess of protactinium oxide, the amount of protactinium in solution, after two days of agitation at room temperature, was proportional to the fluoride concentration (F/Pa approx = 12). Further agitation of these solutions for periods up to six weeks raised the solubility to approximately 200 mg/liter for all solutions.

14. Irradiation Effects on Heterogeneous Systems

14.1 RADIOLYSIS OF WATER IN THE ADSORBED STATE

The study of irradiation effects on heterogeneous systems was continued, using water adsorbed on various solids having high specific surface areas. It was previously observed that when water was adsorbed on silica gel, the yield of hydrogen gas obtained upon radiolysis was greatly enhanced.[1] The mechanism of this phenomenon, however, was not clear, so the study was extended to include alumina, silica-alumina, activated carbon, gold supported on silica gel, platinum supported on silica gel, and various molecular sieves as adsorbents to see if relationships between the properties of the solid and the amount of radiolysis enhancement could be deduced. The goal of these studies is to determine the mechanisms by which adsorption sensitizes molecules to radiation-induced chemical reactions and, if possible, to apply such knowledge to the chemonuclear and radiation-catalytic production of useful chemicals.

Experimental

The beta-radiation source used as a source of ionizing radiation has been described elsewhere.[2] The yield of hydrogen is measured by periodically flushing the gas accumulated in the irradiation vessel through a gas chromatograph. Hydrogen is normally the only radiolysis product observed. The yield is measured as a function of the water content of the system, including structural water present in the adsorbent. The adsorbents are all pretreated by soaking them in distilled water and drying them at 150°C overnight.

The water content of the dried material is estimated from weight loss upon heating to 1000°C. Additional water is added by exposure to water vapor; the amount added is determined by weight gain. At the conclusion of the radiolysis tests, during which a negligible amount of water is destroyed, the irradiation chamber is heated to 150°C, and the emitted water vapor is collected in a Drierite trap to provide a check on the water content. To obtain data points using samples with less water than that contained in the 150°C dried material, the solids were heated to a temperature predetermined by thermogravimetric measurements to give the desired amount of water. Specific surface areas of the adsorbents are given in Table 14.1.

Results

As in the tests with silica gel, the evolution rate of hydrogen by radiolysis of water on the above adsorbents varied with irradiation time. Figure 14.1 shows some typical results for the various

Table 14.1. Specific Surface Areas of Adsorbents

Material	BET Surface Area (m^2/g)
Davison R-566 silica-alumina (13% alumina)	302
Fisher activated alumina	195
Merck acid-washed alumina	188
Norton Zeolon H molecular sieve – unpelleted	398
Silica–5 wt % Pt	730
Silica–9.5 wt % Au	643
Activated carbon	1093

[1] *Chem. Technol. Div. Ann. Progr. Rept. May 31, 1965*, ORNL-3830, pp. 233–35.

[2] N. A. Krohn, *Nucleonics* 23(5), 83 (1965).

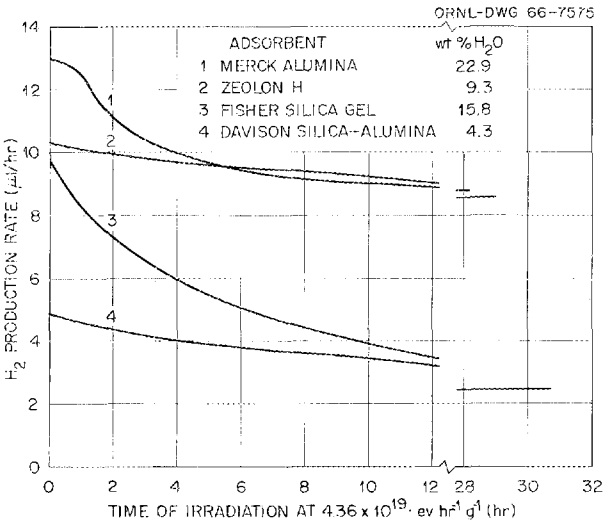

Fig. 14.1. Effect of Irradiation Time on the Hydrogen Yield from the Radiolysis of Adsorbed Water.

types of adsorbents. The rate of hydrogen evolution normally decreases with time under irradiation, but maximum yields can ordinarily be restored by heating the adsorbent in its own water vapor at 150°C for an hour or two. An exception was noted with silica-alumina, where this treatment led to a substantial increase in the hydrogen yield.

Maximum $G(H_2)$ values are shown in Fig. 14.2 as a function of the electron fraction of water. The behavior when silica-alumina is used as the adsorbent is very similar to that previously reported for silica gel, that is, a sharp rise in $G(H_2)$ that reaches a maximum at an electron fraction of water of about 0.11 and then drops off as more water is added. The maximum $G(H_2)$ of 1.85 compares with 1.72 for silica gel, although the specific surface area was only 302 m^2/g, compared with 682 m^2/g for silica gel. Thus, while comparable on a weight basis, the silica-alumina is more than twice as efficient per unit of surface area, perhaps because of the more acidic nature of the surface. The $G(H_2)$ value of 2.12 measured at an electron fraction of water equal to 0.085 appears to be a spurious result.

The curves obtained when using alumina as the adsorbent were markedly different, being characterized by a rather slow increase of $G(H_2)$ with water content, with no sharp maximum. The difference may be caused by differences in the nature of binding of the water. With the silica gels, water was present mainly on the surface, either as silanol groups or as adsorbed water molecules. In the case of alumina, water is present throughout the solid as water of hydration. Again, the greater hydrogen yields from the acid-washed alumina may be related to the presence of more surface acidity as a result of the washing.

The radiolysis of water on molecular sieves was found by Sutherland and Allen to give hydrogen yields proportional to the electron fraction of water, with a $G(H_2)$ of about 0.1 at an electron fraction of 0.1; they concluded that there was no energy transfer from the solid to the adsorbed water.[3] From later studies on the radiolysis of azoethane on magnesium oxide, however, Allen and co-workers suggested that energy-transfer efficiency increased with increasing perfection of crystallinity.[4] Therefore, it was decided to investigate molecular sieves more extensively. Tests with Linde 4A (sodium form) and 5A (calcium form) sieves gave somewhat higher yields than found by Allen, but they were still too low to be of much interest. In line with the idea that acidic sites might be important, however, the molecular sieve Norton

[3] J. W. Sutherland and A. O. Allen, *J. Am. Chem. Soc.* **83**, 1040 (1961).

[4] J. G. Rabe, B. Rabe, and A. O. Allen, *J. Am. Chem. Soc.* **86**, 3887 (1964).

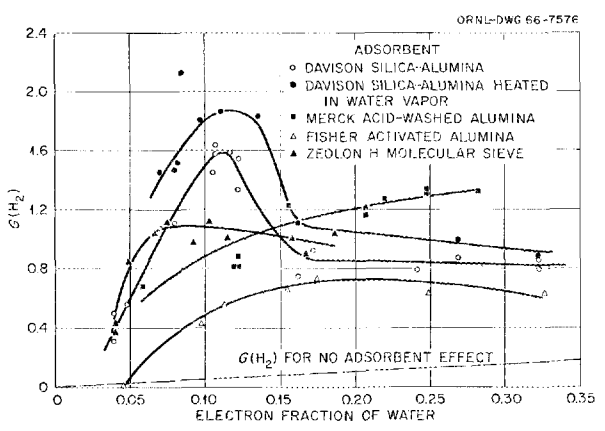

Fig. 14.2. Values of $G(H_2)$ for the Radiolysis of Adsorbed Water.

Zeolon H was tried in the present studies. In this material, sodium ions have been replaced by hydrogen. As shown by the results in Fig. 14.2, the hydrogen yield is greatly enhanced by this particular material, though it is still not as effective as silica gel or silica-alumina. Thus, the crystallinity of the adsorbent does not seem to be important to the enhanced radiolysis.

Activated carbon, platinum-silica, and gold-silica were only briefly investigated as adsorbents. The $G(H_2)$ values were a few hundredths for the first two, just about what would be expected from the electron fraction of water. The gold-silica combination had some effect, the hydrogen yields being about one-fourth of those obtained when using silica gel of comparable surface area. The hydrophobicity of carbon, the affinity of platinum for hydrogen, and the electrical properties of the solids are all involved here, and no firm conclusions can be made from the few experiments carried out.

15. High-Temperature Chemistry

The purpose of this program is to develop and exploit spectrophotometric techniques for studying the properties of aqueous solutions, primarily those of uranium and the transuranium elements. A spectrophotometer, associated cells, and related systems were specially designed for ORNL by the Applied Physics Corporation (APC) to aid in these studies. The spectrophotometer was built by APC, and all the related equipment was built by shops at Oak Ridge. The overall system is designed so that the chemistry of solutions containing alpha-active heavy elements can be studied. The system will permit the study of the solution chemistry and the spectral properties of elements in solution up to the vicinity of the critical point of water, 372°C.

During the time that the spectrophotometer system was under construction and during the installation and checkout period, studies at temperatures up to 95°C were done with a Cary model 14 spectrophotometer on uranyl systems of interest in perchlorate and other media. To aid in the analysis and interpretation of spectroscopic data, computer analyses of spectra and other ancillary experimental techniques were developed.

15.1 FABRICATION AND INSTALLATION OF THE SPECTROPHOTOMETER SYSTEM FOR USE WITH HIGH LEVELS OF ALPHA-ACTIVE ELEMENTS

The spectrophotometer system was constructed by the Applied Physics Corporation, the Engineering and Construction Division at the Oak Ridge Gaseous Diffusion Plant (ORGDP), and the Special Projects Shop at the Y-12 Plant. The overall program for the construction of the spectrophotometer system was started in September 1964, and the main spectrophotometer was delivered by APC in October 1965.

The design of the system is such that solutions containing high levels of alpha-active elements of interest in heavy-element chemistry can be studied after the entire system is moved to a high-level alpha-containment laboratory; this relocation must be preceded by "cold" checkout and operation periods to prove the soundness, safety, and performance of the overall system.

Spectrophotometer

Installation and integration of the basic spectrophotometer unit with the ancillary equipment fabricated locally were begun the first part of October. Electronic instrument modifications necessary to couple the new spectrophotometer into our digital data output system (IBM card) were completed and checked out. Information obtained during several days of acceptance testing at APC showed that the resolution of the machine is somewhat better than that specified for the Cary model 14 spectrophotometer. The special high-vacuum cell compartment, which was fabricated at ORGDP, was not fully completed at the time of the tests, but this did not preclude adequate optical testing. Modifications were made to almost all items of the overall system; a number of changes in the spectrophotometer were made during its construction, as well as after its installation.

Cell Compartment

It was found that, when the cell compartment was evacuated, a deflection (maximum, about 0.050 in.) of the walls ($\frac{1}{2}$- and $\frac{3}{4}$-in.-thick T6 aluminum) occurred. This was eliminated by adding internal bracing, which was arranged so as not to interfere

with the cells and other internal pieces. Work was also necessary on the structural design of high-temperature fluid-line penetrations of the vacuum-chamber cell compartment. These lines can be disconnected; they are flexible and vacuum-tight and carry fluid (silicone oil) at temperatures up to 800°F. The cell compartment was examined for leaks in the shop; final tests, however, including those under operating conditions, remain to be done. The wearing of threaded bolt holes in the T6 (high-strength, heat-treated) aluminum was a problem, but it was eliminated by installing hardened steel Helicoil inserts into all threaded holes for compatibility with steel bolting. Now, the aluminum threads take only the load, which is not excessive, and have no abrasive wear from the stainless steel bolts. The cell rocker system will be made operable soon.

Vacuum System

The vacuum system for depressurization of the cell compartment to at least 10^{-6} torr was improperly tested for leaks, and a number of items had to be reworked. If outgassing of the myriad of items inside the cell compartment is a problem (for the most part they cannot be outgassed by baking), the addition of a hermetically sealed VacIon pump to the cell compartment will be indicated. This would be compatible with the use of the silicon solid-state alpha detectors installed inside the cell compartment for leak detection with high-level alpha operations.

A Consolidated Vacuum Corporation mass-spectrometer-type helium leak detector was put into service and is performing adequately.

Pump-Loop Heating System

The pump-loop heating system, which supplies thermostated high-temperature silicone heat-transfer fluid to the cell jackets and is intimately connected with the emergency and programmed cooling system, was delivered in December 1965. It was also "cold" tested for leaks (helium leak test). It has been partially installed, but has yet to be debugged electrically and mechanically and to be coupled to the cells via the cell vacuum compartment. This system underwent numerous necessary design changes and equipment item changes during fabrication.

Auxiliary Services

The installation of services, both to the facility and to the individual equipment items, is almost completed. This includes main power supply, electrical distribution and heavier power wiring, liquid-nitrogen and gas supplies, and all the standard laboratory services necessary for the spectrophotometer and other ancillary systems. The spectrophotometer monochromator was thermostated. An auxiliary roughing pump was provided for evacuation of the cell compartment before transferring the pumping load to the vacuum system.

Control Console System

The control console system (Fig. 15.1), fabricated at ORGDP, was completed and installed. A number of changes and additions are not shown. The equipment was preliminarily checked out while it was in the shop; detailed testing of the individual components is about 50% complete. A significant amount of miswiring in the control console system caused difficult checkout problems; these are being solved one by one. Making minor changes in the local shops rather than returning the items to the manufacturer was found to be more expedient from the point of view of convenience and time required, except in cases of significant equipment malfunctions and long-term warranty.

Part of the temperature control and programming system, designed and built by Minneapolis-Honeywell, was returned for changes and rework. The set-point generator and paper-tape reader did not perform according to specifications or the design intent.

A tape-read pulse supply, not included in the original design but necessary for the operation of the punched-paper-tape reader, was provided by the use of a Hamner timer.

Absorption Cells

Two of the three cells needed, and the essential parts, were fabricated. The cell body and an exploded view of the internal parts for one-half of the cell are depicted in Fig. 15.2. Tubing, valving, and pressure, differential pressure, and temperature transducers are not shown. The third cell will not be made until operating experience has been obtained with the present design, since operation

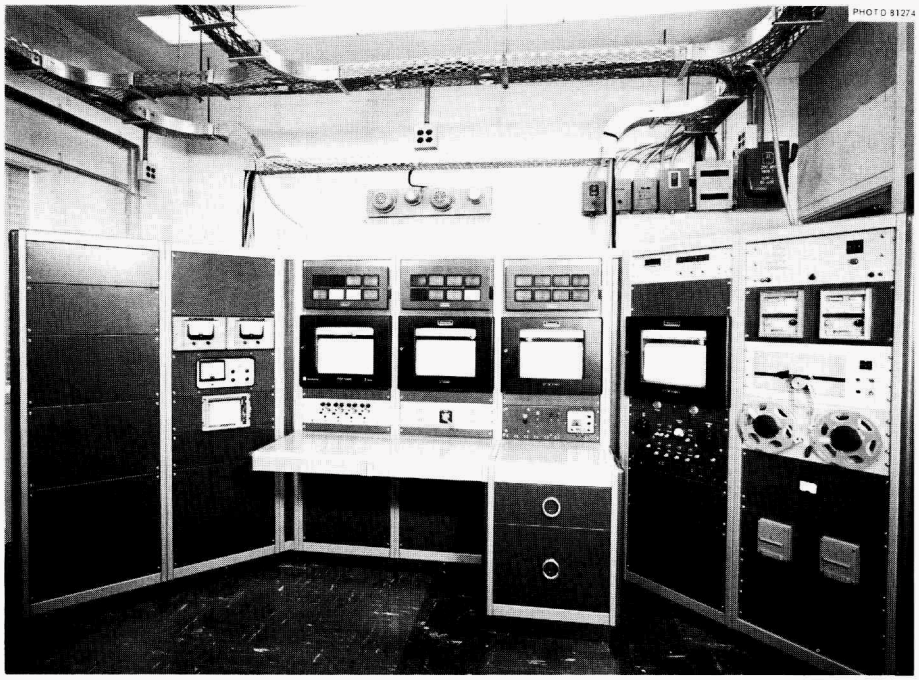

Fig. 15.1. Control Console System for the Spectrophotometer. The temperature control and programming system can be seen at the right side. None of the spectrophotometric, data acquisition, or other auxiliaries are shown in this early photograph.

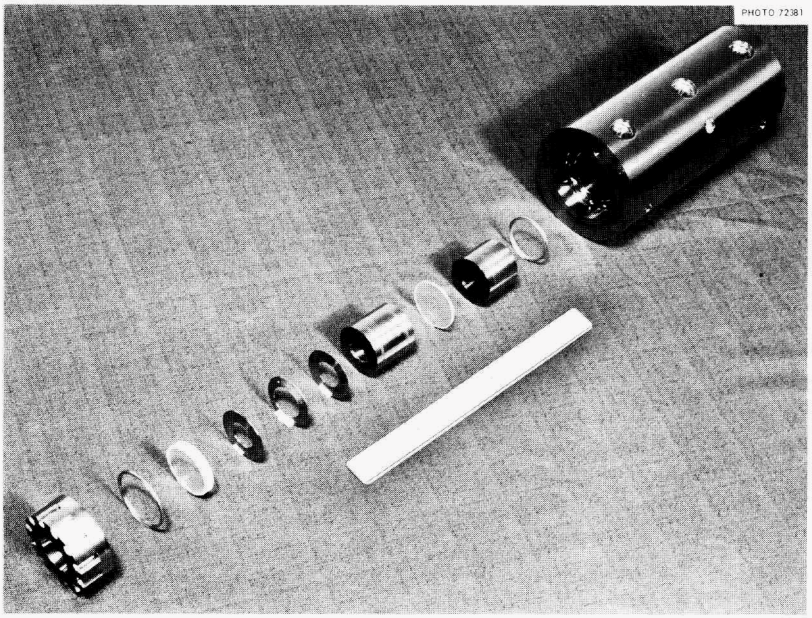

Fig. 15.2. Disassembled Absorption Cell Showing Parts for the Assembly of One-half of the Cell. No valving, tubing, or pressure and temperature monitoring transducers are shown. The parts are, from right to left: cell body, inner Haskel seal, inner filler body, inner sapphire window, outer filler body, thickness spacer disk, Bellville spring, outer window spacer disk, outer sapphire window, outer Haskel seal, window retaining flange.

may suggest some necessary or desirable improvements. The present cell design is the result of (1) a considerable amount of work and experience with the prototype and (2) extensive calculations to improve the design and performance of the cell and the window.

A major difficulty was encountered in attaching the heating-system lines to the cells (inside the vacuum chamber). The originally specified self-sealing quick disconnects were found to be incapable of operating at the specified temperature because of the failure of organic elastomer seals (no such self-sealing couplings are currently available). This necessitated using another type of coupling – a special alloy metal-metal sealing coupling available with brazed-on tubulations, 321 stainless steel in our case. Attaching these couplings (tubulations) to the absorption cells (titanium) in a structurally rigid, leak-free manner proved to be very difficult. A technique reported by NASA for brazing titanium to stainless steels was used to make some test brazes; these were evaluated. Upon confirmation of the soundness of the joint design and the test brazes, the couplings will be attached to the titanium cells.

The sapphire windows required for the initial operations, obtained from two manufacturers, had to be returned for rework because they did not conform to surface-finish specifications. They have now been completed in conformance with specifications.

A beam mask attachment (for vertical clipping of the optical beam and for detection and optical isolation of multiple phases in the cell) was fabricated and tested. Its performance appears, at the moment, to be adequate, although it has not yet been possible to test it with the cell. It may be necessary to modify it later for external indication of position.

15.2 SPECTRAL STUDIES OF IONIC SYSTEMS

The goals of these studies include measurements of transuranium elements such as berkelium, curium, etc., as well as eventual operation at temperatures up to at least the critical point of water (372°C). The spectrophotometer system described above will give us this capability. Until the new spectrophotometer can be made available for this work, interim experiments are being performed along the same lines of interest, at temperatures to about 95°C with the spectrophotometric equipment available. We are also developing certain ancillary equipment. A number of computer techniques and programs were developed and evaluated specifically for the analysis of certain types of spectroscopic data and for other needed calculations. We plan, eventually, to do similar studies with the higher actinide elements under conditions of high levels of alpha activity after relocation of the system.

To interpret the spectroscopic properties of the actinide elements beyond uranium properly, uranium should be understood as well as is possible. However, many basic problems remain concerning uranium and, in particular, the uranyl ion; and a comprehensive theory of the ion with respect to its spectroscopic properties has not been developed.

Studies of the Uranyl Ion Spectrum in Perchlorate Media

We concentrated initially on the uranium system, with the following experimental parameters of particular interest: temperature (25 to 95°C, with our conventional equipment), metal ion (uranyl) and ligand (complexing) concentrations, acidity (complications due to hydrolysis), and ionic strength. Initially, we chose to study perchlorate systems, since they are not only of intrinsic interest but will also serve as reference data for spectral studies of the uranyl ion in certain complexing systems. This series of studies will also serve as a model for studies of the transuranium elements to be carried out later.

An oral presentation of part of this work was given at the Symposium on Molecular Structure and Spectroscopy at the Ohio State University, Columbus, Ohio, June 14–18, 1965, and the work was recently published.[1] The parameters obtained for the absorption and fluorescence spectra of the uranyl ion in perchlorate media with the aid of computer techniques were interpreted with regard to some theoretical models recently proposed for the vibronic level structure. Our results show that some prior inferences concerning the character and distribution of the bands in the UO_2^{2+} spectrum are in error. A careful examination of the profile of the experimental spectra and the structure of the resolved spectra led us to a different assignment of bands into the various levels of a proposed triplet excited state.

---

[1] J. T. Bell and R. E. Biggers, *J. Mol. Spectry.* **18**, 247–75 (1965).

We also measured the ultraviolet (uv) spectrum of the uranyl ion to 1860 A and resolved it into 15 bands (Fig. 15.3), with band 1 corresponding to band 11 of the visible spectrum.[1] As far as we are aware, uv spectra in this detail have not been heretofore reported for UO_2^{2+}.

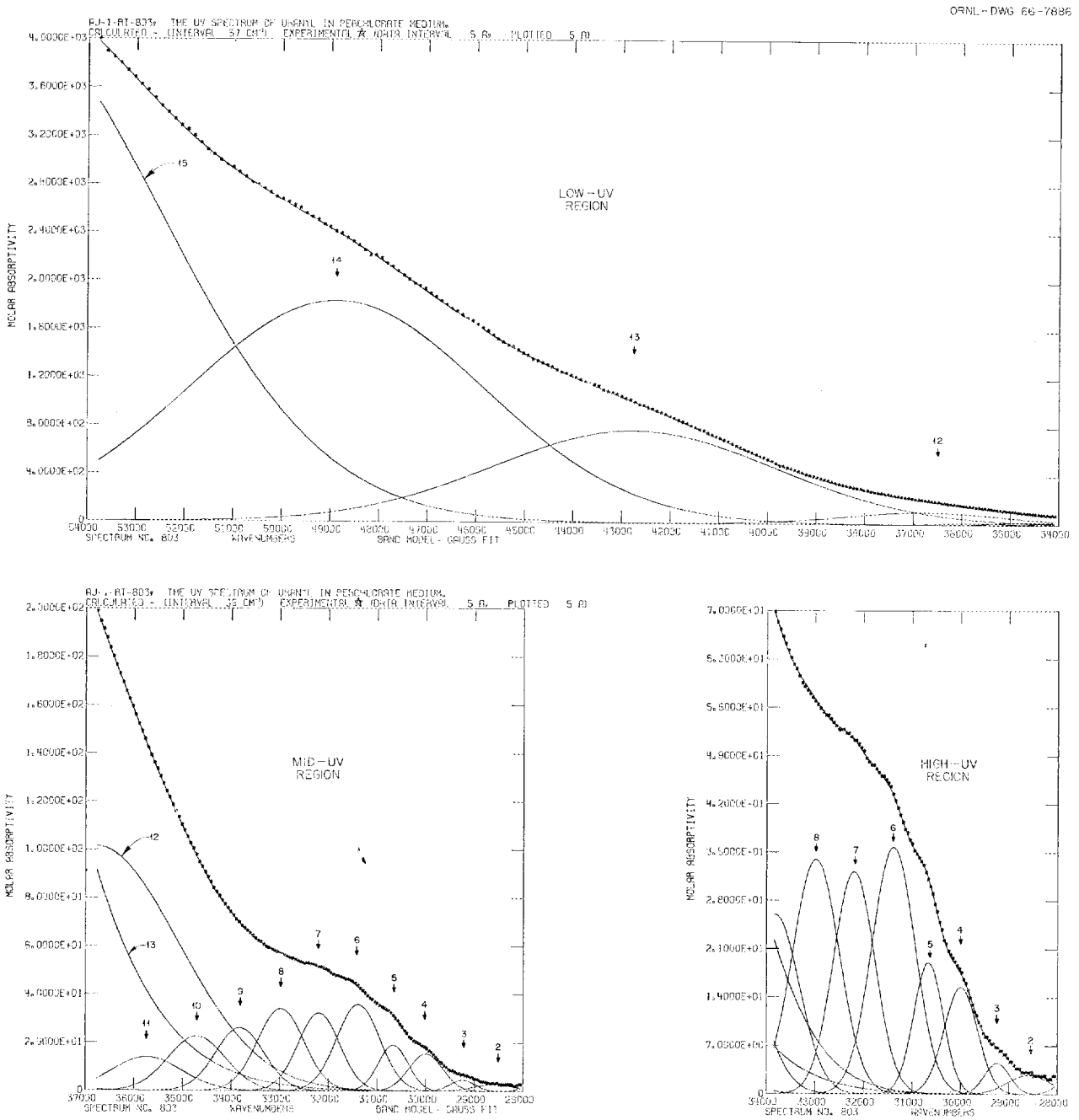

Fig. 15.3. Resolution of the $UO_2(ClO_4)_2$ Spectrum in Aqueous Solution in the Spectral Region 28,000 to 54,000 cm^{-1} (3570 to 1860 A). A comparison of the experimental and the nonlinear least-squares-calculated spectrum showing the resolved bands. $UO_2^{2+} = 0.0966\ M$; $H^+ = 0.112\ M$ ($HClO_4$); temperature, 25.0°C; $\mu = 3.00$ (ionic strength).

Effect of Hydrolysis on the Spectra of UO_2^{2+}

Spectroscopic studies were made on the hydrolysis of the uranyl ion in perchlorate media under quite varied conditions. We conclude, in agreement with some other recently reported work,[2] that much of the previously published work concerning "equilibrium" hydrolysis of the uranyl ion is based on systems not at true equilibrium.

We measured and resolved several series of spectra of the uranyl ion in solutions ranging from those containing excess perchloric acid to those where extensive hydrolysis had occurred. The parameters of the 13 uranyl absorption bands were observed as a function of the hydroxyl number, n, to $n = 0.291$.[3] The results of a linear least-squares fit of the positions, determined from the nonlinear least-squares resolution, for each band from $n = 0$ to 0.208 show that the hydrolysis of the uranyl ion does not affect the uranyl ion transitions. Least-squares fits of the integrated areas for first- and second-order equations gave almost equal standard errors of fit and showed that the increase in the band areas is a linear function of the hydroxyl number to about $n = 0.3$. The low oscillator strengths of the uranyl bands in the visible region indicate that the transitions are forbidden. A uranyl ion model involving a singlet ground state and an excited state consisting of two singlets and one triplet was developed and further refined by McGlynn and Smith.[4] According to this model, the uranyl ion is linear, and the spectrum arises from electronic transitions from O – U – O π molecular bonds to a uranium f orbital. This model is probably the best representation of the uranyl ion at this time.

Kraus and Moore[5] showed in some early work on plutonium that hydrolysis of the plutonyl ion (PuO_2^{2+}) produces changes in all parameters of the absorption spectral bands, although the parameters of the various spectral bands were not studied in detail. Upon increasing hydrolysis, the needle-sharp transition characteristic of PuO_2^{2+} at 8310 A disappears gradually, and the spectrum gradually converts to a less-intense, more-diffuse one, without significant band structure and with very pronounced band shifts toward the red as the bands disappear. We observed no such changes in the band positions for the uranyl ion and agree with Hermans[2] that the complicated U(VI) entities having various charges probably are not encountered at hydroxyl numbers less than 0.3 to 0.5 and surely do not exist near the stoichiometric point ($n = 0$) of the perchlorate salt.

15.3 MEASUREMENT OF DENSITIES OF LIQUIDS AT HIGH TEMPERATURES AND HIGH PRESSURES

As an important adjunct to the program for the spectrophotometric study of solutions at high temperatures and high pressures, a method was devised for measuring the densities of aqueous solutions at accurately measured temperatures and pressures up to the critical points of the solutions. A knowledge of solution densities vs temperature is required to calculate the concentration of species in solutions at temperatures up to the critical point of water (372°C) from the known or measured concentration values of the solutions prepared at about 25°C. A high-temperature, high-pressure autoclave (dilatometer) and related facilities were designed and assembled to permit the accurate measurement of liquid densities under these conditions. The system was improved and was operated over the temperature range 25 to 400°C. The design and mode of operation allow determination of densities of solutions near the critical point to within an error of about 1.2%, with progressively smaller errors at temperatures below the critical point.

The liquid volume of a weighed solution of a known composition is determined by taking an x-ray photograph to show the position of the vapor-liquid interface in a calibrated section of the dilatometer. The density is determined from the

---

[2] M. E. A. Hermans, *The Urea Process for UO_2 Production: Chapter VI, Some Hydrolytic Phenomena of Uranyl Salt Solutions* (thesis), Techn. Hogeschool, Delft, Netherlands, 1964; Euratom RCN-Kema Reactor Development Group, Arnhem, Netherlands; AEC Accession No. 30063, NP-14078, 170 pp., 1964.

[3] The hydroxyl number, n, is defined as the ratio of hydroxyl ion concentration (OH^-) to U(VI) concentration. The hydroxyl ion concentration is taken to be equal to the difference between the U(VI) molarity and the concentration of anions other than OH^-.

[4] S. P. McGlynn and J. K. Smith, *J. Mol. Spectry.* 6, 164–87 (1961).

[5] K. A. Kraus and G. E. Moore, Paper 4.22, *The Transuranium Elements*, vol. 14B, Part II, Plutonium Project Record, National Nuclear Energy Series, ed. by G. T. Seaborg, J. J. Katz, and W. M. Manning, McGraw-Hill, New York, 1949.

weight of the solution and the location of the interface at various temperatures. A prototype high-temperature dilatometer for this use was designed and was constructed entirely from titanium. A recent change in the closure method greatly improved its serviceability.[6] A special furnace and the necessary control instrumentation were also designed and constructed to maintain the autoclave, up to temperatures of about 375°C, in an essentially isothermal state over its entire length of about 18 in. The autoclave can be operated to pressures of about 5000 psi and temperatures of 400°C. The addition of a dilatometer containment chamber with continual recirculation of the atmosphere within it has greatly improved the heat transfer and the coupling to the furnace, with a resulting large increase in its thermal stability and end-to-end thermal equilibrium. With a temperature-measuring and -recording system utilizing a conventional thermocouple (calibrated), the density of water was measured at numerous temperatures up to the critical point. Agreement with steam-table values was obtained to within 0.5% up to about 275–300°C; at higher temperatures, the error increased because the temperature was not known accurately enough.

Computation of the Results

Experience obtained during the development of the facility and the calculation procedures evolved led to the development of a set of computer programs for performing the detailed calculations and plotting the results. The computer program DENSITY calculates the density of an experimental solution from measurements made with the high-temperature, high-pressure dilatometer at each of the temperatures used.

Program STEAM was prepared to generate steam-table data over any temperature span specified up to the critical temperature of water. The following quantities may be obtained: temperature (°C); pressure (in bars, kg/cm^2, atm, and psi); specific volume, liquid (cc/g); density, liquid (g/cc); specific volume, vapor (cc/g); density, vapor (g/cc).

In the density experiments, there is a progressive loss of water to the vapor phase as the temperature is increased. This weight loss can be determined from steam-table data. Proper interpolation techniques must be used, particularly for values from 300°C to the critical point, where the values are pronounced nonlinear functions of the temperature. As was pointed out by Bain in the 1964 steam-table revision, a Bessel function interpolation is most appropriate, and one was used (subroutine BESINT) here.

Program TCT was prepared to plot graphs of thermocouple calibration data, NBS referenced. Each graph covers 10°C, and graphs of such intervals may be obtained from 0 to 400°C. The *y*-axis range is variable. Temperatures may be read with a resolution of at least 0.05°C.

Typical Density Results

The densities of a number of uranyl perchlorate solutions which have been studied spectrophotometrically were measured to 95°C with a pycnometer for comparison with the dilatometer results at higher temperatures (25 to 400°C). At 95°C the results from the dilatometer agreed with those from the pycnometer to within 0.4%.

The density of water was measured at numerous temperatures up to the critical point of water in a number of independent experiments to ascertain the accuracy and reproducibility of the measurements. The results show that, up to about 325°C, the densities are determined to within an average error of about 0.6% or better. From about 325°C to the critical point, the average error does not exceed about 1.2%, and in some experiments it did not exceed 0.7% in this region. The liquid-vapor interface may be determined accurately from the x-ray photograph to within a few degrees centigrade of the critical point; but as the critical point is closely approached, this becomes exceedingly difficult. Measurements were made with uranyl sulfate and perchlorate solutions with equally good results. Also, a series of measurements was made on potassium chloride at various concentrations.

---

[6] A. M. Rom, *Thermally Compensated Closure for Liquid Density Autoclave*, ORNL-TM-1293 (Oct. 14, 1965).

16. Mechanisms of Separations Processes

16.1 ACTIVITIES OF TRI-*n*-BUTYL PHOSPHATE (TBP) IN TBP-HNO_3-H_2O SOLUTIONS

An abstract of a published report[1] summarizing activity studies in the organic phase for the TBP-HNO_3-H_2O system is included in the Summary of this report. There is no further progress to report on this work.

16.2 DETERMINATION OF RADIOISOTOPES BY RESOLUTION OF GAMMA-RAY SPECTRA

Two abstracts of published work[2,3] in the Summary of this report summarize the work completed to date. Several aspects of the mathematical resolution of gamma-ray spectra of radioisotope mixtures by the method of least squares are discussed. Current work, presented below, concerns improvements in accuracy in the determination of radioisotopes.

The mathematical resolution of complex gamma-ray spectra having a considerable overlap of adjacent bands or widely differing radioisotope concentrations for two overlapping bands is difficult, and accuracy is poor in some cases. One method of improving the accuracy of the analysis consists in the use of coincidence counting. (A coincidence event is the simultaneous emission of two gamma rays.) Improved resolution of gamma-ray spectra is achieved by coincidence counting because some of the interfering radioisotopes do not have coincidences and thus are not counted.

To achieve improved resolution by coincidence counting it was necessary to formulate a method of displaying the spectra so that radioisotopes present in the sample can be identified. The problem was to display the 20,000 data points of each spectrum in a small, easily viewed three-dimensional representation. This was done by writing a program that allowed a digital computer to read the output data from the coincidence counter and, with optional smoothing, to plot a permanent record on paper. A typical display of the coincidence spectra of a sample mixture containing five radioisotopes is shown in Fig. 16.1.

A second problem in this area requiring solution was the mathematical resolution of the coincidence gamma-ray spectra. Resolution was achieved by modifying the highly successful ALPHA[2] computer program. Preliminary results obtained with this new program indicate that, for a mixture of ^{106}Ru and ^{131}I, it is possible to measure about 1 part of ^{106}Ru in the presence of 1000 parts of ^{131}I. This represents about a 20 fold improvement in accuracy.

---

[1] W. Davis, Jr., J. Mrochek, and C. J. Hardy, "The System: Tri-*n*-Butyl Phosphate (TBP)--Nitric Acid--Water. I. Activities of TBP in Equilibrium with Aqueous Nitric Acid and Partial Molar Volumes of the Three Components in the TBP Phase," accepted for publication in the *Journal of Inorganic and Nuclear Chemistry*.

[2] E. Schonfeld, *ALPHA -- A Computer Program for the Determination of Radioisotopes by Least-Squares Resolution of the Gamma-Ray Spectra*, ORNL-3810 (1965).

[3] E. Schonfeld, "Improved Accuracy in Determination of Radionuclide Concentrations in Solutions Containing Fast-Decaying Isotopes by Least-Squares Resolution of the Gamma-Ray Spectra," *Proceedings of the 1965 International Conference on Modern Trends in Activation Analysis, Texas A & M University* (in press).

ORNL-DWG 66-715

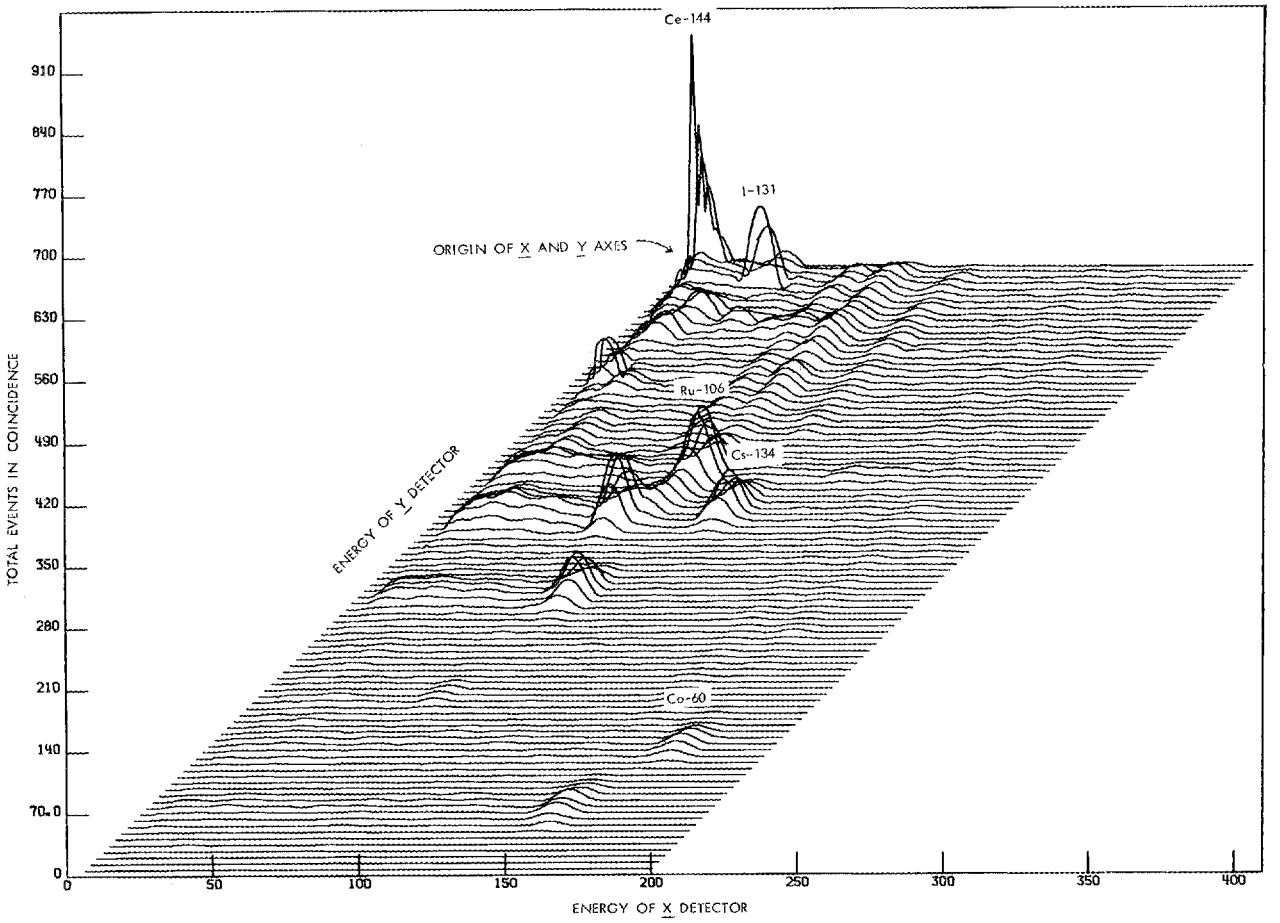

Fig. 16.1. Typical Three-Dimensional Representation of the Coincidence Gamma-Ray Spectra of a Sample. Obtained by programming a digital computer.

17. Chemical Engineering Research

Chemical engineering research is an aggregate of studies which, while generally pertinent to the applied programs of the Chemical Technology Division, are fundamental in nature or pursue attractive new ideas. The fundamental studies usually arise from interesting effects noted during work on programs with more specific commitments. On the other hand, work begun on new ideas frequently becomes part of applied programs as the work matures.

The reported work this year is restricted to the development of the stacked-clone contactor, which, in addition to showing excellent performance characteristics, is proving to be a practical device of a rugged and reliable nature.

17.1 THE STACKED-CLONE CONTACTOR

The stacked-clone contactor is a high-speed solvent extraction device incorporating all the necessary features for processing highly radioactive materials: low holdup, fast response, very short residence time (for the solvent) per stage, and high solution throughput. The contactor consists of a cascade of axially aligned liquid cyclones, or stages. Each stage operates with countercurrent flow of the two liquid phases resulting from the induced underflow. To show a wide range of applicability, the experimental contactor was tested with a variety of chemical systems. Original development work was done with the Amsco-TBP-$NaNO_3$-$UO_2(NO_3)_2$ system at several concentrations and temperatures. Solution throughputs of 3 to 4 liters/min (A/O = 3) and mass transfer efficiencies of 70 to 80% were typical, indicating a solution residence time of 4 sec/stage.

The more recent tests involving seven extraction stages and four aqueous-raffinate polishing stages operating with the following systems resulted in the throughputs (A/O = 3) and mass transfer efficiencies noted below and in Table 17.1:

1. A hexone–water–acetic acid system exhibited throughputs of 7 liters/min and efficiencies from 80 to 90% (a residence time of 2 sec per theoretical stage) at about 25°C. This flow capacity is unusually high, considering the physical properties involved (density, viscosity, interfacial tension). Other solvent extraction devices showed unusual throughputs with this system, which suggests that some other intrinsic physical property influences flooding behavior.

2. A hexone–0.2 *M* acid-deficient $Al(NO_3)_3$–$UO_2(NO_3)_2$ system, featuring aqueous- (continuous-) phase viscosities as high as 5 centipoises, operated with flow capacities of 2.8 and 5.9 liters/min for 1.7 and 1.0 *M* $Al(NO_3)_3$, respectively, and with a mass transfer efficiency near 70% at about 30°C. Again, the hexone solvent was responsible for the high flow capacity, since previous systems having aqueous-phase viscosities as low as 1.3 centipoises exhibited flows of only approximately 1.5 liters/min.

3. Very high organic- (dispersed-) phase viscosities apparently do not affect stacked-clone contactor throughput. Mineral oil (viscosity, 116 centipoises) was run with 0.08 *M* HNO_3 at flows up to 3.9 liters/min at about 30°C. Extraction of benzoic acid in this system, however, was only 30 to 40% efficient, possibly because of a low mass transfer coefficient caused by the high viscosity.

4. Low efficiencies and low extraction rate constants were also observed when benzoic acid was extracted with Amsco, which has a viscosity of only 1.3 centipoises. Flow capacities were 3.8 liters/min at about 30°C.

5. Benzoic acid extraction with N-Paraffins-175 (similar to *n*-dodecane and having physical properties matching those of Amsco) was carried out at flows up to 3.8 liters/min (about 30°C) with efficiencies near 60%.

Table 17.1. Stacked-Clone Contactor Performance and Flow Capacity Data

Continuous Phase	Dispersed Phase	Distributing Species	Density Difference (g/cc)	Viscosity of Continuous Phase (centipoises)	Viscosity of Dispersed Phase (centipoises)	Interfacial Tension (dynes/cm)	Mass Transfer Efficiency (%)	Flow Capacity (liters/min)				Temperature (°C)
								A/O = ½	A/O = 1	A/O = 2	A/O = 3	
0.005 *M* CH_3COOH	Hexone	CH_3COOH	0.198	0.89	0.56	7.1	87	3.48	4.50		6.97	25
1.7 *M* $Al(NO_3)_3$, 0.2 *M* acid-deficient	Hexone	$UO_2(NO_3)_2$	0.474	4.17	0.56	8.1	69		1.95		2.83	30
1.0 *M* $Al(NO_3)_3$, 0.2 *M* acid-deficient	Hexone		0.356	1.88	0.56	7.6		2.79	3.43		5.88	25
0.01 *M* HNO_3	Mineral oil	C_6H_5COOH	0.121	0.84	116.	53	33		2.77		3.88	30
0.01 *M* HNO_3	Mineral oil	C_6H_5COOH	0.124	0.66	57.	52	38				4.29	40
0.08 *M* HNO_3	2-Ethyl-1-hexanol		0.171	0.84	6.6	13.4		1.21	1.43		1.96	30
0.08 *M* HNO_3	N-Paraffins-175	C_6H_5COOH	0.254	0.84	1.34	36	65	2.23	2.64		3.79	30
0.08 *M* HNO_3	N-Paraffins-175	C_6H_5COOH	0.258	0.66	1.10	35	57	2.80	3.32		4.57	40
0.08 *M* HNO_3	Amsco		0.248	0.84	1.28	45			2.78		3.78	25
0.08 *M* HNO_3	Amsco		0.254	0.66	1.07	44		2.71	3.16		4.22	40
0.08 *M* HNO_3	Amsco	C_6H_5COOH	0.248	0.84	1.28	35	35	2.02	2.35		3.15	25
0.08 *M* HNO_3	Amsco	C_6H_5COOH	0.254	0.66	1.07	35	31		2.92		4.01	40
0.08 *M* HNO_3	Amsco		0.253	0.66	1.18	41		3.04	3.60	4.40	4.96	40
Amsco	0.08 *M* HNO_3		0.251	1.18	0.66	40		6.28	5.51	4.92		40
Amsco	66 wt % glycerol, 0.05 *M* HNO_3		0.425	1.10	10.2	27		1.60	1.44	1.29	1.24	40
Amsco	1.7 *M* $Al(NO_3)_3$, 0.3 to 0.9 *M* acid-deficient		0.56	1.10	3 to 4	31 to 35		2.19	2.16	2.14	2.13	40
Amsco	38 wt % dextrose		0.409	1.10	2.35	15.6		1.87	1.82	1.78	1.76	40
Amsco	38 wt % dextrose		0.399	1.33	3.20	12.8		1.47	1.33	1.22	1.17	25
5% TBP–Amsco	1 *M* $NaNO_3$, 2.5 g of U per liter	$UO_2(NO_3)_2$	0.296	1.11	0.73	16.3	85	2.29	2.08	1.87	1.76	40
5% TBP–Amsco, 1.0 g of U per liter	1 *M* $NaNO_3$		0.296	1.11	0.72	16.2		2.19	1.74	1.44	1.32	40
5% TBP–Amsco	1 *M* $NaNO_3$	$UO_2(NO_3)_2$	0.297	1.11	0.72	16	67					40

6. Flooding for a 2-ethyl-1-hexanol–0.08 *M* HNO_3 system – one characterized by a low interfacial tension – occurred at 2.0 liters/min (about 30°C). The interfacial tension for 2-ethyl-1-hexanol was 13 dynes/cm, whereas values from 35 to 50 were common for the other solvents used.

Perhaps the most significant result this year was a demonstration of stacked-clone contactor operation with the solvent phase continuous. This mode is applicable when aqueous-phase viscosities are high, when flow ratios (A/O) less than ½ are desired, and when impurities in feed streams cause emulsions in the aqueous-continuous mode. Several modifications in clone geometry were tested before a suitable arrangement was found. The most disturbing problem was that of formation of double dispersions – dispersions having subminiature organic droplets within the dispersed aqueous drops. Good dispersions up to 80% of flooding resulted when the end clone adjacent to the organic feed point was one having a very strong induced underflow as compared with that of the normal clones. Other extraction stages were identical to those used during operation with the aqueous phase continuous. Of course, the polishing stages for the aqueous raffinate were removed; a gravity settler was installed at the raffinate end; and organic-phase polishers were installed above the aqueous feed point (Fig. 17.1). These polishing clones were identical to the extraction clones.

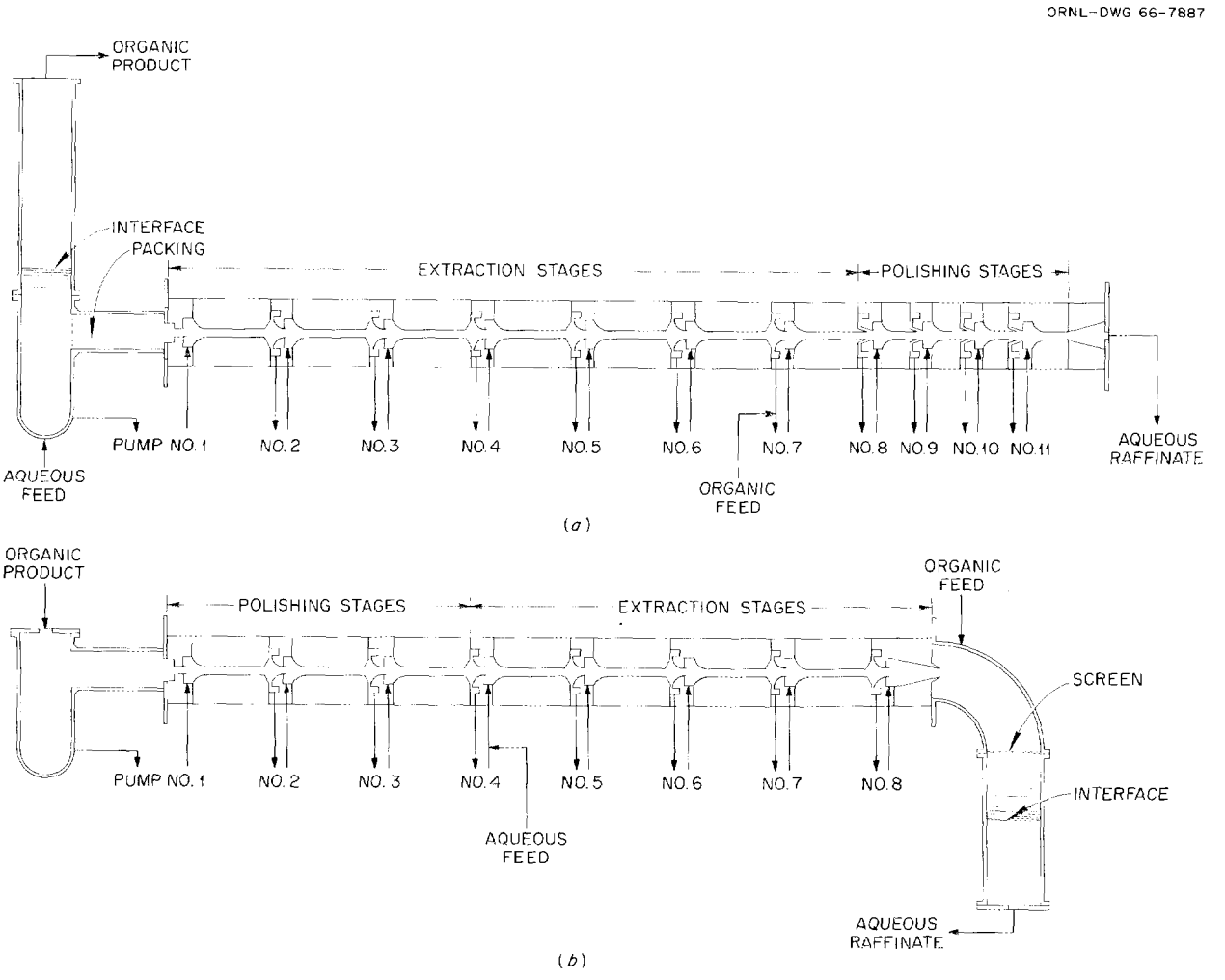

Fig. 17.1. (*a*) Normal Stacked-Clone Contactor Arrangement for Aqueous-Continuous Operation; (*b*) Stacked-Clone Contactor Arrangement for Organic-Continuous Operation.

Flooding occurred in the organic-continuous mode at 6.3 liters/min (A/O = ½, 40°C) for the system Amsco–0.08 *M* HNO_3, and entrainment of aqueous in organic product was <1%.

Additional systems tested (at approximately 40°C) include:

1. an Amsco–66 wt % glycerol system that flooded at 1.6 liters/min (dispersed- or aqueous-phase viscosity = 10 centipoises);
2. an Amsco–38 wt % dextrose system that exhibited flooding at 1.8 liters/min (dextrose viscosity = 2.3 centipoises);
3. an Amsco–acid-deficient 1.7 *M* $Al(NO_3)_3$ system that flooded at 2.1 liters/min (aqueous-phase viscosity of 4 centipoises);
4. a 5% TBP–Amsco–1 *M* $NaNO_3$–$UO_2(NO_3)_2$ system that indicated a flow capacity of 2.2 liters/min.

Mass transfer data for the last system indicated an extraction efficiency of 70 to 80% during operation at a flow ratio (A/O) of approximately ½ and at flows >80% of flooding (Table 17.1).

Tests to determine the effect of feed impurities on contactor operation were conducted by suddenly injecting large quantities of powdered solids (diatomaceous earth, Fuller's earth, or infusorial earths) into the aqueous feed stream. Flow control was not affected as long as the solids remained in the aqueous phase. Tests made with solids that transferred to the organic phase during operation in the aqueous-continuous mode indicated no transfer during operation in the organic-continuous mode; but emulsions contaminated the organic product in both cases.

A 14-stage stacked-clone contactor with integral pumps has been fabricated and installed in a test rack. This plant prototype unit has gone through preliminary testing, with 18% TBP–Amsco–1 *M* $NaNO_3$–$UO_2(NO_3)_2$, and will receive additional attention and evaluation with practical flowsheets.

18. Reactor Evaluation Studies

This program is supported jointly by the Reactor Division and the Chemical Technology Division. It consists of studies of various advanced reactor and fuel-cycle systems to determine engineering and economic feasibility. The work in this Division during the past year included cost studies of shipping fresh and spent nuclear fuel, processing spent fuel (including final waste disposal), and preparing various virgin and recycle fuel materials (oxides, fluorides, metals, etc.) of interest. In addition, computer codes were developed for estimating and optimizing fuel-cycle and overall power costs. Formal studies were made for the ^{233}U value study,[1,2] the HWOCR (Heavy-Water-Moderated, Organic-Cooled Reactor) evaluation,[3] and the forthcoming first two volumes of the new *Nuclear Power Evaluation* series (to supersede the present *Guide to Nuclear Power Cost Evaluation*[4]), in collaboration with the Metals and Ceramics Division and the Reactor Division. Costs of fuel preparation, shipping, and processing were estimated for a variety of reactor types of interest to the Desalination Reactor Program.

18.1 STUDIES OF THE COST OF SHIPPING REACTOR FUELS

The computer program NORA, used to calculate shipping and reprocessing costs, was described in previous annual reports. It was expanded this year to include the calculation of cask criticality by linking NORA with the DTF neutron transport code.[5] This change will add considerably to the usefulness of NORA, since the possibility of cask criticality represented a potential source of error in the shipping cost calculations. No difficulty was found in controlling criticality in any of the cases calculated. When boron was used in the metal structure supporting the fuel elements, effective multiplication factors of the order of 0.3 to 0.6 were obtained under full water moderation and reflection; the safe upper limit is considered to be about 0.9.

In connection with the Reactor Division's project to modernize parts of the *Guide to Nuclear Power Cost Evaluation*,[4] a proposed section on fuel shipping costs was prepared. It presents cost estimating procedures for fresh (new) fuels, spent fuels, recycled gamma-active fresh fuels, and certain fuel chemicals (uranium hexafluoride, uranyl nitrate, thorium nitrate, thorium oxide). Cask design is handled by means of charts and curves based on correlations obtained with NORA. Numerical examples of cask design and cost calculation are included. This information is available separately as an ORNL report.[6]

A study was made of the relative economic advantages of lead, steel, and uranium as shielding materials for shipping casks.[7] Findings showed that the use of uranium shielding could potentially reduce shipping costs appreciably, especially

[1] L. L. Bennett, *A Study of the Fuel Value of U^{233}*, ORNL-TM-1499 (to be issued).

[2] J. T. Roberts, E. D. Arnold, F. E. Harrington, A. L. Lotts, and R. Salmon, *A Study of Costs and Other Factors Associated with Processing, Fabrication, and Shipment of Recycled Thorium-Uranium Fuels*, ORNL-TM-1463 (to be issued).

[3] P. R. Kasten, F. E. Harrington, J. T. Roberts, and R. Salmon, *An Evaluation of Heavy-Water-Moderated, Organic-Cooled Reactors*, ORNL-3921 (to be issued).

[4] *Guide to Nuclear Power Cost Evaluation*, TID-7025, vols. 1–5 and Suppl. I (March 1962–April 1963).

[5] W. W. Engle, M. A. Boling, and B. W. Colston, *DTF-II, A One-Dimensional Multigroup Neutron Transport Program*, NAA-SR-1095 (to be issued).

[6] R. Salmon, *Estimation of Fuel Shipping Costs for Nuclear Power Cost Evaluation Purposes*, ORNL-3943 (March 1966).

[7] L. B. Shappert and R. Salmon, *Shipping Cost Comparisons of Lead-, Steel-, and Uranium-Shielded Casks*, ORNL-3918 (January 1966).

Table 18.1. Spent-Fuel Shipping Costs[a]

Fuel Type	Burnup of Reference Material (Mwd/metric ton)	Reference Material per Cask (kg)	Shipping Cost of Reference Material ($/kg)	Shipping Cost [mills/kwhr (electrical)]
AICE,[b] 37-rod cluster	10,000	3200	2.31	0.028
	15,000	3200	2.37	0.019
	20,000	2800	2.70	0.016
	25,000	2400	2.96	0.014
B&W,[c] 66-rod cluster	15,000	1852	4.78	0.038
	20,000	1852	4.82	0.029
	25,000	1620	5.58	0.027
B&W,[c] 5-ring cylinder	15,000	2916	3.21	0.026
	20,000	2499	3.56	0.021
	25,000	2499	3.62	0.017

[a]Cooling time, 120 days; rail shipment, 1000 miles each way; maximum weight of loaded cask, 240,000 lb; casks shared among 15 reactors; costs are in $/kg reference material charged to reactor; reference material is total uranium for the AICE type and total uranium plus thorium for the B&W type.

[b]A design by Atomics International and Combustion Engineering.

[c]A design by Babcock and Wilcox Co.

where vehicle capacity is limited to about 25 tons, as in shipment by truck. For any given cask weight, the uranium-shielded cask has a fuel capacity much larger than that of either lead- or steel-shielded casks; this is clearly advantageous, since shipping cost is considered to be roughly in inverse ratio to fuel load per cask.[8] In the larger cask sizes (70 to 100 tons), however, the advantage of uranium is less clear, because heat-removal capacity is more likely to be the limiting factor in deciding how much fuel can be carried per cask. Thus, from a shielding point of view, a 100-ton uranium cask might carry four times as much fuel as a lead cask of the same weight, but the problem of removing several hundred kilowatts of decay heat might make the load advantage academic. (It should be noted here that shipping regulations require that the design rate of heat removal be maintained safely under loss-of-coolant conditions, with all mechanical cooling systems inoperative.[9]) No economic advantage was foreseen in the use of all-steel casks, since their fuel capacities are less than those of lead-shielded casks. Its economic potential notwithstanding, the commercial use of uranium-shielded casks will depend largely on the price and availability of uranium and on developing economical fabrication techniques.

Table 18.2. Recycled Gamma-Active Fresh Fuel Shipping Costs[a]

	B&W 66-Rod Cluster	B&W 5-Ring Cylinder
Costs, $/kg (U + Th)		
Handling	$ 0.11	$ 0.08
Insurance	0.14	0.14
Freight	1.38	0.91
Cask amortization	0.43	0.40
Total shipping cost	$ 2.06	$ 1.53
Weight of filled cask, thousands of pounds	179	172
U + Th per cask, kg	4630	6665
Heat removal per cask, kw	0.6	0.9

[a]Rail shipment, 1000 miles each way; maximum cask weight, 240,000 lb; casks shared among 15 reactors; cask length, 4 elements end-to-end; costs are in $/kg reference material shipped.

[8]M. W. Rosenthal, J. T. Roberts, and R. Salmon, *A Comparative Evaluation of Advanced Converters*, ORNL-3686 (January 1965).

[9]Code of Federal Regulations, Title 10, Part 71, "Transport of Licensed Material" (proposed), *Federal Register* **30**, 15748 (1965).

As part of the HWOCR evaluation,[3] shipping costs were estimated for a 1000-Mw (electrical) reactor of this type, using several different fuel designs. These included a 37-rod cluster (SAP-clad uranium carbide), a 66-rod cluster (SAP-clad uranium and thorium oxides), and a nested cylinder (Zircaloy-clad uranium and thorium). (SAP is a sintered dispersion of 5 to 15% Al_2O_3 in aluminum.) Tables 18.1–18.3 show the calculated shipping costs for spent fuel, recycled gamma-active fresh fuel, and non-gamma-active fresh fuel respectively. The economic assumptions and "ground rules" for this study were similar to those used in the evaluation of advanced converters.[8] The gamma activity in the recycled fuel comes from the daughters of ^{232}U and ^{228}Th.

Table 18.3. Non-Gamma-Active Fresh Fuel Shipping Costs[a]

	AICE 37-Rod Cluster	B&W 66-Rod Cluster	B&W 5-Ring Cylinder
Handling	$ 0.04	$ 0.05	$ 0.05
Insurance	0.03	0.08	0.06
Freight	0.20	0.21	0.19
Containers	0.06	0.10	0.08
Total shipping cost	$ 0.33	$ 0.44	$ 0.38

[a]Truck shipment, 1000 miles each way; maximum load, 46,000 lb; containers shared among 15 reactors; costs are in $/kg reference material [U or (U + Th)] shipped.

18.2 COSTS OF PREPARING NUCLEAR FUEL MATERIALS

The preparation of nuclear fuel material consists of the procedures necessary to convert makeup and recycle material to the proper chemical and physical form for fuel fabrication. Costs of such processing are usually included in fabrication costs.

The preparation of fuel material for the HWOCR study included:

1. Conversion of 1.16% enriched UF_6 to UO_2 for the carbide-fueled HWOCR-U by the process method for normal feed material production.
2. Conversion of partially decontaminated nitrate product solutions from the reprocessing plant to urania-thoria for the oxide-fueled HWOCR-Th or to pressed thorium powder and uranium billets for the metal-fueled HWOCR-Th. Required makeup uranium of high enrichment was converted from UF_6 to UO_3 for oxide fuel or to UF_4 for metal fuel.

Table 18.4 summarizes the estimated costs for the fuel materials above and states the ground rules of the HWOCR study. These estimates may

Table 18.4. Summary of Estimated Costs[a] of Preparing Fuel Material

Reactor	Fixed Charge Rate[b] (%)	Costs ($/kg) for Throughputs of: 1 Metric Ton/Day		4 Metric Tons/Day		10 Metric Tons/Day	
		Capital	Total	Capital	Total	Capital	Total
HWOCR-U	22	2.79	6.41			0.82	1.84
	15	1.90	5.52			0.56	1.58
HWOCR-Th							
Urania-thoria	22	4.92	9.75	2.32	4.30		
	15	3.35	8.18	1.58	3.56		
Uranium-thorium	22	5.78	13.49	2.56	6.90		
	15	3.94	11.65	1.74	6.08		

[a]260 days/year on stream; fuel material preparation assumed to be done in an integrated processing-preparation-fabrication facility.

[b]Annual fixed charge rate on capital investment.

be connected by a straight line on a log-log graph to obtain the cost for throughputs other than those listed.

The costs reported for the HWOCR-U fuel material are the sum of previously developed[10] UF_6-to-UO_3 costs and a new estimate for the conversion of UO_3 to UO_2 by hydrogen reduction in a fluid bed.

The costs for the sol-gel ThO_2-UO_2 are modifications of an earlier study[11] to reflect the ground rules of this study and a consistent method for all fuel material estimates.

The costs for the metal fuel facility are based on a heavily shielded thorium-metal powder line and an enriched uranium billet line.

18.3 COST STUDIES OF SPENT-FUEL PROCESSING

Advanced Converter Fuels

For the HWOCR evaluation,[3] cost estimates for spent-fuel processing were prepared for SAP-clad uranium carbide, SAP-clad thorium-uranium oxide, and Zircaloy-clad thorium-uranium fuels. These estimates were made under assumptions somewhat different from those for the advanced converter evaluation,[8] given in last year's annual report;[12] hence for comparison purposes, the processing costs for the six earlier advanced converters were reestimated on the new basis. All the estimates are summarized in Table 18.5.

Like the earlier advanced-converter evaluation, the estimates assume that, in each case, the processing plant is designed to serve a nuclear economy of 15,000 Mw (electrical) of the particular reactor under consideration. This basis gives an advantage to high-burnup reactors, other things being equal, in that a smaller processing plant is required for an economy of a given size. High-burnup reactors are given an even greater advantage if the size of the processing plant is arbitrarily made the same for all reactors and if the plant is assumed to be fully loaded at all times. Using single-purpose plants as the basis of comparison avoids the complication of trying to divide costs between two different products in the same plant.

In the earlier advanced converter evaluation, processing capital and operating costs were based on modifications of and scaling between 1961 Du Pont estimates[13] for 0.907- and 9.07-metric ton/day plants and on 1965 ORNL cost estimates[14] for final waste disposal. The estimates in Table 18.5 are based on modifications of and scaling between 1963 Nuclear Fuel Services (NFS) estimates[15] for a 1.0-metric ton/day plant and 1964–65 Du Pont estimates[16–18] for 9.07-metric ton/day plants, and on 1965–66 ORNL cost estimates for final disposal.[19] The new estimates are from 20 to 40% lower than the earlier ones.

Most of the variation in unit processing costs in Table 18.5 is caused by differences in processing plant size, total annual capital, and operating costs scaling with about the 0.34 power of the daily throughput rate in this study. Differences in fuel type (uranium vs thorium, oxide vs carbide vs metal, Zircaloy-clad vs SAP-clad vs graphite matrix, etc.) contributed about 10% of the variation. Differences in waste characteristics (differences in amounts of fission products caused by differences in burnup and thermal efficiency, and differences in bulk inert material caused by differences in fuel type and process flowsheets) contributed about 7 to 8% of the variation.

---

[10] F. E. Harrington *et al.*, *Fuel Cycle Costs for a Plutonium Recycle System*, ORNL-3501 (January 1964).

[11] J. M. Chandler and F. E. Harrington, *A Study of Sol-Gel Fuel Preparation Costs for SSCR and HTGR Reactors*, ORNL-TM-1109 (Apr. 8, 1965).

[12] *Chem. Technol. Div. Ann. Progr. Rept. May 31, 1965*, ORNL-3830 (November 1965).

[13] W. H. Farrow, Jr., *Radiochemical Separations Plant Study, Part II — Design and Cost Estimates*, DP-566 (March 1961).

[14] J. O. Blomeke, R. L. Bradshaw, J. J. Perona, and J. T. Roberts, *Estimated Costs for Management of High-Activity Power Reactor Processing Wastes*, ORNL-TM-559 (May 1963).

[15] "Chemical Processing Plant," Hearing Before the Joint Committee on Atomic Energy, May 14, 1963, U.S. Govt. Printing Office, 1964.

[16] R. J. Christl, J. E. Crawley, and C. S. Otto, *Radiochemical Separations Plant Study, Limited Maintenance — Case VII*, DP-930 (September 1964).

[17] V. R. Thayer, E. I. du Pont de Nemours and Co., unpublished study of HWOCR-Th fuel processing (June 1965).

[18] V. R. Thayer and J. F. Proctor, E. I. du Pont de Nemours and Co., unpublished study of HWOCR-U fuel processing (August 1965).

[19] J. O. Blomeke, R. Salmon, J. T. Roberts, and R. L. Bradshaw, "Estimated Costs of High-Level Waste Management," *Proc. Symp. Solidification and Long-Term Storage of Highly Radioactive Wastes, Richland, Wash., Feb. 15–18, 1966* (to be issued).

Table 18.5. Cost Estimates of Spent-Fuel Processing for Advanced Converter Reactors

Basis: Single-purpose plants serving 15 reactors of a given design; 1000 Mw (electrical) each; 80% reactor load factor; burnup approximately equal to the estimated economic optimum; 260 processing days per year

	PWR	SSCR	HWR-U	HWR-Th	HTGR[a]	SGR	HWOCR-U	HWOCR-Th	
								Oxide	Metal
Reference material burnup, Mwd/metric ton	21,248	29,580	12,540	23,000	48,500	16,750	15,000	20,000	20,000
Thermal efficiency, %	31.1	31.2	26.8	26.1	44.4	43.6	34.8	34.8	34.8
Throughput rate, metric tons/year	663	475	1300	730	206	600	839	629	629
Processing rate, metric tons/day	2.55	1.83	5.00	2.81	1.00[b]	2.31	3.23	2.42	2.42
Total capital investment, millions of dollars	40.0	34.4	52.2	40.0	31.0	41.3	46.4	38.0	38.0
Operating cost, millions of dollars per year	4.00	3.44	5.22	4.00	3.10	4.13	4.64	3.80	3.80
Total waste disposal charge, millions of dollars per year	2.15	2.36	2.35	2.63	1.91	1.93	3.02	3.02	2.21
Unit costs at 15%/year FCR[c]									
$/kg	18.3	23.1	11.8	17.3	46.9[d]	20.4	17.4	19.9	18.6
mills/kwhr (electrical)	0.116	0.104	0.147	0.120	0.092	0.117	0.139	0.119	0.111
Unit costs at 22%/year FCR[c]									
$/kg	22.5	28.1	14.7	21.1	57.4[d]	25.3	21.3	24.1	22.8
mills/kwhr (electrical)	0.142	0.127	0.181	0.147	0.113	0.144	0.170	0.144	0.137

[a]HTGR case assumes separate processing of the thorium and uranium particles.

[b]Processing rate for thorium particles. The rate for the enriched uranium particles is much lower.

[c]Annual fixed-charge rate on total capital investment.

[d]Average cost per kilogram of reference material (thorium plus uranium charged to reactor).

Optimization of Plant Size in an Expanding Economy

The cost studies described above assume that the processing plants operate at a constant full load equal to the requirements of the assumed static nuclear economy. A dynamic economy which starts small and grows over a period of years cannot expect to experience processing costs as low as those equivalent to a static economy of the same size at a given time. The processing plant can be oversized initially and start up with a low load, or spent fuel can be stockpiled initially so that the plant, when built, can start up with a higher load. The alternatives involve economics of scale, cost penalties associated with operation at less than full load, and cost penalties associated with inventory and storage charges on stockpiled fuel.

There should be an optimal stockpiling period and an optimal plant size, depending on the assumed growth rate and on economic parameters.

The general problem of optimizing plant size is quite complex, requiring computer calculations with such techniques as dynamic programming.[20,21] We are developing such an analysis as applied to fuel-cycle plants for advanced converter and breeder reactors to aid in our reactor evaluation studies. For the present, however, we are using less-general solutions to the problem, based on making enough simplifying assumptions to permit rapid hand calculations for estimating purposes. A simplified mathematical model similar to that of Manne[22] was developed for this purpose. It assumes that the economy grows linearly with time, that is, that the amount of spent fuel produced each year increases at a constant rate and that the planning horizon is infinite. It further assumes that the fuel is backlogged for y years, paying inventory and storage costs, at which time a plant of processing capacity mx comes on stream. The cycle is repetitive, with plants of size mx coming on stream every x years starting at year y. For our simplified model it can be shown that for a given x the optimal value of y is determined by Eq. (1):

$$ry + e^{-ry} = 1 + \frac{1}{2}\left(\frac{r^2Kx^a}{vm^{1-a}}\right) . \qquad (1)$$

For a given value of y the optimal value of x is determined by Eq. (2):

$$\frac{r^2Kx^a}{vm^{1-a}}\left[a\left(\frac{e^{rx}-1}{rx}\right)-1\right] = e^{ry} - e^{-ry} - 2ry. \qquad (2)$$

For x and y optimized simultaneously, Eq. (3) is applicable:

$$2a = \frac{rx}{e^{rx}-1}\left(\frac{e^{ry}+e^{-ry}-2}{e^{-ry}+ry-1}\right). \qquad (3)$$

In these equations, m is the growth rate of the annual spent-fuel production rate (such that mt is the production rate at time t), r is the effective discount interest rate for present-worth calculations, K is the capitalized cost of building and operating a processing plant of unit annual processing capacity, a is the cost-scaling factor for processing plants (such that the capitalized cost of building and operating a plant of size mx is Km^ax^a), and v is the value (for inventory charge purposes) of a unit amount of fuel. In general the present-worth-levelized processing cost per unit amount of fuel is given by Eq. (4):

$$p = v\left\{\frac{1 - e^{-ry}\left[e^{-ry} + 2ry - (r^2Kx^a/vm^{1-a})\right]}{1 - e^{-rx}}\right\}. \qquad (4)$$

The optimal (minimum) value of p (for x and y both optimized simultaneously) is given by Eq. (5):

$$\frac{p}{v} = \frac{1 - e^{-ry}(2 - e^{-ry})}{1 - e^{-rx}} . \qquad (5)$$

For $y = 0$ (no stockpiling of fuel), Eqs. (2) and (3) give

$$\frac{rx}{e^{rx}-1} = a , \qquad (6)$$

which is also Manne's result for this case. Manne's result with stockpiling disagrees with ours, since he used a different model for the cost of stockpiling.

To demonstrate this approach to reactor evaluation from the fuel processing viewpoint, a hypothetical nuclear economy growing at a rate of 1000 Mw (electrical) per year is considered. For PWR fuel processing, reasonable values of the parameters might be as follows: m = 44 metric tons/year^2, v = \$100,000/metric ton, r = 0.1 year^{-1}, a = 0.34, and K = \$8,800,000/(metric ton/year)^a. Trial-and-error solution of Eqs. (1) and (2) gives x = 21.4 years and y = 4.9 years. Equation 5 gives p = \$17,000/metric ton, which is equivalent to 0.108 mill/kwhr (electrical). For HTGR fuel the parameters would be the same except for m = 13.7, $v = 4 \times 10^5$, and $K = 9.4 \times 10^6$. In this case the optimal results are x = 20.6 years, y = 3.55 years, and p = \$41,000/metric ton or 0.081 mill/kwhr (electrical). If stockpiling is not permitted (y = 0), the optimal value of x becomes 18.7 in both cases, with p = \$22,900/metric ton for PWR and p = \$53,400/metric ton for HTGR. Thus, optimizing the stockpiling period saves about 25% in these cases.

[20] L. Thiriet, C. Oger, and P. deVaumas, *Long Term Developments in Irradiated Natural Uranium Processing Costs, Optimal Size and Siting of Plants*, CEA-R2642 (Geneva A/Conf/28/P/98) (1964).

[21] R. E. Bellman and S. E. Dreyfus, *Applied Dynamic Programming*, Princeton Univ. Press, 1962.

[22] A. S. Manne, *Econometrica* 29(4) 632–49 (1961).

At this point such a comparison between PWR and HTGR should be regarded as qualitative rather than quantitative, since the mathematical model is oversimplified and the numerical values of the parameters (m, v, r, a, and K) are subject to errors of estimation and also differences of opinion. This approach does, however, provide a less-arbitrary method of arriving at comparable processing costs for different reactor types than did our previous approaches of either specifying a fixed throughput (such as 1 or 10 metric tons/day) or a fixed nuclear economy [such as 15,000 Mw (electrical)]. Computer codes now being developed should permit more complicated (more accurate) mathematical models to be used for evaluation purposes.

18.4 COMPUTER CODE FOR STUDIES OF OVERALL POWER COSTS

Last year's annual report[12] described the development of a computer code (POWERCO) for calculating the cost of electricity produced by nuclear power plants. A report covering this work was written and will be issued.[23] The code uses a fundamental method of calculation that does not depend on fixed-charge rate. Equations are given for the exact calculation of fixed-charge rates and average fuel working capital under various conditions. The true role of these quantities in the determination of power cost is discussed in detail.

Additional progress was made in the formulation of codes for some of the component fuel-cycle costs. Computer code TASCO was written, covering the calculation of the cost of storing high-level liquid wastes in tanks on either a permanent or an interim storage basis. This code was used in an economic study by Blomeke *et al.*, in which optimal tank sizes were determined for acid and neutralized wastes under various economic conditions.[24]

18.5 SHIELDING DESIGN CODE FOR FUEL-HANDLING FACILITIES

SDC, a FORTRAN code designed for the IBM 7090 computer, was developed for calculating the gamma-shielding requirements for chemical processing, fabrication, or fuel-handling facilities.[25]

SDC can handle 13 source geometries (point, line, disk, plane, slab, cylinder with shield at side, cylinder with shield at end, sphere, ring, rod cluster, skew line, annular cylinder with shield at side, and annular cylinder with shield at end) either unshielded or shielded (by slab shields).

Materials of construction for shield, cladding, or source volume may be selected from a list of 17.

As many as 12 gamma-energy groups, covering an energy range from 0.10 to 10 Mev, with corresponding source strengths, may be used to describe the gamma spectrum.

Integration of the basic exponential-attenuation point kernel over the various geometries was the method chosen for calculating the uncollided gamma flux. Biological dose rate was obtained by multiplying this uncollided flux by the product of a flux-weighted buildup factor and a dose-conversion factor.

SDC was used successfully in several design jobs to evaluate shield thickness and dose rates. The average machine time was less than 0.01 hr per evaluation. Dose-rate determinations, where compared with experiment or other calculations, were conservative (+0 to 50%).

---

[23] R. Salmon, *A Procedure and a Computer Code (POWERCO) for Calculating the Cost of Electricity Produced by Nuclear Power Stations*, ORNL-3944 (March 1966).

[24] J. O. Blomeke, E. J. Frederick, R. Salmon, and E. D. Arnold, *The Costs of Permanent Disposal of Power-Reactor Fuel-Processing Wastes in Tanks*, ORNL-2873 (September 1965).

[25] E. D. Arnold and B. F. Maskewitz, *SDC, A Shielding-Design Calculation Code for Fuel-Handling Facilities*, ORNL-3041 (March 1966).

19. Preparation and Properties of Actinide-Element Oxides

The purpose of this program is to determine the microstructural, surface-chemical, and colloid-chemical properties that control the behavior of thoria, urania, and other oxides of metals of importance in the development of sol-gel processes. Techniques developed for thoria will be extended to studies of urania and plutonia as well as other actinide-element oxides.

19.1 FUNDAMENTAL STUDIES OF THORIA SOLS AND GELS

Viscosities of Dilute Thoria Sols

The viscosities of thoria sols (116-A crystallite) were measured at solids volume fractions of 0.041 and lower, at the optimum dispersion pH (2.70) of thoria. The fractional surface coverage of the thoria by nitrate ion is about 0.46. Values of reduced viscosity $(\eta/\eta_0 - 1)/\phi$ are tabulated (Table 19.1) for various solids volume fractions ϕ and for various temperatures, along with the nominal prolate spheroidal axial ratios for the particles, as calculated by the method of Simha.[1] The viscosities at the highest solids volume fractions probably reflect particle-particle interaction rather than particle shape.

At pH 2.70 the axial ratios at solids volume fractions (concentrations) of 0.00513 and higher are similar to those at pH 2, but below this concentration the flocs of particles tend to come apart, unlike the flocs at pH 2 or 3.6.[2] The sol then can be dispersed more easily at pH 2.70 than at the higher and lower pH values. However, this optimum state is evident only at low concentrations; at the higher concentrations a floc that appears to be in dynamic equilibrium with the individual particles is the dominant form of the hydrodynamically effective particles.

Rheology of Concentrated Thoria Sols

Flow curves (Fig. 19.1) were determined at pH 2.70 for 4.0 to 8.8 *M* thoria sols (116-A crystallites). The 8.0 and 8.8 *M* sols were actually soft gels that were pseudoplastic above the yield stress. At lower concentrations the sols behaved as simple pseudoplastics. Unlike the high-acid sols of Sturch,[3] these sols at pH 2.70 did not show complex thixotropic and rheopectic behavior.

Electrophoretic Studies of Thoria Sols

A major effort during the past year was the study of the electrophoretic behavior of thoria sols with a moving-boundary apparatus. At least two electrophoretic mobilities were repeatedly observed for the same thoria sol.

Sols were prepared by dispersing in distilled water some oxalate-precipitated thoria (140-A crystallite) that had been calcined at 800°C. Aliquots (100 ml) were then dialyzed in about 7 liters of HNO_3 solution (pH 3). The 1 and 0.33 *M* sols were so optically dense that only the leading edge (fastest-moving boundary if more than one boundary is present) of the ascending boundary

[1] R. Simha, "Effect of Shape and Interaction on the Viscosity of Dilute Solutions of Large Molecules," *Proc. Intern. Rheol. Congr., 1st Congr., 1948*, pp. II-68, II-76, North-Holland, Amsterdam, 1949.

[2] *Chem. Technol. Div. Ann. Progr. Rept. May 31, 1965*, ORNL-3830, p. 280.

[3] E. Sturch, *A Study of the Viscosity of Thoria Sols*, ORNL-TM-258 (June 13, 1962).

Table 19.1. Reduced Viscosities of Dilute Thoria Sols (116-A Crystallites) Measured at pH 2.70

Solids Volume Fraction, ϕ	Temperature (°C)	Reduced Viscosity	Nominal Prolate Spheroidal Axial Ratio
0.041	19.90	34.4	19.1
	25.50	30.0	17.5
	33.08	25.8	16.1
0.0205	19.89	16.1	11.2
	24.82	14.9	10.5
	33.07	13.4	9.9
0.01025	19.89	11.6	8.9
	25.40	11.0	8.5
	31.89	10.5	8.2
0.00513	19.72	9.4	7.6
	25.44	9.1	7.4
	33.10	8.4	6.9
0.00256	19.89	6.9	5.8
	25.43	6.2	5.3
	33.11	5.9	5.0
0.00128	19.89	5.6	4.8
	25.45	4.8	4.2
	30.07	2.5	1

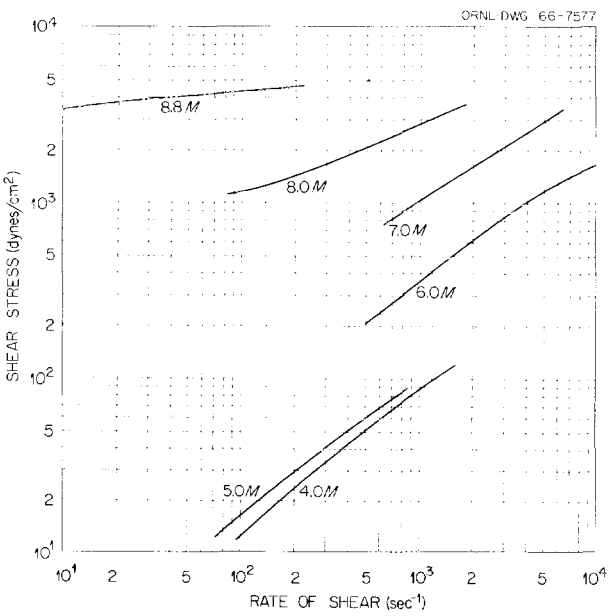

Fig. 19.1. Flow Curves for Thoria Sols of Varying Thoria Concentration.

and the trailing edge (slowest-moving boundary if more than one boundary is present) of the descending boundary could be observed. However, 0.1 and 0.033 *M* sols were sufficiently transparent to allow observation of the schlieren pattern (refractive-index gradient) throughout both channels of the electrophoretic cell. Two moving boundaries were observed in both the 0.1 and the 0.033 *M* sols in both the ascending and descending channels of the cell, indicating that all the sol particles did not possess the same effective charge density. The results are summarized in Table 19.2. The fastest-moving boundaries in the ascending and descending channels have the same electrophoretic mobility, as do the slowest-moving boundaries in the two channels; however, they are not enantiographs (mirror images). The most intense boundary in the ascending channel corresponds to the fastest-moving boundary; in the descending channel, however, the slowest-moving boundary is most intense. Other oxalate-precipitated thoria showed similar behavior.

Table 19.2. Electrophoretic Mobility of Thoria Sols (140-A Crystallites)

Sol Concentration (moles/liter)	Field Strength (v/cm)	Electrophoretic Mobility [$cm^2/(v \cdot sec)$]	
		Fastest Boundary	Slowest Boundary
		$\times 10^{-4}$	$\times 10^{-4}$
1	1.47	9.86 right[a]	1.36 left
0.33	1.51	5.39 right	2.13 left
0.1	1.12	6.8 right	3.5 left
0.033	1.22	3.84 right 3.83 left	3.51 right 3.50 left

[a]The right and left channels contain the descending and ascending boundaries respectively.

Table 19.2 shows that the electrophoretic mobility depends strongly on the sol concentration. This indicates that an unpredicted long-range interaction of the electrostatic fields of the colloidal particles might be occurring. To determine if crystal size or shape could be the cause of this unexpected observation, about 2 ml of "electrophoretically pure" thoria was collected with a macro preparative cell and the Beckman model H sampler, which was modified to handle thoria sols. Electron photomicrographs of the sol samples for each of the electrophoretically different regions were obtained. No marked difference in crystal size or shape was noted. The crystal habit appears to be predominantly octahedral or cubo-octahedral throughout; however, a mixture of cubic and octahedral habit cannot be ruled out.

A "CO_2-free" thoria sol was prepared by repeatedly peptizing thoria OXO-500 gel in concentrated HNO_3 under argon. All subsequent operations, including loading the electrophoresis cell, were done in a dry box with a constant argon purge. The electrophoretic pattern observed for the CO_2-free sol appears to be essentially the same as that for untreated thoria. However, when the same sol was saturated with CO_2, it showed essentially only one electrophoretic band, which was considerably slower than those for the CO_2-free sol.

Preliminary studies with ammonia-precipitated thoria showed essentially only one electrophoretic band. Multiple electrophoretic bands, then, are not common for all thoria. Further investigations to determine the origin of this anomaly are under way on these and other types of thoria. These studies will also be extended to urania and to other actinide-element oxides.

Preparation and Properties of Iron-Thoria Cermets and Mixtures

The feasibility of using the sol-gel process for dispersion hardening of metals or increasing the thermal conductivity of refractory oxides was studied, using iron-thoria cermets and mixtures.

These cermets and mixtures were made by mixing nitrate-stabilized α-Fe_2O_3 and ThO_2 sols in preparations varying in concentration from 2% Fe to 2% ThO_2 and by calcining in hydrogen the mixed gels made by drying these sols at 80°C in air. The iron sol was made by the method of Bradfield.[4] The thoria sols were made by peptizing calcined oxalate-derived thoria in dilute HNO_3. Electron photomicrography of the iron sol particles showed the predominant form to be an elongated, platy aggregate of fine, centrosymmetric particles. The aggregates, in overall shape, were similar to the iron sol particles shown by Overbeek,[5] but were not as elongated or as definite. A typical aggregate size was about 1600 by 800 A and consisted of parallel strings of centrosymmetric particles about 50 A in diameter. The iron crystal phase was identified as α-$Fe_2O_3 \cdot H_2O$ by x-ray

[4]R. Bradfield, *J. Am. Chem. Soc.* **44**, 965–74 (1922).

[5]J. Th. G. Overbeek, *Colloid Science*, vol. 1, ed. by H. R. Kruyt, p. 77, Elsevier, New York, 1952.

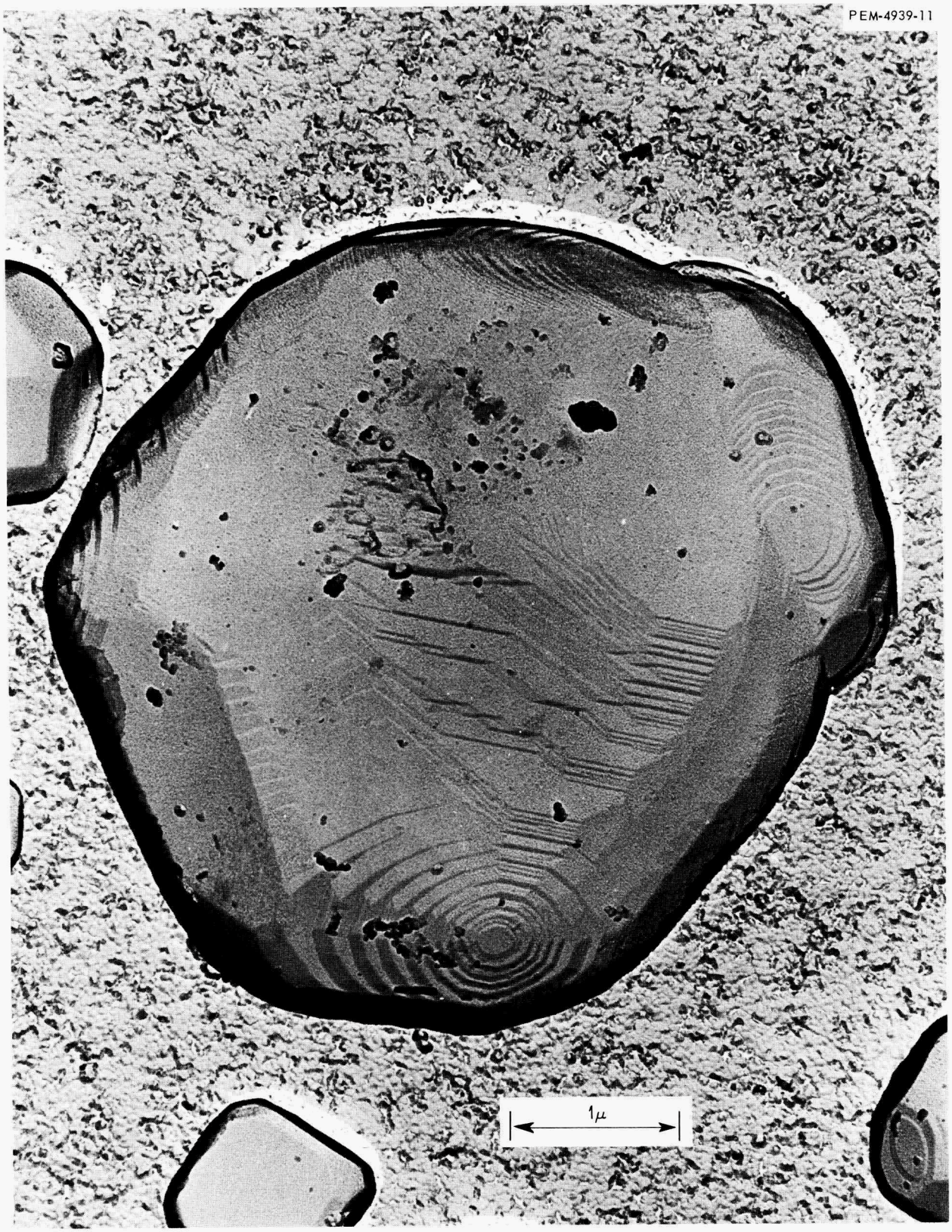

Fig. 19.2. Iron Crystals in 7.8% Iron-Thoria Cermet.

analysis, but the line intensities were insufficient for determining crystal size.

The x-ray analysis of the products calcined at 1100°C is presented in Table 19.3. The two products with highest iron compositions were made with the 116-A thoria (initial crystal size), and the rest were made with the 202-A thoria. The pattern of crystal growth is reasonable, but iron appears to possess anomalous, exaggerated grain growth at the intermediate compositions. Electron photomicrographs of replicas of fracture surfaces of these cermets reveal a grain structure whose characteristic dimensions do not agree quantitatively with the x-ray line broadening measurements; however, the pattern of exaggerated crystal growth at the intermediate compositions is again shown. Electron photomicrographs showed that the grain size of the 2% iron mixture was about 1 to 2 μ, while that of the 7.8% iron sample was about 2 to 10 μ. Figure 19.2 shows the grains of iron in the 7.8% iron cermet. The smaller well-formed grains at the edges are characteristic of the typical grains of the 2% iron sample, whereas the "overgrown" crystal shown in the center is observed frequently in the 7.8% sample. Metallographs show that thoria tends to be the interstitial continuous phase, even at proportions as low as 2%. However, the overall homogeneity of the mixture of phases appears fair for the high-iron sample and moderately good for the high-thoria sample. These samples are now being tested for strength and thermal conductivity.

Table 19.3. X-Ray Analysis of 1100°C-Calcined Iron-Thoria Cermets and Mixtures

Composition (% α-iron)	Crystallite Size (A)	
	Iron (110) Plane	Thoria (111) Plane
98	304	180
87	2500	210
70	2500	244
46	850	200
22	480	270
7.8	360	409
2	*a*	755

[a]Insufficient line intensity for measurement.

19.2 SURFACE AND SINTERING PROPERTIES OF SOL-GEL-DERIVED THORIA

The work reported in this section was done under subcontract with the University of Utah, under the direction of M. H. Wadsworth.

Sintering of Thoria Gels

The initial densification of thoria gel prepared from steam-denitrated thorium nitrate was studied by isothermal shrinkage measurements. The gel showed shrinkage (1) from water loss at temperatures below 600°C, and (2) from plastic flow and grain-boundary diffusion sintering from 600 to 1000°C. An initial, rapid 5% linear shrinkage of the gel was activated by temperature increase and adsorbed water vapor. Then an additional 6% shrinkage occurred by grain-boundary diffusion sintering. Measurements in nitrogen–water vapor and argon-hydrogen suggested O^{2-} vacancies as the diffusion-controlling species. The activation energy for diffusion sintering in air was 39.0 kcal/mole.

Calcined thorium oxalate powder compacts also showed isothermal grain-boundary diffusion shrinkage, but with an activation energy of only 18.9 kcal/mole. Perhaps this can be attributed to a high vacancy concentration in the relic structure left by initial calcination.

Low-Temperature Shrinkage of Thoria Gel

The linear relationship of the weight loss and the volume change of thoria gel undergoing shrinkage below 500°C was determined experimentally. This linearity allows theoretical significance to be given to the shrinkage equation, which was empirically found to be obeyed:

$$(L/L_0)^2 - (L/L_0)^3 = b(\log t + \log c) \ , \qquad (1)$$

where

L = length of sample,

L_0 = original length of sample,

t = time,

b = constant,

c = constant.

The constants are found by theory to be composed of the following theoretical and measured quantities:

$$b = \frac{2.303RTP_0}{3S\alpha} , \qquad (2)$$

$$c = \frac{\alpha k}{hR} \frac{fW_0 - W}{W_0} - \Delta F_0^{\ddagger}/RT , \qquad (3)$$

where

R = the gas constant,

T = absolute temperature,

α = a free-energy correction coefficient,

k = Boltzmann's constant,

h = Planck's constant,

f = weight fraction of water in the sample,

W_0 = initial sample weight,

W = sample weight at time t,

$\Delta F_0^{\ddagger}$ = initial activation energy for shrinkage,

P_0 = initial sample bulk density,

S = constant of proportionality between weight loss and volume shrinkage.

Equation (3) assumes that the free energy of activation is a linear function of the weight loss according to the equation

$$F^{\ddagger} = F_0^{\ddagger} + \alpha \frac{W}{W_0} . \qquad (4)$$

The weight loss here refers only to chemisorbed species. Physical water appears to play no role in low-temperature shrinkage; it merely fills the interstices between particles and produces no shrinkage when removed. Most physically adsorbed water is removed by simple room-temperature evacuation of the gel at 3 μ Hg. The remainder is removable by heating to 150°C. Heating from 150 to 500°C removes chemisorbed water and nitrate from the gel.

Preliminary data indicated a value of α of 1.33×10^3 kcal/mole, which leads to a correction term, $\alpha W/W_0$, of from 10 to 40 kcal/mole. This is a very large value, and suggests that the free energy of activation of shrinkage is strongly dependent on the amount of water and nitrate present.

Infrared Spectroscopy of Thoria Gel

Infrared spectroscopy of the nitrate and water in thoria gel was extended to the near-infrared region. A broad absorption band extending from 2.6 to 4.3 μ was found. In addition, peaks occurred at 2.2, 1.9, 1.4, and possibly 0.58 μ. The peak at 1.9 μ is a combined O–H stretching and H_2O deformation band for physically adsorbed water. The peaks at 1.4 and 2.2 μ are controversial, but they also appear in silica gel. Some suggested assignments of these peaks are the first overtone of the O–H stretching mode and combination of H_2O deformation, or combination of the SiOH deformation fundamental; or the peaks might result from absorption in the crystal lattice.

The nitrato absorption band at 1030 cm^{-1} is increased in intensity by removal of physically adsorbed water at room temperature. Evacuation to 10^{-2} μ Hg and heating of the gel to 150°C causes some of this band to become a doublet, with sharp peaks at 850 and 800 cm^{-1}. The peaks cannot be positively identified, but they are thought to result from nitrato nitrate association with surface hydroxyls. Heating to 300°C causes a decrease in the nitrato doublet at 1000 and 1030 cm^{-1}, removes the 850 cm^{-1} peak, and sharpens the 800 cm^{-1} peak.

Grain Growth and Densification of Thoria Gel

The effects on grain growth and densification of firing in nitrogen and in hydrogen were studied. Little difference in either densification or grain growth was noted up to 900°C. At 1050°C, however, the hydrogen-fired sample densified to 10.0 after only 60 min, whereas 530 min was required in nitrogen. Presoaking the samples at 900°C in their respective atmospheres did not alter the qualitative differences in densification and grain growth noted at 1050°C. Samples presoaked at 900°C showed a density of 9.94 in nitrogen after 880 min; in hydrogen the density was 9.99 after 10 min. The same pattern was followed for firing at 1150°C. In nitrogen a density of 10.01 was achieved in 150 min; in hydrogen this density was reached in 30 min.

19.3 URANIA GEL OXIDATION

Urania (but not thoria) sols and gels are sensitive to air oxidation. Preliminary efforts were made to evaluate this problem, and to determine the kind and extent of safeguards necessary to obtain valid, reproducible results in the study of such materials.

Urania gel having an initial O/U mole ratio of 2.05 was allowed to spontaneously oxidize in air. When the ratio exceeded 2.35, oxidation caused severe reduction of area (from 72 m^2/g to 17 m^2/g and less). Figure 19.3 shows the effect of oxidation on the x-ray diffraction powder pattern of the urania. Initially, there was a peak characteristic of the (111) diffraction line of 30-A urania crystallites. The extremely rich pattern shown for the composition $UO_{2.45}$ could not be identified as that of any of the known uranium oxides or hydrates of uranium oxides. However, many of the lines were found to correspond to an unidentified component of hydrated UO_3 prepared by steam hydrolysis of ammonium diuranate. The x-ray pattern of the oxidized urania is thought to result from a mixture of two hydrates of uranium oxide, both of which were hitherto unreported.

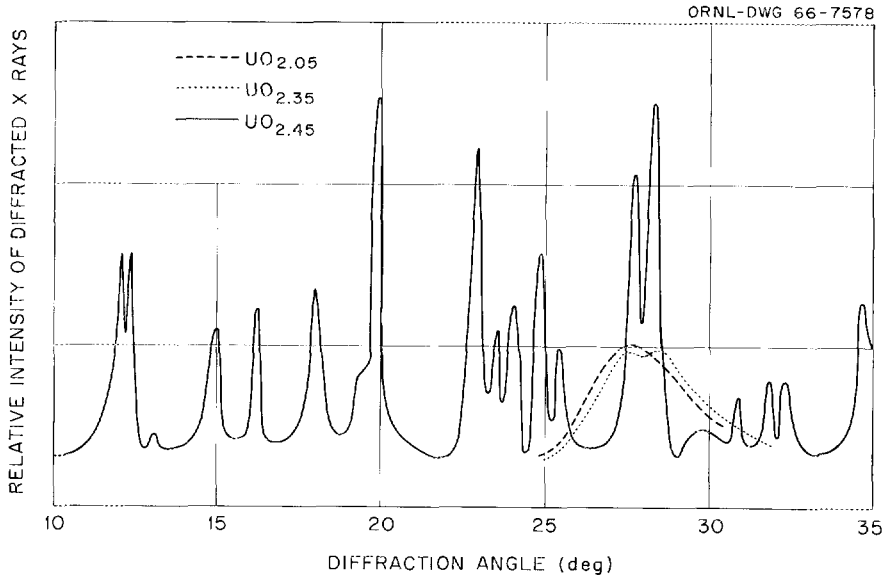

Fig. 19.3. X-Ray Diffraction of Partially Oxidized Urania Gel.

20. Assistance Programs

The Chemical Technology Division provided assistance to others on several projects. The Eurochemic Assistance Program was continued. Under this program, the Laboratory is coordinating the exchange of information between Eurochemic and the various AEC sites and is currently supplying the U.S. Technical Advisor to Eurochemic during the construction and start-up periods. Engineering assistance on the disposal of high-radioactivity-level solid waste in salt was provided the Health Physics Division. This work was completed in November 1965. Assistance on alpha-laboratory design included the preparation of a detailed design study for a 32-laboratory alpha facility. The program on fuel shipping safety studies was expanded to provide more theoretical and experimental data to ensure that the shipping of spent nuclear fuels can be done in the safest possible manner in order to provide near-absolute protection to the public.

Additional irradiation-contamination-decontamination evaluation tests were made on selected protective coatings and plastics. Evaluation of commercial protective coatings to gamma radiation and to fission product contamination in a simulated reactor accident was continued. A new procedure for determining the decontaminability of protective coatings was developed and tested.

20.1 EUROCHEMIC ASSISTANCE PROGRAM

The Laboratory continued to coordinate the Eurochemic Assistance Program for the exchange of information between Eurochemic and the several AEC sites included in the program. In addition, the Laboratory is supplying the services of the U.S. Technical Advisor, E. M. Shank, who will remain at Mol, Belgium, during the construction and start-up phases of the Eurochemic plant.

During the past year, 494 USAEC-originated documents and 80 drawings and miscellaneous items of information were sent to Eurochemic. Twenty-five Eurochemic documents written in English were received, reproduced, and distributed. In addition, two Eurochemic reports (French) were translated for distribution in English.

Construction of the Eurochemic facility was completed, and the checkout of equipment and cold runs are now in progress. The plant is now scheduled to go "hot" during October 1966.

20.2 DEMONSTRATION OF THE DISPOSAL OF SOLID, HIGH-LEVEL RADIOACTIVE WASTE IN SALT

Project Salt Vault, the Health Physics Division's field demonstration of the disposal of highly radioactive waste in salt, was placed in hot operation in November 1965 with the storage of 14 short-cooled Engineering Test Reactor (ETR) fuel assemblies in a salt mine at Lyons, Kansas. The equipment designed and developed in the Chemical Technology Division was tested during cold runs made during September, using operating instructions prepared for the transfer and storage of radioactive material. The first runs were cold and proved highly beneficial in checking out the operating procedures and potential pitfalls that would have been costly in the hot runs. Several minor equipment changes were made to simplify or improve the operations, and the instructions were reworked to provide for maximum safety. Five hundred curies of ^{60}Co in each of two canisters were used in the next runs in October; these runs were very useful in scouting radiation levels in the various operating areas. Radiation streaming in excess of tolerance from a construction joint in the shipping cask was found. This was eliminated by

adding an extra shielding band of $2\frac{1}{2}$ in. of lead to the cask over the joint. The band was fabricated from field measurements on the cask and installed at the site. Radiation readings with the ^{60}Co source were reduced from 60 mr/hr to about 6. When the cask was loaded with 14 ETR fuel assemblies, the maximum cask reading was 45 mr/hr at contact. The reading for the above-ground working area when the cask was in position for charging the fuel assemblies to the mine was less than 1 mr/hr, and the transporter shield with the loaded assemblies in the mine also showed less than 1 mr/hr. Radiation streaming from the fuel assemblies in the storage hole was about 2 r/hr immediately over the hole. Supplementary scatter shields filled with lead shot were fabricated and installed, reducing the level to less than 10 mr/hr at the floor level immediately over the storage holes.

Fuel loading into the canisters at the National Reactor Test Station was accomplished with little difficulty after development of the appropriate hot-cell loading techniques. Using equipment developed and built at the Laboratory, remote loading of the canisters into the cask in the large hot cell went smoothly. Radiation damage to the ethylene glycol coolant was more severe than expected and led to gassing of the coolant. The cooling system was cleaned out, and the ethylene glycol was replaced with demineralized water; an ion exchange column was added to the system in an additional effort to keep the system clean. No further difficulty was encountered with the cooling system during transit between Idaho and Kansas or during operations at Kansas.

20.3 HIGH-LEVEL ALPHA LABORATORY

Detailed design and cost evaluation studies for a high-level alpha laboratory were continued and have culminated in the preparation of a design package suitable for use by an architect-engineer. The laboratory, which will be administered by the Analytical Chemistry Division, is estimated to cost about $5,000,000. It will be located in Melton Valley and will occupy an area of about 50,000 ft^2. In addition to office, service, and cold-laboratory support facilities, the building will contain thirty 16- by 32-ft alpha laboratories, a 32- by 88-ft high-bay area, and a 32- by 64-ft shielded glovebox area. These will provide analytical, chemical, metallurgical, and chemical engineering facilities with capabilities for handling up to 100 curies of ^{239}Pu equivalent and lesser amounts of alpha-gamma- or alpha-neutron-emitting materials.

Since the project has been put off until fiscal year 1968, no further detailed design will be done during the interim; however, in an effort to effect additional construction economies, several alternative building arrangements are being evaluated.

20.4 FUEL-SHIPPING SAFETY STUDIES

To provide technical backup data for Federal Regulations (10 CFR 72) designed to ensure the safety of spent fuel shipments by public carriers, both theoretical and experimental studies are being made. The scope of this program was increased materially during the past year.

It is presently realized that there is a distinct lack of information concerning minimum standards of good engineering practice in the design, fabrication, and testing of shipping containers for transporting radioactive materials. To overcome these shortcomings and to provide standard methods of container analysis, a program was undertaken to provide design information in a number of different areas.

Formulas to be used by the design engineer to calculate the maximum stress produced in a cask used to ship radioactive materials when it is subjected to internal pressure were developed. These are presented in the report *Structural Analysis of Shipping Casks, Vol. 1, Analysis of a Shipping Cask Subjected to Internal Pressure* (ORNL-TM-1312). The formulas take into account the elasticity of lead shielding and will predict the thickness of the cavity wall for casks of both prismatic and cylindrical configurations.

Volumes 2 and 3, which cover closures, lifting and tie-down devices, and the required thickness of the outer cask shell to resist puncture, have been completed in draft form.

This information will provide standard methods of cask analysis and reporting. Additional work this coming year in all phases of cask design will cover areas of heat transfer, shielding, materials, fabrication, criticality, testing, and maintenance.

The shipping cask manual[1] (ORNL-TM-681) prepared last year is being upgraded by ORNL and

[1] *Chem. Technol. Div. Ann. Progr. Rept. May 31, 1965*, ORNL-3830, p. 269.

Battelle Memorial Institute, under a subcontract, for reissue as an AEC-sponsored monograph.

20.5 EVALUATION OF RADIATION RESISTANCE AND DECONTAMINABILITY OF SELECTED PROTECTIVE COATINGS

Tests to evaluate commercial protective coatings for use in reactor containment vessels, spent-fuel processing plants, and laboratories handling radioactive materials were conducted by exposing sample coatings to (1) gamma radiation, (2) fallout of radioactive fission products from the plasma-jet volatilization of irradiated UO_2 in a 1350-ft^3 vessel, and (3) a tentative standard decontamination test. The Nuclear Safety Pilot Plant group conducted the volatilization test with coated specimens supplied by the Chemical Technology Division.

Radiation-Tolerance Testing

Seventy-five commercial coatings, applied to steel, stainless steel, concrete, and Fiberglas, were exposed to ^{60}Co gamma radiation at an intensity of 1×10^6 r/hr at 40 to 50°C in demineralized water and in air. Three newly tested coatings surpassed the previous high (5×10^9 r) radiation resistance[2] in demineralized water; these were (1) Carboline Company's system K, which consisted of a modified phenolic (Phenoline 368) embedded in glass cloth and Phenoline 368 seal coat; this coating failed at 8.3×10^9 r by blistering and loss of adhesion; (2) Varni-Lite Corporation's No. S-0900 epoxy system, which failed at 8.0×10^9 r by blistering; and (3) Amercoat No. 1762 with No. 66 epoxy seal coat, which failed at 7.9×10^9 r by chalking. There is also evidence of improved radiation tolerance in air, since many (19 of 75) of the newer coatings appear to be serviceable after an exposure of 1×10^{10} r. A summary of these recent tests is given in Table 20.1.

Studies of Contamination due to a Simulated Reactor Excursion

Protective-coating and control specimens were exposed in the Nuclear Safety Pilot Plant to an atmosphere contaminated with radioactive fission products from plasma-jet volatilization of natural UO_2 that had been irradiated to an average neutron exposure of 4.5×10^{10}. About 0.6 curie of total mixed-fission-product gamma radiation (after cooling for seven days) was airborne in this test. The amount of radionuclides deposited on the samples was measured and compared. The contaminants were identified and measured by scanning the specimens with a gamma-ray spectrometer before decontamination.

A polyester coating retained the least amount of radionuclides; the three best vinyls and epoxies retained about 32 and 36% more respectively. Coatings exhibiting the least retention of the ten radionuclides (^{131}I, ^{147}Nd, ^{239}Np, ^{132}Te, ^{103}Ru, ^{141}Ce, ^{99}Mo, ^{95}Zr-Nb, ^{137}Cs, ^{140}Ba-La) were as follows:

Vinyls

No. 33, Amercoat Corporation
No. SX-1666, Devoe and Raynolds Company
Nukem-40, Amercoat Corporation

Epoxies

No. R4-74F, Plas-Chem Corporation
No. R4-74E, Plas-Chem Corporation
No. SX-1655, Devoe and Raynolds

Modified Phenolics

Phenoline 300, Carboline Company
Phenoline 305, Carboline Company
No. 7122, 7133X, Wisconsin Protective Coating Company

Polyester

Liquid glass No. 5301, Stanley Chemical Company

Chlorinated Rubber

No. SX-1661, Devoe and Raynolds Company

Inorganics

Dimetcote-4, Amercoat Corporation
Dimetcote-3, Amercoat Corporation

Improved Test to Determine Decontaminability of Coatings

A standard (ASTM type) test for evaluating the decontaminability of protective coatings and paints does not now exist. A previous procedure included the use of 3 *M* (17.2%) HNO_3, which in some cases

[2] *Chem. Technol. Div. Ann. Progr. Rept. May 31, 1965*, ORNL-3830, pp. 296–98.

attacked and removed a surface layer from some of the coatings. Furthermore, the contaminating solution (a solution of mixed fission products in nitric acid) became more concentrated in nitric acid as the solution evaporated to dryness on the specimens, again resulting in surface attack and false results.

A new approach to the evaluation of decontaminability is being developed. The specifications and procedure are summarized below:

1. Contaminants consist of mixed fission products from spent fuel (20,000 Mwd/ton burnup, cooled one year).
2. Contaminants are dissolved in 8 *M* HNO_3 solution, which is to be adjusted to a pH of 4 at the time of application.
3. Radionuclides to be deposited on coupons include ^{144}Ce-Pr, ^{106}Ru-Rh, ^{95}Zr-Nb, and ^{137}Cs-^{137m}Ba at 6×10^4 to 2×10^5 dis min^{-1} nuclide^{-1}.
4. Contaminated coupons are to be immersed successively in: (*a*) agitated tap water at room temperature, (*b*) agitated weak acid solution of $C_2H_2O_4$ (0.4 *M*), NaF (0.05 *M*), and H_2O_2 (0.3 *M*), at room temperature, (c) agitated weak acid solution (as above) at 80°C.
5. Radionuclides originally deposited and remaining after each decontamination step are measured and identified by a gamma-ray spectrometer.

The decontaminability of several paints was measured to evaluate the utility of the test, and the results are summarized in Table 20.2. The first water wash removed all of the ^{137}Cs-^{137m}Ba, and the other contaminants were removed generally to the extent of 50 to 90% for all types of coupons. Plate glass was the most completely decontaminated material; after the water wash, no ^{95}Zr-Nb remained. Other coupons were not as readily cleaned as the glass; however, epoxy SX-1346 gave up about 98% of the ^{95}Zr-Nb. After the 80°C mild-acid wash, the contaminants on the glass and Varni-Lite S-0900 had reached the lower limit of detection, providing an overall decontamination factor of 600. Ruthenium-106 was the most difficult element to remove.

Table 20.1. Gamma-Radiation-Resistance Rating of Several Protective Coatings

Radiation source: ^{60}Co at 1×10^6 r/hr
Temperature: 40 to 50°C
Manufacturers are listed in alphabetical order

Manufacturer	Coating	Substrate	Exposure Under Demineralized Water (r)	Effect[a]	Exposure in Air (r)	Effect[a]
Amercoat Corporation	Epoxy, No. 1762 and No. 66	Concrete	7.9×10^9	A	6.2×10^9	D
	Epoxy, No. 4000 Bondstrand pipe	Fiberglas	1.0×10^{10}		1.0×10^{10}	
	Polyester, No. 5000 Bondstrand pipe	Fiberglas	1.0×10^{10}		1.0×10^{10}	
	Inorganic, Dimetcote-3	Steel			2.2×10^{10}	
	Inorganic, No. 1741	316 steel	9.6×10^8	C	1.0×10^{10}	F
	Inorganic, Dimetcote-4	Steel	3.9×10^9	G	1.0×10^{10}	
	Epoxy, No. 1762 and No. 66 gloss	Concrete	2.2×10^9	C	4.2×10^9	B
	Epoxy, No. 1762 and No. 1732	Concrete	1.7×10^9	C	4.2×10^9	B
	Vinyl, No. 1762 and No. 33HB	Concrete	1.2×10^9	C	3.2×10^9	A,B
	Epoxy, No. 1762 and No. 74	Concrete	1.7×10^9	A,B,C	2.7×10^9	B
	Vinyl, No. 1762 and No. 88	Concrete	1.2×10^9	C	2.7×10^9	A,B
	Vinyl, No. 1762, No. 88, and No. 99	Concrete	1.2×10^9	C	2.7×10^9	A,D
Carboline Company	Modified phenolic, system K	Concrete	5.8×10^9	C,D	1×10^{10}	
	(Phenoline 368)	Steel	8.3×10^9	C,D	1×10^{10}	
	Modified phenolic, system C	Concrete	3.6×10^9	C,D	8.3×10^9	B,C
	(Phenoline 300)	Steel	6.3×10^9	A,B	1×10^{10}	
	Modified phenolic, system H	Concrete	2.6×10^9	C	1×10^{10}	
	(Phenoline 368)	Steel	6.3×10^9	C	1×10^{10}	
	Modified phenolic, system G	Concrete	4.7×10^9	C	1×10^{10}	
	(Phenoline 368)	Steel	4.7×10^9	C	1×10^{10}	
	Modified phenolic, system I	Concrete	4.7×10^9	C	1×10^{10}	
	(Phenoline 368)	Steel	3.6×10^9	C	1×10^{10}	
	Modified phenolic, system F	Concrete	No test		7.8×10^9	C
	(Phenoline 300-368)	Steel	3.6×10^9	C	6.8×10^9	C
	Modified phenolic, system J	Concrete	2.1×10^9	A	4.7×10^9	B,C
	(Phenoline 305)	Steel	2.1×10^9	A	1×10^{10}	
	Modified phenolic, system A	Concrete	4.3×10^9	A,C	3.2×10^9	C
	(Phenoline 300)	Steel	4.7×10^9	C	7.1×10^9	B,C
	Modified phenolic, system B	Concrete	2.6×10^9	C	5.6×10^9	B,C
	(Phenoline 305)	Steel	3.6×10^9	C	7.1×10^9	C

Table 20.1 (continued)

Manufacturer	Coating	Substrate	Exposure Under Demineralized Water (r)	Effect[a]	Exposure in Air (r)	Effect[a]
	Modified phenolic, system D	Concrete	2.1×10^9	A,E	6.0×10^9	C
	(Phenoline 300)	Steel	4.7×10^9	A,E	1×10^{10}	
	Modified phenolic, system E	Concrete	2.1×10^9	A	6.0×10^9	C
	(Phenoline 300)	Steel	2.1×10^9	A	6.8×10^9	B
Devoe and Raynolds	Epoxy (No. 4), 46612, 43614	Steel	1.0×10^9	C	1.0×10^{10}	
	Catalyzed epoxy (No. 2), 46612, OX-1055	Steel	1.57×10^9	C	1.0×10^{10}	
	Modified epoxy (No. 3), ReNew Coat	Concrete	2.9×10^9	A	1.0×10^{10}	
	Epoxy (No. 3), 46612, SX-1346	Steel	2.0×10^8	C	1.0×10^{10}	
	Acrylic (No. 1), MX-140, MX-142, MX-145	Steel	2.0×10^8	C	1.0×10^{10}	
	Chlorinated rubber (No. 2C), SX-1662, SX-1661	Concrete	3.2×10^8	C	1.0×10^{10}	
	Vinyl (11-S), 46610, SX-1667	Steel	8.5×10^8	C	1.0×10^{10}	C
	Epoxy (1-C), SX-1655, SX-1655	Concrete	1.3×10^9	C	8.97×10^9	C
	Epoxy (FS-3C), Catalyzed 46000, SX-1665	Steel	1.58×10^9	A,B,E	$>7.0 \times 10^9$	
	Vinyl (FS-5), SX-1666	Steel	1.8×10^8	C	$>7.0 \times 10^9$	
	Epoxy (FS-4), RB-1304, SX-1665	Steel	9.0×10^8	C	3.87×10^9	C
	Epoxy (FC-6), SX-1665	Concrete	1.4×10^9	A,B	$>7.0 \times 10^9$	
	Epoxy (FC-3), OX-1055	Concrete	1.4×10^9	A,B	$>7.0 \times 10^9$	
	Epoxy (FC-2), Catalyzed 48101, OX-1055	Concrete	1.4×10^9	A,B	$>7.0 \times 10^9$	
	Epoxy (FS-3B), Catalyzed 46000, SX-1665	Steel	9.0×10^8	C	$>7.0 \times 10^9$	
	Epoxy (FS-2), Catalyzed 46610, 46613, 46614	Steel	5.4×10^8	C	$>7.0 \times 10^9$	
	Epoxy (FC-8), SX-1029	Concrete	1.4×10^9	C	2.68×10^9	A,C
	Epoxy (FS-3A), Catalyzed 46000, SX-1665	Steel	9.0×10^8	C	2.8×10^9	C
	Acrylic (FC-7), MX-148	Concrete	1.8×10^8	C	2.68×10^9	B,D
	Epoxy (FG-6), SX-1655(FG)	Concrete	1.5×10^9	A	$>5.0 \times 10^9$	
	Epoxy (FG-5), SX-1665(FG)	Concrete	1.5×10^9	A,C	2.5×10^9	C
	Epoxy (FG-3), OX-1055(FG)	Concrete	1.5×10^9	A	$>5.0 \times 10^9$	
	Epoxy (FC-4), SX-1665	Concrete	1.4×10^9	A,C	1.7×10^9	C
	Catalyzed epoxy (No. 2), OX-1055	Concrete	1.57×10^9	C	1.53×10^9	B
	Epoxy (FG-4), SX-1665(FG)	Concrete	1.5×10^9	C	1.5×10^9	C
	Epoxy (1-S), 4600, SX-1655	Steel	8.5×10^8	C	1.0×10^{10}	C
	Chlorinated rubber (No. 2C), SX-1662, SX-1661	Steel	3.2×10^8	C	1.0×10^{10}	B,C,D
	Epoxy (FC-1), Catalyzed 48101, SX-1346	Concrete	5.4×10^8	C	$>7.0 \times 10^9$	
	Chlorinated rubber, (No. 6), 14700, 47212, 47201	Steel	2.0×10^8	A,C	9.5×10^9	B

Table 20.1 (continued)

Manufacturer	Coating	Substrate	Exposure Under Demineralized Water (r)	Effect[a]	Exposure in Air (r)	Effect[a]
	Epoxy (FS-6), RB-1033, SX-1029	Steel	1.8×10^8	C	2.2×10^9	C
	Vinyl (10-C), No. SX-1667 and 1666	Concrete	5.28×10^8	C	1.87×10^9	A,B
	Chlorinated rubber (No. 5), 4600, 47212N, 47201	Steel	2.0×10^8	A,C	1.53×10^9	B
	Epoxy (No. 1), OX-1055 and SX-1346	Concrete	2.0×10^8	C,D	1.5×10^9	B
	Vinyl (FC-9), L-10429, PVS	Concrete	1.8×10^8	C,D	9.0×10^8	D
	Acrylic (FS-1), 303, MX-145, MX-148	Steel	9.0×10^8	C	5.4×10^8	B,D
	Epoxy (FC-5), SX-1665	Concrete	1.4×10^9	A,B	$>7.0 \times 10^9$	
Hughson Chemical Company	Polyurethane, Z552 (B)	Concrete	1.0×10^9	C	$>6.0 \times 10^9$	
		Steel	1.0×10^9	D	4.6×10^9	B
	Polyurethane, Z051, (C-1)	Steel	1.0×10^9	C,E	4.6×10^9	B
	Polyurethane, Z051, (C-3)	Steel	1.68×10^8	C	4.6×10^9	B
	Polyurethane, Z552, (A)	Concrete	1.0×10^9	C	$>6.0 \times 10^9$	
		Steel	1.68×10^8	C	2.9×10^9	B
	Polyurethane, Z001, (D)	Steel	5.0×10^8	C,E	4.6×10^9	B
	Polyurethane, Z452, (E)	Steel	5.0×10^8	D	4.6×10^9	B
	Polyurethane, Z051, (C-2)	Steel	1.68×10^8	C	1.3×10^9	C
	Polyurethane, Z051, (C-4)	Steel	1.68×10^8	C	1.0×10^9	C
Varni-Lite Corporation	Epoxy, S0900	Concrete	8.0×10^9	C	1.0×10^{10}	
		Steel	(Not in H_2O)		1.0×10^{10}	
	Epoxy, industrial	Concrete	8.56×10^8	C	4.0×10^9	B
		Steel	(Not in H_2O)		1.0×10^{10}	
	Epoxy, S0800	Concrete	8.56×10^8	C	3.0×10^9	B,C
		Steel	(Not in H_2O)		3.0×10^9	B,C
	Epoxy, industrial special	Concrete	8.56×10^8	C	1.9×10^9	C
		Steel	(Not in H_2O)		1.9×10^9	C
Wisconsin Protective Coating Company	Modified phenolic (No. 5), 7155, FG, 7133H	Steel	3.0×10^9	B,E	1.4×10^{10}	
	Modified phenolic (No. 4), 7100H, FG, 7133H	Steel	1.1×10^9	C	1.4×10^{10}	
	Modified phenolic (No. 2), 9028, 7155, FG, 7133H	Concrete	3.0×10^9	B	7.2×10^9	B
	Modified phenolic (No. 1), 9028, 7100H, FG, 7133H	Concrete	2.7×10^9	C	4.2×10^9	C
	Epoxy (No. 3), 9028, 9009-1	Concrete	3.0×10^9	C	2.7×10^9	B,C
	Epoxy (No. 6), 9009-1	Steel	3.0×10^9	B	2.7×10^9	B

[a]Radiation effect: A – coating chalked; B – coating embrittled; C – coating blistered; D – loss of adhesion; E – interfacial area attack; F – rough, sandlike surface; G – bleeding of binder materials.

Table 20.2. Results of Decontaminability Test: Comparison of Results for Overall Factors with Factors for Ruthenium

Test Coupon	Initial Radioactivity (dis/min)	Final Radioactivity (dis/min)	Overall Decontamination Factor	Decontamination Factor for ^{106}Ru
	$\times 10^5$			
Controls				
Plate glass	5.18	<550	>900	>800
Stainless steel, 304L (2-B finish)	5.66	1.01×10^3	560	185
Teflon sheet	6.00	2.43×10^3	247	185
Polyethylene sheet	5.30	1.81×10^3	293	112
Test Coatings				
Amercoat Corp.				
No. 99 semigloss (vinyl)	5.72	3.65×10^3	156	56
No. 33 HB (vinyl)	5.20	3.56×10^4	14	29
No. 66 (epoxy)	5.26	7.64×10^4	7	7
Carboline Co. coatings				
Phenoline 300 (modified phenolic)	4.72	1.93×10^4	24	13
Phenoline 305 (modified phenolic)	6.14	2.65×10^4	23	10
Phenoline 368(H), (modified phenolic)	5.34	2.77×10^4	19	13
Phenoline 368(G), (modified phenolic)	5.27	3.73×10^4	14	8
Devoe and Raynolds Corp.				
No. SX-1346 (epoxy)	5.97	4.75×10^3	125	52
No. SX-1667 (vinyl)	5.39	4.50×10^3	120	40
No. SX-1666 (vinyl)	5.80	5.80×10^3	100	35
No. 47201 (chlorinated rubber)	5.34	5.47×10^3	97	32
No. SX-1661 (chlorinated rubber)	5.34	7.12×10^3	75	25
No. SX-1665 (epoxy)	4.99	6.94×10^3	72	35
No. SX-1665(B), (epoxy)	4.88	7.03×10^3	69	39
No. 46614 (epoxy)	5.20	8.09×10^3	64	29
No. MX-145 (acrylic)	5.46	2.18×10^4	20	8
David E. Long Corp.				
Series-A (vinyl)	5.39	1.19×10^4	45	19
Pittsburg Plate Glass Co.				
No. UC-9647 (epoxy)	5.34	5.61×10^4	9	17
No. U-8134 (vinyl)	5.76	8.55×10^3	66	44
Vami-Lite Corp.				
No. S-0900 (epoxy)	5.34	<900	>590	>330
Industrial special (epoxy)	5.75	7.51×10^3	78	30
No. S-0800 (epoxy)	5.94	1.36×10^4	44	18
Industrial (epoxy)	5.84	2.25×10^4	26	26
Wisconsin Protective Coating Co.				
Plasite 7155 (modified phenolic)	5.53	1.62×10^4	34	14
Plasite 7100 (modified phenolic)	4.82	2.40×10^4	20	15
Plasite 7122 (modified phenolic)	4.39	3.14×10^4	14	10

21. Water Research Program

Work by the Chemical Technology Division on the Water Research Program is reported directly to the Office of Saline Water, and only an abstract appears in this report (see the Summary).

22. Chemistry of Carbides and Nitrides

The basic chemistry of uranium, thorium, plutonium, and other carbides and nitrides is being investigated, particularly in aqueous and gaseous systems. This work has application in connection with the processing of power reactor fuels (Sect. 1), reactor safety, and high-temperature materials development (Sect. 8). Most of the work to date has consisted in studies of the hydrolysis of uranium and thorium carbide specimens that were carefully characterized by means of advanced analytical and metallographic techniques. Since the specimens were well characterized, information on the uranium-carbon and thorium-carbon phase diagrams was a natural by-product of this work. During the past year, the reactions of thorium carbides with sodium hydroxide solutions and the effect of phase distribution on the hydrolysis of uranium monocarbide-dicarbide mixtures were studied. Information on the high-temperature region of immiscibility in the uranium-carbon system was also obtained. The results of these studies were reported in the open literature;[1–3] consequently, only a brief summation of the main conclusions is given here.

Hydrolysis of the thorium carbides in 2 to 18 *M* NaOH at 80°C gave practically the same results as obtained with water.[1] The monocarbide yielded ThO_2 and 90 ml (STP) of gas per gram of carbide. The gas consisted of 83% methane, 13% hydrogen, and small quantities of C_2 to C_8 hydrocarbons. The dicarbide ($ThC_{1.95}$) yielded ThO_2, a nonvolatile wax, and a gas composed of about 35% hydrogen, 30% ethane, 4% methane, 25% unsaturated C_2 to C_8 alkenes, and small amounts of C_3 to C_8 alkanes. Although the composition of the gas was not affected by changes in the NaOH concentration, the volume of evolved gas did vary. The total volume of gas evolved [ml (STP) per gram of carbide] was about 49 ml/g with 0 to 6 *M* NaOH, 53 ml/g with 12 *M* NaOH, and 55 ml/g with 18 *M* NaOH.

In studies of the hydrolysis of as-cast and heat-treated uranium monocarbide-dicarbide mixtures,[2] it was shown that complex polymerization reactions occur between the single C units from the monocarbide and the C_2 groups from the dicarbide. The polymerization was evidenced by the fact that less gas was evolved and more wax was formed than expected from a physical mixture of the two compounds. The extent of polymerization of C and C_2 groups was dependent on the distribution of the phases throughout the mixture. A physical mixture of mono- and dicarbides hydrolyzed to give the products expected from the respective pure components. As-cast mixtures, which had very fine platelets of the mono- and dicarbides dispersed uniformly throughout the specimens, showed maximum deviation from the behavior expected from a binary mixture. Specimens that had been heat-treated at 1820 to 2130°C and which contained relatively large isolated areas of monocarbide and dicarbide within the sample, but still considerable contact between the phases, exhibited hydrolysis properties that were intermediate to those obtained with the physical mixture and the as-cast specimens.

The high-temperature region where uranium mono- and dicarbides are immiscible was determined[3] by examining the room-temperature microstructures of specimens having compositions between $UC_{1.1}$ and $UC_{1.8}$ that had been prepared by decomposing monocarbide-sesquicarbide and sesquicarbide-dicarbide mixtures at temperatures of 1820 to 2130°C. The low-carbon miscibility

[1] M. J. Bradley, M. D. Pattengill, and L. M. Ferris, *Inorg. Chem.* **4**, 1080 (1965).

[2] M. J. Bradley and L. M. Ferris, *J. Inorg. Nucl. Chem.* **27**, 1557 (1965).

[3] M. B. Sears, L. M. Ferris, and R. J. Gray, *J. Electrochem. Soc.* **113**(3), 269 (1966).

boundary, which occurs between $UC_{1.1}$ and $UC_{1.2}$ (5.2 and 5.7% carbon), is nearly composition-invariant between 1820 and 2070°C. The high-carbon miscibility boundary occurs at about $UC_{1.65}$ (7.7% carbon) at 1820°C, and the solubility of the monocarbide in the dicarbide phase increases linearly with increasing temperature. The peak of the immiscible region occurs at about $UC_{1.2}$ (5.7% carbon) and at a temperature above 2070°C.

23. Industrial Applications of Nuclear Energy

Large, dual-purpose nuclear reactors have shown great promise as sources of energy for desalting seawater. However, there is some question concerning the ability of seaside areas to utilize the large blocks of power [3000 to 5000 Mw (electrical)] that may be produced by proposed nuclear desalting stations. Certainly, if the area is highly industrialized, a fraction of the power could be put into the existing system. But most of the arid and semiarid regions of the world are not industrialized sufficiently to use the power, and it must be transmitted elsewhere at a penalty of about 0.2 mill/kwhr per 100 miles of transmission.[1] Obviously, plants for producing industrial chemicals at the site of a nuclear desalting station would provide a ready market for power and eliminate transmission losses.

Industrial-nuclear combinations may have promise for immediate applications as well as for future ones. Many areas are now considering 800- to 1000-Mw (electrical) reactors to serve as power stations. The rate of increase in cost with reactor size is very favorable, and the cost difference between building a 1200-Mw (electrical) instead of a 1000-Mw (electrical) reactor would be small. The extra power could be used in plants for the on-site synthesis of useful chemicals such as ammonia-based fertilizer for the surrounding area and, in this way, also eliminate or greatly reduce transportation costs. Since hydrogen enters the synthesis of ammonia, the efficient production of hydrogen by electrolyzing water is of primary concern.

The production of ammonia was selected as having promising potential because of its importance as a fertilizer, and an economic study of its production, using electricity from a nuclear desalination reactor, was made by Blanco and others.[2] The study assumed the use of a new, advanced type of electrolytic cell, which has been studied here (see Sect. 23.2). Other studies now in progress include the direct fixation of nitrogen from nitrogen-oxygen mixtures (Sect. 23.3) and the use of oxygen, ozone, or nuclear heat or electricity for treating waste waters, such as sewage (Sect. 23.4).

23.1 ECONOMICS OF HYDROGEN AND AMMONIA PRODUCTION VIA THE ELECTROLYSIS OF WATER, USING LOW-COST NUCLEAR POWER

A study of the economics of hydrogen and ammonia fertilizer production by the electrolysis of water was made to serve as an example of how large blocks of low-cost nuclear power predicted for the foreseeable future could be used.[2] Also, the cost of ammonia production at a nuclear desalination site via electrolysis was compared with the cost using the conventional steam-methane reforming process.

As a result of this study, it was concluded that an ammonia fertilizer plant can be an economical consumer of power from a large nuclear desalination station. The cost of producing ammonia by the electrolytic route, using 1.6-mill/kwhr power, with financing typical of the chemical industry, could be competitive with the cost based on the use of natural gas at 44¢ per million Btu's with no oxygen credit, or with natural gas at 29¢ per million Btu's allowing an oxygen credit of $4 per ton. The latter price for natural gas compares favorably with the 34¢ per million Btu's average

[1] Economic Planning Committee, Canadian Nuclear Association, "Nuclear Generation in Canada (1965–85)," 64 CNA-110.

[2] R. E. Blanco *et al.*, *An Economic Study of the Production of Ammonia Using Electricity from a Nuclear Desalination Reactor Complex*, ORNL-3882 (1966).

industrial price in the United States in 1963. The use of power from light-water reactors at a cost of 2.5 to 3.0 mills/kwhr could produce ammonia in the near future at remote locations for less than $40 per ton, which is within the range of our estimate of the current cost of ammonia production, including shipping costs, of $30 to $45 per ton.

The cost of producing ammonia via electrolysis at the desalination reactor site was determined and compared with that for producing hydrogen by steam-methane reforming plants currently in existence. The cost of natural gas was also examined since this is the most important cost in the production of ammonia by reforming. Selected examples of ammonia production costs for the water electrolysis process are shown in Table 23.1. For comparison, the natural-gas price required to manufacture ammonia at the same cost in a reforming plant is also included. Very large ammonia plants (3000 tons/day) that might be associated with large desalination reactors (by 1980) producing 1.6-mill/kwhr power are represented along with smaller plants (300 tons/day) that could be considered for the near future where power rates in the range of 2.5 to 3.0 mills/kwhr are available. The production costs given in Table 23.1 may be compared with published costs of $20 to $40 per ton disclosed in the literature. Production costs over the power-cost range of 1 to 3.5 mills/kwhr are given in Fig. 23.1. The current wholesale price of anhydrous ammonia in the United States is $92 per ton, but this includes the manufacturing cost ($20 to $40 per ton), plant storage costs ($10 to $15 per ton), transportation costs ($10 to $15 per ton), and selling expenses.

Other studies in progress include surveys of the chemical and metallurgical industries to determine other processes that could be installed at such a nuclear-industrial site. An example of one such combination is illustrated in Fig. 23.2.

Table 23.1. Examples of Ammonia Production Costs

Ammonia Plant Capacity (tons NH_3/day)	Return on Investment (%/year)	Ammonia via Electrolysis			Ammonia via Reforming	
		Electric Power Cost (mills/kwhr)	Electrolytic Oxygen Credit ($/ton O_2)	Ammonia Production Cost ($/ton NH_3)	Competitive Natural Gas Cost ($/$10^6$ Btu)	Ammonia Production Cost ($/ton NH_3)
3000	15[a]	1.6	0	27.60	44	27.60
3000	4[b]	1.6	0	20.00	41	20.00
3000	15[a]	1.6	4	22.00	29	22.00
3000	4[b]	1.6	2	17.20	33	17.20
3000	4[b]	0.8[c]	2	13.40	21	13.40
300	4[b]	2.5	0	34.80	67	34.80
300	4[b]	2.5	2	32.00	59	32.00
300	4[b]	3.0	0	39.00	80	39.00

[a]After income tax.

[b]Assuming no income tax.

[c]Off-peak power.

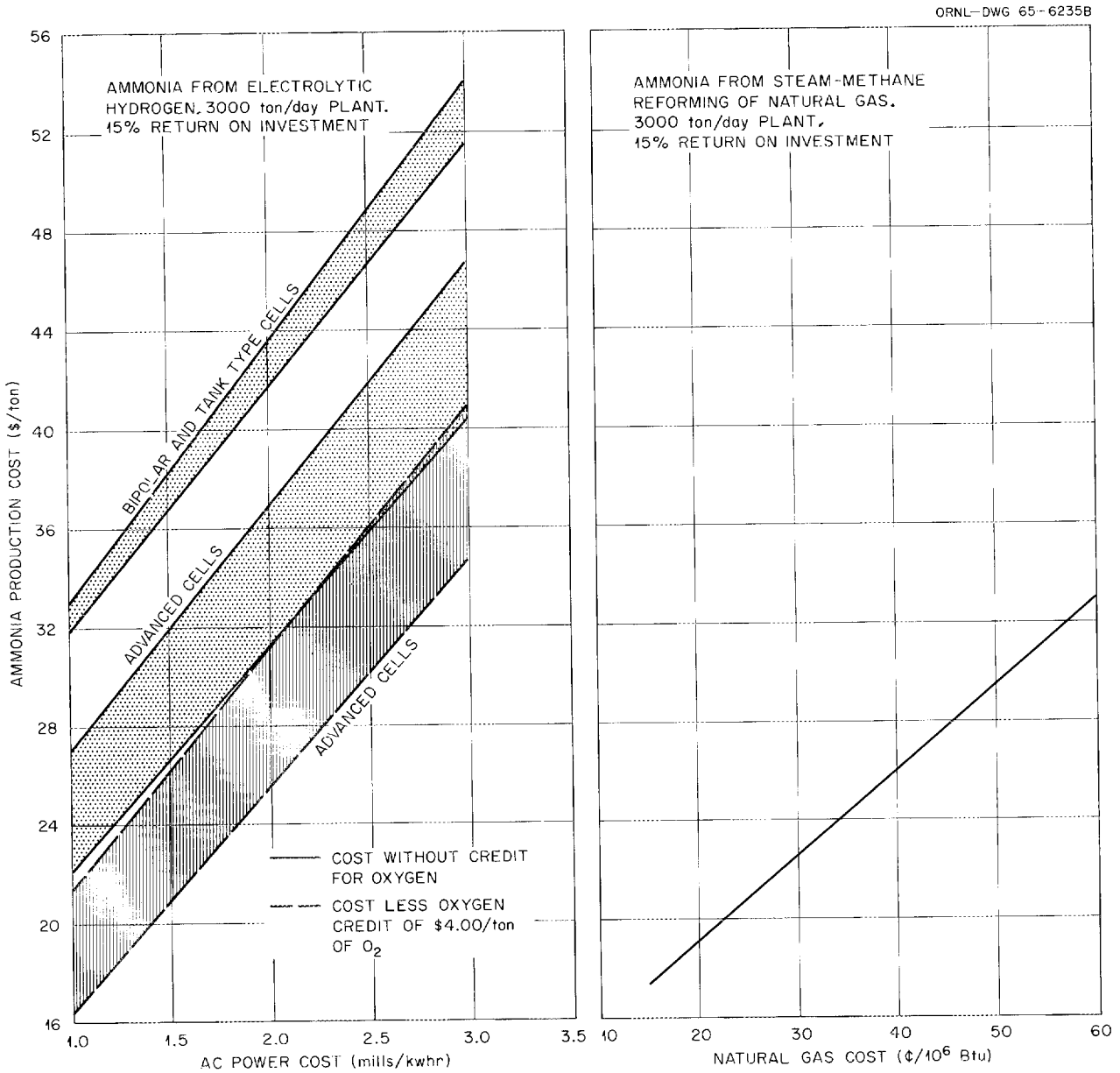

Fig. 23.1. The Cost of Ammonia Manufacture via Water Electrolysis and Steam-Methane Reforming Are Compared as a Function of the Costs of Power and Natural Gas. The effect of oxygen credit for the electrolysis system is also given.

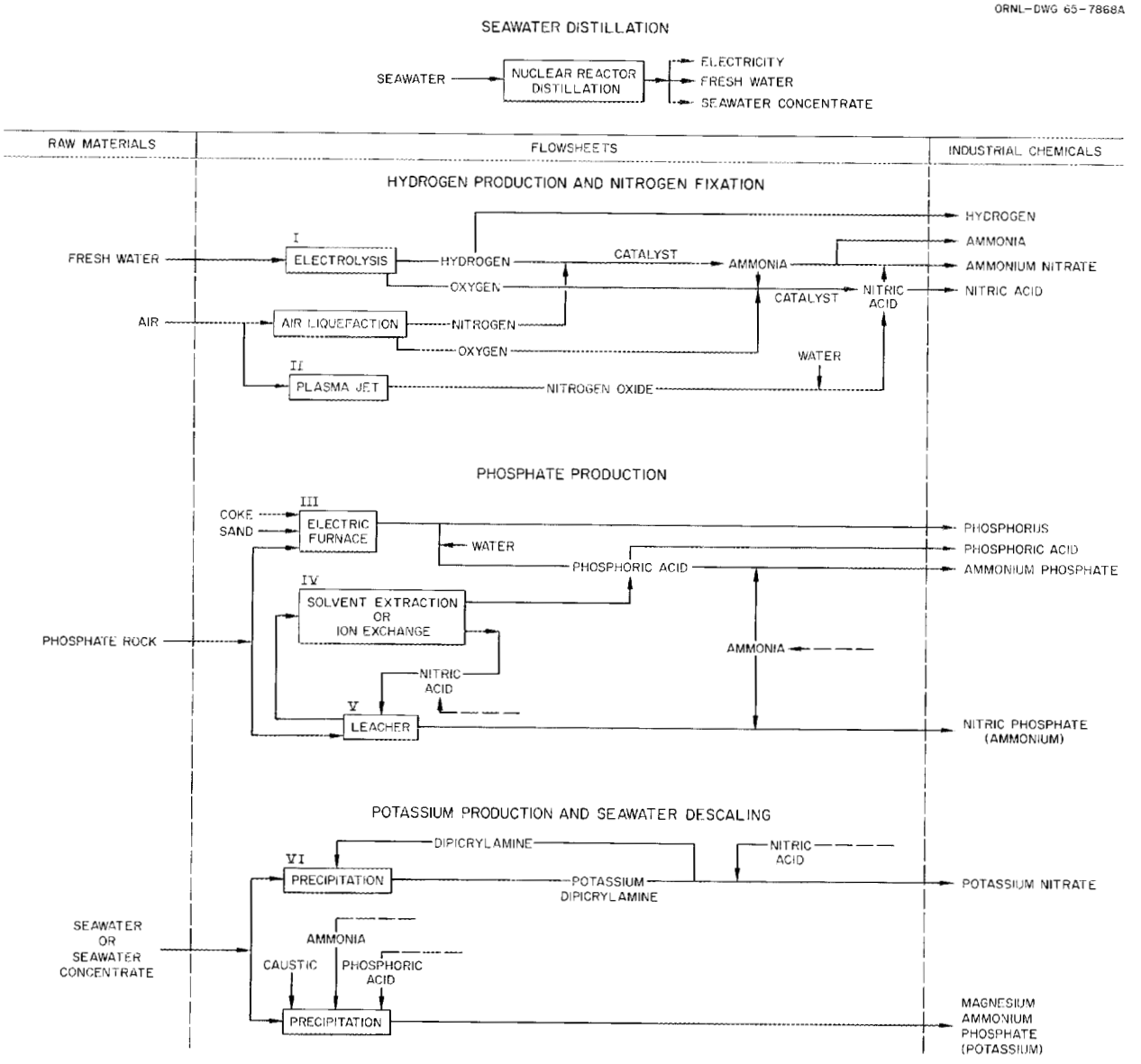

Fig. 23.2. A Multipurpose Industrial Complex That Uses the Electricity, Fresh Water, and Seawater Available at a Desalination Reactor to Produce Industrial Chemicals.

23.2 PRODUCTION OF HYDROGEN BY THE ELECTROLYSIS OF WATER

A study of the economics of the production of ammonia by using electrolytic hydrogen had showed promise when low-cost nuclear byproduct power was used. The study[1] indicated that new, advanced electrolytic cells producing hydrogen for an ammonia plant could permit the plant to compete economically with one using the steam-methane reforming process (using natural gas), provided the capital costs of electrolytic plants could be minimized. One approach to lower capital costs would be operation at high current densities, thus decreasing the number of cells required. An experimental program was initiated to investigate various means of reducing capital costs while maintaining or improving electrolytic cell efficiencies.

Status and Progress

A new, advanced electrolysis cell capable of good cell efficiency at high current densities is being studied in the laboratory. The cell, developed for fuel-cell applications[3] and oxygen production in submarines,[4] has been operated at temperatures up to 90°C and current densities up to 1633 ma/cm^2 (1517 amp/ft^2), with the limitation on current density being dictated by the size of the laboratory power supplies. Cell efficiencies, determined by dividing the calculated thermodynamically reversible voltage at the cell temperature (90°C) by the measured cell voltage, ranged from 63.8% at a current density of 500 ma/cm^2 to 53.8% at 1633 ma/cm^2. Typical tank-type electrolyzers such as the Trail cell operate at current densities of less than 100 ma/cm^2 and efficiencies of about 50%.[5]

The cell has been operated intermittently with daily startups and shutdowns for three months, with no observable deterioration of efficiency. These results suggest that off-peak power at a 50% reduction in power cost might be used and thus result in additional savings in the production of hydrogen. Data on the durability of the cells at high current densities have not yet been obtained.

The Electrolysis Cell and Electrolyte Circulation System

Figure 23.3 shown an exploded view of the cell. The two porous nickel electrodes are are separated by a thin asbestos membrane impregnated with 26 to 35% KOH. The electrodes are porous nickel with average pore size of 12 μ and 85% void space; dimensions are 1.6 × 1.6 × 0.03 in. The membrane is 0.010-in.-thick asbestos paper. Electrolyte (26 to 35% KOH) is circulated in the channels behind each electrode to replace electrolyzed water by diffusion and to supply cooling at high current densities as shown in Fig. 23.4.

The electrolyte is circulated through the cell from a reservoir kept at constant temperature. Before entering the cell, it is split into two streams and, after passing through the cell, flows through individual gravity gas separators where the electrolysis products, hydrogen and oxygen, are exhausted at atmospheric pressure (Fig. 23.4). Carbonate in the reagent-grade KOH is removed by precipitation, and Ascarite drying tubes at all system openings prevent contamination with CO_2 from the air. Carbonate contamination was in most cases less than 0.05%, with the maximum being 0.09%.

Current Supply and Electrical Measuring Equipment

Direct current was supplied by a voltage-current-regulated power supply with an output of 0 to 25 amp and less than 0.02% or 1 ma output current change for ±9% ac line variation. The high-impedance measuring circuit consisted of a high-stability bucking supply, a voltage divider, two follower amplifiers, and a recorder. Sensitivity was better than ±1 mv. Only measurements of total cell voltage can be made when using direct current, since the configuration of this cell and the use of high current density preclude the use of Luggin capillaries and reference electrodes.

---

[3] R. J. Jasinski, *Advan. Chem. Ser.* **47**, 95 (1965).

[4] Contract NObs 90502, awarded by U.S. Navy, June 1964.

[5] B. P. Sutherland, *Trans. Electrochem. Soc.* **85**, 183 (1944).

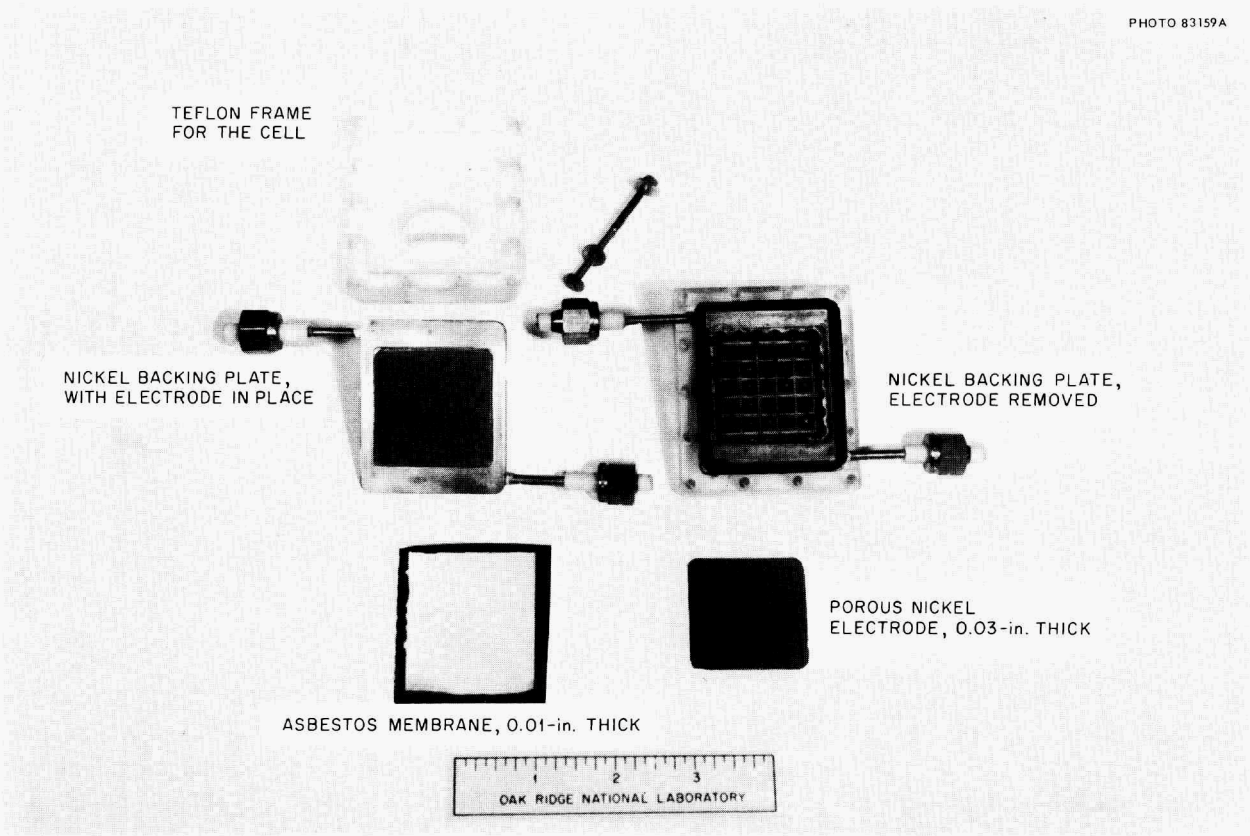

Fig. 23.3. Exploded View of a New Electrolytic Cell Incorporating Porous Nickel Electrodes for the Electrolysis of Water to Produce Hydrogen.

To obtain independent measurements of polarization voltage and internal resistance voltage in electrolytic cells of the dimensions used in this investigation, it is necessary to make use of the current-interrupter technique. The cell is subjected to a periodically interrupted current load, and, by means of electronic circuitry, the polarization voltage of the cell is measured during the current-off period and the *IR* drop through the electrolyte and membrane is measured during the current-on period. Kordesch and Marko[6] developed a simple measurement circuit for this technique; later, Pollnow and Kay[7] built an improved, transistorized version. Our measuring circuitry is almost the same as the latter authors' except that we used the high-impedance circuitry and recorders for readout. Half-wave rectified alternating current (unidirectional) is provided by using a silicon controlled rectifier and firing circuit. The current is kept constant by the use of a motor-driven Variac, which is actuated when the current changes from its set-point value. This power supply is capable of delivering up to 22 amp (average).

Results

The cell (Fig. 23.3) has been operated at temperatures up to 90°C and at current densities up to 1633 ma/cm^2 (1517 amp/ft^2) with direct current, and up to 1350 ma/cm^2 with half-wave rectified alternating current.

The total cell voltage of an electrolysis cell is made up of several components, as shown in

[6]K. Kordesch and A. Marko, *J. Electrochem. Soc.* **107**, 480 (1960).

[7]G. F. Pollnow and R. M. Kay, *J. Electrochem. Soc.* **109**, 648 (1962).

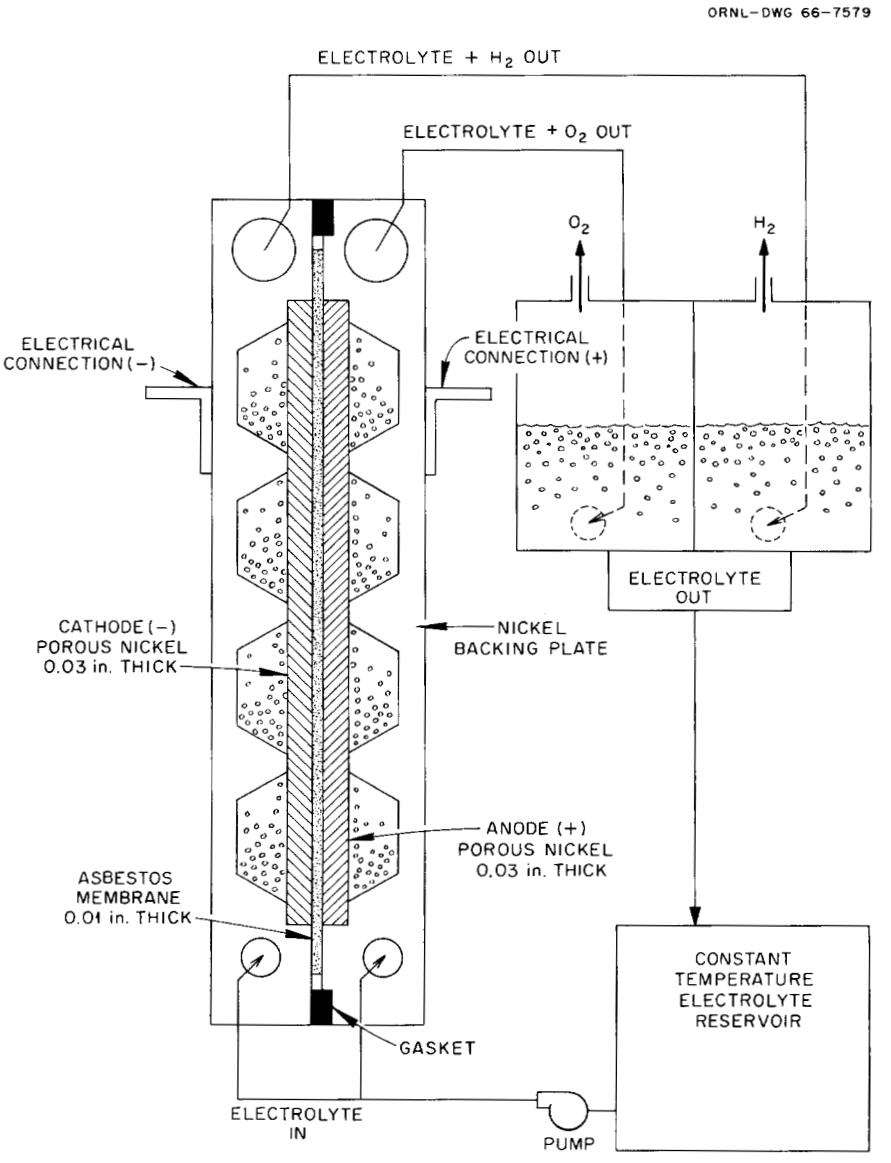

Fig. 23.4. Schematic Diagram of Electrolysis Cell and Electrolyte Circulation System.

Eq. (1):

$$E_{cell} = E_{rev} + \omega_{anode} + \omega_{cathode} + E_{IR} \ . \quad (1)$$

The term E_{rev} is the thermodynamically reversible decomposition voltage of water (1.175 v at 90° and 1.184 v at 80°C). The terms ω_{anode} and $\omega_{cathode}$ represent the anode and cathode overvoltages, and E_{IR} is the potential drop due to the resistivity of the electrolyte and membrane. With the current-interrupter technique (without individual reference electrodes) we are able to make independent measurements of the *IR*-free cell voltage [the sum of the first three terms of Eq. (1)] and the *IR* drop [the last term of Eq. (1)]. The *IR*-free cell potential and the total cell voltage (obtained by adding *IR*-free and *IR*-drop terms) for pulsed current and the total cell voltage for direct current are shown in Fig. 23.5 as a function of current density at two temperatures. The data show that pulsed current affects cell voltage differently than direct current, with higher cell voltage observed

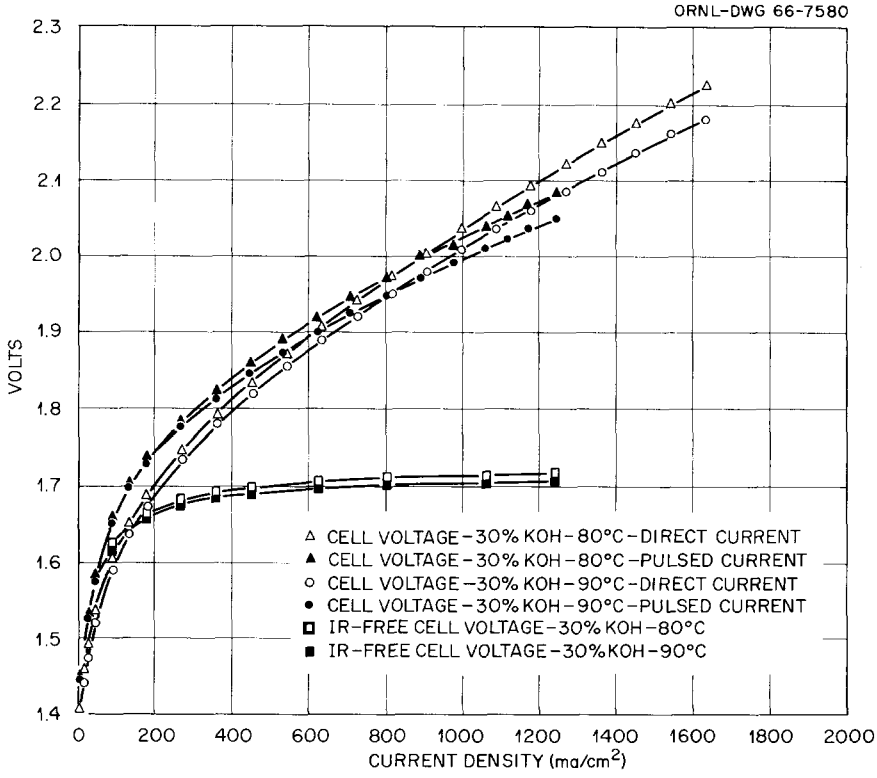

Fig. 23.5. Cell Voltages and IR-Free Cell Voltages Measured with Direct Current or Half-Wave Rectified Alternating Current (Unidirectional) Supplied to the Electrolytic Cell.

for the pulsed current at low current density and higher cell voltage observed for direct current at high current density. The reason for this is not known, but it is not a function of the measuring circuitry, since measurements of average current delivered by the pulsed-current source were calibrated by measuring voltage drop across a calibrated shunt resistor with an integrating digital voltmeter.

Determinations of current efficiency were made by measuring the volume of hydrogen evolved. At 80°C, 28% KOH, and a current density of 1179 ma/cm^2, the measured efficiency using direct current was 95.7%. Under the same conditions except with a slightly lower current density, 1152 ma/cm^2, current efficiency was 94.5% with pulsed current. This difference is within the experimental error of the measurement. Current efficiencies of 98 to 99% were measured at 600 ma/cm^2 using direct current.

A defect in the circulation pump caused contamination of the electrolyte with iron. Analysis showed the ferric iron concentration to be 8 to 10 μg/ml and the ferrous iron concentrations to be 0.8 to 1 μg/ml. When the cell was disassembled, about 30 to 40% of the back side of the cathode was covered with a deposit of Fe_3O_4. This deposit had not caused any noticeable deterioration of cell efficiency, and the hydrogen gas was being evolved through the deposit, as shown by a multitude of tiny pinholes in it.

23.3 DIRECT FIXATION OF NITROGEN WITH A PLASMA TORCH

Nitrogen can be fixed as nitric oxide by heating air or other oxygen-nitrogen mixtures to very high temperatures. The nitric oxide can be recovered from the reaction mixture if the mixture is cooled quickly. The maximum concentration of nitric oxide occurs at about 3500°K. For the equimolar nitrogen-oxygen system, the maximum equilibrium concentration is 6.6 mole % NO, compared with

5.6% for air. One of the major problems in such high-temperature processes is that of cooling or quenching the reaction mixture to obtain the desired product without excessive energy losses. Quenching rates on the order of a million degrees Kelvin per second are required to obtain the bulk of the equilibrium concentration of nitric oxide formed at 3500°K. Such rates have been achieved by many investigators with fluidized beds, expansion chambers, nozzles, cooled tubes or probes, and by injection of cold components into the product mixture.

Status and Progress

Studies were carried out on the high-temperature direct fixation of nitrogen with a plasma torch and auxiliaries such as a condenser and gas scrubbers (Fig. 23.6). Nitrogen was heated to temperatures of 3000 up to 10,000°K. To obtain nitrogen as oxides, oxygen was injected into the nitrogen plasma and the hot reactants were quenched very rapidly. The yields of fixed nitrogen, expressed as mole % nitric oxide in the final mixture, varied from 1.3 to 5.3. The energy utilization, expressed as grams of nitrogen fixed per kilowatt-hour, varied from 1 to 6.6. The latter value is about 45% of that obtained in the Birkeland-Eyde arc process used in the early 1900's. Kinetic considerations show that the gases were quenched at a rate that is on the order of a million degrees per second or greater.

In these studies, the nitrogen and oxygen flow rates varied from 9.5 to 19 liters/min and the N_2/O_2 flow rate ratio was nominally 1. Power to the torch ranged from 4 to 20 kw, and about 40% was lost to the water used to cool the electrodes. The pressure in the system varied from 685 to 728 mm Hg. Data were collected over periods of 15 to 30 min. For a given nitrogen-oxygen flow rate, the percentage of nitrogen fixed is nearly independent of the power to the torch; however, the energy utilization is higher, the lower the power to the torch (Fig. 23.7 and Table 23.2). Over the range of conditions studied, the best

ORNL-DWG 66-7581

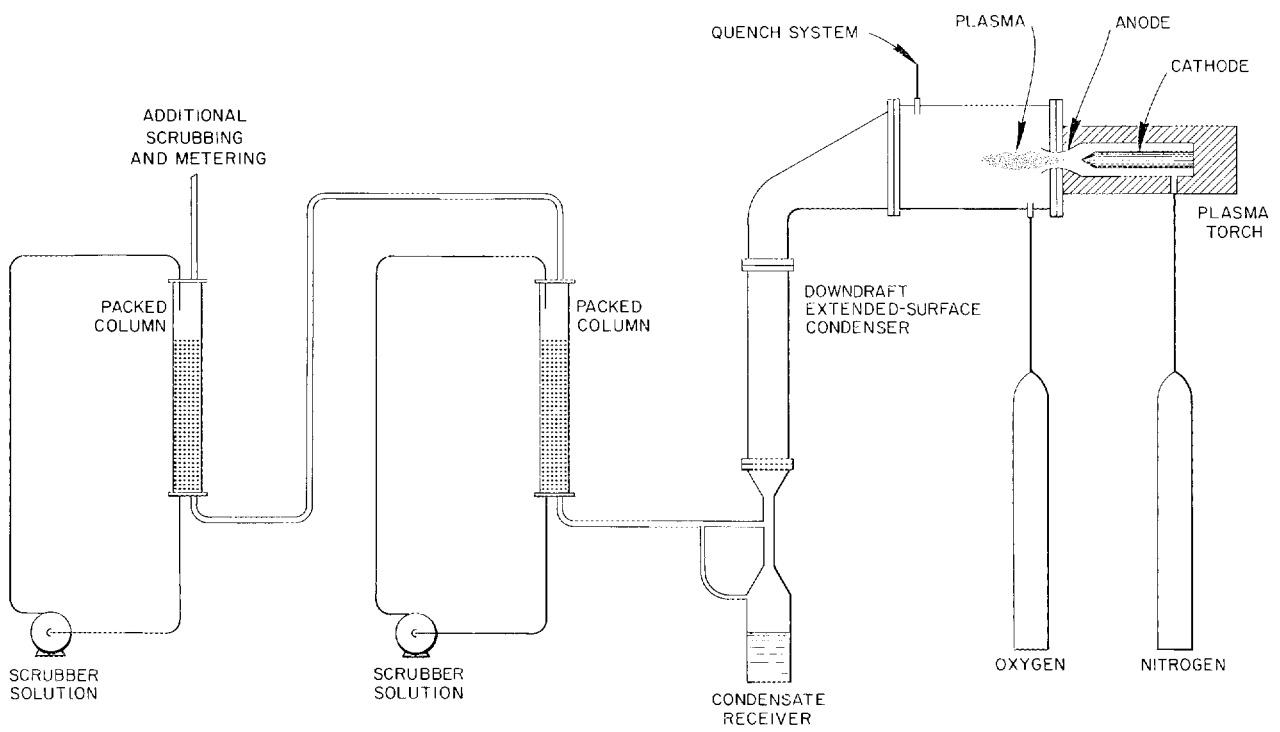

Fig. 23.6. Schematic Diagram of Apparatus Used for High-Temperature Direct Fixation of Nitrogen Studies.

Table 23.2. Yields of Fixed Nitrogen Obtained with a Nitrogen Plasma and Spray Quench

Experiment Number	Flow Rate (liters/min)		Power to Torch (kw)	Nitric Oxide in Final Gas (vol %)	Energy Utilization (grams fixed nitrogen/kwhr)
	N_2	O_2			
1	17	12	20	2.4	1.6
2	19	19	6.8	2.9	6.0
3	19	19	6.4	2.1	4.8
4	19	19	6.3	2.3	5.2
5	19	19	6.0	2.0	4.6
6	19	19	5.8	2.7	6.6
7	19	19	5.4	2.3	6.1

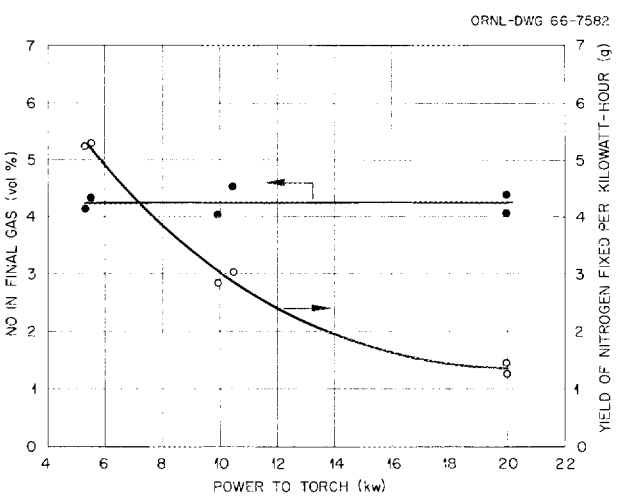

Fig. 23.7. Yield of Fixed Nitrogen as a Function of Power. Conditions: N_2 plasma; flow rate of $N_2 = O_2 =$ 9.5 liters/min; spray quench.

energy utilization – which is not coincident with the best percentage of fixed nitrogen – was obtained with the highest flow rate and the lowest power at which the torch would operate stably.

23.4 WASTE-WATER TREATMENT

Large nuclear power stations can effect cost reductions in waste-water treatment by using lower-cost electricity and process heat to produce chemical reagents such as ammonia, chlorine, hydrogen peroxide, oxygen, and ozone for use in conventional and advanced water treatment processes. This application of nuclear energy will depend on the physical locations of the reactor and the waste-water-treatment plants.

Initial efforts were concentrated on oxygen-consuming tertiary treatment processes. Oxygen can be produced at an attractive price by conventional distillation or electrolysis of water if low-cost electricity is made available. Oxygen costs were calculated for 500- to 1000-ton/day plants by using power costs of 2 to 5 mills/kwhr for both high-pressure (450 psig) and low-pressure (0.5 to 5.0 psig) plants supplying 95% oxygen. Costs, based on government financing and 25-year amortization, totaled from $3.19 per ton for 2-mill power to $4.19 per ton for 5-mill power for a 1000-ton/day low-pressure oxygen plant, and from $3.69 per ton for 2-mill power to $5.03 per ton for 5-mill power for a 1000-ton/day high-pressure oxygen plant.

The wet-air oxidation (Zimmermann) process for treating sludge from sewage disposal was discussed with key personnel of Zimpro, a Division of Sterling Drugs, Inc., to consider reducing the costs of the process by using oxygen instead of air. Although considerable investigation and pilot plant work would be required before a plant could be designed for oxygen, the idea is attractive. Estimates based on a plant processing 1000 tons/day of sewage solids at 3% solids concentration and accomplishing 70% reduction of chemical oxygen demand were made. The plant would consist of eleven 100-ton/day units, of which 10 would be in continuous operation – the

capacity that would be required for a city the size of Chicago in the 1980's. Preliminary estimates based on oxygen production using 2-mill power indicate that a plant operating on oxygen rather than air would be cheaper by about $3 per ton of sludge processed or $3000 per day. The cost of operation, including amortization, would be about $15 per ton of sludge processed. Building and power substation costs are not included and will raise the cost of processing. The costs will be higher for the air plant, however, than for the oxygen plant because of the higher power requirements and the building space required for the air compressors.

Publications, Speeches, and Seminars

ASSISTANCE PROGRAMS

Goeller, H. E., E. M. Shank, and W. M. Sproule, *List of Information Sent to and Received from the Eurochemic Co., January 1, 1965 Through June 30, 1965 (Categorized)*, ORNL-TM-685, Suppl. 4 (Aug. 30, 1965).

Goeller, H. E., E. M. Shank, and W. M. Sproule, *List of Information Sent to and Received from the Eurochemic Company, July 1, 1965 Through December 31, 1965 (Categorized)*, ORNL-TM-685, Suppl. 5 (Feb. 3, 1966).

Salmon, Royes, *Estimation of Fuel-Shipping Costs for Nuclear Power Cost-Evaluation Purposes*, ORNL-3943 (March 1966).

Shappert, L. B., and R. Salmon, "Shipping Cost Comparisons for Lead-, Steel-, and Uranium-Shielded Casks," to be presented at the AEC Traffic Management Conference, Las Vegas, Nev., May 10–12, 1966; also published in the Proceedings.

Shappert, L. B., and R. Salmon, *Shipping Cost Comparisons for Lead-, Steel-, and Uranium-Shielded Casks*, ORNL-3918 (March 1966).

CHEMICAL ENGINEERING RESEARCH

Chester, C. V., *The Effect of Ionizing Radiation on Coalescence Rates in Liquid-Liquid Systems*, ORNL-TM-1283 (December 1965), submitted to the University of Tennessee for a Doctor of Philosophy Degree (October 1965).

Groenier, W. S., R. A. McAllister, and A. D. Ryon, *Flooding in Perforated-Plate Pulsed Extraction Columns: A Survey of Reported Experimental Data and Correlations, and the Presentation of New Correlations with Physical Properties, Operating Variables, and Column Geometry*, ORNL-3890 (March 1966).

Jury, S. H., *The Interaction of Multiple Coils on a Cylindrical Induction Heating Load*, ORNL-TM-1352 (Dec. 28, 1965).

Scott, C. D., and J. S. Newman, "Heat Storage in Tunnel Walls," submitted for publication in *The International Journal of Heat Transfer*.

Whatley, M. E., "The Stacked-Clone Contactor: A High Performance Hydroclone Solvent Extraction Device," presented at the Annual Technical Meeting of the South Texas Section of the American Institute of Chemical Engineers, Houston, Tex., Oct. 22, 1965; also published in the program announcement for the meeting.

CHEMICAL PROCESSING FOR THE MOLTEN-SALT REACTOR EXPERIMENT

Scott, C. D., and W. L. Carter, *Preliminary Design Study of a Continuous Fluorination–Vacuum-Distillation System for Regenerating Fuel and Fertile Streams in a Molten Salt Breeder Reactor*, ORNL-3791 (January 1966).

Whatley, M. E., L. E. McNeese, W. L. Carter, C. D. Scott, R. B. Lindauer, and J. R. Hightower, "Engineering Development of On-Site Processing for Molten Salt Breeder Reactors," presented at the Second International Thorium Fuel Cycle Symposium, Gatlinburg, Tenn., May 3–6, 1966; also published in the Proceedings.

CHEMISTRY OF PROTACTINIUM

Campbell, D. O., "Protactinium Chemistry Studies," presented at the colloquium "The Physical Chemistry of Protactinium," Paris, France, July 2–8, 1965.

CLASSIFIED

Culler, F. L., Jr., *Rover Report for December 1964–January 1965*, ORNL-TM-1088 (Mar. 19, 1965) (classified).

CURIUM PROCESSING

Vaughen, V. C. A., and R. D. Baybarz, "Curium Processing Experience," presented at the ANS National Topical Meeting, Augusta, Ga., Mar. 20–23, 1966; also published in the Proceedings.

FLUORIDE VOLATILITY PROCESSING

Bennett, M. R., G. I. Cathers, R. P. Milford, W. W. Pitt, Jr., and J. W. Ullmann, "Fused-Salt Fluoride-Volatility Process for Recovering Uranium from Spent Aluminum-Based Fuel Elements," *Ind. Eng. Chem. Process Design Develop.* 4, 387 (1965).

Carr, W. H., R. E. Brooksbank, F. G. Kitts, and R. G. Nicol, "Processing Short Cooled Aluminum Base Fuels in the Molten-Salt Fluoride-Volatility Pilot Plant," presented at the 150th National Meeting of the American Chemical Society, Atlantic City, N.J., Sept. 12–17, 1965.

Guthrie, C. E., *Fluidized Bed Volatility – Process Design for BrF_5 Fluorination and UF_6 Recovery*, ORNL-TM-1206 (July 28, 1965).

Katz, S., "Preparation of MF_6·NaF Complexes with Uranium, Tungsten, and Molybdenum Hexafluoride," *J. Inorg. Chem.* 5, 666 (May 1966).

Mann, S., and E. L. Youngblood, *Decontamination of the ORNL-Molten Salt Fluoride-Volatility Pilot Plant After Processing Irradiated Zirconium-Uranium Alloy Fuel*, ORNL-3891 (February 1966).

Miller, P. D., W. E. Berry (BMI), and R. P. Milford, "Corrosion in the Fluidized-Bed Volatility Process," presented at the 15th Annual AEC Corrosion Symposium, Oak Ridge, Tenn., May 23–25, 1966.

DEVELOPMENT OF THE THORIUM FUEL CYCLE

Brooksbank, R. E., J. P. Nichols, and A. L. Lotts, "The Impact of Kilorod Operational Experience on the Design of Fabrication Plants for ^{233}U-Th Fuels," presented at the Second International Thorium Fuel Cycle Symposium, Gatlinburg, Tenn., May 3–6, 1966; also published in the Proceedings.

Buxton, S. R., M. H. Lloyd, and C. J. Hardy, "Analysis and Significance of Rare-Earth Oxides Produced by a Sol-Gel Method," presented at the Third International Materials Symposium on Ceramic Microstructure, Berkeley, Calif., June 14–16, 1966.

Ferguson, D. E., B. A. Hannaford, and E. L. Nicholson, "Status of Process Development for Thorium-Bearing HTGR Fuels," to be presented at the 12th Annual Meeting of the American Nuclear Society, Denver, Colo., June 19–23, 1966.

Gens, T. A., D. M. Helton, and S. D. Clinton, *Laboratory Preparation of Uranium Nitride Microspheres by a Sol-Gel Technique*, ORNL-3879 (November 1965).

Haas, P. A., and S. D. Clinton, "Preparation of Thoria and Mixed-Oxide Microspheres," presented at the 150th National Meeting of the American Chemical Society, Atlantic City, N.J., Sept. 12–17, 1965.

Haas, P. A., and S. D. Clinton, *Preparation of Thoria and Mixed-Oxide Microspheres*, ORNL-TM-1281 (October 1965).

Haas, P. A., S. D. Clinton, and A. T. Kleinsteuber, "Sol-Gel Process Development and Oxide Microsphere Preparation," presented at the Canadian Chemical Engineering Conference, Quebec, Canada, Oct. 25–27, 1965.

Haas, P. A., W. D. Bond, M. H. Lloyd, and J. P. McBride, "Sol-Gel Process Development and Microsphere Preparation," presented at the Second International Thorium Fuel Cycle Symposium, Gatlinburg, Tenn., May 3–6, 1966.

Helton, D. M., *Dispersion of a Liquid Stream by an Electrical Potential: Applications to the Preparation of Thoria Microspheres*, ORNL-TM-1395 (Jan. 17, 1966).

McBride, J. P., *Preparation of UO_2 Microspheres by a Sol-Gel Technique*, ORNL-3874 (February 1966).

Nicholson, E. L., "Recent Developments in Thorium Fuel Processing," presented at the Second International Thorium Fuel Cycle Symposium, Gatlinburg, Tenn., May 3–6, 1966.

Wymer, R. G., and J. H. Coobs, "Preparation, Coating, Evaluation, and Irradiation Testing of Sol-Gel Oxide Microspheres," presented at Nuclear and Engineering Ceramics Conference, Harwell, England, Oct. 25–27, 1965; to be published in *Ceramics Journal*.

MISCELLANEOUS

Bell, J. T., and R. E. Biggers, "The Absorption Spectrum of the Uranyl Ion in Perchlorate Media. Part I. Mathematical Resolution of the Overlapping Band Structure and Studies of the Environmental Effects," *J. Mol. Spectry.* **18**, 247–75 (1965).

Blake, C. A., Jr., and D. J. Crouse, "Plowshare Participation of Oak Ridge National Laboratory," presented at the Fourth Annual Plowshare Review Meeting, Denver, Colo., Mar. 1–2, 1966.

Godbee, H. W., *Thermal Conductivity of Magnesia, Alumina, and Zirconia Powders in Air at Atmospheric Pressure from 200°F to 1500°F*, ORNL-3510 (April 1966).

Godbee, H. W., and W. T. Ziegler, "Thermal Conductivities of MgO, Al_2O_3, and ZrO_2 Powders to 850°C. I. Experimental," *J. Appl. Phys.* **37**(1), 40–55 (January 1966).

Godbee, H. W., and W. T. Ziegler, "Thermal Conductivities of MgO, Al_2O_3, and ZrO_2 Powders to 850°C. II. Theoretical," *J. Appl. Phys.* **37**(1), 56–65 (January 1966).

Klitgaard, J., and J. H. Goode, *Evaluation of Small Modified CEN Mixer-Settlers for the Extraction of Uranium and Thorium in a Hot Cell Facility*, ORNL-TM-1256 (Aug. 30, 1965).

Krohn, N. A., and R. L. Pearson, *Examination of Irradiated UO_2 Particles from Aerojet General Nucleonics*, ORNL-TM-1150 (June 14, 1965).

Landry, J. W., "Into Plowshares and Pruning Hooks," presented to Oak Ridge Council of Knights of Columbus, Oak Ridge, Tenn., June 10, 1965.

Landry, J. W., "Project Plowshare – the Constructive Application of Nuclear Explosives," presented at the U.S. Army Nuclear Science Seminar, Oak Ridge, Tenn., July 28, 1965.

Landry, J. W., "Civilian Applications of Nuclear Explosives," presented to the 1965 Exhibit Managers of the American Museum of Atomic Energy, Oak Ridge Institute of Nuclear Studies, Oak Ridge, Tenn., July 30, 1965.

Landry, J. W., "Nuclear Explosives in the Service of Man," presented to the Oliver Springs Lions Club, Oliver Springs, Tenn., Sept. 13, 1965.

Landry, J. W., "Into Plowshares and Pruning Hooks," presented to the Oak Ridge Catholic Women's Club, Oak Ridge, Tenn., Sept. 16, 1965.

Landry, J. W., "Project Plowshare: The Peaceful Uses of Nuclear Explosives," presented under the Oak Ridge National Laboratory Traveling Lecture Program to the student chapter of the American Nuclear Society, University of Virginia, Charlottesville, Va., Sept. 28, 1965.

Landry, J. W., "Industrial Applications of Nuclear Explosives," presented to the West Kentucky Engineers' Club, Paducah, Ky., Oct. 12, 1965.

Landry, J. W., "Engineering with Nuclear Explosives," presented to the Oak Ridge Subsection of the American Society of Mechanical Engineers, Oak Ridge, Tenn., Oct. 21, 1965.

Landry, J. W., "Scientific and Industrial Applications of Nuclear Explosives," invited paper presented at the 75th Meeting of the Tennessee Academy of Science, including the Collegiate Division, Oak Ridge, Tenn., Dec. 10, 1965.

Landry, J. W., "Industrial and Scientific Uses of Nuclear Explosives," presented under the Oak Ridge Traveling Lecture Program at Mississippi State University, College Station, Jan. 6, 1966.

Landry, J. W., "The Reformed Sword," presented under the Oak Ridge Traveling Lecture Program at LeMoyne College, Memphis, Tenn., Feb. 17, 1966.

Landry, J. W., "Nuclear Explosives: Creative Resource for Progress," presented at Kickoff Dinner of Chattanooga Engineers' Club, Chattanooga, Tenn., Feb. 21, 1966.

Landry, J. W., "Into Plowshares and Pruning Hooks," presented at the President's Dinner of the Tennessee State Association of B'nai B'rith, Oak Ridge, Tenn., Mar. 12, 1966.

Landry, J. W., "Peaceful Nuclear Explosives," presented to Lenoir City Methodist Men's Club, Mar. 28, 1966.

Landry, J. W., "A Foreseeable Boom in the Petroleum and Earth-Moving Industries," presented to Atlanta Section of Society of Automotive Engineers, Atlanta, Ga., May 2, 1966.

Nichols, J. P., *Calculations of Concrete Shields for Fission Sources*, ORNL-TM-1167 (June 17, 1965).

Paxton, E. L., Jr., Chairman of Tennessee-Tombigbee Waterway Authority; R. A. Winkel, Superintendent of Paducah Gaseous Diffusion Plant; Tom Butler, interviewer; and J. W. Landry; "Constructive Nuclear Explosives and the Tennessee-Tombigbee Waterway Project," an interview on "Accent," WPSD Television, Paducah, Ky., Nov. 10, 1965.

Roddy, J. W., and J. Mrochek, "Activities and Interaction in the Tri-*n*-butyl Phosphate–Water System," presented at the 151st ACS Meeting, Pittsburgh, Pa. (Mar. 28–31, 1966); to be published in the *Journal of Inorganic and Nuclear Chemistry.*

Rom, A. M., *Thermally Compensated Closure for Liquid Density Autoclave,* ORNL-TM-1293 (Oct. 14, 1965).

Watson, C. D., *et al.*, "Policy and Procedures Used in the United States for Decontaminating Hot Cells," presented at the International Symposium on Working Methods in High Activity Hot Laboratories, Grenoble, France, June 15–18, 1965.

Watson, C. D., and G. A. West, "A Ten Year Look at Protective Coatings (Paints) in the Nuclear Industry," presented at the 22nd Annual NACE Conference and 1966 Corrosion Show, Miami Beach, Fla., Apr. 18–22, 1966.

PATENT

Coleman, C. F., "Recovery of Uranium and Zirconium from Aqueous Fluoride Solutions," U.S. Pat. 3,243,257 (Mar. 29, 1966).

POWER REACTOR FUEL PROCESSING

Arnold, E. D., "Formation of ^{236}Pu and ^{232}U in Slightly Enriched Power Reactors," to be presented at the 12th Annual Meeting of the American Nuclear Society, Denver, Colo., June 19–23, 1966.

Bradley, Mildred J., L. M. Ferris, and R. J. Gray, "High-Temperature Immiscibility of Uranium Mono- and Dicarbides," *J. Electrochem. Soc.* **113**(3), 269 (March 1966).

Cathers, G. I., R. E. Blanco, L. M. Ferris, R. W. Horton, and R. P. Milford, "Use of Fluidized Beds as a Head-End Processing Method," presented at the 150th National Meeting of the American Chemical Society, Atlantic City, N.J., Sept. 12–17, 1965.

Farrell, J. B., and P. A. Haas, "Oxidation by Nitric Acid and Oxygen (Pressurized Aqueous Combustion) of Nuclear Graphite," presented at the 150th National Meeting of American Chemical Society, Atlantic City, N.J., Sept. 12–17, 1965.

Ferris, L. M., *Acid Leaching of Products from the Fluidized-Bed Combustion of Graphite-Base Reactor Fuels and the HF-O_2 Disintegration of Stainless Steel- and Zirconium-Clad Oxide Fuels,* ORNL-3876 (November 1965).

Ferris, L. M., "Solubility of Uranyl Fluoride in Hydrofluoric Acid–Nitric Acid Solutions at 25°C," *J. Am. Chem. Soc.* **87**, 5377 (1965).

Gens, T. A., *Chloride Volatility Experimental Studies: The Reaction of U_3O_8 with Carbon Tetrachloride and Mixtures of Carbon Tetrachloride and Chlorine,* ORNL-TM-1258 (Aug. 26, 1965).

Gens, T. A., *Thermodynamic Calculation of the Yield of Uranium Nitride During Carbothermic Reduction of Uranium Oxide in the Presence of Pure Nitrogen or Nitrogen Mixed with Hydrogen or Inert Gas,* ORNL-TM-1264 (Sept. 16, 1965).

Gens, T. A., *Thermodynamic Calculations Relating to Chloride Volatility Processing of Nuclear Fuels. IV. The Gas-Phase Reduction of Uranium Pentachloride and Hexachloride to Solid Tetrachloride with Carbon Monoxide,* ORNL-TM-1340 (Oct. 14, 1965).

Gens, T. A., *Vapor Pressures of Gaseous Products from Chemical Reactions of Sol-Gel Fuels,* ORNL-TM-1418 (Feb. 10, 1966).

Goode, J. H., "The Release of Tritium and ^{85}Krypton to the Atmosphere During Processing of ThO_2-UO_2 Reactor Fuel," submitted for presentation at the 12th Annual Meeting of the American Nuclear Society, Denver, Colo., June 20–23, 1966.

Haas, P. A., and L. M. Ferris, "Dissolution of Graphite-Base Reactor Fuels by Pressurized Aqueous Processes," presented at the 150th National Meeting of the American Chemical Society, Atlantic City, N.J., Sept. 12–17, 1965.

Irvine, A. R., A. L. Lotts, and A. R. Olsen, "The Thorium-Uranium Recycle Facility," presented at the Thirteenth Conference on Remote Systems Technology, Washington, D.C., Nov. 15–18, 1965; also published in the Proceedings.

Irvine, A. R., A. L. Lotts, and A. R. Olsen, "The Thorium-Uranium Recycle Facility Design," *Transactions of the American Nuclear Society*, December 1965.

Nicholson, E. L., L. M. Ferris, and J. T. Roberts, *Burn-Leach Processes for Graphite-Base Reactor Fuels Containing Carbon-Coated Carbide or Oxide Particles*, ORNL-TM-1096 (Apr. 2, 1965), presented at the EURATOM symposium at Brussels, Belgium, June 10–11, 1965.

Nicholson, E. L., L. M. Ferris, J. R. Flanary, J. H. Goode, B. A. Hannaford, J. W. Landry, J. G. Moore, R. H. Rainey, C. D. Watson, and H. O. Witte, "Recent Developments in Thorium Fuel Processing," presented at the Second International Thorium Fuel Cycle Symposium, Gatlinburg, Tenn., May 3–6, 1966; also published in the Proceedings.

Ullmann, J. W., *ORNL Facilities Capable of Contributing to Plutonium Fuel Cycle Development*, ORNL-TM-1268 (November 1965).

Witte, H. O., *Survey of Head-End Processes for the Recovery of Uranium and Thorium from Graphite-Base Reactor Fuels*, ORNL-TM-1411 (Feb. 3, 1966).

Witte, H. O., and L. M. Ferris, *Ball-Milling of Graphite-Base Reactor Fuel*, ORNL-TM-1412 (Feb. 3, 1966).

PROGRESS REPORTS

Blake, C. A., Jr., K. B. Brown, and D. J. Crouse, *Chemical Applications of Nuclear Explosions (CANE): Progress Report for July 1 to September 30, 1965*, ORNL-TM-1275 (Sept. 30, 1965).

Blake, C. A., Jr., K. B. Brown, and D. J. Crouse, *Chemical Applications of Nuclear Explosions (CANE): Progress Report for October 1 to December 31, 1965*, ORNL-TM-1394 (Jan. 21, 1966).

Blake, C. A., Jr., K. B. Brown, and D. J. Crouse, *Chemical Applications of Nuclear Explosions (CANE): Progress Report for January 1 to March 31, 1966*, ORNL-TM-1496 (Apr. 20, 1966).

Blanco, R. E., and F. L. Parker, *Waste Treatment and Disposal Semiannual Progress Report, July–December 1965*, ORNL-TM-1465 (Mar. 24, 1966).

Brown, K. B., and C. A. Blake, Jr., *Chemical Applications of Nuclear Explosions (CANE): Progress Report for January 1 to June 30, 1965*, ORNL-TM-1191 (July 20, 1965).

Burch, W. D., *Transuranium Quarterly Progress Report for Period Ending November 30, 1964*, ORNL-3847 (September 1965).

Burch, W. D., *Transuranium Quarterly Progress Report for Period Ending February 28, 1965*, ORNL-3880 (December 1965).

Ferguson, D. E., and staff, *Chemical Technology Division Annual Progress Report for Period Ending May 31, 1965*, ORNL-3830 (November 1965).

Whately, M. E., *Unit Operations Section Monthly Progress Report, March 1965*, ORNL-TM-1103 (June 1965).

Whatley, M. E., *Unit Operations Section Quarterly Progress Report, April–June 1965*, ORNL-3868 (December 1965).

Whatley, M. E., *Unit Operations Section Monthly Progress Report, November 1964*, ORNL-TM-1090 (February 1966).

Whatley, M. E., *Unit Operations Section Quarterly Progress Report, July–September 1965*, ORNL-3916 (March 1966).

Wymer, R. G., and D. A. Douglas, Jr., *Status and Progress Report for Thorium Fuel Cycle Development for Period Ending December 31, 1963*, ORNL-3611 (July 1965).

SEPARATIONS CHEMISTRY RESEARCH

Baybarz, R. D., "Synthesis and Evaluation of Several Polyaminopolycarboxylic Acids for Group Separation of Transplutonium from Lanthanide Elements by Solvent Extraction," presented at the 9th Conference on Analytical Chemistry in Nuclear Technology, Gatlinburg, Tenn., Oct. 11–13, 1965.

Blake, C. A., Jr., and J. M. Schmitt, "Stability of Aromatic Diluents and Solvent Extraction Reagents in Radiochemical Processing," presented at the International Conference on the Chemistry of the Solvent Extraction of Metals, Harwell, England, Sept. 27–29, 1965.

Coleman, C. F., "Amine Sulfate Extraction Mechanism and Amine Extraction Metal Separations," presented at the Gordon Research Conference on Ion Exchange, New London, N.H., Aug. 2–6, 1965.

Coleman, C. F., and J. W. Roddy, "Mass Action and Non-Ideality in Extraction by Amine Sulfate," for presentation at the International Conference on Solvent Extraction Chemistry, Goteborg, Sweden, Aug. 29–Sept. 1, 1966.

Crouse, D. J., and D. E. Horner, "Unexpected Rate Effects in the Extraction of Rare Earths by Di(2-ethylhexyl)phosphoric Acid," presented at the International Conference on the Chemistry of the Solvent Extraction of Metals, Harwell, England, Sept. 27–29, 1965.

Egan, B. Z., and W. D. Arnold, "The Purity, Properties, and Analytical Determination of 4-sec-Butyl-2-(α-methyl-benzyl)phenol (BAMBP)," submitted for publication in *Analytical Chemistry*.

Kelmers, A. D., "Separation of Transfer Ribonucleic Acids," presented at ACS monthly Analytical meeting at ORINS, Dec. 1, 1965.

McDowell, W. J., and C. F. Coleman, "Extraction of Alkaline Earths from Sodium Nitrate Solutions by Di(2-ethylhexyl)phosphate in Benzene: Mechanisms and Equilibria," *J. Inorg. Nucl. Chem.* **28**, 1083 (May 1966).

McDowell, W. J., and C. F. Coleman, "Interface and Transferring Species in Amine Extraction of Uranium," for presentation at the International Conference on Solvent Extraction Chemistry, Goteborg, Sweden, Aug. 29–Sept. 1, 1966.

Pearson, R. L., and A. D. Kelmers, "Separation of Transfer Ribonucleic Acids by Hydroxylapatite Columns," to be published in *J. Biol. Chem.* **241**(3), 767–69 (February 1966).

Seeley, F. G., and D. J. Crouse, "Extraction of Metals from Chloride Solutions with Amines," submitted for publication in the *Journal of Chemical and Engineering Data*.

Weaver, Boyd, "Separations Techniques in Rare Earth Analysis," presented at the Eastern Analytical Symposium, New York, Nov. 18–20, 1965.

Weaver, Boyd, "Chemical Differences Between the Lanthanides and Trivalent Actinides," pp. 415–25 in *Rare Earth Research*, vol. III (ed. by LeRoy Eyring), Gordon and Breach, New York, 1965.

SOLVENT EXTRACTION TECHNOLOGY

Crouse, D. J., K. B. Brown, and F. G. Seeley, "Primary Amine Extraction of Beryllium from Sulfate Liquors," presented at the International Conference on the Chemistry of the Solvent Extraction of Metals, Harwell, England, Sept. 27–29, 1965.

Leuze, R. E., R. D. Baybarz, F. A. Kappelmann, and Boyd Weaver, "Behavior of the Transplutonium Elements in Solvent Extraction Systems," presented at the International Conference on Chemistry of Solvent Extraction of Metals, Harwell, England, Sept. 27–29, 1965.

Roddy, J. W., and C. F. Coleman, "Activity Coefficients and Aggregation Numbers in the Tri-*n*-octylamine–Sulfuric Acid–Benzene System," to be presented at the 152nd American Chemical Society Meeting, New York, Sept. 11–16, 1966.

Weaver, Boyd, and F. A. Kappelmann, "Preferential Extraction of Lanthanides over Trivalent Actinides by Monoacidic Organophosphates from Carboxylic and Aminopolyacetic Acids," to be presented at the 152nd American Chemical Society Meeting, New York, Sept. 11–16, 1966.

TRANSURANIUM ELEMENT PROCESSING

Baybarz, R. D., "Dissociation Constants of the Transplutonium Element Chelates of 1,2 Diaminocyclohexanetetraacetic Acid," *J. Inorg. Nucl. Chem.* **28**, 1055 (1966).

Buxton, S. R., C. J. Hardy, and M. H. Lloyd, "The Preparation and Nature of Rare-Earth Hydroxide Sols, and Implications on Transplutonium Element Oxides," for presentation at the 12th Annual Meeting of the American Nuclear Society, Denver, Colo., June 19–23, 1966.

Ferguson, D. E., "Production of Transplutonium Elements," *Encyclopedia of Science and Technology*, McGraw-Hill Book Company (1966 Yearbook).

Katz, S., and G. I. Cathers, "A Gas Sorption-Desorption Separation of Plutonium and Uranium Hexafluoride," to be presented at the American Chemical Society, New York, Sept. 11–16, 1966.

Vaughen, V. C. A., and R. D. Baybarz, "Recovery and Purification of Gram Quantities of ^{243}Am, ^{244}Cm, and ^{242}Cm," presented at the 150th National Meeting of the American Chemical Society, Atlantic City, N.J., Sept. 12–17, 1965.

WASTE TREATMENT AND DISPOSAL

Blanco, R. E., W. Davis, Jr., H. W. Godbee, L. J. King, J. T. Roberts, W. C. Yee, *et al.*, "Recent Developments in Treating Low and Intermediate Level Radioactive Waste in the United States," presented at the Symposium on Practices in the Treatment of Low and Intermediate Level Radioactive Wastes, Vienna, Austria, Dec. 6–10, 1965.

Blanco, R. E., "Waste-Byproduct Production," presented at the Nuclear Power Briefing for Utility Executives, Southern Interstate Nuclear Board, Oak Ridge, Tenn., Jan. 20–21, 1966.

Blanco, R. E., J. O. Blomeke, and J. T. Roberts, "Future Magnitude and Proposed Solutions of the Waste Disposal Problem," presented at the Symposium on the Solidification and Long-Term Storage of Highly Radioactive Wastes, Richland, Wash., Feb. 14–18, 1966.

Blomeke, J. O., E. J. Frederick, R. Salmon, and E. D. Arnold, *The Costs of Permanent Disposal of Power-Reactor Fuel-Processing Wastes in Tanks*, ORNL-2873 (September 1965).

Blomeke, J. O., Lee Gemmell, and W. H. Kline, "Economics of Radioactive Waste Management at Oak Ridge National Laboratory, Argonne National Laboratory, and Brookhaven National Laboratory," presented to the Panel on Economics of Radioactive Waste Management, IAEA, Vienna, Dec. 13–18, 1965.

Blomeke, J. O., R. Salmon, J. T. Roberts, R. L. Bradshaw, and J. J. Perona, "Estimated Costs of High-Level Waste Management," presented at the Symposium on Solidification and Long-Term Storage of Highly Radioactive Wastes, Richland, Wash., Feb. 15–18, 1966.

Clark, W. E., H. W. Godbee, and C. L. Fitzgerald, *Laboratory Development of Processes for Fixation of High-Level Radioactive Waste in Glassy Solids. 3. Wastes from the Purex Solvent Extraction Process*, ORNL-3640 (June 1965).

Clark, W. E., R. E. Blanco, J. C. Suddath, C. W. Hancher, H. W. Godbee, J. M. Holmes, and C. L. Fitzgerald, "Pot Calcination and Rising Level Pot Glass Processes for Converting Highly Radioactive Wastes to Solids," presented at the 150th National Meeting of the American Chemical Society, Atlantic City, N.J., Sept. 12–17, 1965.

Clark, W. E., H. W. Godbee, and C. L. Fitzgerald, "Laboratory Development of Pot Processes for Solidification of Radioactive Wastes," presented at the Symposium on Solidification and Long-Term Storage of Highly Radioactive Wastes, Richland, Wash., Feb. 14–18, 1966.

Davis, W., Jr., P. A. Haas, J. M. Holmes, A. H. Kibbey, L. J. King, and E. Schonfeld, "Foam Separation Studies and Pilot Plant Tests," presented at the USSR delegation visit, ORNL, June 8–9, 1965.

Davis, W., Jr., A. H. Kibbey, and E. Schonfeld, *Laboratory Demonstration of the Two-Step Process for Decontaminating Low-Radioactivity-Level Process Waste Water by Scavenging-Precipitation and Foam Separation*, ORNL-3811 (October 1965).

Fitzgerald, C. L., H. W. Godbee, M. H. Davis, and W. E. Clark, *A Computer Code for Storing and Retrieving Data and Developing Improved Solids for Fixation of Highly Radioactive Wastes*, ORNL-3824 (March 1966).

Godbee, H. W., "Disposal of Intermediate-Level Radioactive Waste," presented at the USSR delegation visit, ORNL, June 8–9, 1965.

Godbee, H. W., W. E. Clark, and C. L. Fitzgerald, "Physical Properties of Solids Incorporating Simulated Radioactive Wastes," presented at International Symposium on Solidification and Long-Term Storage of Highly Radioactive Wastes, Richland, Wash., Feb. 14–18, 1966.

Goode, J. H., *Fixation of Intermediate Level Radioactive Waste in Asphalt: Hot-Cell Tests*, ORNL-TM-1343 (Nov. 18, 1965).

King, L. J., W. C. Yee, J. M. Holmes, J. T. Roberts, and R. E. Brooksbank, "Ion Exchange Studies and Pilot Plant Tests," presented at Russian waste disposal delegation visit, ORNL, June 8–9, 1965.

King, L. J., and M. Ichikawa, *Pilot Plant Demonstration of the Decontamination of Low Level Process Wastes by a Recycle Scavenging-Precipitation Ion-Exchange Process*, ORNL-3863 (December 1965).

Schaffer, W. F., Jr., W. J. Boegly, Jr., F. L. Parker, R. L. Bradshaw, F. M. Empson, and W. C. McClain, "Project Salt Vault: Design and Demonstration of Equipment," presented at International Symposium on the Solidification and Long-Term Storage of Highly Radioactive Wastes, Richland, Wash., Feb. 14–18, 1966.

Suddath, J. C., and J. O. Blomeke, *An Economic Analysis of High-Level Waste Management for Fluidized-Bed Volatility Processing of Power Reactor Fuels*, ORNL-TM-1441 (Apr. 1, 1966).

Suddath, J. C., C. W. Hancher, and J. M. Holmes, "Engineering Development of the Pot Processes for Solidification of Radioactive Waste," presented at International Symposium on Solidification and Long-Term Storage of Highly Radioactive Wastes, Richland, Wash., Feb. 14–18, 1966.

Yee, W. C., *The Selective Removal of Mixed Phosphates from Water Streams by Activated Alumina*, ORNL-TM-1135 (Nov. 22, 1965).

Yee, W. C., "The Selective Removal of Mixed Phosphates from Water Streams by Activated Alumina," presented at American Water Works Association Meeting, Portland, Ore., June 27–July 2, 1965, also published in *J. Am. Water Works Assoc.* **58**, 239–47 (February 1966).

Yee, W. C., and W. Davis, Jr., "Effects of Gamma Radiation on Cation Exchange Resin in a Flowing Water System," *Nucl. Sci. Eng.* **24**, 1–5 (January 1966).

URANIUM FUEL CYCLE SOL-GEL PROCESSES

Haire, R. G., and M. H. Lloyd, "Development of a Sol-Gel Process for the Preparation of Dense Oxide Forms of PuO_2," to be presented at the 12th Annual Meeting of the American Nuclear Society, Denver, Colo., June 19–23, 1966.

SEMINARS

1965		
June 1	Separation of Transfer-RNA	A. D. Kelmers
June 8	Studies on Fission Product Recovery – A Status Report	D. E. Horner
June 15	UO_2 Sol-Gel Process Development (classified)	J. P. McBride W. D. Bond
June 22	Chemistry of Cesium Extraction by Phenols	B. Z. Egan
June 29	Status Report on TALSPEAK Process Developments	Boyd Weaver
Aug. 2–13	Lecture Series – Technical Advancement Program Thermodynamics Lectures	J. J. Martin (University of Michigan)
Dec. 21	The Resolution of Complex Overlapping Spectra	J. T. Bell
1966		
Feb. 1	Hot Flowsheet Demonstration (Talspeak, Cerex, Dapex) – Curium Recovery Facility	F. A. Kappelmann J. E. Bigelow
Feb. 8	Project Salt Vault – Design and Demonstration of Equipment	W. F. Schaffer, Jr.
	Estimated Costs of High-Level-Waste Management	J. O. Blomeke
Feb. 15	The Potential Uses of Activated Carbons for the Adsorption of Metallic Ions	E. A. Sigworth (West Virginia Pulp and Paper Co., Chemicals Division)
Feb. 22	Project Plowshare: Application to Copper Ores	W. D. Arnold F. J. Hurst
Feb. 25	Densification of Thoria	M. E. Wadsworth
Mar. 1	Extraction of Alkalies and Alkaline Earths by HDEHP	W. J. McDowell
Mar. 8	Activity Measurements in the Water, Sulfuric Acid, Trioctylamine, Diluent System	J. W. Roddy
Mar. 15	Plowshare, Possible Applications: Stimulation of Gas Production from Wells and Recovery of Oil for Shales	C. A. Blake

Mar. 22	Waste Disposal by Hydrofracture	H. O. Weeren
Mar. 29	Thermal Conductivity of Sheared Fuel Elements	H. W. Godbee
Apr. 12	Rare-Earth Sol-Gel Development, and Application of Spectroscopy to the Study of Sol-Gel Processes	C. J. Hardy
Apr. 19	Plutonia Sol-Gel Development	R. G. Haire
May 24	Comments on Design and Construction of TURF	A. R. Irvine J. W. Anderson
May 31	Laboratory Testing of the Fluid-Bed Volatility Process	J. C. Mailen

CHEMICAL TECHNOLOGY DIVISION

D. E. FERGUSON, DIRECTOR
NANCY BEACH, SECRETARY
ELAINE HICKMAN, SECRETARY
A. T. GRESKY, SPECIAL ASSIGNMENT
H. B. WHETSEL,[†] REPORTS EDITOR

H. B. GRAHAM, ADMINISTRATIVE ASSISTANT
JUNE REDMOND, SECRETARY
W. O. GREEVER, PROCUREMENT
LUCILLE KUYKENDALL, SECRETARY

LONG RANGE PLANNING COMMITTEE
J. T. ROBERTS, CHAIRMAN
E. D. ARNOLD
C. E. GUTHRIE
R. SALMON
J. W. ULLMANN
MARGARET WALLS, SECRETARY
TECHNICIAN: P. P. HAYDON

CHEMICAL DEVELOPMENT SECTION A

R. G. WYMER, SECTION CHIEF
R. E. LEUZE, ASSISTANT SECTION CHIEF
ALICE McWILLIAMS, SECRETARY
D. M. HELTON, TECHNICIAN
C. F. KECK, TECHNICIAN
A. S. LYLE, TECHNICIAN
R. G. MANSFIELD, TRANSLATIONS

FUEL CYCLE STUDIES

W. D. BOND, GROUP LEADER
A. T. KLEINSTEUBER
A. B. MESERVEY
K. J. NOTZ
T. A. GENS
TECHNICIANS: D. E. SPANGLER
C. W. GREENE
E. R. JOHNS

RADIATION CHEMISTRY

N. A. KROHN
TECHNICIAN: D. H. NEWMAN

ALPHA MATERIAL PROCESSING

M. H. LLOYD, GROUP LEADER
R. D. BAYBARZ, PROBLEM LEADER, *TRANSURANIUM*
S. R. BUXTON
R. G. HAIRE
R. L. JOLLEY
C. J. HANDY[2]
P. B. ORR
J. D. HOESCHELE
TECHNICIANS: R. L. HICKEY
S. A. McCOSH
O. K. TALLENT
J. T. WIGGINS

PROTACTINIUM CHEMISTRY

D. O. CAMPBELL, PROBLEM LEADER
J. M. CHILTON

SOL-GEL PROCESS

J. P. McBRIDE, GROUP LEADER
L. E. MORSE
W. L. PATTISON

ACTINIDE OXIDES

K. H. McCORKLE
F. J. SMITH
TECHNICIAN: J. F. TALLEY

SPECTROPHOTOMETER PROGRAM

R. E. BIGGERS,[1] PROBLEM LEADER
J. T. BELL

CHEMICAL DEVELOPMENT SECTION B

R. E. BLANCO, SECTION CHIEF
IRENE REED, SECRETARY
BRENDA MOSES, SECRETARY
J. E. FARMER, DRAFTSMAN

MECHANISMS OF SEPARATION STUDIES (SOLVENT EXTRACTION, FOAM SEPARATION, WATER ELECTROLYSIS)

W. DAVIS, JR., GROUP LEADER
A. H. KIBBEY
J. E. MROCHEK
E. SCHONFELD
P. WACE[1]

WASTE STUDIES

W. E. CLARK, GROUP LEADER
H. W. GOODBEE[2]
W. C. YEE
N. S. S. RAJAN[2]
F. LAUDE[2]
TECHNICIANS: G. D. DAVIS
C. L. FITZGERALD
W. E. SHOCKLEY
R. L. TAYLOR[3]

POWER REACTOR FUEL PROCESSING

T. A. GENS, *MATERIALS DEVELOPMENT*
TECHNICIAN: E. R. JOHNS

J. R. FLANARY, GROUP LEADER, *FLOWSHEET DEMONSTRATION ON RADIOACTIVE FUELS*
J. H. GOODE
H. O. WITTE[2]
TECHNICIANS: L. A. BYRD
R. C. SHIPWASH
G. E. WOODALL
O. L. KIRKLAND

L. M. FERRIS, GROUP LEADER, *HEAD-END AND HTGR FUEL PROCESSING*
M. B. SEARS
K. S. WARREN
TECHNICIANS: J. F. LAND
C. T. THOMPSON

R. H. RAINEY, GROUP LEADER, *CLOSE COUPLED PROCESSING*
J. G. MOORE
R. H. SHIGLEY[3]
TECHNICIAN: R. C. LOVELACE

G. I. CATHERS, GROUP LEADER, *VOLATILITY PROCESSING*
M. R. BENNETT
S. KATZ
J. C. MAILEN
C. E. SCHILLING
H. F. SOARD
TECHNICIANS: T. E. CRABTREE
C. J. SHIPMAN

H. W. GOODBEE,[2] *NUCLEAR DESALINATION - INDUSTRIAL CHEMICAL PROCESSES*
TECHNICIAN: G. D. DAVIS[2]

CHEMICAL DEVELOPMENT SECTION C

K. B. BROWN, SECTION CHIEF
ANN HENSLEY, SECRETARY

BIOCHEMICAL SEPARATIONS

A. D. KELMERS, GROUP LEADER
B. Z. EGAN
R. L. PEARSON
J. F. KEISS
C. D. SCOTT, SPECIAL ASSIGNMENT TO BIOLOGY DIVISION
TECHNICIAN: D. E. HEATHERLY

SEPARATIONS PROCESSES AND FISSION PRODUCT RECOVERY

D. J. CROUSE,[1] GROUP LEADER
W. D. ARNOLD[1]
D. E. HORNER
F. J. HURST[2]
F. G. SEELEY
TECHNICIAN: W. B. HOWERTON

SEPARATIONS CHEMISTRY RESEARCH

C. F. COLEMAN, GROUP LEADER, *FUNDAMENTAL CHEMISTRY AND SALINE WATER PROGRAM*
W. J. McDOWELL
R. W. RHEAR
J. W. RODDY
TECHNICIANS: G. N. CASE
J. P. EUBANKS
J. E. THOMPSON

C. A. BLAKE,[1] GROUP LEADER, *DESCRIPTIVE CHEMISTRY OF SEPARATIONS SYSTEMS*
J. M. SCHMITT
TECHNICIAN: W. E. OXENDINE

B. WEAVER, GROUP LEADER, *SEPARATIONS AND CHEMISTRY OF ACTINIDES AND LANTHANIDES*
TECHNICIANS: R. R. COLLINS
R. R. SHOUN

PLOWSHARE PROGRAM

C. A. BLAKE[2]
D. J. CROUSE[1]
W. D. ARNOLD[1]
F. J. HURST[2]
J. M. SCHMITT[2]

UNIT OPERATIONS SECTION

M. E. WHATLEY, SECTION CHIEF
A. D. RYON,[†] ASSISTANT SECTION CHIEF
PATSY SILLER, SECRETARY
JANE POSEY, SECRETARY

FUEL CYCLE STUDIES AND THORIUM UTILIZATION

P. A. HAAS, GROUP LEADER
S. D. CLINTON
C. C. HAWS, JR.
J. J. PERONA
TECHNICIANS: R. D. ARTHUR
E. W. BROWN
D. A. McWHIRTER
F. A. SKELLIE[3]

FLUORIDE VOLATILITY PROCESS AND MSR PROCESSING

R. W. HORTON, GROUP LEADER
J. R. HIGHTOWER, JR.
R. S. LOWRIE
L. E. McNEESE
W. W. PITT, JR.
W. M. WOODS
TECHNICIANS: J. BEAMS
V. L. FOWLER
F. G. KILPATRICK
J. D. SHANLEVER[2]

SOLVENT EXTRACTION DEVELOPMENT

A. D. RYON,[†] GROUP LEADER
F. L. DALEY
L. O. FINSTERWALDER[2]
W. S. GROENIER
TECHNICIANS: G. JONES, JR.
K. LADD
C. H. TIPTON

CHEMICAL ENGINEERING RESEARCH

J. C. SUDDATH,[‡] GROUP LEADER
C. V. CHESTER[4]
S. H. JURY[4]
J. T. LONG
J. S. WATSON
TECHNICIANS: R. O. PAYNE
W. G. SISSON[5]

WASTE PROCESSING STUDIES

J. C. SUDDATH,[‡] GROUP LEADER
C. W. HANCHER[2]
TECHNICIANS: J. S. TAYLOR
D. E. WILLIS

POWER REACTOR FUEL PROCESSING

C. D. WATSON,[†] GROUP LEADER
B. C. FINNEY
B. A. HANNAFORD
H. F. JOHNSON[4]
G. A. WEST
TECHNICIAN: F. L. ROGERS

BIOCHEMICAL SEPARATIONS

C. D. WATSON,[†] GROUP LEADER
C. W. HANCHER[2]
H. O. WEEREN
TECHNICIANS: G. B. DINSMORE
J. C. ROSE

PROCESS DESIGN SECTION

H. E. GOELLER, SECTION CHIEF
W. E. UNGER, ASSISTANT SECTION CHIEF
E. M. SHANK, *EUROCHEMIC ASSISTANCE*
W. M. SPROULE,[*] TECHNICIAN
J. W. LANDRY, *PLOWSHARE PROGRAM*
W. G. STOCKDALE, *ECONOMIC STUDIES*
P. L. ROBERTSON, *COST ESTIMATES*
R. SALMON,[7] *COMPUTER COST STUDIES*
F. E. HARRINGTON, *SMALL-PLANT STUDIES*
S. F. SCOTT[2]
W. F. SCHAFFER, JR., *WASTE DISPOSAL IN SALT*
W. L. CARTER, *MSRR PROCESSING STUDIES*
J. P. NICHOLS, *SHIELDING STUDIES*
M. KINOSHITA[2]
L. B. SHAPPERT,[1] *FUEL-TRANSPORT SAFETY*
J. M. HOLMES, *INDUSTRIAL CHEMICAL STUDIES*
J. R. RICH, RADIATION CONTROL OFFICER
B. F. BOTTENFIELD, *HLAL DESIGN*
MAY E. PEPPER, SECRETARY
JO B. DeCARLO, SECRETARY
M. SUE DAMEWOOD, SECRETARY
PATRICIA J. TRENT, SECRETARY
MARY S. BROWN, SECRETARY
K. F. STOOKSBURY, CLERK
S. A. THURMER,[8] CLERK

DRAFTSMEN
D. E. DUNNING,[9] CHIEF
S. H. BEASLEY[9] — G. K. FORD[9]
J. W. DAY — BARBARA A. HISE
B. G. DeVALL — L. C. HUBBARD[9]
H. W. FALLON[2] — R. P. OLIVER[9]
A. J. FARMER — J. D. PHILLIPS[9]
J. N. WHEELER[9]

TRANSURANIUM PROGRAM

W. D. BURCH,[4] GROUP LEADER
F. L. PEISHEL, *SPECIAL EQUIPMENT*
C. H. LeMASTER,[3,4] *CRITICAL-PATH SCHEDULE*

THORIUM FUEL CYCLE

A. R. IRVINE, GROUP LEADER
J. W. ANDERSON,[4] *CONSTRUCTION LIAISON*
J. P. JARVIS,[4] *CONSTRUCTION LIAISON*
R. V. FOLTZ,[4] *CONSTRUCTION LIAISON*
J. M. CHANDLER, *PROCESS EQUIPMENT*
J. W. SNIDER, *PROCESS EQUIPMENT*
G. B. BERRY,[4] *PROCESS EQUIPMENT*
C. H. LeMASTER,[3,4] *CRITICAL-PATH SCHEDULE*

VOLATILITY STUDIES

R. P. MILFORD, GROUP LEADER
S. MANN, *SAMPLING AND ACCOUNTABILITY*
F. W. MILES, *RADIATION AND PLUTONIUM*
L. B. SHAPPERT,[1] *MECHANICAL EQUIPMENT*
J. D. YOUNG,[3] TECHNICIAN
B. B. KLIMA, *PROCUREMENT*
G. E. PIERCE,[10] *PROJECT LIAISON*
J. T. HUFFSTETLER,[4] *CRITICAL-PATH SCHEDULE*

POWER REACTOR FUEL PROCESSING

E. L. NICHOLSON, GROUP LEADER
J. KLITGAARD,[7] *SOLVENT EXTRACTION*
L. E. McGINNIS,[11] *HTGR FUELS*

WASTE STUDIES

J. O. BLOMEKE, GROUP LEADER
A. M. ROM, *WASTE IN ASPHALT*
E. J. FREDERICK, *FBVPP WASTE*
A. SHIMOZATO[2]

PILOT PLANT SECTION

R. E. BROOKSBANK, SECTION CHIEF
R. B. LINDAUER, *MSRR PROCESSING PLANT DESIGN*
BOBBIE HOYLE, SECRETARY
JANET MASON, SECRETARY
NANCY NEXLER, SECRETARY
E. C. BRANTLEY, CLERK
R. B. WATERS, DRAFTSMAN

FLUORIDE VOLATILITY PROCESS

W. H. CARR, GROUP LEADER
R. G. HICOL
R. J. SHANNON
E. L. YOUNGBLOOD[12]

SOL-GEL DEMONSTRATION

F. G. KITTS, PROBLEM LEADER
TECHNICIANS: S. E. SHELL
R. F. PURKEY

CURIUM RECOVERY FACILITY

V. C. A. VAUGHEN, GROUP LEADER
F. A. KAPPELMANN
W. T. McDUFFEE
W. R. WHITSON
TECHNICIANS: W. T. GOSTIC
W. A. LINDSEY
D. K. TAYLOR
C. S. WADDELL

RADIOCHEMICAL OPERATIONS

J. R. PARROTT, GROUP LEADER, *THORIUM UTILIZATION, PLANT SAFETY, ^{233}U HANDLING*
W. A. SHANNON
TECHNICIANS: J. E. KERLEY
J. H. WALKER

TRU FACILITY

W. D. BURCH, GROUP LEADER
J. E. BIGELOW
F. R. CHATTIN
E. D. COLLINS
W. W. EVANS
L. J. KING
J. L. MATHERNE
J. M. TURLEY
J. E. VAN CLEVE[12]
O. O. YARBRO

TECHNICIANS:
K. P. BAYNE[13] — C. L. JOHNSON[13]
C. K. BOATMAN — R. R. LAXSON
J. H. BROCK — J. B. OVERTON
W. J. BRYAN — D. B. OMSLEY
H. S. CALDWELL — C. L. SHEPHERD
T. L. DOUGLASS — R. C. SHIPWASH
J. T. EAST[13] — W. M. SPROULE
J. H. GROOVER — B. J. STRADER[13]
M. C. HILL — H. C. THOMPSON
C. H. JONES — A. V. WILDER

---

[*]ON LOAN TO CIVIL DEFENSE STUDIES, ORNL
[†]ON LOAN FROM TECHNICAL INFORMATION DIVISION
[‡]DUAL CAPACITY
[1]ASSIGNED TO THIS PROBLEM BY THE ANALYTICAL CHEMISTRY DIVISION
[2]GUEST SCIENTIST FROM ABROAD
[3]CO-OP STUDENT
[4]CONSULTANT, UNIVERSITY OF TENNESSEE
[5]ON LOAN TO CHEMISTRY DIVISION
[6]PART TIME FROM PILOT PLANT SECTION
[7]PART TIME (NOW WITH LONG RANGE PLANNING COMMITTEE)
[8]SUMMER EMPLOYEE
[9]ON LOAN FROM GENERAL ENGINEERING AND CONSTRUCTION DIVISION
[10]ON LOAN FROM PLANT AND EQUIPMENT DIVISION
[11]ON LOAN FROM GENERAL ATOMIC
[12]ON LOAN TO ARGONNE NATIONAL LABORATORY
[13]METALS AND CERAMICS DIVISION

ORNL-3945
UC-10 – Chemical Separations Processes for Plutonium and Uranium

INTERNAL DISTRIBUTION

1. Biology Library
2–4. Central Research Library
5. Laboratory Shift Supervisor
6. Reactor Division Library
7–8. ORNL – Y-12 Technical Library Document Reference Section
9–28. Laboratory Records Department
29. Laboratory Records, ORNL R.C.
30–31. E. L. Anderson
32. S. E. Beall
33. Arnold Berman
34. D. S. Billington
35. C. A. Blake
36. R. E. Blanco
37. J. O. Blomeke
38. C. J. Borkowski
39. R. E. Brooksbank
40. G. E. Boyd
41. J. C. Bresee
42. R. B. Briggs
43. K. B. Brown
44. F. R. Bruce
45. W. D. Burch
46. W. H. Carr
47. G. I. Cathers
48. J. M. Chandler
49. W. E. Clark
50. C. F. Coleman
51. J. A. Cox
52. D. J. Crouse
53. F. L. Culler
54. W. Davis, Jr.
55. D. A. Douglas
56–185. D. E. Ferguson
186. L. M. Ferris
187. J. R. Flanary
188. J. L. Fowler
189. J. H. Frye, Jr.
190. J. H. Gillette
191. H. E. Goeller
192. A. T. Gresky
193. W. R. Grimes
194. P. A. Haas
195. Richard Hamburger
196. J. P. Hammond
197. C. S. Harrill
198. A. Hollaender
199. R. W. Horton
200. A. R. Irvine
201. W. H. Jordan
202. M. T. Kelley
203. J. A. Lane
204. C. E. Larson
205. R. E. Leuze
206. M. H. Lloyd
207. R. S. Livingston
208. H. G. MacPherson
209. F. C. Maienschein
210. R. A. McNees
211. R. P. Milford
212. D. R. Miller
213. E. C. Miller
214. K. Z. Morgan
215. L. Nelson
216. E. L. Nicholson
217–218. R. B. Parker
219. R. E. Pahler
220. R. H. Rainey
221. J. T. Roberts
222. A. D. Ryon
223. A. F. Rupp
224. H. E. Seagren
225. M. J. Skinner
226. A. H. Snell
227. J. C. Suddath
228. E. H. Taylor
229. V. C. A. Vaughen
230. W. E. Unger
231. B. J. Young
232. C. D. Watson
233. B. S. Weaver
234. A. M. Weinberg
235. M. E. Whatley
236. G. C. Williams
237. R. G. Wymer
238. J. J. Katz (consultant)
239. C. W. J. Wende (consultant)
240. P. H. Emmett (consultant)
241. C. E. Winters (consultant)

EXTERNAL DISTRIBUTION

242. J. A. Swartout, 270 Park Avenue, New York 17, New York
243. Sylvania Electric Products, Inc.
244. Research and Development Division, AEC, ORO
245. Dr. Barendregt, Eurochemic, Mol, Belgium
246. Giacomo Calleri, CNEN, c/o Vitro via Bacdisseras, Milano, Italy
247. D. J. Carswell, Radiochemical Laboratory, The New South Wales University of Technology, P.O. Box 1, Kensington, Sydney, N.S.W., Australia
248. E. Cerrai, Laboratori CISE, Casella Postale N. 3986, Milano, Italy
249. David Dryssen, The Royal Institute of Technology, Department of Inorganic Chemistry, Kemisträgen 37, Stockholm 70, Sweden
250. Syed Fareeduddin, Indian Rare Earths Ltd., Army and Navy Building, 148 Mahatma Gandhi Road, Bombay 1, India
251. J. M. Fletcher, United Kingdom Atomic Energy Authority, Atomic Energy Research Establishment, Harwell, Berks, England
252. W. A. Graf, Manager, Plant Design, Atomic Products Division, General Electric Company, Box 450, Palo Alto, Calif.
253. H. Irving, Department of Inorganic Chemistry, University of Leeds, Leeds, England
254. T. Ishihara, Chemical Engineering Laboratory, Japan Atomic Energy Research Institute, Tokyo, Japan
255. A. S. Kertes, Hebrew University, Jerusalem
256. Jorgen Klitgaard, Eurochemic, Mol. Belgium
257. Y. Marcus, Israel Atomic Energy Commission, Tel Aviv, Israel
258. E. Glueckauf, Atomic Energy Research Establishment, Harwell, Berks, England
259. P. Rengnaut, C.E.N. Fontenay-aux-Roses, Boite Postale No. 6, Fontenay-aux-Roses, Sein, France
260. R. Rometsch, Eurochemic, Mol. Belgium
261. A. J. A. Roux, Director of Atomic Energy Research, South African Council for Scientific and Industrial Research, Box 395, Pretoria, South Africa
262. Jan Rydberg, Department of Nuclear Chemistry, Chalmers Tekniska Hogskola, Gibraltargatan 5 H. Goteborg, Sweden
263. M. Shaw, AEC, Washington
264. Erik Svenke, Director, Department of Chemistry, Atomic Energy Company, Stockholm 9, Sweden
265. D. G. Tuck, Associate Professor, Department of Chemistry, Simon Fraser University, Burnaby 2, British Columbia, Canada
266. B. F. Warner, United Kingdom Atomic Energy Authority, Production Group, Windscale and Calder Works, Sellafield, Seascale, Cumberland, England
267. R. A. Wells, Dept. of Scientific and Industrial Research, National Chemical Laboratory, Teddington, Middlesex, England
268. M. Zifferero, Comitato Nazionale per l'Energia, Nucleare, Laboratorio Trattamento Elementi Combustibili, c/o Instituto di Chemica Farmaceutica e Tossicologica dell 'Universita, Piazzale delle Scienze, 5, Rome, Italy
269. M. Claude Jean Jouannaud, Department Head, Plutonium Extraction Plant, Marcoule (Gard), France
270. Prof. Louis Gutierrez-Jadra, Director de Planta Pilotos e Industriales, Junta de Energia Nuclear, Ciudad Universitaris, Madrid (3), Spain
271. W. G. Belter, AEC, Washington
272. J. A. Lieberman, AEC, Washington
273. W. H. Regan, AEC, Washington
274. H. Bernard, AEC, Washington
275. P. Schmid, Federal Institute for Reactor Research, Wurenlingen, AG, Switzerland
276. Atou Shimozato, Nuclear Reactor Design Section, Nuclear Power Plant Department, Hitachi Ltd., Hitachi Works, Hitachi-Shi, Ibaraki-Ken, Japan

277. R. S. Brodsky, Division of Naval Reactors, Atomic Energy Commission, Washington, D.C. 20545
278. Theodore Rockwell III, Chairman, AIF Safety Task Force, MPR Associates, Inc., 815 Connecticut Avenue, N.W., Washington, D.C. 20006
279. Guenther Wirths, NUKEM, Hanau, Germany
280. Riki Kobayashi, Professor, Rice University
281. W. W. Grigorieff, Assistant to the Executive Director, Oak Ridge Associated Universities

282–461. Given distribution as shown in TID-4500 under Chemical Separations Processes for Plutonium and Uranium